FUNDAMENTALS OF RADIOCHEMISTRY

D.D. Sood

A.V.R. Reddy

N. Ramamoorthy

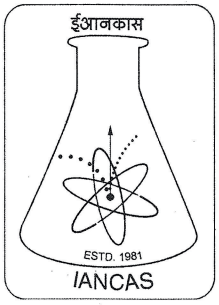

INDIAN ASSOCIATION OF NUCLEAR CHEMISTS AND ALLIED SCIENTISTS

Printed by : Sharda Stationery & Xerox
Shop No. 4, Arjun Centre,
Govandi East,
Mumbai - 400088
Tel. : 9869004377

First Edition : 2000
Second Edition : 2004
Third Edition : 2007
Fourth Edition : 2010
Reprinted : 2022

For copies and other information, please write to:

Secretary,
Indian Association of Nuclear Chemists and Allied Scientists
C/o Radiochemistry Division
Bhabha Atomic Research Centre
Trombay, Mumbai 400 085
INDIA
FAX: +91 22 25505151

About IANCAS

The Indian Association of Nuclear Chemists and Allied Scientists (IANCAS) was founded in 1981 with an objective of popularizing nuclear sciences among the scientific community in the country. Under its mandate, IANCAS is continuously promoting the subject of nuclear and radiochemistry, and use of radioisotopes & radiation sources in education, research, agriculture, medicine and industry by organizing seminars, workshops and publishing periodical thematic bulletins. With its enthusiastic Life Members from all over the country and overseas, IANCAS has become one of the popular platforms for popularizing the subject of nuclear and radiochemistry across the country. The Association's activities can be seen on its website: www.iancas.org.in.

IANCAS brings out quarterly thematic bulletins on the topic of relevance to the nuclear science and technology with the financial support from BRNS. The Association's popular book on "***Fundamentals of Nuclear and Radiochemistry***", "***Introduction to Radiochemistry***" and "***Experiments in Radiochemistry"*** is widely sought amongst the academia, researchers and students of DAE, non-DAE units and Universities. Another popular book of INCAS is "***Nuclear Materials***" which has been translated into Arabic, Hindi, Marathi and Telugu. Till December 2022, IANCAS has published 78 Thematic Bulletins and several special Bulletins. All IANCAS Books and Bulletins are available for free download on its website: www.iancas.org.in.

As a part of outreach programs, IANCAS conducts workshops on "*Radiochemistry and Applications of Radioisotopes*" at various universities, institutes, schools and colleges. These workshops play paramount role in motivating the young researchers and encourage them to accept the subject of radiochemistry and applications of radioisotopes. With the support from BRNS, a set of G.M. Counter / NaI(Tl) detector(s) are donated to the host institute of each National Workshops for their academic use. Similarly, IANCAS is also conducting one-day school Workshops to encourage and popularize the nuclear and radiochemistry subject amongst the young students. These workshops are conducted by the IANCAS main body and its four regional chapters (Southern Regional Chapter at Kalpakkam, Tarapur Chapter, Northern Regional Chapter at Amritsar, and Eastern Regional Chapter Bhubaneswar) covering the entire nation.

IANCAS is the co-organizer of biennial Symposia on Nuclear and Radiochemistry, popularly known as NUCAR. NUCAR series of Symposia covers the scope of nuclear chemistry, nuclear probes, chemistry of actinides, fission and activation products, nuclear and radioanalytical techniques, applications of radioisotopes in medical, agriculture and industries, nuclear safeguards, NUMAC & nuclear forensics, and nuclear instrumentation. In its series, the 16^{th} biennial NUCAR-2023 Symposium will be organized at DAE Convention Centre, Anushakti Nagar, Mumbai in May 2023.

To encourage scientists / researchers actively pursuing activities in this discipline, IANCAS has instituted several awards. ***Dr. M.V. Ramaniah Memorial Award*** is conferred annually to an outstanding scientist for their significant contributions and lifetime achievements in the field of nuclear and radiochemistry. **Dr*. Tarun Datta Memorial Award*** is given annually to a young scientist (below 45 years of age) with minimum 5 years of research experience in the field of nuclear and radiochemistry and applications of radioisotopes. IANCAS also gives ***Prof. H.J. Arnikar Best Thesis Award*** annually for the Ph.D. research in the nuclear and radiochemistry area. Additionally, IANCAS also gives about 20 best paper awards to young researchers for presetting their work in NUCAR symposia.

To achieve the excellent in its cause for popularizing the nuclear sciences through electronic media, IANCAS has its own website (www.iancas.org.in) which is updated regularly. Information about the workshops, Awards and various activities of IANCAS are available on the website. All the publications of IANCAS including bulletins and books are available in free downloadable form.

Seraj A. Ansari
General Secretary, IANCAS
September 5, 2022

Table of Contents

Chapter 1	The Beginning of Nuclear Sciences	1
Chapter 2	Nuclear Properties	8
Chapter 3	Nuclear Models	26
Chapter 4	Radioactivity	48
Chapter 5	Nuclear Decay Processes	66
Chapter 6	Interaction of Radiation with Matter	88
Chapter 7	Radiation Detection	104
Chapter 8	Nuclear Reactions	136
Chapter 9	Nuclear Fission and Nuclear Fusion	158
Chapter 10	Nuclear Reactors	178
Chapter 11	Particle Accelerators	205
Chapter 12	Production and Separation of Isotopes	221
Chapter 13	Applications of Radioisotopes in Physico-Chemical Investigations	253
Chapter 14	Radioanalytical Techniques and Applications	264
Chapter 15	Applications of Radioisotopes in Agriculture and Industry	289
Chapter 16	Applications of Radioisotopes in Healthcare	298
Chapter 17	Applications of Radioisotopes in Biology	323

Chapter 18	Radiochemical Separations	335
Chapter 19	Radiation Chemistry	347
Chapter 20	The Actinide Elements	367
Chapter 21	Health Physics	388
Chapter 22	Radioactive Waste Management	417
Appendix I	Fundamental Constants	439
Appendix II	Some Conversion Factors	440
Appendix III	Some α emitting Radioisotopes Used for Energy Calibration	441
Appendix IV	Some Pure Beta Emitters	442
Appendix V	Some Isotopes Used as Gamma Ray Energy Calibration Standards	443
Appendix VI	Nuclear Data of some Gamma Ray Emitting Radioisotopes used as Detection Efficiency Standards	444
Appendix VII	Q Value Equation of Nuclear Reaction	446
Appendix VIII	The Laboratory and Center of Mass Coordinate Systems	448
Appendix IX	Angular Momentum in Nuclear Reactions	451
Appendix X	Breit - Wigner Relation	454
Appendix XI	Table of Nuclides	455

Chapter 1
The Beginning of Nuclear Sciences

Discoveries of X-rays by Wilhelm Conrad Röntgen in November 1895 and radioactivity by Henri Becquerel in February 1896 had profound effect on the fundamental knowledge of matter. These two discoveries can be treated as the beginning of the subject 'Radiochemistry'. Röntgen found that some invisible radiation produced during the operation of cathode ray tube caused luminescence on a card board coated with barium platinocyanide which was placed at a distance. He called this radiation X-rays. He established that X-rays can penetrate opaque objects like wood and metal sheets. Henri Becquerel, in his investigation to establish a relation between fluorescence and emission of X-rays, stumbled upon the discovery of radioactivity. Becquerel discovered that crystals of a fluorescent uranium salt emitted highly penetrating rays which were similar to X-rays and could affect a photographic plate. Based on subsequent experiments, it was observed that uranium salts, fluorescent or not, emitted these rays and the intensity of the rays was proportional to the amount of uranium present in these salts. These rays were called uranic rays. Marie Curie christened the phenomenon as 'Radioactivity'. One of the interesting observations by Marie and Pierre Curie was that uranium ores were more radioactive than pure uranium and also more radioactive than a synthetically prepared ore similar to the ore. Foresight and further work by Curies led to the discovery of new elements polonium and radium. It is worth recording the monumental efforts made by Curies to isolate significant quantities of radium. Starting from two tonnes of pitchblende residue, from which much of the uranium had been removed, they obtained 100 mg of radium chloride. Madam Curie determined the atomic weight of radium as 226.5 and also prepared radium metal by electrolysis of the fused salt. All the separation work was carried out in a cow shed!! This accomplishment represented the culmination of their scientific faith and perseverance.

α, β, γ-radiations

The emanations from radioactive substances were found to have three components, called α, β and γ radiations. From the nature of their deflection in electric and magnetic fields, α-particles were recognised as having positive charge, β-particles as having negative charge and γ-radiation as electromagnetic radiation. The α-particles were found to be less

penetrating compared to β-particles and γ-radiation. Later, Rutherford conclusively proved, by spectroscopic measurements, that α-particles were doubly charged helium ions.

Transformation Hypothesis

Observation of emanations from thorium salts and compounds of radium, led Rutherford and Soddy to conclude (i) a radioactive element undergoes transformation and an atom of a new element is formed, (ii) the radiations are accompaniment of these changes and (iii) radioactive process causes a subatomic change within the atom. These conclusions were drawn when the existence of nucleus was not known, neutron was not discovered, isotope concept was not proposed and the source of energy of the emitted radiations was a big puzzle!!

Radioactive Decay Law

In 1902, Rutherford and Soddy proposed the theory of radioactive disintegration. They proposed that "the disintegration of the atom and expulsion of a charged particle leaves behind a new system lighter than before and possessing physical and chemical properties quite different from those of the original parent element. The disintegration process, once starts, proceeds from state to state with measurable velocities in each case". This would mean that the rate of decay of an active species in unit time is proportional to the total number of atoms of that species present at that time. Rate of disintegration (-dN/dt) continuously changes as the number of atoms (N) are changing (decreasing).

$$-\frac{dN}{dt} = N\lambda \qquad (1.1)$$

where λ is a proportionality constant known as the decay constant. Solving eqn. 1.1, one obtains

$$N = N_0\, e^{-\lambda t} \qquad (1.2)$$

where N_0 is the number of atoms present initially. In 1905, E. Von Schweilder formulated the radioactive decay law $N = N_0\, e^{-\lambda t}$ based on the decay probability (P) of a particular atom in a given time interval (Δt) (Details are given in Chapter 4). It may be noted that the observable is the radioactivity, rather than number of atoms. Radioactivity is the product of number of atoms (N) and the decay constant (λ).

Radioactive Equilibrium

When a radioactive atom (parent) decays, it transforms into another atom of a different element (except in γ transition). e.g. ^{14}C decays by emitting β^- and the product is ^{14}N is formed, which is stable. In this case, ^{14}C decays exponentially and ^{14}N grows exponentially with time. On the other hand, there are many cases where the product

(daughter) is also radioactive. In such cases, the daughter grows with time, not exponentially, but reaches a maximum value of radioactivity. As long as the combined parent-daughter system is undisturbed, depending on the decay constants of parent and daughter, the activities of both will be in a constant ratio. This condition is called 'radioactive equilibrium' condition. e.g. ^{226}Ra undergoes α-decay and its daughter ^{222}Rn also undergoes α-decay but at a faster rate compared to ^{226}Ra. After about 12-13 days, activity of ^{222}Rn and ^{226}Ra will be in constant ratio (near to 1). More details are given in Chapter 4.

Natural Radioactive Elements

Elements (isotopes) having atomic number greater than bismuth are radioactive. For example, ^{238}U undergoes α-decay with ^{234}Th as the product, ^{234}Th further undergoes β^- decay

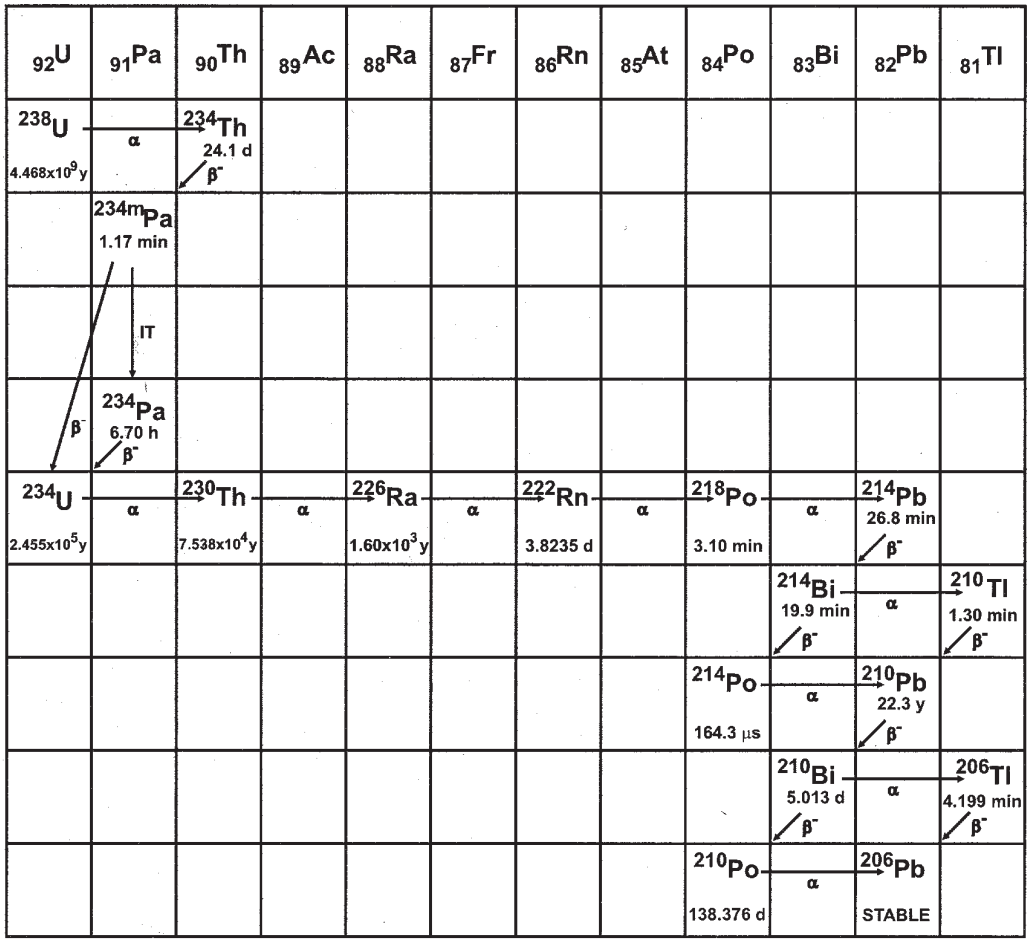

Fig. 1.1 The uranium series [Nuclear data are taken from J.K. Tuli, Nuclear Wallet Cards, 5th ed (1995), Brookhaven National Laboratory, Upton, New York].

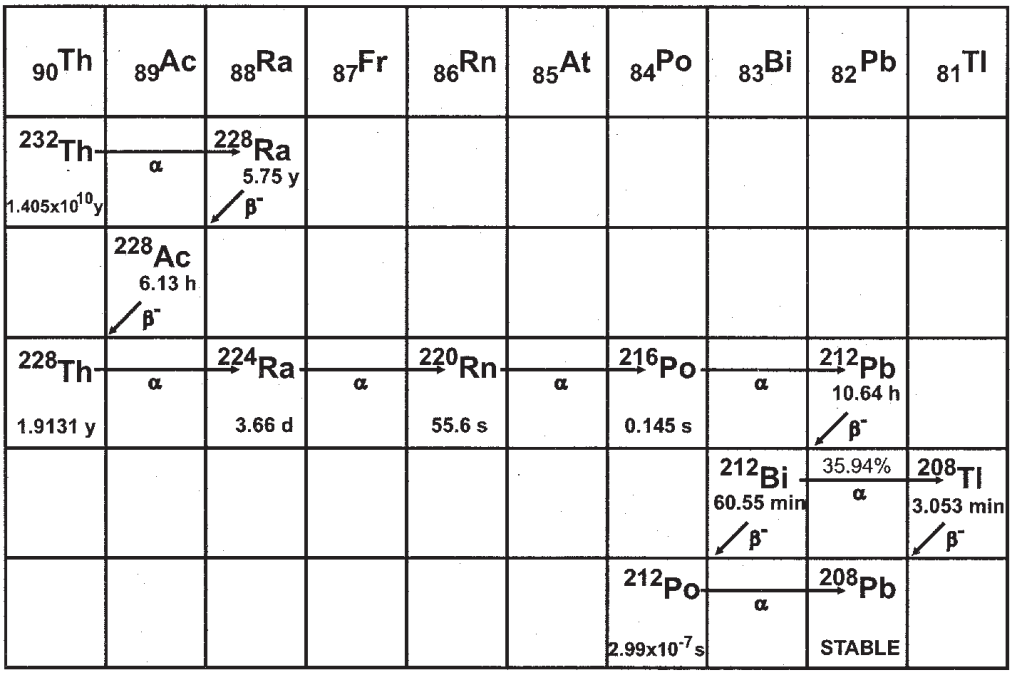

Fig. 1.2 The thorium series [Nuclear data are taken from J.K. Tuli, Nuclear Wallet Cards, 5th ed (1995), Brookhaven National Laboratory, Upton, New York].

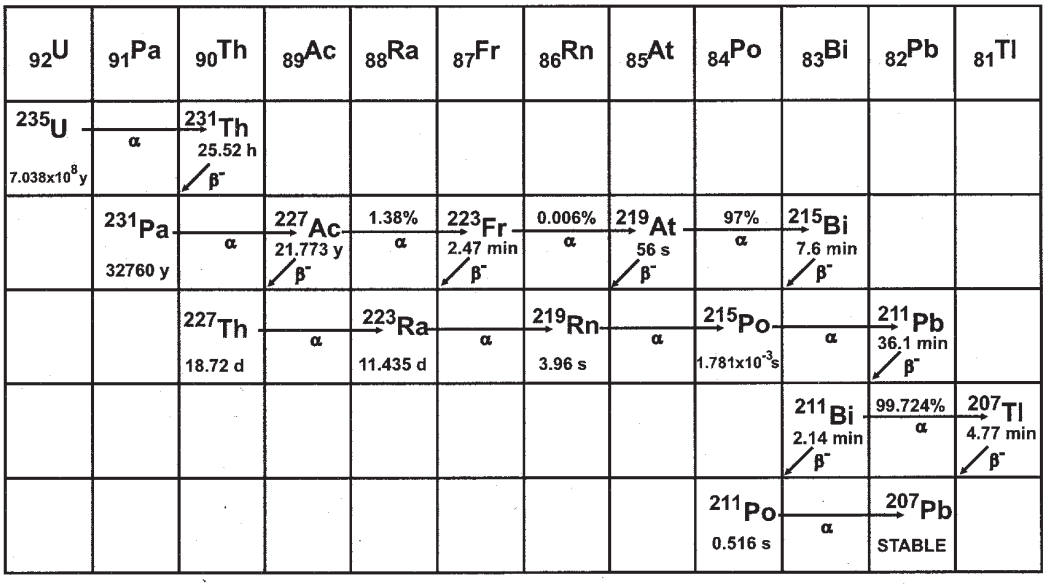

Fig. 1.3 The actinium series [Nuclear data are taken from J.K. Tuli, Nuclear Wallet Cards, 5th ed (1995), Brookhaven National Laboratory, Upton, New York].

with ^{234}Pa as the product. The chain continues until the stable end product ^{206}Pb is reached (Fig. 1.1). All the radioisotopes present in this chain form a family or series. This family is known as uranium series or ^{238}U series or 4n + 2 series since the mass number of all the members has a reminder of 2 after dividing by 4. Similarly, Thorium series, starting from ^{232}Th and ending at ^{208}Pb is known as 4n series (Fig. 1.2). Actinium series, starting from ^{235}U and ending at ^{207}Pb is known as 4n+3 series (Fig. 1.3). Other radioisotopes present in nature are shown in Table 1.1. In addition, tritium (^{3}H) and ^{14}C are continuously produced by cosmic ray induced nuclear reactions in the atmosphere. Another series of radioisotopes

Table 1.1 - Naturally occurring radioactive substances other than members of 4n, 4n+2 and 4n+3 series

Active substance	Type of Disintegration[a]	Half-life (y)	Isotopic abundance (%)	Stable Disintegration Products
^{40}K	β^-, EC, β^+	1.277×10^9	0.0117	^{40}Ca, ^{40}Ar
^{50}V	EC, β^-	1.4×10^{17}	0.250	^{50}Ti, ^{50}Cr
^{87}Rb	β^-	4.75×10^{10}	27.835	^{87}Sr
^{113}Cd	β^-	9.3×10^{15}	12.22	^{113}In
^{115}In	β^-	4.41×10^{14}	95.7	^{115}Sn
^{123}Te	EC	$> 1 \times 10^{13}$	0.908	^{123}Sb
^{138}La	EC, β^-	1.05×10^{11}	0.0902	^{138}Ba, ^{138}Ce
^{144}Nd	α	2.29×10^{15}	23.8	^{140}Ce
^{147}Sm	α	1.06×10^{11}	15.0	^{143}Nd
^{148}Sm	α	7×10^{15}	11.3	^{144}Nd
^{152}Gd	α	1.08×10^{14}	0.20	^{148}Sm
^{176}Lu	β^-	3.73×10^{10}	2.59	^{176}Hf
^{174}Hf	α	2.0×10^{15}	0.162	^{170}Yb
^{187}Re	β^-	4.35×10^{10}	62.60	^{187}Os
^{190}Pt	α	6.5×10^{11}	0.011	^{186}Os

[a]The symbols EC, β^- and β^+ stand for electron capture, negatron decay and positron decay, respectively; these decay modes are described in Chapter 5.

[Nuclear data are taken from J.K. Tuli, Nuclear Wallet Cards, 6th ed (2000), Brookhaven National Laboratory, Upton, New York].

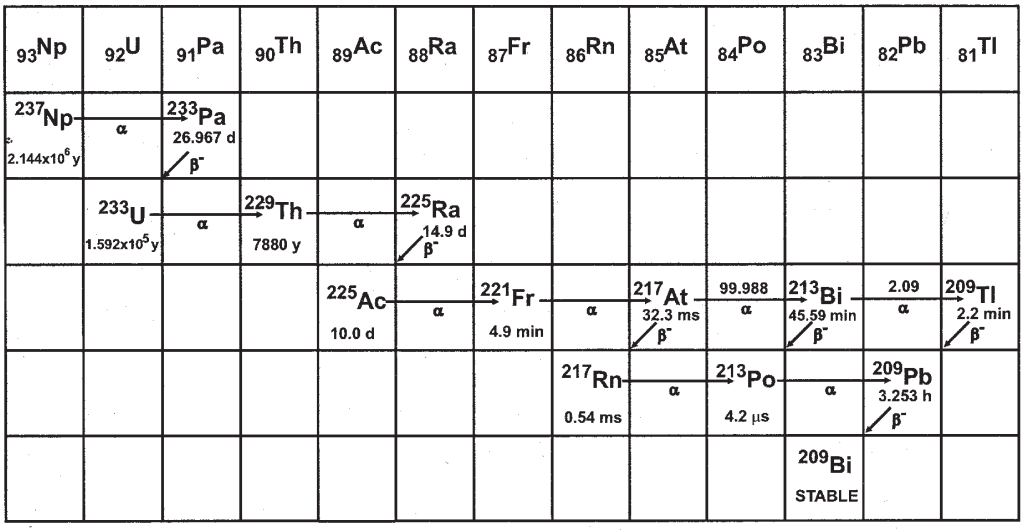

Fig. 1.4 The 4n + 1 series [Nuclear data are taken from J.K. Tuli, Nuclear Wallet Cards, 5th ed (1995), Brookhaven National Laboratory, Upton, New York].

starting from ^{237}Np and ending with ^{209}Bi, known as 4n+1 series is an artificial series (Fig. 1.4). Uranium-233, a member of this series, is a fissile isotope.

Artificial Radioactive Elements

Rutherford discovered the first nuclear reaction when he was investigating the possibility of α induced transmutation on various targets. In 1919, he postulated the transmutation of ^{14}N as per the following reaction.

$$^{14}_{7}\mathrm{N} + ^{4}_{2}\mathrm{He} \rightarrow ^{17}_{8}\mathrm{O} + ^{1}_{1}\mathrm{H} \qquad (1.3)$$

In 1932, similar studies by his student Chadwick involving α bombardment of boron lead to the discovery of neutron.

$$^{10}_{5}\mathrm{B} + ^{4}_{2}\mathrm{He} \rightarrow ^{13}_{7}\mathrm{N} + ^{1}_{0}\mathrm{n} \qquad (1.4)$$

In the same year positron, an antiparticle of electron, was discovered by Anderson. In 1934, Irene and Federic Joliot Curie, in their studies on production of positrons by bombardment of aluminium with α-particles, found that the product formed continued to emit positrons even after the α-source was removed (Eqns. 1.5 and 1.6). They separated phosphorus as posphine, measured its half-life and concluded that the product formed was a radioactive element.

$$^{27}_{13}\mathrm{Al} + ^{4}_{2}\mathrm{He} \rightarrow ^{30}_{15}\mathrm{P} + ^{1}_{0}\mathrm{n} \qquad (1.5)$$

$$^{30}_{15}\mathrm{P} \rightarrow ^{30}_{14}\mathrm{Si} + \beta^{+} \qquad (1.6)$$

This heralded the beginning of artificial production of radioisotopes. With the construction of accelerators and nuclear reactors, a large number of radioisotopes have been produced. ^{233}U has been produced by neutron irradiation of ^{232}Th as follows:

$$^{232}Th + n \rightarrow {}^{233}Th \xrightarrow{\beta^-} {}^{233}Pa \xrightarrow{\beta^-} {}^{233}U \qquad (1.7)$$

^{233}U undergoes α-decay leading to a series of products upto the stable end product of ^{209}Bi (Fig. 1.4). Currently research on producing heavy elements using heavy ion accelerators is being pursued.

Bibliography

1. S. Glasstone, Sourcebook on Atomic Energy, 3rd Ed., Affiliated East West Press Pvt. Ltd. (1967).
2. G. Friedlander, J.W. Kennedy, E.S. Macias and J.M. Miller, Nuclear and Radiochemistry, 3rd Ed., John Wiley & Sons Inc., New York (1981).
3. G.R. Choppin and J. Rydberg, Nuclear Chemistry: Theory and Applications, Pergamon Press, Oxford (1980).
4. Frontiers in Nuclear Chemistry, Eds. D.D. Sood, A.V.R. Reddy and P.K. Pujari, IANCAS Publication, Mumbai (1996).
5. R.D. Evans, The Atomic Nucleus, Tata-McGraw-Hill Book Co., New York (1978).
6. I. Kaplan, Nuclear Physics, 2nd Ed., Addision Wesley, Cambridge, Massachusetts (1963).
7. W.R. Nitske, The Life of Wilhelm Conrad Röntgen-Discoverer of X-rays, The University of Arizona Press, USA (1971).
8. A. Romer, The Discovery of Radioactivity and Transmutation, Dover, New York (1964).
9. H. Becquerel, *Comp. Rend.*, **122** (1896) 420, 501.
10. P. Curie and Mme S. Curie, *Compt. Rend.*, **127** (1898) 175.
11. T.J. Trenn, The Self Splitting Atom - The History of Rutherford- Soddy Collaboration, Taylor and Francis Ltd., London (1977).
12. F. Joliot and I. Curie, *Nature*, **133** (1934) 201.
13. H. Langevin-Joliot, In Artificial Radioactivity, Eds. K.N. Rao and H.J. Arnikar, Tata-McGraw Hill, New Delhi (1985).

Chapter 2
Nuclear Properties

Introduction

Path breaking experiments by J.J. Thomson and others towards the end of the 19th century had a profound effect on the study of atomic structure. Carrying out different experiments, Thomson proved that negatively charged electrons are the fundamental constituents of all atoms. As the atoms are electrically neutral, the total negative charge must be equal to the total positive charge. Thomson proposed the plum pudding model in which the atom consisted of positive charged matter of uniform density in which electrons are distributed such that numerically the total negative charge due to electrons is equal to the total positive charge. Accordingly the diameter of the sphere consisting of the positive charge is same as the size of the atom ($\sim 10^{-8}$ cm). Emission of positively charged alpha particles by radioactive atoms indicated that atoms also contain positively charged constituents. However, Thomson's model could not explain the subsequent observations made by Rutherford in the experiments on scattering of α-particles by atoms.

Discovery of the Nucleus

One of the most spectacular observations was made by Rutherford in the experiments on the scattering of α-particles by thin metallic foils which eventually led to the discovery of the atomic nucleus. This discovery gave an impetus to a series of experiments that revolutionised the understanding of nuclear structure. A brief description of Rutherford's experiment is given here.

A collimated beam of α-particles was projected onto a thin gold foil and the α-particles coming out of the foil, at different angles with respect to the incident beam, were measured using a scintillation screen in a dark room. Most of the α-particles passed through the thin foil undeflected as if there was no matter in the foil to obstruct the passage of these fast moving α-particles (Fig. 2.1). A few of them were scattered which was attributed to the electrostatic forces between the α-particles and the charges in gold atoms. The most important observation was that on an average one in 8000 α-particles was scattered through

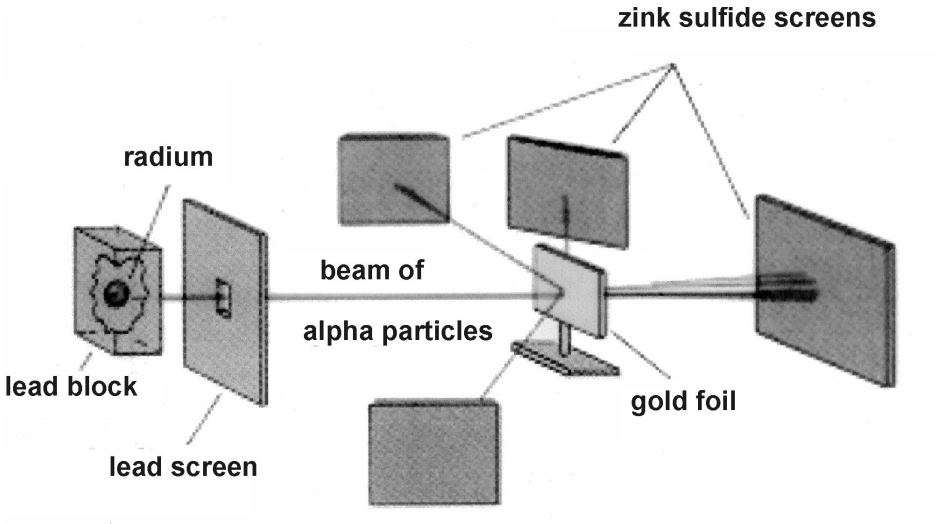

Fig. 2.1 Scattering of alpha particles by gold atoms in a thin foil.

an angle greater than 90^{o}. This large angle scattering could not be explained by the then known theories/models of the atom. Rutherford proposed that the large angle scattering could be due to a single encounter with a massive and positively charged centre in the atom which is responsible for producing an intense electric field. He called this centre as 'nucleus'. He suggested that the positive charge and entire mass are concentrated in this small region, surrounded by orbiting electrons. From these experiments, nuclear size (~10^{-13} cm) and the charge were first determined. After experimentally verifying the scattering formula proposed by Rutherford, the concept of his "Nuclear atom" was accepted, though the nature of nuclear force that is responsible for holding such a massive part (~10^{14} g/cc) in the atom was not known. Success of the nuclear atom is more due to the vision of Rutherford, as at that time, the existence of neutron was not known and it was difficult to account for both mass and charge in the nucleus. Subsequent experiments by many workers, notably Chadwick, firmly established that neutron also is one of the constituents of the nucleus.

Nomenclature and Classification of Nuclides

Nucleus of an atom consists of neutrons and protons, together called nucleons. A nucleon is about 1837 times heavier compared to the mass of an electron. As discussed above, most of the mass to the atom is provided by protons and neutrons of the nucleus. The sum of neutrons (N) and protons (Z) in a nucleus is called its mass number (A). Mass number is an integer close to its actual mass. Since atom is electrically neutral, each atom has the same number of electrons (Z) as that of protons. Z is known as atomic number. An atomic nucleus is often referred to as 'nuclide' and represented as ${}^{A}_{Z}X_{N}$ where X is the chemical symbol of the element. e.g. Uranium-235 is represented as ${}^{235}_{92}U_{143}$. Often neutron number is not written i.e. ${}^{235}_{92}U$. Sometimes, even atomic number is not written as the chemical symbol

uniquely represents an element and therefore, atomic number is known from the chemical symbol. e.g., ^{235}U, ^{12}C, ^{16}O etc. Nuclides are classified depending on mass, atomic and neutron numbers.

Isotopes

Nuclides having same atomic number (Z) but different mass number (A) are called isotopes. They occupy the same place in the periodic table and are chemically similar. e.g., ^{1}H, ^{2}H and ^{3}H are isotopes of hydrogen and ^{234}U, ^{235}U and ^{238}U are isotopes of uranium.

Isobars

Isobars are those nuclides having same mass number (A) but different neutron number (N) and atomic number (Z). e.g. $^{135}_{52}Te$, $^{135}_{53}I$, $^{135}_{54}Xe$ and $^{135}_{55}Cs$ are isobars with mass number A = 135. They belong to different chemical elements. Another set of isobars is $^{15}_{8}O$ and $^{15}_{7}N$. In this case, neutron number and proton number in the pair of isobars are interchanged. Such a pair of isobars is called "mirror nuclides".

Isotones

Nuclides having same number of neutrons are called isotones. e.g. $^{3}_{1}H$, $^{4}_{2}He$ and $^{5}_{3}Li$ have neutron number of 2. But both A and Z are different and thus they are chemically different.

Isomers

Nuclides having same A and Z are known as isomers of an isotope. They differ in energy of the nucleus, e.g., ^{60m}Co and ^{60}Co are isomers of ^{60}Co; and ^{137m}Ba and ^{137}Ba are isomers of ^{137}Ba. Superscript 'm' represents metastable or isomeric state and is one of the excited states of a nucleus which has measurable life time. Isomers deexcite mainly by γ-ray emission. In some cases, more than two isomeric states have been found; e.g., ^{124g}Sb (60.2 d) is unstable and has two isomers: $^{124m1}Sb$ (93 s) and $^{124m2}Sb$ (20.2 min).

Nuclear Properties

Static properties of nuclei like mass, energy, size and shape; mechanical properties like spin and moments are described below. Also a brief description of excited states is given.

Nuclear Mass and Binding Energy

Mass of a nucleus (M) is a direct measure of its energy content (E) as given by Einstein's equivalence of mass and energy

$$E = Mc^2 \qquad (2.1)$$

where c is the velocity of light. The mass of a nucleus is always smaller than the combined mass of its constituent nucleons. The difference between the two is called mass defect or binding energy (B) of the nucleus. Binding energy of a nucleus of mass number A, charge Z and atomic mass M(A,Z) is defined as

$$B = ZM_H + (A\text{-}Z)M_n - M\,(A,Z) \qquad (2.2)$$

where M_H and M_n are masses of hydrogen atom and neutron respectively and the values are 1.007825 and 1.008665 atomic mass units (amu)[1] respectively. Literature data on atomic masses of hydrogen and other isotopes incorporate mass of electrons, and can be used in the calculation of binding energy. For example, binding energy of ^{4}He is calculated as follows:

Helium nucleus contains 2 protons and 2 neutrons and its measured mass is 4.002603 amu. From eqn.2.2,

$$B = 2M_H + 2M_n - M\,(^4\text{He})$$

$$= 2 \times 1.007825 + 2 \times (1.008665) - 4.002603$$

$$= 0.030377 \text{ amu} = 28.2962 \text{ MeV}.$$

It means that when a ^{4}He nucleus is formed by combining 2 free protons and 2 free neutrons, a mass of 0.030377 amu is defected and an equivalent energy of 28.2962 MeV is liberated. Since this energy is liberated when the ^{4}He nucleus is formed, it is called binding energy of ^{4}He. The formation of ^{4}He from 4 protons is the reaction that is taking place in the Sun and stars and is known as thermonuclear reaction. This energy is the source for the light and heat we are receiving from the Sun. It may be noted that in this process, the Sun is losing 4.2 million tonnes of mass per second. Since the Sun is very massive, it turns out to be a very small fraction of the Sun's mass.

Binding energy of ^{56}Fe nucleus is 492.248 MeV and that of ^{238}U nucleus is 1801.647 MeV. Binding energy is a measure of stability. To compare binding energy of different nuclides, it is customary to express binding energy per nucleon (B/A) which is known as

---

[1] amu is energy unit in terms of mass. Mass of ^{12}C is taken as 12 amu and 1 amu is equal to 1/12th of the mass of ^{12}C. Thus

1 amu = $1.66053886 \times 10^{-27}$ kg

$\therefore$ Energy equivalent of 1 amu is obtained using eqn. 2.1, $E = 1.66053886 \times 10^{-27} \times (2.99792458 \times 10^8)^2$

$= 1.4924179 \times 10^{-10}$ Joule.

The energy units used in nuclear sciences are eV, keV (1000 eV) and MeV (10^6 eV) where eV is the energy required to raise one electron through a potential difference of one volt.

1 eV = 1.602189×10^{-12} erg.

$$\therefore \text{ 1 amu} = \frac{1.4924179 \times 10^{-10}}{1.602189 \times 10^{-19}} \text{ eV} = 931.5 \text{ MeV}$$

In nuclear science, energy is expressed in either amu or MeV

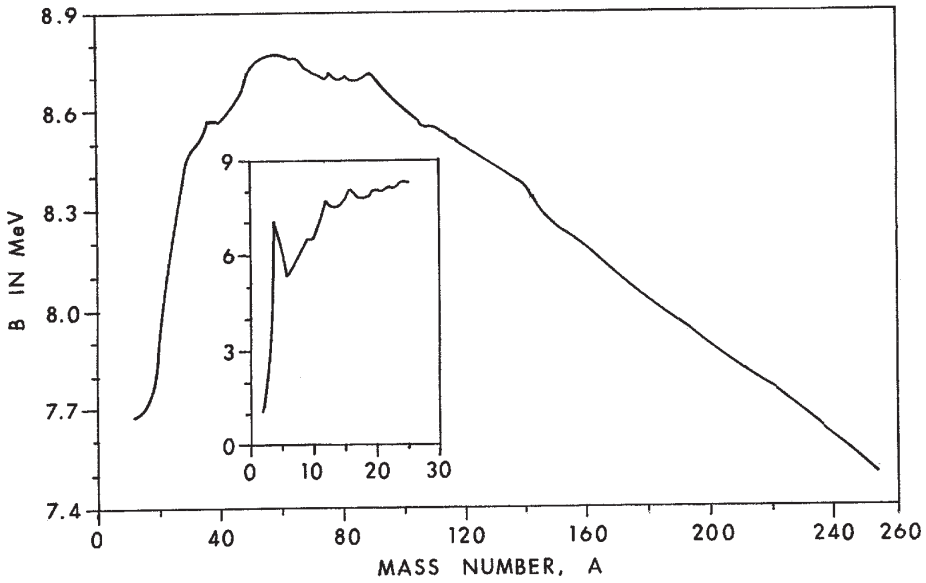

Fig. 2.2 Average binding energy curve [Introduction to Radiochemistry, A.V.R. Reddy and D.D. Sood, IANCAS Publication, 1997, p.6].

average binding energy. Average binding energy is remarkably constant for most of the nuclides with A = 60 to 200 having values in the range of 7.4 to 8.8 MeV. A plot of average binding energy as a function of mass number is known as binding energy curve and is shown in Fig. 2.2.

Much of the present knowledge about the structure of nuclei and the forces between nucleons is derived from the measured masses of nuclei. Most of these have been obtained either by mass spectrometry or by measurements of the energy released in radioactive decay, or energy released/absorbed in nuclear reactions. Experimental nuclear masses are available for most of the isotopes except those which are having very short half-lives. In the literature, generally mass excess $\Delta M(=M-A)$ rather than mass values are given.

Nuclear Radius and Density

Nuclear volumes are nearly proportional to nuclear masses. This means that nuclear density in all nuclei is same. Assuming the nucleus to be spherical, the density of the nuclear matter turns out to be about 10^{17} kg/m^3 or 10^8 tonnes/cm^3. It follows that nuclear matter is extremely dense compared to ordinary matter[2]. The force that holds the nucleons has to be very strong, attractive and at the same time very short-ranged, operative over a distance of

[2]"Although nuclear matter is dense, nuclei are not densely packed with nucleons". This is an important assumption in the success of the nuclear shell model (see Chapter 3).

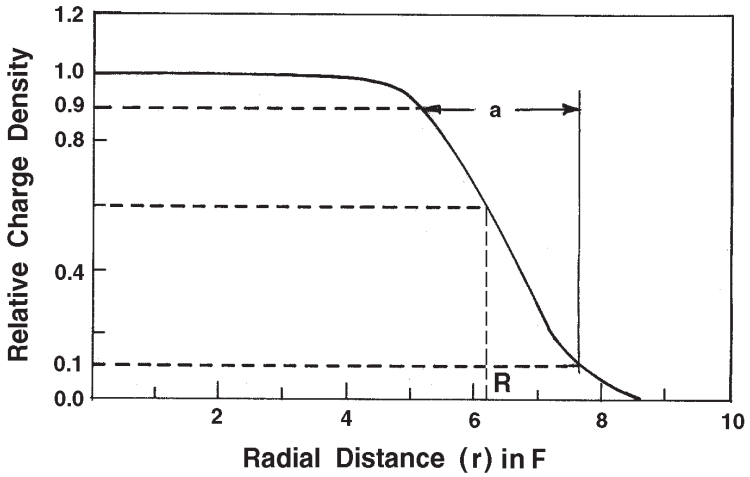

Fig. 2.3 Nuclear density profile as a function of radial distance [R. Hofstadter, Ann. Rev. Nucl. Sci. 7 (1957) 231].

the order of 10^{-15} m. Experimental methods are now available to determine the size and shape of the nuclei. For such studies, wave-length of probing particles should be of the order of the size of nuclei. Hence ordinary light with wavelength of about 10^{-7} m cannot be used. Energetic neutrons, protons and electrons are used as projectiles and the scattering intensity as a function of the angle is measured. For protons and neutrons, a few MeV energy is sufficient, whereas over 100 MeV electrons are required to be used for the same purpose. But electron has the advantage that it interacts with nucleus by familiar coulomb force whereas neutron and proton interact by nuclear force, the exact nature of which is not known. Experiments are performed for many nuclei and the charge distribution obtained are similar in shape for all nuclei. Charge density remains nearly constant from the centre upto a distance and gradually falls off as shown in Fig. 2.3. Mass distribution (density) is qualitatively same as that of charge distribution. Assuming that neutrons and protons have same density distribution, the mass distribution, $\rho(r)$, can be represented by eqn. 2.3.

$$\rho_{(r)} = \frac{\rho_{(0)}}{1+\exp\left[\dfrac{(r-R)}{a}\right]} \qquad (2.3)$$

where $\rho_{(0)}$ is the density at the centre and r is the radial distance The distance in which the density varies from $0.9\,\rho(0)$ to $0.1\,\rho(0)$ is called skin thickness, 'a' (see Fig.2.3). The distance corresponding to $0.5\,\rho(0)$ is taken as nuclear radius (R). A general set of parameters that fits a large body of data are given below:

$\rho_{(0)} = 1.6 \times 10^{14}$ nucleons/m^3 = 0.165 nucleons/F^3

---

[3]F is called Fermi and is equal to 10^{-15}m.

$$R = 1.28\ A^{1/3}\ F \text{ and } a = 0.55\ F$$

Since $\rho_{(0)}$ is constant for all nuclei, one can write

$$\rho_{(0)} \cdot V = \text{mass} \propto A$$

$$\frac{4}{3}\pi R^3 \propto A$$

$$\text{or } R \propto A^{1/3}$$

$$R = r_0 \cdot A^{1/3} \qquad (2.4)$$

R increases smoothly with $A^{1/3}$, i.e. nuclear volume is proportional to A.

Nuclear Force

Nucleons in a nucleus are bound by forces that are different than the familiar gravitational, electrostatic forces of attraction and weak interactions involved in β-decay. Gravitational force is attractive but between two protons its magnitude is 10^{39} times less than the repulsive electrostatic force. At the small distances at which protons are present in the nucleus, the electrostatic repulsion would be quite high and a strong attractive force would be essential to hold protons (nucleons) together. However, since we know that size of all nuclei is small, the nuclear forces, though very strong and attractive, must have a short range ($\sim 10^{-15}$ m). Nuclear force is thus attractive, short ranged and very strong. These forces are equally attractive between p-p, n-n and n-p. The nuclear force does not extend beyond the nuclear dimensions. In fact it is effective only among neighbouring nucleons and falls off more rapidly than $1/r^2$ where r is radial distance.

Nuclear Potential

For simplicity, nuclear potential is assumed to be of the form of a square well. Fig. 2.4 depicts the potential energy of a nucleus as a function of radial distance. It is the shape of the potential energy profile obtained using a charged particle probe like proton. The first part upto r = R represents potential due to attractive forces and the potential beyond nuclear radius is due to Coulombic repulsion. Nuclear potential (V(r)) is represented as

$$V(r) = 0 \qquad \text{for } r > R$$

$$V(r) = -V_0 \qquad \text{for } r \leq R \qquad (2.5)$$

Usually V_0 is around 30 MeV and the negative sign signifies attractive nature of nuclear forces. Though the nuclear potential outside nuclear dimensions is expected to be zero, the repulsive force due to protons has to be considered in the context of overall potential energy diagram. In this model, quite unrealistically, the nuclear potential becomes zero sharply at r = R. Nuclear potential can also be described by considering nucleus as a simple harmonic

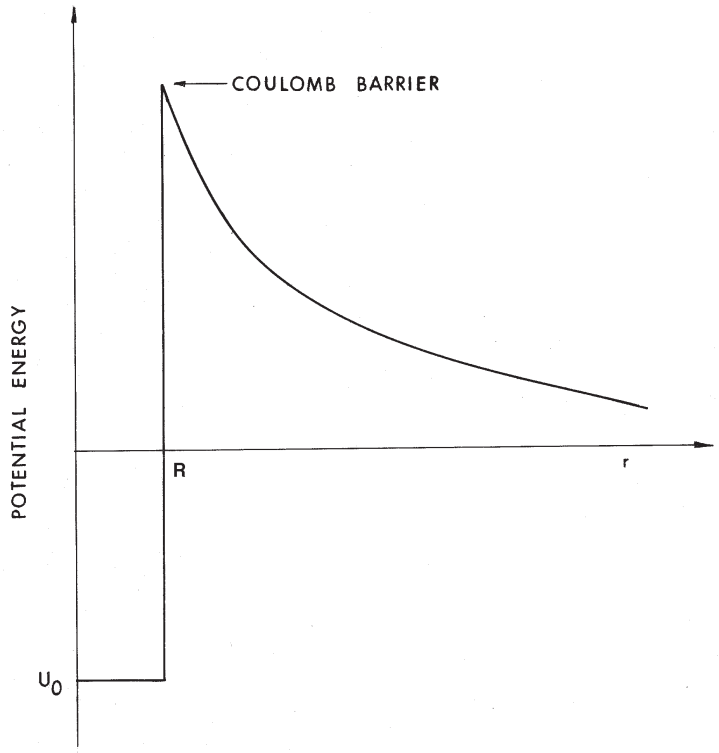

Fig. 2.4 Schematic of potential energy (PE) diagram of a nucleus. Inside the nuclear dimension, PE is negative (attractive) and outside it is positive (repulsive coulombic).

oscillator. In this case, potential energy diagram is represented by eqn. 2.6. In this model, the potential becomes infinity at r = R, which is also unrealistic. Realistic potential might be in between these two extremes and the details are beyond the scope of this book.

$$V(r) = -V_0\left[1-\left(\frac{r}{R}\right)^2\right] \qquad (2.6)$$

Quantum Numbers and Nuclear Spin

Observation of hyperfine structure in atomic spectra indicated that atomic nuclei must possess angular momenta. Net angular momentum of a nucleus is called nuclear spin (I).

Analogous to the vector model for atomic electrons, it is possible to visualise individual nuclear properties through a similar model which represents quantum mechanical results.

Quantum Numbers

The state of a nucleon is described by four quantum numbers, as in the case of atomic electrons. They are principal (n), orbital (l), magnetic (m_l) and spin (s) quantum numbers. Each bound individual particle is associated with principal quantum number n which can take positive values 1, 2, 3 .... . In the non-coulombic field, as in the case of nucleons, n is the sum of radial quantum number (ν) and orbital quantum number (l). Thus $n = \nu + l$. The orbital quantum number l is having values $l = 0, 1, 2 .... (n-1)$. The associated symbols for different l values are s(l=0), p(l=1), d(l=2) etc., as adopted in atomic spectroscopy. The orbital magnetic quantum number (m_l) is the component of l in a specified direction, e.g., applied magnetic field. m_l can have ($2l$+1) integer values between -l and l. The spin quantum number (s) has the value of ½ for all elementary particles, which obey Fermi-Dirac statistics. s value for neutron as well as proton is ½.

Total Angular Momentum State for a Particle (j)

It is equal to vector sum of its orbital and spin angular momenta and is a positive number. Each state can split into two levels with j values of l+½ and l-½. For example, $d_{5/2}$ state has a j value of 5/2.

Nomenclature of Nucleon States

Each nucleon can fully be described by four quantum numbers n, l, m_l and s. Pauli exclusion principle is applicable to neutrons and protons. For example, $^{1}d_{3/2}$ state has a l value of 2. Its j value is 3/2 means that it is a j = l-s state. Principle quantum number n is not represented explicitly. In $^{1}d_{3/2}$, 1 corresponds to radial quantum number (ν) and therefore, n will be 3 as $n = \nu + l$. Similarly, $^{2}f_{7/2}$ state has l=3, s=½ and therefore, it is a l+s state. The n value of this state is 5. In the case of nucleons, a neutron and a proton can have same set of four quantum numbers, as neutrons and protons occupy separate set of levels.

Nuclear Spin

As defined above, net angular momentum is called nuclear spin (I). In a nucleus, protons pair with protons and neutrons pair with neutrons. Protons of a pair align opposite to each other resulting in zero spin and thus even number of protons in a nucleus will have all protons in pairs. Same is the case with even number of neutrons. Thus, for an even-even nucleus, the net nuclear angular momentum in the ground state will be zero. A nucleus having even number of protons and odd number of neutrons, e.g., ^{13}C, can be treated as having an e-e core + 1 neutron. The angular momentum of the nucleus (nuclear spin) will be the orbital angular momentum of the last neutron which will be an half integral value. Similarly an odd-even nucleus will have an half integral nuclear spin due to the last proton. In the case of odd-odd nuclei, they will have nuclear spin of integer multiples which would be result of vectorial addition of contributions from the unpaired neutron and proton. Ground state nuclear spins of ^{12}C(e-e), ^{13}C(e-o), ^{13}N(o-e) and ^{14}N(o-o) are 0, 1/2, 1/2 and 1 respectively.

Parity

Parity is a nuclear property connected with the symmetry of the wave function. A system is said to have odd or even parity according to whether or not the wave function for the system changes sign when the signs of all the space coordinates are changed.

In mathematical terms,

If $\Psi(x,y,z) = \Psi(-x,-y,-z)$, then even parity and

If $\Psi(x,y,z) = -\Psi(-x,-y,-z)$, then odd parity

Parity of an isolated system like its total energy, momentum, angular momentum and statistics is conserved. The parity of a system is $(-1)^l$ where l is angular momentum quantum number, and + and - values correspond to even and odd parity respectively.

Magnetic Moments

An electrically charged particle having angular momentum revolves about a centre or spins about its own axis, behaving like a small magnetic dipole, and possesses a magnetic moment. For example, electron has a unit magnetic moment (μ) called Bohr magneton (μ_B) and is given by

$$\mu_B = \frac{e\hbar}{2\,mc} = 9.274 \times 10^{-21} \text{ erg/gauss} \qquad (2.7)$$

Where c is the velocity of light and m and e are respectively mass and charge of an electron. Similarly for a proton, expected intrinsic magnetic moment is 1 μ_N, where μ_N is known as nuclear magneton and is given by

$$\mu_N = \frac{e\hbar}{2\,m_p\,c} = 5.050 \times 10^{-24} \text{ erg/gauss} \qquad (2.8)$$

and m_p is the mass of the proton. Neutron being a particle with zero charge, is not expected to have magnetic moment. However, the measured magnetic moments for p and n are 2.792 μ_N and -1.913 μ_N respectively. These values indicate that both proton and neutron are not simple particles like electron but they may have structure. The negative sign for magnetic moment of neutron indicates that the negative charge is concentrated at the periphery and is overbalancing the effects of equal amount of positive charge near the centre.

Nuclei that have non zero nuclear spin (I) show magnetic moments. It is expressed in terms of nuclear gyromagnetic ratio (g) as

$$\mu = gI \qquad (2.9)$$

Nuclear spins and magnetic moments can be determined from hyperfine structure in atomic spectra. Several resonance techniques are also used for this purpose.

Quadrupole Moments

Quadrupole moment is a measure of deviation of a nucleus from spherical symmetry. If positive charge on a nucleus is distributed in a perfect spherical symmetrical manner, then its quadrupole moment (Q) is zero. The fact that Q is not zero for many nuclei means that nuclear charge has an asymmetric distribution. A positive Q value means that the charge distribution is elongated in the direction of the spin axis and the shape of the nucleus is prolate. On the other hand, if Q is negative, nucleus will be of oblate shape. Quadrupole moments are observed in those nuclei which have nuclear spin greater than 1/2.

The interaction of quadrupole moments with the electric field produced by electrons in the atom gives rise to hyperfine splitting of electronic energy levels that are observed in the atomic spectra. Techniques like optical spectroscopy and nuclear resonance absorption are used to measure Q values. For example $Q = 2 \times 10^{-30}$ m^2 for ^{14}N and -0.5×10^{-30} m^2 for ^{17}O.

Statistics

All nuclei and elementary particles are known to obey either Bose-Einstein or Fermi-Dirac statistics. Particles like protons, neutrons, electrons, positrons and neutrinos have a spin of 1/2 and obey Fermi-Dirac statistics. These particles are called Fermions. Nuclei having integer spin follow Bose-Einstein statistics and are called Bosons. Fermions obey Pauli's exclusion principle whereas Bosons do not.

If the wave function representing a nucleus does not change sign with the interchange of space and spin coordinates, the wave function is called symmetrical and nuclides/particles follow Bose-Einstein statistics. Whereas if the sign of the wave function is changed, then the wave function is called antisymmetric and particles obey Fermi-Dirac statistics.

In Fermi-Dirac statistics, a completely defined quantum state can be occupied by only one particle and hence Pauli's exclusion principle is applicable. e.g., protons, electrons etc. Such a restriction is not applicable to those particles that follow Bose-Einstein statistics, e.g., photon and pion. A nucleus will obey Bose-Einstein or Fermi-Dirac statistics depending upon whether it contains even or odd number of nucleons.

Excited State of the Nucleus

Just as the atomic spectrum is due to transition of an electron from ground state to excited state and subsequent deexcitations, gamma spectrum arises due to deexcitation of excited states of a nucleus. Measurement of properties like energies, spins and parity as well as the transition probabilities between excited states or from an excited state to ground state are important in understanding nuclear structure. Studying the properties of excited states of the nucleus constitutes the branch of nuclear spectroscopy.

Nuclear Stability

The elements in the universe are formed by nucleo-synthesis and observed abundance of stable nuclides must be related to the mechanism by which the elements originated and the characteristics of nuclear forces. Frequency distribution of nuclides, neutron to proton ratio in the stable nuclides and average binding energy variation with mass number have provided with some clues about nuclear forces. These systematics are used to arrive at the empirical rules regarding nuclear stability. Some of the observations of stable nuclides are explained in terms of nuclear models.

Frequency Distribution of Stable Nuclides

The observed relative abundances of elements are clearly related to nuclear properties of their stable isotopes rather than chemical properties. In the earth crust 85% of the elements have stable nuclei corresponding to even-even configuration. e.g., $^{16}_{8}O$ (48%) and $^{28}_{14}Si$ (26%). About 13% of elements have odd Z, but their principal isotopes have even-N. Abundances of the elements in the earth crust and the principal isotopes of these elements are given in Table 2.1. These numbers indicate that the nuclear stability is linked to pairing of nucleons. Elements having isotopes with paired configurations (e-e nuclei) are the most abundant.

The frequency distribution of stable nuclides is given in Table 2.2. It is seen that even-even nuclides are more stable. There are 81 stable elements that exist in nature. Out of

Table 2.1 - Weight % abundance of major elements in the earth's crust

	Even Z					Odd Z		
Element	O	Si	Fe	Ca	Mg	Al	Na	K
Weight % abundance	48	26	5	3.5	2.0	8.5	2.8	2.5
Principal isotope	$^{16}_{8}O$	$^{28}_{14}Si$	$^{56}_{26}Fe$	$^{40}_{20}Ca$	$^{24}_{12}Mg$	$^{27}_{13}Al$	$^{23}_{11}Na$	$^{39}_{19}K$

Table 2.2 - Frequency distributions of stable nuclides

Z	N	A = Z + N	Number of stable nuclides
even	even	even	165
even	odd	odd	55
odd	even	odd	50

these, 20 are monoisotopic and rest are multiisotopic. All except Be of these 20 stable monoisotopic elements have odd Z. Elements Tc (Z = 43) and Pm (Z = 61) do not have stable isotopes. There are 10 stable isotopes for Sn (Z = 50), 6 for Ca (Z = 20) and 4 for Pb (Z = 82). Similarly stable isotones are maximum for N = 50 (6) and N = 82 (7).

From these data, following conclusions are drawn.

(i) Even-even nuclides are most stable. Neutrons tend to pair with neutrons and protons tend to pair with protons. Pairing is associated with nuclear stability.

(ii) Stability of nuclides containing at least one class of even nucleons, e-o or o-e, is comparable. It reflects in the existence of comparable number of stable isotopes (Table 2.2).

(iii) Odd-odd nuclides are least stable.

(iv) Extra stability is associated with configuration having Z = 2, 8, 20, 50, 82 and/or N = 2, 8, 20, 50, 82, 126. These are called magic numbers.

Neutron to Proton Ratio

A plot of neutron number (N) vs proton number (Z) is given in Fig. 2.5. Stable isotopes are confined to a narrow region known as stability line. Any deviation from the stability line results in the instability. e.g., $^{55}_{25}$Mn is a stable nuclide. $^{56}_{25}$Mn with one additional neutron is unstable. It decays with a half-life of 2.5789 h. $^{17}_{8}$O is another stable nuclide. By adding a

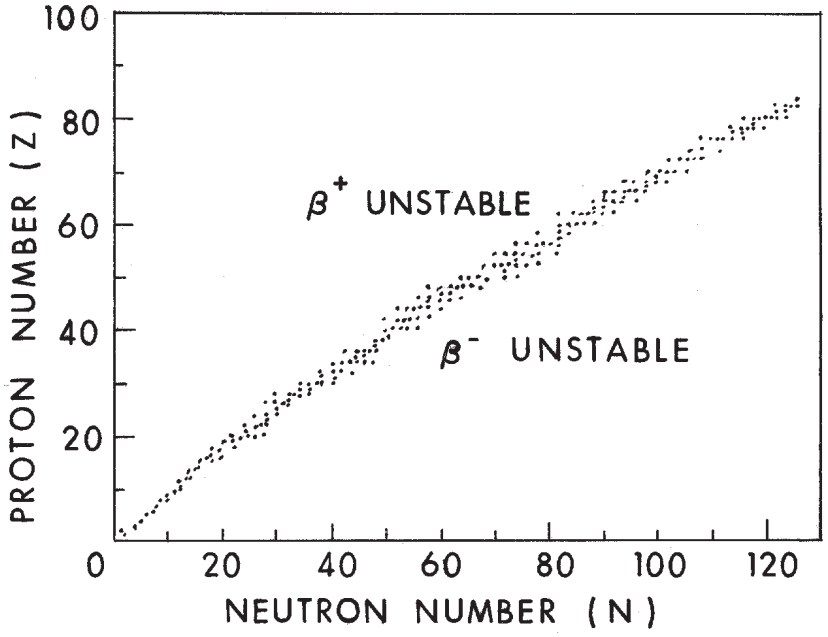

Fig. 2.5 N/Z curve for stable nuclides (line of stability).

proton, $^{18}_{9}F$ is obtained which is unstable. It decays with a half-life of 109.77 min. In fact, by bombarding stable isotopes with neutrons or protons, N/Z ratio of the resulting nucleus is changed and often the resulting nuclides are radioactive. This is the cardinal principle used in the production of radioisotopes.

From Fig. 2.5, it is observed that N/Z ratio remains as 1 upto mass number 40 and then slowly increases. e.g. N/Z values for ^{40}Ca, ^{56}Fe and ^{209}Bi are 1.00, 1.16 and 1.52 respectively. With increase in mass number (or Z), Coulombic repulsion due to protons increases; which results in destabilisation. To off-set this effect and maintain stability, more neutrons are needed and N/Z increases with A (or Z). Beyond A = 209, there is no stable nuclide as they are unstable with respect to α-decay, and some also undergo spontaneous fission (SF). Uranium is the last naturally occurring element and elements upto 112 have been artificially produced. Synthesis of higher Z elements is extremely difficult because of their short half-lives with respect to SF decay. In fact, SF puts the limit beyond which periodic table cannot be extended.

Since a large number of elements have stable isotopes, the stability line appears like a strip that widens out at higher Z values. The nuclides on the neutron rich side decay by β^- emission and those on the proton rich side undergo β^+ decay or electron capture to attain the stability. As mentioned earlier, nuclides above A = 209 undergo α-decay and in the region above A = 240 and Z = 92 nuclides are also unstable towards SF decay. This region is called sea of instability. Calculations have shown that there could be an island of stability around Z = 126 and N = 184, though, so far, experiments are not successful to synthesize elements in the island of stability or Super Heavy Element (SHE) region.

Beta Stability of Odd A and Even A Isobars

It is found that family of isobars having odd A has one stable nuclide. e.g. mass chain A = 131 has twelve isobars : ^{131}In, ^{131}Sn, ^{131}Sb, ^{131}Te, ^{131}I, ^{131}Xe, ^{131}Cs, ^{131}Ba, ^{131}La, ^{131}Ce, ^{131}Pr and ^{131}Nd, out of which ^{131}Xe is the only one stable nuclide. On the other hand, two or three stable nuclides are observed in the case of even A family of isobars. For example, for A = 132, ^{132}Xe and ^{132}Ba are stable nuclides. Similarly for A = 130, ^{130}Te and ^{130}Xe are stable nuclides. Less frequently three stable nuclides are also observed. For example, for A = 124, ^{124}Sb, ^{124}Te and ^{124}Xe are stable nuclides.

Binding Energy Curve

Average binding energy (B/A) is directly related to nuclear stability. From Fig. 2.2, B/A initially rises very sharply upto A = 20, then gradually reaches a maximum around A = 60 (Fe, Ni and Co region) and slowly decreases from there onwards. Additionally, in the lower mass region (inset in Fig. 2.2), a periodic structure is observed. The initial rise is due to decrease in surface to volume ratio with increasing A. For light nuclides, most of the nucleons will be at the surface of the nucleus and hence deprived of nuclear binding from all sides. e.g., in ^{2}H both nucleons are on the surface, hence it has a low binding energy. With increase in A, a larger fraction of nucleons are inside the nucleus compared to the nucleons at

the surface. Nucleons inside the nucleus are bound from all sides (saturation) than at the surface. Consequently binding energy per nucleon rises. After A = 60, the Coulombic repulsion due to protons becomes significant and hence average binding energy slowly decreases with increasing mass number (or Z). The following conclusions can be drawn from the average binding energy curve.

(i) For majority of nuclides, B/A is roughly constant in the range of 7.4 to 8.8 MeV. This is called saturation of binding energy.

(ii) Periodic recurrence of maxima at ^{4}He, ^{12}C, ^{16}O, ^{20}Ne, ^{40}Ca and ^{208}Pb shows that these nuclides are more stable compared to their neighbours. These nuclides have certain combinations of nucleons (N or Z = 2, 8, 20 etc.). They are more stable, indicating that the internal arrangement of nucleons inside the nucleus dictates the nuclear stability.

(iii) Decrease in B/A values with increase in A indicates that Coulombic repulsion due to protons increases rapidly ($\propto Z^2$) compared to attractive forces ($\propto A$).

Separation Energy of the Last Nucleon

The energy required to remove one neutron from a nucleus is called the separation energy of the last neutron (S_n). It can be written in terms of masses of nuclides and neutrons as

$$S_n(Z,A) = M(Z, A-1) + M_n - M(Z,A) \quad (2.10)$$

The S_n also can be defined as the energy released when a neutron is added to a nucleus (Z, A-1) to form another nucleus (Z,A). This quantity is analogous to the ionisation potential of an atom. Similarly separation energy of the last proton (Sp) is defined as the energy required to separate one proton from a nucleus and can be written as

$$S_p(Z,A) = M(Z-1, A-1) + M_H - M(Z,A) \quad (2.11)$$

Separation energies of neutron and proton are calculated using the masses of nuclides and neutron/proton. Eqns. 2.10 and 2.11 can also be written in terms of binding energy as given below.

$$S_n(Z,A) = B(Z,A) - B(Z,A-1) \quad (2.12)$$

$$S_p(Z,A) = B(Z,A) - B(Z-1,A-1) \quad (2.13)$$

The systematics of separation energies of last nucleons provide information on pairing energy and extra stability associated with magic numbers. In Table 2.3, computed values of S_n for gallium isotopes are given. From the table, it is clear that energy required to remove a neutron from gallium isotopes having even number of neutrons is more indicating that a paired neutron is tightly bound in the nucleus. This extra stability is origin of pairing energy. Pairing energy of neutrons (δ_n) can be calculated from the separation energies as

$$\delta_n(Z,A) = 0.5[S_n (Z, \text{even A}) - S_n (Z, A-1)] \quad (2.14)$$

Table 2.3 - Separation energies of last neutron of some gallium isotopes

Isotope	^{73}Ga	^{72}Ga	^{71}Ga	^{70}Ga	^{69}Ga	^{68}Ga	^{67}Ga	^{66}Ga
N	42	41	40	39	38	37	36	35
S_n	9.21	6.52	9.31	7.65	10.31	8.28	11.23	9.14
δ_n	1.35		0.83		1.02		1.05	

and the values for gallium isotopes are also given in Table 2.3. The value of pairing energy for very light nuclides is around 2 MeV and it reduces to around 1 to 1.2 MeV as the mass number increases.

Separation energy of the last neutron for strontium isotopes with neutron number around N=50 are calculated and given in Table 2.4. Similarly Table 2.5 contains the separation energy values for some isotones with Z around 50. These data can be used to understand the extra stability brought in by the presence of shell closures, known as magic numbers. The variation is also shown in Fig. 2.6 and 2.7. Differences in separation energies are mainly due to the pairing energy. However, around N=50 or Z=50, the difference is quite dramatic. The extra difference is due to the presence of magic number of N=50 or Z=50.

Table 2.4 - Separation energies of last neutron of some strontium (Z=38) isotopes

Isotope	^{94}Sr	^{93}Sr	^{92}Sr	^{91}Sr	^{90}Sr	^{89}Sr	^{88}Sr	^{87}Sr	^{86}Sr	^{85}Sr
N	56	55	54	53	52	51	50	49	48	47
S_n	6.75	5.46	7.29	5.80	7.81	6.36	11.11	8.43	11.48	8.53

Table 2.5 - Separation energies of last proton of some isotones (N=70)

Isotope	^{117}Ag	^{118}Cd	^{119}In	^{120}Sn	^{121}Sb	^{122}Te	^{123}I	^{124}Xe	^{125}Cs
Z	47	48	49	50	51	52	53	54	55
Sp	9.41	11.36	8.31	10.66	5.78	8.04	4.92	6.77	3.88

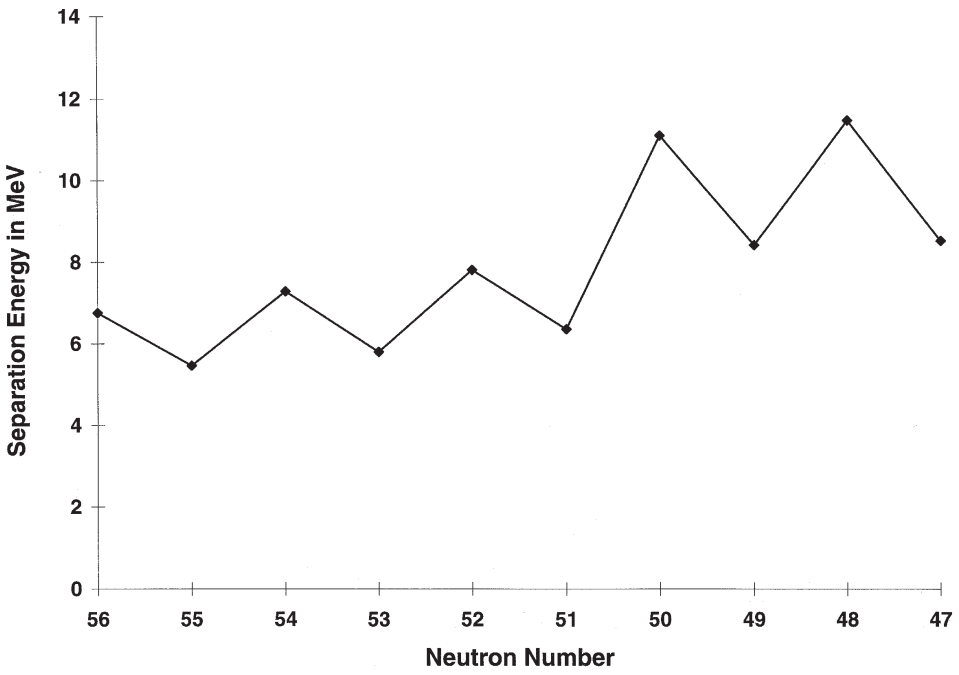

Fig. 2.6 Variation of separation energy with neutron number.

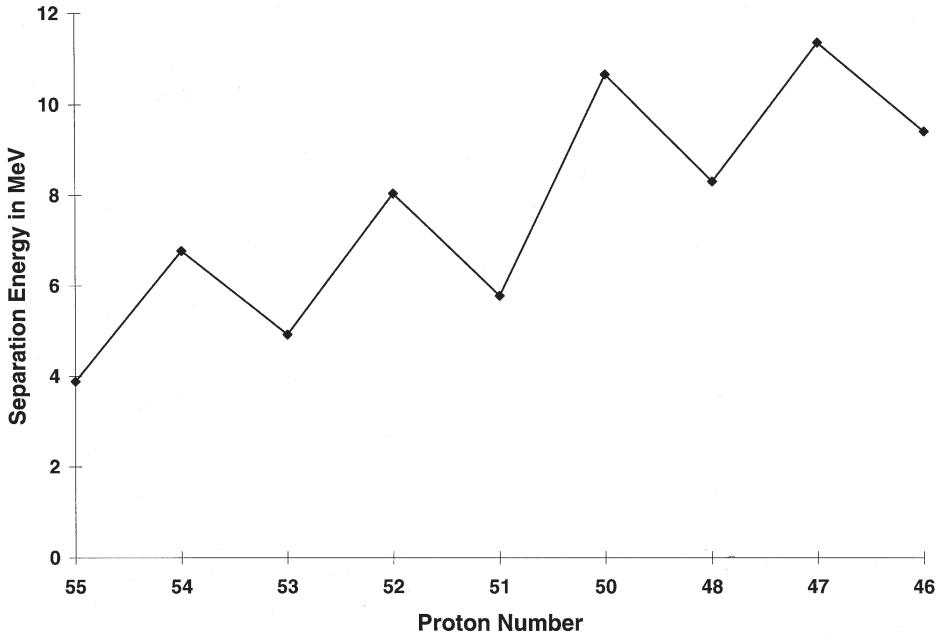

Fig. 2.7 Variation of separation energy with proton number.

Bibliography

1. R.D. Evans, The Atomic Nucleus, Tata-McGraw-Hill Book Co., New York (1978).
2. B.L. Cohen, Concepts of Nuclear Physics, Tata McGraw-Hill (1971).
3. I. Kaplan, Nuclear Physics, 2nd Ed., Addision Wesley, Cambridge, Massachusetts (1963).
4. G.R. Choppin and J. Rydberg, Nuclear Chemistry: Theory and Applications, Pergamon Press, Oxford (1980).
5. G. Friedlander, J.W. Kennedy, E.S. Macias, J.M. Miller, Nuclear and Radiochemistry, 3rd Ed., John Wiley & Sons Inc., New York (1981).
6. S. Glasstone, Sourcebook on Atomic Energy, 3rd Ed., Affiliated East West Press Pvt. Ltd. (1967).
7. Introduction to Radiochemistry, A.V.R. Reddy and D.D. Sood, IANCAS Publication, Mumbai (1997).
8. H.J. Arnikar, Essentials of Nuclear Chemistry, 4th Ed., Wiley Eastern (1990).
9. J.M. Blatt and V.F. Weisskopf, Theoretical Nuclear Physics, Wiley, New York (1952).
10. E. Rutherford, *Phil. Mag. Ser. 6*, **21** (1911) 669.
11. F. Soddy, *Ann. Rept. Chem. Soc*., **7** (1911) 285.
12. H.A. Bethe and R.F. Bacher, *Revs. Mod. Phys.*, **8** (1936) 82.
13. F. Bilter and H. Feshbach, *Phys. Rev.*, **92** (1953) 837L.
14. L.W. Alvarez and R. Cornog, *Phys. Rev*., **56** (1939) 613L.

Chapter 3
Nuclear Models

Nuclear Models are developed with an aim to explain the complex inter-relationships between nucleons when they aggregate to form nuclei. A number of nuclear models are proposed with different sets of assumptions and each of them could explain some experimental observations. Some models are : independent particle model / shell model, liquid drop model (LDM) and statistical model. Presently, no single model can explain all the observations.

Summary of Experimental Observations

Some of the important experimental observations related to nuclei which form the basis for nuclear models, are listed below.

1. The density of the nucleus is constant throughout the nucleus except near its surface.
2. Average binding energy is almost constant for most of the nuclei and its variation with mass number, A, is small but shows a definite trend.
3. In a family of isobars, β-decay energy is related to mass differences.
4. α-decay energies show systematic variation as a function of N and Z.
5. ^{235}U undergoes fission with thermal neutrons.
6. There is a finite upper boundary for N and Z of nuclides (drip lines) produced in nuclear reactions and nuclides heavier than ^{238}U are non-existent in nature.
7. Nuclear angular momenta (spin), I, of ground state are zero for even-even nuclei, integral multiples of 1/2 for odd A nuclei and non-zero integers for odd-odd nuclei.
8. Mirror nuclei have same value of I.
9. Magnetic moments (μ) have a relationship with I.
10. Electric quadrupole moments (Q) vary systematically with Z or N.

11. Existence of isomers and their prominence in the regions of N or Z = 40 to 50 and 70 to 80.

12. Parity change of nuclei in β-decay is followed by γ-deexcitation.

13. Discontinuities in the binding energy around the values of N or Z equal to 50, 82 and 126.

14. Discontinuities in the separation energy of the last nucleon around the values of N or Z equal to 50, 82 and 126.

15. Extra stability is associated with nuclides having N and/or Z : 2, 8, 20, 28, 50, 82, 126 (magic numbers).

16. Stable end products in the decay series of 4n, 4n+1, 4n+2 and 4n+3 corresponding to Pb (Z=82) or Bi (N=126)

17. Higher number of stable isotones with N=82, 126 and stable isotopes with Z=50 and 82.

18. Existence of resonance cross-section in (n,γ) reactions. High neutron capture cross section for ^{135}Xe (N=81).

19. Wide spacing of low-lying excited levels in nuclei.

Observations 1 to 6 are well explained by LDM whereas shell model explains observations 8 to 18. Observation 19 is the basis for statistical model. In this book, only LDM and shell model are described.

Liquid Drop Model

This model is essentially a collective model. A drop of liquid has constant density and binding energy per molecule. The same is true for a nucleus. In liquids, the Van der Waals force which is attractive and large for nearest neighbours and repulsive at smaller distances is responsible for this property. In the case of a nucleus, it is the exchange force that gives saturation property. The exchange force between a pair of nucleons is mediated by a particle called pi-meson (π^+, π^-, π^0). Interaction between pairs of nucleons can be viewed as:

$$p + n \rightarrow n' + \pi^+ + n \rightarrow n' + p$$
$$n + p \rightarrow p' + \pi^- + p \rightarrow p' + n$$
$$n + n \rightarrow n' + \pi^0 + n \rightarrow n' + n'$$
$$p + n \rightarrow p' + \pi^0 + p \rightarrow p' + n'$$
$$p + p \rightarrow p' + \pi^- + p \rightarrow p' + p'$$

where the prime quantities are used to indicate that the original pair of nucleons have exchanged their coordinates.

Assumptions of Liquid Drop Model

(i) Nucleus is like a droplet of incompressible and homogeneous liquid, and all nuclei have the same density. Interaction between nucleons is strong.

(ii) Nuclear force is spin and charge independent i.e. there is no difference in the magnitude of the force between n-n, p-p and n-p.

(iii) Nuclear force is having a short range character and is effective between nearest neighbours only.

Semi-Empirical Mass Formula (Von Weizsacker's Mass Formula)

It is possible to calculate the mass of a nuclide with mass number A and atomic number Z provided the binding energy (B) of the nucleus is known. B can be calculated on the basis of liquid drop model (LDM), using certain constants, neutron number and proton number of the nucleus. These constants are evaluated using some experimental quantities. The formula for B is called semi empirical mass formula. Mass of any unknown nuclide (isotope) can be calculated using this formula.

Binding energy formula derived using LDM, consists of five energy terms: volume energy (B_v), surface energy (B_s), coulomb energy (B_c), asymmetry energy (B_a) and pairing energy (B_p).

Volume Energy

It was seen that for stable isotopes binding energy per nucleon (B/A) is fairly constant over a large range of masses (Fig. 2.2). Thus, it can be written as

$$B/A = \text{Constant}$$

$$B_v = a_v \, . \, A \qquad (3.1)$$

where, a_v is a constant which has to be evaluated and v refers to volume. In the constant density model, volume of a nucleus is proportional to its mass and therefore, to its mass number (A).

In a nucleus, if each nucleon interacts with the remaining (A-1) nucleons, then there would be $A(A-1) \simeq A^2$ interactions. But from the eqn. 3.1, it is seen that B_v is proportional to A and not A^2. This indicates that each nucleon interacts only with its nearest neighbours and is a consequence of the short range and saturation character of nuclear forces.

Surface Energy

The nucleus has a surface and the nucleons at the surface interact only with half as many nucleons as the nucleons in the interior of the nucleus. Nucleons at the surface, therefore, are less strongly bound compared to those in the interior of the nucleus giving rise to the surface energy term (similar to surface tension in the case of a liquid drop). This energy (B_s) is proportional to the number of nucleons near the surface which is proportional to the

surface area of the nucleus. It is a correction for over estimation of volume energy and hence results in reduction in B.

$$B_s \propto 4\pi R^2$$

Considering the constant density of nucleus it was shown by eqn. 2.4 that $R = r_0 A^{1/3}$

$$\therefore B_s = -a_s A^{2/3} \qquad (3.2)$$

where a_s is a proportionality constant. The -ve sign implies destabilisation due to surface energy and hence reduction in B.

The fraction of the nucleons in contact with the surface is approximately equal to $4\pi A^{-1/3}$. For light nuclei like ^3He, this works out to be greater than unity indicating that all the nucleons are near the surface. In fact, for light nuclei, majority of the nucleons are near the surface and thus surface energy would be more. As the volume increases this term levels off. Further, surface energy would be minimum for nuclides with spherical shape. According to LDM, ground state of the nucleus is always spherical.

Coulomb Energy

Coulomb repulsion between protons is a long range force and it causes destabilisation of nucleus. Hence binding energy is reduced due to inter-proton repulsion. It can be shown that, for an uniform charged sphere of charge Z and radius R, the Coulomb energy B_c is

$$B_c \alpha \frac{3}{5} \times \frac{Z^2 e^2}{R} \cong -\frac{3e^2}{5r_0} \times \frac{Z^2}{A^{1/3}} \cong -a_c \frac{Z^2}{A^{1/3}} \qquad (3.3)$$

where a_c is a constant. The negative sign implies destabilisation due to Coulombic energy and hence reduction in B. With increasing atomic number, this energy becomes significant.

Asymmetry Energy

In the case of light elements, the number of neutrons is equal to the number of protons. But heavy nuclei always contain more neutrons than protons to provide enough total attractive force to compensate the Coulomb repulsion. At the same time neutron excess brings in instability. It is true also for nuclei which have more protons than neutrons.

This term has a single particle origin. Let us assume that both neutron and proton are independently constituting Fermi gas confined in potential wells of equal depth. Then for a nucleus with N = Z, Fermi energy (energy of the last occupied nucleon in the ground state) for n and p will be equal. For N>Z, Fermi level for neutron will be greater than that of proton and hence there will be a tendency to trade off the Fermi level of neutrons by beta decay. If there are more protons than neutrons, then the asymmetry due to (Z-N) excess protons will also lead to the same extent of instability. Thus in a nucleus, there will be asymmetry energy proportional to $(N-Z)^2$ which represents the extent of destabilisation due to excess neutrons or protons. B_a is also inversely proportional to A because the binding energy contribution per

neutron-proton pair is proportional to the probability of having such a pair within a certain volume (determined by the range of nuclear forces). Thus

$$B_a = - a_a \times \frac{(N - Z)^2}{A}$$

$$= - a_a \times \frac{(A - 2Z)^2}{A} \qquad (3.4)$$

where, a_a is a constant.

Pairing Energy

It is seen from the pattern of abundance of stable nuclides and separation energy of the last neutron and proton that even-even (e-e) nuclides are more stable than odd-even (o-e), even-odd (e-o) or odd-odd (o-o) nuclides. To account for this, a term called pairing energy (B_p) is added to the binding energy formula. This is given as:

$$B_p = + \delta \text{ for e-e nuclides}$$
$$B_p = 0 \text{ for o-e and e-o nuclides} \qquad (3.5)$$
$$B_p = -\delta \text{ for o-o nuclides}$$

where,

$$\delta = a_p A^{-1/2} \qquad (3.6)$$

and a_p is a constant.

The evaluation of δ is empirical and in some references δ is given as proportional to $A^{-3/4}$ and accordingly a_p value will be different.

Total Binding Energy and Mass of a Nucleus

A relation for the total binding energy of a nucleus is obtained by combining all the energy terms as :

$$B = B_v + B_s + B_c + B_a + B_p$$

$$B = a_v A - a_s A^{2/3} - a_c \frac{Z^2}{A^{1/3}} - a_a \frac{(A - 2Z)^2}{A} \pm a_p A^{-1/2} \qquad (3.7)$$

The relation is known as semiempirical mass formula. The constants a_v, a_s, a_c, a_a and a_p are empirically determined. Binding energy of stable nuclides is calculated using their known masses. The values of B for a few nuclides are used to solve for a_v, a_s, a_c, a_a and a_p. Approximate values of these constants expressed in MeV, are

$a_v = 14.1 \pm 0.2$ MeV; $a_s = 13 \pm 1$ MeV;
$a_c = 0.595 \pm 0.02$ MeV; $a_a = 19 \pm 0.9$ MeV;

a_p = +1.2 MeV for e-e nuclei, 0 for (o-e) and (e-o) nuclei, and -1.2 MeV for o-o nuclei.

Mass of a nucleus is given by eqn. 3.8.

$$M(A,Z) = Z\,M_H + (A\text{-}Z)\,M_n - B \qquad (3.8)$$

where M_H and M_n are masses of hydrogen atom and neutron respectively. Since binding energy is in MeV, masses also have to be expressed in MeV.

Worked Example

Binding energy of a nucleus can be calculated using LDM semi empirical formula with the constant given above.

For ^{59}Co, A = 59 and Z = 27. Value of $a_p = 0$ as ^{59}Co is e-o nucleus. Substituting these values in eqn. 3.7.

$$B = 14.1 \times 59 - 13\,(59)^{2/3} - 0.595\,\frac{(27)^2}{(59)^{1/3}} - 19 \times \frac{5^2}{59}$$

$$= 831.9 - 197.02 - 111.42 - 8.05$$
$$= 515.41 \text{ MeV}$$

$$\therefore \frac{B}{A} = 8.736 \text{ MeV}$$

This can also be calculated using the experimental masses of the neutrons, hydrogen atom and neutron in eqn. 3.8.

$$B = Z \times M_H + (A\text{-}Z)M_n - M\,(A,Z)$$

$$= 27 \times 1.007824 + 32 \times 1.008665 - 58.93320$$

$$= 0.55533 \text{ amu}$$

$$= 517.29 \text{ MeV}$$

$$\therefore \frac{B}{A} = 8.767 \text{ MeV}$$

These two values are in close agreement.

However, the differences between calculated and experimental values are large for the nuclei whose Z or N correspond to magic numbers.

Applications of the Semi-Empirical Mass Formula

Masses of unknown nuclei can be calculated using semi empirical formula. These calculations are extremely useful in nuclear reactions. Using LDM, predictions can be made

regarding nuclear stability with respect to beta decay, alpha decay and spontaneous fission. It is also useful to calculate nuclear radius constant (r_0).

Nuclear Radius Constant

The binding energy difference in the case of mirror nuclei (e.g., ^{15}O and ^{15}N) is proportional to $A^{2/3}$. For mirror nuclei, |N-Z| = 1 and N and Z are exchanged. Mass number A is same for both the nuclei. Therefore, in the binding energy formula, only coulomb term is different, all others being same.

$$DB = \left(- a_c \times \frac{Z^2}{A^{1/3}} \right) - \left(- a_c \times \frac{N^2}{A^{1/3}} \right)$$

$$= - \frac{a_c}{A^{1/3}} (Z^2 - N^2)$$

$$= - \frac{a_c}{A^{1/3}} (Z-N)(Z+N)$$

$$= a_c \times \frac{A}{A^{1/3}}$$

$$= a_c \times A^{2/3} \qquad (3.9)$$

This can be used to calculate nuclear radius constant. It is also known that for a spherical nucleus having uniform charge distribution,

$$a_c = \frac{3e^2}{5\, r_0} \qquad (3.10)$$

$$\therefore \Delta B = a_c \times A^{2/3}$$

$$= \frac{3e^2}{5\, r_0} \times A^{2/3}$$

$$\therefore r_0 = \frac{3\, e^2 \cdot A^{2/3}}{5 \cdot \Delta B} \qquad (3.11)$$

Since we know that r_0 is related to nuclear radius (R) as

$$R = r_0 \times A^{1/3}$$

R can be calculated.

The value of the radius constant has been found as $r_0 = 1.28$ F (1 Fermi = 10^{-15} m) from the data on mirror nuclei.

Beta Decay

In a family of isobars, β-decay is observed. In the case of β-decay, mass number A remains constant and Z changes by one unit. However, there are small differences in the masses of a given family of isobars which show a parabolic dependence on Z.

From eqns. 3.7 and 3.8, after rearrangement of co-efficients of Z and A, a relation for M(A,Z) is obtained as:

$$M(A,Z) = \alpha A + \beta Z + \gamma Z^2 \pm \delta \tag{3.12}$$

where,

$$\alpha = M_n\left(a_v - a_s - \frac{a_a}{A^{1/3}}\right) \tag{3.13}$$

$$\beta = 4a_s - (M_n - M_H) \tag{3.14}$$

$$\gamma = \left(\frac{4a_s}{A}\right)\left(1 + \frac{A^{2/3}}{4\frac{a_a}{a_c}}\right) \tag{3.15}$$

and α, β and γ are known as local constants of a family of isobars.

From eqn. 3.12, it can be concluded that for constant A, M(A,Z) has a parabolic dependence on Z. The vertex of the parabola corresponds to the most stable charge (Z_0) for a given A. This can be found out by differentiating eqn. 3.12 with respect to Z and equating it to zero

$$\left|\frac{\delta M(A,Z)}{\delta Z}\right|_A = \beta + 2\gamma Z_0 = 0$$

Hence $Z_0 = -\frac{\beta}{2\gamma}$ (3.16)

If the values of mass formula constants are substituted into eqn. 3.16, then dependence of Z_0 on A comes out as

$$Z_0 = \frac{A}{(0.015\,A^{2/3} + 2)} \tag{3.17}$$

Two examples of β-decaying isobaric chains involving odd A and even A are given below and also shown in Figs. 3.1 and 3.2.

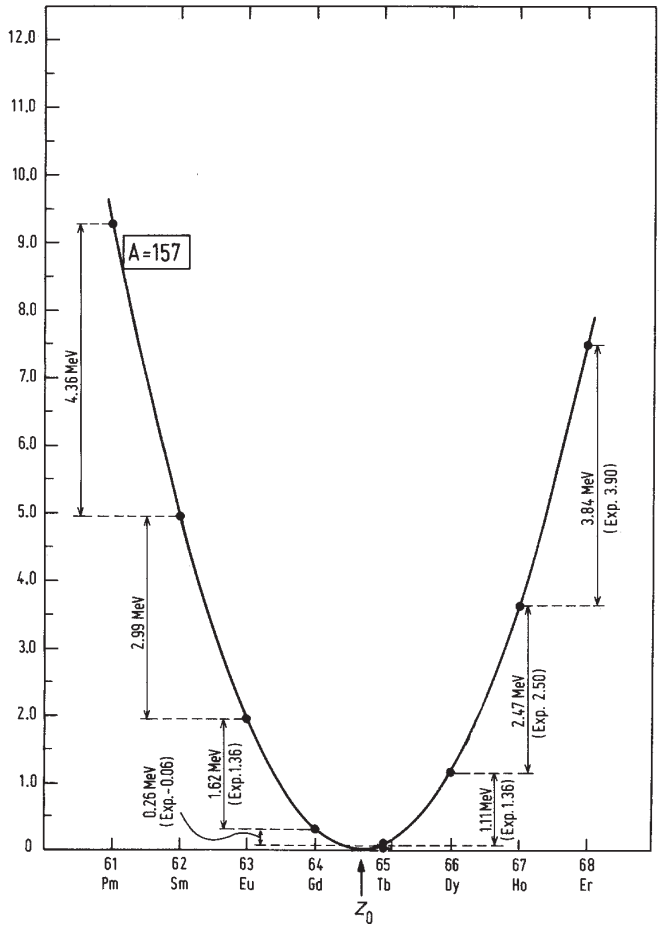

Fig. 3.1 Mass parabola for odd isobaric chain (A =157). Values given in the parantheses are experimentally observed values [Nuclear and Radiochemistry, G. Friedlander, J.W. Kennedy, E.S. Macias and J.M. Miller, 3rd Ed., John Wiley (1981) p.46].

A = 157; Odd mass number (Fig. 3.1)

$$^{157}_{61}\text{Pm} \xrightarrow{\beta^-} {}^{157}_{62}\text{Sm} \xrightarrow{\beta^-} {}^{157}_{63}\text{Eu} \xrightarrow{\beta^-} {}^{157}_{64}\text{Gd} \xrightarrow{\beta^-} {}^{157}_{65}\text{Tb} \xleftarrow{\beta^+} {}^{157}_{66}\text{Dy} \xleftarrow{\beta^+} {}^{157}_{67}\text{Ho} \xleftarrow{\beta^+} {}^{157}_{68}\text{Er}$$

A = 156; Even mass number (Fig. 3.2)

$$^{156}_{61}\text{Pm} \xrightarrow{\beta^-} {}^{156}_{62}\text{Sm} \xrightarrow{\beta^-} {}^{156}_{63}\text{Eu} \xrightarrow{\beta^-} {}^{156}_{64}\text{Gd} \xleftarrow{\beta^+} {}^{156}_{65}\text{Tb} \xrightarrow{\beta^-} {}^{156}_{66}\text{Dy} \xleftarrow{\beta^+} {}^{156}_{67}\text{Ho} \xleftarrow{\beta^+} {}^{156}_{68}\text{Er}$$

For odd-A, one mass parabola is observed. The most stable charge (Z_0) can be found from eqns. 3.16 and 3.17 and this may be a fractional number. The integer nearest to Z_0 will correspond to stable charge ($^{157}_{65}$ Tb in the above example).

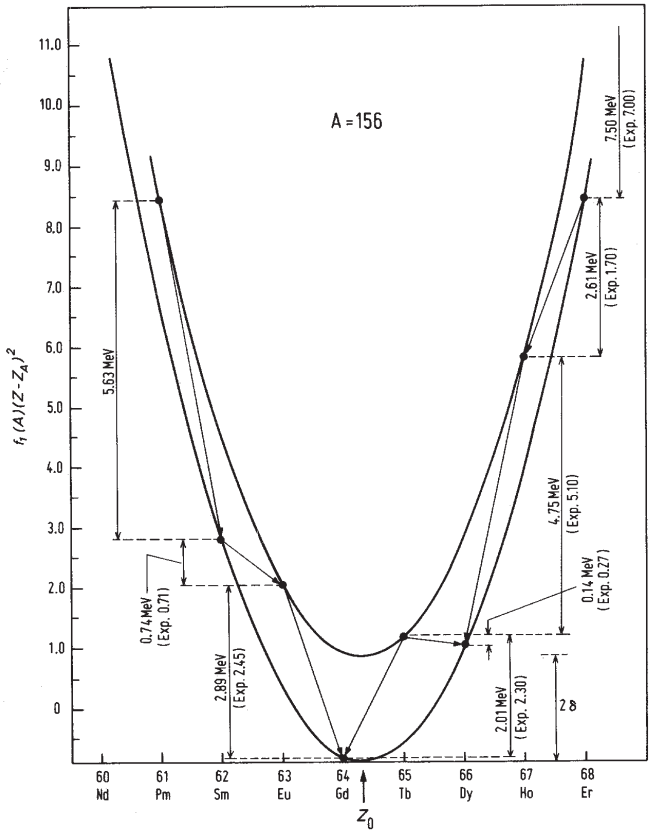

Fig. 3.2 Mass parabolae for even A (A = 156). Values given in parantheses are the experimentally observed values [Nuclear and Radiochemistry, G. Friedlander, J.W. Kennedy, E.S. Macias and J.M. Miller, 3rd Ed., John Wiley (1981) p.47].

For $Z < Z_0$, nuclei are β^- unstable and $(N/Z) > (N/Z)_0$

For $Z > Z_0$, nuclei are β^+ unstable and $(N/Z) < (N/Z)_0$

For even A, two parabolae corresponding to o-o and e-e nuclides exist. The vertex of o-o parabola is separated from the vertex of e-e parabola by 2δ. The masses for o-o nuclei are represented by the upper parabola while that of e-e nuclei lie on the lower parabola. Because of this, two stable isobars with even Z are observed. It is, therefore, expected that ^{156}Tb could decay to form both ^{156}Gd and ^{156}Dy, which indeed is the case. Even though the mass of ^{156}Gd is lower than that of ^{156}Dy, the decay of $^{156}\text{Dy} \rightarrow {}^{156}\text{Gd}$ is precluded because the possibility of double β-decay is negligibly small (not observed so far). Hence both ^{156}Gd and ^{156}Dy are stable.

From eqn. 3.17, it is seen that when A is very small, first term in the bracket can be neglected with respect to 2. Thus for low A elements $Z_0 \approx A/2$ (N=Z). As A increases, the first

term becomes significant and $Z_0 < A/2$ or $N > Z$ for stable nuclei. This explains the deviation of beta stability line from N = Z curve with increasing A.

Stability Against Alpha Decay

Liquid Drop Model (LDM) is very useful to find out whether a nucleus is stable against alpha decay or not. Calculations based on LDM predict that nuclei with A > 150 are energetically unstable with respect to alpha decay. The Q_α value, i.e. decay energy associated with α-decay of a nucleus ${}^{A}_{Z}X$ can be calculated from the differences in the mass of nucleus ${}^{A}_{Z}X$ and the combined mass of the product nucleus ${}^{A-4}_{Z-2}Y$ and alpha particle. Reduction of the Coulomb instability or increase in binding energy is the main driving force for alpha decay. For example, Binding energies of ^{232}U, ^{228}Th and α are 1765.931 MeV, 1743.050 MeV and 28.295 MeV, respectively. The combined BE of ^{228}Th and α (1771.345 MeV) is greater than the BE of ^{232}U (1765.931 MeV). Thus ^{232}U is expected to undergo α-decay and indeed it is α unstable nucleus.

It is also observed that in a family of isotopes, Q_α-values decrease as A increases. For isobars, Q_α value increases with atomic number due to higher Coulomb instability. In the case of ^{210}Po (N=126), Q_α-value is found to be much lower than that is expected from LDM. The extra stability associated with N=126 is responsible for this.

Stability Against Spontaneous Fission

LDM predicts spherical shape for the ground state of a nucleus so as to have minimum surface energy. But it is seen that around A=200, Coulomb energy becomes sufficient to make the nucleus unstable against alpha decay. Around A=230, nuclei become unstable against spontaneous fission (SF). In the spontaneous fission, a nucleus undergoes division into two nearly equal fragments accompanied by the release of a large amount of energy (≈200 MeV). For example, ^{238}U decays by α (4.468×10^9 y) and SF (10^{16} y) and ^{252}Cf also decays by α (2.85 y) and SF (85 y). A brief description of nuclear fission is given here whereas details are included in Chapter 9.

If the nucleus is deformed say, to some ellipsoidal shape by preserving the volume (necessary to keep the density constant), surface energy tends to restore the spherical shape to keep itself to a minimum. But decrease of Coulomb energy with deformation on the other hand favours deformation. For lighter nuclei, surface energy is very dominant whereas Coulomb instability is not very high. For nuclei with A>230, the gain in Coulomb energy (ΔE_C) due to deformation starts becoming comparable to the loss of surface energy (ΔE_S) and distortion of nuclear shape becomes easier. A typical plot of potential energy as a function of deformation is given in Fig. 3.3. Potential energy reaches a maximum at certain deformation and then starts falling off sharply. This point of maximum is called saddle point and the energy difference between saddle point and the ground state is called fission barrier (analogous to activation energy for a chemical reaction). A parameter, called fissility parameter (χ) is defined as:

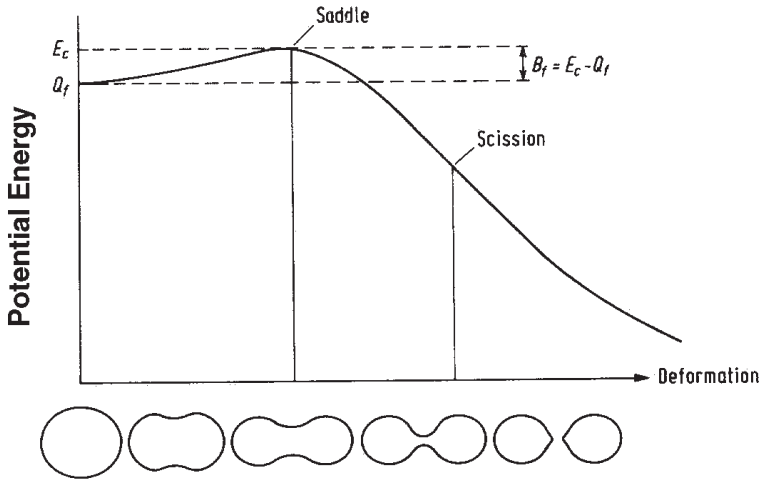

Fig. 3.3 Liquid Drop Potential Energy as a Function of Deformation [Nuclear and Radiochemistry, G. Friedlander, J.W. Kennedy, E.S. Macias and J.M. Miller, 3rd Ed., John Wiley (1981) p.72].

$$\chi = \frac{(Z^2 / A)}{50} \qquad (3.18)$$

Nuclides for which $\chi < 1$, a finite fission barrier exists. If $\chi > 1$, fission barrier vanishes and nuclides undergo spontaneous fission. Hence, according to LDM, heavy elements upto with $\chi < 1$ can be produced.

Merits of Liquid Drop Model

Liquid drop model has been extensively used to explain the gross properties of nuclei i.e. the properties which vary smoothly with the composition of nuclei (A,Z). These properties are:

(i) Constant nuclear density and nearly constant B/A.

(ii) Systematic deviation of N/Z ratio of stable nuclides from N=Z curve.

(iii) Mass differences in the family of isobars

(iv) Systematic variation of alpha decay energies with A and Z.

(v) Instability of heavy nuclei (A>230) against spontaneous fission.

Short comings of the Liquid Drop Model

(i) It is inconsistent with the p-p and n-n pairing effect prominently observed in natural abundances of stable nuclides and enhanced binding energy for even-Z and even-N nuclides.

(ii) The model is incompatible with closed shell effects as revealed by the periodicity in a large number of nuclear properties recurring at magic numbers of protons and neutrons.

(iii) The model ignores independent motion of nucleons, the single particle spin, parity and magnetic moment effects

Nuclear Shell Model

By the time LDM was established, a large number of empirical evidences was collected that showed that nuclides with proton and/or neutron number equal to 2, 8, 20, 28, 50, 82 and 126 are comparatively more stable. These numbers are called magic numbers. The extra stability associated with magic numbers could not be explained by LDM. A few of the observations are discussed here.

(i) Number of stable isotones is maximum for N = 50 (6) and N = 82 (7).

(ii) Number of stable isotopes is large for even Z nuclides; 10 for Sn (Z = 50), 6 for Ca (Z = 20) and 4 for Pb (Z = 82), compared to their neighbours with atomic number Z±1.

(iii) The most abundantly nuclides in the universe are those with magic number of protons or neutrons or both, e.g., $^{16}_{8}O$, $^{40}_{20}Ca$, $^{88}_{38}Sr$, $^{89}_{39}Y$, $^{90}_{40}Zr$, $^{118}_{50}Sn$, $^{138}_{56}Ba$, $^{139}_{57}La$, $^{140}_{58}Ce$, $^{208}_{82}Pb$, etc.

(iv) The beta decay of a nuclide is favoured if the resulting daughter product is having magic number of protons or neutrons or both. These nuclides will have a short half-life and emitted beta particle will have high β_{max}. e.g., $^{86}_{35}Br$ (55.1 s), $^{136}_{53}I$ (83.4 s).

(v) The alpha decay of a nuclide is favoured if the resulting daughter product is left with magic number of protons or neutrons or both. The nuclide will have a short half-life and emitted alpha particle will have high E_α. e.g., $^{212\,m}_{84}Po_{128}$ (45.1 s, 8.78 MeV), $^{213}_{85}At_{128}$ (0.125 μs, 9.08 MeV). On the contrary alpha emitter already having magic number of protons or neutrons would be expected to be long lived and emit alpha particles of lower energy. e.g., $^{210}_{84}Po_{126}$ (138.376 d, 5.31 MeV).

(vi) The heaviest stable nuclide occurring in nature is $^{209}_{83}Bi$ (N = 126).

(vii) $^{87}_{36}Kr$ (N = 51) and $^{137}_{54}Xe$ (N = 83), when formed in excited states via beta decay from their precursors, emit neutrons. This shows that the one neutron excess of 50 or 82 is loosely bound. (Just as ionisation potentials of alkali metals are very low).

(viii) Separation energy of last neutron or proton for nuclei having magic number is very high (just as ionisation potentials of noble gases are very high). e.g., $^{208}_{82}Pb$ (7.38 MeV).

(ix) Neutron absorption cross-sections are lowest for nuclides having N = 20, 50, 82, 126 (just as electron affinity of noble gases) as compared to their neighbouring nuclides. e.g., $^{136}_{54}Xe_{82}$ (0.16 b), $^{135}_{54}Xe_{81}$ (2.65 x 10^6 b). It should be noted that the large cross-section in the case of ^{135}Xe (N = 81) is attributed to the ease with which a nucleus tries to attain magic number configuration (N = 82).

These observations indicate that magic numbers (2, 8, 20, 28, 50, 82, 126) correspond to closed shell configurations for a nucleus, similar to the closed shell configurations for electrons in noble gases (2, 10, 18, 36, 54, 86). Apart from magic numbers, there are other nuclear properties like spin, parity and well defined excited states which necessitated invoking of a model based on single-particle behaviour of the nucleons.

M.G. Mayer, and Haxel, Jensen and Suess independently introduced nuclear shell model in 1949 to explain the magic numbers by proposing a strong spin-orbit interaction. This assumption gained acceptance due to its success in explaining experimental observations.

Nuclear shell model is based on the assumption that each nucleon moves independently in an average potential generated by the interactions among the remaining nucleons. This essentially means that interaction among the nucleons is weak so that mean free path of nucleons is larger than the nuclear dimension. In other words, nucleons move inside the nucleus in a collision-free path. This is in sharp contrast to the assumption of liquid drop model where it is assumed that interactions among nucleons are strong so that mean free path of the nucleons is smaller than the nuclear dimension. This apparent contradiction can be qualitatively explained by taking recourse to Pauli's exclusion principle. Nucleons are fermions and obey Pauli's exclusion principle which states that no two similar particles can occupy the same state. In the ground state of nucleus, all the available states upto Fermi level are filled with particles. If a collision takes place between two nucleons then this should alter the states of the colliding nucleons but no such states are available in the ground state as they are all filled. Hence the assumption that nucleons essentially move in a collision free path inside the nucleus is fairly valid. But in reality, collisions do occur, which alter the course of the nucleons.

Shell Model Potential

If the nucleus is assumed to have a sharp surface, the density of nuclear matter would be constant from its centre, right upto the surface and becomes zero outside its radius. The potential generated by nuclear matter would then be expected to vary inversely with density distribution. That is why the simplest choice of potential for shell model calculations is the square well potential given by :

$$V(r) = -V_0 \quad r \leq R$$
$$= 0 \quad r > R \qquad (3.19)$$

where, R = nuclear radius and V_0 = depth of the potential. The negative sign indicates that the potential is attractive.

Another commonly used potential for calculation of shell model states is the three dimensional simple harmonic oscillator (S.H.O.) potential given by :

$$V(r) = -V_0 \left[1-\left(\frac{r}{R} \right)^2 \right] \qquad (3.20)$$

The value of V(r) is equal to V_0 at the centre and reaches to 0 where r = R and increases dramatically outside nuclear dimensions which is unrealistic.

Shell Model States

Once the potential is chosen, Schordinger equation can be set up and solved to obtain the energy states. For the three dimensional isotropic harmonic oscillator potential, the solution is given as

$$\varepsilon_N = (n_1 + n_2 + n_3 + 3/2)\ \hbar\omega_0$$

$$= (N + 3/2)\ \hbar\omega_0 \qquad (3.21)$$

where ω_0 is the oscillator frequency and it is related to the depth of the potential, which is equal to $\sqrt{\frac{2V_0}{MR^2}}$ where M is the mass of a nucleon . N is the sum of n_1, n_2 and n_3 which are positive integers specifying the wave function in the three dimensions. N can take the values of 0, 1, 2 .....

In spherical polar coordinates, N is given by :

$$N = 2(n-1) + \ell \qquad (3.22)$$

where, ℓ is the orbital angular momentum of the system and the values of ℓ are N, N-2, N-4, ... 0 or 1, and n is the radial quantum number with the values of 1,2,3,....

The magnitude of total orbital angular momentum (L) is given by

$$L\hbar = \sqrt{(\ell(\ell+1)}\ \hbar \qquad (3.23)$$

The nomenclature for energy states is borrowed from atomic spectroscopy. i.e. $\ell = 0$ corresponds to an s state and $\ell = 1$ corresponds to a p state and so on so forth. Unlike in atomic spectroscopy, 3s means that the s state is appearing for the third time. The values of n and ℓ are 3 and 0 respectively and satisfies the eqn. 3.22. Thus a 3s state corresponds to N = 4. The other states for N = 4 are 1g (n = 1 and $\ell = 4$) and 2 f (n = 2 and $\ell = 2$). Thus the states 3s, 2d and 1g belong to N = 4 energy state and incidentally has the same energy. i.e. the states 3s, 2d and 1g are degenerate states. Another point to note is that the energy states in a given N value will all have either even ℓ value or odd ℓ value. Hence these degenerate states have

same parity. Occupancy of each state is as per atomic spectroscopy. An s state can accommodate 2 nucleons and a p state 6 nucleons. The possible states with occupancy are given below.

ℓ	0	1	2	3	4	5	6
state	s	p	d	f	g	h	i
Occupancy $2(2\ell+1)$	2	6	10	14	18	22	26
N	0	1	2	3	4	5	6
Possible states	s	p	s,d	p,f	s,d,g	p,f,h	s,d,g,i
Occupancy	2	6	12	20	30	42	56
Cumulative occupancy	2	8	20	32	62	104	160

An energy gap appears whenever there is a change in the quantum number N. Protons and neutrons are separately filled in the energy levels. In ^{16}O, there are eight protons and eight neutrons. 8 protons occupy 1s and 1p levels. Similarly eight neutrons will occupy 1s and 1p levels.

Spin-orbit Interaction

Sequential filling of nucleons using the above described scheme could produce shell closure corresponding to numbers 2, 8, 18, 20, 34, 40, 58, 68 etc. Experimental evidences support shell closure at 2, 8, 20, 28, 50, 82 and 126. These magic numbers could be reproduced by proposing a strong interaction between the orbital angular momentum (ℓ) and intrinsic angular momentum (s); known as ℓ-s coupling. In ℓ-s coupling scheme each ℓ state is split-up into two states with j values given by (ℓ + 1/2) and (ℓ -1/2). Thus an s-state becomes $s_{1/2}$, p-state splits into $p_{3/2}$ and $p_{1/2}$, d-state splits into $d_{5/2}$ and $d_{3/2}$ and so on. The energy of $j = \ell + 1/2$ is lower than that of $j = \ell - 1/2$. Occupancy of a j state is 2j + 1. e.g., $d_{3/2}$ accommodates 4 nucleons.

By introducing the ℓ-s coupling, the magic numbers 2,8, 20, 28, 50, 82 and 126 were reproduced. An energy level diagram is given in Fig. 3.4. Maximum occupancy of each level is shown in the brackets. In the next column, cumulative occupancy upto that level is given. Total number of nucleons at each shell closure is shown in the last column.

Ground States of Nuclei

The nuclear configuration of a given nuclide ${}^{A}_{Z}X_{N}$ is obtained by adding neutrons and protons separately in accordance with the Pauli's exclusion principle to the levels in the order shown in Fig. 3.4, beginning from the bottom of the well till all the protons (Z) and neutrons (N) are accommodated. The depth of the potential well is less for protons than neutrons due to Coulombic repulsion.

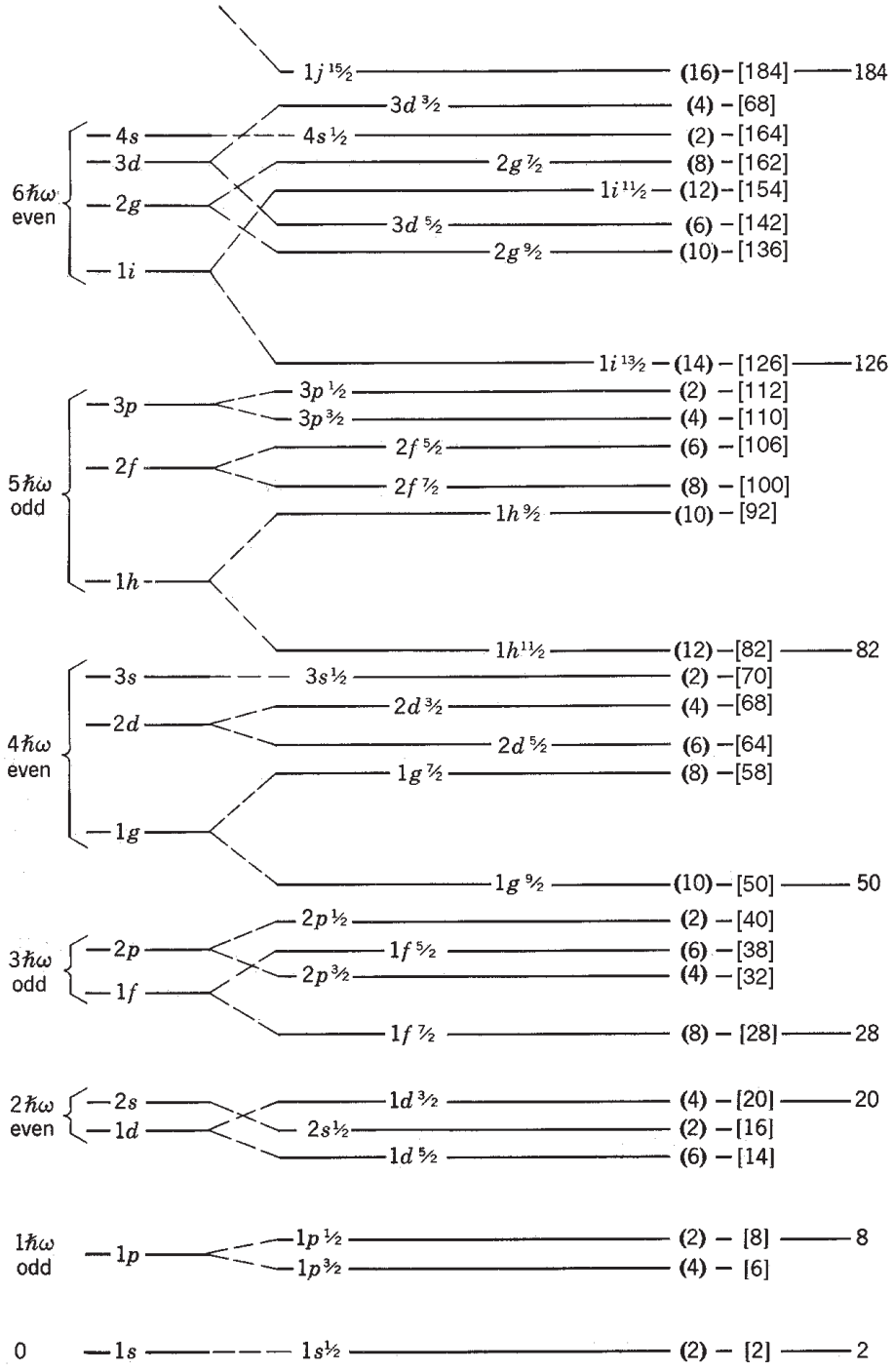

Fig. 3.4 Splitting of Energy Levels of Three Dimensional Isotropic Harmonic Oscillator by Spin-Orbit Coupling [M.G. Mayer and J.H.D. Jenson, Elementary Theory of Nuclear Shell Structure, Wiley, New York, 1955].

Nuclear Spin

While filling electronic levels in an atom, electrons occupy separate levels as far as possible (maximum spin multiplicity). For example, for a p state, first three electrons occupy separate levels and fourth electron pairs with first. On the contrary, in the case of nucleon filling, pairing interaction is strong and nucleons are paired. Neutrons pair with neutrons and protons pair with protons. Thus ground state spin of all even-even nuclei is zero. e.g. $^{16}_{8}O$ has 8 protons and 8 neutrons. Eight neutrons occupy $1s^2_{1/2}$, $1p^4_{3/2}$ and $1p^2_{1/2}$ levels. All 8 neutrons are paired. Similarly 8 protons also occupy a separate set of energy states $1s^2_{1/2}$, $1p^4_{3/2}$ and $1p^2_{1/2}$, and are also paired. Therefore, the net spin of ^{16}O is zero. Ground state spin (I) of o-e nuclei is determined by the j value of the last nucleon occupying the highest energy state, since net spin of the remaining even-even core is zero. Thus nuclei with odd neutron or proton have half- integral spin. In $^{17}_{8}O$, 8 protons occupy $1s^2_{1/2}$, $1p^4_{3/2}$ and $1p^2_{1/2}$ states. First 8 neutrons occupy $1s^2_{1/2}$, $1p^4_{3/2}$, $1p^2_{1/2}$ states and the 9th neutron occupies the next energy level $1d^1_{3/2}$. This unpaired nucleon represents the ground state properties of ^{17}O. For a d state, ℓ value is 2 and all even ℓ values correspond to positive parity. Therefore, spin and parity of ground state of ^{17}O is given as $1d^+_{3/2}$. In the case of $^{13}_{6}C$, 6 protons are paired and 6 of 7 neutrons are paired. Last neutron occupies $1p_{1/2}$ state. Since the neutron occupies $1p_{1/2}$ state, spin of ^{13}C is 1/2 and parity is odd as ℓ is 1. In the case of nuclei with odd Z and odd N, prediction of j is feasible by Nordheim's rule. According to this rule, total spin of the nucleus, equal to the net angular momenta of unpaired proton and neutron (J_T) is given as

$$J_T = |j_p - j_n| \text{ if } [(\ell_p + j_p + \ell_n + j_n)] \text{ is even and } (j_p + j_n) \text{ otherwise} \qquad (3.24)$$

Parity is even if both ℓ_n and ℓ_p are even or odd, and odd otherwise.

e.g. for $^{76}_{33}As_{43}$, 33rd proton is in $1f_{5/2}$ state and 43rd neutron is in $1g_{9/2}$ state. $\ell_p = 3$, $\ell_n = 4$, $j_p = 5/2$ and $j_n = 9/2$. Therefore, $\ell_p + \ell_n + j_p + j_n = 3 + 4 + 5/2 + 9/2 = 14$. It is even.

$$\therefore J_T = |j_p - j_n| = \left|\frac{5}{2} - \frac{9}{2}\right| = 2$$

The parity of ^{76}As is odd because ℓ_n and ℓ_p are odd and even respectively. Thus spin and parity of ground state of ^{76}As is 2^-.

Nuclear Isomerism

The magic shells at 2, 8 and 20 are the consequence of normal sequence of shell model states. The shell closures at 28, 50, 82 and 126 are obtained with $j = \ell + 1/2$ states e.g. $1f_{5/2}$, $1g_{9/2}$, $1h_{11/2}$ and $1i_{13/2}$. The energy gap between the $j = \ell \pm 1/2$ states increases with increase in ℓ values. A direct consequence of this is close spaced energy states of significantly different spin values just before the shell closure configuration. In such cases for nuclei with odd number of nucleons, the last nucleon can occupy either the expected low spin ground state (j_g) or high spin isomeric state (j_m) of slightly higher energy. Deexcitation from the isomeric

state to the ground state results in emission of γ-rays. If the difference in spins of isomeric and ground states is high, higher multipolarities are expected. Emission of γ-rays with high multipolarity is hindered and thus results in measurable life times for the isomers.

$^{95m}_{41}Nb_{54}$: $j_g = 9/2^+$, $j_m = 1/2$; $t_{1/2} = 86.6$ h

$^{131\,m}_{52}Te_{79}$: $j_g = 3/2+$, $j_m = 11/2$; $t_{1/2} = 30$ h

Nuclear Moments

In a nucleus, rotating charged nucleons (protons) can act as small magnets by virtue of the orbital (ℓ) as well as spin (s) motions. The resultant magnetic moment (μ) is given by

$$\mu = g\, I\, \mu_N \qquad (3.25)$$

where, I is nuclear spin, g is the g factor or gyro magnetic ratio which can be obtained experimentally and μ_N is the nuclear magneton. In the case of free neutron I is equal to ½. Neutron being neutral, is not expected to have orbital magnetic moment. However, a spinning neutron shows a negative magnetic moment.

The finite magnetic moment for neutron (-1.913 μ_N) and a large value of μ for proton (2.793 μ_N) indicate that neutron and proton are not simple elementary particles like electron, but have complex structure.

For even A-even Z nuclei, the total spin I = 0 as is the magnetic moment. For odd A nuclei, the total spin is due to the odd nucleon spin and the magnetic moment arises from coupling of μ_ℓ and μ_s depending upon $j = \ell \pm s$ scheme. Schmidt derived the limiting values of magnetic moments for odd-proton and odd- neutron systems. The Schmidt limits of magnetic moment μ in nuclear magnetons (μ_N) for nuclides having odd nucleon are given in Table 3.1.

Table 3.1 - Schmidt's limits for magnetic moments

Nuclei state	$j = l + s$	$j = l - s$
odd proton	$\mu = j + 2.23$	$\mu = j - 2.293\left[\frac{j}{(j+1)}\right]$
odd neutron	$\mu = -1.913$	$\mu = 1.913\left[\frac{j}{(j+1)}\right]$

Two examples are discussed below.

1. $^{59}_{27}Co_{32}$ has j = 7/2, $\mu = 4.64\ \mu_N$. The spin of ^{59}Co is due to the 27th proton which occupies $1f_{7/2}$ level. Therefore, the spin of ^{59}Co should be 7/2 which is a $\ell + 1/2$ level. According to Schmidt limits, magnetic moment should correspond to odd proton, $\ell + s$ case and the measured value of $\mu = 4.64\ \mu_N$ is close to the expected value of 5.73 as per the above expression.

2. Schmidt limits for magnetic moments can be used to arrive at the nucleon spin and hence the spin and the parity of the last occupied nuclear level. In the cases of $^{121}_{51}$Sb and $^{123}_{51}$Sb, 51st proton contributes to the nuclear spin of these isotopes and according to shell model 51st proton occupies $1g_{7/2}$ level. Therefore, nuclear spin for both these nuclei should be 7/2. However, measured spin and magnetic moments in the case of ^{123}Sb are 7/2 and 2.55 μ_N respectively. The μ value is close to the one calculated on the basis of $j = \ell - s$ and hence ℓ is equal to 7/2. Thus the level is $1g_{7/2}$. In the case of ^{121}Sb, I = 5/2 and $\mu = 3.36\ \mu_N$; 5/2 could be due to $g_{5/2}$ or $d_{5/2}$ level. $g_{5/2}$ corresponds to $\ell - s$ state and $d_{5/2}$ corresponds to $\ell + s$ state. By substituting j value (=I), for both the cases, the μ value can be calculated as 4.48 μ_N and 0.86 μ_N, respectively. 4.48 μ_N is closer to 3.36 μ_N. Therefore, this value corresponds to $\ell + 1/2$ case. The level should be $1d_{5/2}$ and spin and parity of ^{123}Sb is $5/2^+$.

Electric Quadrupole Moment

Electric quadrupole moment is the result of deviation of charge distribution from spherical symmetry. If the time average of the volumetric distribution of electric charge within a nucleus deviates from perfect spherical symmetry, the nucleus possesses finite electrical moments.

For a nucleus, two most common deviations from spherical shape occur when it is (i) elongated along Z-axis and (ii) compressed along Z-axis. For such shapes, quadrupole moment can be shown to be

$$Q = \frac{2}{5} \cdot Z(b^2 - a^2) \qquad (3.26)$$

where, Z is atomic number, b and a are semi axes parallel and perpendicular to Z-axis, respectively. For $b > a$, Q is positive and shape is called prolate. For $b < a$, Q is negative and the shape is oblate. If $b = a$, nucleus has spherical shape and $Q = 0$.

Quadrupole moment of a nucleus is determined from hyperfine splitting of spectral lines, microwave absorption spectroscopy, molecular beam resonance method etc. It can be shown that the nuclear spin should be greater than 1/2 to observe quadrupole moment. As a consequence, for nuclei with I = 0 or 1/2, even if the charge distribution deviates from spherical symmetry, their quadrupole moment cannot be determined by the above methods. Quadrupole moments vary systematically with proton and neutron numbers. Nuclei with magic number configuration are spherical and have zero quadrupole moment. For odd-Z, even-N nuclides in which Z corresponds to a closed shell plus a proton, Q is negative

Table 3.2 - Magnetic moments and quadrupole moments of some nuclides

Nuclide	I	$\mu(\mu_N)$	$Q(\times 10^{-30}\ m^2)$	$\eta^{\#}$
$^{1}_{1}H$	1/2	+2.793	0	
$^{2}_{1}H$	1	+0.857	+0.273	+0.095
$^{6}_{3}Li$	1	+0.822	<0.09	<0.005
$^{14}_{7}N$	1	+0.404	+2	+0.027
$^{17}_{8}O$	5/2	-1.894	-0.5	-0.005
$^{37}_{17}Cl$	3/2	+0.0684	-6.21	-0.018
$^{83}_{36}Kr$	9/2	-0.970	+15	+0.012
$^{115}_{49}In$	9/2	+5.50	+116	+0.056
$^{121}_{51}Sb$	5/2	+3.36	-30	-0.013
$^{131}_{54}Xe$	3/2	+0.700	-15	-0.006
$^{175}_{71}Lu$	7/2	+2.90	+590	+0.148
$^{189}_{76}Os$	3/2	+0.7	+200	+0.045
$^{209}_{83}Bi$	9/2	+4.082	-40	-0.008

$^{\#}\eta = 2\ (b-a)/(b+a)$

(oblate). When Z corresponds to one proton less than the closed shell, Q becomes positive (prolate). Large positive Q is exhibited by mid-shell nuclides which are permanently deformed. In the case of e-o nuclides, if the neutron number is one excess over the magic number, e.g. ^{17}O, the Q value is negative (see Table 3.2). On the other hand, if neutron number is one less than magic number, then Q value is positive.

From the Table 3.2, it is clear that Q values change from positive values to negative values around the magic number configuration. For example, Q value for ^{115}In and ^{121}Sb are $116 \times 10^{-30}\ m^2$ and $-30 \times 10^{-26}\ m^2$ respectively and the expected value for tin isotopes (Z = 50) is zero.

Merits of Shell Model

Apart from explaining magic numbers, single particle model is useful to explain the following.

(i) Nuclear spin, parity, magnetic and quadrupole moments.

(ii) Pairing energy (stability of e-e nucleons).

(iii) Discontinuity in nuclear binding energy for magic nuclei.

(iv) Discontinuity in S_n and S_p.

(v) Spectrum of excited states of nuclei.

(vi) Occurrence of nuclear isomers.

Bibliography

1. R.D. Evans, The Atomic Nucleus, Tata-McGraw-Hill Book Co., New York (1978).
2. G. Friedlander, J.W. Kennedy, E.S. Macias, J.M. Miller, Nuclear and Radiochemistry, 3rd Ed., John Wiley & Sons Inc., New York (1981).
3. I. Kaplan, Nuclear Physics, 2nd Ed., Addision Wesley, Cambridge, Massachusetts (1963).
4. B.L. Cohen, Concepts of Nuclear Physics, Tata McGraw-Hill (1971).
5. P. Marmier and E. Sheldon, Physics of Nuclei and Particles, Academic Press, New York (1970).
6. H.J. Arnikar, Essentials of Nuclear Chemistry, 3rd Ed., John-Wiley (1990).
7. J.M. Blatt and V.F. Weisskopf, Theoretical Nuclear Physics, Wiley, New York (1952).
8. S. Glasstone, Sourcebook on Atomic Energy, 3rd Ed., Affiliated East West Press Pvt. Ltd. (1967).
9. Nuclear Chemistry, Vol. 1 and 2, Ed. L. Yaffe, Academic Press, New York (1968).
10. C.F. Von Weizsäcker, *Z. Phys.*, **96** (1935) 431.
11. W.D. Myers and W.J. Swiatecki, *Nucl. Phys*., **81** (1966) 1.
12. C.D. Coryell, *Ann. Rev. Nucl. Sci.*, **2** (1953) 305.
13. O. Haxel, J.H.D. Jensen and H.E. Suess, *Z. Phys.*, **128** (1950) 295.
14. M.G. Mayer, *Phys. Rev.*, **78** (1950) 16.
15. L.W. Nordheim, *Rev. Mod. Phys.*, **23** (1951) 322.

Chapter 4
Radioactivity

Radioactive decay is a spontaneous phenomenon of emission of particles or electromagnetic radiation from an atom (nucleus). Thermodynamic instability of a nucleus is responsible for the spontaneous decay so as to obtain more stable nucleus. Nuclear decay is accompanied by emission of alpha (α), beta (β), gamma (γ), neutron, proton and even heavier particles. Elements (isotopes) that are undergoing nuclear decay are called radioactive elements (isotopes).

The phenomenon of radioactivity was discovered by Henri Becquerel in 1896 and the radiations emitted were called 'Becquerel rays' or 'Uranic rays'. Pierre and Marie Curie concluded that these uranic rays were due to atomic phenomenon, characteristic of the element and not related to its chemical and physical states. They introduced the term 'Radioactivity' for this phenomenon.

The study of radioactivity, which deals with the properties of radioactive elements (isotopes) and the radiations emitted, formed the basis of many important discoveries in the field of atomic and nuclear physics. The scattering of alpha particles by gold atoms led to the idea of existence of a nucleus inside an atom (Chapter 2). Convincing proof of the existence of isotopes came from the analysis of chemical relationships among the natural radioactive elements. The study of disintegration of the nucleus by bombardment with energetic alpha particles led to the discovery of neutrons and in turn the current concept of the nucleus. Bombardment of atoms with various projectiles produces a large number of radioactive isotopes. Production of radioisotopes has added a further dimension to the nuclear research. The study of radiations from both natural and artificial radioactive isotopes showed that the nucleus has energy levels similar to those in the atoms. Nuclear spectroscopy which deals with the study of nuclear energy levels to arrive at the nuclear structure relies on the measurement of radioactivity. Thus radioactivity is very closely related to nuclear physics and nuclear chemistry, and its measurement may help in understanding of the fundamentals of nuclear structure and systematics of nuclear processes. Therefore, it is essential to understand the types of decay, decay kinetics, decay energies and decay theories, and some of these are discussed in this Chapter.

Types of Radioactive Decay

The radioactive decay processes are energetically feasible when the mass of the parent radionuclide is more than the sum of the masses of the products.

$$M_{parent} - M_{prod} = Q > 0 \quad (4.1)$$

In α and β decay, the original (parent) nucleus and the product nucleus have different atomic numbers. The types of nuclear decay processes and the associated changes in nuclear charge and mass numbers are given below.

α-*Decay*

A nucleus undergoing α-decay emits an α-particle which consists of two protons and two neutrons. Atomic and mass numbers of the product nucleus are reduced by 2 and 4 units respectively.

$$^{A}_{Z}X \rightarrow ^{A-4}_{Z-2}Y + \alpha \quad (4.2)$$

e.g. $^{232}_{92}U$ decays to $^{228}_{90}Th$ by α-emission.

$$^{232}_{92}U \rightarrow ^{228}_{90}Th + \alpha \quad (4.3)$$

β-*Decay*

β decay comprises of one of the following three processes: (i) negatron decay (β^-), (ii) Positron decay (β^+) and (iii) Electron Capture (EC). In all the three processes, charge of the resulting product nucleus differs from the starting nucleus by one unit and there is no change in mass number.

In negatron decay, a β^- particle (electron) is emitted along with an antineutrino ($\bar{\nu}$) and the atomic number is increased by one unit. e.g.,

$$^{132}_{53}I \rightarrow ^{132}_{54}Xe + \beta^- + \bar{\nu} \quad (4.4)$$

In the positron decay, a β^+ particle (positron) and a neutrino (ν) are emitted and atomic number is decreased by one unit. e.g.

$$^{22}_{11}Na \rightarrow ^{22}_{10}Ne + \beta^+ + \nu \quad (4.5)$$

In electron capture (EC), one of the orbital electrons of the atom is captured by the nucleus and a neutrino is emitted. Here also, the atomic number of the product nucleus is decreased by one unit. e.g.,

$$^{172}_{71}Lu + e^- \rightarrow ^{172}_{70}Yb + \nu \quad (4.6)$$

β^-, β^+, ν and $\bar{\nu}$ are non-nuclear particles and the moment they are formed, they are emitted.

Gamma Deexcitation

Alpha and β decay quite often leave the daughter product nucleus in excited states. When an excited state of a nucleus undergoes deexcitation, electromagnetic radiation, known as γ-ray, is emitted. e.g.,

$$^{60}_{29}Co^{*} \rightarrow {}^{60}_{29}Co + \gamma \qquad (4.7)$$

Spontaneous Fission

Spontaneous fission is a decay process in which a nucleus undergoes division into two fragments along with emission of 2-3 neutrons. This is prevalent in isotopes of heavy elements, e.g., ^{252}Cf.

$$^{252}_{98}Cf \rightarrow F_1 + F_2 + 3 \text{ neutrons} \qquad (4.8)$$

where F_1 and F_2 are fission fragments.

Kinetics of Radioactive Decay

The rate of decay of a radioisotope is proportional to the number of atoms of that isotope present at that instant. Radioactive decay, thus, follows the first order kinetics.

$$-\frac{dN}{dt} = \lambda N \qquad (4.9)$$

where, N is the number of atoms at any time t and λ is the disintegration constant which has the dimensions of time^{-1}.e.g., s^{-1}. The negative sign implies the decay of atoms. Integration of eqn. 4.9, gives,

$$N = N_0 e^{-\lambda t} \qquad (4.10)$$

where, N_0 is the number of atoms at the initial time. Radioisotopes are estimated by measuring 'radioactivity' or simply 'activity' (**A**), e. the product of decay constant (λ) and the number of atoms present (N) rather than N alone

$$\mathbf{A} = N\lambda \qquad (4.11)$$

Activity has the unit of disintegrations per unit time, generally disintegrations per second (dps). The units of radioactivity are :

1 Becquerel (Bq) = 1 dps

1 Curie (Ci) = 3.7×10^{10} dps

Combining eqns. 4.10 and 4.11, a relation for activity as a function of time is obtained.

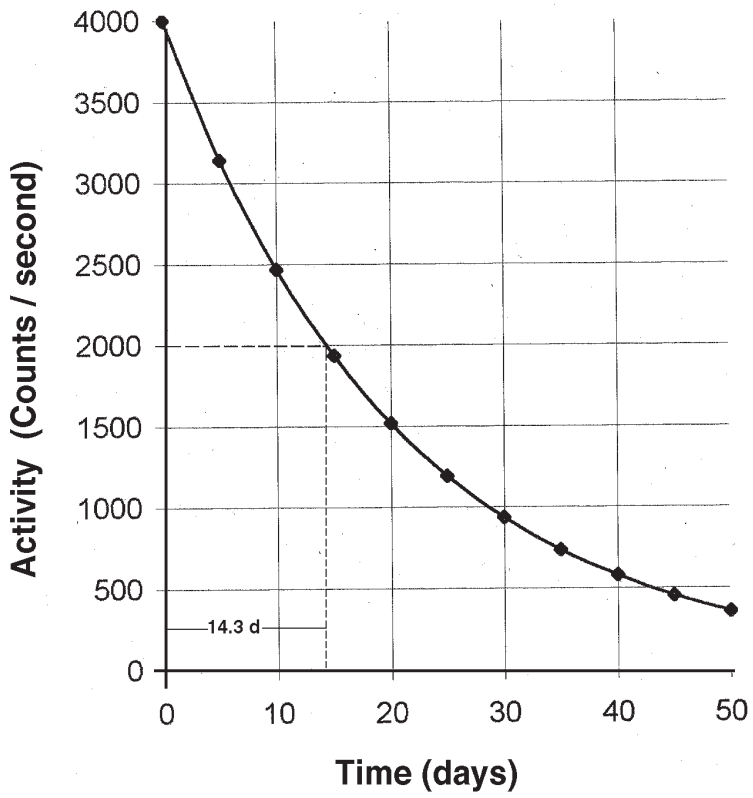

Fig. 4.1 Decay of ^{32}P on a linear plot ($t_{1/2}$ = 14.262 days).

$$\mathbf{A} = A_0 e^{-\lambda t} \qquad (4.12)$$

Activity decreases exponentially as a function of time. A typical activity profile of ^{32}P is shown in Fig. 4.1.

Half-Life

In the radioactive decay, the parent atoms are transformed into the daughter atoms. The time required for the decay of half of the parent atoms to daughter products is defined as the half-life ($t_{1/2}$) of the parent nuclide. Thus $t = t_{1/2}$ when $N = N_0/2$.

Substituting $N = N_0/2$ and $t = t_{1/2}$ in eqn. 4.10 and simplifying, one obtains,

$$1/2 = e^{-\lambda t_{1/2}}$$

$$\text{and } t_{1/2} = \frac{\ln 2}{\lambda} = \frac{0.693}{\lambda} \qquad (4.13)$$

Half-life is a unique characteristic of each isotope. From the Fig. 4.1, it is seen that the activity present at time t = 0 is 4,000 dps. After 14.262 d, it becomes 2,000 dps, i.e. half of the original activity. Therefore by definition, half-life of this nuclide is 14.262 d. Activity after

Table 4.1 - Half-lives and decay constant of some radioisotopes

Nuclide	Half-life	Decay constant s^{-1}	Specific activity dps/μg
^{32}P	14.262 d	5.61×10^{-7}	1.06×10^{10}
^{99}Mo	65.94 h	2.92×10^{-6}	1.77×10^{10}
^{131}I	8.0207 d	9.97×10^{-7}	4.58×10^{9}
^{235}U	7.038×10^{8} y	3.12×10^{-17}	7.90×10^{-2}
^{259}Fm	1.5 s	0.462	1.45×10^{15}

two, three and four half-lives would be 1000, 500 and 250 dps, respectively. Half-life of the radioisotope is determined from the activity profile (Fig. 4.1)

Taking logarithms of eqn. 4.12,

$$\log A = \log A_0 - \lambda t \qquad (4.14)$$

A straight line is obtained when log A is plotted as a function of time on a semilog paper as shown in Fig. 4.2. The slope of this line gives the decay constant from which half-life of the radioactive nuclide is obtained. Half-life can also be determined from Fig. 4.2, by locating the time coordinate corresponding to 2000 dps (as the original activity is 4000 dps). Time corresponding to the activity of 1000 dps is equal to two half-lives as shown in Fig. 4.2.

Half-lives of different radioisotopes can vary from as low as microseconds to billions of years. Half-lives and decay constants of a few radioisotopes are given in Table 4.1. Column 4 in this table gives specific activity of these isotopes. Specific activity is defined as the activity per unit mass.

Statistical Aspects of Radioactive Decay

In 1905, E. Von Schweidler formulated exponential law for radioactive decay in terms of disintegration probabilities. Two assumptions were made. (i) The probability of decay λ is same for all the atoms of the species and (ii) λ is independent of the age of a particular atom. Therefore, the probability p of a radioactive atom disintegrating in a very small time interval Δt is independent of the past history and the present circumstances of the atom, but depends only on Δt.

$$p \propto \Delta t$$

$$p = \lambda \Delta t \qquad (4.15)$$

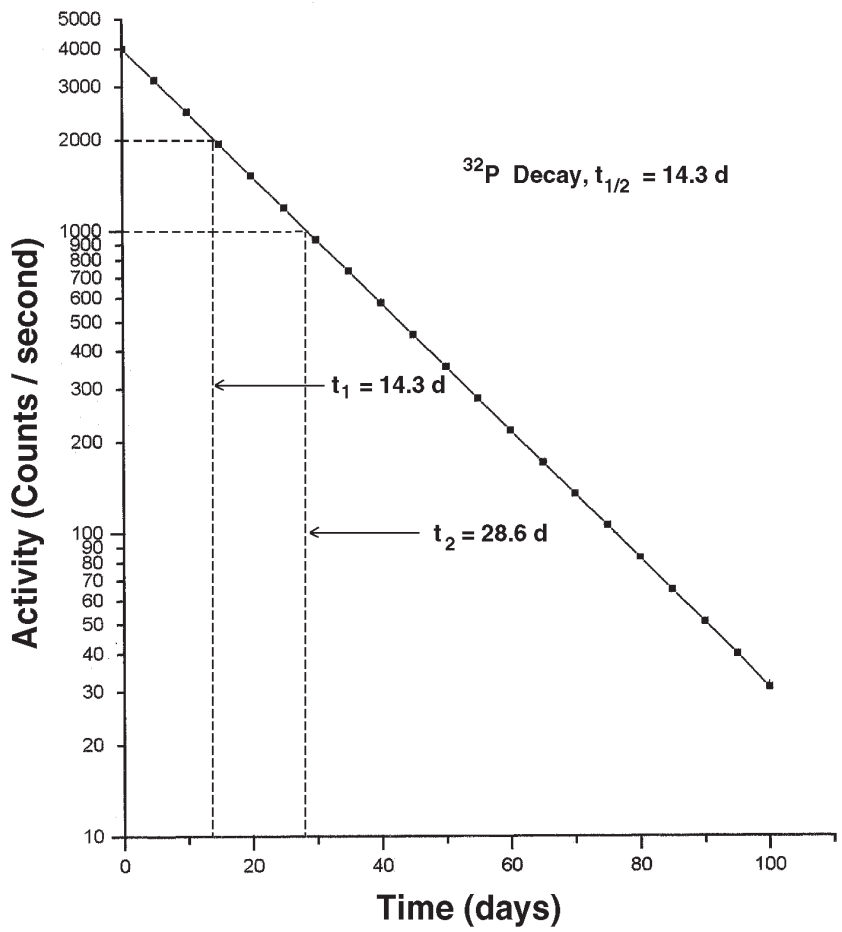

Fig. 4.2 Log of activity as a function of time ($t_{1/2}$ = 14.3 d is obtained from graph. Actual half-life is 14.262 d).

The probability of survival of one nucleus is equal to (1-p). This probability is same for the next interval of Δt. Thus the total probability of the nucleus to survive for n such intervals is

$$(1\text{-}p)^n = (1\text{-}\lambda\Delta t)^n = \left(1-\frac{\lambda t}{n}\right)^n \qquad (4.16)$$

$\because \quad n\ \Delta t = t$

This is the survival probability of the nucleus upto time t. It is known that

$$\lim_{n\to\infty}\left(1-\frac{x}{n}\right)^n = e^{-x} \qquad (4.17)$$

From eqns. 4.16 and 4.17,

$$\lim_{n \to \infty} (1\text{-}p)^n = \left[1 - \frac{\lambda t}{n}\right]^n = e^{-\lambda t} \qquad (4.18)$$

If N_0 is the number of radioactive atoms at time t = 0 of which N are surviving through the time interval t, then this probability is equal to the fraction N/N_0.

i.e. $$\frac{N}{N_0} = (1-p)^n = e^{-\lambda t}$$

$$\therefore N = N_0 e^{-\lambda t} \qquad (4.19)$$

Mean Life

The life time of radioactive isotope varies from 0 to ∞. The average time that an atom of a radioisotope can survive is called mean life (τ) which is obtained by dividing sum of the times of existence of all the atoms by the initial number of atoms. Summation can be replaced by integration as the number of radioactive atoms is infinitely large. The mean life is given by

$$\tau = -\frac{1}{N_0} \int_{t=0}^{\infty} t \, dN$$

[-ve sign indicates the decay of nuclide]

$$= \frac{1}{N_0} \int_0^{\infty} t \cdot \lambda N \, dt = \int_0^{\infty} te^{-\lambda t} dt \qquad (4.20)$$

By partial integration of eqn. 4.20, it can be shown that

$$\tau = \frac{1}{\lambda} \qquad (4.21)$$

From eqns. 4.13 and 4.21, it is clear that the mean life is greater than the half-life by a factor of 1/0.693. This difference is due to the weightage given in the averaging process to the atoms surviving for longer time i.e. beyond the half-life period.

In the following example, half-life, decay constant and mean life time are calculated.

Suppose activity of a radioisotope is decreased to 75% of the original value in 30 days period, its half-life ($t_{1/2}$), decay constant (λ) and mean life time (τ) are calculated as follows:

$A = A_0 e^{-\lambda t}$

A = 75% of the original activity

$$= \frac{75}{100} \times A_0 = \frac{3}{4} A_0$$

$$t = 30 \text{ d}$$

$$\therefore \frac{3}{4} A_0 = A_0 \, e^{-\lambda(30)}$$

$$\frac{3}{4} = e^{-30\lambda}$$

$$\lambda = \frac{\ln\left(\frac{4}{3}\right)}{30} \text{d}^{-1} = 0.00959 \text{ d}^{-1}$$

$$t_{1/2} = \frac{0.693}{\lambda} \text{d} = 72.3 \text{ d}$$

$$\tau = \frac{1}{\lambda} = 104.3 \text{ d}$$

Branching Decay

A nuclide may be unstable towards more than one decay mode. For example, ^{252}Cf decays by spontaneous fission (SF) and alpha decay. Each decay mode has a decay constant called partial decay constant. The total decay constant (λ) of the nuclide is given by the sum of the partial decay constants; $\lambda = \lambda_1 + \lambda_2 + ...$

Let the nuclide X decays to two daughter products Y and Z, having corresponding decay constants as λ_1 and λ_2 respectively.

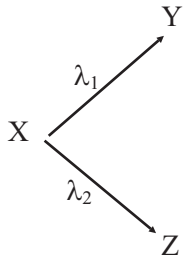

$$\lambda = \lambda_1 + \lambda_2$$

Rate of decay of X is

$$-\frac{dN}{dt} = (\lambda_1 + \lambda_2)N = \lambda N \qquad (4.22)$$

Total half-life of X is related to partial half-lives as

$$\frac{0.693}{t_{1/2}^{X}} = \frac{0.693}{t_{1/2}^{X \to Y}} + \frac{0.693}{t_{1/2}^{X \to Z}}$$

$$t_{1/2}^{X} = \frac{t_{1/2}^{X\to Y} \cdot t_{1/2}^{X\to Z}}{t_{1/2}^{X\to Y} + t_{1/2}^{X\to Z}} \qquad (4.23)$$

Thus the total half-life of X is shorter than any of the individual partial half-lives. e.g., in the case of ^{252}Cf, half- life for SF and α decay are 85 y and 2.85 y, respectively, where as its total half-life is 2.645 y.

Mixture of Radioactive Nuclides

Consider a mixture consisting of two or more radioactive nuclides having different half-lives which are genetically not correlated. In neutron induced reaction of a compound like NaCl, both Na and Cl get activated and ^{24}Na (14.9512 h), ^{36}Cl (3.01 x 10^5 y) and ^{38}Cl (37.24 min) are formed. Similarly neutron induced reaction of Cu results in the formation of ^{64}Cu (12.7 h) and ^{66}Cu (5.120 min). Total activity of such a mixture of radionuclides is given by

$$\begin{aligned} A &= A_1 + A_2 + ... \\ &= A_1^0\, e^{-\lambda_1 t} + A_2^0\, e^{-\lambda_2 t} + ... \end{aligned} \qquad (4.24)$$

where, Ai and A_i^0 are the activities of ith nuclide at times t = t and t = 0 respectively. λ_1, λ_2,.... are decay constants of 1, 2, ..., nuclides respectively. For a mixture of two radionuclides, the activity is given as

$$A = A_1^0\, e^{-\lambda_1 t} + A_2^0\, e^{-\lambda_2 t} \qquad (4.25)$$

Total activity is the sum of the activity of both the isotopes. The decay rate, therefore, depends on the decay constants of both the isotopes. The shape of the activity profile depends on the half-lives. The activity profile of a mixture of two nuclides of which one is short lived and the other is long lived, is given in Fig. 4.3. The initial part is dominated by decay of nuclide with shorter half-life whereas later part solely represents the decay of longer lived nuclide which is a straight line. The half-lives of both the nuclides can be obtained graphically. Since the later part of the profile is due to the decay of longer lived nuclide, a straight line is extrapolated to zero time (curve b). Since curve a, represents total activity of nuclides 1 and 2, by subtracting curve b from curve a, curve c is obtained. Curve c represents the decay of shorter lived nuclide. Thus curves a, b and c represent profiles of total activity, activity of the long lived nuclide and activity of the short lived nuclide, respectively.

Slopes of curves b and c give the decay constants of the long lived and the short lived nuclides, respectively. Corresponding intercepts represent the activity of individual isotopes, at time t = 0.

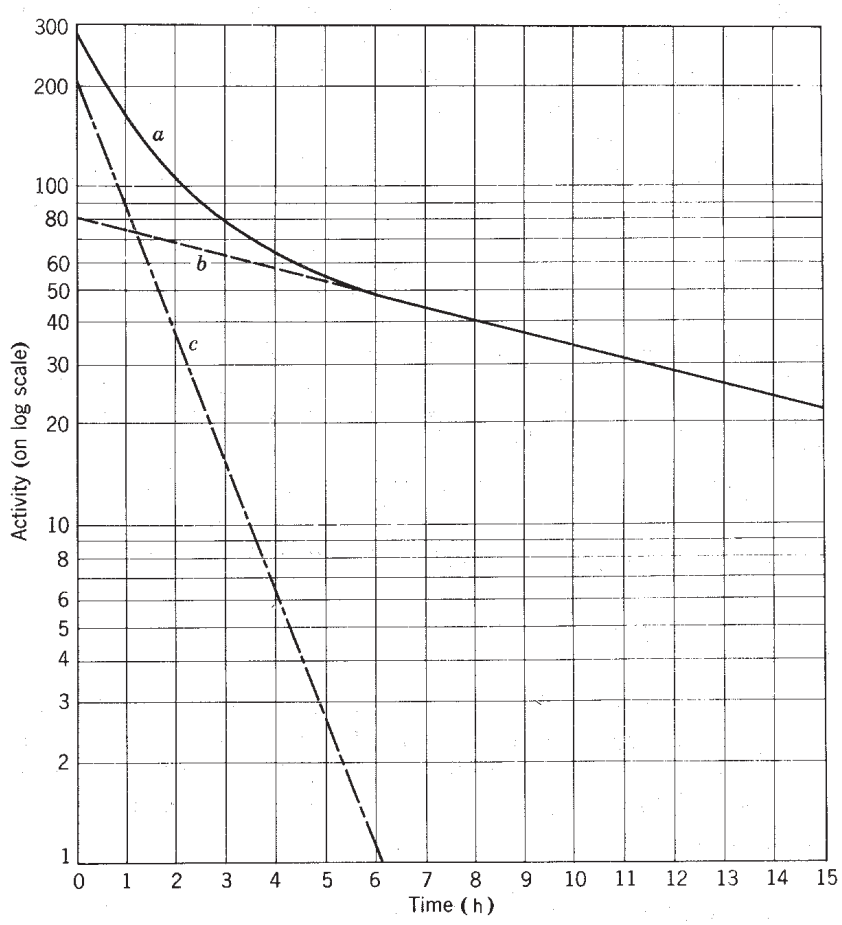

Fig. 4.3 Plot of total activity of mixture of two radioisotopes as a function of time [Nuclear and Radiochemistry, G. Friedlander, J.W. Kennedy, E.S. Macias and J.M. Miller, 3rd Ed., John Wiley (1981) p.192].

Parent-Daughter Equilibria

Growth of Daughter Product

When a nucleus of a radioisotope decays by particle emission, it gets converted into a nucleus of a new atom. For example, ^{131}I disintegrates by β-decay with a half-life of 8.0207 d and its daughter product is ^{131}Xe which is stable. In this β-decay, an atom of ^{131}I becomes an atom of ^{131}Xe. If N atoms of ^{131}I disintegrate, an equal number of ^{131}Xe atoms are accumulated. As the number of atoms of ^{131}I decrease, the number of ^{131}Xe grows as shown in Fig. 4.4. Both curves cross, exactly at a time equal to one half-life. At any given time, the sum of the atoms of ^{131}I and ^{131}Xe would be constant.

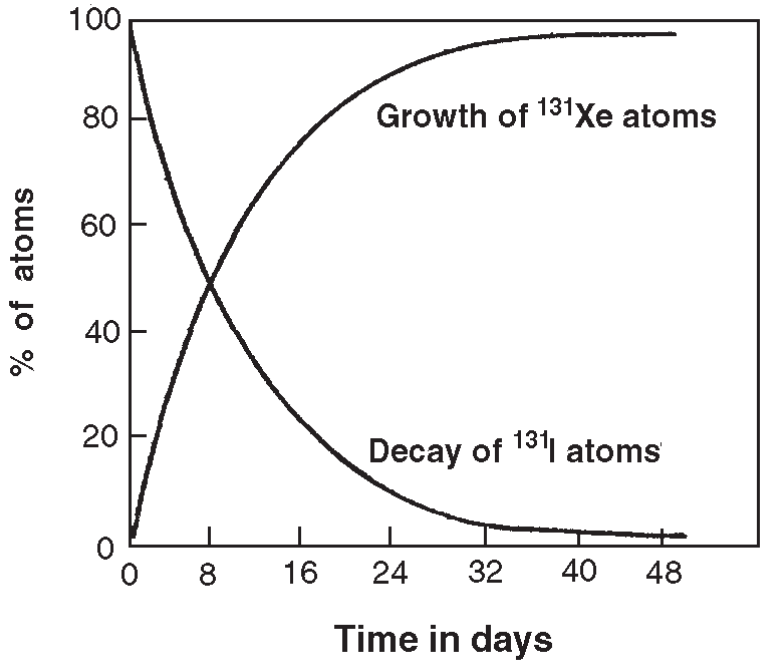

Fig. 4.4 Decay of ^{131}I and growth of ^{131}Xe.

Growth of Radioactive Products

Let us consider the decay of ^{140}Ba.

$$^{140}Ba \xrightarrow{\beta^-} {}^{140}La \xrightarrow{\beta^-} {}^{140}Ce$$

If a purified sample of ^{140}Ba is taken, its decay leads to formation of ^{140}La. Since ^{140}La is also radioactive and decays, only a fraction of ^{140}La formed survives, and its activity grows with time. The formation of ^{140}La is given as

$$\frac{dN_2}{dt} = N_1\lambda_1 - N_2\lambda_2 \qquad (4.26)$$

where, N_1 and N_2 are atoms of ^{140}Ba and ^{140}La present at time t. λ_1 and λ_2 are decay constants of ^{140}Ba and ^{140}La respectively. Solving this differential equation, the number of atoms of ^{140}La present at any time t is obtained.

$$N_2 = \left[\frac{N_1^0\lambda_1}{(\lambda_2 - \lambda_1)}\right][e^{-\lambda_1 t} - e^{-\lambda_2 t}] \qquad (4.27)$$

where, N_1^0 is the number of atoms of ^{140}Ba present at t = 0.

By multiplying both sides of eqn. 4.27 with λ_2, this eqn. can be re-written in terms of activity as

$$A_2 = A_1^0 \left[\frac{\lambda_2}{(\lambda_2 - \lambda_1)} \right] [e^{-\lambda_1 t} - e^{-\lambda_2 t}] \tag{4.28}$$

From the eqn. 4.28, it is clear that A_2 which is zero at t = 0, increases with time. It reaches a maximum value and then starts decreasing.

In the ^{238}U series as seen in Fig. 1.1, many radioisotopes are formed, the end product being ^{206}Pb which is stable. It is possible to calculate the atoms corresponding to any member of the series. It is obtained by setting up the differential equation and solving it. H Bateman gave a relation for the atoms of mth member with an assumption that at t = 0 only the parent is present and $N_2^0 = N_3^0 = \cdots\cdots = N_m^0 = 0$

$$N_m = C_1 e^{-\lambda_1 T} + C_2 e^{-\lambda_2 T} + \cdots\cdots C_m e^{-\lambda_m T} \tag{4.29}$$

where,

$$C_1 = \frac{\lambda_1 \lambda_2 \cdots\cdots \lambda_{m-1}}{(\lambda_2 - \lambda_1)(\lambda_3 - \lambda_1)\cdots\cdots(\lambda_m - \lambda_1)} N_1^0 \tag{4.30}$$

$$C_2 = \frac{\lambda_1 \lambda_2 \cdots\cdots \lambda_{m-1}}{(\lambda_1 - \lambda_2)(\lambda_3 - \lambda_2)\cdots\cdots(\lambda_m - \lambda_2)} N_1^0 \tag{4.31}$$

and so on.

Radioactive Equilibrium

In the cases where daughter product is also radioactive and its half-life is shorter than that of its parent's half-life, then the activity of the daughter product grows with time and is represented by eqn. 4.28. It reaches a maximum and starts decaying with parent's half-life. Time required to reach the maximum activity is called t_{max}. Beyond this time (t_{max}) the ratio of activity of parent and daughter remains almost constant. This condition of constant ratio of parent and daughter activity is called equilibrium. In the cases where the half-life of the daughter product is longer than that of the parent, equilibrium condition is not reached, though the activity of daughter product increases, reaches a maximum and decays with its characteristic half-life.

Total activity of the sample having decaying parent and growing daughter is given as

A = activity of the parent + activity of daughter.

$$= A_1^0 e^{-\lambda_1 t} + A_1^0 \left[\frac{\lambda_2}{(\lambda_2 - \lambda_1)} \right] [e^{-\lambda_1 t} - e^{-\lambda_2 t}] \tag{4.32}$$

where, the first part in the eqn. 4.32 represents the decay of the parent and the second part represents growth and decay of the daughter product on the assumption that pure parent sample was taken to start with ($A_2^0 = 0$).

After a long time t, $e^{-\lambda_2 t} \rightarrow 0$ and the total activity (A) becomes

$$A = A_1^0 e^{-\lambda_1 t} + A_1^0 \left[\frac{\lambda_2}{(\lambda_2 - \lambda_1)}\right] e^{-\lambda_1 t}$$

$$= A_1^0 \left[1 + \left\{\frac{\lambda_2}{(\lambda_2 - \lambda_1)}\right\}\right] e^{-\lambda_1 t}$$

$$= A_1^0 \cdot k \cdot e^{-\lambda_1 t} \qquad (4.33)$$

where k is constant. Therefore, the total activity decreases with the parent's half-life. At this time, the daughter activity can be removed by chemical separation for making a sample of daughter product. Again the daughter product grows and attains equilibrium with the parent. When the equilibrium is attained, the daughter product can be separated. Since parent product is used to generate daughter product repeatedly, it is called a radioisotope generator. For example, ^{99m}Tc (6.01 h) is repeatedly separated from a ^{99}Mo (65.94 h) generator, at an interval of 1 day.

Types of Equilibria

Depending on the decay constants of the parent and daughter products, there are three cases of correlated decay : (i) transient equilibrium, (ii) secular equilibrium and (iii) no equilibrium.

Transient Equilibrium

In the cases where decay constants λ_1 (parent) and λ_2 (daughter) are in the ratio of ~0.1, the equilibrium is called transient equilibrium.

A typical example is

$$^{99}\text{Mo} \xrightarrow{\beta^-} {}^{99m}\text{Tc} \xrightarrow{\text{IT}} {}^{99}\text{Tc} \qquad (4.34)$$

In the case of transient equilibrium, the sum of the parent and daughter activities in an initially pure parent fraction goes through a maximum before the equilibrium is achieved. The total activity profile is shown in the Fig. 4.5 as curve 'a' and is resolved into curves b, c, d and e for determining the half-lives as discussed below.

Curve a: It represents the total activity of the parent and daughter, as given by eqn. 4.32.

Curve b: This line, obtained by drawing a parallel line to the later part of *curve a* starting from the activity A_1^0 at t = 0, represents the decay of pure parent. Slope of this line gives the decay constant of parent product.

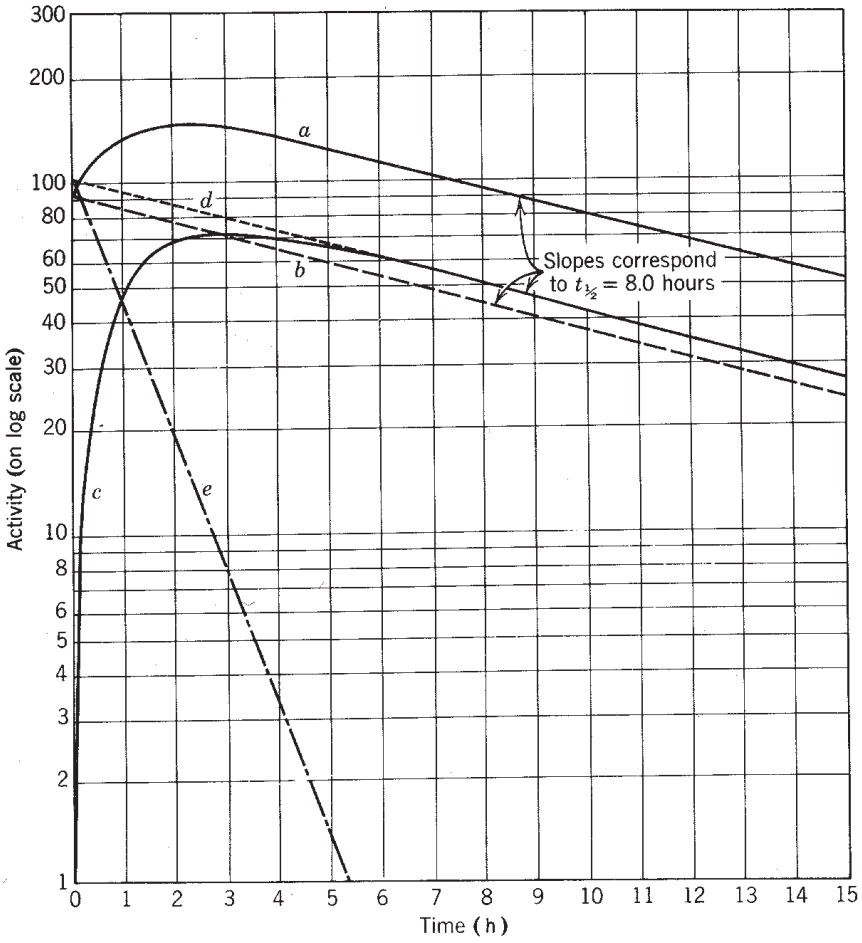

Fig. 4.5 Activity Profile in Transient Equilibrium [Nuclear and Radiochemistry, G. Friedlander, J.W. Kennedy, E.S. Macias and J.M. Miller, 3rd Ed., John Wiley (1981) p.195].

Curve c: This is obtained by subtracting *curve b* from *curve a* and represents the growth of the daughter product from the parent.

After sufficiently long time, $e^{-\lambda_2 t} \rightarrow 0$ and eqn. 4.28 is reduced to

$$A_2 = \left[\frac{\lambda_2}{(\lambda_2 - \lambda_1)}\right] A_1^0 e^{-\lambda_1 t} = \frac{\lambda_2}{\lambda_2 - \lambda_1} \cdot A_1 \qquad (4.35)$$

From this point onwards, daughter product also decays with the half-life of the parent.

Curve d is obtained by extrapolation of later part of *curve c*. The difference between extrapolated part (*curve d*) and corresponding part of *curve c* is due to continuous decay of

daughter product. Since $[\lambda_2/(\lambda_2-\lambda_1)]$ is greater than unity, activity of daughter product is more than activity of parent after equilibrium (eqn. 4.35).

Curve e: It is obtained by subtracting curve c from curve d and represents the decay of the pure daughter fraction.

$$A_1^0\left[\frac{\lambda_2}{(\lambda_2-\lambda_1)}\right]e^{-\lambda_1 t}-A_1^0\left[\frac{\lambda_2}{(\lambda_2-\lambda_1)}\right][e^{-\lambda_1 t}-e^{-\lambda_2 t}]=A_1^0\left[\frac{\lambda_2}{(\lambda_2-\lambda_1)}\right]e^{-\lambda_2 t} \qquad (4.36)$$

Slope of this line gives the half-life of the daughter product. From the measured total activity, one can arrive at the half- lives of both parent and daughter products by graphical analysis as described above.

Secular Equilibrium

If the half-life of the parent isotope is much longer than the half- life of the daughter isotope ($\lambda_2 >> \lambda_1$), then the equilibrium is called secular equilibrium. In this condition, the total activity of the parent and daughter reaches the maximum and does not decrease appreciably for several half-lives of the daughter product. Decay of ^{144}Ce is an example of secular equilibrium.

$$^{144}Ce \xrightarrow[284.893d]{\beta^-} {}^{144}Pr \xrightarrow[17.28\ min]{\beta^-} {}^{144}Nd$$

Recalling eqn. 4.27, the number of atoms of daughter product formed from the pure parent is obtained as

$$N_2 = N_1^0\left[\frac{\lambda_2}{(\lambda_2-\lambda_1)}\right][e^{-\lambda_1 t}-e^{-\lambda_2 t}]$$

For large t, $e^{-\lambda_2 t} \rightarrow 0$ and also $\lambda_2 - \lambda_1 \approx \lambda_2$

$$N_2 = N_1^0\left(\frac{\lambda_1}{\lambda_2}\right)\cdot e^{-\lambda_1 t} = \frac{N_1\lambda_1}{\lambda_2}$$

$$N_1\lambda_1 = N_2\lambda_2 \qquad (4.37)$$

Radioactivity profile for the case of secular equilibrium is shown in Fig. 4.6. It is resolved graphically to obtain the half-lives of parent and daughter products as discussed below :

Curve a : Total activity of an initially pure parent fraction i.e. activity due to parent decay, and growth and decay of the daughter product.

Curve b is obtained by drawing a parallel line to the later part of *curve a* starting from total activity at t = 0. It represents activity due to parent only (large $t_{1/2}$) which is equal to the daughter activity. Slope of this curve is equal to the decay constant of the parent.

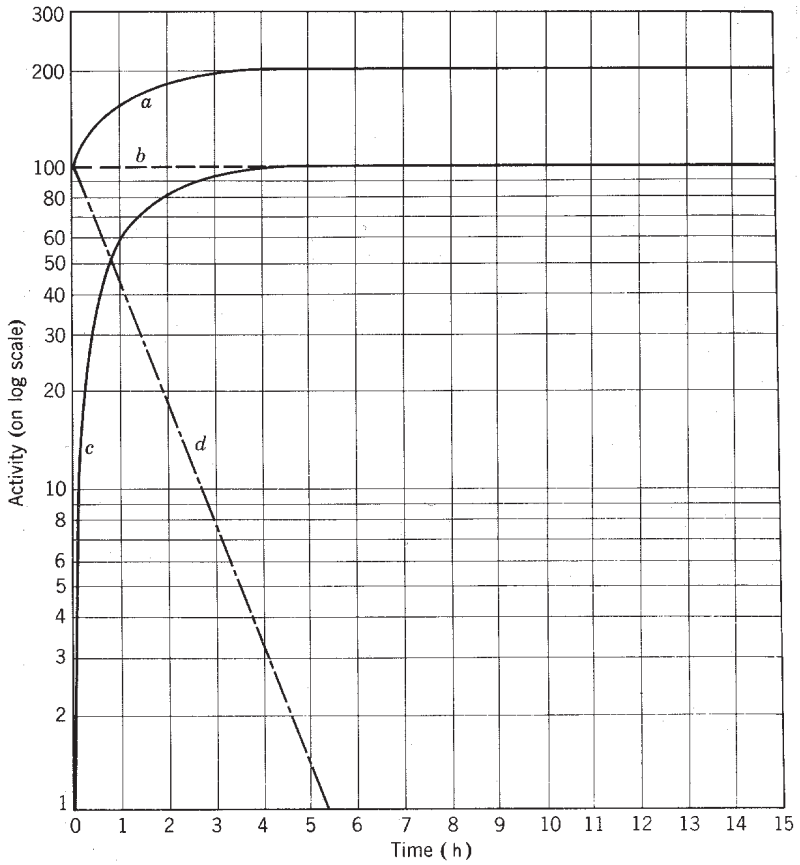

Fig. 4.6 Activity profile in a secular equilibrium case [Nuclear and Radiochemistry, G. Friedlander, J.W. Kennedy, E.S. Macias and J.M. Miller, 3rd Ed., John Wiley (1981) p.196].

Curve c : Growth of daughter activity in pure parent fraction. It is obtained by subtracting *curve b* from *curve a*.

Curve d is obtained by subtracting *curve c* from *curve b* and represents decay of the daughter product. From the slope of *curve d*, half life of the daughter product is determined.

No Equilibrium

If the decay constant of parent is larger than that of the daughter i.e. $\lambda_1 > \lambda_2$, then the parent decays faster than the growth of the daughter product. This does not satisfy the equilibrium condition of constant activity ratio at any point of time after preparing the pure parent sample and, therefore, represents a 'no equilibrium' case. For example, ^{138}Xe is short lived compared to its daughter product ^{138}Cs.

$$^{138}\text{Xe} \xrightarrow[14.08\ \text{min}]{\beta^-} {}^{138}\text{Cs} \xrightarrow[33.41\ \text{min}]{\beta^-} {}^{138}\text{Ba}$$

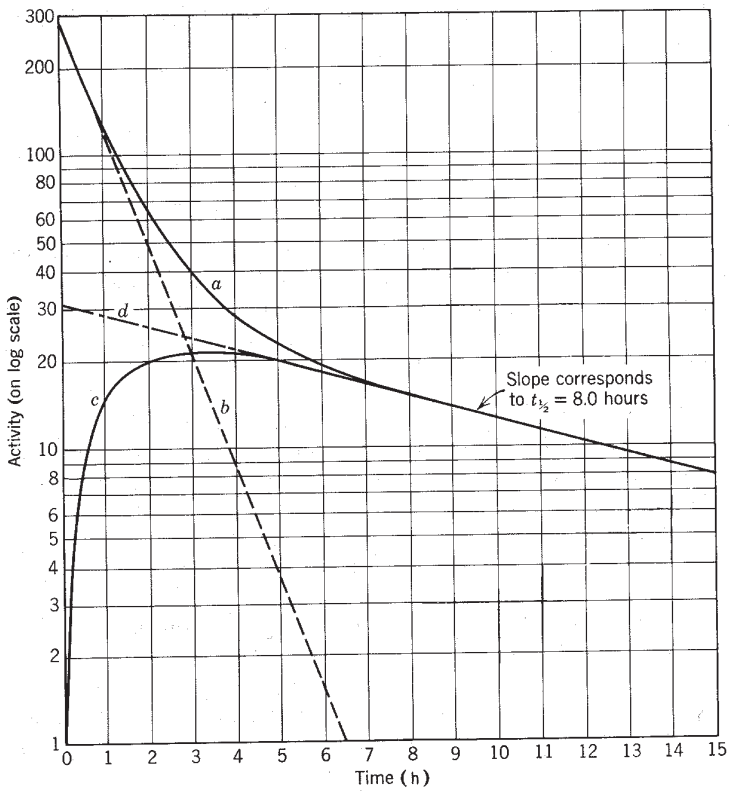

Fig. 4.7 Activity profile in a no equilibrium case [Nuclear and Radiochemistry, G. Friedlander, J.W. Kennedy, E.S. Macias and J.M. Miller, 3rd Ed., John Wiley (1981) p.197].

There will be no rise in the total activity as it is always lower than the activity at any earlier instant. Typical profile of a no equilibrium case is given in Fig. 4.7. The half-lives of both parent and daughter products can be determined graphically. The total activity profile 'a' is resolved into *curves b, c and d*. *Curve b* is obtained by drawing a tangent to *curve a* at t = 0. *Curve c* represents the growth of the daughter and is obtained by subtracting *curve b* from *curve a*. *Curve d* is obtained by extrapolation of *curve c* at large t and represents the decay of daughter. The slopes of *curve b* and *curve d* give the decay constants of parent and daughter respectively.

It may be noted that with the availability of high resolution γ-ray spectrometers, the daughter product activity alone can be measured as a function of time to obtain its growth curve (*curve c* in Figs. 4.5, 4.6 and 4.7). From the growth curve, half-lives of daughter and parent nuclides are determined by graphical analysis. Activity of the parent nuclide alone can also be measured, if parent has a non-interfering γ-line.

Bibliography

1. G. Friedlander, J.W. Kennedy, E.S. Macias, J.M. Miller, Nuclear and Radiochemistry, 3rd Ed., John Wiley & Sons Inc., New York (1981).
2. S. Glasstone, Sourcebook on Atomic Energy, 3rd Ed., Affiliated East West Press Pvt. Ltd. (1967).
3. R.D. Evans, The Atomic Nucleus, Tata-McGraw-Hill Book Co., New York (1978).
4. I. Kaplan, Nuclear Physics, 2nd Ed., Addision Wesley, Cambridge, Massachusetts (1963).
5. H.J. Arnikar, Essentials of Nuclear Chemistry, 4th Ed., John-Wiley (1990).
6. Introduction to Radiochemistry, A.V.R. Reddy and D.D. Sood, IANCAS Publication, Mumbai (1997).
7. Handbook of Radioactivity Analysis, Ed. M.F. L'Annunziata, Academic Press, New York (1998).
8. E. Rutherford and F. Soddy, *Trans. Chem. Soc.*, **81** (1902) 837.
9. F.A. Paneth, *Nature*, **166** (1950) 931.
10. P. Kirkpatnëk, *Phys. Rev.*, **70** (1946) 446A.
11. H. Bateman, *Proc. Cambridge Phil. Soc.*, **15** (1910) 423.

Chapter 5
Nuclear Decay Processes

Instability of a nuclide may result in its decay. A nuclide may undergo α-decay if the combined mass of the product nucleus and the α-particle is lower than the mass of the nuclide under consideration. It is true for all the spontaneous decay processes like β^- decay, γ-deexcitation, spontaneous fission and particle emission. While considering the radioactive decay, it is essential to know the decay rates, energy of the radiation emitted, the decay rate dependence on the energy, and possible theoretical explanation of the observed systematics. Measurement of energies of the radiations provides the basic information for nuclear spectroscopy.

Alpha Decay

Most of the isotopes of elements having Z > 82 are susceptible to α-decay. In the early years of this century, natural decay series were the main sources of α-emitters. The energy of the α-particle is determined from the measured ranges or the velocity of the α-particles.

If an α-particle is subjected to a magnetic field (H), it orbits in a circular path of radius (r). Velocity (v) of the α-particle is related to H and r as

$$v = \frac{q}{M} Hr \qquad (5.1)$$

where q and M are respectively charge and mass of the α-particle. For a given H, v can be determined by measuring radius or for a given orbit of r, H can be adjusted. From the velocity, E_α is calculated. The velocity of α-particles from ^{230}Th (4.685 MeV) and ^{212}Bi (6.0466 MeV) are 1.5018 x 10^7 m/s and 1.7846 x 10^7 m/s respectively.

Fine Structure in α-Spectra

An alpha unstable nuclide may emit mono energetic α-particles or α-particles with different energies (fine structure). When a nucleus is decaying from its ground state to the ground state of product nucleus (g-g transition), then the energy is maximum and this energy

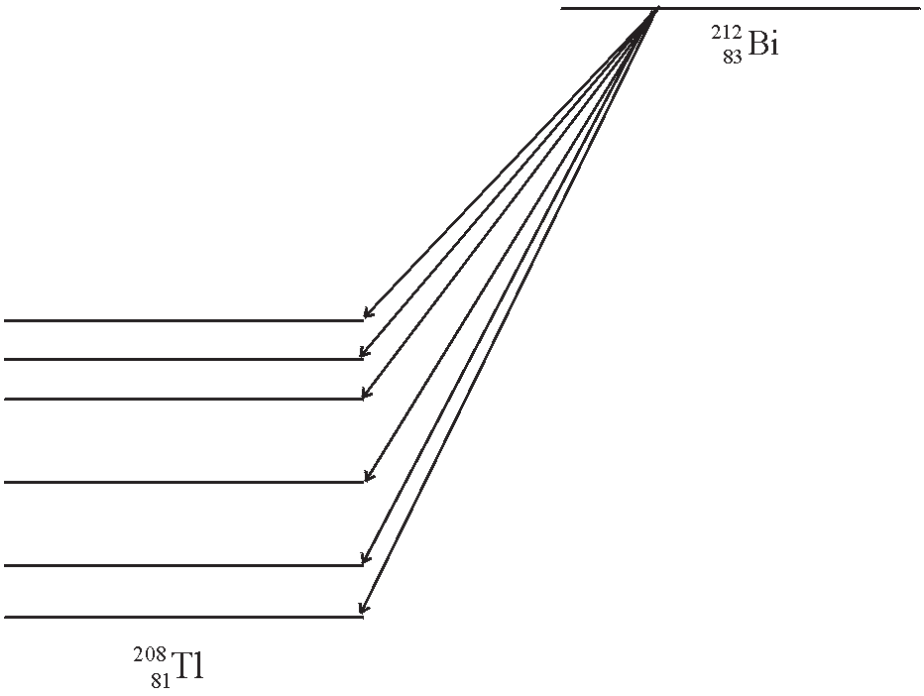

Fig. 5.1 Energy level diagram for the α-decay from ^{212}Bi (Energy is not to scale).

is directly related to the Q value of the α-decay of the nuclide. On the other hand, when the α-decay results in populating excited levels of the daughter products, then the α- energy will be lower than the Q value. In such cases, often α-decay is accompanied by γ-ray emission, e.g., ^{212}Bi undergoes α-decay and has 6 groups of α-particles: 6.230 MeV, 6.163 MeV, 5.874 MeV, 5.730 MeV, 5.711 MeV and 5.584 MeV with different intensities. The 6.230 MeV α-group corresponds to g-g transition. The remaining α-groups are the result of populating excited states of ^{208}Tl. Gamma rays corresponding to the deexcitation of different excited states are observed. Energy level diagram of $^{212}\text{Bi} \xrightarrow{\alpha} {}^{208}\text{Tl}$ is shown in Fig. 5.1. From the g-g transition value, Q value of the α-decay can be calculated or if Q value is known, expected kinetic energy of α-particle can be calculated. The α-decay energy (Q value) is shared by the α-particle (kinetic energy, E_α) and the product (recoil energy, E_R). From momentum conservation Q, E_R and E_α are related as

$$Q = E_\alpha + E_R = E_\alpha \left[1 + \frac{M_\alpha}{M_R} \right] \tag{5.2}$$

where, M_α and M_R are the masses of alpha and recoil product respectively. Use of mass numbers for M_α and M_R yield reasonably accurate values for Q. From the g-g transition of ^{212}Bi, Q is calculated as

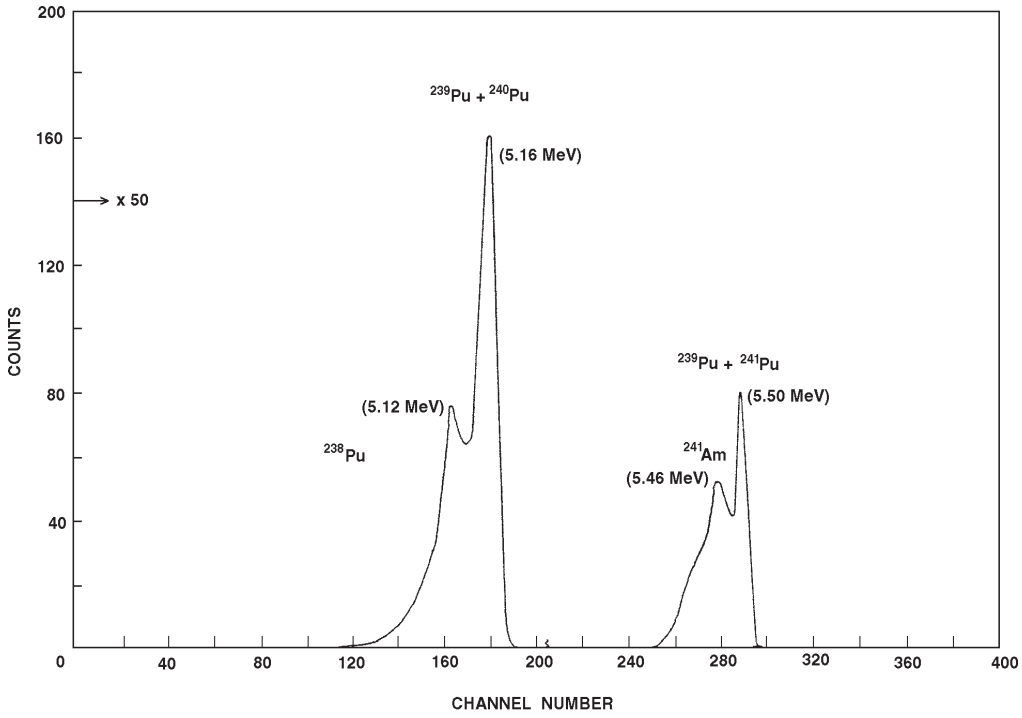

Fig. 5.2 Alpha spectrum of mixed source of $^{238,239,240}Pu$ and ^{241}Am.

$$Q = 6.023 \times \left[1+\frac{4}{208}\right] = 6.139 \text{ MeV}$$

Alpha spectrum consists of discrete lines corresponding to different energies of α-groups and it is easy to identify energies from measured α-spectra using high resolution detectors like silicon surface barrier detectors. A typical spectrum of a mixed source of Am and Pu is shown in Fig. 5.2. Energies of individual α-groups are marked.

Half-life and and Alpha Energy

Half-lives of ^{232}Th and ^{212}Po are 1.405×10^{10} y and 2.99×10^{-7} s whereas Q values are 4.06 MeV and 8.95 MeV respectively. For a change of an energy by two times, the half-life varies in these cases, by a factor of 10^{24}. Longest lived nuclide ^{144}Nd (2.29×10^{15} y) emits lowest energy α-particle (1.8 MeV). Geiger-Nuttal formulated a quantitative relation between decay constant (λ) and range (R) or E_α for isotopes in a given series, e.g., 4n or 4n+2 etc.

$$\log \lambda = A + B \log R \quad (5.3)$$

$$\log \lambda = A' + B' \log E_\alpha \quad (5.4)$$

where A, B and A′, B′ are constants for a given series.

Potential Energy Barrier

It was puzzling that ^{238}U emits spontaneously an α-particle of about 4.5 MeV whereas in the scattering experiments, α-particles of 9 MeV (from ^{212}Po) could not penetrate into the nucleus of ^{238}U. The potential barrier for the α-particles in the field of the nucleus (daughter product) is given by $U(r) = 2ze^2/r$. It follows that at about a distance of $r = 3 \times 10^{-14}$ m, U(r) is about 9 MeV and increases to a maximum value (22 MeV) until the Coulomb law breaks down; i.e. nuclear attraction starts. Unless the α energy is above 22 MeV, the repulsive potential prevents the incident α from entering the nucleus. Yet, α-decay of ^{238}U with α energy of 4.5 MeV has been observed. This could be explained by proposing quantum mechanical tunneling of the potential by α-particle.

Alpha Decay Theory

A theoretical basis for understanding the α-decay was not available until the advent of quantum mechanics. In 1928, Gamow and the team of Gurney and Condon independently explained the relationship between E_α and half-life on the basis of quantum mechanics. It is assumed that the α-particle is preformed and exists for a while within the nucleus before emission. The interaction of the preformed α-particle with residual nucleus, both inside and outside nuclear dimensions is represented in Fig. 5.3. The wave function representing the α-particle does not go abruptly to zero at the wall of the potential barrier (R_1) and has a finite, although small, value outside R_1. Schrödinger wave equation is set up for the α-particle inside nuclear well and solved. The probability (P) for the α-particle of mass M_α to penetrate this barrier is given by

$$P = \exp\left(-\frac{4\pi}{h}\sqrt{2\mu}\int_{R_1}^{R_2}\sqrt{U(r)-T}\ dr \right) \qquad (5.5)$$

U(r) is potential energy as a function of radial distance r, T is the total kinetic energy (sum of the kinetic energy of α-particle and recoil energy of the residual nucleus) and μ is the reduced mass given as

$$\mu = \frac{M_\alpha M_R}{M_\alpha + M_R} \qquad (5.6)$$

From the eqn. 5.5, it is clear that P increases with decrease in barrier height and/or increase in the value of T. For higher E_α values, T is higher and therefore probability for barrier penetration increases.

If the α-particle is considered to be bouncing between the walls of the potential barrier (i.e. under the influence of potential U(r)) with a velocity υ corresponding to a frequency *f*, then *f* can be calculated as

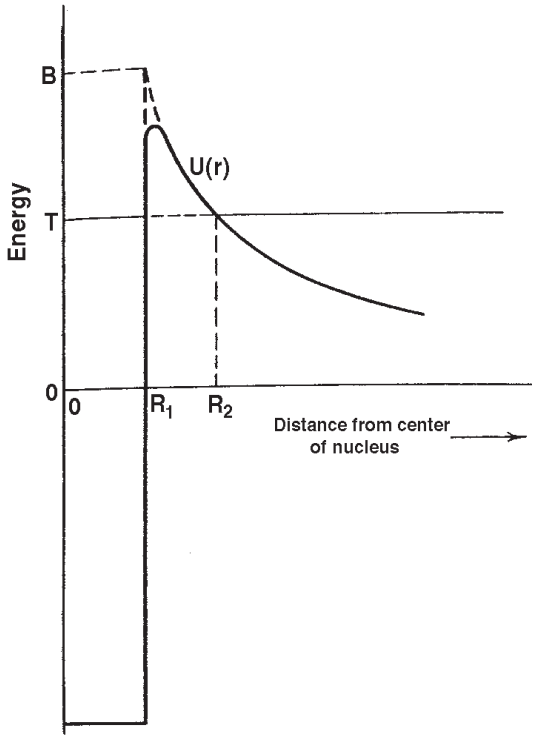

Fig. 5.3 Potential energy for a nucleus+α particle system [Nuclear and Radiochemistry, G. Friedlander, J.W. Kennedy, E.S. Macias and J.M. Miller, 3rd Ed., John Wiley (1981) p.59].

$$f = \frac{\upsilon}{2R_1} \approx \frac{h}{2\mu R_1^2} \text{ as } \upsilon = \frac{h}{\mu R_1} \tag{5.7}$$

The de Broglie wavelength $h/\mu\upsilon$ is taken as equal to R_1. The product of P and *f*, is the decay probability of the radionuclide to undergo α-decay and is given by

$$\lambda \approx \frac{h}{2\mu R_1^2} \exp\left[-\frac{4\pi}{h}\sqrt{2\mu}\int_{R_1}^{R_2}\sqrt{U(r)-T}\ dr\right] \tag{5.8}$$

Solution for eqn. 5.8 is given by (details are beyond the scope of this book)

$$\lambda \approx \frac{h}{2\mu R_1^2} \exp\left\{-\frac{8\pi Zze^2}{h\upsilon}\cos^{-1}\sqrt{\frac{T}{B}} - \sqrt{\frac{T}{B}\left(1+\frac{T}{B}\right)}\right\} \tag{5.9}$$

where,

Table 5.1 - Comparison of calculated decay constants with experimental data

Alpha emitter	T (MeV)	R_1 x 10^{13} cm[a]	λ_{calc} (s^{-1})	λ_{exp} [b] (s^{-1})
^{144}Nd	1.9	7.950	2.7 x 10^{-24}	1.0 x 10^{-23}
^{148}Gd	3.27	8.014	2.6 x 10^{-10}	2.2 x 10^{-10}
^{210}Po	5.408	8.878	1.0 x 10^{-6}	5.80 x 10^{-8}
^{214}Po	7.835	8.927	4.9 x 10^{3}	4.93 x 10^{3}
^{226}Th	6.448	9.072	2.6 x 10^{-4}	2.95 x 10^{-4}
^{228}Th	5.521	9.095	8.0 x 10^{-9}	8.35 x 10^{-9}
^{230}Th	4.767	9.118	1.7 x 10^{-13}	2.09 x 10^{-13}
^{232}Th	4.080	9.142	7.8 x 10^{-19}	1.20 x 10^{-18}
^{254}Fm	7.310	9.390	1.3 x 10^{-4}	5.1 x 10^{-5}

[a]Radii were calculated from formula $R_1 = (1.30\ A^{1/3} + 1.20) \times 10^{-15}$ m

[b]The λ values listed are partial decay constants for ground-state α transitions only.

$$B = \frac{Zze^2}{R_1} = \frac{2Ze^2}{R_1} \qquad (5.10)$$

Using eqn. 5.9, λ values for α-decay of many nuclei were calculated with R_1 value as the sum of nuclear radii of the daughter product ($1.30 \times A^{1/3} \times 10^{-15}$ m) and the α-particle (1.20×10^{-15} m). The agreement between calculated values and experimental values is good (Table 5.1). Gamow's theory, in general, explained the variation of half-life as a function of E_α. However, in the case of o-o, o-e and e-o nuclei, there are large deviations in the calculated half-lives from the measured values. Also when the daughter product or the α-decaying nucleus has a neutron shell N = 126, e.g., ^{210}Po or a proton shell Z = 82, e.g., ^{206}Pb, then the agreement is not good. It is important to note that despite the constraints that were used in this theory viz. (i) preformation of α-particle inside a nucleus, (ii) use of square well potential and (iii) arbitrary assumption of alpha radius as 1.20 F, the theory could explain the experimental observations reasonably well.

Nuclear Structure Effects

One of the assumptions in the theory, discussed above, is the preformation of α-particle inside a nucleus. It is easily conceivable, that an α-particle is preformed in an e-e nucleus than in an e-o or o-e or o-o nucleus. This involves either breaking an existing nucleon

pair or leaving the daughter product in an excited state. In either case, the probability of α-decay for the g-g transition becomes lower.

The decay energies (Q_α) decrease as a function of mass number for an element (Z). However, abrupt changes are observed if the parent nucleus is having a magic number of neutrons and/or protons. The Q_α value for $^{212}_{84}Po_{128}$ is 8.953 MeV with a half life of 0.299 μs. In this case, the daughter product is $^{208}_{82}Pb_{126}$ is a doubly magic shell configuration nucleus. α-decay is highly favoured as it results in extra stability. Most of the Po isotopes are α-unstable as the decay product is having more stable configuration with Z = 82 (Pb) compared to the parent nucleus with Z = 84. Let us examine the α-decay of $^{213}_{85}At_{128}$ and $^{211}_{85}At_{126}$. In the former case, the daughter product will be $^{209}_{83}Bi$ with N = 126, and therefore, the decay is favourable. In the latter case, the parent is having N = 126, thus the α-decay is less probable. This reflects in the half- lives and Q_α values of these nuclides. For $^{213}_{85}At$, Q_α and $t_{1/2}$ are 9.25 MeV and 0.125 μs respectively, whereas for $^{211}_{85}At$, they are 5.98 MeV and 7.214 h respectively. In fact, α-branch for $^{211}_{85}At$ is 49% and competing mode of decay is EC with 51%. It has to be noted that spin and parity of initial and final nuclei are not at all discussed. A complete discussion on these aspects is beyond the scope of this book.

Beta Decay

After the discoveries of neutron and artificial radioactivity, a large number of β unstable radioisotopes have been produced, which paved the way for understanding the decay modes and nuclear structure. In the β-decay process, mass number remains constant, but atomic number changes by one unit. The three processes β^- decay, β^+ decay and electron capture (EC) together are known as β-decay. Energy spectrum in the emission of β-particles differs from that of α-particles. A discrete energy spectrum is observed in α-decay where the α-energy is related to the disintegration energy. In the case of β-decay, the energy spectrum is continuous. However, the end point energy of β-spectrum (β_{max}) is related to the disintegration energy. This continuous energy spectrum posed serious challenges and could not be explained based on the theories available at that time and required new and bold assumptions.

Energetic Conditions

Mass difference between β-unstable nuclide and its daughter product is the Q_β value of β-decay. The energetic conditions for a nuclide of mass M_Z to undergo β-decay are

β^- decay : $M_Z > M_{Z+1}$

β^+ decay : $M_Z > M_{Z-1} + 2m_e$

Electron capture : $M_Z > M_{Z-1}$

where, Z is the atomic number of the parent nucleus and m_e is the rest mass of the electron. Nucleus that have higher N/Z compared to corresponding ratio of stability line $(N/Z)_0$ are prone to β^- decay. On the other hand, those nuclides having lower N/Z compared to $(N/Z)_0$ are prone to β^+ decay and / or EC decay. For β^+ decay 2 $m_e c^2$ is the energy threshold. Therefore, for the nuclides with low Q_β values, EC is the decay process, whereas above this threshold β^+ decay and EC are competing decay modes.

Energy and Velocity of β*-particles*

Energy of β-emitters vary from a few keV upto even 15 MeV, though for most, the β_{max} value does not exceed 4 MeV. Velocities of β-particles (v) are as high as 0.995 c, where c is velocity of light. Therefore β-particles must be treated relativistically. Velocities of the β-particles are measured by means of deflection of the path of the particles in a magnetic field. The velocity is related to the magnetic field (H) applied and radius of curvature (r) by eqn. 5.11.

$$Hr = 1704.5\ \beta \sqrt{1-\beta^2} \tag{5.11}$$

where β = v/c. Values of H compiled as a function of v/c for a given r are available. From experimental value of H, v/c can be calculated using the tables. From the v/c, kinetic energy (T) of β particles can be calculated as

$$T = \frac{0.511}{\sqrt{1-\beta^2}} \tag{5.12}$$

Thus both energy and v are determined.

β*-Decay and Conservation Laws*

As stated earlier β-spectrum is continuous from zero to a maximum value (β_{max}). This β_{max} corresponds to the energy difference between initial and final states (Q value for β^- decay). A typical energy spectrum is shown in Fig. 5.4. In a transition from one discrete state (parent) to another discrete state (daughter), the emitted β-particles have shown different energies which appeared as a violation of energy conservation. Half-life of the nuclide remained same whichever portion of the energy spectrum was used for measurement.

Nuclear spin has not been conserved as mass number of initial and final nuclei in β-decay remains same (either odd or even). Nuclear spin should be either half integral or integral whether a nucleus is odd or even. The emitted electrons have half unit of spin. Thus spin is not conserved. Accordingly statistics are also violated.

These apparent violations could be solved by a bold postulation made by Pauli in 1930 that in each β disintegration an additional unobserved particle called neutrino is emitted.

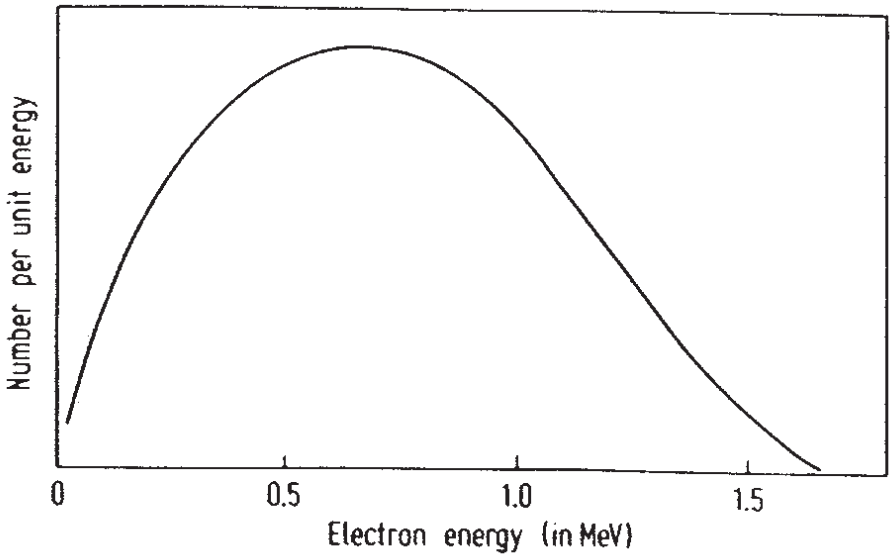

Fig. 5.4 Beta spectrum of ^{32}P [E.N. Jensen et al., Phys. Rev. ***85*** *(1952) 112].*

This neutrino is a Fermion. It was assigned zero charge, spin 1/2, almost no mass and carries away the energy and momentum in each β-decay process to conserve energy and momentum. Existence of neutrinos was experimentally confirmed in 1956 in the inverse process, in which a proton captures a neutrino to give a neutron. It is also proved that neutrinos emitted in β^- and β^+ are different, the former being antineutrino. In the EC, monoenergetic neutrinos are emitted. Careful measurements of β-decay energy spectrum and determination of masses of parent and daughter products gave an upper limit of 200 eV for the neutrino mass.

Fermi's Theory of β*-decay*

Fermi's theory of β-decay was patterned after the electromagnetic theory of light emission. Fermi considered that the β-particle and neutrino are created when a bound neutron is converted to a bound proton, the same way a photon is produced in an electromagnetic transition from one energy level to another. In the theoretical consideration, electro-magnetic field is replaced by electron-neutrino field. The electron-neutrino interaction is weaker than the electromagnetic interaction and in contrast to strong interaction between nucleons. The probability N(p)dp that a β-ray with momentum between p and p+dp will be emitted in unit time is given by

$$N(p)\,dp = = \frac{2\pi}{\hbar}\left[|\psi_e(0)|^2\ |\psi_v(0)|^2\ M_{if}^2\ g^2\ \frac{dn}{dE_0}\right] \qquad (5.13)$$

where Ψ_e and Ψ_v are wave functions of electron and neutrino whose probabilities of finding at the nucleus are $|\Psi_e\ (0)|^2$ and $|\Psi_v\ (0)|^2$ respectively, M_{if} represents the matrix element

characterising the transition from initial to final nuclear state, and the $|M_{if}|^2$ is a measure of the extent of overlap between the wave functions of initial and final nuclear states; g is the Fermi constant whose numerical value is empirically determined as $\sim 10^{-49}$ cm^3 erg. The density factor dn/dE_0, known as statistical factor, is the density of the final states of the system in the electron momentum interval of p and p + dp. The characteristic bell shape of the β-ray spectrum is determined by the statistical factor.

Statistical Factor

Kinetic energy is shared by electron (E_e) and neutrino (E_ν), with a negligibly small fraction of the energy going as recoil energy of the final (daughter) product.

$$E_0 = E_\nu + E_e \tag{5.14}$$

But momentum is conserved between the electron, neutrino and the final nucleus. This allows to write the momentum of neutrino (q) in terms of its kinetic energy ($E_\nu = E_0 - E_e$)

$$q = \frac{1}{c}(E_0 - E_e) \tag{5.15}$$

and for the electron

$$p = \frac{1}{c}\sqrt{E_e(E_e + 2m_e c^2)} \tag{5.16}$$

The number of electron states in the volume element $4\pi p^2.dp$ corresponding to momentum interval of p and p+dp is $\frac{4\pi p^2 dp}{h^3}$. The number of neutrino states in the momentum interval q and q + dq is $\frac{4\pi q^2 dq}{h^3}$, where h^3 is the volume of the phase space in the momentum intervals of p and p+dp and q and q+dq. From the uncertainty principle the volume in the six dimensional phase space; characterised by three space coordinates, x, y, z and three momentum coordinates P_x, P_y, P_z is given by

$$\Delta x \,.\, \Delta y \,.\, \Delta z \,.\, \Delta p_x \,.\, \Delta p_y \,.\, \Delta pz = h^3 \tag{5.17}$$

The number of translational states in a certain volume and in a certain momentum is taken as the number of unit cells in the phase space.

Total number of final states is given by

$$dn = \frac{4\pi p^2}{h^3}\, dp \cdot \frac{4\pi q^2}{h^3}\, dq \tag{5.18}$$

Total number of states per unit range of energy is

$$\frac{dn}{dE_0} = \frac{16\pi^2}{h^6} \cdot p^2 dp \cdot q^2 dq \cdot \frac{1}{dE_0} \tag{5.19}$$

It can be shown by differentiating eqn. 5.15 at a given constant energy of electron,

$$dq = \frac{dE_0}{c} \tag{5.20}$$

and therefore

$$\frac{dn}{dE_0} = \frac{16\pi^2}{h^6 c^3} \cdot p^2 \ (E_0 - E_e)^2 \ dp \tag{5.21}$$

$\frac{dn}{dE_0}$ is the relative probability that the β-ray momentum will be between p and p+dp, also between E_e and E_e+dE_e. Therefore, it has a parabolic dependence on energy E_e as shown in Fig. 5.4.

Both momentum (p) and energy (E_e) are expressed as dimension-less quantities η and W respectively.

$$\eta = \frac{p}{m_0 c} = \frac{mv}{(m_0 c)_2} = \frac{E(MeV)}{0.511} \tag{5.22}$$

and $$W = \frac{mc^2}{m_0 c^2} = \frac{E + m_0 c^2}{m_0 c^2} = \frac{E(MeV)}{0.511} + 1 \tag{5.23}$$

Eqns. 5.22 and 5.23 are rearranged to get

$$W^2 = \eta^2 + 1 \tag{5.24}$$

Eqn. 5.21 can be rewritten as

$$\frac{dn}{dE_0} = \left[\frac{16\pi^2 m_0^5 c^4}{h^6}\right] \ \eta^2 \ [W_0 - W]^2 \ d\eta \tag{5.25}$$

The statistical factor $\eta^2 \ (W_0\text{-}W)^2 \ d\eta$ gives an excellent representation of the shape of allowed β-ray spectra in low Z nuclides (Fig. 5.4).

Nuclear Coulomb Factor

Atomic nucleus has positive charge and β^- particles are negatively charged. Thus β^- emission is decelerated by positively charged nucleus and the lower side of energy spectrum will show higher intensity. On the other hand in β^+ decay, β^+ particles are accelerated due to repulsion from positively charged nucleus. This results in depletion of low energy β^+ particles, as shown in Fig. 5.5. Also, β^+ has to penetrate Coulomb barrier between itself and

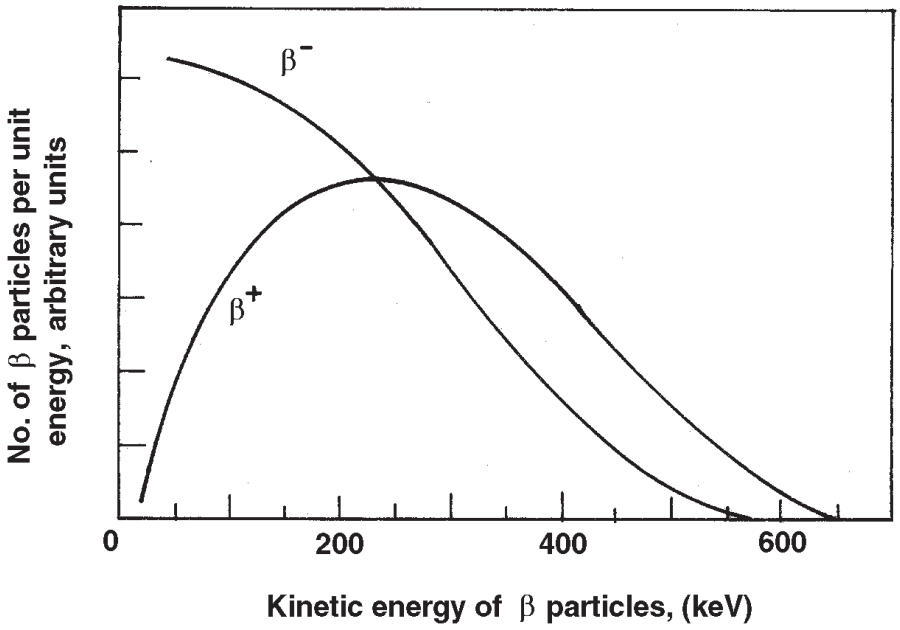

Fig. 5.5 Beta energy spectrum of ^{64}Cu [J.R. Reitz, Phys. Rev. 77 (1950) 10].

nucleus. This reduces the intensity of β^+ decay. Thus the net result is highly depleted low energy part and generally reduced intensity in the entire spectrum. Effect of nuclear Coulomb potential (F (Z,W)) is given by

$$F(Z,W) = \frac{2\pi y}{1-e^{-2\pi y}} \tag{5.26}$$

$$\text{where } y = \frac{\pm Z}{137\beta} \cong \pm Z\alpha\frac{W}{\eta} \tag{5.27}$$

+Z for β^- decay and -Z is for β^+ decay where Z is the atomic number of the daughter product and $\alpha = \frac{e^2}{\hbar c} \simeq \frac{1}{137}$ is the fine structure constant.

Screening by Electrons

Atomic electrons also affect emission of β^- and β^+. Screening by atomic electrons reduces β^- ray emission by about 2% for Z~50 and affects further with increasing Z. For β^+ emission the probability increases by about 37% for Z~50 and dramatically increases with higher Z.

Comparative Half-lives : log ft values

The probability of β-decay per unit time in a momentum interval dη or energy interval dW can be obtained by combining eqns. 5.13, 5.24 and 5.25 as

$$P(W)\,dW = \frac{64\pi^2\, m_0^5\, c^4 g^2}{h^7} |M_{if}|^2\; F(Z,W)\; W(W^2-1)^{1/2}\; (W_0 - W)^2\; dW \qquad (5.28)$$

Integrating eqn. 5.28 between 1 to W_0, the total probability per unit time for a β particle emission is obtained as

$$\int_1^{W_0} P(W)dW = \frac{64\pi^2\, m_0^5\, c^4\, g^2}{h^7}\; |M_{if}|^2 \cdot \int_1^{W} F(Z,W)\cdot W(W^2-1)^{1/2}\; (W_0 - W)^2\; dW \qquad (5.29)$$

and is equal to the decay constant λ. It can be written as

$$\frac{\ln 2}{t_{1/2}} = \lambda = \int_1^{W_0} P(W)dW = \frac{|M_{if}|^2 \cdot f_0}{\tau_0} \qquad (5.30)$$

where $$\frac{1}{\tau_0} = \frac{64\pi^4\, m_0^5\, c^4 g^2}{h^7} \qquad (5.31)$$

and f_0 is the integral in eqn. 5.29. Eqn. 5.30 is rewritten as

$$f_0 \,.\, T_{1/2} = \frac{0.693\,\tau_0}{|M_{if}|^2} \qquad (5.32)$$

Often $f_0\; t_{1/2}$ is written as ft and it can be thought of as the half- life corrected for differences in Z and W_0. Eqn. 5.32 becomes.

$$ft = \frac{\text{Universal constant}}{|M_{if}|^2} \qquad (5.33)$$

Approximate relations for f values are obtained with empirical evaluation as

$$\log f_{\beta^-} = 4.0 \log E_0 + 0.78 + 0.02\, Z - 0.005\,(Z-1) \log E_0 \qquad (5.34)$$

$$\log f_{\beta^+} = 4.0 \log E_0 + 0.79 - 0.007\, Z - 0.009\,(Z+1)\left[\log\left(\frac{E_0}{3}\right)\right]^2 \qquad (5.35)$$

$$\log f_{EC} = 2.0 \log E_0 - 5.6 + 3.5\; \log (Z+1) \qquad (5.36)$$

where E_0 is the β_{max} expressed in MeV and Z is the atomic number of the daughter product.

Selection Rules

Transitions in which electron and neutrino do not carry away angular momentum are expected to have largest probability and are called 'allowed' transitions. Transitions are classified depending on the changes in l (Δl), spin (ΔI) and parity ($\Delta\pi$). Transitions with ΔI = 0 or 1 and $\Delta\pi$ = NO are called allowed transitions and should have the allowed shape and similar ft values. However, 'ft' values were found to have a range in the allowed transitions from 10^3 to 10^9. This may be due to the fact that $|M_{if}|^2$ is not same for $\Delta I = 0, \pm 1$ and $\Delta\pi = NO$.

The electron and neutrino emission with orbital angular momenta (l) other than zero is possible. With increase in l values, the probability of emission decreases rapidly. β-transition with l = 1, 2, 3 ... are classified as first, second, third .... forbidden transition. A few example are given in Table 5.2.

Table 5.2 - Classification of β-transition and selection rules

Type	Example	β_{max} (MeV)	log ft[a]	ΔI	Δl	$\Delta\pi$
Super allowed	$^{1}n \rightarrow {}^{1}H$	0.78	3	0	0	No
Allowed	$^{35}S \rightarrow {}^{35}Cl$	0.17	4-7	0	0	No
Allowed (l-forbidden)	$^{32}P \rightarrow {}^{32}S$	1.71	6-12	0	1	Yes
First forbidden	$^{139}Ba \rightarrow {}^{139}La$	2.27	6-15	1	1	Yes
	$^{137}Cs \rightarrow {}^{137m}Ba$	0.51		2	1	Yes
Second forbidden	$^{137}Cs \rightarrow {}^{137g}Ba$	1.17	11-15	2	2	No
Third forbidden	$^{87}Rb \rightarrow {}^{87}Sr$	0.27	17-19	3	3	Yes
Fourth forbidden	$^{115}In \rightarrow {}^{115}Sn$	0.63	~23	4	4	No

[a]Note : Ranges of log ft values are approximate

A few examples are discussed below to understand the log ft values and selection rules.

^{137}Cs decays by β^- emission and populates two states in the daughter product ^{137}Ba and the decay scheme is shown in Fig. 5.6. The calculated log ft values for E_{β^-} values of 1.17 MeV and 0.51 MeV are given in Table 5.3.

The log ft value obtained for the transition involving E_0 = 1.17 MeV is 12.2 and the transition corresponds to second forbidden type. The ΔI should be ±2 of ^{137}Cs $(7/2^+)$and parity of ^{137}Ba is same as that of ^{137}Cs. Accordingly ground state of ^{137}Ba should have a spin of $I = \frac{7}{2} \pm 2 = \frac{11}{2}$ or $\frac{3}{2}$. On the other hand, the log ft value for excited state (E_{β^-} = 0.51 MeV)

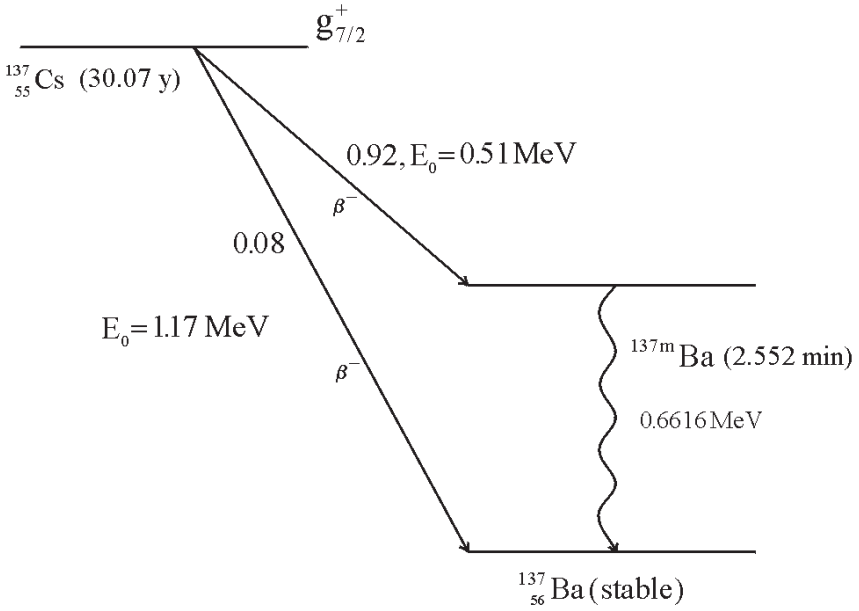

Fig. 5.6 Decay scheme of ^{137}Cs.

Table 5.3 - E_0 and log ft values for the decay of ^{137}Cs.

E_0 (MeV)	log f	Branching	t(s)	log ft
1.17	2.13	0.08	1.187×10^{10}	12.2
0.51	0.79	0.92	1.032×10^{8}	8.8

is 8.8 which belongs to first forbidden type. Then its spin is that of ^{137}Cs ±2 and associated with parity change. It is also known that γ-decay of ^{137m}Ba to ground state of ^{137}Ba is long delayed with a half-life of 2.552 min. Also ground state of ^{137}Ba is assigned a value of $(3/2)^+$ from magnetic moment measurements. Thus the excited state (^{137m}Ba) is assigned a spin value of 11/2 with a negative parity. The nuclear state thus is $11/2^-$. Since the spin difference between m → g state is 4 with a change in parity, the emission of γ-decay is associated with higher order multipolarities and the γ-deexcitation has low probability, which will be discussed in the next part.

A more complicated, but of importance is the decay of ^{87}Br and its daughter product ^{87}Kr. The decay scheme is given in Fig. 5.7.

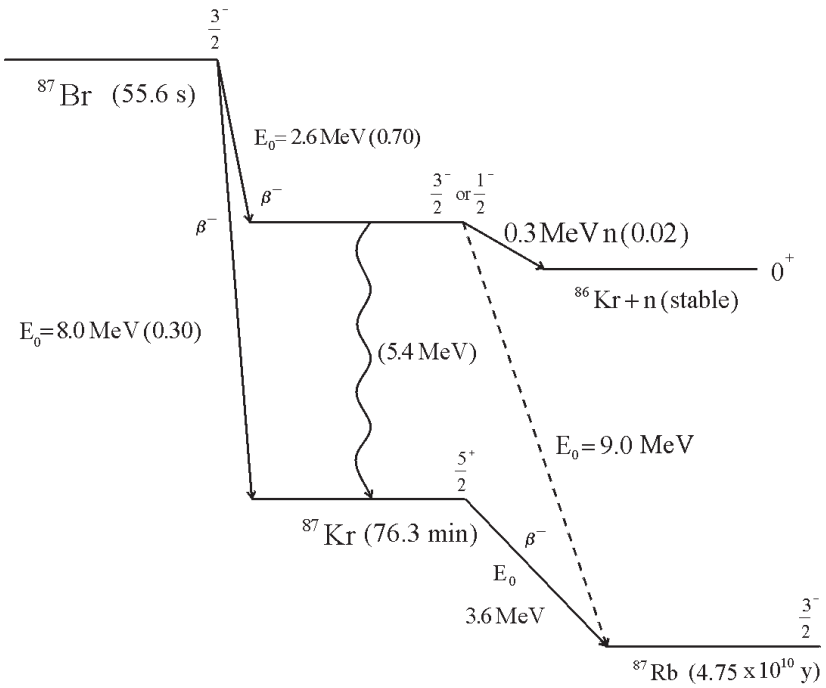

Fig. 5.7 Partial decay scheme of ^{87}Br (Life time of ^{87m}Kr is very short. The delayed neutrons are emitted from this level)

The log ft values for the two transitions from ^{87}Br with E_0 values of 2.6 MeV and 8.0 MeV are 4.83 and 7.08, respectively, which are calculated using eqn. 5.34 and are given in Table 5.4. Ground state of ^{87}Br is $p_{3/2}$ and log ft value for E_0 = 2.6 MeV suggests that this transition, populating the excited state 5.4 MeV of ^{87}Kr, is an allowed transition. Therefore, $\Delta l = 0$, $\Delta I = 0$ or 1 with no parity change. Thus the excited level can be characterised as a $p_{3/2}$ or $p_{1/2}$ state. The other transition is assigned as $d_{5/2}$ state, though expected state from single particle shell model is $g_{7/2}$.

The most interesting part of this system is the decay of 5.4 MeV excited state of ^{87}Kr. This energy is 0.3 MeV excess over the combined mass of ^{86}Kr and a neutron. It means that the neutron separation energy is 5 MeV and therefore 5.4 MeV level is an unbound level of ^{87}Kr. The deexcitation of the level can be by one of the three modes: (1) emission of a neutron with a kinetic energy of 0.3 MeV, (ii) Decay to ground state of ^{87}Kr by 5.4 MeV γ-emission and (iii) Decay to ground state of ^{87}Rb by emission of a β with E_0 = 9.0 MeV. Though the β-transition is allowed ($p_{3/2} \rightarrow p_{3/2}$), it is not observed as the energy involved is high. 2% is the branching for neutron emission and the remaining is by γ-deexcitation. Neutron emission is delayed by the decay of ^{87}Br (55.5 s) as this depends on the population of 5.4 MeV level of ^{87}Kr subsequent to the decay of ^{87}Br.

Table 5.4 - E_0 and log ft values for the decay of ^{87}Br

Isotope	E_0 (MeV)	log f	Branching	t(s)[a]	log ft
$^{87}_{35}Br$	2.6	2.93	0.70	79.28	4.83
	8.0	4.81	0.30	185	7.08
$^{87m}_{35}Br$	9.0	5.01	~ 0	large	large

[a]Half-life x branching

Gamma Transitions

Deexcitation Processes

The product nucleus in α-decay or β-decay may be left in either an excited state or ground state; more frequently in an excited state. Excited states may also arise as a result of nuclear reactions or because of direct excitation from the ground state. An excited state returns to the ground state or reaches less excited state mainly by emission of electromagnetic radiation known as gamma radiation. Energy of the γ-rays is between a few keV and about 7 MeV. By measuring the γ-ray energy, useful information on the structure of the product nucleus is obtained. The γ-ray energies can be measured with a crystal spectrometer. Solid state germanium and Si(Li) detectors are frequently used for measuring γ-ray energies.

Internal conversion (IC) is a competing mode of deexcitation process. Internal conversion is the result of interaction between nucleus and extra nuclear electrons leading to emission of an electron. In the process, energy of the excited nuclear level is transferred to the nearest orbital electron which is emitted if it gains an energy more than its binding energy. Kinetic energy of the earlier electron is equal to the difference between the energy of the nuclear transition and its binding energy.

Deexcitation of a nucleus in yet another mode is probable, if the energy available is more than $2 m_o c^2$ (1022 keV). It is possible that the excited nucleus creates simultaneously an electron (e^-) and a positron (e^+). Since this pair of particles are non-nuclear, they are emitted the moment they are formed with kinetic energy equal to half of the excess energy over 1022 keV. It is to be noted that it is an uncommon mode of deexcitation and also it is an example where energy is converted to mass in the form of e^- and e^+ pair.

Since in all these processes, deexcitation of an excited nucleus is taking place, all are called γ-transitions as there is no change in A and Z. Only the first process is accompanied by the emission of γ-rays.

Life times of Excited States

The life times of excited states are around 10^{-12} s, though there are quite a few exceptions. In certain cases, the excited states are found with measurable and long life times,

and are known as 'isomers'. e.g., ^{137m}Ba has a half life of 2.552 min. ^{99m}Tc (6.01 h); ^{125m}Xe (56.9 s), ^{129m}La (0.56 s) and ^{210m}Bi (3.04 x 10^6 y) are some examples of isomers. If the differences of spin (I) and energy (E) between the levels are large, then existence of isomers is possible. Gamma decay from an isomeric state is called isomeric transition (IT). The systematics of isomer life times and their dependence on energy and spin changes played an important role in the development of nuclear shell model.

Multipole Radiation and Selection Rules

Gamma radiation arises from purely electromagnetic effects that may be due to changes in charge and current distributions in nuclei. Charge distributions give rise to electric moments and current distributions to magnetic moments. Correspondingly γ-ray transitions are classified as electric and magnetic. Gamma ray carries away integral units of angular momenta (l). The emitted γ-rays with l values of 1, 2, 3... units of $\hbar$ are called dipole quadrupole, octupole ... radiations, respectively. It is represented as El or Ml. e.g. E2 means electric quadrupole; M3 means magnetic octupole ($2^3 \rightarrow$ octupole).

The electric and magnetic multipole radiations differ in parity in such a way that an electric 2^l pole radiation has a parity of $(-1)^l$ whereas magnetic 2^l multipole radiation has $(-1)^{l+1}$ parity. Angular momenta (l) associated with 2^l pole radiation are governed by $I_i + I_f \geq l \geq |I_i - I_f|$ where I_i and I_f are nuclear angular momenta of initial and final states involved in the γ-transition. If the transition is from 2^+ to 3^+, then l can have integral values from 1 to 5. Since there is no change in parity, odd l values are associated with magnetic multipolarity and even l values with electric multipolarity. Thus the multipolarities associated with this transition are M1, E2, M3, E4 and M5. But in reality only lowest in the case of electrical and lower two in the case of magnetic multipolarities are probable. In this case the multipolarities of γ-ray would be a mixture of M1 and E2. A point to be noted is that if there is no parity change, electric multipolarity will be even and magnetic will be odd; as in the above case. If there is a parity change, odd electric multipolarity and even magnetic multi polarity are observed.

The selection rules discussed above are given in Table 5.5.

Table 5.5 - Selection rules and multipolarities in the γ-decay.

ΔI	0	0	1	1	2	2	3	3
Δπ	No	Yes	No	Yes	No	Yes	No	Yes
Transition type	M1, E2	E1	M1,E2	E1	E2	M2, E3	M3, E4	E3

It should be noted that the transition from 0 to 0 ($I_i = 0$ and $I_f = 0$) cannot take place as photon carries away atleast an l value of 1 unit. Transitions with parity change and $\Delta I = 0$ are possible. In the case of no change in parity ($\Delta\pi$ = NO), deexcitation may occur by internal

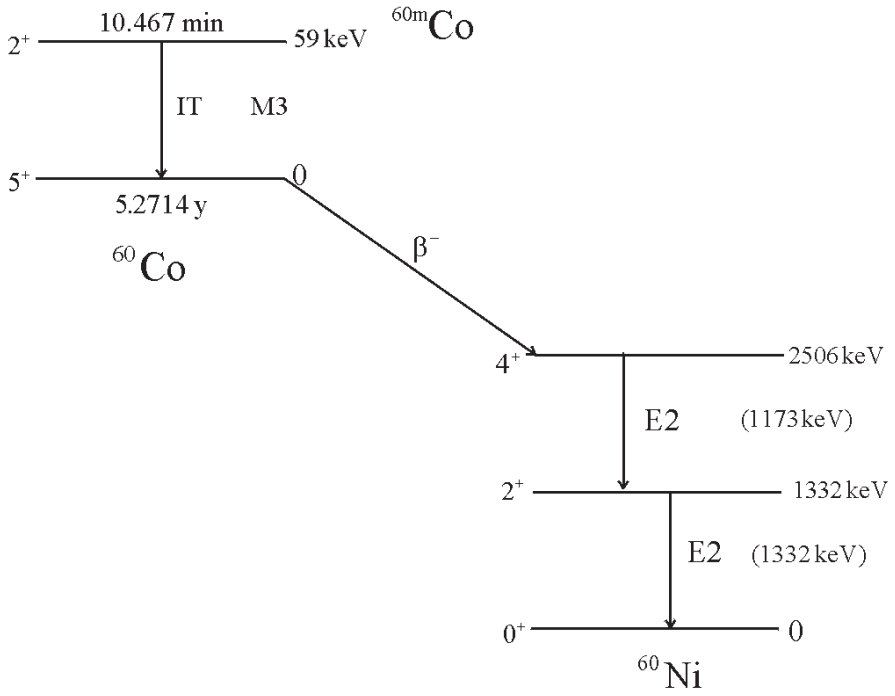

Fig. 5.8 Decay scheme of $^{60m}Co \rightarrow {}^{60}Co \rightarrow {}^{60}Ni$.

conversion, e.g., ^{72}Ge. Other possibility is pair production if the energy is more than 1.022 MeV; e.g., ^{16}O (6.05 MeV state).

These selection rules can be applied to arrive at the multipolarities of the γ-rays from IT of ^{60m}Co (E_γ = 59 keV) and γ-rays of ^{60}Co (E_γ = 1173 keV and 1332 keV). The decay scheme of ^{60m}Co is shown in Fig. 5.8. In the case of ^{60m}Co → ^{60}Co, the transition is $2^+ \rightarrow 5^+$ with no parity change. Electric even multipoles and magnetic odd multipoles are associated with the γ-rays of 59 keV. I_i = 2 and I_f = 5. The γ-rays can have *l* values of 3, 4, 5, 6, 7. Associated multipolarities are M3, E4, M5, E6, M7. The γ-rays will be M3 type competed by E4 as higher orders will be of very low probability. In fact experimental observation is that 59 keV is mainly of M3 type.

The β^- decay of ^{60}Co populates excited states 2506 keV (4^+) and 1332 keV (2^+) of ^{60}Ni. Deexcitation is through emission of cascade γ-rays of 1173 keV ($4^+ \rightarrow 2^+$) and 1332 keV ($2^+ \rightarrow 0^+$). In both the cases, there is no parity change. Therefore, the γ-rays will have electric even multipolarities and magnetic odd multipolarities. In the case of $4^+ \rightarrow 2^+$, *l* values will be 2, 3, 4, 5, 6 and therefore E2, M3, E4, M5 and E6 are the expected multipolarities. The experimental observation is of E2 transition. Similarly the transition of $2^+ \rightarrow 0^+$, will be purely E2 type as $I_i - I_f = 2$ and $I_i + I_f = 2$ and no parity change.

By measuring the multipolarities and energies of γ-rays, valuable information on nuclear structure in terms of spin and parity and energy of excited states can be arrived at.

Gamma Decay Constant

A complete theory of γ-transition requires the use of the quantum theory of radiation and detailed description of quantum states of the nucleus; which is not dealt with here. The interaction potential between the nucleus and electromagnetic radiation can be expressed as an infinite series of powers of R/ƛ where R is nuclear radius and ƛ is the de Broglie wavelength of the electromagnetic radiation. The transition probability is proportional to $\left(\frac{R}{ƛ}\right)^{2l}$. The wavelength of radiation is given by

$$ƛ = \frac{\hbar}{p} = \frac{\hbar c}{E} \tag{5.37}$$

This can be written as

$$ƛ = \frac{197}{E(MeV)} \times 10^{-15}\ m \tag{5.38}$$

$$\text{Thus}\ \ \frac{R}{ƛ} = \frac{R_0 \cdot A^{1/3}\ E(MeV)}{197} \tag{5.39}$$

which is always less than 0.1. Therefore, the transition probability decreases drastically with increase in *l* value

The decay probability (λ) for a gamma transition is related to $\frac{R}{ƛ}$ and *l* as given in eqn. 5.40 and 5.41.

$$\lambda_{El} = 2\pi\nu \frac{e^2}{hc} \cdot S\left(\frac{R}{ƛ}\right)^{2l} \tag{5.40}$$

$$\lambda_{Ml} = 2\pi\nu \frac{e^2}{hc} \cdot (10\ S)\left(\frac{h}{MCR}\right)\left(\frac{R}{ƛ}\right)^{2l} \tag{5.41}$$

where λ_{El} and λ_{Ml} are respectively decay probabilities for emission of electrical and magnetic multipoles of order 2^l, ν is the frequency of emitted radiation and M is the mass of a nucleon. The quantity (S) is *l* dependent and is given by

$$S = \frac{2(l+1)}{l\,[1 \times 3 \times 5 \ldots\ldots (2l+1)]^2}\left(\frac{3}{l+3}\right)^2 \tag{5.42}$$

With increase in *l* value, the values of S decrease drastically as given in Table 5.6

Table 5.6 - Values of S as a function of *l*.

l	1	2	3	4	5
S	2.5×10^{-1}	4.8×10^{-3}	6.25×10^{-5}	5.3×10^{-7}	3.1×10^{-9}

From eqn. 5.42, it may be observed that higher multipole emission is less probable (see Table 5.6). In view of this, even though γ-ray may carry different *l* values, lowest multipoles are more probable as discussed in the case of decay of ^{60}Co. From eqns. 5.40 and 5.41, it is clear that electric mulitpole radiation emission is more probable compared to magnetic multipole radiations and the ratio is given by,

$$\frac{\lambda_{El}}{\lambda_{El}} = \frac{1}{10} \cdot \left[\frac{R}{h/MC}\right]^2 = 4.4\, A^{2/3} \qquad (5.43)$$

where A is the mass number of the nucleus emitting γ-rays.

Internal Conversion (IC) Coefficients

As mentioned earlier, internal conversion is an alternative to γ-deexcitation, in which an electron is emitted. Kinetic energy of the emitted electrons (E) is given as

$$E = E_d - E_B \qquad (5.44)$$

where E_d is the difference in the energy of initial and final nuclear levels and E_b is the binding energy of the emitted electron. The ratio of the rate of the IC to the rate of γ-emission is known as the internal conversion coefficient (α). It can also be calculated as the ratio of the converted electrons to the number of γ-rays emitted. The α can have values from 0 to ∞. The values of α from K, L, M etc. shells are termed as α_K, α_L, α_M etc. respectively. If E is more than E_B of K-shell electron, then K-shell electron can be emitted. Depending on the value of E, conversion electrons of different energies can be produced with distinct energy and they appear as discrete lines in the electron spectrum. By adding appropriate binding energy to the measured energy values of conversion electrons, the transition energies are obtained.

Auger Electron Emission

Auger electron emission is a competing process to X-ray emission. In an excited atom which has a core electron removed, a vacancy exists. This vacancy is filled by jumping of an electron from higher levels. In the process, a characteristic X-ray of the atom is emitted with an energy equal to the difference of binding energies (E) of these two electrons. It is possible that this energy could be transferred to a neighbouring electron which is then emitted from the atom and this process is called Auger electron emission.

Suppose a vacancy exists in K-shell of an excited atom and it is filled by an electron from L_I shell. The energy excess E_K-E_{L_I} would be the energy of X-ray emitted. On the other hand, if the energy is transferred to a neighbouring electron in L_{II} shell, then that electron (Auger electron) would be emitted with a kinetic energy equal to (E_K-E_{L_I}) - $E_{L_{II}}$.

Bibliography

1. G. Friedlander, J.W. Kennedy, E.S. Macias and J.M. Miller, Nuclear and Radiochemistry, 3rd Ed., John Wiley & Sons Inc., New York (1981).
2. I. Kaplan, Nuclear Physics, 2nd Ed., Addision Wesley, Cambridge, Massachusetts (1963).
3. R.D. Evans, The Atomic Nucleus, Tata-McGraw-Hill Book Co., New York (1978).
4. S. Glasstone, Sourcebook on Atomic Energy, 3rd Ed., Affiliated East West Press Pvt. Ltd. (1967).
5. Nuclear Chemistry, Vol. 1 and 2, Ed. L. Yaffe, Academic Press, New York (1968).
6. Alpha, Beta and Gamma ray spectroscopy, Ed. K. Scigbahn, North Holland Press, Amsterdam (1966).
7. H.J. Arnikar, Essentials of Nuclear Chemistry, 3rd Ed., John-Wiley (1990).
8. H. Geiger and H.M. Nuttall, *Phil. Mag.*, **22** (1911) 613.
9. I. Perlman, A. Ghiorso and G.T. Seaborg, *Phys. Rev.*, **77** (1950) 26.
10. G. Gamow, *Z. Phys.*, **51** (1928) 204.
11. R.W. Gurney and E.V. Condon, *Nature*, **122** (1928) 439.
12. H.J. Mang, *Ann. Rev. Nucl. Sci.*, **14** (1964) 1.
13. E. Fermi, *Z. Phys.*, **88** (1934) 161.
14. J.B. Gerhart, *Phys. Rev.,* **95** (1954) 288L.
15. S. Raman and N.B. Gove, *Phys. Rev.*, **C7** (1973) 1995.
16. F. Reines, *Ann. Rev. Nucl. Sci.*, **10** (1960) 1.
17. M. Goldhaser and R.D. Hill, *Rev. Mod. Phys.*, **24** (1952) 179.

Chapter 6
Interaction of Radiation with Matter

The passage of radiation through matter results in the deposition of its full / partial energy in the medium traversed by the radiation and may cause ionisation and excitation of atoms. If the ionisation / excitation is measured, then it serves as the basic signal to detect the presence of radiation and often its quantitative measurement. Nuclear radiations are detectable only through their interaction with matter. Radiation detection, therefore, depends on the manner in which the radiation interacts with the material of the detector. For measurement and characterisation of nuclear radiations, it is necessary to understand the interaction of various radiations with matter through which they are passing.

Nuclear radiations are broadly classified into two categories: (i) charged particulate radiations, e.g., p, e^-, e^+ and α and (ii) uncharged radiations, e.g., n and γ. Charged particulate radiations interact with the electrons of the medium through familiar Coulombic forces and lose their energy. On the other hand, uncharged radiations undergo interaction in two steps or they pass through matter without interacting. In favourable conditions neutrons collide with nuclei of the atoms in matter and may get captured resulting in nuclear reactions. Neutron detection is based on those nuclear reactions involving emission of charged particles. Photons either are absorbed in the medium or scatter the electrons in the medium. In both cases, electrons are produced which interact with the medium.

Heavy Charged Particles

Heavy charged particles, such as alpha particles, interact with matter through a series of primary collisions. The interaction takes place between positive charge of particulate radiations and negative charge of orbital electrons within the medium. This results in the dissociation of molecules and ionisation/excitation of atoms and molecules. Ionisation is easily measurable and often used for the detection of the positively charged particle radiations. The maximum energy transferred to an electron of mass m_0 in a single collision with charged particle of mass M and kinetic energy E is given by $4 Em_0/M$. A 4 MeV alpha particle transfers about 2 keV energy to an electron in a single collision. The energy transferred decreases with slowing down of the α-particle. Therefore, an α-particle of 4 MeV energy has to undergo many collisions before it loses all its energy and the particle is

stopped. On an average, the energy imparted to an electron by the α-particle is about 100-200 eV. Many of these electrons, or δ-rays, cause further secondary ionisation. About 60-80% of the ionisation produced by the charged particle interaction is due to the secondary ionisation, though it is difficult to determine the exact ratio of primary to secondary ionisation. When the velocity of the charged particle becomes comparable to the velocity of the K-shell electron, then the particle starts picking up electrons and loses its charge. When the velocity of the charged particles becomes comparable to that of valence electrons, then the particles start making elastic collisions with the atomic electrons in the medium rather than exciting the atomic electrons. This gives rise to nuclear stopping.

High energy charged particles may also undergo nuclear reactions with the nuclei of the interacting medium. However, nuclear reactions have a small cross section as compared to the Coulombic interaction with electrons.

Stopping Power

The linear stopping power 'S' for a charged particle in a given medium (absorber) is defined as the differential energy loss of that particle as a function of the path length (x) traversed by the particle

$$S = -dE/dx \tag{6.1}$$

The term S is also called specific energy loss or rate of energy loss or specific ionisation. The specific energy loss is related to number density (N) and atomic number (Z) of the medium. Bethe has derived an expression correlating S with the characteristics of the particle and the medium. A simplified version of Bethe's formula is given in eqn. 6.2.

$$S = NB \frac{4\pi e^4 z^2}{m_0 \upsilon^2} \tag{6.2}$$

where

$$B = Z \left[\ln \frac{2m_0 \upsilon^2}{I} - \ln\left(1 - \frac{\upsilon^2}{c^2}\right) - \frac{\upsilon^2}{c^2} \right] \tag{6.3}$$

where z is the charge of the particle, υ is the velocity of the particle, c is velocity of light, m_0 is the rest mass of electron and *I* is the average excitation and ionisation potential of the absorber. This relation is applicable only when the charged particle is totally ionised. Eqn. 6.2 is valid for the charged particles with velocities that are large compared to the velocity of orbital electrons. In the case of non-relativistic charged particles with velocity smaller as compared to the velocity of light, only the first term in eqn. 6.3 is important and eqn. 6.2 is reduced to

$$-\frac{dE}{dx} = \frac{4\pi z^2 e^2}{m_0 \upsilon^2} \cdot NZ \left(\ln \frac{2m_0 \upsilon^2}{I} \right) \tag{6.4}$$

The stopping power is inversely proportional to the energy of the charged particle. The plot between -dE/dx and the distance of penetration (x) for α-particle is shown in Fig. 6.1 and the plot is known as 'Bragg Curve'. The rate of energy loss is low in the initial stages because the charged particle is moving so fast that it has only a short time for interaction with the electrons. The time a charged particle spends within a given distance is proportional to $1/\upsilon$, which would be low in the initial stages. The energy of the particle is reduced as it passes through the matter resulting in increased specific ionisation along its path. This will reach a maximum when the velocity of the charged particle becomes comparable to the velocity of the orbital electrons of the medium. At this stage the charged particle starts picking up electrons and the rate of energy loss starts diminishing. Further, during atomic collisions, -dE/dx gets greatly reduced as the ion will pick up and then lose electrons many times near the end of the path.

Energy loss is a statistical process. Even a beam of mono energetic charged particles will be having distributed energies along their path in the medium. This 'energy straggling' reflects in the enhanced width of the Bragg curve (last part of the Fig. 6.1).

The thickness of the absorber is generally measured in grams per cm^2 which is the product ρx where ρ and x are the density and thickness of the absorber respectively. This unit is convenient for expressing thickness as this gives a better description of the amount of material in a thin absorber foil. Mass stopping power is defined as the ratio of -dE/dx and the

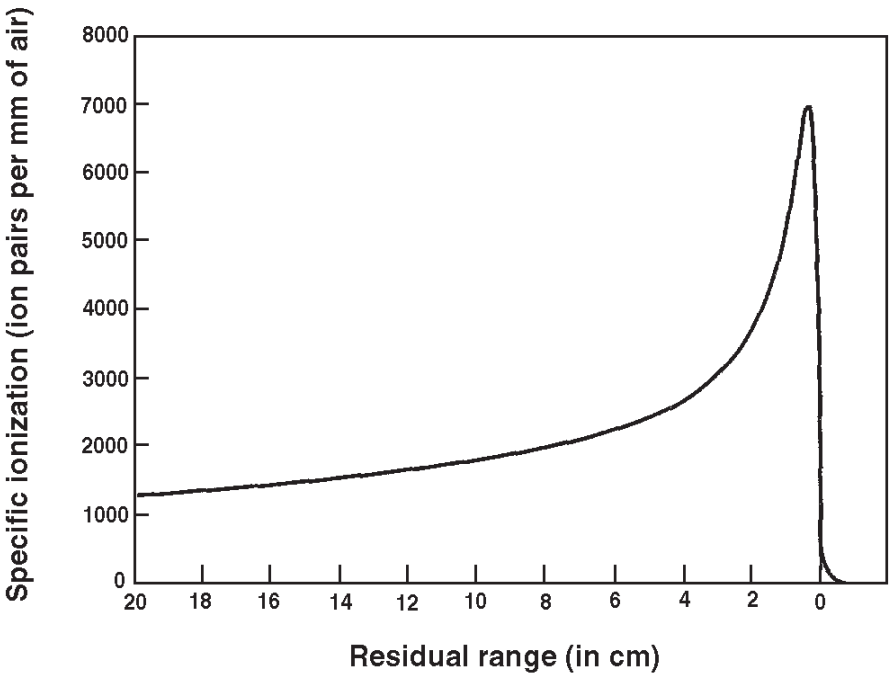

Fig. 6.1 Bragg curve for monoenergetic α particles.

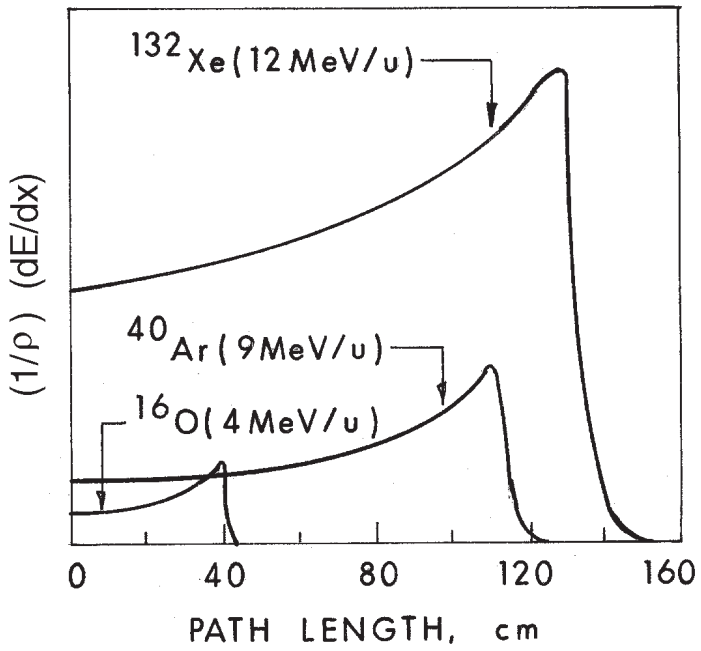

Fig. 6.2 Bragg curves for heavy ion in methane.

density (ρ) of the medium. Mass stopping power as a function of path length in methane gas, for a few charged particles of different energies, are given in Fig. 6.2. These curves are important to decide the detector specifications for the measurement of charged particles.

Range of Heavy Charged Particles

The distance travelled by a charged particle before coming to rest is known as its range (R). Range depends on the absorber material and the type as well as the energy of the charged particle. Ranges of positively charged particles are determined by absorption method either with thin metallic absorbers or with a gas in a container whose pressure can be varied. A typical plot of distance travelled in the absorber and the intensity of the charged particles is shown Fig. 6.3. Heavy charged particles suffer only small deflection due to collisions with atomic electrons and therefore, they travel in a straight line along the initial direction. For small values of absorber thickness, energy of the charged particles is reduced with no attenuation of the charged particles. Therefore, number of charged particles remains same. As the thickness of the absorber approaches the range, rapid fall in the number of charged particles is observed. The thickness of the absorber at which the number of transmitted particles becomes nearly half (the differential range is maximum) is called mean range (R_m). The range of all the monoenergetic charged particles is not identical and there is a small variation which is called range straggling, as is seen in Fig. 6.3. Sloping portion of the curve when extrapolated, cuts the X-axis at R_e and this is called extrapolated range (R_e). If, instead

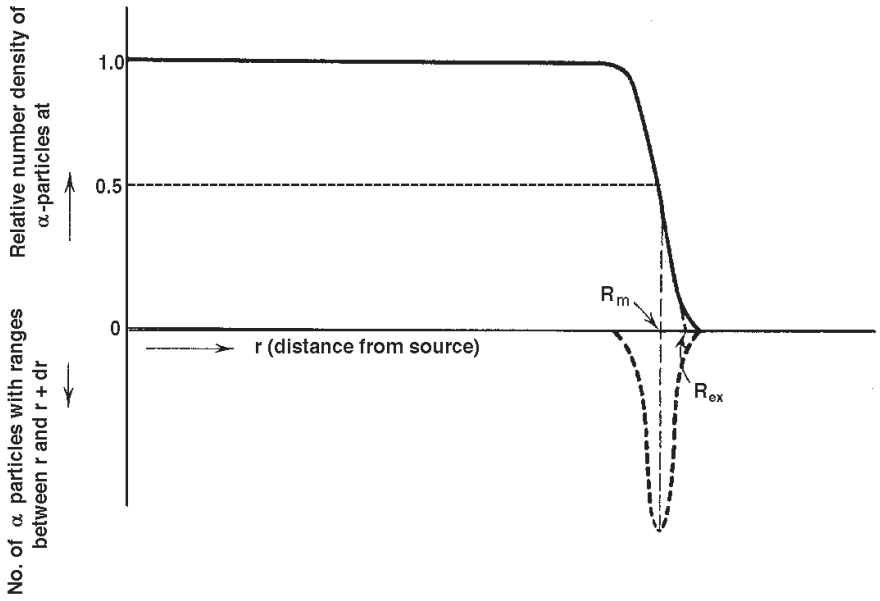

Fig. 6.3 Number of α-particles from a point source as a function of distance from the source (full curve) and the derivative (heavy dashed curve) [Nuclear and Radiochemistry, G. Friedlander, J.W. Kennedy, E.S. Macias and J.M. Miller, 3rd Ed., John Wiley (1981) p.209].

of extrapolation, this curve is differentiated with respect to X, a nearly Gaussian curve is obtained with peak at a distance (R_m) which is called the mean range. Range of a charged particle is related to its energy (E_0) by

$$R = \int_{E_0}^{0} \frac{1}{(dE / dx)} dE \qquad (6.5)$$

Ranges can be computed from specific energy loss. The integration is generally carried out by numerical methods, as there is no single relation that is applicable to the entire energy region.

Scaling Laws

The mean range (R^1_m) of a charged particle in an absorber of density ρ_1 and atomic weight A_1 can be calculated from the mean range R^0_m in another absorber with density ρ_0 and atomic weight A_0 by using Bragg Kleeman relation

$$\frac{R^1_m}{R^0_m} = \frac{\rho_0 \sqrt{A_1}}{\rho_1 \sqrt{A_0}} \qquad (6.6)$$

This relation is based on the assumption that the ranges in different type of media are additive. Thus the range of a charged particle (R^c_m) in a compound, made up of several atomic species, can be computed with the knowledge of the ranges for the constituent atoms as

$$R^c_m = \frac{M_c}{\sum_i n_i \left(\frac{A_i}{R^i_m} \right)} \tag{6.7}$$

where, R^i_m is the range of the charged particle in a medium made up of ith element in the compound, A_i is the atomic weight of the element and M_c is the molecular weight of the compound. The mean range of a 5 MeV alpha particle in air at STP is 3.5 cm. Mean ranges of charged particles as a function of energy can be computed in different media. The general range - energy relation can be approximated by the expression. $R = a E_0^b$ where a and b are empirical constants whose values depend on the type of the charged particle but vary slowly with energy. The value of b is nearly constant (between 1.7 and 1.8) for ions that are completely stripped off electrons.

Electrons

The interaction of fast moving electrons with matter is very similar to that of heavy charged particles. Electrons lose their energy in a medium by collisional losses through Coulombic interactions with the electrons in the medium. The average energy loss per ion pair formed is about 35 eV in air which is same for heavy charged particles. The primary ionisation by electrons accounts for about 20-30% of the total ionisation. When compared with heavy charged particles, fast electrons lose energy at a lower rate. The mean deflection of an incident electron in the medium is large compared to a heavy particle and it follows a tortous path (Fig. 6.4). Large deviations in the path are possible because its mass is nearly equal to that of the orbital electrons, with which it is interacting and a much larger fraction of its energy can be lost in a single encounter. Some times electron-nucleus interactions occur which can change the electron direction abruptly. High energy electrons may also lose energy in radiative collision process. When an electron is accelerated in the electric field of a nucleus, radiation is emitted and it is known as Bremsstrahlung radiation.

Specific Energy Loss

For collisional interaction of fast electrons, Bethe derived a relation for the specific energy loss (-dE/dx) of fast electrons as given by eqn. 6.8

$$-\left(\frac{dE}{dx}\right)_c = \frac{2\pi e^4 NZ}{m_0 \upsilon^2} \left[\ln \frac{m_0 \upsilon^2 E}{2I^2 (1-\beta^2)} - \ln 2\left(\sqrt{1-\beta^2} - 1 + \beta^2\right) + (1-\beta^2) + \frac{1}{8}\left(1-\sqrt{1-\beta^2}\right)^2 \right] \tag{6.8}$$

where, $\beta = \upsilon/c$, υ and c are velocity of fast moving electrons and velocity of light respectively, and other symbols carry same meaning as described in eqns. 6.2 and 6.3. Since

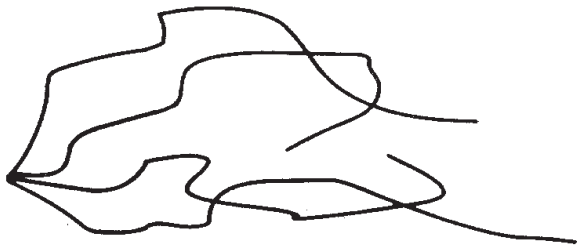

Fig. 6.4 Path of β particles while passing in matter [G.F. Knoll, Radiation Detection and Management, John Wiley & Sons, New York (1979) p.44].

the velocity of electrons of high energy are comparable to the velocity of light, relativistic corrections are incorporated in the above equation.

From classical theory, any charge must radiate energy when accelerated. Deflection of the electrons due to their interactions with the absorber corresponds to such acceleration. The energy loss by this radiative process is given by

$$-\left(\frac{dE}{dx}\right)_{\gamma} = \frac{NEZ\,(Z+1)e^4}{137\,m_0^2\,c^4}\left[\ln\frac{2E}{m_0\,c^2} - \frac{4}{3}\right] \qquad (6.9)$$

In eqn. 6.9, the numerator consists of E and Z^2 terms, indicating that energy loss by radiative process becomes important for high energy electrons while passing through heavy elements, e.g., lead. In the light elements like Al and also for low energy electrons, radiative loss is unimportant. The total specific energy loss for electrons is the sum of collisional and radiative losses and is given by eqn. 6.10.

$$\frac{dE}{dx} = \left(\frac{dE}{dx}\right)_c + \left(\frac{dE}{dx}\right)_{\gamma} \qquad (6.10)$$

The ratio of specific energy losses is approximated as

$$\frac{\left(\frac{dE}{dx}\right)_c}{\left(\frac{dE}{dx}\right)_{\gamma}} \sim \frac{EZ}{700} \qquad (6.11)$$

where, E is expressed in units of MeV. Typically for β-particle of energy upto 2 MeV, in the light Z absorbers, like Al, radiative losses correspond to a small fraction (<4%). On the other hand for a 4 MeV β particle, while passing through lead, radiative loss will be about 45%.

Cerenkov Radiation

When the phase velocity of a charged particle (υ) moving in a medium is greater than the speed of light (c) in the same medium, light is emitted. This light is known as Cerenkov radiation. A bluish halo observed in nuclear reactors, spent fuel ponds and storage pools for ^{60}Co sources is due to Cerenkov radiation. Emission of Cerenkov radiation is possible only with the particles that move with relativistic velocities, e.g., high energy electrons. Additionally, refractive index (μ) of the medium should be high to observe Cerenkov radiation, e.g., electrons of E = 265 keV have a velocity of 0.751 c. These electrons while passing through a medium with μ = 1.332, have a phase velocity of μβ = 1.013 c and, therefore, Cerenkov radiation is emitted. This radiation can be used for the detection of electrons and the detectors are known as Cerenkov detectors. These detectors are 'threshold' type detectors.

Range of Electrons

It is difficult to define the range for fast electrons as the electron's total path length is considerably greater than the distance of penetration along its initial direction. This is due to the scattering the fast moving electrons experience, during the Coulombic interaction with the orbital electrons of the medium. Collision with orbital electrons may lead to change in direction of the electrons; and thus may not reach the detector kept in line with the source for measuring the transmitted electrons. Thus even a thin absorber can reduce the flux of electrons in an attenuation experiment. In Fig. 6.5, experimental set up to measure the transmission of electrons (mono energetic electrons to begin with) through an absorber of

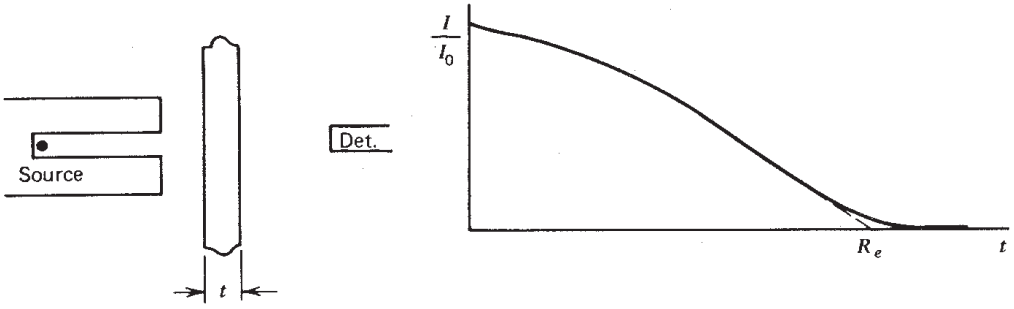

Fig. 6.5 Transmission curve for monoenergetic electrons. R_e is the extrapolated range [G.F. Knoll, Radiation Detection and Management, John Wiley & Sons, New York (1979) p.46].

thickness t is shown. A plot of the number of transmitted electrons versus the absorber thickness is also given in Fig. 6.5. It can be noticed that there is a continuous decrease in the electron flux which gradually reduces to zero with increase in thickness. Extrapolation of the linear portion of the curve to zero intensity represents the absorber thickness required to assure that almost no electrons can penetrate the entire thickness. This extrapolated range is also known as practical range. Range for electrons is much larger as compared to alpha

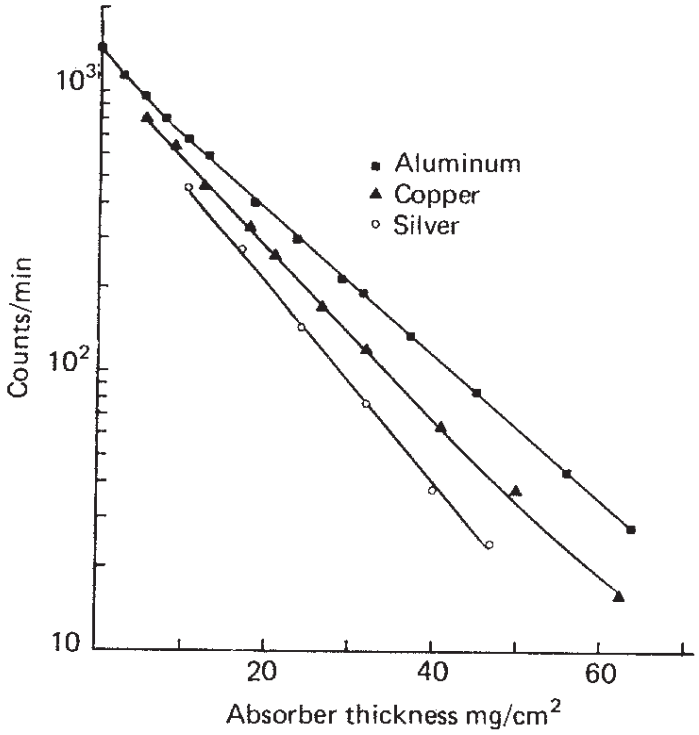

*Fig. 6.6 Transmission curves for beta particles from ^{185}W (endpoint energy of 0.43 MeV) [T. Baltakmens, Nucl. Inst. Meth., **142** (1977) 535].*

particles of same energy. e.g., range of 1 MeV electrons would be around 2 mm in low density materials and about 1 mm in moderately dense materials, whereas a thin paper can stop 4 MeV α-particles.

Absorption of β-particles

Beta particles emitted by a radioisotope have energies ranging from zero to the end point energy. The absorption curve for beta particles is different from the one shown in Fig. 6.5, which is for mono energetic electrons. Low energy β-particles are rapidly absorbed even in a small thickness of the absorber and thus the initial slope of the curve is greater. In Fig. 6.6 transmission curves for β particles from ^{185}W in different absorbers are given.

Back Scattering

A significant fraction of the electrons striking a material may be reflected back as a result of single or multiple scattering processes. An electron entering one surface of an absorber may undergo sufficient deflection so that it re-emerges from the surface through which it entered. This phenomenon is known as back scattering. The ratio of the measured

activity of a β-source with a reflector to that without a reflector is known as the back scattering factor. Backscattering increases with increase in the thickness of the absorber, until it is about one third of the range of electrons.

Electromagnetic Radiation

X-rays and γ-rays are electromagnetic radiations. They interact with matter in many ways and three modes of interaction are important from the radiation detection point of view. These are: photoelectric absorption, compton scattering and pair production. In these processes, full or partial energy of the photons is transferred to electrons as kinetic energy. In photoelectric absorption and pair production, the entire energy of the photon is transferred to the medium and in compton scattering the full energy is not transferred. There is a possibility that a few of the γ-rays may pass through the matter without interacting, which is not the case with charged particles. Thus the absorption of photons in matter is expected to be exponential, with half thickness much greater than the range of electrons of the same energy. Average specific ionisation produced in the γ-ray interaction is less than 10% of that caused by an electron of same energy and therefore, ranges are much greater. The ionisation observed for γ-rays is almost entirely secondary in nature. The average energy loss per ion pair formed remains the same i.e. 35 eV in air.

Photoelectric Absorption

In this process a photon interacts with an absorber atom in which the photon completely disappears and an energetic electron is ejected from one of the bound shells of the atom (Fig. 6.7). The interaction is with the atom as a whole and does not take place with free electrons. The probability of emission of K electrons is higher than the electrons in the other shells if the energy of the photons (hν) is higher than the binding energy of the K- electrons. The energy of the photoelectron (E_e) is given by $E_e = h\nu - E_b$ where E_b is the binding energy of the electron.

When a photoelectron is ejected, the atom is in the ionised form with a vacancy in one of its shells. This vacancy is quickly filled up either by rearrangement of electrons of the

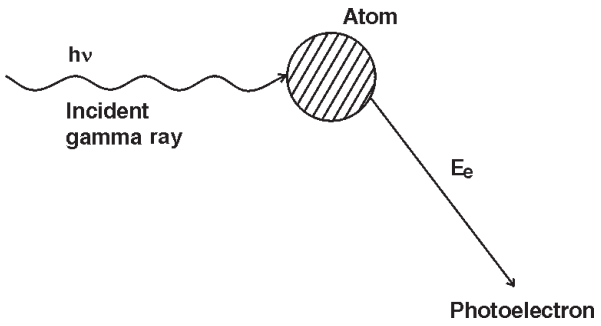

Fig. 6.7 Schematic representation of the photo-electric absorption process.

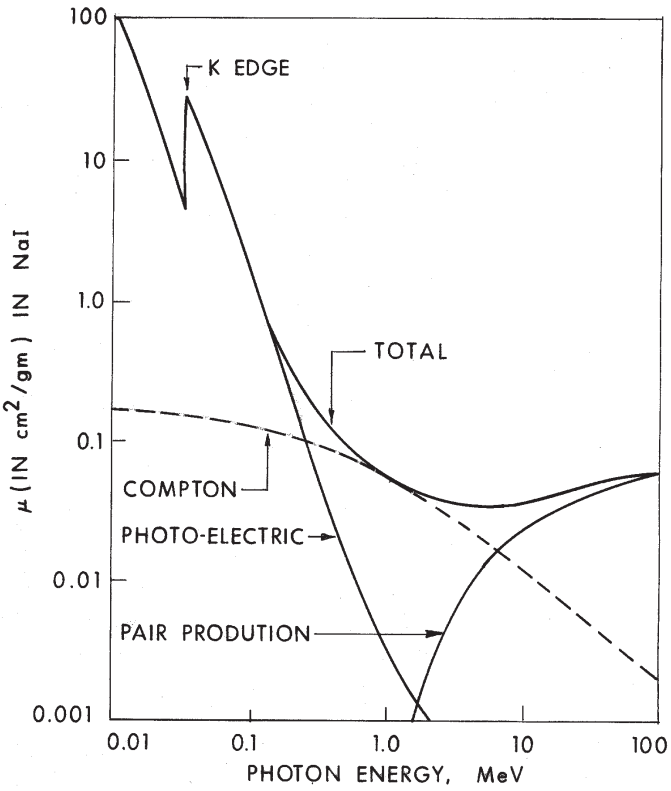

Fig. 6.8 Energy dependence of the various γ-ray interaction processes in sodium iodide [G.R. White, Natl. Bur. Stds. (US), Report 1003, 1952].

atom or from the medium. This results in production of one or more characteristic X-ray photons. These X-ray photons may either be absorbed in the medium or escape. These X-rays can deposit their energy by photoelectric absorption. Thus the photoelectric effect is characterised by the total absorption of the photon energy with in the medium. In some cases, the emission of Auger electrons may compete with the emission of characteristic X-rays.

The photoelectric process is the main interaction mode of relatively low energy (< 1 MeV) gamma rays. This interaction is enhanced for the absorber material with high atomic number, e.g., lead. Photoelectric absorption cross-section (τ) for photons of energy hν is given by an approximate relation.

$$\tau \propto \frac{Z^n}{h\nu^{3.5}} \qquad (6.12)$$

where Z is the atomic number of the atoms of the medium and n varies between 4 and 5. From the eqn. 6.12 it is clear that τ is large for low energy photons and heavy elements of the medium. High Z materials are, therefore, preferred for γ-ray detectors and also for shielding.

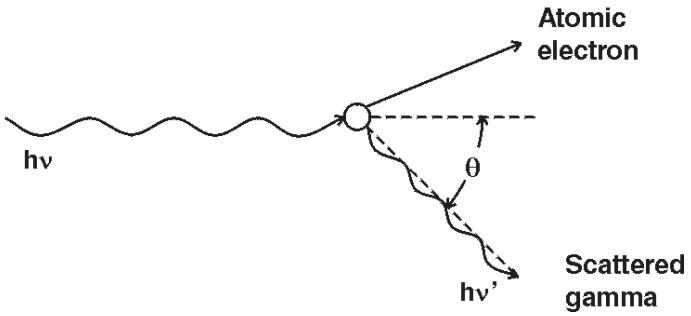

Fig. 6.9 A schematic representation of Compton scattering.

Variation of τ as a function of photon energy in the medium of NaI is given in Fig. 6.8. It decreases as a function of energy. However, a sharp rise is seen at energies corresponding to the binding energies of the electron of the absorber medium (atoms).

Compton Scattering

In the Compton scattering process a gamma ray interacts with a free or weakly bound electron and transfers part of its energy to the electron (Fig. 6.9). This interaction involves the outer, least tightly bound electrons in the atom of the medium. In the process, the incoming photon is scattered through an angle (θ) with respect to its original direction. From the conservation of momentum and energy, a relation for the energy of the scattered photon (hν′) at an angle θ can be obtained as

$$h\nu' = \frac{h\nu}{1+\frac{h\nu}{m_0 c^2}(1-\cos\theta)} \qquad (6.13)$$

where, m_0 is the rest mass of the electron. The difference of hν and hν′ is the kinetic energy of the electron that is ejected in the compton scattering. For very small angles of scattering, the energy of the scattered γ-ray is slightly less than the incident gamma ray energy. It is maximum, when the photon is back scattered ($\theta = 180^o$). Thus in the compton scattering, electrons of energies ranging from 0 ($\theta = 0^o$) to ($h\nu - 0.5\ m_0c^2$) are produced. This results in the continuous response in the detectors and therefore, is not very useful in γ-ray spectrometry. Compton scattering predominates for photons with energies between 1 and 5 MeV for high Z materials and over a wide range of energies in the low Z materials. Because compton scattering involves the least tightly bound electron, the nucleus has only a minor influence and the cross section (σ) is nearly independent of atomic number. It depends on electron density, which is proportional to Z/A and nearly constant for all the materials. σ is a slowly varying function of gamma energy (dashed line in Fig. 6.8). σ is also proportional to Z of the medium.

Pair Production

A γ-ray with energy greater than twice the rest mass of electron (1.022 MeV), under the influence of the strong electromagnetic field in the vicinity of a nucleus, can create an electron and positron pair. In this interaction, the gamma ray is absorbed and the nucleus of the absorber material receives negligibly small amount of recoil energy to conserve momentum. Pair production has a threshold of 1.022 MeV, which is needed to produce a positron. The excess energy of the γ-ray over 1.022 MeV is shared between electron and positron as kinetic energy as shown below

$$h\nu - 1.022 = E_{e^-} + E_{e^+} \quad (6.14)$$

where, E_{e^-} and E_{e^+} are kinetic energies of positron and electron respectively. This interaction does not take place when $h\nu \leq 1.022$ MeV and becomes very important when the energy is in the region of 5 MeV and above.

The positron and electron produced in this interaction slow down in the medium and produce ionisation and excitation. After losing kinetic energy, the positron combines with an electron in the medium and gets annihilated producing two gamma rays of 511 keV (m_0c^2) each. These two gamma rays move in opposite direction. They may interact with the medium or escape. If both the gamma rays of 511 keV are absorbed in the gamma ray detector, then it corresponds to the full energy deposition in the detector. On the other hand if one or both annihilation gamma rays escape then the energy deposited accordingly is either $h\nu - m_0c^2$ or $h\upsilon - 2m_0c^2$. The cross section for the pair production is low around the threshold, slowly increases with energy and becomes dominant mode of interaction in the high energy region (see Fig. 6.8). There is no single expression that could quantitatively relate the cross section for pair production (k). It could be expressed as

$$k \propto Z^2 \ln (h\nu - 2m_0c^2) \quad (6.15)$$

Total Cross-Section and Dependence on energy and Z

Cross-section for photo electric effect (τ) decreases rapidly with increase in energy barring around absorption edge (Fig. 6.8). Cross-section for compton scattering (σ) varies slowly with energy as indicated in the Fig. 6.8. Pair production has a threshold of 1.022 MeV. Cross-section for pair production (k) increases with increase in energy and becomes a dominant mode of interaction at high energy. Total cross-section (μ) as a function of energy in NaI material is given in Fig. 6.8.

$$\mu = \tau + \sigma + k \quad (6.16)$$

The cross-sections for all the three processes increase with Z of the medium. This is understandable that these interactions depend on the number of electrons available with the absorber atoms and therefore the cross-sections increase with increase in Z.

Gamma-ray Attenuation

When a beam of monoenergetic gamma rays are collimated and passed through an absorber, there will be a decrease in its intensity. The three processes described above would remove gamma photons from the beam either by absorption or by scattering. This can be characterised by a fixed probability of occurrence per unit length in the absorber. Sum of these probabilities is the probability per unit path length and is given by μ (eqn. 6.16), the linear attenuation coefficient. If I and I_0 are intensities of γ-ray beam after and before passing through an absorber of thickness x, then they are related as

$$I = I_0 \, e^{-\mu x} \tag{6.17}$$

μ varies with density of the absorber. For a given material and γ-ray energy, mass attenuation coefficient (μ/ρ) does not change with physical state of the absorber and is, therefore, used instead of μ.

$$I = I_0 \, e^{-(\mu/\rho)\rho x} \tag{6.18}$$

In radiation measurement, mass thickness (ρx) with units of mg/cm^2 is used instead of thickness (cm).

Neutrons

Neutrons do not have charge and, therefore, cannot interact with the electrons in the matter by means of coulomb force. Neutrons travel through matter much more easily than other nuclear particles, of similar energy, such as α, p, e^- and e^+. Neutrons do not face a coulomb barrier to enter into or collide with a nucleus and get scattered or captured in the process. Collisions of neutrons with nucleus results in scattering of neutrons (elastic or inelastic). On the other hand, capture of a neutron by a nucleus may lead to emission of other particle/radiation or division of the nucleus (nuclear fission). The relative probabilities of the various types of neutron interaction change dramatically with neutron energy. A brief description of neutron interaction of different types is presented in the following.

Elastic Scattering

In elastic scattering, a part of kinetic energy of the neutron is transferred to a nucleus as recoil energy (E_R). In this process, kinetic energy is conserved. The recoil energy of the nucleus is given by

$$E_R = E_n \frac{4A}{(1+A)^2} \cos^2 \theta \tag{6.19}$$

where, E_n is the kinetic energy of the neutron, A is the mass number of the nucleus and θ is the scattering angle. For example, if a 2 MeV neutron collides with hydrogen atom, then the energy transferred is equal to 2 $\cos^2 \theta$. In the case of head-on collision, ($\theta = 0$), E_R works about to be 2 MeV, indicating that full energy can be transferred to hydrogen atom. If a

neutron undergoes a head-on collision with ^{197}Au, then only about 2% of energy is transferred. Nuclides of lower mass like H, D and ^{9}Be are good moderators for slowing down of fast neutrons.

Inelastic Scattering

In inelastic scattering, neutron is scattered by the nucleus and a part of the kinetic energy is transferred to the nucleus and the nucleus is left in an excited state. The excited nucleus, in most cases, deexcites by γ-emission. In this process, kinetic energy is not conserved, but total energy is conserved. Inelastic scattering and subsequent secondary γ-rays play an important role in the shielding of high energy neutrons but are undesirable complication for detection of fast neutrons based on elastic scattering.

Neutron Capture

As there is no Coulomb barrier for neutron interaction, neutron can come very close to a nucleus and may get captured by the nucleus. Probability (cross-section) for this nuclear reaction is high with slow neutrons. Cross-section(σ) decreases with increase in neutron energy. A few reactions involving capture of thermal neutrons (E_n = 0.025 eV) which are of importance in neutron detection, are given below :

$$^{10}B + n \rightarrow {}^{7}Li + {}^{4}He \qquad \sigma = 3840 \text{ b} \qquad (6.20)$$

$$^{6}Li + n \rightarrow {}^{3}H + {}^{4}He \qquad \sigma = 940 \text{ b} \qquad (6.21)$$

$$^{235}U + n \rightarrow \text{fission} \qquad \sigma = 583 \text{ b} \qquad (6.22)$$

Neutron Attenuation

The range of neutrons in matter through which neutrons travel is a function of neutron energy and the cross-section (σ). The reduction in neutron intensity (*I*) in unit area after passing through a thickness of x of a given material is given by

$$I = I_0 \, e^{-n\sigma x} \qquad (6.23)$$

where I_0 is the initial intensity and n is the number of nuclei per cm^3 of the material (absorber). Half-value thickness ($x_{1/2}$) that is required to reduce intensity of neutron beam to half of its original value is given by

$$x_{1/2} = \frac{0.693}{n\sigma} \qquad (6.24)$$

For example, if neutrons of energy 10 keV are travelling in water. For 10 keV neutrons, the σ is 20 b.

$$n = \frac{6.023 \times 10^{23}}{18} \times 2 = 0.0668 \text{ x } 10^{24} \text{ H nuclei / cm}^3$$

$$\sigma = 20 \times 10^{-24} \text{ cm}^2$$

$$x_{1/2} = \frac{0.693}{n\sigma} = 0.51 \text{ cm}$$

For neutrons of 0.03 eV, $\sigma = 50$ b

$$x_{1/2} = \frac{0.693}{0.0668 \times 10^{24} \times 50 \times 10^{-24}} = 0.21 \text{ cm}$$

Interaction of neutrons with oxygen atoms is negligible compared to that with hydrogen atoms and, therefore, is ignored. Knowledge of half value thickness is important for determining dimensions of detectors as well as for calculating neutron shield dimensions. Often in neutron detectors, moderation of neutrons is carried out to enhance the capture cross-section and hence detection sensitivity.

Radiation Protection

As a consequence of interaction of radiation with matter, ionisation and excitation are produced in the matter. This also leads to dissociation of molecules and in some cases displacement of atoms. If the matter is a human body, then all these effects can lead to different chemical changes in the cells. Radiation exposure, thus may result in adverse effects in living organisms. External radiation, ingested or inhaled radioactive materials produce similar effects. The study of biological effects, their relation to intensity and energy, type of radiation etc. and the preventive steps form the basis for the subject of `Radiation Protection' which is dealt separately in this book (See Chapter 21).

Bibliography

1. R.D. Evans, The Atomic Nucleus, Tata-McGraw-Hill Book Co., New York (1978).
2. G.F. Knoll, Radiation Detection and Measurement, John Wiley & Sons, New York (1979).
3. G. Friedlander, J.W. Kennedy, E.S. Macias and J.M. Miller, Nuclear and Radiochemistry, 3rd Ed., John Wiley & Sons Inc., New York (1981).
4. I. Kaplan, Nuclear Physics, 2nd Ed., Addision Wesley, Cambridge, Massachusetts (1963).
5. S. Glasstone, Sourcebook on Atomic Energy, 3rd Ed., Affiliated East West Press Pvt. Ltd. (1967).
6. L.C. Northcliffe, *Ann. Rev. Nucl. Sci.*, **13** (1963) 67.
7. H.A. Bethe and J. Ashkin, Passage of Radiation through Matter, In Experimental Nuclear Physics, Vol. 1, Ed. E. Segre, Wiley, New York (1953).

Chapter 7
Radiation Detection

Radiation detection methods are based on measurement of the charge produced due to interaction of radiation as it passes through detector volume. The net result of the radiation interaction is the appearance of an electric charge within the active volume of the detector[1]. The interaction times are so short[2] that the deposition of radiation energy can be considered as instantaneous and charge appears in the detector at zero time. This charge must be collected to form the basic signal for radiation detection. Charge is collected by applying an electric field across the detector. Time required for charge collection greatly varies from one detector to another[3] depending on the mobility of charge carriers in the detector and the average distance to be travelled. The charge collected is so small that it has to be amplified. The amplified signal is further processed to obtain intensity (total number) of radiations of all energies (gross counting) OR intensity as a function of energy (spectrometry).

Detectors are operated either in current mode or pulse mode[4]. In pulse mode operation, interaction of each individual quantum of radiation is recorded. Thus only in pulse mode the information on the energy of each radiation is obtained. In the current mode, average current, produced in the interaction of radiation, is measured. It depends on the product of interaction rate and the charge per interaction. Thus in this mode, the average event rate and charge produced per event are obtained. This mode of measurement is highly useful where the event rate is high and pulse mode operation becomes impractical.

There are a variety of radiation detectors. They can be classified based on the detector material used and/or type of measurement that can be made. e.g., gas filled detectors in which ionisation produced is measured. Some materials absorb energetic radiations and produce scintillation that can be measured. Yet another class of detectors are based on using

[1]It is true for gas based and semiconductor detectors. For scintillation detectors, the emitted light in detector gets converted to charge and multiplied in a photo multiplier tube.
[2]Interaction or stopping time is about a few nano seconds in gases and a few picoseconds in solids.
[3]Charge collection time in gas based detectors can be as long as a few milliseconds where as in semiconductors, it is a few nanoseconds.
[4]Mean square voltage (MSV) mode is used in some specialised cases and is not discussed here.

semiconductor materials like Ge and Si. Another class of gas filled detectors like BF_3, ^3He and ^4He are exclusively used for neutron detection. Principles of detectors with some applications are described in the following.

Gas Filled Detectors

Several of the oldest and most widely used radiation detectors are based on measuring the effects produced when ionising radiation passes through a gas filled chamber. While passing through the gas, radiation produces ionisation or excitations along its path. Left to themselves the positive ions and electrons that are produced may recombine. But if an electric field is applied, positive ions start migrating to the cathode and electrons towards anode. If the field strength, applied voltage per unit length, is high enough to prevent recombination during migration, then all the charge reaches the respective electrodes. Measurement of this charge gives an indication of the presence of ionising radiations. Quantitative information can easily be obtained from the measured charge which is related to the strength of the ionising radiation.

There are three types of detectors that work on the basis of measuring ionisation produced in a gas. These are ion chambers, proportional counters and Geiger Müller (GM) counters. They differ mainly in the strength of the electric field applied and the details would be discussed under each topic. Ion-pair[5] formation, multiplication and discharge processes that take place in a gas filled detector under the influence of applied electric field are described here. A typical gas filled detector consists of a metallic enclosure that is either sealed or fabricated in a such way to permit a continuous flow of the fill gas. The outer wall generally serves as a cathode where as a thin wire, a plate or a rod, that is centrally placed and insulated from the cathode, serves as an anode. Cross sectional view of a simple gas filled detector is given in Fig.7.1.

Pulse Height Variation with Applied Voltage

Gas filled detectors can be characterised by the effects created by different applied field strengths. Passage of radiation through matter like fill gas, produces ion-pairs which can be collected by applying a potential across the electrodes. The pulse size[6] produced by collection of charges depends on the field strength, the type of radiation and the energy of radiation. Variation of pulse size (height) as a function of applied voltage is given in Fig.7.2.

Ionisation and Recombination Region

At low field strength, there is a competition between recombination of ion pairs formed and collection of these ion pairs. Since all the ions are not collected, pulse height is

[5]Interaction of radiation with fill gas produces a positive ion and an electron. These two together are called an ion-pair. On an average 35 eV of energy is needed to produce an ion pair

[6]Ion pairs formed in the interaction of a single event when collected at the electrode form a pulse and the pulse size is related to the number of ion pairs, that are collected.

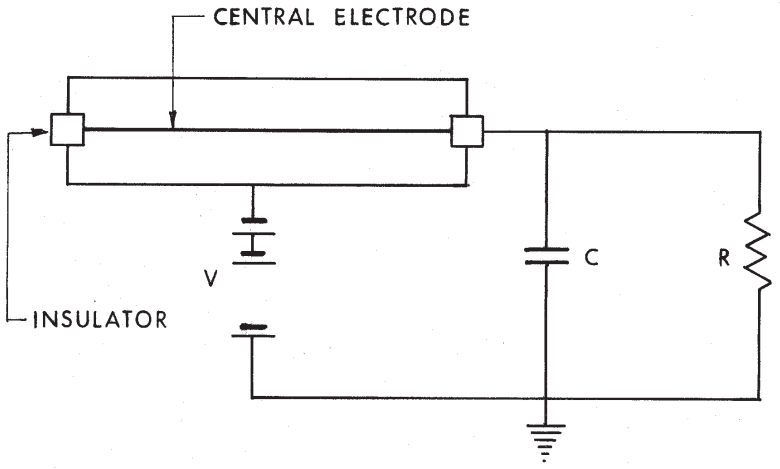

Fig. 7.1 Schematic diagram of a gas filled detector for pulse operation V : Applied voltage; C : Capacitor; R : Resistance.

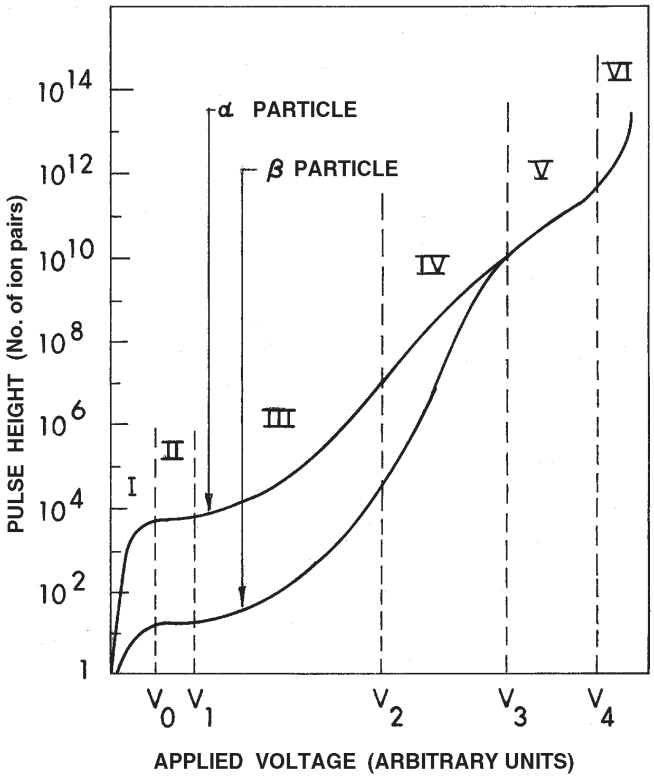

Fig. 7.2 Variation of pulse height with applied voltage in a gas filled detector [Nuclear and Radiochemistry, G. Friedlander, J.W. Kennedy, E.S. Macias and J.M. Miller, 3rd Ed., John Wiley (1981) p.247].

accordingly small and increases with increase in applied voltage. Thus a rise in pulse height is observed when the applied voltage is increased as shown in region I of Fig. 7.2.

Saturation Region

As the applied voltage is increased, more and more ion pairs reach the electrodes and at a certain field strength all the ion pairs produced are collected. A further increase in the field strength does not increase the pulse height as all the ion-pairs formed are collected, resulting in saturation (constant) pulse height, as shown in region II of Fig. 7.2. Pulse height in this region is directly proportional to the ionisation produced by incident radiation. Thus this region is very useful for radiation detection and to obtain information on the energy of radiation and intensity. Gas filled detectors operating in this region are called ion chambers.

An example is worked out here to calculate the charge produced by 1000 Bq of radioactive sample that emits 4 MeV α-radiation.

A 4 MeV α-particle produces about $\sim \frac{4 \times 10^6}{35} = 1.14 \times 10^5$ ion pairs/Bq

$\therefore$ Total number of ion pairs produced by 1000 Bq = 1.14×10^8

This corresponds to a charge of $1.14 \times 10^8 \times 1.6 \times 10^{-19}$ C = 1.8×10^{-11} C

This much charge is produced in 1 s and is equal to 1.8×10^{-11} A of current.

For β and γ radiations under similar conditions, the corresponding charges are different, as the linear energy transfer is different. The design of ion chambers may be tailored so that information on radiation energy and intensity can be obtained.

Proportional Region

The pulse height or ion current in a gas filled detector eventually increases if the applied voltage is increased further. Migrating primary ions[7] acquire higher kinetic energy under higher field strength. If this kinetic energy is more than the binding energy of electron of the fill gas, then further ionisation in the gas is possible. With increasing field strength, a large number of additionally produced ions, mainly electrons, are accelerated and ionisation in the detector gas is multiplied[8]. This multiplication is as high as 10^4 for each primary ion. Total number of ion pairs is still proportional to the primary ions at a given applied voltage. The gas filled detectors operating in this region are called 'proportional counters' (Region III).

---

[7]Ions produced due to the direct interaction of radiation are called primary ions. Ions produced in the multiplication are called secondary ions.

[8]Most of the pulse height in the proportional region is due to secondary ionisation known as gas multiplication.

If the voltage is fixed and multiplication factor (M) is 10^4, then the ion pairs for the 4 MeV α-particle discussed in the previous example would be 1.18×10^{12} and accordingly pulse height will be enhanced. In the case of β and γ radiation, the specific ionisation is lower and the range is higher. This results in lower pulse height. Hence discrimination between α, β and γ radiation is possible.

Limited Proportional Region

If voltage is further increased, though multiplication increases, proportionality is lost. This is because electrons reach anode faster, whereas positive ions being bulkier, they migrate slowly. The positive ions form a charge cloud in the detector which is slow to disperse as it drifts towards cathode and the field strength gets altered. This leads to reduction in the rate of multiplication. Thus increasing further voltage produces non-linear effects. These effects mark the onset of the region of limited proportional region (region IV, Fig. 7.2) where multiplication increases but linearity is lost. Therefore, this region is not useful for radiation measurement.

Geiger Müller Region

Further increase in voltage leads to a different situation (region V). The space charge created by positive ions completely dominates and determines the subsequent fate of the pulse. This positive space charge, while drifting towards the cathode forms a sheath of positive charge across the anode and reduces the field strength. The field strength is reduced below the value necessary for multiplication. The process is then self limiting. When the same total number of positive ions are produced regardless of the number of primary ions that are created by the interaction of radiation, the process of multiplication will be terminated. Then each output pulse from the detector is of same amplitude and no longer reflects any properties of the incident radiation. Typically pulse height is of the order of a few volts.

Geiger Discharge

While electrons migrate towards anode, they may collide with fill gas molecules resulting in excitation of molecules/atoms. These excited molecules / atoms deexcite by emitting photons in the visible and UV region. If one of these photons interacts by photoelectric absorption either on cathode surface or with constituents of the fill gas, a photo electron is produced, which can subsequently migrate towards anode and will trigger another avalanche. This effect is negligible in the proportional region (region III, M is 10 to 10^4) where as it becomes very significant in the GM region (region V, M $\simeq 10^8$ -10^{10}). Increase in applied voltage beyond GM region, would require a large build up of positive charge needed to terminate the multiplication process which is not possible as the source of enhanced multiplication is triggered by photoelectric process and not ionisation process. Therefore, pulse height begins to increase with voltage leading to discharge of the fill gas. If the detector is operated in this region of voltages, then its life time is reduced and has to be discarded.

Ionisation Chambers

Ion chambers are the simplest of all the gas filled detectors. All the charge produced by the interaction of radiation with the fill gas in the detector volume is collected through the application of electric field (region I, Fig. 7.2). Ion chambers can be operated both in pulse and current modes.

Argon, He, H_2, N_2, air and methane are a few fill gases that are used in ion chambers. Energy required for producing an effective ion pair, on an average, is about 30-35 eV although ionisation potentials range between 10-20 eV. There are other mechanisms like collision and excitation of molecules in which energy of incident radiation is spent and these processes are non-ionisation processes. The drift of positive ions and electrons under the applied voltage constitutes an electric current. For a given volume of detector and constant radiation source strength the rate of ion-pair formation and, therefore, ion current is constant. Measurement of this ion current is the basic principle of ionisation chambers. The chamber is made of a non-porous material, the electrodes are usually parallel plates and the fill gases have pressures of a few tenths of a bar upto a few bars. A typical cross sectional view of an ionisation chamber and corresponding current voltage characteristics are shown in Figs.7.3a and 7.3b respectively. The output signal registered by the electric circuit can be flow of current (current mode) or a charge or voltage pulse (pulse mode).

Some of the applications of ion chambers are calibration of radioactive sources, radioactivity dose monitors, radiation survey instruments and measurement of radioactive gases. Ionisation chambers are also useful in charged particle spectroscopy, e.g., measurement of α-particles and fission fragments. Due to significant differences in their mass and energy, pulse heights for these two are different. Individual pulses corresponding to α and fission fragments are measured, taking care that dimensions of the detector are larger than the ranges of these charged particles. These detectors are used to measure low α

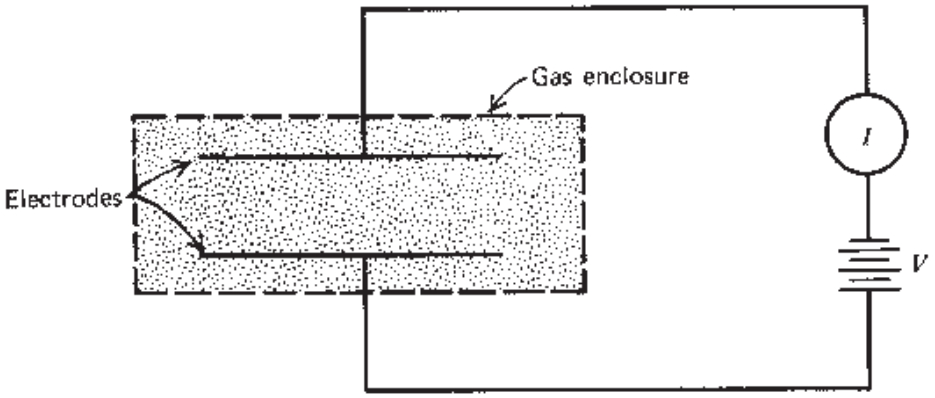

Fig. 7.3a Cross-sectional view of an ion chamber [G.F. Knoll, Radiation Detection and Management, John Wiley & Sons, New York (1979) p.136].

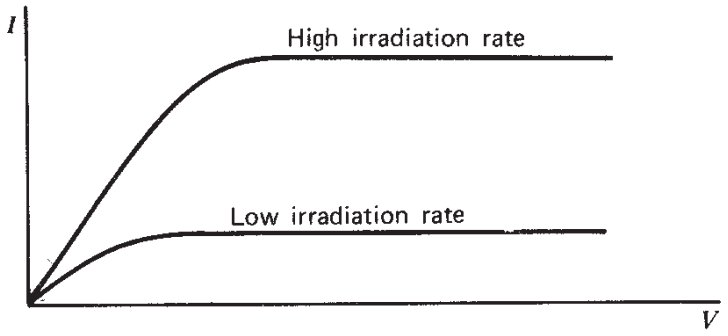

Fig. 7.3b The current-voltage characteristics in an ion chamber [G.F. Knoll, Radiation Detection and Management, John Wiley & Sons, New York (1979) p.136].

active samples in presence of large amount of β-radiation and low fission rates in presence of large α-particle fluxes taking advantage of pulse height discrimination.

Proportional Counters

Proportional gas ionisation detectors (proportional counters) operate at a higher voltage gradient than ion chambers (Region III, Fig. 7.2). Proportional counters are almost always operated in pulse mode. They rely on the gas multiplication to amplify the charge created by interaction of radiation with the fill gas. As discussed above, multiplication is a consequence of increasing the electric field within the gas to a sufficiently high value. There is a threshold value of the electric field for the onset of gas multiplication. In typical cases, it is about 10^6 V/m at atmospheric pressure. Therefore, the geometry of the detector becomes very important. A cylindrical tube with a thin anode wire is the general configuration of a proportional counter and a cross sectional view of such a proportional counter for measuring radiation that penetrates into the tube, is shown in Fig. 7.4. For less penetrating radiations like α, windowless flow proportional counter is used. In this counter, source is introduced normally with a leak tight rotating platform into the detector volume and the fill gas flows through the detector. Efficiency of this detector is nearly 50% for α-counting

The fill gas should not form anions and should not contain components with high electron attachment coefficient. Nobel gases like argon meet this requirement optimally. Gas mixtures like P-10 having 90% argon and 10% methane is most commonly used fill gas. Methane exchanges the excitation energy from excited atoms of argon and discharges the energy by non-radiative processes. Thus it inhibits the deexcitation of excited argon atoms by emission of UV light which may create an electron by photoelectric absorption and that electron under applied voltage may trigger an avalanche.

Proportional counters have good efficiency for α, β and other charged particles. For γ and X-ray measurement, detection efficiency is low. High Z gases are used as fill gases. e.g.,

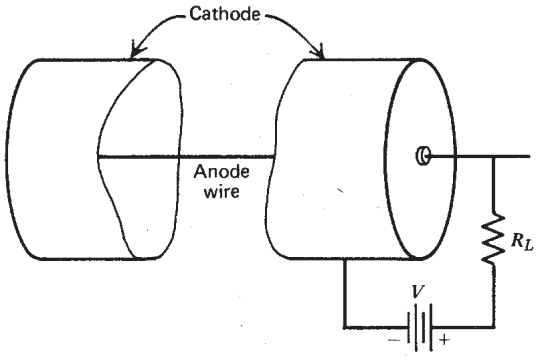

Fig. 7.4 Cross-sectional view of a proportional counter [G.F. Knoll, Radiation Detection and Management, John Wiley & Sons, New York (1979) p.163].

argon is replaced by krypton or xenon. Also, often fill gas is pressurised. The spectroscopy of low energy X-rays is one of the most important applications of proportional counters. The photo electrons formed in the X-ray interaction are fully absorbed by the fill gas to produce primary ionisation.

Since these counters operate with a multiplication factor around 10^4 and the pulse height is proportional to the number of primary ions formed, these detectors are useful for measurement of energy in addition to their intensity of the radiations. Since pulse heights for α and β are significantly different (See Fig.7.2), both α and β can effectively be counted using proportional counters. Thermal neutrons are measured using fill gases like BF_3 and ^3He. Parallel plate avalanche counters, position sensitive detectors etc. are different types of proportional counters with special applications.

Geiger Müller (G.M.) Counters

G.M. counter is one of the oldest radiation detectors. Due to its simplicity, low cost and ease of operation, it still continues to be used for radiation measurements in various areas of research. Gas multiplication is very high compared to that in the proportional counters. It is of the order of 10^8-10^{10} and, therefore, large pulses are produced in G.M. counters. In G.M. counters, a situation is created in which an avalanche can trigger a second avalanche at a different position in the tube, and a self propagating chain reaction results. This reaches a self limiting point as discussed above and, therefore, information on the energy of radiation is lost.

Fill gases for G.M. counters are helium or argon. G.M. counters are sealed tubes with thin windows and a cross-sectional view of a GM tube is shown in Fig. 7.5. The positive ions slowly drift away from the anode wire and ultimately arrive at the cathode, the inner wall of the counter. They are neutralised by combining with electrons from the cathode surface. In this process, an amount of energy equal to the ionisation energy of the gas minus the energy required to eject the electron from the cathode surface is liberated. If this liberated energy

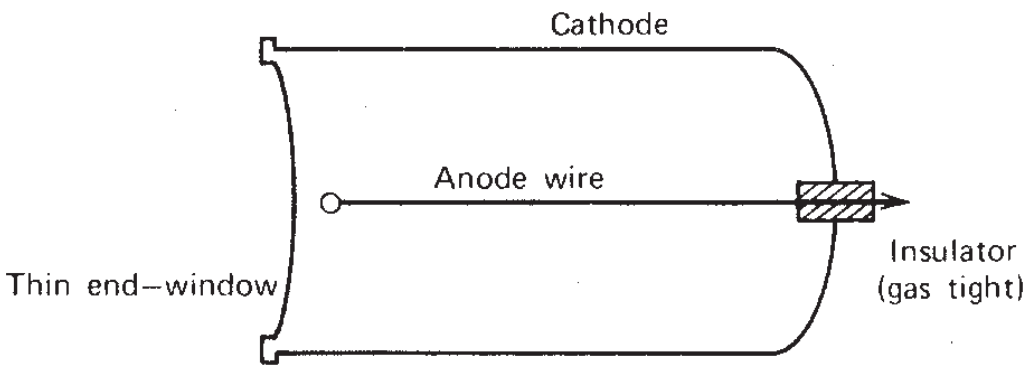

Fig. 7.5 A cross-section of a typical end window Geiger tube [G.F. Knoll, Radiation Detection and Management, John Wiley & Sons, New York (1979) p.209].

also exceeds the effective energy to produce an electron at cathode surface (cathode work function), it is energetically possible that another electron can be ejected out. This electron will then drift towards the anode and trigger another avalanche, leading to a second full Geiger discharge. The entire cycle will now be repeated. Under these circumstances the G-M counter, once initially triggered would produce a continuous output of pulses. This multiple pulsing can be prevented either by external quenching or internal quenching.

For external quenching, operating voltage is lowered below the threshold electronically for the period till all the ions are collected. Internal quenching is achieved by adding a suitable gas having lower ionisation potential and a more complex molecular structure than the fill gas. Multiple pulsing is prevented through the mechanism of charge transfer collisions. The primary ions have a tendency to transfer the positive charge to the quench gas molecules. When they are neutralised at the cathode, the excess energy may go into dissociation of the more complex molecules. Examples of quench gases are ethyl alcohol and ethyl formate with a typical concentration of 5-10%.

Organic quenched tubes may typically have a limit of about 10^9 counts and thus limiting its life time. If halogens (chlorine or bromine) are used as quenchers the tube can have infinite life time. Halogen molecules undergo atomic dissociation subsequent to exchanging the energy from the excited atoms of helium or argon. They dissipate the energy non-radiatively and recombine to form halogen molecules.

The building up of the positive charge in space ensures that a considerable period of time must pass before a second Geiger discharge is generated in the G.M. tube. During this period, if another ionising event occurs, a second pulse will not be observed because gas multiplication is prevented (self-limiting situation). During this period, the G.M. tube is 'dead' and information about any radiation interaction that takes place in the tube will be lost. In typical G.M. tubes, the dead time is of the order of 50-100 μs.

G.M. counters are useful for gross counting particularly β-γ counting. G.M. tubes are used in the survey meters. Once the radiation enters the tube, efficiency is 100%. A special window has to be arranged for α-counting. In the case of γ-ray counting, efficiency depends on the probability of interaction of γ-rays with fill gas, Normally efficiency for γ-counting is low.

Scintillation Detectors

Darkening of a photographic plate and scintillation of fluorescent materials are the oldest techniques for radiation measurement. Any material that luminesces in a suitable wavelength region, when ionising radiation passes through it, can serve as a scintillator. The emission could be due to fluorescence or phosphorescence. The intensity of emitted light is a measure of incident radiation energy. Interaction of radiation with the scintillator results in producing photons in the visible region (scintillations). These photons undergo photo electric effect and eject electrons when they strike the cathode of a photomultiplier tube (PMT) that is mounted with the scintillator. These electrons are multiplied with a series of dynodes in PMT and collected at the anode to produce a signal representative of the primary radiation.

The ideal scintillator should possess the following properties:(i) It should convert the radiation energy into detectable light with high efficiency, (ii) conversion should be proportional to deposited energy, (iii) scintillator material should be transparent to the emitted light, (iv) the decay time of the induced luminescence should be short ($\sim 10^{-9}$ s) for fast signal generation, (v) material should be of good optical quality to make detectors in large size and desired shape and (vi) its refractive index should be near to glass (~1.5) to permit efficient coupling with the PMT. Inorganic scintillators like thallium activated NaI and CsI, and Bismuth Germanate (BGO), organic scintillators like anthracene and stilbene, liquid mixtures and plastics are often used as materials for scintillation detectors. No material meets all the properties listed above. Inorganic materials often are used for γ-ray spectroscopy and organics are used for β-spectroscopy and fast neutron detection.

Organic Scintillators

The fluorescence process in organics can be observed from a given molecular species independent of its physical state: as a solid, liquid, vapour or even as a part of a multi component solution. Absorption of radiation energy results in excitation of molecules of scintillator from ground state to higher energy states (Fig.7.6). Scintillation light is emitted in the transitions from excited states S_{10} to one of the vibrational states of the ground state (S_{00} to S_{03}) with a decay time of around 10^{-9} s. Deexcitation through a triplet state would be very slow (phosphorescence) and is not useful for radiation measurement. Anthracene and stilbene are two good solid organic scintillators. Anthracene has a higher scintillation efficiency where as stilbene is useful for pulse discrimination to distinguish between charged particles and electrons.

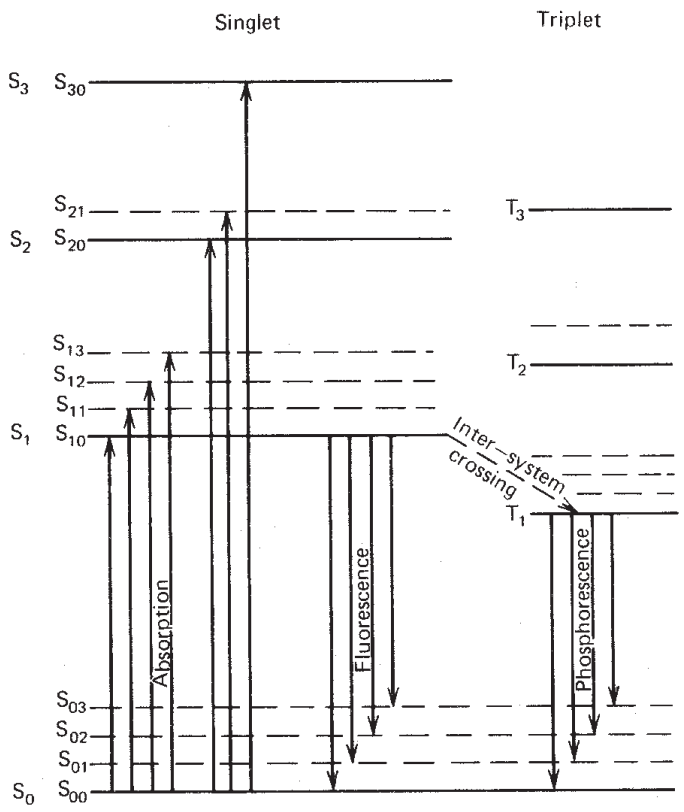

Fig. 7.6 Energy levels of an organic molecule with p-electron structure [G.F. Knoll, Radiation Detection and Management, John Wiley & Sons, New York (1979) p.217].

Organic liquid mixtures are versatile scintillator materials for radiation measurement. Scintillation cocktail is composed of a solvent like dioxan or toluene, a scintillator like PPO (2,5 diphenyl oxazole) and a wavelength shifter like POPOP (1,4-bis-2- (5-phenyl oxazolyl)-benzene). The solvent is the main stopping medium for the radiation and must be chosen to give efficient energy transfer to the scintillating solute. Scintillation light corresponds to the UV region. Photocathodes of most of the PMTs are not compatible with UV light. A wavelength shifter like POPOP is therefore used in the cocktail. It has intermediate energy levels. If the deexcitation is via these levels then the wavelength is shifted from UV to visible region. While dealing with aqueous solutions, like HNO_3 there is a possibility that quenching of scintillations (chemical quenching) can take place. A fourth component like TOPO is added to complex such quenchers and thus TOPO acts as an anti quenching agent. Naphthalene is added to increase the shelf life of the cocktail mixture. Now-a-days ready made liquid scintillation cocktails are commercially available.

Liquid scintillators are useful for α, β counting and also for spectroscopy. Large volume samples can also be measured. Nearly 100% efficiency is obtained using liquid

scintillations. Taking special precautions, low energy β-emitters like ^{3}H and ^{14}C are measured.

Plastics are another class of scintillators that are commercially available. Scintillators like PPO, wavelength shifter like POPOP and a monomer such as styrene are mixed and polymerised to produce plastic scintillators. Plastic scintillators have fast timing response and are very useful in nuclear spectroscopy. Large plastic scintillators are used as anti coincidence shields in low level activity measurements.

Inorganic Scintillators

Sodium iodide activated with 0.1 to 0.2% of Tl is by far the most widely used inorganic scintillator. CsI(Tl), CsI(Na) and bismuth germinate (BGO) are other inorganic scintillators. The scintillation mechanism depends on the energy states determined by the crystal lattice of the material. The valence band (representing electrons bound to lattice sites) and conduction band (representing free electrons that migrate throughout the crystal) of an activated crystalline scintillator are shown in Fig.7.7. The band gap is of the order of 5-6 eV. A charged particle[9] passing through the detection medium produces a large number of electron-hole pairs by elevation of electrons from valence band to conduction band. Deexcitation leads to emission of photons in the UV region as band gap is large. To shift the wavelength of emitted photons to visible region, crystals are doped with activator impurities like Tl which form the intermediate bands (Fig.7.7). Electrons and holes formed move freely in the crystal. The hole drifts to the location of an activator site and ionises it. Electron moves freely until it encounters an ionised activator, combines with it, and neutralised activator deexcites by emitting light in the visible region. Typical half-lives of such excited states are about 10^{-7} s. Alternately an electron and hole, known as exciton, also move freely until an activator atom is seen. An excited activator is formed which can undergo deexcitation by emission of light. Competing modes like phosphorescence are not useful for measurement.

Though the band gap is 5-6 eV, on an average about 20 eV is required to produce a photon. Taking into account the efficiency of light collection and photoelectric absorption of the cathode of PMT, about 100-200 eV of energy is required to produce an electron at photocathode, limiting resolution of the detector[10] to 7-10% at 662 keV.

The high density (3.7 g cm^{-3}) of NaI and high Z of iodine make NaI(Tl) a very popular γ-ray detector. A 3" x 3" NaI(Tl) crystal is commonly used as a detector. Both flat and well type detectors are in use. A typical γ-ray spectrum obtained using a NaI(Tl) is discussed later in this Chapter, along with the γ-ray spectrum obtained using a Ge detector.

---

[9]In the case of gamma ray detection, electrons produced in the gamma ray interaction act as the representatives of the gamma rays.

[10]Resolution of a detector is the capability of producing separate signals corresponding to two or more nearby radiation energies.

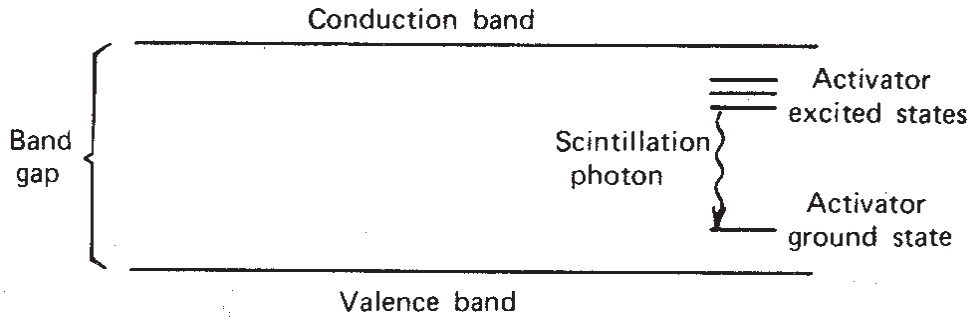

Fig. 7.7 Energy band structure of an activated crystalline scintillator [G.F. Knoll, Radiation Detection and Management, John Wiley & Sons, New York (1979) p.228].

Semiconductor Detectors

A semiconductor detector can be compared to an ionisation chamber. Use of denser material has advantages for stopping higher energy particles and also for the detection of radiation of low specific ionisation. Interaction of radiation with semiconductors results in lifting electron from valence band to conduction band, leaving a hole in the valence band. Electron moves through the crystal. Hole also moves by successive electron exchanges between neighbouring sites. Electron and hole together are charge carriers and signatures of interaction of radiation. Energy required to produce a charge carrier pair is larger than the band gap as some of the energy is spent in other modes like lattice vibration. This situation is analogous to ionisation in the gas filled detectors. Silicon and Germanium are the two best semiconductors that are being used as radiation detector material. The band gap for Ge and Si are 0.67 eV[11] and 1.12 eV respectively and the energy required to produce an effective charge carrier pair is 2.96 eV and 3.76 eV respectively for Ge and Si. Therefore, a large number of charge carriers are produced in these detectors compared to NaI(Tl) detectors and this reflects in good energy resolution.

In a pure semiconductor, electrons and holes would be created by thermal excitation also and ideally the number of electrons should be equal to the number of holes. Such a material is called intrinsic semiconductor. In practice, it is difficult to get an intrinsic material. Small impurities (either inherent or doped) will cause imbalance in the number of charge carriers which dominate the electrical properties of semiconductors.e.g., intrinsic hole or electron densities are 1.5 x 10^{10} cm^{-3} for Si and 2.4 x 10^{13} $cm\text{-}^{3}$ for Ge at room temperature. If a donor impurity like P is present at a concentration of 2 ppm, i.e. 10^{17} atoms/cm^3, the electron density would be 10^{17} cm^{-3} and the hole density would be about 2 x 10^3 cm^{-3} as the product of e^- and h^+ density should be same for intrinsic and doped materials. In this case, electrons are majority carriers and such materials are called n-type

[11]The band gap for Ge is low and to reduce thermal noise, Ge detectors have to be operated at low temperatures by cooling to liquid nitrogen temperature.

semiconductors. Similarly materials doped with group III element would be p-type with holes as majority carriers. Heavily doped materials are called n^+ type and p^+ type materials respectively. They have very high conductivity and are useful for electrical contacts with semiconductor devices.

When a p-type material is brought in contact with an n-type material (taking care to reduce leakage current), electrons from n-type diffuse across the junction and holes from p-type also diffuse across junction resulting in the formation of a depletion region. If a reverse bias is applied across the junction (+ve on n-type and -ve on p-type side), providing a field of the order of 10^3 Vcm^{-1}, the depth of the depletion region is increased. This results in extremely low leakage current and useful for radiation detection. This is the active volume of a detector. Electron-hole pairs produced in the depletion region due to interaction of radiation will be swept out of the depletion region by the applied electric field and their motion constitutes the basic signal for radiation measurement.

Silicon surface barrier detectors, Ge(Li), Si(Li) and HPGe are a few important types of semiconductor detectors. All these detectors are useful for spectroscopic measurements.

Surface Barrier Detectors and α-spectroscopy

An n-type material is used in a surface barrier detector. Its surface is etched and a thin gold layer is deposited on it by evaporation for electrical contact. Gold evaporation is carried out such that an oxide layer between gold and silicon is formed which acts as a surface barrier. This behaves like a true junction. It may be because a thin oxidised film under the metal surface acts as a p-type layer. By applying high voltage, depletion depths upto 2 to 3 mm have been achieved. Silicon surface barrier detectors are very useful for charged particle spectroscopy.

A typical α-spectrum obtained for ^{241}Am using silicon surface barrier detector is shown in Fig. 7.8. The intrinsic shape of an α-peak is expected to be a gaussian, but always a left tailing is observed. Though the α-source[12] is kept in a vacuum chamber connected to α-spectrometer, degradation in α-energy is prevalent. The α-particles coming out of the source undergo degradation in the source, at the dead layer of the detector and in the travel path as absolute vacuum is not achievable. Resolution is calculated considering only right part of the peak from the centroid. Typical values of resolution are around 15-20 keV at 5.486 MeV of ^{241}Am. By locating peak centroid and using a calibration plot, α-energy is calculated. Area under the α-peak is proportional to the source strength. By using the pre-determined detection efficiency, abundance and peak area, α-source strength is determined.

---

[12] α-sources are prepared by special methods like electrodeposition and electrospraying. Monomolecular layers are ideal, though a definite thickness sources only can be prepared. Electrodeposition from organic medium under high tension field is one of the proven techniques for α-source preparation.

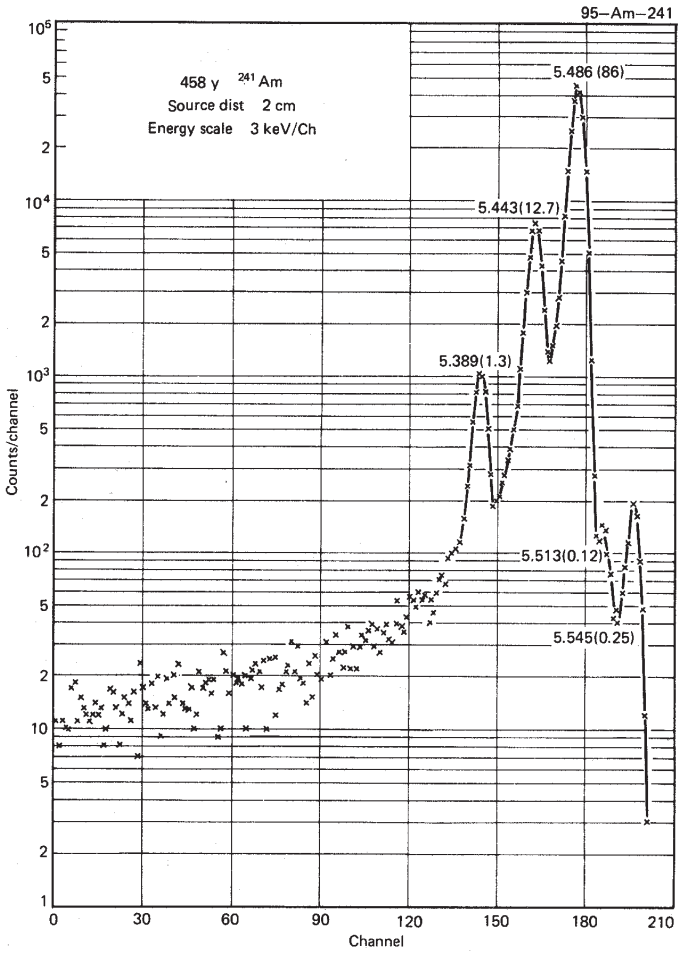

Fig. 7.8 Upper portion of the ^{241}Am alpha spectrum as recorded by a high-resolution surface barrier detector [R.N. Chanda and R.A. Deal, 1N-126, (1970)].

Germanium Detectors and γ-ray Spectroscopy

Germanium detectors are useful for γ-ray spectroscopic measurements. Unlike in α-measurements, thick detectors are required for γ-ray measurements. Therefore, large volume Ge crystals are used as detectors. Two types of Ge detectors are available: (1) Li drifted Ge known as Ge(Li) and (2) High Purity Germanium known as HPGe detectors. In Ge(Li) net impurity concentration is reduced to create a compensated material by doping with equal number of atoms of opposite type. The process of lithium ion drifting is used to compensate the material after the crystal is grown. Compensated materials with thickness of upto 2 cm have been achieved. Ge(Li) detector has always to be maintained at liquid nitrogen temperature.

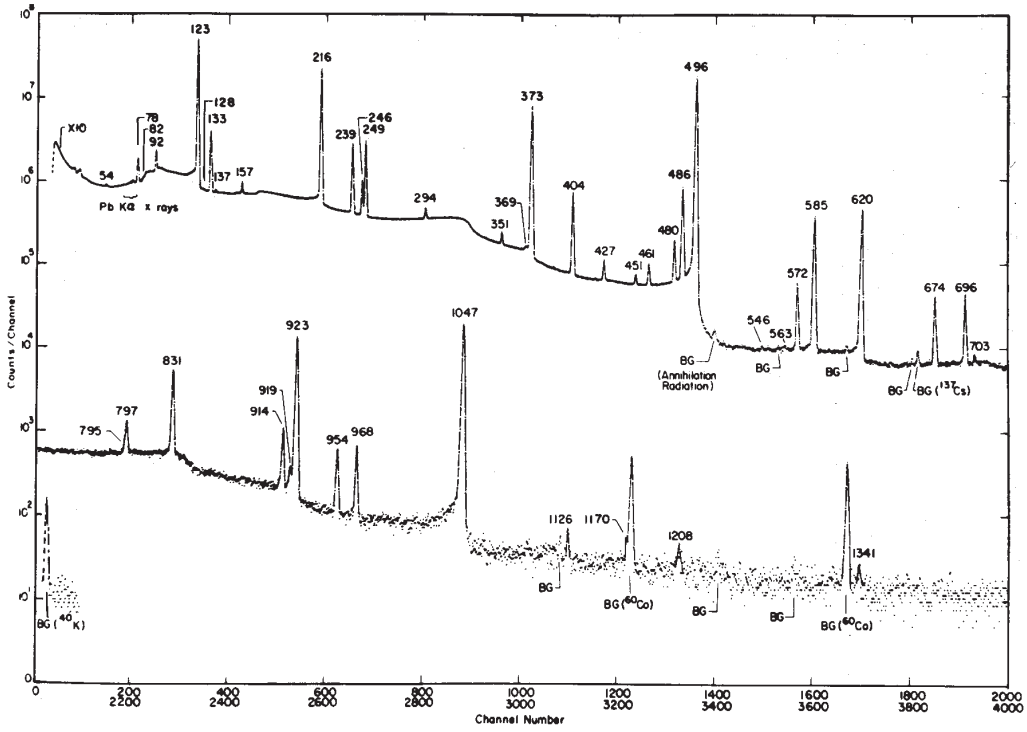

*Fig. 7.9 Gamma-ray spectrum of ^{131}Ba obtained with 65 cm^3 Ge(Li) detector. Peaks are labelled with the γ-ray energies in keV; those marked BG are background lines. The upper (lower-energy) curve is displaced upward by a factor 10 [R.J. Gehrke et al. Phys. Rev., **C14** (1976) 1896].*

High purity Germanium detectors were developed in mid 1970's with impurity levels around 10^{10} atoms/cm^3. Starting with bulk germanium, using zone refining technique, the impurity levels are progressively reduced by locally heating the material and slowly passing the melted zone from one end to the other end. Impurities are transferred to molten zone and swept away from the sample. Impurity levels are brought down by repetition of this process. HPGe has to be maintained at liquid nitrogen temperature, before applying high voltage. Otherwise detector can be stored at room temperature.

Both HPGe and Ge(Li) of same size have nearly identical performance characteristics vis-a-vis energy resolution and detection efficiency. A typical γ-ray spectrum of ^{131}Ba is shown in Fig. 7.9. The high resolution of Ge(Li) results in well resolved γ-ray spectrum. Centroids correspond to γ-ray energy and peak area under each γ-ray peak is proportional to the corresponding γ-ray intensity. Detection efficiency varies approximately as photoelectric cross-section (see Fig. 6.8). To compare the capabilities of Ge(Li) and NaI(Tl),

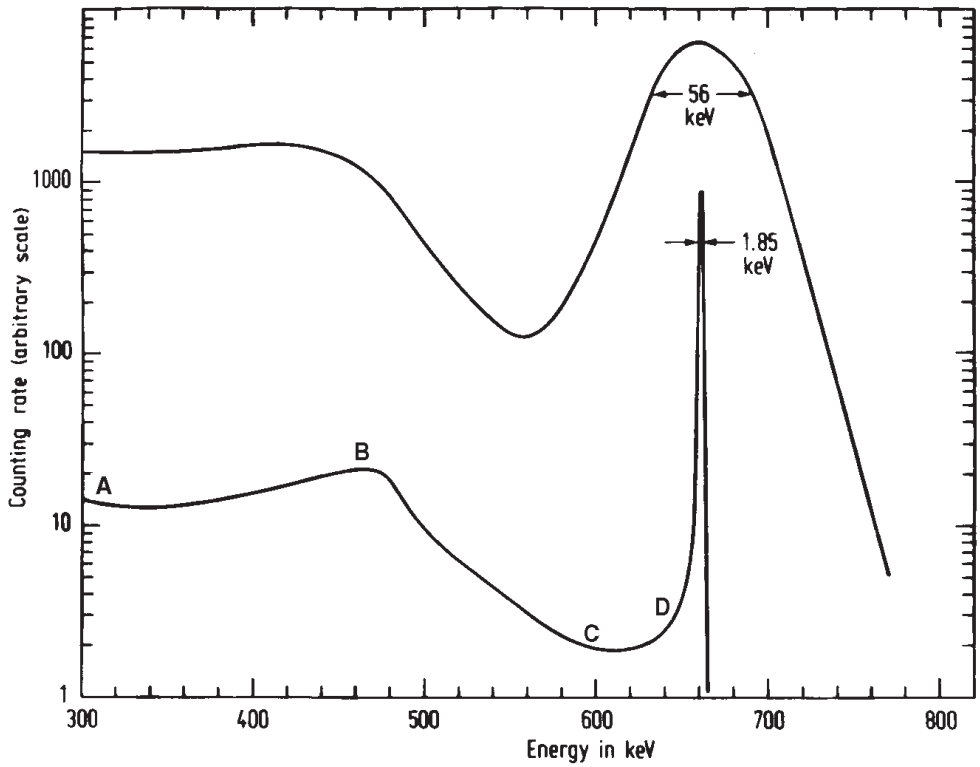

Fig. 7.10 Gamma-ray spectrum of ^{137}Cs taken with a 7.5 cm x 7.5 cm NaI(Tl) scintillation detector (top curve) and with a 50 cm^3 Ge(LI) semiconductor detector (bottom curve). The FWHM is shown for each photopeak [Nuclear and Radiochemistry, G. Friedlander, J.W. Kennedy, E.S. Macias and J.M. Miller, 3rd Ed., John Wiley (1981) p.259].

a γ-ray spectrum of ^{137}Cs is shown in Fig. 7.10. Upper spectrum is obtained using NaI(Tl) detector and the lower one is obtained with a Ge(Li). From the figure it is clear that the resolution of Ge(Li) is superior to NaI(Tl). On the other hand, efficiency of NaI(Tl) is more than Ge(Li). Lower left side upto about 480 keV region (AB) is due to compton scattering and BC region represents compton edge. The region CD represents the compton multiscattering. Peak to compton ratio (ratio of the response of peak maximum to peak minimum at the left side) is a measure of quality of the detectors. Peak to compton ratios of about 60 are achieved for HPGe. Typical resolutions for Ge(Li) and HPGe are about 1.5 to 1.8 keV at 1333 keV.

Si(Li) Detectors and X-ray Spectroscopy

Large depletion Si(Li) detectors are obtained by lithium drifting into Si crystals. The process is similar to the one described for Ge(Li). Si(Li) detectors are very useful for X-ray

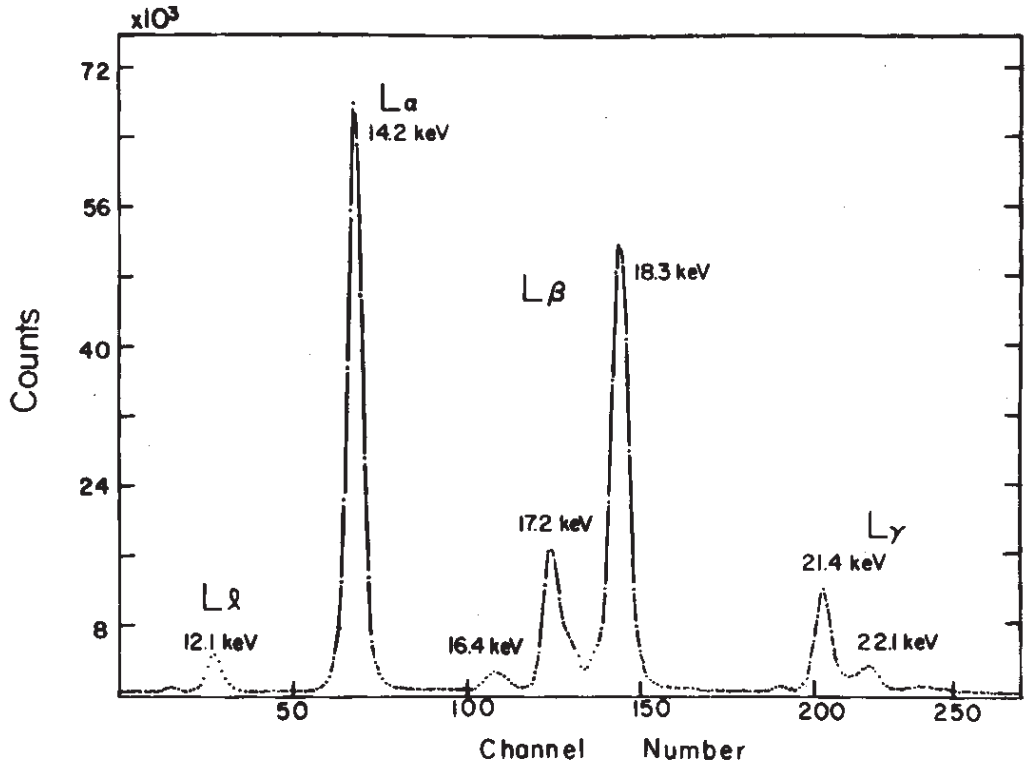

*Fig. 7.11 Spectrum of plutonium L-X rays taken with a Si(Li) detector of 4 mm diameter and 3 mm sensitive depth [E.S. Macias and M.R. Zalulsky, Phys. Rev., **A9** (1974) 2356].*

measurements. A typical X-ray spectrum of plutonium using Si(Li) detector is shown in Fig. 7.11. The resolution of Si(Li) detectors is excellent, e.g., 150 eV at 15 keV.

Sample preparation for γ-ray spectroscopy and X-ray spectroscopy are not that critical as compared for α-spectroscopy. However, thin samples are needed particularly in the case of low energy X-ray spectroscopy.

Miscellaneous Detectors

Photographic Films

In 1896, Becquerel used photographic films and blackening or fogging after chemical development was used to measure the intensity of radiation in the experiments that led to the discovery of the phenomenon of radioactivity. Film badges are used to measure the cumulative dose received by the radiation workers. In the autoradiograph techniques, films are used to measure the distribution of the tracer.

Ordinary photographic films consist of an emulsion of silver halide grains suspended in a gelatine matrix and supported with a glass or cellulose acetate film. Ionising radiation sensitises the silver halide grains which remain intact for indefinite period until they are developed. The extent of darkening of emulsion is due to the cumulative effects of individual interactions and, therefore, are used for dose measurements. They are also used in the radiographic measurements using photographic emulsions.

Thermoluminescence Dosimeters (TLD)

Some of the inorganic crystals when exposed to radiation produce electron-hole pairs which are trapped by impurities present in the crystals. If the crystals are heated, they emit light which has a bearing on the energy and intensity of radiation that interacted with the crystals. By measuring the light, the total radiation exposure can be estimated. LiF and $CaSO_4$ doped with Mn impurity are a few examples of thermoluminescent materials. Small capsules containing about 50-100 mg of these crystals are used in TLDs which are worn by the radiation workers while working in the radiation environment. Cumulative exposure dose is determined by measuring the emitted light when they are electrically heated.

Solid State Nuclear Track Detectors

Ionising radiations, having high linear energy transfer (LET), while passing through a dielectric material create a trail of damaged molecules along their path. In some materials, the tracks are made visible upon etching in a strong acidic or basic solution. The damaged molecular tracks are etched faster than the bulk and look like pits on the surface. These tracks are counted using a microscope. The commonly used track-etch materials are quartz, mica, silica glass, flint glass, polyethylene terephthalate, lexan, makrofol, cellulose triacetate and cellulose nitrate.

Cerenkov Detectors

When a fast moving charged particle passes through an optically transparent medium with a refractive index (μ) greater than 1, then light is emitted. This light is called Cerenkov light. The condition for emitting Cerenkov radiation is $\beta\mu > 1$ where β is the ratio of the particle velocity in the medium to the speed of light in vacuum. For example, electrons of a few MeV energy in water emit Cerenkov light and it is measured using a PMT. Cerenkov detectors have some similarities with scintillation detectors. Some properties are quite different. The light is emitted over a very short period, of the order of picoseconds in solids or liquids. The timing properties of the detectors are limited by PMTs. Choice of Cerenkov medium is made from materials with good optical transmission properties and no scintillation component, with a value of μ between 1.2 and 1.33, e.g., lucite and glasses. Light output in best of the detectors is about 103 times inferior to any good scintillator. Cerenkov light is produced in the direction of the particle in a narrow cone. These detectors are used in high energy particle physics experiments.

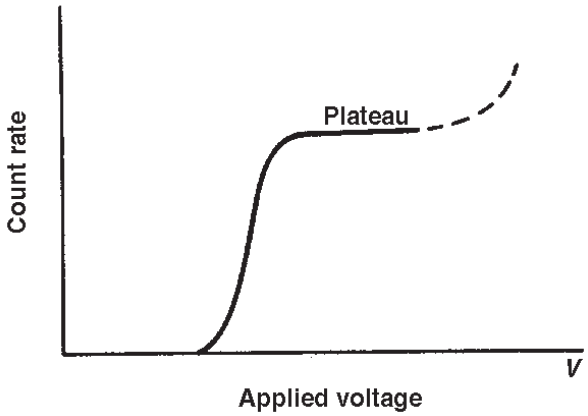

Fig. 7.12 Plateau of a proportional counter.

Important Features of Detectors

Some of the important features of detectors such as counting curves, plateaus, energy resolution, dead time and detector efficiency are described below:

Counting Curves and Plateaus

When detectors are operated in pulse mode, the pulses from the detector are fed to a counting device with a fixed pulse height discrimination level (H_d). The signal pulses exceeding H_d only get registered by the counting circuit. This is generally used to cut off the noise or background. The gain of the counting system is adjusted to find the optimum value for carrying out the desired counting. In some types of radiation detectors such as Geiger-Muller tubes and scintillation counters, the gain can conveniently be varied by changing the applied voltage to the detector. The gain may not change linearly with voltage. The operating voltage is a region in which count rate due to a radiation source of fixed strength remains constant for a given settings of the equipment and it is called plateau of the detector. A typical plateau for a proportional counter is shown in Fig. 7.12.

Energy Resolution

The ability of a detector in distinguishing two radiations of nearby energies is called the resolution of the detector. The energy resolution of a detector can be determined from the response function (differential pulse height distribution) of the detector which is gaussian. The energy resolution is defined as the full width at half maximum (FWHM) of the distribution of a mono energetic radiation.

The resolution (**R**) for energy E is given by

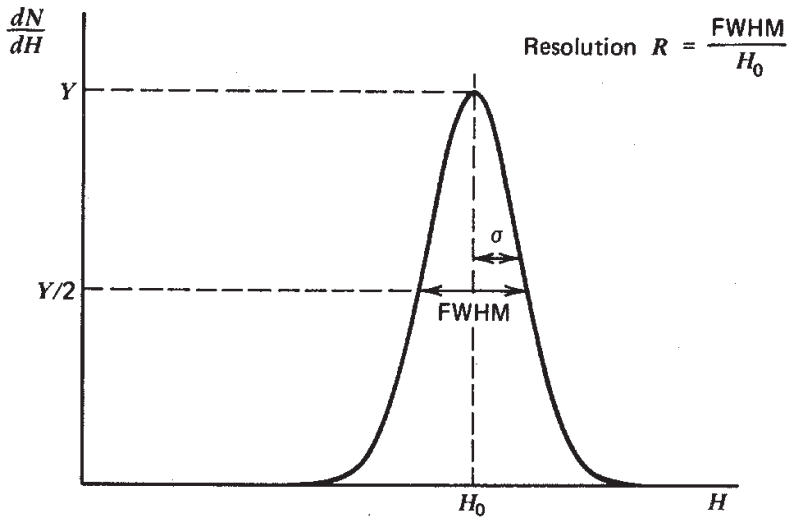

Fig. 7.13 Definition of detector resolution [G.F. Knoll, Radiation Detection and Management, John Wiley & Sons, New York (1979) p.115].

$$\mathbf{R} = \frac{\text{FWHM}}{\text{E}} = 2.35\frac{\sigma}{\text{E}} \qquad (7.1)$$

where, σ^2 is the variance of the gaussian distribution. The FWHM is shown in Fig. 7.13.

Ideally the response of a detector for γ-rays is a line spectrum. The observed response is a Gaussian distribution with a width that reflects resolution of the detector (see Fig. 7.13). This width is the result of fluctuations observed in the response for a monoenergetic γ-rays. The sources of fluctuations are

(i) Drift in the operating characteristics of the detector during the course of the measurement,

(ii) Random noise within the detector and instrumentation system and

(iii) Statistical fluctuations arising from the discrete nature of production of the measured signal of the detector.

An estimate of the statistical fluctuations can be made assuming that the formation of charge carriers is a Poisson process. Number of charge carriers (N) produced for a given energy (E) is given as

$$\text{N} = \frac{\text{E}}{\text{W}} \qquad (7.2)$$

where, W is the energy required to produce one ion pair. The standard deviation (σ) of the number of ion pairs (N) expected from Poisson distribution would be

$$\sigma = \sqrt{N} = \sqrt{\frac{E}{W}} \tag{7.3}$$

From eqns. 7.1 and 7.3, FWHM is given by

$$FWHM = 2.35\ \sigma = 2.35.\ \sqrt{N}\ \alpha\ \sqrt{E} \tag{7.4}$$

Thus R, due to statistical fluctuation of production of charge carriers is given by

$$R = \frac{FWHM}{E} = 2.35\frac{\sigma}{E} \tag{7.5}$$

From eqns. 7.4 and 7.5,

$$R\ \alpha\ \frac{1}{\sqrt{E}}$$

The typical values for the % resolution of semiconductor diode detectors is in the range of 0.1% to 0.3% and of scintillation detectors is about 7-10%. Smaller the value of the energy resolution, better is the detector in distinguishing two radiations of close by energy.

Fano Factor

Careful measurements of the energy resolution of some types of radiation detectors have shown that the achievable values for R can be lower by a factor of 3 or 4 than that predicted by the statistical fluctuations. Hence the processes that give rise to the formation of each individual charge carrier are not independent and therefore the total number of charge carriers cannot be described by simple Poisson statistics. The correction factor is defined as the Fano Factor (F):

$$\text{Fano Factor (F)} = \frac{\text{Observed variance}}{\text{Poisson predicted variance}}$$

The observed energy resolution (R) is represented as:

$$R = \frac{FWHM}{E} = 2.35\frac{\sqrt{FN}}{E}$$

$$= 2.35\sqrt{\frac{F}{N}} \tag{7.6}$$

The Fano Factor (F) has different values for different detectors. For semiconductor detectors it is ~0.1 and for proportional counters, it is about ~1.0. Smaller the value of F, smaller is R and hence better is the resolution.

Detection Efficiency

If all the radiation quanta incident on the detector deposit their energy in the detector, then the intrinsic detection efficiency will be 100%. The intrinsic efficiency (ε_{int}) of a detector is defined as

$$\varepsilon_{int} = \frac{\text{Number of pulses recorded}}{\text{Number of radiations incident on the detector}}$$

In practice, it is important to know the absolute efficiency (ε_{abs}) of the detector rather than its intrinsic efficiency.

$$\varepsilon_{abs} = \frac{\text{Number of pulses recorded}}{\text{Number of radiations emitted by the source}}$$

The absolute efficiency (E_{abs}) of a detector depends on the detector material, radiation energy, physical thickness of the detector in the direction of the incident radiation and counting geometry. However, it is difficult to obtain 100% efficiency due to the constraints of limited detector size, range of radiation, geometry between the source and detector, self absorption etc.

In the γ-ray spectroscopy, efficiency of the detector varies as a function of energy. Gamma spectrum of a source of known strength is acquired in a fixed source to detector geometry. The number of full energy events corresponding to the γ-rays are obtained by integrating the total peak area (PA) under a gamma ray peak (E_γ). Efficiency is calculated as the ratio of PA to the intensity (emission rate) of the gamma ray and is plotted as function of energy. The total efficiency depends on the distance between the source and sample in addition to the intrinsic efficiency of the detector.

Detector Dead Time

Radiation produces a pulse in the detector consequent to its interaction. While this pulse is being processed, detector is not available (dead) for processing the next pulse that might be generated during this interval. Because of the random nature of radioactive decay, there is always some probability that a true event will be lost because it occurs too quickly following a preceding event. The minimum time of separation required to record two successive events as two separate pulses is called the dead time (T) of the counting system. The dead time losses increase with the increase in count rate.

In the case of non-paralysable detectors, the dead time period is a fixed duration and any pulse appearing in this period is lost. While in the case of paralysable detectors, if another pulse occurs during the dead period, the latter is extended by the same duration of dead time. The dead time behaviour of a detector, however, is intermediate between these two extremes. Let the true and observed count rates be n and m respectively. In the non-paralysable case the detector is dead for the fraction mT and the rate at which events are lost is equal to nmT. This loss can also be equated to n-m. Thus

$$n - m = nmT$$

or $$n = \frac{m}{1 - mT} \qquad (7.7)$$

Similarly it can be shown that for paralysable case

$$m = ne^{-nT} \qquad (7.8)$$

The common methods for measuring the dead time of a counting system are (i) two source method and (ii) decaying source method.

In the two source method, the two sources of true count rate plus background rate n_1 and n_2 are counted in the detector independently as well as together in a fixed source to detector geometry. Let the true count rate plus background rate of combined sources be n_{12} and the background rate be n_b. n_1, n_2 and n_{12} are related as

$$n_{12} - n_b = (n_1 - n_b) + (n_2 - n_b)$$

i.e. $$n_{12} + n_b = n_1 + n_2 \qquad (7.9)$$

In the non-paralysable case the true count rate can be represented in terms of respective observed count rates by combining eqns. 7.7 and 7.9.

$$\frac{m_{12}}{1 - m_{12}T} + \frac{m_b}{1 - m_bT} = \frac{m_1}{1 - m_1T} + \frac{m_2}{1 - m_2T} \qquad (7.10)$$

This equation is solved for T as

$$T = \frac{X(1 - \sqrt{1 - Z})}{Y} \qquad (7.11)$$

where $$X = m_1m_2 - m_bm_{12}$$

$$Y = m_1m_2(m_{12} + m_b) - m_bm_{12}(m_1 + m_2)$$

$$Z = Y\frac{(m_1 + m_2 + m_{12} - m_b)}{X^2} \qquad (7.12)$$

Nuclear Electronics

Nuclear electronics play an important role in radiation detection and measurement. Depending on the requirement, instrumentation and specifications vary. Radiation measurement can broadly be classified into two categories : Gross counting and Energy spectrometry. In the gross counting, all the events that produce an output pulse in the detector with an amplitude greater than the discriminator threshold (H_d) are counted. The discriminator setting is just sufficient to reject the noise from the amplifier. A typical block diagram is given in Fig. 7.14. In this set up, no information on the energy of the incoming

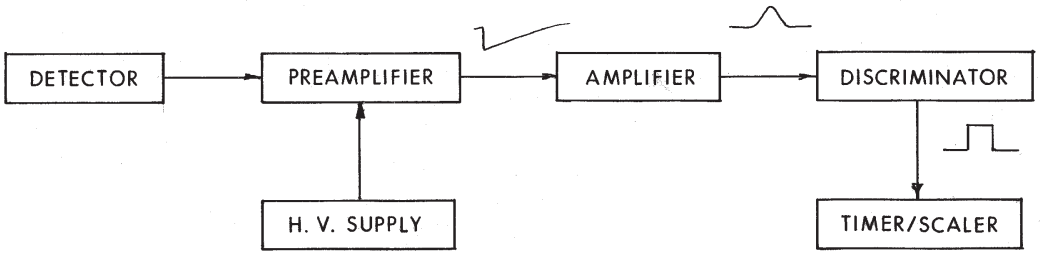

Fig. 7.14 Simple counting system.

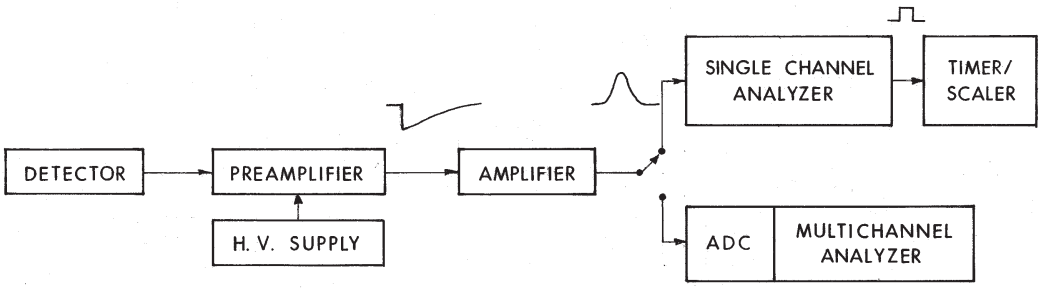

Fig. 7.15 Energy spectrometry system

radiation is obtained. On the other hand in the energy spectrometry, the events are sorted out on the basis of pulse height that depends on the energy of the incoming radiation. Intensity of radiation as a function of pulse height, known as spectrum, is measured. A block diagram for energy spectrometry system is shown in Fig. 7.15.

Functions of various blocks in the system are briefly described below:

Detectors

(a) For alpha particles : Silicon Surface Barrier (SSB) detector and gas proportional counters

(b) For gamma radiation: NaI(Tl), Ge(Li) and HPGe detectors

Pre-Amplifier

Preamplifier is an interface between the detector and the rest of the counting system. Its main function is to convert the charge produced in the active volume of the detector to a proportional voltage pulse compatible with the main amplifier input. It also provides an optimal coupling between the detector and counting system by:

(a) Minimising the degradation of the low signal obtained from the detector, before reaching the amplifier, by its physical proximity to the detector. Preamplifier is located as close as possible to the detector so that the inter connecting cable capacitance is minimum.

(b) Matching the high output impedance of the detector to the low input impedance of the amplifier. The input stage of the preamplifier uses a field effect transistor (FET) which has high input impedance.

Characteristics of the Pre-Amplifier

(a) Charge sensitivity: Pulse voltage (V) developed across the detector due to the charge (Q) collected is given by:

$$V = \frac{Q}{C} \tag{7.13}$$

where C is the detector capacitance. The proportionality between the charge (hence energy) and the voltage of the pulse will be maintained only if C is constant. In the case of semiconductor detectors, the capacitance does not remain constant, thereby, necessitating a charge sensitive preamplifier whose output voltage is independent of input capacitance and is proportional to the charge collected.

(b) Output shape and voltage: The output pulse may be either +ve or -ve. It has a very small rise time (of the order of ns) which is characteristic of the charge collection time of the detector. The decay time of the pulse is made quite large (50-100 μs) so that the full charge collection from the detector with widely differing collection times is ensured before significant decay of pulse sets in. The conversion gain is of the order of a few mV per MeV (typically 500 mV/MeV for Ge). Normally voltage gain is not expected at this stage. The output stage will be a driver to drive the pulse into the 93 ohm cable.

(c) Connectors provided in a preamplifier:

1. LV Power supplies (normally 9-pin; minimum 5 pin required)
2. HV input (SHV/MHV)
3. HV output (SHV/MHV) for detector in some cases
4. Preamplifier output (BNC)
5. TEST input (BNC)

Amplifier

The long-tailed output pulses from the preamplifier are not suitable for subsequent analysis. They are shaped and amplified using a linear amplifier to a suitable level before feeding to the analysing units.

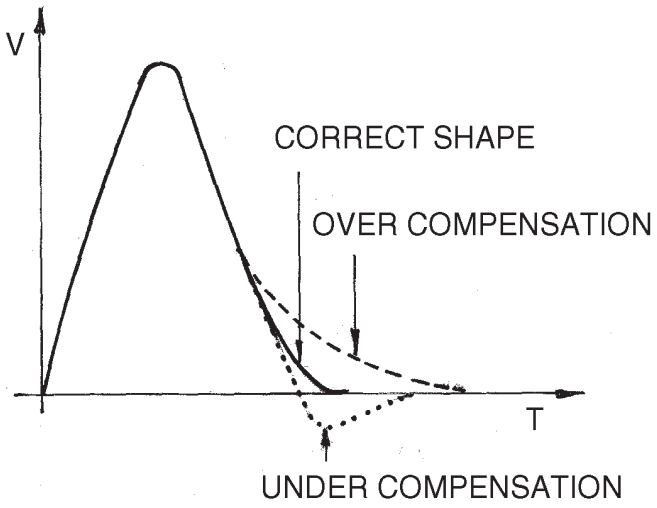

Fig. 7.16 Pole-zero compensation.

Characteristics of the Amplifier

(a) Shaping: From the point of view of signal to noise ratio, the best practical shape is a gaussian. Hence the long tail pulse from preamplifier is converted into gaussian shape by a set of differentiation and integration circuits. The time constant is selected from front panel in steps of 1, 2, 4, 6, 8 ... μs. Higher time constants (6 or 8 μs) are selected for better resolution and lower time constants (1 or 2 μs.) are chosen for higher count rate applications.

(b) Amplification: Input to the amplifier from the preamplifier is in the range of a few mV, whereas input for analysers is in the range of 0-10V. The signal has to be amplified. Normally amplifier gain of upto 3000 is provided and is selected from front panel by COARSE and FINE controls, to suit the analysis.

(c) Pole-zero: The circuitry for pulse shaping produces a bad side effect - a negative lobe for unipolar pulses (Fig. 7.16). Since this affects adversely the further processing, it is eliminated using a pole- zero cancellation circuit whose fine adjustment potentiometer is accessible from front panel. This is adjusted experimentally by observing the amplifier output on an oscilloscope (Fig. 7.16). Pole zero adjustment has to be ensured whenever a preamplifier is newly connected or the time constant of the amplifier is changed.

(d) Base line restorer (BLR): This is a circuitry for bringing back the baseline of the amplifier to zero immediately after the pulse. BLR avoids any shift in the baseline which could happen when high count rates are encountered.

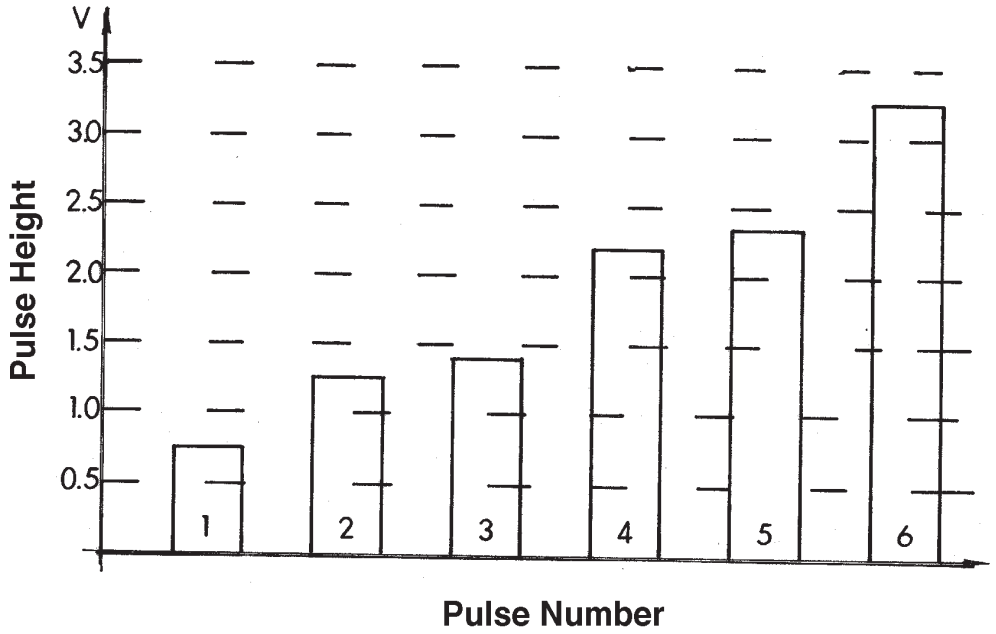

Fig. 7.17 SCA operation.

Single Channel Analyser

Single channel analyser (SCA) produces a logic pulse (normally upto 10V) for every-input pulse, satisfying a set of conditions. This unit has two discriminators called the Lower and Upper Level Discriminators (LLD and ULD). There are three modes of operation:

(a) Differential: LLD is 0-10 V and ULD is 0-2 V above LLD. This is a WINDOW mode where the output is recorded only when the input pulse height is between the levels of LLD and ULD.

(b) Integral: Any input pulse whose height is greater than the LLD produces a logic output. The ULD is not effective. This is equivalent to a simple discriminator.

(c) Normal: Here ULD is 0-10 V and is independent of LLD. The output occurs when input pulse lies between the LLD and ULD.

These three aspects are depicted in the Fig. 7.17 as described below:

(a) Differential: LLD = 1.0 V and ULD = 0.5 V. Pulses 2 and 3 are counted.

(b) Normal: LLD = 1.0V and ULD = 2.5V. Pulses 2, 3, 4 and 5 are counted.

(c) Integral: LLD = 1.0 V and ULD = XXXX. Pulses 2, 3, 4, 5 and 6 are counted.

Note that pulse 1 is not counted in all the three modes as its height is less than LLD in all the cases. LLD is often used to discriminate unwanted low energy pulses.

Timer - Scaler Unit

Both Timer and Scaler units are usually incorporated in a single module as they are invariably used together in the counting systems.

(a) Timer Unit: This unit is used to control the scaler to count for a definite interval of time. It operates with a high precision crystal oscillator clock. The time interval (normally variable from 1 to 9999 s) can be selected by switches. Elapsed time display and switches for START, STOP and RESET are provided on the front panel.

(b) Scaler unit: This unit counts the pulses fed to its input when the GATE input (obtained from the Timer unit) is high. Front panel will have counts display and switch for RESET of counter. It is desirable to have a discriminator incorporated in the unit to prevent noise, from being counted

High Voltage (HV) Unit

This unit is used to provide BIAS voltages for detectors. It is highly regulated (0.1%) and normally provides variable voltage from zero to a maximum of 5 KV of either polarity (selectable through a switch). The front panel will usually have an ON/OFF switch, polarity indicator, meter to read HV, potentiometer to vary the HV and a connector for taking out the HV. The HV unit used for NaI(Tl) system should have higher current capacity so that it can supply current to the photomultiplier tube bleeder circuit. Current capacity of 300 μA for semiconductor detectors and 1 mA for NaI(Tl) detectors are usually provided in the HV unit.

Multichannel Analyser

One of the basic functions of the multichannel analyser (MCA) is Pulse Height Analysis (PHA) by which pulses are sorted according to their heights and stored in different channels. It can be thought of conceptually as a stack of single channel analysers. An Analog to Digital Converter (ADC) is used to achieve this objective. The MCA has functionally two parts. (1) the ADC and (2) the analyser.

The ADC

The function of the ADC is to convert the input pulse height to a proportional digital (binary) value often called the channel number. The Wilkinson type ADC works on the principle of charging a capacitor to the peak voltage of the pulse and discharging it at constant current (Fig. 7.18). The discharge time (which is then proportional to peak height) is used to open the gate of a counter to which highly stable clock pulses from a crystal oscillator (normally 100 MHz) are fed. The number of counts recorded in the counter is thus proportional to the pulse height and is referred to as the channel number and contents of the channel is incremented by one. Since a definite time is taken for the conversion of an input pulse (of the order of 10-100 μs), the system cannot accept the next pulse for processing if it

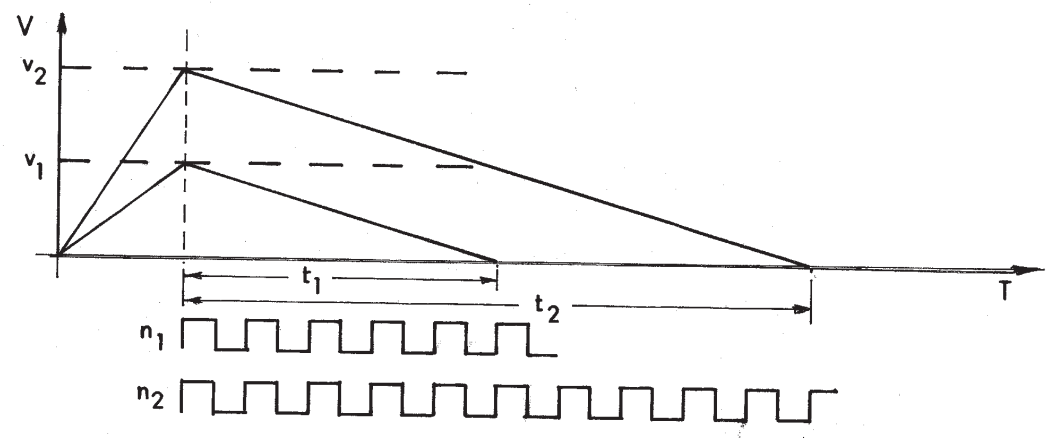

Fig. 7.18 ADC operation.

arrives during this time. To compensate for this dead time, provision is made to stop the timer clock from advancing during this period (LIVE time mode). In all gamma ray spectroscopic counting, timer is set for LIVE time counting. Apart from this, the ADC will also have a provision for cutting off unwanted pulses from being converted with the help of SCA in NORMAL mode, ADC gain selection, digital offset etc. There will also be a percentage dead time indicator. The resolution of an ADC is expressed in number of bits or conversion gain. For example, a 12 bit ADC has a conversion gain of 4K (2^{12}). Better resolution is achieved when the number of bits is high.

The Analyser

The analyser consists of storage memory, monitor, keyboard for user interaction, output devices like printer, plotter etc. and preferably a storage device like floppy or hard disk to store programmes and data. For each input pulse to the ADC, the analyser increments the counts by one in the memory location whose address is the channel number output by the ADC.

In all modern MCAs the output of the ADC will be connected to the bus of a microprocessor or a computer through interface cards so that full utility of the computer is exploited for all the functions of MCA like displaying the spectrum, analysis of data, its storage and report making. The user interaction is through interactive software so that persons not initiated into computer programming can also use the system without difficulty. Now, IBM-PC compatible plug-in cards are available which, when plugged into a personal computer (PC), will facilitate the PC to be used as an MCA. This arrangement has become extremely popular with experimenters because: (1) an MCA can easily be configured by adding just a plug-in card and (2) the PC can continue to be used as a computer while the data acquisition is in progress.

Nuclear Instrument Modular (NIM) System

Nuclear instrument modules (NIMs) are standardised instruments based on the International engineering specifications adopted in 1964 by the US Atomic Energy Commission and the National Bureau of Standards (US AEC Report TID-20893, July 1964). The standardisation encompasses mechanical and electrical specifications to provide various advantages to NIM users. The advantages include:

- Instrument interchangeability
- System optimisation
- Reduced cost
- Ease of configuring
- Reduced inventory of spare units
- Interchange between installations
- Convenient servicing
- Availability of compatible instruments from different manufacturers
- Reduced down time

An existing system can be updated with new modules to meet the ever increasing experimental demands and technology advances.

NIM system has an empty BIN with a power supply unit mounted at its backside as a starting basic unit. Standard voltages of ±6V, ±12 V and ±24 V are provided by the power supply unit on specified pins in 12 sockets mounted inside the bin. 12 single width MODULES can be plugged into the bin. Modules can be made in single width or in multiple widths form and they can make use of the power supplies available from the bin. As power supply requirements of individual modules, characteristics of input and output pulses, connectors, cables, etc. are standardised and specified, modules from different manufacturers can easily be integrated into any experimental system.

Bibliography

1. G.F. Knoll, Radiation Detection and Measurement, John Wiley & Sons, New York (1979).
2. G. Friedlander, J.W. Kennedy, E.S. Macias, J.M. Miller, Nuclear and Radiochemistry, 3rd Ed., John Wiley & Sons Inc., New York (1981).
3. Handbook of Radioactivity Analysis, Ed. M.F. L'Annunziata, Academic Press, New York (1998).
4. J. Tölgyessy and M. Kyrs, Radioanalytical Chemistry, Vol. 1 and 2, Ellis Horword Ltd., England (1989).

5. W.J. Price, Nuclear Radiation Detectors, 2nd Ed., Methuen and Co., London (1964).

6. C.A. Colmenares, *Nucl. Inst. Meth.*, **114** (1974) 269.

7. G. Charpak et al., *ibid*, **62** (1968) 262.

8. H. Oeshger and M. Wahlen, *Ann. Rev. Nucl. Sci.*, **25** (1975) 423.

9. J.B. Birks, The Theory and Practice of Scintillation Counting, Pergamon, New York (1964).

10. T. Aoyama and T. Watanabe, *Nucl. Inst. Meth*., **197** (1982) 357.

11. B.D. Wilkins, M.J. Flun, S.B. Kaufman, C.E. Gross and E.P. Steinberg, *Nucl. Inst. Meth.*, **92** (1971) 381.

12. P.W. Nicholson, Nuclear Electronics, Wiley-Interscience, London (1974).

13. Principles of Radiochemistry, Eds. D.D. Sood, N. Ramamoorthy and A.V.R. Reddy, IANCAS Publication (1994).

Chapter 8
Nuclear Reactions

When two nuclear particles (two nuclei or a nucleus and a nucleon) approach each other within a distance of 10^{-15} m, they experience a strong nuclear interaction. This process is called a nuclear reaction and involves a redistribution of energy and momentum. In turn it may give rise to the emission of particles from the interacting system. By adding a proton to ^{12}C, it can be changed to ^{13}N. This nuclear reaction is similar to a chemical reaction in which one chemical substance is converted to one or more compounds/elements. Another example of a nuclear reaction is that in which a neutron of an element is replaced by a proton, e.g., $^{23}_{11}Na + p \rightarrow ^{23}_{12}Mg + n$, where by adding a proton to ^{23}Na, ^{24}Mg is formed which disintegrates into $^{23}Mg + n$. There are innumerable examples of such reactions in which a nucleus is changed to another nucleus. This change could be brought in by addition of particles such as p, n, α, γ, ... and/or by emission of α, γ, n, p ... In a nuclear reaction, like in chemical reactions, energy could be absorbed or released. If the energy is absorbed, then the reaction is endoenergetic (endoergic) reaction and if the energy is released, then it is exoenergetic (exoergic) reaction.

Discovery of Nuclear Reaction

A brief description of the first nuclear reaction that was produced in laboratory by E. Rutherford in 1919 is given here before describing details of nuclear reactions. The experimental arrangement is simple and elegant as shown in Fig. 8.1. It consisted of a chamber filled with nitrogen and a radioactive source containing ^{214}Po, which is an alpha emitter. The source is collimated to provide a narrow beam of α-particles. These particles interact with nitrogen and are eventually stopped by a metal foil mounted on the wall of the chamber. Behind this foil a ZnS screen is placed. When scintillations were observed on the ZnS screen, it could only be explained by conceiving the idea that the nucleus of ^{14}N undergoes transmutation after interacting with alpha particles and long range ionising particles were produced which could penetrate the metal foil placed at the end of the collimator. In another set of experiments these radiations were deflected using the magnetic field. From the extent of deflections, it was identified that the emitted radiations were ionised hydrogen atoms or more precisely protons. From this unequivocal proof of proton emission,

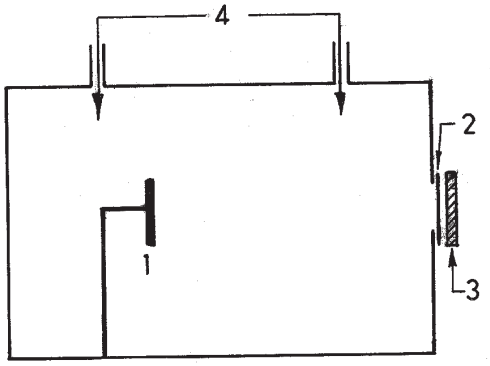

Fig. 8.1 Cross sectional view of Rutherford's experimental arrangement.
1. Radioactive source on a holder, 2. Metal foil (Ag), 3. ZnS screen, 4. Gas inlets.

it was concluded that ^{14}N absorbs an α-particle to form ^{18}F, which disintegrates to give a proton and ^{17}O. This experiment demonstrated nuclear transmutations and opened a new chapter called 'Nuclear Reactions'. It is to be noted that this discovery was made when the existence of neutron was not known.

Notation

The above reaction can be written as

$$^{14}_{7}N + ^{4}_{2}He \rightarrow {}^{17}_{8}O + ^{1}_{1}H \qquad (8.1)$$

In a chemical reaction, chemical substances taking part in the reaction are called reactants and the resulting compounds are called products. In nuclear reactions, the notation is slightly different. In the above example, ^{14}N is known as the target and the α's are called projectiles. Projectiles bombard the target. Emitted particles, protons in this case, are called ejectiles and the remaining nucleus (product nucleus) is called "residual nucleus" or product. The reaction shown in eqn. 8.1 is also represented by Bethe's notation as

$$^{14}N\ (\alpha,p)\ ^{17}O \qquad (8.2)$$

Conservation Laws

A considerable amount of information about nuclear reactions can be obtained as a result of the application of conservation laws; which impose definite restrictions on the course of the reactions. Certain physical quantities like nuclear charge, nucleon number, mass and energy, the momentum, and angular momentum are conserved. These are discussed considering the above reaction $^{14}_{7}N\ (\alpha,p)^{17}O$.

1. Nuclear charge Z: Before the reaction Z = 7 + 2 = 9 and after the reaction also it is 8+1 =9. Therefore, charge is conserved.

2. Mass (nucleon) number A: Before the reaction it is 14 + 4 = 18. After the reaction it is 17 + 1 = 18. Therefore, mass number is conserved

3. Mass and Energy : Mass (M) and energy (E) are conserved. It can be written as

$$M_1 + E_1 + M_2 + E_2 = M_3 + E_3 + M_4 + E_4 \quad (8.3)$$

where 1,2,3 and 4 refer to the projectile, target, ejectile and product respectively, and in the example shown in eqn. 8.2, they are respectively α, ^{14}N, p and ^{17}O.

4. Linear Momentum : Sum of the initial momenta of the projectile and target is equal to the sum of the momenta of the products

5. Angular Momentum : The sum of nuclear spin of projectile and target and orbital angular momentum between them remains constant before and after the reaction.

Apart from these quantities, parity and statistics also follow the conservation laws, whereas, the magnetic dipole moment and electric quadruple moment are not conserved as these are determined by the internal structure of nuclei.

Energetics of Nuclear Reactions

Like in chemical reactions, nuclear reactions are always accompanied by release or absorption of energy. In a chemical reaction the heat of the reaction arises from the binding energy of electrons in the molecules and is of the order of a few kcals/mole or a few eV/molecule. Likewise, the energy associated with a nuclear reaction (Q value) arises from the binding energy of nucleons in a nucleus which is of the order of a few MeV/atom. Thus the Q value of a nuclear reaction is about 10^6 times that of a chemical reaction.

The mass-energy conservation in a nuclear reaction is given by eqn. 8.3. The Q value is given by the difference between the masses of reactants and products as discussed earlier. To put it quantitatively,

$$Q = (M_1 + M_2) - (M_3 + M_4) \quad (8.4)$$

and the Q value is calculated using exact masses. A positive Q value corresponds to energy release (exoergic reaction) while negative Q corresponds to absorption of energy (endoergic reaction). It is equivalent to state that there could be mass gain or mass loss in a nuclear reaction, taking Einstein's equation into consideration. The Q value can be computed using the masses of the reactants and products, that are available in standard compilations.

The Q value for ^{14}N (α,p) ^{17}O is calculated as follows. Masses of ^{14}N and ^{4}He are 14.003074 amu and 4.002603 amu respectively. Masses of ^{17}O and ^{1}H are 16.99913 amu and 1.007825 amu respectively. The combined mass of $^{14}N + ^{4}He$ is lower than that of $^{17}O + ^{1}H$ by 0.001278 amu and is equal to 1.19 MeV. This is called Q value of the reaction. In this case, it is negative, Q = -1.19 MeV. This means that energy has to be supplied for this reaction to take place. Such reactions are called threshold reactions wherein unless Q equivalent amount of energy is supplied, reaction will not take place.

The Q Value Equation

One of the important applications of nuclear reactions is to obtain energetic particles. Neutron sources of varying energy can be made by (p,n) and (d,n) reactions on light mass targets, e.g.,

$$^{2}_{1}D + ^{3}_{1}H \rightarrow ^{4}He + n \qquad Q = 17.6 \text{ MeV} \tag{8.5}$$

$$^{1}_{1}H + ^{7}_{3}Li \rightarrow ^{7}_{4}Be + n \qquad Q = -1.64 \text{ MeV} \tag{8.6}$$

In these reactions the outgoing particle's (neutron) energy depends on the emission angle (θ) with respect to the projectile beam direction and the incident particle energy. Using conservation of linear momentum, and mass and energy, a relation for Q is obtained as

$$Q = E_1\left(\frac{M_1}{M_4} - 1\right) + E_3\left(\frac{M_3}{M_4} + 1\right) - 2\frac{\sqrt{M_1 M_3 E_1 E_3}}{M_4}\cos\theta \tag{8.7}$$

where, E_1 and E_3 are kinetic energies of the projectile and the ejectile respectively. Kinetic energy of the target (E_2) is assumed as zero as it is at rest. M_1, M_2, M_3 and M_4 are masses of projectile, target, ejectile and the product respectively. This equation is called Q value equation of a nuclear reaction. Details of the derivation and different cases are discussed in Appendix VII. This equation is useful to arrive at the energy levels of the product from the measured kinetic energy of different ejectile groups.

Threshold Energy of a Reaction

The minimum energy of the projectile which is required to induce a reaction is known as the threshold energy of the reaction. When a projectile (a) is incident on a target (A), a fraction of the kinetic energy of the projectile, that is $E_1.M_2/(M_1 + M_2)$ is available in the centre of mass system. (Details of centre of mass system and lab system are given in Appendix VIII). The remaining energy goes into the recoil energy. For endoergic reactions the energy available in the CM system must be equal to the Q value i.e. the minimum energy to initiate the reaction. The threshold energy, therefore, is equal to

$$E_{th} = -Q\,\frac{(M_1 + M_2)}{M_2} \tag{8.8}$$

The combined potential energy of the projectile and the target is lower than the potential energy of the products. Therefore, kinetic energy of projectile is utilised to raise the potential energy of the reactants for the reaction to proceed. For the reaction $^{14}N(\alpha,p)\,^{17}O$ to take place kinetic energy of the α particle should at least be equal to $-Q(M_1 + M_2)/M_2$. For good approximation, mass numbers can be used to calculate this value. $E_{th} = +1.19 \times 18/14 = 1.53$ MeV. Minimum energy of α should be 1.53 MeV.

In the case of charged particle induced reactions, Coulomb barrier (V_c) hinders the reaction at energies lower than V_c where

$$V_c = \frac{Z_1 Z_2 e^2}{R_1 + R_2} = \frac{Z_1 Z_2 e^2}{R_0 \left(A_1^{1/3} + A_2^{1/3}\right)} \quad (8.9)$$

where Z, R and A denote the nuclear charge, radius and mass number respectively. Thus for charged particle induced reactions, the E should be atleast equal to V_c. In the case where the reaction has both potential energy threshold and coulomb barrier, then the minimum energy should be either $V_c.(M_1+M_2)/M_2$ or $-Q(M_1 + M_2)/M_2$ which ever is larger.

To understand this, consider the case of $^{14}N(\alpha,p)^{17}O$ where 7.7 MeV α-particles from ^{214}Po were used by Rutherford. The potential threshold was 1.53 MeV. In this reaction, both α and ^{14}N are having charge and hence there would be a Coulomb barrier equal to

$$V_c = \frac{1.44 \times 2 \times 7}{1.5\ (4^{1/3} + 14^{1/3})} = 3.36 \text{ MeV}$$

V_c is higher than E_{th}. Therefore, the KE of α-particle in C.M. system should be more than V_c for the reaction to take place. Excitation energy (E*) for this reaction is [(7.7 x 14/18) - 1.53] = 4.80 MeV. Where does this energy go? E* is shared by both proton and ^{17}O. Proton gets a major share of this (17/18 E*) in the form of its kinetic energy and the remaining (1/18 E*) goes to ^{17}O as recoil energy.

It is interesting to note that protons with slightly lower energy can also be emitted. Accordingly product nucleus gets slightly lower recoil energy. Where does the remaining energy disappear? It will be retained by the product nucleus, not in the form of KE, but as potential energy (PE). This means that nucleus is formed in a potentially higher state or excited state. This excess energy could be dissipated, generally, by γ-emission and the nucleus attains ground state/lower excited state configuration. By measuring kinetic energy of different groups of ejectiles, information on the structure of the product nucleus is obtained.

Another interesting example is α-induced reaction of ^{232}Th. The reaction of alpha on ^{232}Th has both potential energy threshold and coulomb barrier. The values of Q, E_{th} and V_c are calculated for alpha induced reaction of ^{232}Th.

Excess masses (ΔM = M-A) of ^{232}Th, α and ^{236}U are 35.444, 2.425 and 42.441 MeV respectively. Q is calculated using eqn. 8.10 as -4.57 MeV.

$$Q = M_{Th} + M_\alpha - M_U \quad (8.10)$$

Since Q is negative, it is endoergic reaction and has a potential energy threshold. Thus,

$$E_{th} = -Q \times \frac{236}{232} = 4.57 \times \frac{236}{232} = 4.65 \text{ MeV}$$

This reaction also has a Coulomb barrier (V_c) because both alpha and thorium have charge and is given by

$V_c = 1.44 \times 92 \times 2/(1.5(232^{1/3} + 4^{1/3})) = 22.35$ MeV

The minimum energy required to overcome this Coulomb barrier is $V_c \times 236/232 = 22.75$ MeV, which is greater than E_{th}. Therefore, we have to supply an energy equal to 22.75 MeV, in the form of kinetic energy of α-particles for the reaction to take place. However, out of this 22.75 MeV, only 4.65 MeV will be spent to take care of potential threshold. Remaining energy will appear as excitation energy of ^{236}U.

In the case of α-induced reaction of ^{232}Th, suppose α-particles of 30 MeV are used, then the excitation energy (E*) of the compound nucleus ^{236}U is

$$E^* = E_{CM} + Q = 30 \times \frac{232}{236} - 4.57 = 24.92 \text{ MeV}$$

Since the excitation energy is greater than fission barrier (about 6.5 MeV) fission is one of the prominent modes of deexcitation.

In the case of neutron induced reactions like (n,γ) reactions, the Q value is always positive. As neutron has no charge, there is no Coulomb barrier for neutron induced reactions. Binding energy released when neutron is fused with the target is available as excitation energy of the compound nucleus. Therefore, neutron induced reactions take place with nuclei of all isotopes with the neutrons of all energies.

Reaction Cross-section

The probability of a nuclear reaction is expressed in terms of the cross section (σ). It represents the cross-sectional area offered by a nucleus to the projectile for the reaction to occur. Cross-section, therefore, has units of area, cm^2. Since cm^2 is very large unit compared to nuclear dimensions, a smaller unit called barn, b is used to express cross section. b is equal to 10^{-24} cm^2 is a practical unit for reaction cross section.

Cross section (σ) can be related to the number of events leading to formation of a particular product and the number of projectiles; e.g., in $^{14}N(\alpha,p)^{17}O$, the ratio of atoms of ^{17}O formed to the rate of α particles is related to cross section.

$$\sigma = \frac{\text{Number of products nuclei of one type per second per target nucleus}}{\text{Number of projectiles per unit area per second}}$$

Cross section varies with projectile energy and therefore, cross section, has to be quoted at a particular energy. Some typical cross section values are given in Table 8.1.

From the above relation for cross-section, reaction rate (R) can be written as

$$R = N \sigma I \qquad (8.11)$$

Table 8.1 - Cross section data for some reactions

Reaction	Projectile energy	Cross-section in barns
$^{6}Li\ (n,\alpha)^{3}H$	0.025 eV	940
$^{3}He(n,p)^{3}H$	0.025 eV	5327
$^{2}H(n,\gamma)^{3}H$	0.025 eV	0.0053
$^{10}B(n,\gamma)^{11}B$	0.025 eV	0.5
$^{10}B(n,\alpha)^{7}Li$	0.025 eV	3837
$^{127}I(n,\gamma)^{128}I$	0.025 eV	6.2
$^{54}Fe(\alpha,p)^{57}Co$	20 MeV	0.6
$^{54}Fe(\alpha,pn)^{56}Co$	35 MeV	0.65
$^{51}V(\gamma,\alpha)^{47}Sc$	18 MeV	0.0003
$^{63}Cu(p,n)^{63}Zn$	16 MeV	0.38
$^{63}Cu(p,n)^{63}Zn$	20 MeV	0.50
$^{235}U(n,f)$	0.025 eV	583
$^{235}U(n,f)$	10 keV	4

where N is the number of target nuclei per cm^2 of a thin foil, σ is the cross section and *I* is the intensity of the beam of projectile (per second) used. The eqn. 8.11 is valid only if the beam loss in the target is negligible.

Determination of Cross Section

Reaction Rate Method

Cross section of a nuclear reaction is determined by measuring the reaction rate in a target having N nuclides per cm^2 with a beam of *I* particles per second. These data are used in eqn. 8.11 and the σ is calculated. Cross section for proton (20 MeV) induced reaction on ^{63}Cu with the emission of neutron is 0.5 b (Table 8.1).

Similarly σ for the neutron induced reaction is determined by measuring the reaction rate R. For neutron induced reactions the neutron flux is expressed as neutrons per cm^2 per second and the rate of the reaction (R) is given as

$$R = N \sigma \phi \qquad (8.12)$$

where N is total number of nuclei in the sample. Unlike in charged particle reactions, sample is completely immersed in neutron flux. Substituting the values of R, N and ϕ, σ is calculated.

If the product formed is radioactive, then σ can be obtained by measuring the radioactivity of the product. Accordingly eqns. 8.11 and 8.12 can be modified in terms of radioactivity of the product and its decay constant as follows. Reaction rate is replaced by dNi/dt, where i represents product i formed in the reaction. Taking into account the decay of the product during irradiation, eqn. 8.12 is modified as

$$A_i = N \sigma \phi (1 - e^{-\lambda_i t}) \qquad (8.13)$$

where A_i is the activity formed in the irradiation of the target for a duration of time t and λ_i is the decay constant of the nuclide formed. By measuring the activity A_i and substituting the values of N, ϕ, t and λ_i in eqn. 8.13, σ can be calculated.

An example to calculate cross section of ^{98}Mo : A 1mg target of natural molybdenum (24.1% ^{98}Mo) is irradiated for 66 hours in a thermal neutron flux of 10^{14} n/s/cm^2. At the end of the irradiation if the activity of ^{99}Mo formed in the sample is 9.6 x 10^6 dps, calculate the cross section for ^{98}Mo(n,γ)^{99}Mo. Also calculate the activity of ^{99}Tc (6.01 h half-life)[1] after 24 hours of cooling.

Solution:

Number of ^{98}Mo atoms (N) = $\frac{6.023 \times 10^{20}}{95.94} \times 0.241 = 1.51 \times 10^{18}$

Neutron flux (ϕ) = 10^{14}cm^{-2} s^{-1}

Time of irradiation = 66 h

Half life of ^{99}Mo = 65.94 h

Activity formed (A_i) = 9.6 x 10^6 dps

From eqn 8.13, σ can be calculated as

---

[1]Half life of ^{99m}Tc is 6.01 h and is the daughter product of ^{99}Mo

^{99}Mo $\rightarrow$ ^{99m}Tc

After 1 day of cooling time, ^{99m}Tc will be in equilibrium with ^{99}Mo. Activities of ^{99}Mo and ^{99m}Tc are almost equal (see Chapter 4, transient equilibrium)

Activity of ^{99}Mo after 1 day of cooling = $9.6 \times 10^6 \times e^{-\frac{0.693}{65.94} \times 24}$ =7.5 x 10^6 dps

$\therefore$ Activity of ^{99m}Tc = 7.5 x 10^6 dps

^{99m}Tc is the work horse of radiopharmaceuticals and is daily milked from ^{99}Mo-^{99m}Tc generator

$$\sigma = \frac{A_i}{N\phi\ (1 - e^{-\lambda_i t})}$$

$$= \frac{9.6 \times 10^6}{1.51 \times 10^{18} \times 10^{14} \left(1 - e^{-\frac{0.693}{65.94} \times 66}\right)}$$

$$= 1.272 \times 10^{-25}\ cm^2 = 0.127\ b$$

Beam Attenuation Method

When there is a significant attenuation of beam intensity in the target, *I* is not constant before and after passing through the target. The reduction in beam intensity (d*I*) is equivalent to the reaction rate and is given as

$$\therefore\ -dI = I\ N\ \sigma\ dx \qquad (8.14)$$

On integration of eqn. 8.14, relation between intensity before (I_0) and after (I) passing through the target, is obtained as

$$I = I_0\ e^{-N\sigma x} \qquad (8.15)$$

For measurement of beam attenuation, macroscopic cross section (Σ) is used where

$$\Sigma = N\ \sigma\ (cm^{-1}) \qquad (8.16)$$

In beam attenuation measurements, the effect of the entire target substance, whether it is a single isotope or an isotopic mixture or compound, is measured.

Excitation Function

Profile of cross section as a function of projectile energy is called excitation function. Nuclear reaction cross section varies as a function of energy of the projectile (E). In the case of charged particle induced reaction, there is a coulombic threshold for the reaction. When E is more, then this reaction takes place and σ starts increasing (Fig. 8.2). If the excitation energy is more than binding energy of proton, neutron, α ...., then these particles can be emitted from the compound nucleus. This process of emitting particles is called particle evaporation. Peaks (resonance) could be observed in excitation function. Resonance peaks are observed when the projectile energy matches with one of the energy levels of compound nucleus (CN). Therefore, investigations on excitation functions give information on the structure of the compound nucleus. In the case of neutrons, σ generally decreases with increase in E (Fig. 8.3), barring resonances.

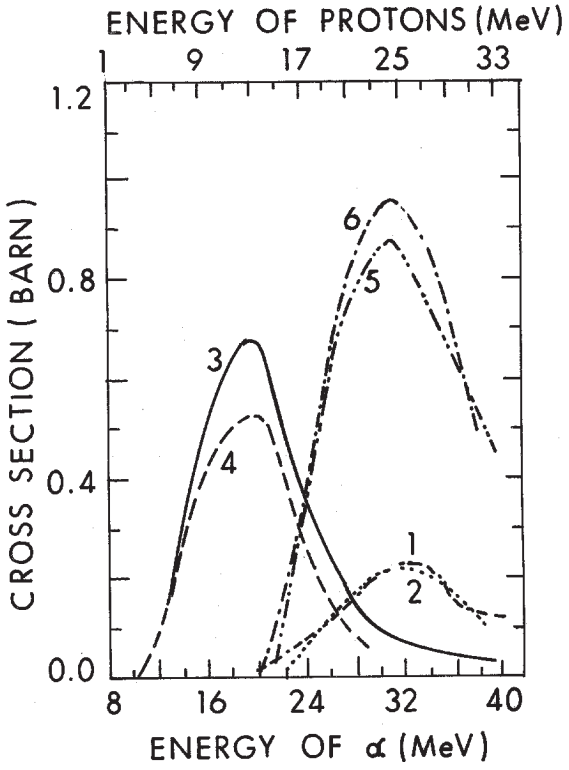

*Fig. 8.2 Excitation functions for 1. $^{63}Cu(p,2n)^{62}Zn$; 2. $^{60}Ni(\alpha,2n)^{62}Zn$; 3. $^{60}Ni(\alpha,n)^{63}Zn$; 4. $^{63}Cu(p,n)^{63}Zn$; 5. $^{63}Cu(p,pn)^{62}Cu$; 6. $^{60}Ni(\alpha,pn)^{62}Cu$ [S.N. Ghoshal, Phy. Rev., **80** (1950) 939].*

Angular Momentum in Nuclear Reactions

Maximum cross section that a nucleus can offer for a projectile is πR^2 where R is the sum of the radii of target and projectile. However, there are instances where σ is larger than πR^2. For example, thermal neutron induced reactions such as

$^{10}B(n,\alpha)^{7}Li$ $\sigma = 3840b$

$^{6}Li(n,\alpha)^{3}H$ $\sigma = 940b$

Reaction cross-sections quoted here are larger by orders of magnitude than the cross sectional area of the target nucleus. This can be explained only by bringing quantum mechanical concept of the wave nature of the neutron. It can be shown that σ is not just proportional to πR^2 but to $\pi(R + \lambda\!\!\!^{-})^2$ where $\lambda\!\!\!^{-}$ is the de Broglie wavelength of the incident particle.

It may be noted that due to their high cross section for thermal neutrons, ^{10}B and ^{6}Li are good detector materials for thermal neutrons.

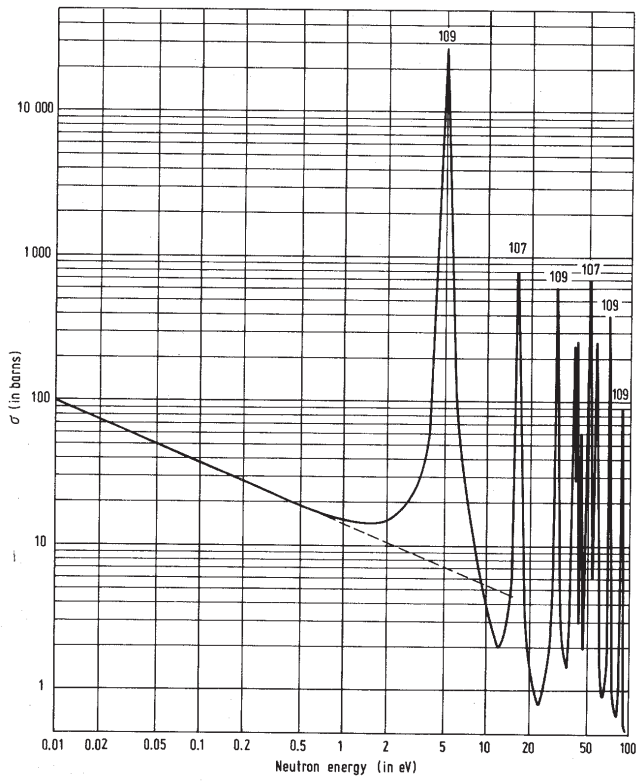

Fig. 8.3 Neutron cross section of silver as a function of energy [Nuclear and Radiochemistry, G. Friedlander, J.W. Kennedy, E.S. Macias and J.M. Miller, 3rd Ed., John Wiley (1981) p.134].

$$\therefore \sigma = \pi(R + \lambda\!\!\!^{-})^2 \qquad (8.17)$$

(Details of the derivation of eqn. 8.17 are given in Appendix III along with angular momentum barrier). For low energy neutrons, it can be shown that $\lambda\!\!\!^{-}$ is very large compared to the nuclear radius. i.e. $\lambda\!\!\!^{-} >> R$, thus

$$\sigma \propto \pi\, \lambda\!\!\!^{-2} \qquad (8.18)$$

On the other hand, high energy neutrons will have smaller $\lambda\!\!\!^{-}$, much less than R and σ will be proportional to πR^2. It should be noted that the values derived by these relations are the maximum values for σ.

Nuclear Reaction Theory

A large body of nuclear data consisting of excitation functions, energetics, emitted particles, their distribution etc. are being obtained in the nuclear reactions. To understand the

process or mechanism of nuclear reactions, some models are proposed with certain assumptions. Some of the successful models that explain most of the observed data are compound nucleus (CN) model, optical model and direct interaction model. The CN model and direct interaction models are briefly described here.

When a projectile bombards a target, the particle can either pass through the nucleus without reacting or it can be absorbed by the target forming a compound nucleus (CN). Alternatively at higher energy, the particle may react with only a part of target nucleus which can be either knocked out or captured by the projectile (direct reaction)

Compound Nucleus Model

This model was proposed by N. Bohr in 1936. In this model the reaction occurs in two steps namely, (i) the capture of the projectile by target nucleus forming a compound nucleus (CN) in excited state and (ii) deexcitation of CN either by evaporation of particles or gamma emission. The two steps are assumed to be independent of each other. Thus, the reaction can be written as

$$a + A \rightarrow C \rightarrow B + b \tag{8.19}$$

Cross section for these two steps can be represented by $\sigma_{A \rightarrow C}$ and $\sigma_{C \rightarrow B}$. The overall cross section is given as product of the cross section of the two steps

$$\sigma_{A \rightarrow B} = \sigma_{A \rightarrow C} \cdot \sigma_{C \rightarrow B} \tag{8.20}$$

The projectile upon entering the target nucleus and forming the compound nucleus, equilibrates its kinetic energy with all nucleons randomly. The excitation energy (E^*) of the CN is given by

$$E^* = E_{CM} + Q \tag{8.21}$$

where E_{CM} is the kinetic energy of the project in centre of mass (CM) system. An example is described to calculate E^* and possible deexcitation modes.

$$^{27}_{13}\mathrm{Al} + ^{1}_{0}\mathrm{n} \rightarrow ^{28}_{13}\mathrm{Al}^* \rightarrow ^{27}_{12}\mathrm{Mg} + ^{1}_{1}\mathrm{p} \tag{8.22}$$

In this reaction, neutron is captured by ^{27}Al to form a CN ^{28}Al and ^{28}Al is in excited state. What could be its excitation energy? Masses of ^{27}Al and ^{1}n are 26.98154 and 1.00866 amu, respectively whereas mass of ^{28}Al in ground state is 27.98191 amu. Thus Q value of this exoergic reaction is 26.98154+ 1.00866 - 27.98191= 0.00829 amu = 7.72 MeV. If the KE of neutron is 1 MeV, then $E^* = \frac{27}{28} \times 1 + 7.72 = 8.68$ MeV. This energy is not concentrated with any particular nucleon, rather it is distributed randomly. All the 28 nucleons share the 8.67 MeV excitation energy. Let us assume that all the energy is with a single nucleon, say a proton. We know that generally the separation energy for a nucleon is around 8 MeV i.e. if a nucleon has about 8 MeV energy, it might be separated from the nucleus. In our example, E^* being 8.67 MeV, it could lead to emission of a proton, if all the E^* is with a proton. In fact, in a

CN, due to continuous collisions among nucleons (quasi-stationary state), a nucleon (or few nucleons) acquires enough KE above separation energy leading to its emission. By this argument, two things should be clear: (i) when projectile is captured by target, energy equilibration is very fast and (ii) emission of particle or deexcitation is a slow process. That is why in CN type of reactions, the history of formation of CN is forgotten. Formation of CN and deexcitation are two independent steps.

This can also be understood in terms of life time of CN which is of the order of 10^{-15} to 10^{-14} s. A 1 MeV neutron travels with a velocity of about 10^7 m/s and the nuclear dimension is of the order of 10^{-14} cm. Therefore, time required to travel across nuclear dimensions (either to form CN or to escape the target nucleus without forming CN) is of the order of 10^{-21} s which is much smaller as compared to life time of CN. Due to this long life time of CN, it forgets how it has been formed. If a CN is formed in two or three different ways, its deexcitation is independent of its formation. This has been demonstrated by Ghoshal experiments which are discussed later. It may be noted that if CN exists in quasi-stationary states, these states are called virtual states or virtual levels. Virtual states decay by the emission of particles, where as bound levels decay by γ emission. Population of virtual levels or bound levels, depends on the extent of E^* available to CN. The energy of the emitted particle shows a Maxwellian behaviour owing to statistical nature of the decay of CN.

The independent hypothesis of the entrance channel (formation of CN) and exit channels (modes of deexcitation) in a compound nucleus reaction has been confirmed by the famous Ghoshal experiments. ^{64}Zn was produced by two different entrance channels as shown below;

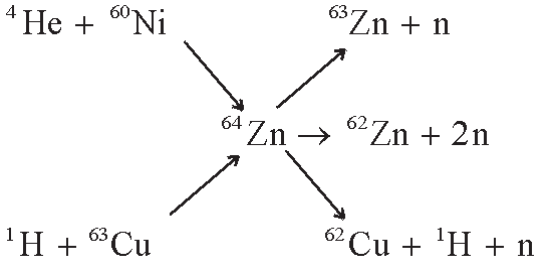

^{64}Zn deexcites by three exit channels as shown above. Excitation functions for the two sets of entrance channels and three exit channels are shown in Fig. 8.2.

The excitation function can experimentally be determined by measuring the evaporation residues at various projectile energies. For charged particle induced reactions, stacked foil arrangement for irradiation of several target foils was used. For ^{60}Ni + ^{4}He reaction, energy of α was increased upto 40 MeV. Similar experiments were carried out for ^{63}Cu + p reaction. It was observed that the ratio of pn and 2n emission probabilities is independent of the mode of formation, that is,

$$\frac{\sigma(\alpha,pn)}{\sigma(\alpha,2n)} = \frac{\sigma(p,pn)}{\sigma(p,2n)} \qquad (8.23)$$

This can be seen from Fig. 8.2

Energy Dependence of Cross Section in CN Reactions

The cross section varies as a function of projectile energy as explained under excitation functions. Experimentally, cross sections are determined at different projectile energies. In the case of neutron induced reactions, separate irradiations are necessary for neutrons of different energy. The evaporation residues can be assayed for their beta and gamma activities. From the measured activities, after appropriate corrections, σ can be evaluated for different evaporation residues (exit channels). Excitation function for neutron induced reaction of Ag is shown in Fig. 8.3. If a few exit channels are weakly formed (low yields) and also if there are many exit channels, radiochemical separations are necessary to observe weak channels.

Low Energy Neutron Induced Reactions

In this case the excitation energy of the CN is slightly more than the neutron binding energy which is shared by many nucleons in the nucleus. The probability for concentration of this excitation energy on a particular nucleon is, therefore, extremely low and the CN decays by emission of gamma rays i.e. (n,γ). However, in the case of low Z targets (n,p) and (n,α) reactions may also compete with (n,γ) reaction. Typical excitation functions for slow neutron induced reactions show a slowly decreasing cross section with increasing neutron energy followed by sharp resonances (Fig. 8.3). The spacing between the resonances is large (few eV to keV). The small width of resonances indicates that the lifetime of the compound nucleus states is about 10^{-14}-10^{-15} seconds as expected form the Heisenberg's uncertainly principle.

Breit and Wigner derived a formula for the cross sections in the resonance region taking into account of decay widths (Γ) and the spins of projectile (a), target (A) and the compound nucleus as I_a, I_A and I_C respectively, and is given by

$$\sigma(n,\gamma) = \pi\lambda\!\!\!^{-2} \frac{(2I_C + 1)}{(I_a + 1)(2I_A + 1)} \frac{\Gamma_n \Gamma_\gamma}{(E - E_0)^2 + (\Gamma/2)^2} \qquad (8.24)$$

E is the energy of the neutron and E_0 is the resonance energy. Details of the derivation are given in Appendix X.

de Broglie wavelength $\lambda\!\!\!^{-}$ is related to the velocity of the neutron (v) as $\lambda\!\!\!^{-} = \hbar/mv$ where m is the mass of neutron. All other factors in the eqn. 8.24 can be shown to be constant except Γ_n which is proportional to neutron velocity v. Thus

$$\sigma(n,\gamma) \propto (v/v^2) = \text{const}/v \qquad (8.25)$$

This explains the 1/v behaviour of cross section in low energy neutron induced reactions as shown in Fig. 8.3 with dotted line.

Fast Neutrons and Charged Particle Induced Reactions

The excitation energy of the CN formed by fast neutron induced reactions and charged particle induced reactions is high. With increasing excitation energy, the spacing between nuclear levels decreases and reaches continuum region. The deexcitation of CN from the continuum region is followed in terms of the statistical model. According to this model the relative probabilities of various exit channels are determined by their relative state densities.

The excitation functions for various evaporation residues show broad curves with growth and decay type of behaviour as new channels open up at higher energies (see Fig. 8.2). The energy spectra of evaporated particles show Maxwellian pattern. For highly excited nuclei, the energy distribution of emitted neutrons is expected to be

$$n\, d(E_n) = \text{const.} E_n \exp\left[-\frac{E_n}{T}\right] d(E_n) \qquad (8.26)$$

where $n\, d(E_n)$ is the number of neutrons having energy between E_n and $E_n + dE_n$ and T is the nuclear temperature of residual nucleus evaluated at its maximum excitation energy. T has the dimension of energy and is analogous to kT in classical Maxwellian distribution. However, if the emitted particle is a charged particle, then the Coulomb barrier suppresses the low energy particles.

The signatures of CN formation are, (i) Maxwellian type of evaporation spectra, and (ii) Angular distribution of emitted particles are symmetric around 90 degrees. Deviation from this can be regarded as departure from CN mechanism.

Types of Reactions

Scattering Reactions

In a nuclear reaction A(a,b)B, a and A are projectile and target, respectively and b and B are the outgoing ejectile and product nucleus respectively. In most of the nuclear reactions, a and b are either a nucleon or a cluster of few nucleons e.g. protons, neutrons, alpha particles etc. If the outgoing particle (ejectile) is identical to the incident particle, the reaction is called scattering. If the energy of the target nucleus is left unchanged in the process, it is called elastic scattering, whereas, if the target nucleus is left in an excited state, it is called inelastic scattering. An example of elastic scattering is given below.

e.g., $^{12}C\ (n,n')^{12}C \qquad (8.27)$

In this example, a neutron in the vicinity of ^{12}C gets scattered, i.e. its direction is changed and kinetic energy is reduced. It means that ^{12}C is set into motion by the neutron at the expense of

its own KE. The outgoing particle is, therefore, the original neutron with lower KE. KE of the projectile is changed but total KE is conserved and PE is not changed. This is one of the most probable reactions that takes place in moderation of neutrons in a nuclear reactor.

Inelastic scattering is a similar reaction, where the projectile and ejectile are same but both KE and PE are changed, and total energy is conserved.

e.g., $^{125}I\ (p,p')^{125}I^{*}$ (8.28)

Here also, like in the earlier example, KE of the projectile is reduced; but this energy has been utilised to excite the target nucleus ^{125}I to a higher energy and thus its PE changed. Elastic scattering is possible with all energies of projectile whereas inelastic scattering needs a minimum energy corresponding to the first excited state in the target nucleus. Excited nucleus deexcites by gamma decay.

Alpha Induced Reactions

Alpha particles emitted by natural radioisotopes were the only projectiles available for the study of nuclear reactions before the discovery of neutrons and construction of accelerators. Alpha being a charged particle, energy of α should be more than coulomb barrier (V_c). Energy of α-particles emitted in the α-decay is low (4-8 MeV) and these low energy alphas can produce reaction only in low Z nuclides. That is why studies were limited to light mass nuclides until the availability of accelerator produced α particles. Many reactions were investigated with alphas of low energy, particularly for the production of protons and neutrons, e.g.,

$$^{10}_{5}B\,(\alpha,p)\,^{13}_{6}C \tag{8.29}$$

$$^{23}_{11}Na\,(\alpha,p)\,^{26}_{12}Mg \tag{8.30}$$

$$^{9}_{4}Be(\alpha,n)\,^{12}_{6}C \tag{8.31}$$

Alpha induced reaction of ^{9}Be mentioned here is the famous reaction by which Chadwick discovered neutron. He estimated mass of the neutron as roughly same as that of a proton. Chadwick improved his estimation of neutron mass between 1.005 and 1.008 amu from the data obtained in another reaction.

$$^{11}_{5}B\,(\alpha,n)\,^{14}_{7}N \tag{8.32}$$

This estimate, in the absence of accurate data on atomic masses and non-availability of sophisticated measuring equipment, is very close to the actual value of neutron mass, 1.008983 amu. Another historically important alpha induced reaction that led to the discovery of artificial radioactivity by Joliots is

$$^{27}_{13}Al(\alpha,n)\,^{30}_{15}P \tag{8.33}$$

The continuous emission of positrons, even after stopping the reaction inducing projectiles, led to the conclusion that the product formed (^{30}P) was radioactive. Phosphorous was separated as phosphine and its half-life was measured. These experiments heralded the discovery of artificial radioactivity. Now with the availability of accelerator produced high energy α beams, α induced reactions are extended to the entire nuclide chart.

The $^{9}_{4}\mathrm{Be}(\alpha, n)$ reaction can profitably be used for production of neutrons in a neutron generator. Alpha particles are continuously made available by radioisotopes such as ^{241}Am, ^{239}Pu, and ^{238}Pu. A stable beryllium alloy in the form MBe_{13}, where M is the actinide metal, is prepared. Each α particle emitted by ^{241}Am has an opportunity to interact with ^{9}Be. However, neutron yield is around 1% or less as most of the α's get stopped rather than producing the desired reaction. In the case of ^{241}Am/Be source, 70-80 neutrons are produced per 10^6 alphas emitted.

Neutron Induced Reactions

Neutron induced reactions are a special class by themselves. Since neutron do not have charge, there is no Coulomb barrier for neutron interaction with the nucleus. Therefore, neutrons of any energy can induce reactions with all the nuclides in the entire nuclide chart. As discussed earlier, the (n,γ) reactions have positive Q value. Another interesting aspect is that the reaction cross sections with low energy neutrons are much larger compared to those by medium and high energy neutron induced reactions as discussed earlier. Nuclear reactor is a vast source of neutrons of different energy. There are other reactions which produce neutrons of definite energy which can be used as projectiles. Neutron induced reactions lead to the production of different ejectiles of the type (n,p) (n,α) etc. or simply to production of radioisotopes by (n,γ) reactions.

$$^{27}_{13}\mathrm{Al}\,(n,\alpha)\,^{24}_{11}\mathrm{Na} \qquad (8.34)$$

$$^{10}_{5}\mathrm{B}\,(n,\alpha)\,^{7}_{3}\mathrm{Li} \qquad (8.35)$$

$$^{14}_{7}\mathrm{N}\,(n,p)\,^{14}_{6}\mathrm{C} \qquad (8.36)$$

$$^{135}_{54}\mathrm{Xe}\,(n,\gamma)\,^{137}_{54}\mathrm{Xe} \qquad (8.37)$$

$$^{115}_{49}\mathrm{In}\,(n,\gamma)\,^{116}_{49}\mathrm{In} \qquad (8.38)$$

$$^{232}_{90}\mathrm{Th}\,(n,\gamma)\,^{233}_{90}\mathrm{Th} \qquad (8.39)$$

An important nuclide ^{233}U for energy production, is produced by irradiating ^{232}Th followed by two successive β-decays as shown below.

$$^{232}_{90}\mathrm{Th} \xrightarrow{\beta^-} {}^{233}_{91}\mathrm{Pa} \xrightarrow{\beta^-} {}^{233}_{92}\mathrm{U} \qquad (8.40)$$

Proton Induced Reactions

Protons are obtained from accelerators, with energy of a few keV upto GeV. In the low energy region, reactions of the type (p,n), (p,γ) and (p,α) are observed.

$$^{27}_{13}\text{Al}\,(p,\gamma)\,^{28}_{14}\text{Si} \tag{8.41}$$

$$^{23}_{11}\text{Na}\,(p,n)\,^{23}_{12}\text{Mg} \tag{8.42}$$

$$^{9}_{4}\text{Be}\,(p,\alpha)\,^{6}_{3}\text{Li} \tag{8.43}$$

$$^{7}_{3}\text{Li}\,(p,\alpha)\,\alpha \tag{8.44}$$

Last mentioned reaction is of historical significance by which experimental proof for Einstein's mass energy relationship was obtained. In this reaction ^{7}Li was bombarded with low energy (≈0.5 MeV) protons. The resulting intermediate $^{8}_{4}$Be is very unstable nuclide. It disintegrates into two α particles. Since masses of $^{7}_{3}$Li, p and α are accurately known as 7.016004, 1.007825 and 4.002603 amu respectively, Q for this reaction can be calculated as 0.01862 amu = 17.35 MeV. Knowing the KE of p and α, Q value is calculated and the value is 17.33 MeV. This proves that whatever mass is lost in the reaction $^{7}_{3}\text{Li} + p \rightarrow 2\alpha$, equivalent energy is liberated as Q of the reaction.

Another interesting reaction is

$$^{11}_{5}\text{B} + p \rightarrow \left[\,^{12}_{6}\text{C}\right] \rightarrow 3\alpha \tag{8.45}$$

It is an example of multiple particle production. When proton energy is more than 20 MeV, excitation energy of the compound nucleus will be sufficient to emit more particles leading to more than one evaporation residues. In Fig. 8.2 excitation function for proton induced reaction with ^{63}Cu is shown. In the case of proton induced reaction, (p,n) exit channel is prominent upto 15 MeV of proton energy. Around 15 MeV, (p,pn) channel competes with (p,n) channel. Around 25 MeV, (p,n) channel becomes negligible where as (p,pn), (p,2n) and (p,p2n) channels become prominent. If the energy is further increased compound nucleus formation becomes less probable and direct reactions may take place.

Deuteron Induced Reactions

Deuteron is an interesting projectile as it is a loosely bound system with a low binding energy of only 2.22 MeV. Deuteron reactions in the low energy region are often of the type (d,n) or (d,p), i.e. one nucleon is ejected and the other one is retained by the target nucleus. In most of the cases, Q-value is positive.

$$^{12}_{6}\text{C}\,(d,p)\,^{13}_{6}\text{C} \tag{8.46}$$

$$^{31}_{15}\text{P}\,(d,p)\,^{32}_{15}\text{P} \tag{8.47}$$

$$^{7}_{3}\text{Li}\ (d,n)\ ^{8}_{4}\text{Be} \tag{8.48}$$

$$^{9}_{4}\text{Be}\ (d,n)\ ^{10}_{5}\text{B} \tag{8.49}$$

There are other reactions in which particles other than n and p are produced.

$$^{16}_{8}\text{O}\ (d,\alpha)\ ^{14}_{7}\text{N} \tag{8.50}$$

Very interesting reaction is deuteron on deuteron target in which (d,p) and (d,n) channels are observed.

$$\text{d(d,p)}\ ^{3}_{1}\text{H} \tag{8.51}$$

$$\text{D(d,n)}\ ^{3}_{2}\text{He} \tag{8.52}$$

CN formed is ^{4}He and both the exit channels leading to p and n production are probable.

Photon Induced Reactions

Reactions leading to disintegrations by photon are called photo-disintegration reactions or photon nuclear reactions. Since binding energy of deuterium is very low, if energy greater than 2.22 MeV is supplied to deuterium nucleus, in principle it has to be disintegrated into proton and neutron. When deuterium is exposed to γ-rays, neutrons are produced. This reaction can be represented as

$$^{2}_{1}\text{H}\ (\gamma,n)\ ^{1}_{1}\text{H} \tag{8.53}$$

Similarly neutron in ^{9}Be is very loosely bound. By irradiating with photons of at least 2.62 MeV, (γ,n) reaction takes place

$$^{9}_{4}\text{Be}\ (\gamma,n)\ ^{8}_{4}\text{Be} \tag{8.54}$$

If the photon energy is not sufficient to excite the nucleus to virtual levels, particle emission is not possible. However, the nucleus dissipates energy by deexcitation. Such reactions are represented as (γ,γ′)

$$^{83}\text{Kr}\ (\gamma,\gamma')\ ^{83}\text{Kr} \tag{8.55}$$

$$^{199}\text{Hg}\ (\gamma,\gamma')\ ^{199}\text{Hg} \tag{8.56}$$

Photons of high energy (>10 MeV) are produced by allowing accelerated electrons to fall on metallic targets such as tungsten. These photons are useful to study photo nuclear reactions.

$$^{31}_{15}\text{P}\ (\gamma,n)\ ^{30}_{15}\text{P} \tag{8.57}$$

At higher energies, reactions of the types (γ,np) and (γ,2n) are probable. If the energy is greater than 25 MeV, photon induced reaction of ^{12}C leads to production of three α's.

$$^{12}C + \gamma \rightarrow 3\alpha \qquad (8.58)$$

The reaction 8.58 is interesting and provides proof for Eiensteins relation of mass-energy equivalence. In this, reaction energy is converted to mass. Let us examine the masses before and after the reaction

Mass of ^{12}C = 12.00000 amu

Mass of 3 α particles = 3 x 4.002603 = 12.007809 amu

Mass of the reactants is lower than mass of the products. This gain in mass resulted after absorbing energetic photon (25 MeV)

Heavy Ion Induced Reactions

Projectiles heavier than α are called heavy ions. Accelerators are the sources for production of these ions. Reactions involving heavy ions have higher V_c. Thus energy required is higher than the reactions induced by p, d and α. This will result in higher E^* for CN. Therefore, large number of exit channels are possible in these reactions. This topic itself is a special subject and detailed discussion is beyond the scope of this book. However, a few examples are cited here

$$^{14}_{7}N\left(^{14}_{7}N,^{13}_{7}N\right)^{15}_{7}N \qquad \text{transfer reaction} \qquad (8.59)$$

$$^{93}_{41}Nb\ (^{12}C,2n)\ ^{103}_{47}Ag$$

$$(^{12}C,\alpha)\ ^{101}_{44}Rh \qquad \text{Case of many exit channels} \qquad (8.60)$$

$$(^{12}C,\alpha)\ ^{103}_{46}Pd \text{ etc.}$$

Heavy ion reactions are very effectively used for the production of higher Z elements such as Bk and Cf. After a few nucleons' evaporation from the compound nucleus, these elements are formed. Without going into further discussion, a few examples are cited below:

$$^{238}_{92}U\left(^{14}_{7}N,\alpha 5n\right)^{253}_{97}Bk \qquad (8.61)$$

$$^{238}_{92}U\left(^{12}_{6}C,6n\right)^{244}_{98}Cf \qquad (8.62)$$

$$^{240}_{94}Pu\left(^{12}_{6}C,4n\right)^{248}_{100}Fm \qquad (8.63)$$

$$^{244}_{96}Cm\left(^{13}_{6}C,4n\right)^{253}_{102}No \qquad (8.64)$$

$$^{252}_{98}Cf\left(^{10}_{5}B,5n\right)^{257}_{103}Lr \qquad (8.65)$$

$$^{242}_{92}Pu\left(^{22}_{10}Ne,4n\right)^{260}_{104}Rf \qquad (8.66)$$

$$^{243}_{95}\mathrm{Am}\left(^{22}_{10}\mathrm{Ne},4\mathrm{n}\right)^{261}_{105}\mathrm{Db} \quad (8.67)$$

$$^{249}_{98}\mathrm{Cf}\left(^{18}_{8}\mathrm{O},4\mathrm{n}\right)^{263}_{106}\mathrm{Sg} \quad (8.68)$$

$$^{209}_{83}\mathrm{Bi}\left(^{54}_{24}\mathrm{Cr},\mathrm{xn}\right)^{263-\mathrm{xn}}_{107}\mathrm{Bh} \quad (8.69)$$

$$^{208}_{82}\mathrm{Pb}\left(^{58}_{26}\mathrm{Fe},\mathrm{xn}\right)^{266-\mathrm{xn}}_{108}\mathrm{Hs} \quad (8.70)$$

$$^{209}_{83}\mathrm{Bi}\left(^{58}_{26}\mathrm{Fe},\mathrm{xn}\right)^{267-\mathrm{xn}}_{109}\mathrm{Mt} \quad (8.71)$$

$$^{208}_{82}\mathrm{Pb}\left(^{62}_{28}\mathrm{Ni},^{1}_{0}\mathrm{n}\right)^{269}_{110}\mathrm{Ds} \quad (8.72)$$

It may be noted that the exit channels mentioned above are favourable channels out of many possible channels. In the above reactions projectile energy is maintained to just cross the Coulombic barrier leaving the CN with 20-40 MeV of excitation. In these reactions, another competing and prominent exit channel is nuclear fission.

Recommended names for elements 104, 105, 106, 107, 108, 109 and 110 are Rutherfordium (Rf), Dubnium (Db), Seaborgium (Sg), Niels Bohrium (Bh). Hassium (Hs), Meitnerium (Mt) and Darmstadtium (Ds) respectively.

Direct Reactions

In this type of reactions the incident projectile collides with one, or at most a few nucleons in the target nucleus, some of which may thereby be directly ejected. Alternately incident particle may leave the target nucleus after losing a part of its energy in a few collisions. Thus compound nucleus is not formed and the kinetic energies of the emitted particles are usually higher than those evaporated from compound nucleus.

Transfer Reactions

The most common type of direct reactions are pick up like (p,d) or stripping like (d,p) and (d,n) reactions which are collectively referred to as transfer reactions. In such reactions, the target like product is formed in discrete angular momentum states and, therefore, the outgoing particle is preferentially emitted at a particular angle. The spectra of outgoing particles, therefore, show pronounced resonances corresponding to discrete energy states being populated in product nucleus and angular distributions are peaked in forward direction and have structures indicative of angular momentum effects. Transfer reactions are, therefore, useful for determination of energy, spin and parity of excited states of nuclei.

Bibliography

1. R.D. Evans, The Atomic Nucleus, Tata-McGraw-Hill Book Co., New York (1978).

2. G. Friedlander, J.W. Kennedy, E.S. Macias, J.M. Miller, Nuclear and Radiochemistry, 3rd Ed., John Wiley & Sons Inc., New York (1981).

3. S. Glasstone, Sourcebook on Atomic Energy, 3rd Ed., Affiliated East West Press Pvt. Ltd. (1967).

4. I. Kaplan, Nuclear Physics, 2nd Ed., Addision Wesley, Cambridge, Massachusetts (1963).

5. Nuclear Chemistry, Vols. 1 and 2, Ed. L. Yaffe, Academic Press, New York (1968).

6. Frontiers in Nuclear Chemistry, Eds. D.D. Sood, A.V.R. Reddy, P.K. Pujari, IANCAS Publication, Mumbai (1996).

7. E. Rutherford, *Phil. Mag.*, **6(XXVII)** (1913) 488.

8. I. Curie and F. Joilot, *Compt. Rend.*, **198** (1934) 254.

9. C.W. Li, W. Whaling, W.A. Fowler and C.C. Lauritsen, *Phys. Rev.*, **83** (1951) 512.

10. J.M. Blatt and V.F. Weisskopf, Theoretical Nuclear Physics, Wiley, New York (1952).

11. N. Bohr, *Nature*, **137** (1936) 344.

12. W.U. Schroeder and J.R. Huizenga, *Ann. Rev. Nucl. Sci.*, **27** (1977) 465.

13. S. Hofmann et al., *Z. Phys.*, **A350** (1995) 277.

14. G.T. Seaborg, *Ann. Rev. Nucl. Sci.*, **18** (1958) 53.

Chapter 9

Nuclear Fission and Nuclear Fusion

Soon after the discovery of radioactivity at the turn of the last century, the possibility that the atom could be a source of enormous energy was realised. Rutherford and Soddy suggested that all atoms possess large amounts of energy. They wrote in 1903 "...the energy latent in the (radioactive) atom must be enormous compared with ordinary chemical change. Now the radioelements differ in no way from other elements in their chemical and physical behaviour ... Hence there is no reason to assume that this enormous store of energy is possessed by the radioelements alone. It seems probable that atomic energy in general is of a similar high order of magnitude, although the absence of (radioactive) change prevents its existence being manifested". Now it is clear that the above statement is prophetic. Atom is indeed a store house of energy and in exo-energic nuclear reactions like nuclear fission and nuclear fusion, enormous amount of energy is released.

In nuclear fission, a heavy nucleus like ^{235}U, when bombarded with thermal neutrons, undergoes division releasing a large amount of energy of about 200 MeV[1]. This process is also accompanied by the emission of 2 to 3 neutrons which makes it possible to have a chain reaction (see Chapter 10) for sustained production of energy. In nuclear fusion two light nuclei like T and D combine and in the process an energy of 17.6 MeV is released. Energy released in nuclear fusion reaction, is more intense than in the nuclear fission of ^{235}U or ^{239}Pu. The energy released in these two reactions can be explained using the average binding energy curve (Fig. 2.2, Chapter 2). Average binding energy of the products formed in both these reactions, is higher than the average binding energy of the reactants. The large amount of energy released makes the reactions very important in nuclear technology and also in the context of current energy scenario.

[1] In the complete fission of 1 gram of ^{235}U, 8.2×10^{17} ergs of energy is released, which is equal to 1MW of power production per day. To obtain the same amount of energy, 3 tons of coal or 2300L of petrol has to be combustioned. This shows that nuclear energy is more than million times energy intense compared to chemical energy.

Nuclear Fission

Discovery of Nuclear Fission

Discovery of nuclear fission can be traced back to the neutron discovery and the subsequent experiments by Fermi et al. for production of transuranium elements by irradiation of uranium with neutrons. Fermi et. al. reported in 1934 that atleast four activities distinguished by their half lives, could be identified. On absorption of a neutron, ^{238}U becomes ^{239}U and ^{239}U undergoes β decay to form element 93. β decay of element 93 results in the formation of element 94. It thus appeared that several activities resulted with atomic number 93, 94 and may be higher. These results attracted the attention of many chemists. Ida Noddack criticised those results, conjectured the process of breaking the nucleus subsequent to the absorption of neutron and proposed that activities that were observed by Fermi et.al could be due to isotopes of known elements. It is history, now, that she did not pursue her ideas further. With an objective of separating the invisible amounts of new activities formed, chemists tried to separate them by using carriers with similar chemical properties; e.g. Ba carrier for Ra, La carrier for Ac and so on. Hahn and Strassmann separated three new activities along with barium and proposed that these could be isotopes of radium. Daughter products of these were separated with lanthanum carrier and attributed to actinium isotopes. But all the time they were having a problem of understanding the possibility of (n,α) reaction on ^{238}U to form radium isotopes. Joliot Curie and Savitch using fractional crystallisation found that activities remained with lanthanum fraction rather than with barium fraction and concluded that the new isotope was of lanthanum rather than that of actinium. These results were not acceptable to Hahn and others. Hahn and Strassmann carried out detailed work on separation of Ra and Ba using fractional crystallisation. To their bewilderment, they found that activity was inseparable from barium fraction and daughter product activity was inseparable from lanthanum fraction. Very reluctantly and cautiously they reported the results in January 1939, stating that these new activities were due to isotopes of Ba, La and Ce and not due to Ra, Ac and Th as reported earlier. They also suggested that this could happen only if fragmentation of the nucleus occurred. They performed another series of experiments to find the possible activities of complementary products of Ba and La around mass number A = 90-100 and atomic number 35. They could separate isotopes of Sr (Z=38), Y (Z=39) and Kr (36). From these results together with their earlier findings, they could conclude that the nucleus was undergoing division. Hahn was awarded 1944 Nobel Prize in Chemistry for the discovery of the fission of heavy nuclei.

Meitner and Frisch recognised that if a nucleus undergoes division to form two products of comparable mass, the products should fly off with high velocity due to mutual Coulombic repulsion. Total kinetic energy was estimated to be around 200 MeV. Within a fortnight of the announcement by Hahn and Strassmann, Meitner and Frisch experimentally measured high energy release associated with this reaction. This phenomenon of division of nucleus was named as nuclear fission (analogous to the cell division in living organism) by a biologist W.A. Arnold who was working at that time with G. Hevesy in Copenhagen.

Fission Process

Various stages of the fission process starting from compound nucleus formation to the formation of fission products are depicted in Fig. 9.1 A heavy nucleus ($^{A}_{Z}X$) of mass A > 200 such as uranium forms a compound nucleus after absorbing a neutron and acquires certain excitation energy (E^{*}). The compound nucleus ($^{A+1}_{Z}X$) deexcites by (i) emission of prompt gamma rays to its ground state, or (ii) undergoes beta decay and forms an element of higher charge ($^{A+1}_{Z+1}X$) or (iii) undergoes α decay and forms an element of lower charge and mass ($^{A-4}_{Z-2}U$) or (iv) undergoes nuclear fission. Compound nucleus having excitation energy undergoes continuous deformation, in the fission mode. While the nucleus deforms, the repulsive Coulomb energy and attractive surface energy change continuously. When the disruptive Coulombs forces overcome attractive forces due to surface energy, the nucleus undergoes division into two fragments ($^{A1}_{Z1}F1$ and $^{A2}_{Z2}F2$). They move in opposite directions due to mutual Coulombic repulsion which ultimately reflects in their kinetic energy. The fragments are formed in excited state and emit neutrons (ν_1 and ν_2), and gamma rays. Resulting products ($^{A_1\nu_1}_{Z_1}F1$, $^{A_2\nu_2}_{Z_2}F2$) have higher N/Z ratio compared to stable nuclei and undergo β decay to attain stability with stable end products $^{A_1\nu_1}_{Z_3}P1$ and $^{A_2\nu_2}_{Z_4}P2$.

Energy Liberated in Fission

About 200 MeV of energy is liberated in nuclear fission. It can be calculated from the average binding energy of the fissioning nucleus and products. If we recall the average binding energy curve in Chapter 2, compound nucleus ^{236}U has an average binding energy (B/A) of 7.6 MeV. Thus the total binding energy of ^{236}U is equal to 7.6 x 236 = 1793.6 MeV. Similarly the products have B/A around 8.5 MeV. Assuming that the average mass of fission products is around 120, total binding energy of both fragments is equal to 236 x 8.5 = 2006 MeV, which is greater than the binding energy of ^{236}U. The difference, equal to 212.4 MeV, is liberated in the fission process. This is an approximate estimate as exact values of B/A for each fragment are not taken. The most direct method is to calculate the mass difference before and after the fission reaction for a given mass division[2]. Energy liberated in nuclear fission is calculated below from the mass difference between a pair of products and uranium and neutron. e.g. on absorption of a neutron, ^{235}U undergoes division as shown below:

$$^{235}U + n \rightarrow \left[^{236}_{92}U \right] \rightarrow ^{103}_{42}Mo + ^{133}_{50}Sn \qquad (9.1)$$

ΔM (M-A) for ^{235}U, n, ^{103}Mo and ^{133}Sn are 40.914, 8.071, -80.85 and -70.97 MeV respectively. The Q value for this mass division is calculated as

---

[2]Mass division in nuclear fission is not unique. Therefore, the products need not be same for energy fissioning atom of ^{235}U. Accordingly energy released will not be same in each split.

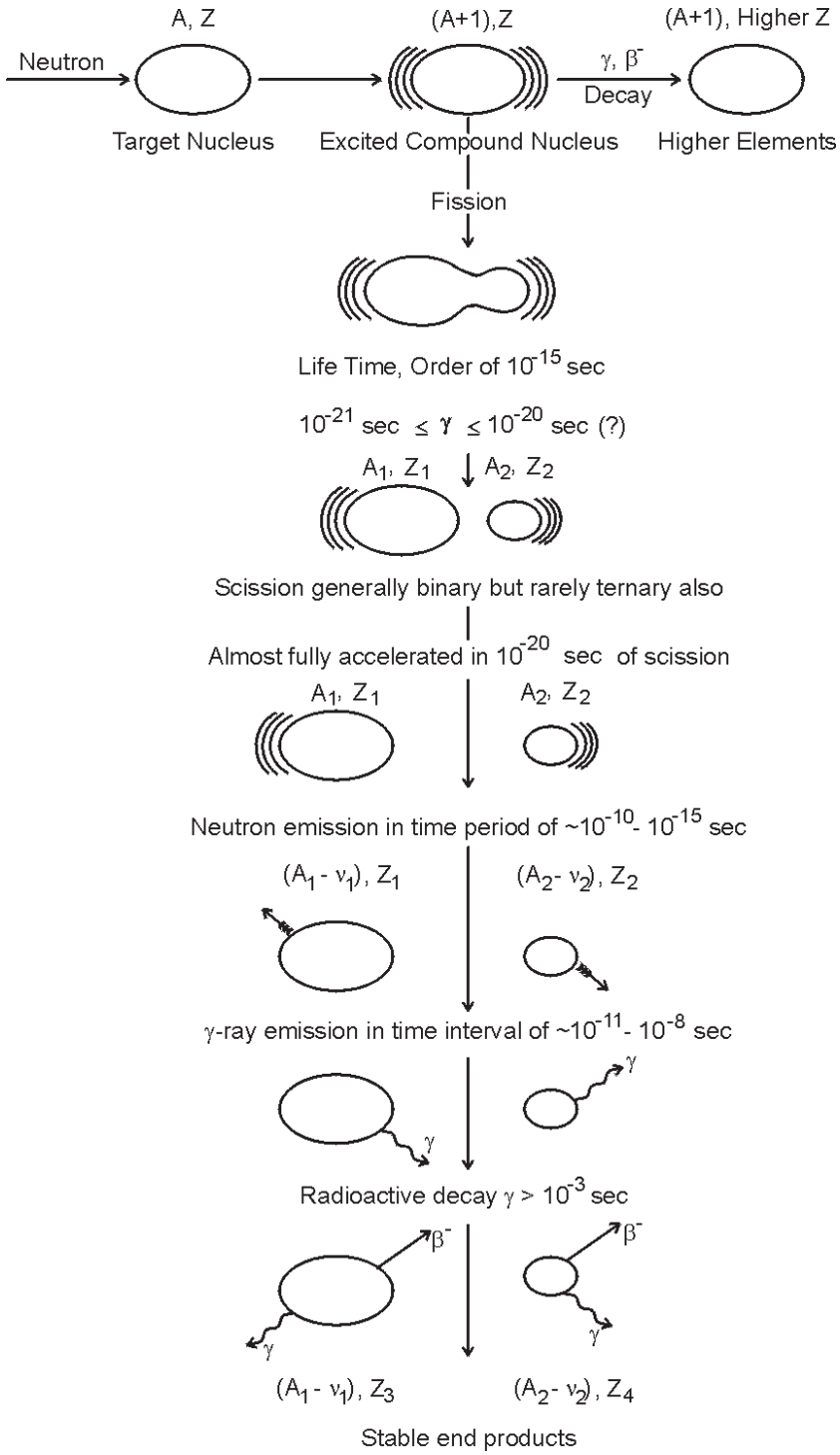

Fig. 9.1 Schematic diagram of fission process.

$$Q = (\Delta m)\, c^2$$

$$= \left(M_{^{235}U} + M_n\right)c^2 - (M_{^{103}Mo} + M_{^{133}Sn})c^2$$

$$= \Delta M_{^{235}U} + \Delta M_n - \Delta M_{^{103}Mo} + \Delta M_{^{133}Sn} = 200.81 \text{ MeV}$$

On an average for different mass divisions, 'Q' value is about 200 MeV. The energy liberated in the fission process appears in several forms. It is approximately distributed into the kinetic energy of the fragments (168 MeV), kinetic energy of the prompt neutrons (5 MeV), prompt gamma ray energy (7 MeV), beta energy (8 MeV), neutrino energy (12 MeV) and gamma ray energy from the products (7 MeV).

Fission Cross-Sections

Fission cross sections (σ_f) are larger for the nuclides with odd neutron number nuclides. e.g., ^{235}U, ^{239}Pu and ^{242}Am. In the case of light mass nuclides like ^{169}Tm and ^{197}Au, σ_f for thermal neutron induced reaction is very low and not measurable. However, these nuclides undergo nuclear fission when bombarded with 30-40 MeV charged particles like α and p. In such cases, neutron emission and other particle emission are competing exit channels. In contrast, nuclear fission is the main reaction in the case of thermal neutron induced reactions of actinide nuclides. The σ_f values for $^{235}U(n_{th},f)$ and $^{239}Pu(n_{th},f)$ are 583 b and 742 b respectively. In the energy region upto 0.1 eV, σ_f follows 1/v law, where v is the neutron velocity. At neutron energies around 1 MeV and greater, σ_f becomes fairly independent of neutron energy and is around l-2 b. With increase in neutron energy, σ_f increases by a step function. A typical excitation function for neutron induced fission of ^{238}U is shown in Fig. 9.2. With increase in kinetic energy of projectiles, it is possible to produce nuclear fission in lighter elements around $Z \geq 85$.

Fission Barrier

Minimum energy required for a nucleus to undergo fission is called fission barrier or critical energy. It is some what similar to activation energy in a chemical reaction where in an activated intermediate is formed which might lead to the formation of products in the chemical reaction. In the case of nuclear fission, a fissioning nucleus has to attain a critical shape, similar to a saddle, for the nucleus to undergo fission. This intermediate structure has more potential energy (PE) compared to the PE of the nucleus in ground state. Difference between these two PE's is called fission barrier. If the E^* of CN exceeds the fission barrier, then fission reaction can take place. e.g., fission barrier of ^{235}U is 5.6 MeV. After absorbing a thermal neutron it forms a CN ^{236}U with an excitation energy of 6.5 MeV. Therefore, ^{235}U is fissionable with thermal neutrons. Nuclides which undergo fission with neutrons of all energies, including thermal neutrons are called fissile nuclides. It can be shown that this barrier height depends on Z^2/A of fissioning nucleus. The larger the value of Z^2/A, lesser is the barrier height. These aspects are discussed in fission theory. Experimentally fission barriers are determined for a large variety of actinide nuclides. One of the methods is to use

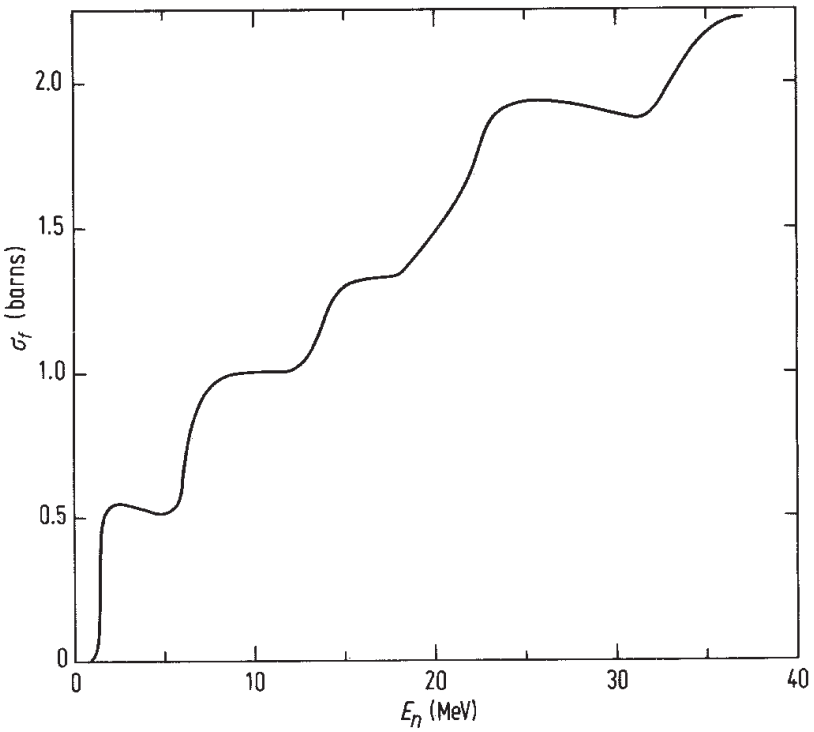

Fig. 9.2 Fission cross-section of ^{238}U for neutron upto 37 MeV [Nuclear and Radiochemistry, G. Friedlander, J.W. Kennedy, E.S. Macias and J.M. Miller, 3rd Ed., John Wiley (1981) p.160].

photons of different energies and measure the fission product activity so as to locate fission threshold.

Fission Theory

Meitner and Frisch explained the fission process using the liquid drop model of the nucleus. Bohr and Wheeler gave a quantitative explanation of the fission process in their classic paper of 1939. It is postulated that nuclear attractive forces tend to keep the nucleus in stable state akin to the surface tension to maintain liquid drop in a stable form resisting distortion. For a drop of liquid to be broken into two smaller drops or for a nucleus to undergo fission, there must be considerable distortion which will be only possible if additional energy is available. A nucleus like ^{235}U after absorbing a thermal neutron forms a compound nucleus and the binding energy gained is available to the CN as excitation energy. This E^* is the driving force to cause distortion of nucleus. Fission is viewed as a continuous evolution of nuclear shape starting from nearly spherical compound nucleus to two well separated fragments. Considering the nucleus as an uniformly charged sphere, the potential energy associated with the nuclear deformation is calculated. The binding energy of the nucleus

based on LDM is calculated as the sum of volume, Coulombic, surface, asymmetric and pairing energies. During deformation of a nucleus only Coulombic (E_c) and surface energies (E_s) are modified and are given below

$$E_s = E_s^0 \left(1 + \frac{2}{5}\alpha_2^2\right) \tag{9.2}$$

$$E_c = E_c^0 \left(1 - \frac{1}{5}\alpha_2^2\right) \tag{9.3}$$

where, α_2 is the deformation parameter along the symmetric axis. E_s^0 and E_c^0 are surface and Coulombic energies of spherical liquid drop nucleus of charge Z and mass A and are given by

$$E_s^0 = 17.94 \left(1 - 1.7826 \left[\frac{A - 2Z}{A}\right]^2\right) \cdot A^{2/3} \text{ MeV} \tag{9.4}$$

$$E_c^0 = 17.94 \frac{0.71\, Z^2}{A^{1/3}} \text{ MeV} \tag{9.5}$$

From eqns. 9.2 and 9.3, the changes in E_s and E_c are given by

$$\Delta E_s = E_s - E_s^0 = \frac{2}{5}\alpha_2^2 \cdot E_s^0 \tag{9.6}$$

$$\Delta E_c = E_c - E_c^0 = -\frac{1}{5}\alpha_2^2 \cdot E_c^0 \tag{9.7}$$

These changes ΔE_s and ΔE_c reflect in the potential energy of the nucleus. With increase in deformation, potential energy of the nucleus increases due to ΔE_s and decreases due to ΔE_c. The potential energy variation as a function of deformation is shown in Fig. 9.3. The transition point of balance of magnitudes of ΔE_s and ΔE_c corresponds to the maximum potential energy, known as saddle point, which the nucleus must pass to undergo fission. The scission point is the configuration at which nucleus will undergo division. The potential energy excess over the ground state energy is called fission barrier; as shown in Fig. 9.4. Fission barriers for actinides are in the range of 5 to 7 MeV. From eqns. 9.6 and 9.7, it is expected that the nucleus undergoes fission when $|\Delta E_s| = 2\,|\Delta E_c|$. Fissility parameter ($\chi$), a measure of the tendency of a nucleus to undergo to fission is derived from the above condition as

$$\chi = \frac{E_c^0}{2\,E_s^0} \simeq \frac{Z^2}{50.13\,A} \tag{9.8}$$

For χ less than unity, the nucleus is stable with respect to small distortions. For the nuclides with $\chi > 1$, there will be no potential energy barrier to inhibit spontaneous division of the

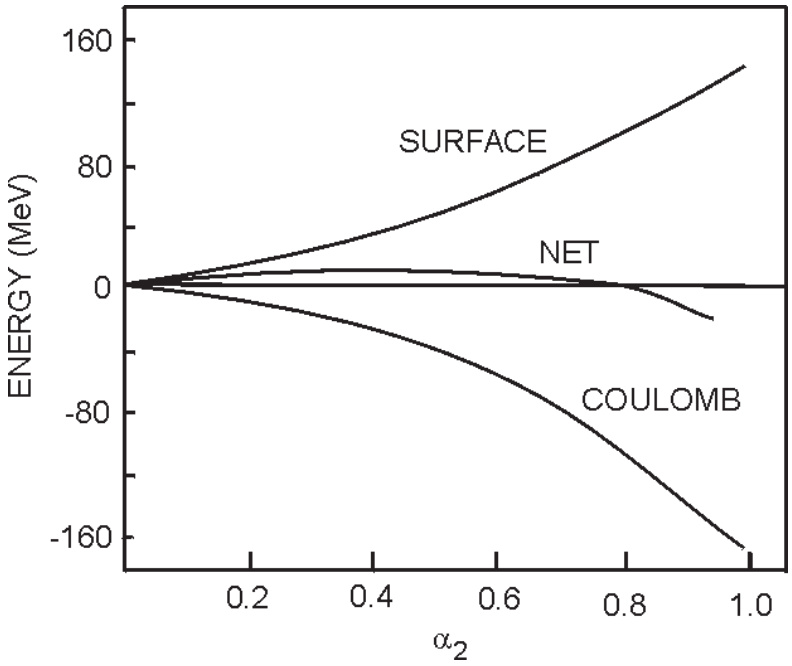

FIg. 9.3 Surface, Coulombic and net deformation energies as a function of α_2.

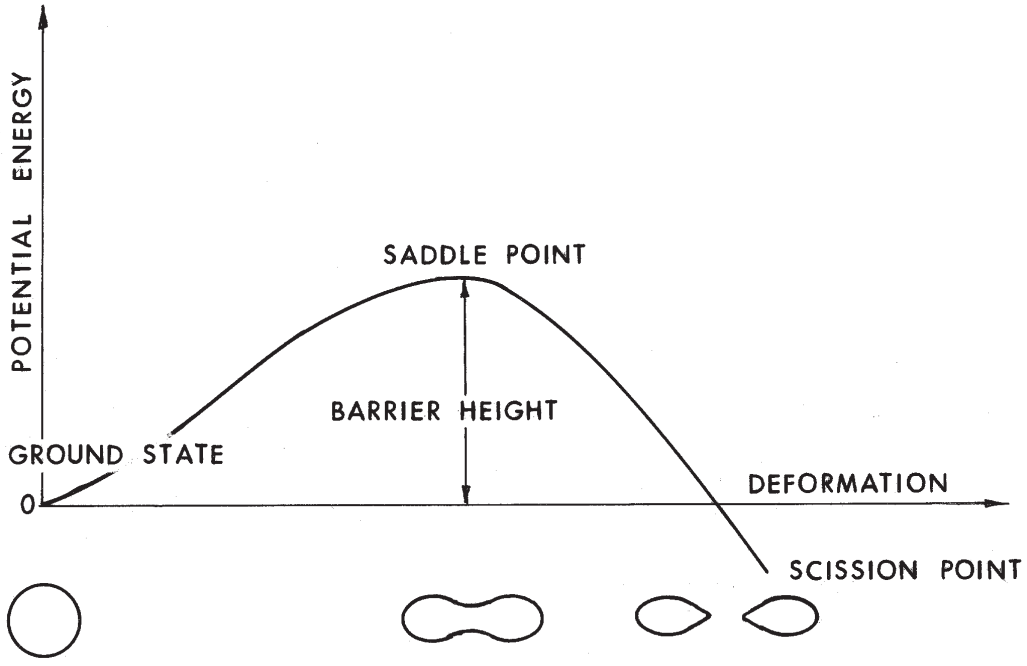

Fig. 9.4 Liquid drop potential energy as a function of deformation.

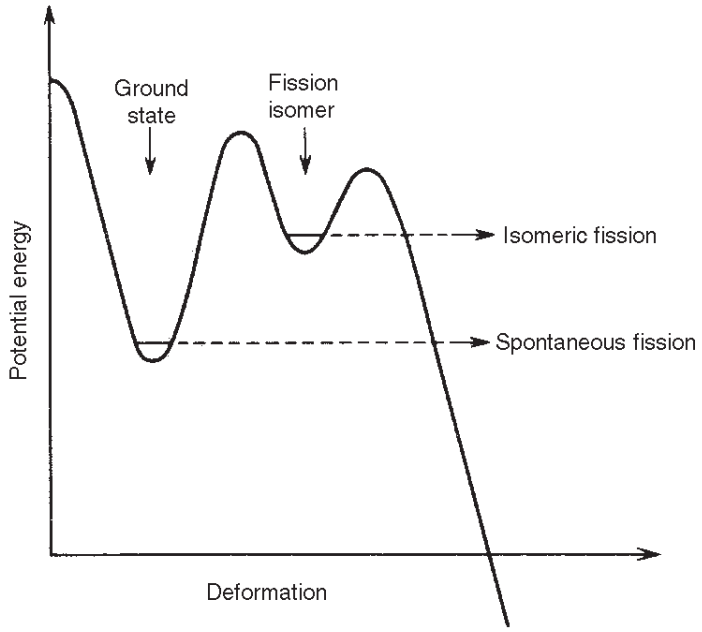

Fig. 9.5 Potential-energy diagram showing double-humped fission barrier [Nuclear and Radiochemistry, G. Friedlander, J.W. Kennedy, E.S. Macias and J.M. Miller, 3rd Ed., John Wiley (1981) p.73].

nucleus. It corresponds to a Z^2/A value > 50. Using eqn. 9.8, it can be estimated that around Z=115 and A=265, all nuclei undergo fission instantaneously. This puts a limit for extending the periodic table.

This model is useful to explain the existence of fission barrier, energy release and other features. However, near constancy of barrier height for actinides, asymmetric mass division, existence of fission isomers etc. could not be addressed by this model. By superimposing deformation dependent nuclear shell and nucleon pairing energy on LDM potential, Strutinsky calculated the potential energy as a function of deformation. He showed that fission barriers for actinides are double humped as shown in Fig. 9.5. A nucleus encounters two barriers and two valleys before it reaches scission point to undergo fission. For isotopes of elements with Z = 92 to 94, both the barriers are having comparable heights. If a nucleus is trapped between the two barriers of comparable heights, then the nucleus will have a finite life time before it tunnels through one of the barriers. These nuclear states are called 'fission isomers' or 'shape isomers'. If the isomer tunnels through the second barrier, it undergoes fission known as 'isomeric fission' (IF). On the other hand if the same nucleus penetrates first barrier and reaches ground state, then it is called γ-deexcitation. If the nucleus tunnels through both barriers from its ground state and undergoes fission, it is called 'spontaneous fission' (SF). SF is a decay process from ground state and IF can be observed only in the induced reactions. Isomeric fission has very short half lives. e.g., Half lives for IF in the cases of ^{236m}Pu and ^{242m}Am are 0.03 ns and 14 ms, respectively.

Observations

Some of the experimental observations of this complex reaction are :

(i) Nucleus undergoes division giving different products. i.e. the products formed are not same in each division resulting in a mass distribution of the products. Mass number of the fragments varies from 70 to 160 whereas atomic number varies from 30 to 65.

(ii) Similarly the kinetic energy of all the products is not same and, therefore, there is a distribution of kinetic energy. Kinetic energy of the fragments is calculated by measuring the range of the fragments in different media. The range of the fragments in air varies from 1 to 2 cm whereas, it varies from 4 to 6 mg/cm^2 in aluminium.

(iii) For every neutron consumed, two or more neutrons are produced in the fission and this aspect was investigated with keen interest which resulted in the demonstration of nuclear chain reaction (see Chapter 10 for details). Neutrons produced in each division are different and so is their kinetic energy. On an average 2.41 neutrons are produced in the thermal neutron induced fission of ^{235}U.

(iv) On an average 8 to 9 prompt gamma rays are emitted in each fission. Prompt gammas have an energy distribution.

(v) Reaction probability (cross section) for fission of ^{235}U is much larger with thermal neutrons than with fast neutrons which could be understood in terms of 1/v law dependence of cross sections for neutron induced reactions.

(vi) Nuclei having odd number of neutrons (^{235}U, ^{239}Pu etc.) are more fissile compared to those having even number of neutrons (^{238}U, ^{240}Pu etc.). This can be explained by considering the excitation energy of the compound nuclei in the cases of ^{235}U and ^{238}U and the fission barriers associated with them. The excitation energy of ^{236}U*, formed by the addition of thermal neutron to ^{235}U, is 6.5 MeV whereas the fission barrier is 5.6 MeV. The absorbed neutron pairs with the unpaired neutron of ^{235}U and pairing energy is released. On the other hand the excitation energy of ^{239}U* is 4.9 MeV whereas the fission barrier is 6.1 MeV. Therefore, fast neutrons of about 1.2 MeV are needed to cause fission in ^{238}U where as thermal neutrons (0.025 eV) are sufficient to cause fission in ^{235}U.

(vii) Some fission products such as ^{87}Br and ^{136}I emit neutrons. These neutrons are emitted after some delay (after β decay) and, therefore, called delayed neutrons.

In the β-decay of fission products like ^{87}Br, the daughter product is ^{87}Kr (neutron number is 51 which is +1 of magic number 50). Neutron emission from the excited states of nuclides like ^{87}Kr is probable as the resulting product ^{86}Kr will be stable as it has a neutron magic number 50. There are five prominent groups of delayed neutrons as shown in Table 9.1 and these neutrons play an important role in the control of nuclear reactors.

Table 9.1 Yields of delayed neutrons in the thermal neutron induced fission of ^{233}U, ^{235}U and ^{239}Pu

Half-life (s)	% of delayed neutrons			Energy (MeV)
	^{233}U	^{235}U	^{239}Pu	
0.43	0.018	0.085	0.04	0.40
1.52	0.062	0.241	0.105	0.67
4.51	0.086	0.213	0.112	0.41
22.0	0.058	0.166	0.094	0.57
55.6	0.018	0.025	0.012	0.25
Total	0.24	0.73	0.36	

Delayed neutron emitters are clustered just above N = 50 and 82 closed neutron shells, as a result of low binding energy for the last odd neutron.

Measurements on mass yields, kinetic energy, neutron emission, prompt gamma emission, cross sections, angular distribution of fragments etc. constitute the experimental investigations in nuclear fission. Mass, kinetic energy and charge distribution studies are discussed in what follows:

Mass Distribution

The mass and charge of the products formed in the fission are in the range of A=70-160 and Z=30-65, having a wide range in the yields (0.0001 % to 7%), as shown in Fig. 9.6. The nature of the yield distribution of the products is predominantly asymmetric with maximum yield of about 7%. The peaks are around A=90-100 in the lighter mass region and around A=134-144 in the heavier mass region. Interestingly the yield around A=117 corresponding to the symmetric mass division is low (0.01%). The two peaks and the valley are the features of the mass distribution in the low energy fission.

There are about 400 fission products with half lives ranging from less than a second to tens of years. Fission products are neutron rich compared to the stable nuclides of the same mass number and undergo β^- decay. A typical isobaric chain A=135 is given here alongwith half lives of isobars.

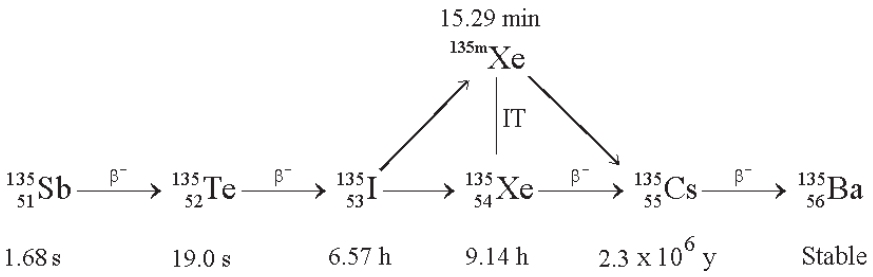

(9.9)

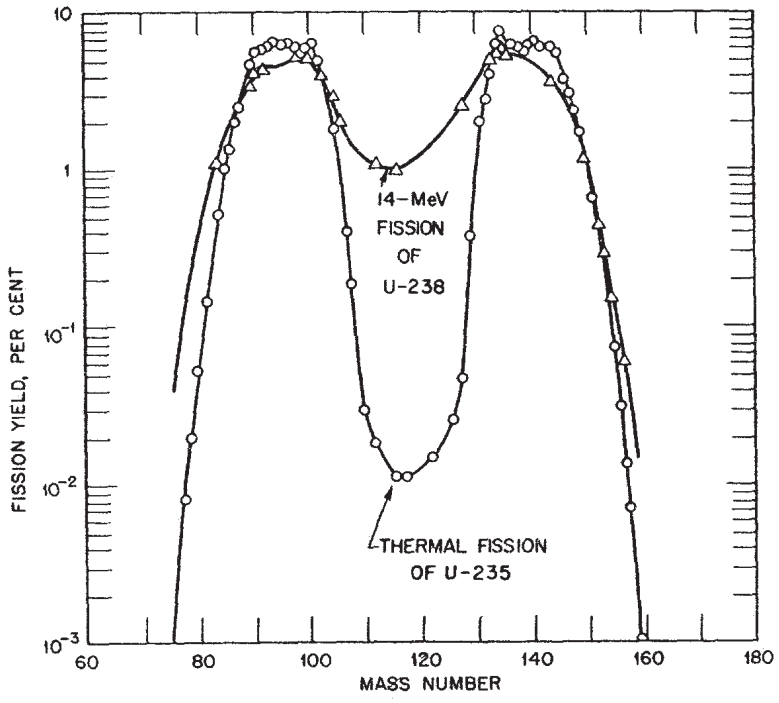

Fig. 9.6 Fission yield as a function of mass number for thermal-neutron fission of ^{235}U and 14 MeV neutron fission of ^{238}U [S. Glasstone, Sourcebook on Atomic Energy, 3rd Ed., Affiliated East West Press Pvt. Ltd. (1967) p.483].

The sum of yields of members of an isobaric chain (e.g., A = 135) is called mass yield of that chain. Yield of each individual product is called its independent yield. In the case of A=135,

$$\text{Independent yield of } {}^{135}_{51}\text{Sb } (IY_{51}) = \frac{\text{No. of } {}^{135}\text{Sb atoms formed}}{\text{Total fission atoms}} \qquad (9.10)$$

$$\text{Mass yield of A} = 135 = IY_{51} + IY_{52} + IY_{53} + ... + IY_{56} \qquad (9.11)$$

To determine the yields experimentally, the number of atoms of a given mass formed in fission have to be estimated. Radiochemical measurements are commonly used for this.

A target of the fissile isotope, e.g., ^{235}U is prepared on a suitable backing. It is irradiated in a reactor with a known neutron flux (ϕ). The products formed are absorbed in a catcher such as aluminium foil. The activities of the individual products are measured either by direct gamma ray spectrometry or by measuring the activities of the radiochemically separated products from the catcher foils. The activity of a given mass (A_i) is related to mass yield (Y_i) by eqn. 9.12.

$$A_i = N \sigma \phi Y_i \left(1 - e^{-\lambda_i t}\right) \qquad (9.12)$$

where, N is the number of fissile atoms in the target, σ is the fission cross-section, ϕ is the neutron flux, λ_i is the decay constant of the product i, and t and T are the periods of irradiation and cooling respectively.

The yields of many masses have to be determined to obtain the mass yield curve. The yields are plotted as a function of mass of the product and the area under the curve is summed and normalised to 200%. From the normalised curve, yields of the products are obtained that could not be determined experimentally.

More than 70% of the yields are concentrated in two groups around A=90-100 and A=134-140. In the low energy fission, mass distribution is predominantly asymmetric and heavy peak position is around mass 139-140 which is attributed to the influence of double magic shell configuration (deformed shells). In the case of neutron induced fission of ^{239}Pu, the heavy peak position remains same as that in ^{235}U (n_{th}, f) where as the light peak gets shifted to right by about 3 mass units.

The width of the distribution of the two peaks is around 12-14 mass units. The peak to valley ratio for ^{235}U (n_{th},f) is about 600 and decreases with increasing mass of the fissioning nucleus. When the kinetic energy of the projectile (n,p,α..) is increased, the yields in the valley start increasing and at around E=100 MeV, mass yield distribution is a single peaked i.e. symmetric division becomes more probable.

Charge Distribution

In a given mass chain there are many isobars. For example in the case of A=135, as described by eqn. 9.9, there are 6 isobars that contribute to the mass yield. Each isobar is formed with a definite yield in the fission process, known as independent yield (as defined in eqn. 9.10). Each isobar is having a different charge or atomic number. The distribution of independent yields of different charges for a given isobaric chain, is called charge dispersion or charge distribution. Charge distribution in low energy fission is characterised by most probable mass (Z_p) and width of the distribution (σ_z), and the independent yield of each charge is represented by eqn. 9.13.

$$\text{I.Y.} = \int_{Z-0.5}^{Z+0.5} \frac{1}{\sqrt{2\pi\sigma^2}} \exp\left(\frac{(Z - Zp)^2}{2\sigma^2} \right) dz \qquad (9.13)$$

By measuring more than two independent yields, Z_p and σ_z can uniquely be determined. Z_p is discussed in terms of displacement from the unchanged charge distribution (Z_{UCD}) of fissioning nucleus. σ_z values reflect the influence of the nuclear shell effects and nucleon pairing. Radiochemical separations are very useful in charge distribution investigations.

Kinetic Energy Distribution

Kinetic energy of the fragments is in the inverse proportion to their masses. The heavier fragments have lower kinetic energy with peak around 70 MeV and the lighter fragments have higher kinetic energy with peak around 100 MeV. In low energy fission, the

two fragments fly off in opposite direction to conserve momentum. From momentum conservation, it can be shown that kinetic energy ratio is in the inverse ratio of masses. Kinetic energy is determined by measuring the ranges of the fragments in a medium such as aluminium. The average total kinetic energy lies in the range of 160 to 190 MeV. Appreciable change in the kinetic energy is not observed with increase in the energy of the projectile

Spontaneous Fission

Spontaneous fission (SF) is a process akin to radioactive decay, in which division of a nucleus takes place without fission reaction being induced. In fact for many actinide isotopes, SF competes with α-decay. Therefore, reaction rates are calculated in terms of $N\lambda$, λ being the decay constant for SF. Mass distribution, kinetic energy distribution, neutron emission and γ-emission are very similar in both neutron induced fission and SF. As discussed earlier, SF becomes a dominant mode of decay in heavier elements. In the case of $^{238}_{92}U$, half lives for SF and α decay are 10^{16} y and 4.5×10^{9} y respectively, where as in the case of ^{252}Cf these values are 85 y and 2.85 y respectively. SF becomes a major decay mode for isotopes of elements with $Z > 100$ and half lives would be as low as a few s to ms. From these data, it can be concluded that with higher Z and A, $t_{1/2}$ for SF decreases rapidly. SF can be understood as a decay process in which a nucleus from ground state tunnels through the fission barriers. It is depicted in Fig. 9.5 in which potential energy is mapped as a function of symmetric deformation (α_2) parameter.

Charged Particle Induced Fission

Nuclear fission can be induced by charged particles such as p and α. Unlike in the case of neutrons, charged particle induced reactions have a Coulombic barrier (V_c). For example, p induced fission of ^{232}Th has a V_c around 11 MeV and unless that much energy is supplied, fission does not take place. In the case of α induced fission of ^{232}Th, V_c is around 22 MeV. The compound nucleus is ^{236}U. Energy of α should be $\geq 22 \times 236/232$ MeV for fission reaction to take place. It results in a large excitation energy to the CN (^{236}U). When the excitation energy is more than the energy required for particle emission, particles like n, p and α are emitted prior to fission. In the case of 30 MeV α induced fission of ^{232}Th, E^* is equal to 24.92 MeV. Hence $^{236}U^*$ can either undergo fission or emit a neutron leaving the residual nucleus ^{235}U with around 17 MeV excitation energy, which can also undergo fission. This fission is called second chance fission. ^{235}U also can emit a neutron leaving its residual nucleus ^{234}U with around 9 MeV excitation energy. If ^{234}U undergoes fission, then it is called third chance fission as depicted in Fig. 9.7

It is difficult to differentiate the first chance, second chance and third chance fissions. Valley region in the mass yield curve gets filled up in medium energy fission and eventually the mass distribution becomes symmetric with increasing energy of the projectile.

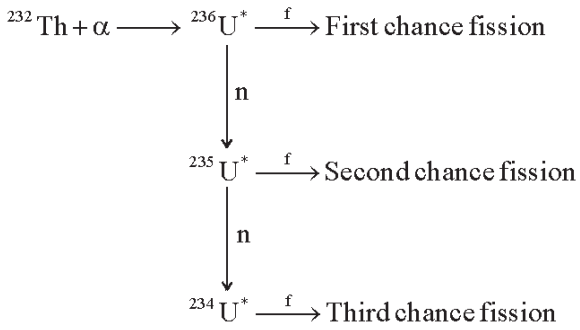

Fig. 9.7 Schematic view of multi chance fission in $^{232}Th + \alpha$

Nuclear Fusion

Nuclear reactions between nuclei of low mass number like p, D, T, ^{3}He and ^{4}He are exoenergic reactions. These being charged particles, face Coulombic barrier. These reactions are brought about by accelerating one of the nuclei. Acceleration is required to attain sufficient kinetic energy to surmount the Coulomb barrier between the reacting nuclei. These reactions are called fusion reactions and are accompanied by the release of energy. e.g., D-T reaction is accompanied by the release of 17.6 MeV of energy. Due to this high energy release, fusion reactions are important to meet the energy requirements of the mankind, if they can be achieved on earth in a sustainable manner. To have practical value, the energy released should be more than the energy consumed. Thermonuclear reactions occurring in the sun and stars are nuclear fusion reactions and are sources of light and heat to mankind. Sun emits electromagnetic radiation at a rate of 4×10^{23} ergs/s and can continue to supply energy for about another 10^{11} years at this rate.

Reactions in the Sun and Stars

Vast amount of energy released by the sun and stars cannot be accounted by chemical reactions and now it is recognised that these are due to nuclear fusion reactions. For fusion of smallest nuclei, e.g., isotopes of hydrogen, the Coulomb barrier is about 0.7 MeV and it corresponds to a temperature of 10^8 K. The reacting atoms (ions) have to be heated and maintained at this temperature for fusion to take place and sustain. At high temperature, gas will be in the form of completely ionised system known as plasma. There are two sets of reactions to account for the energies in stars and sun: Carbon cycle and proton-proton (p-p) chain. In the carbon cycle, carbon acts as a catalyst to facilitate the combination of 4 protons to form a helium nucleus. In p-p chain, starting from p-p interaction, with a series of intermediate reactions, helium nucleus is formed.

Carbon Cycle

The following sequential set of reactions take place in the carbon cycle.

$$^{12}C + p \rightarrow {}^{13}_{7}N + \text{energy} \qquad (9.14)$$

$$^{13}N \rightarrow {}^{13}C + \beta^{+} \quad (9.15)$$

$$^{13}C + p \rightarrow {}^{14}N + \text{energy} \quad (9.16)$$

$$^{14}N + p \rightarrow {}^{15}O + \text{energy} \quad (9.17)$$

$$^{15}O \rightarrow {}^{15}_{7}N + \beta^{+} \quad (9.18)$$

$$^{15}N + p \rightarrow {}^{12}C + {}^{4}He \quad (9.19)$$

In the final step ^{12}C is regenerated and the net reaction is

$$4\ p \rightarrow {}^{4}He + 2\beta^{+} + 26.7\ \text{MeV} \quad (9.20)$$

p-p Chain

The following sequential set of reactions take place in the p-p chain.

$$p + p \rightarrow D + \beta^{+} + \text{energy} \quad (9.21)$$

$$D + p \rightarrow {}^{3}He + \text{energy} \quad (9.22)$$

$$^{3}He + {}^{3}He \rightarrow {}^{4}He + 2p + \text{energy} \quad (9.23)$$

On adding all the reactions, the net result is same as shown in eqn. 9.20, namely the formation of, ^{4}He nucleus from 4 protons.

At low temperatures, p-p chain predominates and as the temperature increases, carbon chain becomes significant. In the sun with an interior temperature of about 1.5×10^{7} K, p-p chain predominates, but at temperatures above 2×10^{7} K, the carbon cycle provides most of the energy.

Fusion Reactions on Earth

The first man made application of light-element fusion reactions came with the development of thermonuclear explosive or hydrogen bomb[3]. Intensive efforts are focused towards achieving controlled thermonuclear reactions in a number of countries.

---

[3]Thermonuclear reactions in stars proceed at a rather slow pace and are thus unsuitable for man-made thermonuclear energy release, whether it takes place explosively in thermonuclear explosive bombs or more slowly in magnetic plasma confinement devices. D-T and D-D reactions were first studied and used in explosive devices. Since in both the cases hydrogen isotopes are used, the name 'hydrogen bomb' is in vogue for thermonuclear explosive devices. Tritium is produced continuously in thermonuclear explosion itself using ^{6}Li D as follows.

$D + T \rightarrow {}^{4}He + n + 17.6\ \text{MeV}$

$^{6}Li + n \rightarrow {}^{4}He + T + 4.8\ \text{MeV}$

To take care of neutron loss and to sustain this chain reaction, it is coupled with a neutron multiplier like ^{238}U or ^{9}Be. ^{6}LiD when used in conjunction with ^{238}U, it produces large amounts of radioactive fission products.

The goal of nuclear fusion research is to develop fusion power plants to generate electricity. It is certain that carbon chain and p-p reactions are difficult to sustain with the available materials for containment of reacting plasma. The promising nuclear fuel for fusion would be hydrogen isotopes deuterium and tritium. Deuterium constitutes 0.0153% of natural hydrogen and can be extracted from water inexpensively. Tritium can be made from lithium by nuclear reactions. The deuterium from one litre of water can produce as much energy as produced in the combustion of 300 L of gasoline. That is why it is said that "deuterium in ocean waters in large quantities is good enough to serve as an inexhaustible source of fuel for fusion reactors".

Some Fusion Reactions and Excitation Functions

A few important reactions which could be of use in controlled fusion are given in the following

$$^{2}H + {}^{2}H \rightarrow {}^{3}He + n + 3.3\ MeV \quad (9.24)$$

$$^{2}H + {}^{2}H \rightarrow {}^{3}H + p + 4.0\ MeV \quad (9.25)$$

$$^{2}H + {}^{3}H \rightarrow {}^{4}He + n + 17.6\ MeV \quad (9.26)$$

$$^{2}H + {}^{3}He \rightarrow {}^{4}He + p + 18.3\ MeV \quad (9.27)$$

$$p + {}^{6}Li \rightarrow {}^{3}He + {}^{4}He + 4.0\ MeV \quad (9.28)$$

$$p + {}^{7}Li \rightarrow {}^{4}He + {}^{4}He + 17.3\ MeV \quad (9.29)$$

Excitation functions for reactions 9.24 - 9.27 are shown in Fig. 9.8. All the reactions have threshold energy and generally cross section rises steeply with increasing energy of the projectile. In the case of D-T reaction, threshold is minimum, and cross section is about 5b at 100 keV. Energy released in the reaction is shared by the products as kinetic energy. In the D-T reaction, of the 17.6 MeV, kinetic energy of ^{4}He and n are 20% and 80% respectively. As mentioned earlier, Coulomb threshold for this reaction is 0.7 MeV and it corresponds to a temperature in the vicinity of 10^{8} K. Both D and T have to be heated and maintained at 10^{8} K for this reaction to sustain. There is no material to contain the plasma at this temperature.

In a D-T reaction based fusion reactor, the supply of reactants is proposed through a breeding cycle for n and T using LiD blankets.

$$D + T \rightarrow {}^{4}He + n$$

$$n + {}^{6}Li \rightarrow {}^{4}He + T$$

Most of the fusion energy would appear in the form of heat in the lithium blanket and power would presumably be extracted by circulating the lithium through a heat exchanger to produce steam for driving a turbine.

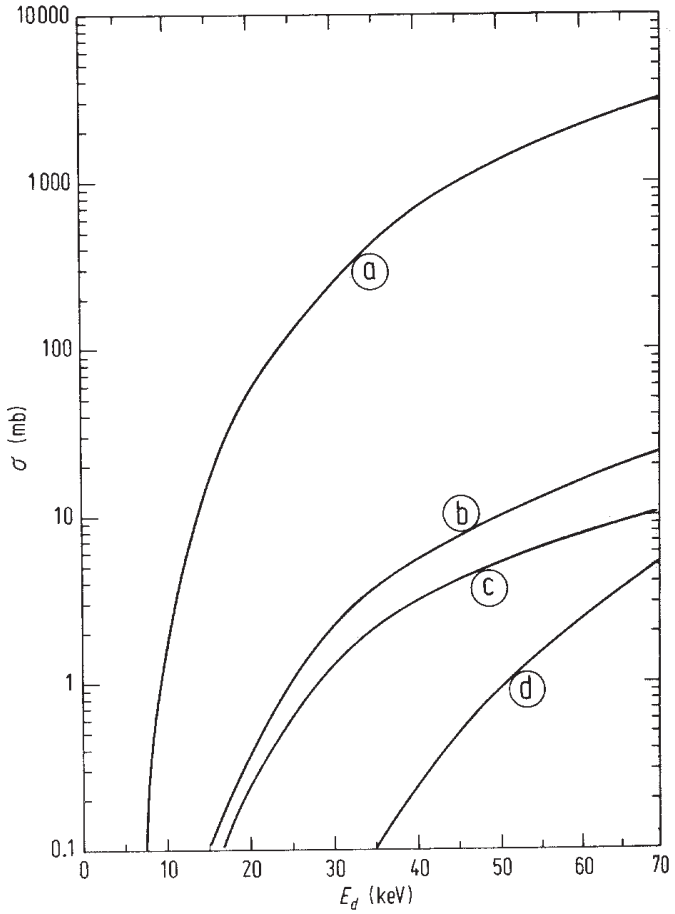

*Fig. 9.8 Excitation functions of some light-element fusion reactions. Curve (a) is for the d-t reaction, curves (b) and (c) are for the d-d reactions and curve (d) is for the d + ^{3}He reaction [R.F. Post, Ann. Rev. Nucl. Sci., **20** (1970) 509].*

Conditions for Fusion

For every reaction, ignition temperature has to be reached in order to achieve fusion ignition. Ignition temperature is defined as the temperature at which the rate of energy production by fusion overtakes the rate of energy loss by Bremsstrahlung radiation produced in close collisions between electrons and nuclei. The ignition temperature for D-T reactions is the lowest and is about 4 x 10^7 K. The plasma produced has to be confined until the break-even point between the energy input and output is reached. It can be expressed as a minimum value for the product of plasma density and confinement time. This product is a constant for a given fusion reaction. e.g. for D-T reaction, it is 10^{14} s/cm^3, and it is known as Lawson Criterion. By keeping high plasma density of the order of 10^{20}-10^{24}/cm^3 for a confinement time of 10^{-6}-10^{-10}s, fusion can be achieved. It should be remembered that along

with Lawson Criterion, ignition temperature has also to be attained for sustaining fusion reaction. Two methods are under study for plasma confinement : (1) magnetic confinement and (2) inertial confinement

Magnetic Confinement

In magnetic confinement, extremely powerful electromagnets are used to contain and insulate fuel plasma. Confinement devices are known as 'magnetic bottles'. In experiments of the 'Tokamak' type, a very high current is induced in a ring shaped plasma contained in toroiodal shape container. Auxiliary heating by microwaves or radiowaves is used to reach temperatures of several hundred million degrees for a few seconds. These values are closer to what is needed in a fusion power plant. Limitations on attainable magnetic fields and other problems limit plasma densities in the range of 10^{12}-10^{17} cm^{-3}. Although in some devices, the D-T ignition temperatures could be reached with best possible efforts, Lawson Criterion is yet to be reached.

Inertial Confinement

In inertial confinement, a high plasma density is produced by using high powered, pulsed beams of lasers for a very short period of time. Pulsed laser beams are directed simultaneously on a pea sized fuel pellet of deuterium tritide (DT) causing it to implode to produce high densities in the range of 10^{25}-10^{26} atoms/cc. Shock wave heating would ignite the pellet. When the fuel is compressed, its inertia holds it together long enough for fusion reactions to occur. In a power plant, it is expected to have about 100 or more pellets explode per second, each producing an energy of 10^{7} J in a time of about 10^{-11} s, in a large chamber. This heat would be used to generate electricity. Neutrons generated would be absorbed in a lithium blanket.

Lasers of various types (Nd, CO_2, iodine) each capable of delivering about 10^{12} w have been developed. In Lawrence Livermore Laboratory, 20 Nd Laser trains capable of delivering 1.2 x 10^{12} w for 0.1 ns are focused on a pellet. It is hoped that technological advances in material science might help to develop structural materials for these reactions, and efficient laser beams to produce power in fusion reactors.

International Thermonuclear Experimental Reactor (ITER) is a joint effort of European Atomic Energy Community, the Government of Japan, the Government of Russian Federation and the Govt. of USA. In about ten years, after ITER built, it is hoped to demonstrate controlled ignition and extended energy production. There are many potential advantages of fusion energy as it is produced from an inexpensive fuel, safe energy source of electricity generation, minimal radioactivity production and environmental friendly.

Bibliography

1. R. Vandenbosch and J.R. Huizenga, Nuclear Fission, Academic Press, New York (1973)

2. E.K. Hyde, Fission Phenomenon in The Nuclear Properties of Heavy Elements, Prentice-Hall Press, Englewood Cliffs, New Jersey (1964).

3. Nuclear Chemistry, Vol. 1 and 2, Ed. L. Yaffe, Academic Press, New York (1968).

4. G. Friedlander, J.W. Kennedy, E.S. Macias and J.M. Miller, Nuclear and Radiochemistry, 3rd Ed., John Wiley & Sons Inc., New York (1981).

5. S. Glasstone, Sourcebook on Atomic Energy, 3rd Ed., Affiliated East West Press Pvt. Ltd. (1967).

6. R.D. Evans, The Atomic Nucleus, Tata-McGraw-Hill Book Co., New York (1978).

7. I. Kaplan, Nuclear Physics, 2nd Ed., Addision Wesley, Cambridge, Massachusetts (1963).

8. J.A. Maniscalco, *Ann. Rev. En.*, **5** (1980) 33.

9. G.A. Cowan, *Sci. Ans.*, **235(1)** (1976) 36.

10. M. Brack et al., *Rev. Mod. Phys*., **44** (1972) 320.

11. O. Hahn and F. Strassmann, *Nature*, **27** (1939) 11.

12. N. Bohr and J. Wheeler, *Phys. Rev*., **55** (1939) 1124.

13. V.M. Strutinsky, *Nucl. Phys*., **A95** (1967) 420.

14. A.V.R. Reddy, Ph.D. Thesis, Sri Venkateswara University (1986).

Chapter 10
Nuclear Reactors

Nuclear reactor is a device in which the fission chain reaction takes place, in a controlled manner, for the production of energy and neutrons. Nuclear fission is the source of energy in a nuclear reactor. In addition to energy, the fission reaction also generates neutrons which are essential for sustaining fission chain reaction. The nuclear reactor is thus a strong source of neutrons. Nuclear reactors are broadly classified as research reactors and power reactors based on their utilisation. In a research reactor the emphasis is on production of neutrons and their utilisation. The energy released by fission is rarely used and is discharged into the environment. In a nuclear power reactor the role of neutrons is only to sustain nuclear chain reaction. In the process, large amount of energy is released which results in the production of heat and is used for electricity generation. Research reactors are extensively used for the production of radioisotopes which have a variety of applications in agriculture, medicine and industry. Research reactors are also used for activation analysis, neutron beam research and silicon doping. Nuclear power reactors are among the major sources of electricity in the world. Currently 438 nuclear power reactors supply about 18 percent of electricity in the world. Nuclear reactors are a clean source of electricity and do not contribute to green house gas emission. If the electricity currently produced by nuclear reactors were to be produced by coal/oil fired plants, there would be additional 2.3 billion tonnes of CO_2 discharged into the atmosphere annually.

Physical Principles

Nuclear Physics Aspects

As mentioned in Chapter 9, fission of each ^{235}U nucleus by neutrons results in the production of about 200 MeV of energy and on an average about 2.42 neutrons. A chemical analogue for energy production is the reaction of carbon (coal) with oxygen to give CO_2 in which 393 kJ of energy is released per gram atom of C (6.023×10^{23} atoms of C). This corresponds to 4.08 eV of energy per C atom. In either case the energy is released by conversion of mass into energy as per Einstein equation $E = mc^2$. However, in a chemical reaction the energy released per atom is very small and the resultant change in mass is negligible. Fission reaction is thus a very concentrated source of energy. Fission of 1 gram of

uranium atoms releases energy equivalent to that released by burning three tonne of coal or 2,300 litres of fuel oil.

Natural uranium has three isotopes namely ^{234}U (0.0054%), ^{235}U (0.7204%) and ^{238}U (99.2742%). Of these, ^{235}U is the main isotope responsible for fission in all uranium fuelled reactors. This is because the compound nucleus ^{236}U formed by thermal neutron absorption gains excitation energy, which is higher than the fission barrier and results in the fission of ^{235}U. Therefore, neutrons of all energies can cause fission of ^{235}U nucleus, and such nuclei are called fissile nuclei. In the case of ^{238}U the compound nucleus formed by thermal neutron capture gains an energy which is less than its fission barrier by about 1 MeV. Therefore, ^{239}U does not split unless the incoming neutron has an energy of about 1 MeV. This aspect is seen clearly by the excitation function plot for the fission of ^{235}U and ^{238}U nuclei as shown in Fig. 10.1.

For ^{235}U it is seen that the fission cross-section is a few hundred barns for neutron of 0.025 eV energy (thermal neutrons, 298 K) and only 1.2 b at 2.5 MeV. For ^{238}U, fission cross-section is negligible till neutron energy reaches 1 MeV and is 0.6 b at 2.5 MeV of neutron energy. The heavier nucleus of uranium is thus not fissile.

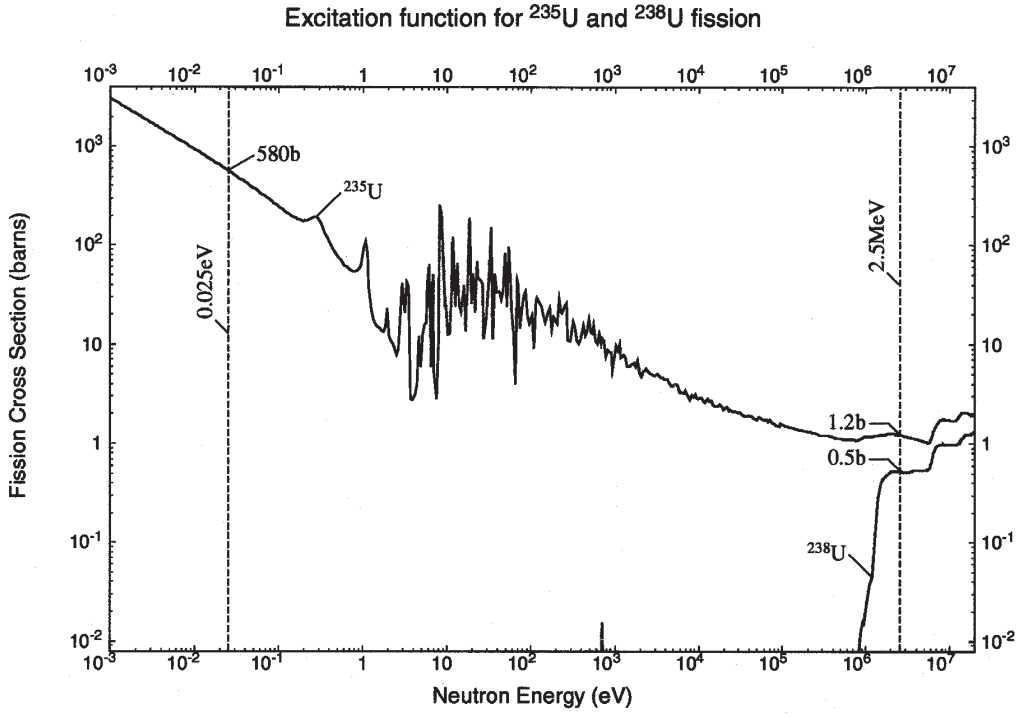

Fig. 10.1 Cross-section of fission reaction induced by neutrons on fissile ^{235}U and fertile ^{238}U nuclei in 640-group presentation. Data are taken from ENDF/B-IV evaluated data library [Courtesy Nuclear Data Section, IAEA, Vienna].

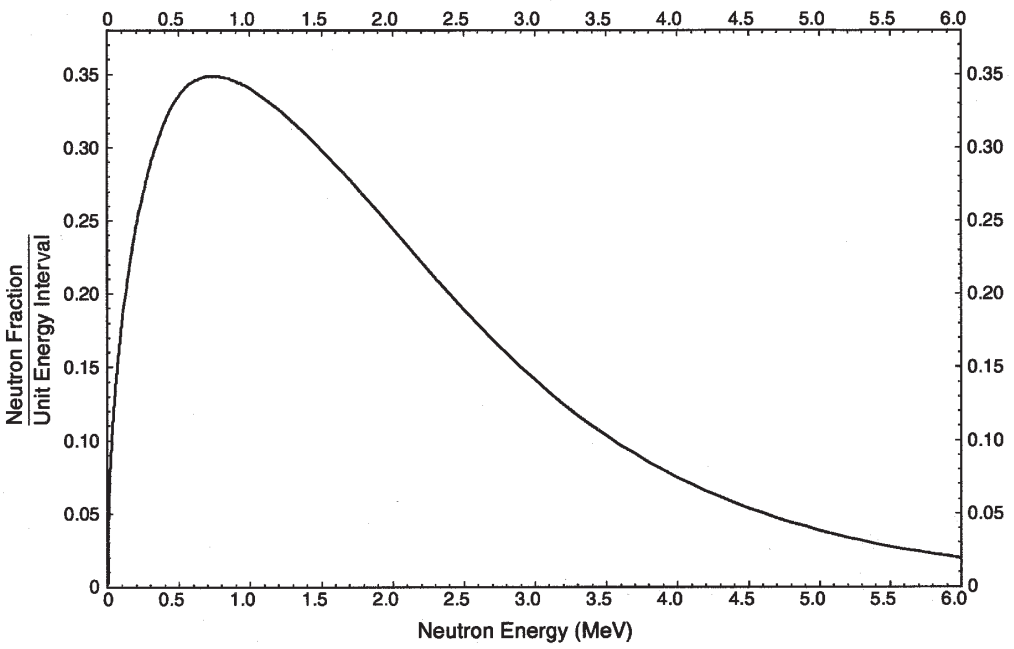

Fig. 10.2 Energy distribution of prompt neutrons formed in fission of ^{235}U induced by neutrons with incident energy 1 MeV. Data are taken from ENDF/B-VI evaluated data library [Courtesy Nuclear Data Section, IAEA, Vienna].

It is also seen that for ^{235}U fission, neutrons of lower energy are more than 200 times as efficient as the neutrons of higher energy. As the chain reaction is maintained by the neutrons produced during fission it is useful to look at the energy of neutrons generated during fission. In the fission reaction, the energy of neutrons is quite variable. A typical energy spectrum for fission neutrons is given in Fig. 10.2. It is seen that bulk of the neutrons have energy in the range of 1-2 MeV. The average neutron energy is approximately 2 MeV.

For sustaining the chain reaction, one has to consider the number of fissile atoms (N), fission cross section (σ) and neutrons produced in each fission. With 0.72% ^{235}U, it is not possible to sustain a fission chain reaction in natural uranium with neutrons generated in fission. Increase of ^{235}U concentration to >10% is required for that purpose. However, it is possible to sustain fission reaction with natural uranium if the energy of neutrons is brought down (neutrons are moderated) as σ increase dramatically with low energy neutrons (Fig. 10.1). Most of the reactors operating in the world use moderated neutrons. The reactors which do not use moderated neutrons are called fast reactors, and these require higher concentration of a fissile isotope as the fission cross-section is in the region of 1-2 barns. In a reactor, neutron energy varies over a wide range. Typical neutron energy spectra for a light water reactor (LWR) and a fast breeder reactor (FBR) are shown in Fig. 10.3.

For slowing down the neutron moderators are required. Elastic and inelastic collisions of neutrons with nuclei are used for moderation. As discussed in Chapter 8, maximum

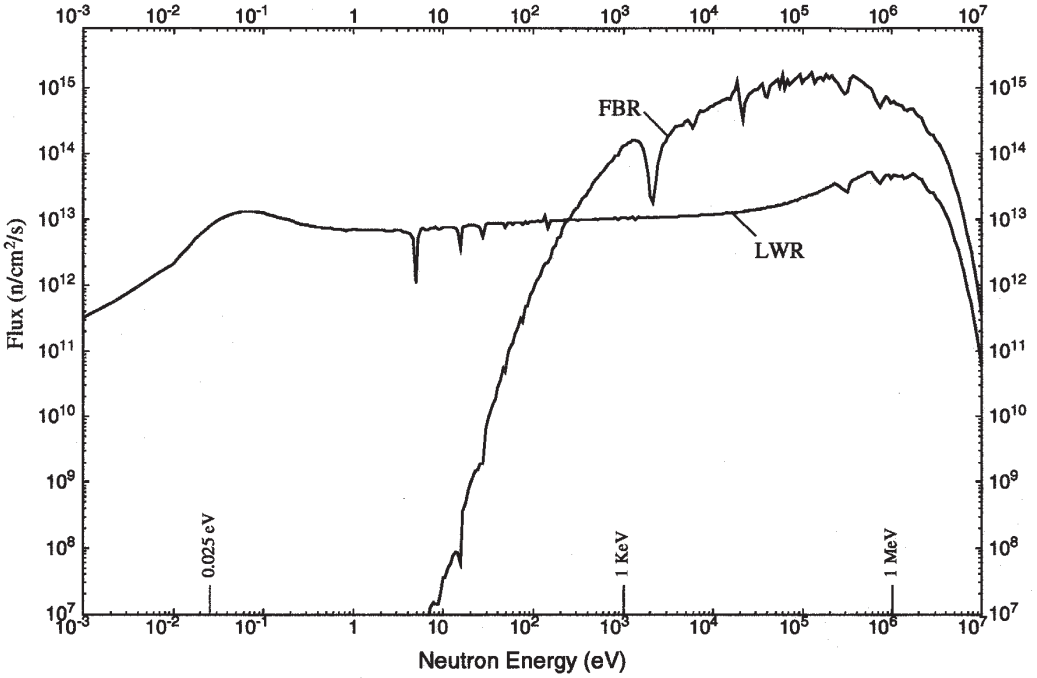

Fig. 10.3 Typical neutron flux density spectra (per unit of energy) for a light water reactor (VVR-1000) and fast breeder reactor (BN-350) [Courtesy Nuclear Data Section, IAEA, Vienna].

energy transfer from a projectile to a target occurs when the two masses are identical or similar. Natural water which contains large quantity of hydrogen is thus used for moderation. The energy of a 1 MeV neutron can be brought down to 0.025 eV in about 18 collisions with hydrogen atoms. Unfortunately, hydrogen is also a good absorber of slow neutrons (σ_c = 0.33 b), resulting in the loss of neutrons.

The use of natural water in a reactor thus requires enhancement of ^{235}U content of uranium. This can be avoided by using other light elements or isotopes which have low neutron absorption cross-section. These include D (σ_c = 0.0005 b) in the form of heavy water (D_2O) and C (σ_c = 0.003 b) in the form of graphite. For water cooled reactor one has to enrich either uranium in ^{235}U content or water in deuterium content. Beryllium (σ_c = 0.0076 b) in the form of beryllium metal or BeO, has also been used in some cases. Number of collisions required to bring neutron energy from 1 MeV to 0.025 eV are 24 for D and 111 for C.

The average energy of thermalised neutrons is dictated by the temperature of the medium. For 298 K it is about 0.025 eV. The average speed of neutrons is given by $13000\sqrt{T}$ cm/s where T is temperature in Kelvin. At 298 K this is 2.2 x 10^3 m/s.

Not all ^{235}U nuclei which absorb a neutron undergo fission. Sometimes the compound necleus ^{236}U deexcites by gamma emission. Typical cross section data for ^{235,238}U and ^{239}Pu

Table 10.1 - Reaction cross-section data (barns) for fissile isotopes

Properties	Isotopes		
	^{233}U	^{235}U	^{239}Pu
Thermal Neutrons (E_n = 0.0253 eV)			
$\sigma_{fission}$	529	585	749
$\sigma_{capture}$	46	99	271
Neutron per fission (ν_p)	2.49	2.42	2.87
Fast Neutrons (E_n = 1.5 MeV)			
$\sigma_{fission}$	1.85	1.24	1.95
$\sigma_{capture}$	0.034	0.0880	0.032
Neutron per fission (ν_p)	2.65	2.56	3.08

(Courtesy Nuclear Data Section, IAEA, Vienna).

with thermal and fast neutron are given in Table 10.1. Uranium-238, which is the major isotope in uranium present in a reactor also undergoes (n,f) and (n,γ) reactions. Cross section for (n,f) reaction with thermal neutrons is negligibly small, and for (n,γ) is significant. The (n,γ) reaction leads to the production of plutonium as

$$^{238}_{92}U + ^{1}_{0}n \rightarrow ^{239}_{92}U \xrightarrow[23.45\ min]{\beta^-} ^{239}_{93}Np \xrightarrow[2.3565\ d]{\beta^-} ^{239}_{94}Pu \qquad (10.1)$$

Plutonium-239, has a half life of 24,110 years. This isotope, ^{239}Pu, also undergoes fission with neutrons of all energies and is, therefore, a fissile isotope. Uranium-238 is, therefore, called a fertile isotope. Through reaction 10.1, partial regeneration of fissile material in a reactor takes place. In fact, a good fraction of energy (10-20%) in a reactor is produced by fission of ^{239}Pu produced *in situ*. Another fertile isotope is ^{232}Th which is the only isotope present in natural thorium. When thorium is irradiated in a nuclear reactor the following nuclear reaction takes place.

$$^{232}_{90}Th + ^{1}_{0}n \rightarrow ^{233}_{90}Th \xrightarrow[22.3\ min]{\beta^-} ^{233}_{91}Pa \xrightarrow[26.967\ d]{\beta^-} ^{233}_{92}U \qquad (10.2)$$

Uranium-233, has a half-life of 1.592 x 10^5 y. It is also a fissile isotope and an important source of nuclear energy for the future.

As discussed in Chapter 9, in the fission process, a large number of fission fragments with masses around 100 and 135 are produced. These are neutron rich with respect to stable nuclides in that mass region and emit neutrons followed by β^- decay. The fission product

half-lives range from a fraction of a second to several hundred years. The fission process thus leads to the production of highly radioactive products, some of them are quite long lived and safe containment of these within the reactor is one of the essential requirements in any reactor design. Further, even after the fuel is taken out, it is essential to ensure safe disposal of the radioactive waste produced in the process of reactor operation.

Reactor Physics Aspects

The fact that 1 g of ^{235}U is equivalent to 2,300 litres of fuel oil in terms of energy production might give an impression that a car may be equipped with 50-100 g of ^{235}U and this would not require refuelling for its life. However, this is outside the realm of reality. Energy by fission can only be harnessed by maintaining a controlled chain reaction, at a specific rate, in a nuclear reactor. As the chain reaction can only be maintained by ensuring that loss of neutrons due to escape (leakage) and non-fission absorptions is small, the nuclear reactor needs a certain minimum size (or quantity of fuel) called 'cirtical' size. This size depends upon a large number of parameters which are studied in reactor physics. Several tonnes of natural uranium along with adequate quantities of D_2O or graphite, would be required for setting up a nuclear reactor. If the concentration of $^{235}U/^{239}Pu$ is increased, the size can be brought down, but still a certain minimum quantity of fuel is required to sustain the chain reaction. So a nuclear reactor does not ever consume all its fuel as the fission chain reaction will stop if adequate quantity of fissile material is not present. Elementary aspects of reactor physics are discussed in the following sub-sections.

Chain Reaction

Reactor physics deals with the theory of nuclear chain reaction. It is seen from Table 10.1 that fission of each ^{235}U nucleus gives rise to, on an average, 2.42 neutrons. If the fissioning nucleus is surrounded by natural/enriched uranium, some neutrons will react with ^{235}U nuclei and cause more fission, while others may leak out or get captured. Continuation of a chain reaction implies that from each fission at least one more fission event is initiated. In more practical sense, it means a growth in the number of fissions in the initial period and then maintaining a steady state when a desirable power level has been reached.

The factor which characterises a fission chain reaction is called the multiplication factor 'k'. If we assume that the mass of uranium is infinite and there is no leakage of neutrons, the multiplication factor is called k_∞. This depends on four main factors.

(i) When a neutron is absorbed in ^{235}U it can either cause fission or get absorbed to form ^{236}U. If each fission, υ neutron are produced. The net number of neutrons produced per neutron absorbed is called η and is given by:

$$\eta = \upsilon \frac{\sigma_f}{(\sigma_f + \sigma_c)} \qquad (10.3)$$

where σ_f and σ_c are fission and capture cross sections respectively.

(ii) These η neutrons have high energy and some of them can cause fission in ^{238}U and each fission event enhances the number of neutrons. The enhancement factor 'ε' is called the fast fission factor. This is the ratio of number of neutrons produced by fission with neutrons of all energies to the neutron number resulting from thermal neutron fission. The number of neutrons thus increases to ηε.

(iii) These ηε neutrons are slowed down by collisions with the moderator nuclei. But in the process of slowing down they pass through an energy range (5 eV) where ^{238}U has resonance absorption of neutrons. If 'p' is the probability for a neutron to escapes capture during thermalisation, called resonance escape probability, then the number of neutrons reaching the thermal energy are ηε p.

(iv) All the ηεp neutrons are not absorbed in ^{235}U to cause fission. Some of them get absorbed in moderator, coolant, structural materials etc. If 'f', the thermal utilisation factor, is the ratio of number of thermal neutrons absorbed in the fuel to cause fission to the total number of thermal neutrons absorbed by all processes then the multiplication factor k_∞ in the absence of neutron leakage is given by

$$k_\infty = \eta\ \varepsilon\ p\ f \qquad (10.4)$$

(v) Neutron being non-charged particle has high probability for escape and a certain amount of leakage takes place in practical system. If 'P' is the probability that the neutrons will not leak out of the system, then the effective multiplication factor 'k_{eff}' is given by

$$K_{eff} = k_\infty\ P \qquad (10.5)$$

Chain reaction would be possible only if k_{eff} is greater than unity. No chain reaction is possible with $k_{eff} < 1$. This implies that for a given system, the value of P should be high, or in other words neutron escape should be minimised. Value of P would be high if volume to surface area ratio is high since the neutrons are produced throughout the volume but escape only from the surface.

To understand the importance of some of these factors let us take the example of natural uranium metal fuel and graphite moderator. If the two are taken in the powder form and homogeneously mixed, the neutrons produced would readily be thermalised. However, it is not possible to sustain a fission chain reaction as $k_\infty < 1$. For this type of system ε is very small. By having uranium in the form of rods put in a graphite matrix (heterogeneous arrangement), it is possible to obtain k_∞ of about 1.05 and sustain a chain reaction. However, this small value of Δk requires that P is large to keep $k_{eff} = 1$. This type of systems are, therefore, large in size.

In all the reactors the value of P is increased by surrounding the core (the region of fission reaction) by a reflector which scatters the neutrons leaking out back into the core. Heavy water, graphite and beryllium are good reflectors for thermal neutrons. Cobalt or stainless steel are used in fast reactors.

A reactor is always started with the help of a neutron source/sources, e.g., americium-beryllium or Sb-Be sources. The source strength can vary from a fraction of a curie to several curies.

Another source of neutrons in a heavy water moderated reactor is the photoneutron reaction of $^{2}H(\gamma,n)^{1}H$. Binding energy of deuteron is 2.2 MeV and hard gammas emitted by some of the fission products cause this reaction. The effect is similar to that of delayed neutrons except that it lasts longer because of the fairly long half-life of the fission products.

Quite often there is a question regarding the possibility of fission chain reaction in ^{238}U or ^{232}Th. These nuclides require neutrons of atleast 1 MeV (preferably > 2 MeV) to cause fission. A large fraction of neutrons produced in the fission process have energies below 1 MeV. Further, a large portion of neutrons with energy greater than 1 MeV undergo inelastic collisions and their energy is reduced to below the optimum value required for fission in ^{238}U or ^{232}Th. Therefore, k_∞ for such systems can not approach unity and self sustaining chain reaction is not possible

Dynamics of Chain Reaction

To understand the dynamics of fission chain reaction, it is necessary to consider its time behaviour. We can divide time in units of neutron life time or the time between its birth as a fission neutron and ultimate absorption by a nucleus. We could thus estimate the number of neutrons from successive generations. If n neutrons are present in a chain reacting system in generation m, then there would be nk_{eff} neutrons in generation m+1. The number of neutrons gained is

$$\Delta n = n\,(k_{eff} - 1) \tag{10.6}$$

If the neutron life time (generation time) is τ, then the rate of change of neutrons is given by

$$\frac{dn}{dt} = \frac{n(k_{eff} - 1)}{\tau} = \frac{nk_{ex}}{\tau} \tag{10.7}$$

where k_{ex}, is the excess multiplication factor and is a measure of the departure of the system from criticality. Upon integration of eqn. 10.7, one gets

$$n = n_0 e^{t(k_{ex}/\tau)} \tag{10.8}$$

where n_0 is the initial neutron number and n is the number after time t. The ratio τ/k_{ex} is called reactor period T.

$$\therefore\ n = n_0\, e^{t/T} \tag{10.9}$$

The reactor period is thus the time required to change neutron number by a factor e. Larger this period, slower is the change in neutron number with time. In the fission reaction essentially all neutrons are promptly released in about 10^{-14} s. A small fraction β (0.73%) is released by the fission products with mean life of 0.43 to 55.7 s (see Chapter 9). Thus there

are two groups of neutrons, prompt neutrons with multiplication factor of k_{eff} (1-β) and delayed neutron with a multiplication factor of k_{eff} β. k_{eff} (1-β) is unity when k_{eff} = 1.0075 and the reactor is described as prompt critical. For thermalised natural uranium system τ is of the order of 10^{-3} s. If k_{ex} based on prompt neutrons were 0.001 then in 10 s, n would be

$$n = n_0 \, e^{10(0.001/0.001)} = n_0 e^{10} = 22,026 \, n_0 \qquad (10.10)$$

The number of neutrons, and therefore, the power level, would go up by a factor of 22,000 in 10 s. It would require extremely fast acting control systems to control a reactor purely based on prompt neutrons. However, when delayed neutrons are also taken into account the average life time of neutrons increases to 0.1 s. In such a case, the number of neutrons in 10 s would be

$$n = n_0 \, e^{10(0.001/0.1)} = n_0 \, e^{0.1} = 1.1 \, n_0 \qquad (10.11)$$

The increase in neutron number, or power, is only 1.1 times. Thus the delayed neutrons play a very crucial role in slowing down neutron multiplication and making a chain reacting system easily controllable.

At this stage it may be useful to get a feeling for the size of chain reacting systems. For simplicity only bare spherical cores, without any reflector are considered. The radius R of a system capable of self sustaining chain reaction is given by

$$R = M \left(\frac{b}{k_{ex}} \right)^{\frac{1}{2}} \qquad (10.12)$$

Where *M* is migration length, the average distance travelled by a neutron in its life time and b is the shape factor which is π^2 for a sphere. *M* varies from about 7 cm for water medium to 50 cm for graphite. For heterogeneous natural uranium - graphite system k_{ex} = 0.05 and critical radius is, therefore, 702 cm. On the other hand, for a highly enriched system (93% ^{235}U) with k_{ex} ~ 0.5 and water moderation, critical radius would be 30 cm. For natural uranium heavy water system, critical radius is about 300 cm. For highly enriched systems with sodium cooling R is about 30 cm.

The actual size of a reactor is of course dependent upon so many other parameters including the need for having a mechanically stable core with proper arrangements for heat removal and control of chain reaction.

Basic Features of a Nuclear Reactor

There are a number of designs for research and power reactors. However, all reactors have some common overall features (Fig. 10.4). Any reactor consists of an active core in which all, or nearly all, nuclear fissions occur. The fissionable material is contained in this core. For reactors using thermalised neutrons, the core also contains a moderator. The core is surrounded by a reflector material. The combination of core and reflector ensures the

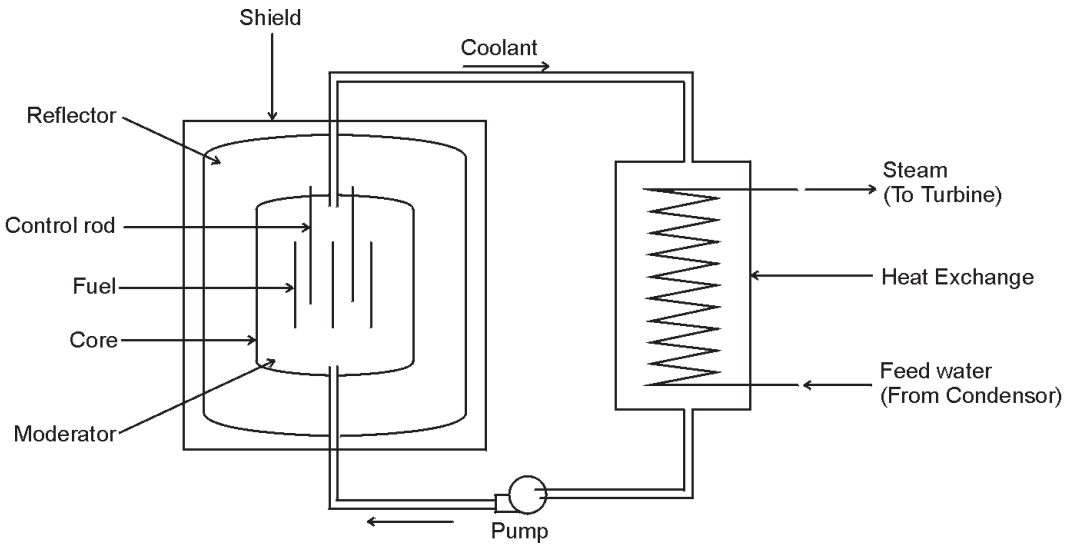

Fig. 10.4 Schematic of a nuclear reactor.

sustenance of fission chain reaction at the required power level. The chain reaction is controlled by having rods of neutron absorbing materials in the core. Essentially in all reactors, particularly power reactors, the core gets heated and a coolant is required to remove the heat. The coolant is cooled in a suitable heat exchanger outside the core and returned back to the reactor. The reactor core and reflector are surrounded by a few meter thick concrete shield which absorbs neutrons, beta rays and gamma rays, coming out of the core-reflector, to protect personnel from radiation exposure. The entire reactor is housed in a leak tight containment to prevent the leakage of radioactivity into the environment should there be an unusual radiation leakage from the reactor. In the current generation of power reactors in India, there is a secondary containment as a measure of added precaution. Further, the power reactors are housed inside an exclusion zone having a radius of 1.6 km. Another zone with a radius of 5 km is a buffer zone in which developmental activity is restricted. These precautions ensure safety of the general public should an untoward incident causes the leakage of radioactivity outside the containment building.

Materials for Nuclear Reactors

The essential materials used in a nuclear reactor are:

(i) Nuclear fuel for sustaining fission reaction

(ii) A sheath/cladding for the fuel such that the fission products, which are radioactive, stay within the fuel and not released into the coolant.

(iii) Moderator for thermalising the neutrons.

(iv) Neutron absorbing material, in the form of rod/plate, to control the fission chain reaction.

(v) Coolant for the removal of heat produced in the fission process and

(vi) Structural materials and reactor vessel.

Other than the fuel and control materials, all materials used should have low thermal neutron absorption cross-section. Most of the materials in a reactor are in continuous use for the entire life (40 y) of the reactor and resistance to corrosion and chemical compatibility are important criteria for the choice of materials.

Nuclear Fuel and Clad

All current research as well as power reactors use solid fuel. Cylindrical or plate configuration is widely prevalent. As the fuel is the heart of the reactor, great attention is paid to its design to ensure successful operation for several years. Even in a power reactor the fuel residence time is one to two years. During the process of fission/energy production, 0.1 to 10% of uranium/plutonium undergoes fission depending upon the design.

Uranium metal, uranium-aluminium alloy or uranium silicide (U_3Si_4) are used as fuels for research reactors. Uranium dioxide is the most prominent fuel for power reactors. For fast reactors $(U,Pu)O_2$ with 20-30% PuO_2, is used as fuel material. Other potential fuel materials for fast reactors are (U,Pu)C, (U,Pu)N and U-Pu-Zr alloy. Uranium metal is used in the form of a rod. Uranium aluminium alloy fuel is a dispersion of UAl_3 in an aluminium matrix which is made in the form of a plate. In this type of fuels always enriched uranium is used. Similarly U_3Si_4 is dispersed in aluminium matrix and used in the form of a plate. Uranium dioxide is always used in the form of pellets having 10 to 14 mm diameter and similar height. Uranium plutonium oxide is also used in the form of pellets of 5-8 mm diameter.

The fuel is always covered with a cladding material to provide the primary barrier between the fuel and the coolant. It has to be chemically compatible with the fuel and the coolant, and strong enough to withstand the pressure exerted due to fuel swelling and accumulation of gaseous fission products. Neutron economy dictates the use of materials with small neutron absorption cross-section. Some typical cladding materials are listed in Table 10.2.

Aluminium is used as clad for plate type fuel elements having UAl_3 or U_3Si_4 dispersed in aluminium matrix. The cladding is rolled along with the fuel during the manufacturing stage to ensure good fuel-clad contact. Aluminium is also used as clad for uranium metal fuel in research reactors. Magnox is used as cladding for uranium metal fuel used in CO_2 cooled reactors. Zirconium alloys in the form of tubes are used for cladding UO_2 fuel pellets. Close contact between fuel and pellet is not required. In fact, the pellet is slightly smaller so that, even after swelling, the pressure of fuel on the clad tube is small. Stainless steel is used as fuel cladding both for some water cooled reactors and sodium cooled reactors using $(U,Pu)O_2$ fuel.

Table 10.2 - Cladding Materials for Nuclear Reactors

Material	Composition	σ_a (0.025 eV) (barn)	Coolant
Alloy 6061	Al-1% Mg, 0.6% Si, 0.3% Cu	0.24	$H_2O < 150^oC$
Magnox	Mg-1% Al, 0.04% Be	0.065	CO_2 upto 550^oC
Zircaloy-2	Zr-1.5% Sn, 0.15% Fe, 0.1% Cr, 0.05% Ni	0.20	H_2O upto 320^oC
Zircaloy-4	Zr-1.5% Sn, 0.2% Fe, 0.1% Cr, <0.0075% Ni	0.20	H_2O upto 320^oC
SS 316 L	Fe-18% Cr, 12% Ni, 2.5% Mo, 2% Mn, <0.04% C	3.1	H_2O upto 320^oC Na upto 600^oC

The fuel plates or rods are quite often made into bundles which are arranged in a reactor core to obtain a fixed geometry. The main objective of fuel design is to obtain maximum power as well as energy from the fuel without any fuel failure. The physical appearance of spent fuel, even after several years of operation, is identical to that of the fresh fuel.

The rate at which the energy is extracted from a particular fuel is called its **specific power** and is measured in terms of magawatts of thermal power (MWt) produced per tonne of the fuel in the reactor. Specific power thus gives a measure of the quantity of fuel used in a reactor having a given power level. The fuel inventory is low if specific power is high. The fuel is cooled at its surface by the coolant. As the energy is produced throughout the fuel, the centre of the fuel is always hotter than the surface. In the case of ceramics like UO_2 the difference can be several hundred degrees. The design ensures that the central part does not melt or undergo any phase change during power production. The specific power is controlled accordingly.

Even with most optimum design one cannot continue to use the fuel beyond a certain limit. After a certain amount of energy has been produced in the fuel element, it is removed from the reactor. The megawatt days of energy produced per tonne of the fuel is called **burn-up** of the fuel. Burn-up of the fuel can be limited by the following factors.

(i) Decrease in the fissile content of the fuel. This is quite often the case with natural uranium fuels.

(ii) Decrease in the reactivity of the fuel due to the accumulation of neutron absorbing fission products.

(iii) Damage to the integrity of the fuel. The reason could be physical stress caused by swelling of the fuel or chemical stress due to the migration of reactive fission products

like I, Cs and Te from within the fuel to the fuel-clad interface. Further, with high burn-up in power reactors, the noble gas fission products (Xe and Kr) are released by the fuel and a pressure of upto 140 kg/cm^2 can build-up inside the fuel pin.

(iv) Damage to the integrity of the clad due to corrosion by coolant/moderator.

Burn-up of a fuel can also be expressed in terms of the percent of U/Pu fissioned. One MWd of thermal energy is produced by the fission of 1 g of uranium. So 1000 MWd/te would mean about 1 kg of fuel undergoes fission per tonne of the fuel charged or burn-up is 0.1 atom percent. In fast reactors, burn-up of the order of 10 atom percent is expected.

Moderator

The concept of moderators was introduced earlier. Light water (H_2O), heavy water (D_2O) and graphite are being used as moderators in research reactors as well as power reactors. When H_2O is being used as a coolant the same water stream acts as a moderator and no separate provision is made. When D_2O is used as a moderator then it is a common practice to separate the moderator and coolant streams, and the coolant can be H_2O or D_2O. With graphite moderator, a wide variety of coolants are used.

Coolant

The choice of coolant is dictated by the following considerations

(i) Good thermal conductivity

(ii) High specific heat (temperature rise is low for a given heat input)

(iii) Compatibility with fuel and structural materials and

(iv) Low neutron absorption cross-section

Light water and D_2O are the most prominent coolants. CO_2 and He have been used in Magnox and high temperature gas cooled reactors. Sodium is the preferred coolant for fast reactors.

Control Rods

In all reactors the reactivity decreases with operation both because of the decrease of fissile content and the increase of fission product concentration some of which are high neutron absorbers. It is almost impossible to replace fuel as it is consumed. Also the operation of a reactor at high specific power requires significantly higher content of fissile material. It is, therefore, essential to have a significant excess reactivity in a reactor. The reactivity is defined as the fractional departure of a system from criticality.

$$\text{reactivity} = k_{ex} / k_{eff} \qquad (10.13)$$

The excess reactivity is provided by having more fuel (>30% more) than required for criticality. At steady power level k_{ex} is zero and so is the reactivity. This is achieved by having control materials which absorb neutrons. Of course reactivity can be decreased by

withdrawal of (i) fuel or (ii) reflector or (iii) moderator or by the insertion of control rods. Primarily control rods are designed to introduce adequate amount of negative reactivity to take care of positive reactivity due to excess fuel.

Another reason for providing excess reactivity is the presence of fission product ^{135}Xe. It is mainly produced by the decay of primary fission product ^{135}Te.

$$^{135}_{52}\text{Te} \xrightarrow[19\text{ s}]{\beta^-} {}^{135}_{53}\text{I} \xrightarrow[6.57\text{ h}]{\beta^-} {}^{135}_{54}\text{Xe} \xrightarrow[9.14\text{ h}]{\beta^-} {}^{135}_{55}\text{Cs} \xrightarrow[2.3 \times 10^6\text{ y}]{\beta^-} {}^{135}_{56}\text{Ba}\ \text{stable} \qquad (10.14)$$

^{135}Xe has a capture cross-section of 2.6×10^6 b for thermal neutrons and is a neutron poison. This high cross-section decreases the value of 'f' and thereby k_{eff}. While the reactor is in operation, the Xe concentration approaches an equilibrium value due to radioactive decay and neutron capture. However, when the reactor is shut down, the ^{135}Xe concentration increases steadily for several hours due to the decay of its precursors, as shown in reaction 10.14, before reaching a maximum after which it decreases slowly. If a reactor is shut down for about 2 hours, the ^{135}Xe concentration may be so high that it may be necessary to wait for a day or two (3 to 5 half-lives of ^{135}Xe) for restarting the reactor. Xenon poisoning is, therefore, an important aspect of the operation of a reactor. Excess reactivity is also provided for Xe override so that the reactor can be restarted even if ^{135}Xe has built up.

There are many other fission products like ^{149}Sm ($\sigma_c = 4.1 \times 10^3$ b) which have high neutron absorption cross section. There would be significant decrease of the reactivity as the fission products build up in the fuel.

The control rods contain boron ($\sigma_c = 759$ b) or cadmium ($\sigma_c = 2450$ b). Boron is often used in the form of boron steel or boron carbide. Cadmium is used in the form of metal or Ag-15%Cd-5%In alloy. Hafnium with $\sigma_c = 2450$ b is also used in metallic form. Control materials are used in a variety of shapes. These include rod type, plate type or cruciform type. Cruciform type rods slide between the fuel assemblies. The rod type are inserted in guide tubes which form a part of the fuel assembly. Control rods can be inserted either from the top or the bottom of the reactor. The control rods are kept fully inserted when the reactor is not in operation. To start up a reactor the control rods are gradually taken out and neutrons from the start-up neutron source initiate the neutron multiplication. The reactivity, which is highly negative with the control rods inserted, gradually comes to zero and a sustained chain reaction starts. Further careful withdrawal of control rods is required to increase power.

History of Nuclear Reactors

Possibility of setting-up a system for fission chain reaction was being explored by Joliot-Curie and co-workers in 1940 using uranium metal as fuel and light water as well as heavy water as moderators. The studies were, however, discontinued in June 1940 with the occupation of Paris by the German army. Just at that time, Otto Frisch predicted that it should be possible to make a nuclear bomb using highly enriched ^{235}U. The British Government set up a committee to verify the prediction of Frisch and the report published in July 1941

confirmed the possibility of producing a bomb. The report also predicted the possibility of using nuclear energy for power production and the production of fissile ^{239}Pu from ^{238}U.

The main thrust of work on nuclear fission was in the United States where Fermi and his team were planning to set up a facility for demonstration of the fission chain reaction. They decided to use graphite as the moderator and since high purity uranium metal was not available, in the initial stages, uranium oxide was used as fuel. The assembly was made by piling bricks of graphite with holes for accommodating uranium oxide spheres of 3.25 inch diameter. Subsequently, a few tonnes of high purity uranium metal bricks were prepared and used in setting up the reactor. Cadmium covered bronze strips were used to control the fission chain reaction. The possibility of sustained fission chain reaction was established in this reactor on December 2, 1942. The maximum reactor power was about 200 watts. Absence of biological shield prevented operation at higher power. Cooling arrangement was not required at this power. The first application of sustained fission chain reaction was for the production of plutonium. The first reactor for this purpose was set up in November 1943 at Oak Ridge National Laboratory, USA which used 35 tonnes of uranium metal as fuel and produced 3.8 MW of heat. This reactor was cooled with air. A graphite lattice with 1248 channels having 39-54 uranium slugs per channel was used. About 4 g of plutonium per day was formed in this reactor. Subsequently, reactors for producing plutonium were set up at various sites in the United States and as well as in UK, France and erstwhile USSR.

Following the second World War, the emphasis of reactor technology shifted towards the development of reactors for other applications. In 1953, US launched a nuclear powered submarine named 'Nautilus'. The first reactor to produce electricity was commissioned in Moscow in June 1954. This was a 5 MWe reactor using uranium oxide as fuel, graphite as moderator and water as coolant. The first reactor to supply electricity for commercial applications was installed in UK in August 1956. The reactor was of 50 MWe capacity using uranium metal as fuel, graphite as moderator and carbon dioxide gas as coolant. The main purpose of this reactor, however, was the production of plutonium required for the military programme. The first reactor solely devoted for civilian application, was set up in the USA in 1957 at Shipping Port. This reactor was of 20 MWe capacity with uranium oxide as fuel, and light water as moderator and coolant. The use of nuclear power reactors in ship propulsion was initiated by the then USSR in 1959 by launching the ice breaker Lenin which had three 90 MWe reactors. Currently, out of the large number of reactors operating in the world, about 600 are being used for submarine and ship propulsion. About 300 reactors are being used for research and isotope production.

Research Reactors

Currently 284 research reactors are operating in the world. One can call Chicago pile as the first research reactor. It was soon followed, in 1944, by a heavy water moderated reactor set up at Argonne National Laboratory, USA. The reactor consisted of a 1.8 m diameter aluminium tank filled with 5900 kg of heavy water. Three tonnes of natural uranium metal in the form of 120 rods, 2.8 cm dia and 1.8 m long, was used as fuel. A 0.6 m

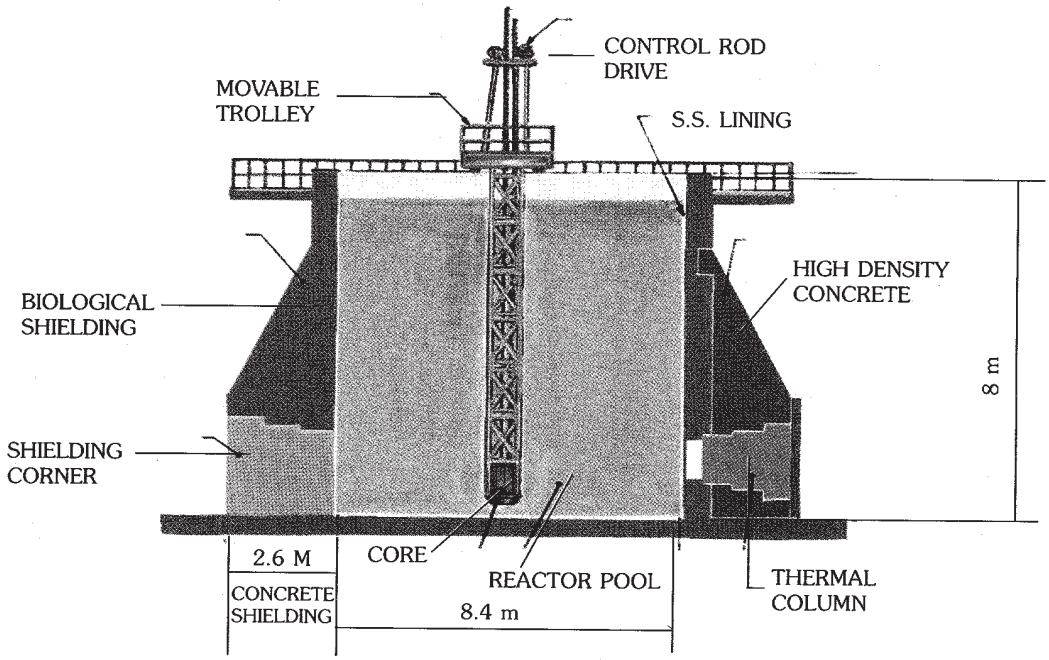

Fig. 10.5 Vertical cross-section of APSARA reactor.

thick layer of graphite blocks acted as reflector. A 10 cm thick thermal shield of Pb-Cd alloy protected the 2.4 m thick concrete biological shield. The moderator itself acted as a coolant for removing 250 kW of heat generated in the reactor. This concept was used to construct 10 MWt research reactor NRX, at Chalk River, Canada, which gave a neutron flux of 6×10^{13} n cm^{-2} s^{-1}. India's 40 MWt CIRUS reactor, built with the help of Canada, has many common features with NRX.

The use of enriched uranium could make the reactor compact. This along with the concept of using water as moderator, coolant, reflector and shield led to the concept of swimming pool reactor first built at Oak Ridge National Laboratory, USA. India's first reactor APSARA, built in 1956, is swimming pool type (Fig. 10.5). An 8.4 m x 2.9 m x 8.0 m deep stainless steel lined pool is used which is surrounded by a concrete shield of 2.6 m thickness in the lower portion having the core. The core lattice has 49 position in 7 x 7 square matrix for fuel bundles. Uranium-aluminium alloy plates with aluminium cladding are used as fuel and uranium has 93% of ^{235}U. Each fuel bundle, with overall dimensions of 73 mm x 73 mm x 905 mm height, has 12 fuel plates. Each plate has 12 g of ^{235}U and the thirty four fuel bundles used contain 4.5 kg of ^{235}U. The reactor has a neutron flux of 10^{12} n cm^{-2} s^{-1} at 1 MWt power.

Dhruva, another research reactor of 100 MWt capacity with a maximum neutron flux of 1.4×10^{14} n cm^{-2} s^{-1} was set up in India in 1985. This is also a uranium metal fuelled and heavy water moderated research reactor.

Table 10.3 - Nuclear power reactors in operation and under construction, December 31, 2001

Country	Reactors in operation		Reactors under construction		Nuclear electricity supplied in 2001	
	No. of units	Total MW(e)	No. of units	Total MW(e)	TW(e).h	% of total
Argentina	2	935	1	692	7	8
Armenia	1	376			2	35
Belgium	7	5712			44	58
Brazil	2	1901			14	4
Bulgaria	6	3538			18	42
Canada	14	10018			72	13
China	3	2167	8	6426	17	1
Czech Rep.	5	2560	1	912	15	20
Finland	4	2656			22	31
France	59	63073			401	77
Germany	19	21283			162	31
Hungary	4	1755			14	39
India	14	2503	2	980	17	4
Iran			2	2111		
Japan	54	44289	3	3696	322	34
Rep. of Korea	16	12990	4	3820	112	39
Lithuania	2	2370			11	78
Mexico	2	1360			8.11*	3.66*
Netherlands	1	450			4	4
Pakistan	2	425			2	3
Romania	1	655	1	650	5	10
Russia	30	20793	2	1875	125	15
South Africa	2	1800			13.34*	6.65*
Slovakia	6	2408	2	776	17	53
Slovenia	1	676			5	39
Spain	9	7524			61	27
Sweden	11	9432			69	44
Switzerland	5	3200			25	36
UK	33	12498			82	22
Ukraine	13	11207	4	3800	72	46
USA	104	97860			769	20
TOTAL	438	353298	32	28438	2544	20.1

*IAEA estimates.
Note : Total includes 6 units in operation and 2 under construction in Taiwan, China.
Source: IAEA Power and Information System (PRIS), RBS No.2, 2002 edition.

Nuclear Power Reactors

Unlike in a research reactor, where the heat produced is rejected into a water body or atmosphere, heat is the primary product of interest in a power reactor. Nuclear power reactor in fact, serves the same purpose as the coal/oil fired boiler in a conventional power plant. Generation of steam for running a turbine is the main focus in a nuclear power reactor. If steam is generated at atmospheric pressure, the temperature is 100°C. The Carnot efficiency of an engine working with 100°C steam source and 25°C sink would be

$$\text{Carnot Efficiency} = \frac{373 - 298}{373} = 0.2 \qquad (10.15)$$

which means that only 20% of the heat generated would be converted to electricity. Higher efficiency can be achieved by having the steam at high temperature which is possible by pressurising water. The critical temperature and pressure of water are respectively 374°C and 220 atmospheres. In a reactor the water is pressurised to about 100-150 atmospheres to obtain temperature in the region of 300°C. Also in most practical systems, the sink temperature would be about 100°C. In practice thermodynamic efficiency is 30-35%. In research reactors the power was specified in terms of MWt. In power reactors, the power is specified in terms of MWe, which is about 1/3rd of the thermal power. So even in a power reactor, 2/3rd of the heat produced is rejected to water body or atmosphere (through cooling towers).

Currently more than 400 nuclear power reactors are operating in the world and providing about 20.1% of the approximate total electricity generated (See Table 10.3).

Power reactors are quite often classified on the basis of the type of coolant used. Some of the prominent types which are in operation for the production of electricity in the world are given below along with the total net electricity capacity.

1. 86 Boiling Water Reactors (BWR) - 74,880 MWe
2. 207 Pressurised Water Reactors (PWR) - 196,682 MWe
3. 34 Pressurised Heavy Water Reactors (PHWR) - 16,515 MWe
4. 15 Light Water Cooled Graphite Moderated Reactors (LWGR) - 10,219 MWe
5. 18 Gas Cooled Reactors (GCR) - 2,930 MWe
6. 14 Advanced Gas Cooled Reactors (AGR) - 8,380 MWe
7. High Temperature Gas Cooled Reactors (HTGR) - None at present
8. 3 Liquid Metal Cooled Fast Breeder Reactors (LMFBR) - 1,039 MWe
9. 50 Pressurised Water Reactors of Russian Type (WWER) - 32,458 MWe

The reactors which use light water as moderator/coolant require enrichment of uranium, e.g., BWR, PWR and LWGR. Similarly, if the cladding material used absorbs neutrons, enrichment of uranium is required, e.g., AGR.

The **Boiling Water Reactor** uses uranium oxide fuel having 1.5 to 3% of ^{235}U. Zircaloy is used as cladding and the reactor is housed in a strong stainless steel vessel. Water flowing through the reactor is used as coolant as well as moderator and is pressurised to 70 atm pressure so that the water boils at about 285°C and good efficiency of conversion of thermal energy to electrical energy is obtained in the turbine. Total installed capacity for this type of reactors in the world is 74,880 MWe. A schematic view of the reactor is shown in Fig. 10.6. In India, the reactors at Tarapur Atomic Power Station are Boiling Water Reactors.

Fuel and cladding for **Pressurised Water Reactors** are similar to the BWR. In this case, however, the pressure in the reactor is kept at 145 atm such that water does not boil inspite of reaching a temperature of 310°C. The reactor vessel, therefore, should be stronger than that used for BWR. This super-heated water is transported to a heat exchanger to produce steam and returned back to the reactor. The steam generated in the heat exchanger is used for producing electricity. This is the most popular reactor type in the world and the total present installed capacity is 196,682 MWe. In India, the two 100 MWe reactors being set up at Kudankulam are of this type.

The **Pressurised Heavy Water Reactor** is based on the use of natural uranium oxide fuel with zircaloy cladding. Unlike the two concepts discussed in the previous paragraphs, this concept does not make use of a large pressure vessel for containing the core components. Instead, the fuel is contained in a number of pressure tubes which are installed horizontally in a large vessel called 'Calandria'. The heavy water used for moderating the neutrons is filled in the Calandria and is kept cooled (<85°C). The control rods are installed in the Calandria.

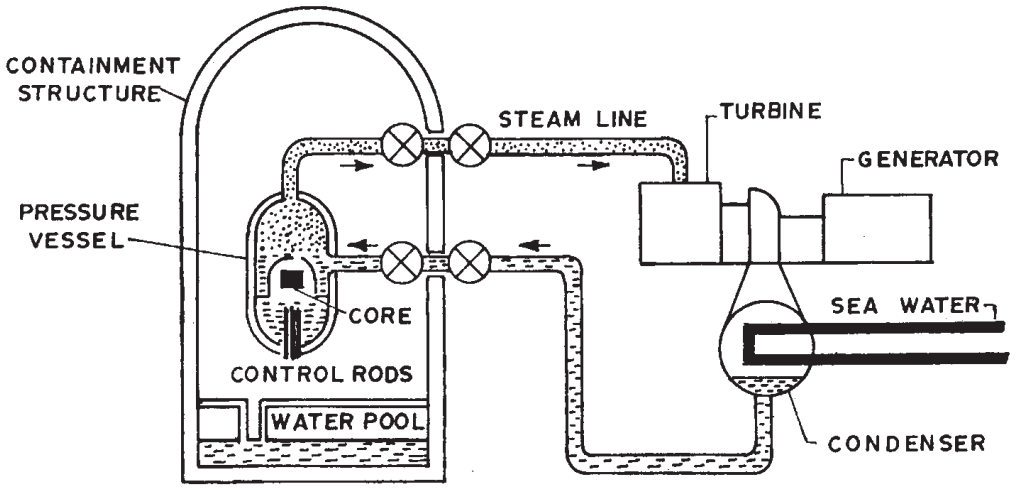

Fig. 10.6 Boiling Water Reactor (BWR).

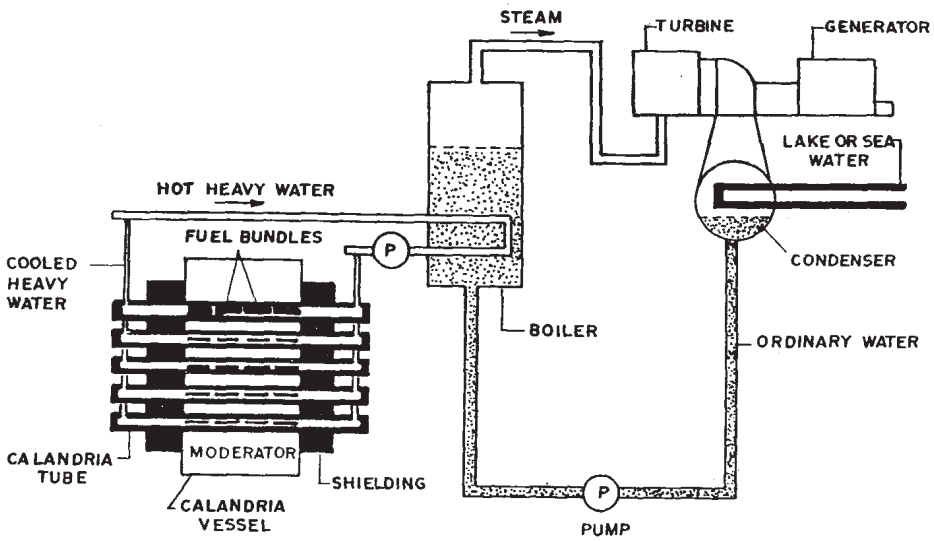

Fig. 10.7 Pressurised Heavy Water Reactor (PHWR).

Heavy water used for cooling the fuel circulates through the pressure tubes at a pressure of 85 atm at a temperature of about 300°C. A schematic view of this reactor is shown in Fig. 10.7. Total installed capacity of this type of reactors is presently 16,515 MWe.

The first reactor which produced electricity was a **Light Water cooled and Graphite moderated Reactor** in the then USSR. This reactor is also a pressure tube type reactor just like PHWR but the pressure tubes are vertical. Uranium oxide enriched to 1.5 to 2% is used as fuel and Zr is used as cladding. Graphite blocks stacked together constitute the moderator and light water flowing through the pressure tubes is used as coolant. This reactor concept is used only in the USSR and the present operating capacity is 10,219 MWe. The reactor in the infamous accident at Chernobyl was of this type. This reactor, even though very successfully operated in the then USSR for many years, has some inherent unsafe features and would not be licensed for operation in India or many other countries.

Gas Cooled Reactors were developed in UK and France based on the experience of plutonium production reactors. In this concept, natural uranium metal clad in magnox, (a magnesium alloy), is used as fuel. These reactors are, therefore, sometimes called Magnox reactors. Graphite is used as a moderator and carbon dioxide gas as a coolant. Average temperature of the coolant is 400°C and the pressure is 20 atmospheres. The total installed capacity of this type of reactors is 2,930 MWe.

Building on the concept of Gas Cooled Reactors, UK developed the **Advanced Gas cooled Reactor**. This reactor also uses carbon dioxide as the coolant and graphite as moderator. However, the fuel is in the form of UO_2 pellets, having 1.2 to 2.3% of ^{235}U, clad in stainless steel tubes. The outlet temperature of coolant gas in this reactor is 650°C and the

Table 10.4 - Neutron balance in Light Water Reactors (100 fissions, 259 neutrons)

Neutrons lost		Neutrons absorbed in U/Pu without fission		Neutrons causing fission in U/Pu	
Structure Materials	45	Pu	27	Pu	32
Fission Products	14	^{235}U	15	^{235}U	63
		^{238}U	58	^{238}U	5
↓		↓		↓	
Activation Products		Produce Pu and higher actinides		Energy and 259 neutrons	

coolant pressure is 40 atm. These reactors are operated only in UK and the present installed capacity is approximately 8,380 MWe.

High Temperature Gas Cooled Reactor concept is different from the other reactor concept in that it does not use conventional metallic cladding. The fuel is in the form of microspheres (0.2 mm dia) of $(U,Th)C_2$ or $(U,Th)O_2$ which are coated with layers of graphite and silicon carbide as cladding. These coated microspheres are mixed with carbon and made into fuel elements of desired shape. Graphite and helium are respectively used as moderator and coolant. Uranium enrichment is in the range of 20 to 90%. The outlet temperature of helium coolant is 740°C and the pressure is about 50 atm. Only two power reactors of this type have operated in the world : one was of 330 MWe capacity in the USA and the other of 300 MWe capacity in Germany. Currently, South Africa, Japan and Germany are having a second look at this concept.

Conversion and Breeding

Plutonium is a byproduct in the operation of uranium fuelled nuclear reactors. With the establishment of nuclear power reactors, about 100 te of plutonium is produced every year in the nuclear power reactors by conversion of fertile ^{238}U into plutonium. The extent of the conversion of ^{238}U to plutonium varies from reactor to reactor. It depends upon the number of neutrons produced per fission in the reactor and the processes which absorb neutrons. At steady state, the number of neutrons present in a reactor is equal to the number of neutrons consumed by various nuclear reactions. As a typical illustration, neutron balance for 100 fissions in a light water reactor is given in Table 10.4. On an average, 100 fissions lead to the release of 259 neutrons in this type of reactor. Out of these, 100 neutrons are required to sustain the fission chain reaction. Another 100 neutrons are lost by absorption in plutonium and uranium. When these neutrons are absorbed by fertile isotopes like ^{238}U or ^{240}Pu, fissile isotopes ^{239}Pu and ^{241}Pu are produced. However, absorption of the neutrons by ^{239}Pu, ^{235}U or ^{241}Pu, without resulting in fission, is wasteful in terms of neutron economics. About 59 neutrons on an average are lost by absorption in structural materials and fission

products. Majority of the fission (63%) is caused in ^{235}U but a significant fraction (32%) also takes place in plutonium isotopes. A small fraction (5%) of fission takes place in ^{238}U due to fast neutrons.

The ratio of fissile isotopes produced to the fissile isotopes consumed is called the conversion ratio. In the light water reactors, the conversion ratio is approximately 0.55 meaning thereby that for every 100 atoms of ^{235}U lost, we gain 55 atoms of fissile plutonium. In the Pressurised Heavy Water Reactors, the neutron economy is better, and the conversion ratio of 0.7 is possible. The annual production of plutonium from various reactors depends on the conversion ratio as well as the burn-up of the fuel. Annual production of plutonium from different types of reactors of 1000 MWe capacity is as follows :

(i) Light Water Reactors - 220 kg

(ii) Pressurised Heavy Water Reactors - 500 kg

(iii) Gas Cooled Reactors - 700 kg

It is seen that the production of plutonium in a reactor is dependent upon the neutron balance. If the neutrons produced from fission can be more, or if the loss in the structural materials can be reduced, then it should be possible to get better production of plutonium. This has been achieved in fast breeder reactors which make use of a very special nuclear property of plutonium. Fig. 10.8 shows the neutrons released per neutron absorbed for various fissile isotopes as a function of neutron energy. At neutron energy below 1 eV, the fission of ^{233}U yields maximum neutrons. However, when we go towards energies of the order of 1 MeV, the neutrons released in the fission of plutonium starts increasing rapidly and approaches a figure of 3.4 at 10 MeV. When the number of neutrons released per of neutron absorbed is more than 2.0, it is possible to produce more fissile material. Average energy of neutrons released in fission reaction is about 1.1 MeV. Thus with the use of fast neutrons and plutonium fuel, it should be possible to have a large conversion ratio. In fact, this conversion ratio exceeds unity and therefore, such reactors are called breeder reactors. In practice, however, even when no moderators are used, neutrons do slow down due to interaction with structural materials and the components of the fuel. The breeding ratio would thus be dependent on various design parameters.

A typical neutron balance in a fast reactor having mixed uranium plutonium oxide as fuel is given Table 10.5. At steady state, 100 fissions lead to the generation of 292 neutrons. The relative % contribution to the total fission by various nuclides are : 84% by Pu, 13% by ^{238}U and 3% by ^{235}U. Out of these 292 neutrons, 100 neutrons are used to continue fission chain reaction. About 153 neutrons are absorbed by the fuel materials which lead to the production of fissile plutonium and 39 are lost by capture in structural materials and fission products. In France, fast reactors using oxide fuel have successfully achieved a breeding ratio of 1.25. Use of fuels which permit a faster spectrum of neutrons can lead to better breeding. Use of mixed carbide or nitride fuel is expected to give a breeding ratio of 1.3 to 1.4 and the use of metallic plutonium alloys can give a breeding ratio of 1.5. The concept of breeding is illustrated further in Fig. 10.9 by taking the case of a 1000 MWe breeder reactor.

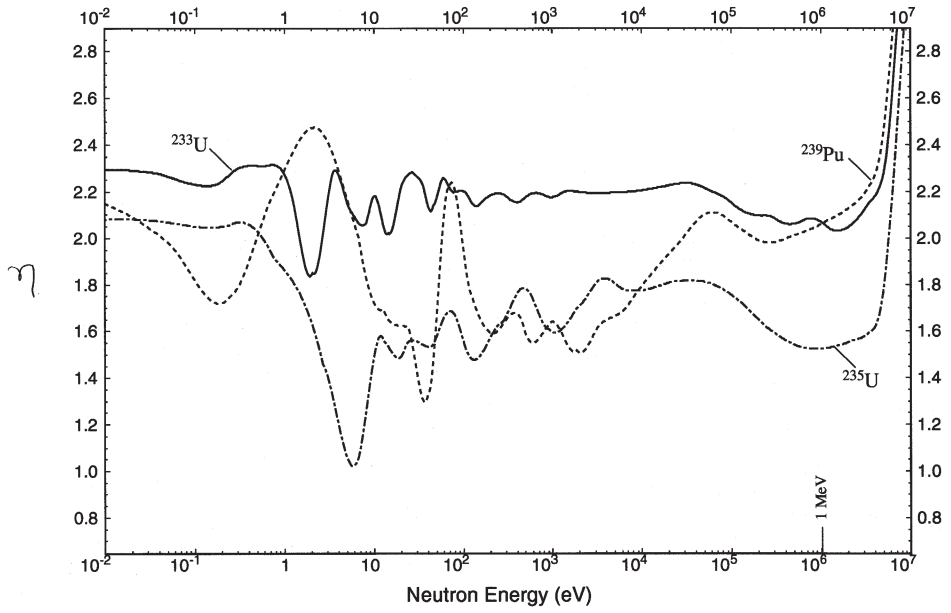

Fig. 10.8 Number of neutrons released per one absorbed neutron (η) as a function of neutron energy. Data are taken from ENDF/B-VI evaluated data library (Courtesy Nuclear Data Section, IAEA, Vienna).

Usually η is determined for thermal and epithermal neutron energy, below inelastic scattering threshold as:

$$\eta = \frac{\sigma_f \nu_f}{\sigma_f + \sigma_{n,\gamma}}$$

The following generalisation was used for a whole energy region in conditions when other reaction cross-sections are negligible.

$$\eta = \frac{\sigma_f \nu_f + \sigma_{inel} + \sigma_{n,nf} + 2(\sigma_{n,2n} + \sigma_{n,2nf}) + 3(\sigma_{n,3n} + \sigma_{n,3nf})}{\sigma_f + \sigma_{n,\gamma} + \sigma_{inel} + \sigma_{n,2n} + \sigma_{n,3n}}$$

Table 10.5 - Neutron balance in Fast Reactors (100 fissions, 292 neutrons)

Neutrons lost		Neutrons absorbed in U/Pu without fission		Neutrons causing fission in U/Pu	
Structure Materials	33	Pu	32	Pu	84
Fission Products	6	^{238}U	121	^{238}U	13
				^{235}U	3
↓		↓		↓	
Activation Products		Pu and higher actinides		Energy and 292 neutrons	

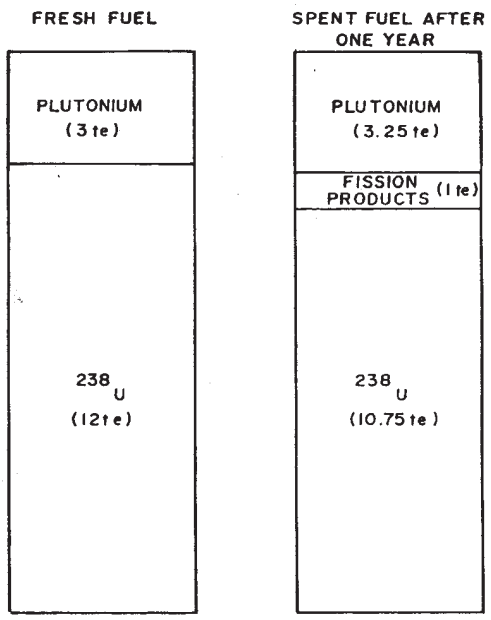

Fig. 10.9 Concept of a breeder as illustrated by (U,Pu)O_2 fuelled 1000 MWe FBR.

This plant would have about 3 te of plutonium and 12 te of ^{238}U in the fresh fuel. Production of 1000 MWe power for one year in this plant would consume about one te of fissile material. The spent fuel would then contain 3.25 te of plutonium, one te of fission products and 10.75 te of ^{238}U. Thus there is a net gain of plutonium by conversion of ^{238}U. Out of the 3.25 te, 3 te should go back to the reactor for continuing energy production but 0.25 te can be used for setting up of new reactors. Thus the use of plutonium and fast breeders can lead to multiplication of the nuclear power capacity in a country. In India, the uranium resources of 86,000 tones can be used to install Pressurised Heavy Water Reactors of only 10,000 to 12,000 MWe capacity. However, the depleted uranium left and plutonium produced in these reactors, can be used in fast breeder reactors leading to an installed capacity of 350,000 MWe. Utilisation of plutonium is thus a very important component of India's nuclear energy programme.

Liquid Metal Cooled Fast Breeder Reactor is based on the use of fast neutrons and, therefore, no moderator is required. The use of fast neutrons permits more efficient conversion of ^{238}U to ^{239}Pu. As no moderator is used in the reactor, the fissile material concentration has to be significantly high and currently, a mixed oxide of uranium and plutonium containing 25% of plutonium oxide is used as fuel. This fuel is clad in stainless steel tubes and cooled by liquid sodium metal. Sodium coolant temperature and pressure are respectively 620°C and 3 atm. The reactor core in surrounded by elements containing UO_2 blanket for efficient breeding of plutonium. A schematic view of this reactor is shown in Fig. 10.10. Countries which have experience in operating this type of power reactors include

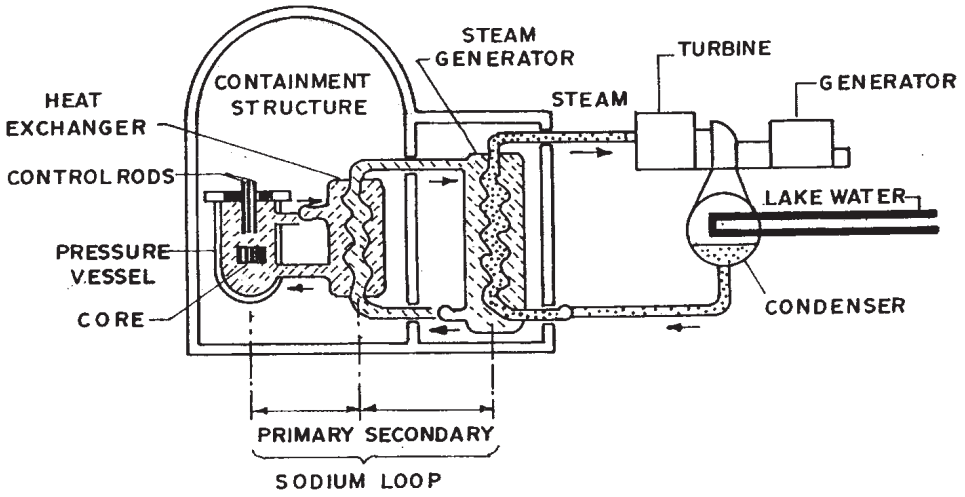

Fig. 10.10 Liquid Metal Fast Breeder Reactor (LMFBR).

France (250 MWe and 1200 MWe), UK (250 MWe), the then USSR (300 MWe and 600 MWe) and Japan. Research in this area is also being pursued in China and India.

Inherent Safety Features of Reactors

In power reactors, control rods have to be operated frequently to maintain the power generation as per the demand of electricity or to compensate for the depletion of fissile isotopes. Control rods are slightly withdrawn from the reactor in order to increase the power. The growth of power in the reactor is very rapid and, therefore, very fast acting control rods are provided for safe operation of the reactor. In addition, the design is suitably optimised so that any sudden increase in power would be opposed by inherent properties of the fuel, moderator and coolant systems. All reactors are thus designed to have a negative temperature coefficient of power. This ensures that at no stage, the nuclear reactor goes out of hand and safe conditions are always maintained.

Controlled and minimal release of fission products to the environment is the main concern of a reactor designer. There are many barriers to prevent the fission products from entering the environment. The fuel matrix itself provides the first barrier for the release of fission products. The second barrier is provided by the fuel cladding. The third barrier is provided by the closed circuit coolant system which normally carries away any released activity. The fourth barrier is provided by the pressure vessel or the pressure tube. If the radioactivity comes out of the pressure vessel or the pressure tubes, into the reactor building, it cannot escape from there because these buildings are of leak tight construction. Only controlled release takes place through properly filtered and monitored routes. The reactor building itself has an isolation zone of 1.6 km and a buffer zone of 5 km radius so that in the

very unlikely event of any release of radioactivity from the reactor building, provision for adequate dilution of radioactivity is facilitated.

The nuclear reactor is thus provided with adequate design and other safety features which ensure that the common man is not exposed to radiation even in the unlikely event of an accident. The exposure due to radiation released from the nuclear reactor during its normal operation is an insignificant fraction of the radiation received by man from natural environmental radionuclides. Every hour a total of 30,000 atoms of radium, polonium, bismuth and lead decay in our lungs, 0.4 million secondary cosmic ray particles traverse our body and about 15 million ^{40}K atoms, which are part of the overall potassium in our body, decay in our body. Besides this, we receive radiation due to terrestrial natural radioisotopes, medical check up etc. which are not known to cause any harmful effects. From experience at all nuclear power stations, it has been observed that in the neighbourhood of these reactors, the contribution to the radiation by the power reactors is less than one percent of the natural background. This is insignificant considering that the natural background itself may vary by more than 100% from place to place.

Bibliography

1. G.I. Bell, S. Glasstone, 'Nuclear Reactor Theory', Van Nostrand, Reinhold, New York (1970).
2. J.R. Marsh, 'Introduction to Nuclear Engineering', Addison Wesley, Reading (1977).
3. S. Glasstone, A. Sesonke, `Nuclear Reactor Engineering', Van Nostrand Reinhold, New York (1987).
4. R. Stephenson, 'Introduction to Nuclear Engineering', McGraw-Hill Book Co. Inc., New York (1954).
5. A.M. Jacobs, 'Basic Principles of Nuclear Science and Reactors', Van Nostrand Princeton, New Jersey (1960).
6. Y. Ronen, 'CRC Handbook of Nuclear Reactor Calculations', CRC Press, Boca Raton (1986).
7. A.V. Nero, 'A Guidebook to Nuclear Reactors', University of California Press, Berkeley (1979).
8. I.R. Cameron, 'Nuclear Fission Reactors', Plenum Press, New York (1982).
9. J.K. Pickard, 'Nuclear Power Reactors', Van Nostrand, Princeton, New Jersey (1957).
10. D. Jakeman, 'Physics of Nuclear Reactors', English University Press, London (1966).

11. E.L. Zebroski, 'Advanced Nuclear Reactors : Current Developments and Future Prospects', Elsevier, Amsterdam (1998).

12. Proceedings of the 1st International Conference on 'The Peaceful Uses of Atomic Energy', Geneva, United Nations, New York (1956).

13. Proceedings of the 2nd International Conference on 'The Peaceful Uses of Atomic Energy', Geneva, United Nations, New York (1958).

14. Proceedings of the 3rd International Conference on 'The Peaceful Uses of Atomic Energy', Geneva, United Nations, New York (1964).

15. Proceedings of the 4th International Conference on 'The Peaceful Uses of Atomic Energy', Geneva, International Atomic Energy Agency, Vienna (1972).

Chapter 11
Particle Accelerators

The study of interaction of alpha particles with matter led Rutherford to the discovery of nucleus. Soon there was a lot of interest in the study of charged particle interaction with matter to probe deeper into the structure of matter. Electrons, which were readily produced by the thermionic emission from a hot filament and protons which could be produced by the ionisation of hydrogen atom, did not have adequate kinetic energy for this type of investigation and the idea of acceleration of these particles by increasing their energy through electrostatic interaction was born. When an electron or a proton travels across a potential difference of one volt, it gains an energy of one electron volt. To provide energy in the range of naturally occurring alpha particles (4-8 MeV), a potential drop of a few million volts would be required. In fact today one talks about charged particle energies of a teraelectron volt (10^{12} eV) to probe matter. Though this energy appears high this would, in fact, be the energy consumed by a mosquito in a short flight. As a result of acceleration the speed of a charged particle could be substantially increased. For example, an electron having 2 MeV energy would be travelling at 98% of the speed of light. Obviously, the speed of a proton would be about 1/43 times less for the same energy. The primary requirement for providing energy to a charged particle is therefore a source of high voltage. In late 1920s, it was very difficult to think of voltages above 10,000V. This barrier was overcome by R.J. Van de Graaff at Princeton University, USA, in 1931 and by J.D. Cockroft and E.T.S. Walton at University of Cambridge, UK, in 1932. Simultaneously research was pursued in many other institutions to find ways to overcome the need for very high voltages for particle acceleration. The concept of resonance linear accelerator using high voltage alternating fields, was demonstrated by R. Wideröe in 1928. E.O. Lawrence and M.S. Livingston demonstrated the principle of magnetic resonance accelerator in 1931. Essentially all accelerators use electric fields, steady, alternating or induced, to accelerate the particles. In most of the cases, magnetic fields are used to contain and focus the beam. Most of the particle accelerators today are essentially based on these concepts and are briefly described in this Chapter.

Constant Voltage Accelerators

Two essential components of an accelerator are the source of energy, a high voltage system in this case, and an evacuated tube through which the charged particle can travel, during acceleration, without any collisions. The maximum energy gain of the accelerated particles is dictated by the voltage used for acceleration.

Cockroft Walton Accelerator

This was the first accelerator used to accelerate protons and study nuclear reactions. Publication of the results in 1932 gave wide attention to this concept. The schematic of the machine is shown in Fig. 11.1. The primary source of energy was a high voltage transformer which could provide alternating current at 100 kV. This energy source was connected to a cascade voltage multiplier having two columns of capacitors. These two columns are cross-connected through diodes which allow conduction in one direction only as indicated. This voltage source is connected to the acceleration tube as shown. Voltage multiplier, in principle, charges capacitors in parallel and discharges them in series. The voltages at all points across the stack oscillate over a range of 2V, where V is voltage from the transformer.

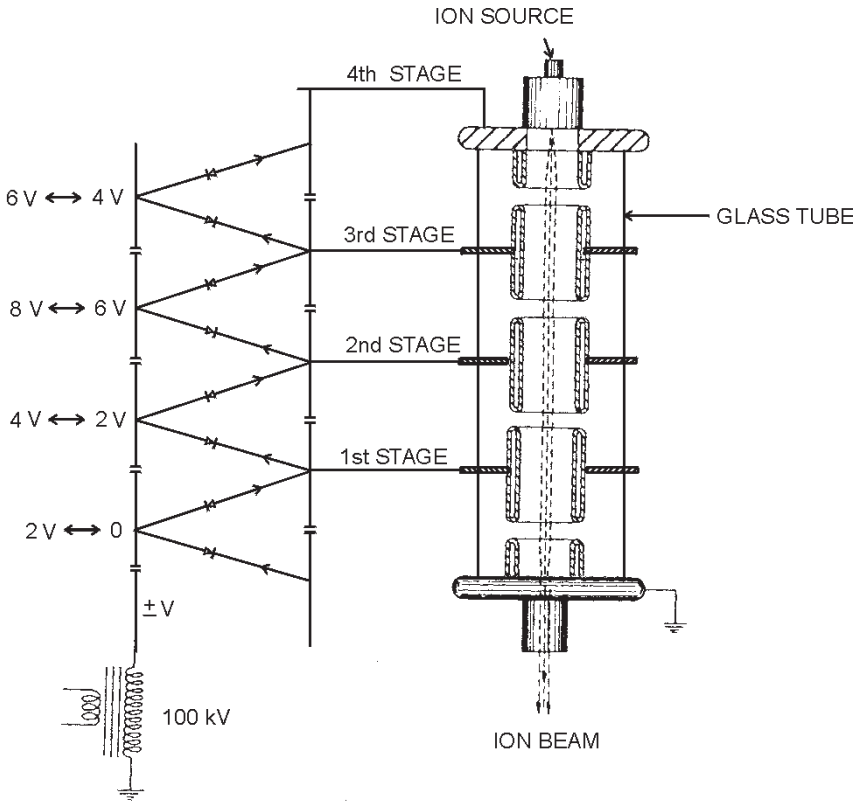

Fig. 11.1 Schematic of a Cockroft-Walton accelerator with four voltage multiplier stages.

As voltage on the stack oscillates, charge is transferred stepwise through rectifiers from ground to the terminal. At any stage N, the voltage is expected to be 2 VN. Cockroft and Walton used a 4 stage stack to obtain 710 keV protons which were used to bombard lithium. The nuclear reaction produced two alpha particles. They received Nobel Prize for their work in 1951.

Protons of 710 keV could be obtained instead of 800 keV expected for the 4 stages. This is because at voltages exceeding 500 kV, ripple from power drain due to instability of corona discharge and stray capacitance reduce the available voltage. G. Reinhold improved the concept of voltage multiplier by developing a symmetrical cascade rectifier. This employs two transformers and two capacitors stacks. Both these stacks feed one fixed-voltage capacitor stack. Using this type of device it has been possible to go upto 2.5 MV. By enclosing the power supply in sulphur hexaflouride (high voltage insulator) filled chamber, it was possible to obtain voltage upto 4 MV. The Cockroft Walton generator is simple and still widely used for accelerating electrons (Nissan High Voltage Co.) and for producing accelerated particles for injection into other machines.

Each stage of the voltage multiplier is connected to a metallic tubular electrode (Fig. 11.1). The particle thus gets accelerated across the gap between the two electrodes. This configuration also helps to focus the beam. Even when we use a single high voltage outlet source, it is divided into several intervals by the use of resistors as shown in Fig. 11.2.The path followed by a charged particle is shown in the figure. As the particle comes out of the drift tube and enters the gap, it experiences defocusing by the electric field. But well before exiting the next tube, there is a focusing effect. This phenomenon keeps the beam focused.

Van de Graaff Generator

Van de Graaff demonstrated in 1929, the high voltage generation with belt charging. The charge is continuously accumulated on a metallic sphere which serves as a high voltage source. A schematic of such a machine is shown in Fig. 11.3. One end of the belt made from

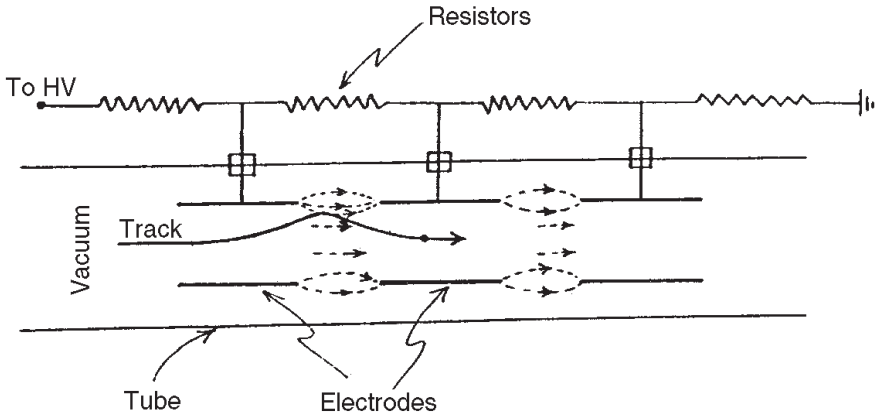

Fig. 11.2 Particle accelerating tube showing the focusing effect by the electric field lines at the gap.

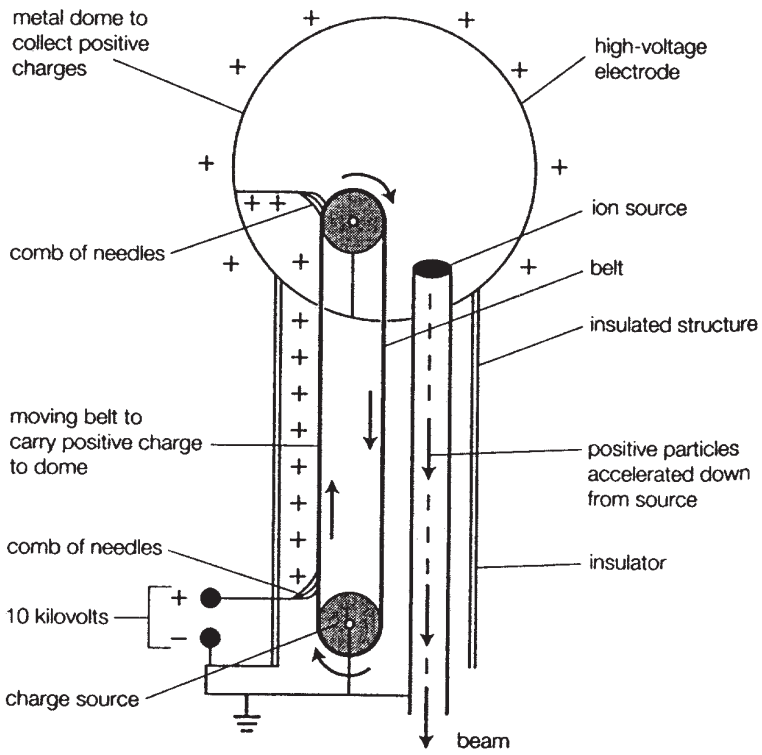

Fig. 11.3 Schematic of a Van de Graaff high-voltage electrostatic accelerator.

an insulating material like neoprene, is mounted on a pulley connected to the grounded end of the structure and the other end on a pulley housed in a large high voltage spherical terminal. The belt is charged at the lower end by a comb of sharp needles with points close to the belt and maintained at a high voltage of 10-50 kV. The entire structure is housed in a leak proof container which is filled with SF_6 at high pressure (5-7 kg/cm^2). The gas near the needle points is ionised by the intense electric field, and the resulting corona discharge transfers the charge to the belt which carries it up. If the comb has positive potential then the electrons produced in discharge are attracted by it and positive charge is carried by the belt. The charge is transferred to the high voltage electrode by another comb of needles from which it passes to the outer surface of the terminal. A carefully designed Van de Graaff generator can give potentials upto 20 MV to apply to an accelerator tube.

Tandem Accelerators

In 1958 High Voltage Engineering developed a technique to use high voltage V to accelerate singly charged particles to gain energy of 2 eV. This type of device is called Tandem accelerator and is schematically shown in Fig. 11.4. An ion source yields a beam of particles, say protons, which are accelerated to a low energy by an auxiliary high voltage source. This beam passes through a region containing a gas at low pressure where some of the protons take up two electrons to form H^- ions by charge exchange with the gas. The

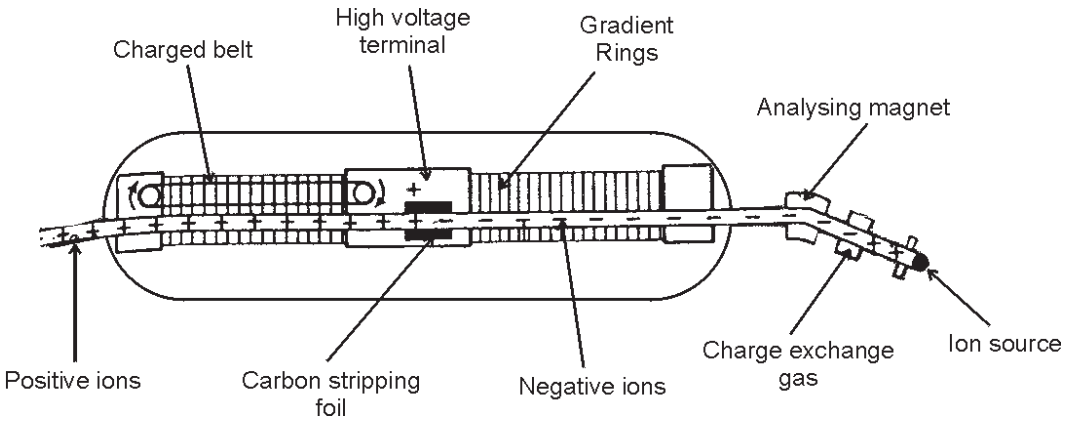

Fig. 11.4 Two stage Tandem Accelerator.

mixture of ions passes through a magnetic field which deflects the negatively charged hydrogen ions into the accelerator. This beam of negative ions is then accelerated towards the positive high voltage terminal. In this terminal the beam passes through a thin carbon foil which strips off the electrons changing the negatively charged beam (most of it) to a positively charged beam, i.e. protons. These are now repelled by the positive terminal and further accelerated through the second part of the accelerator tube. An analyser magnet at the outlet is used to direct particles of the desired energy to the target. The Folded Tandem Ion Accelerator (FOTIA) at BARC is of tandem type designed for 14 MeV proton beam.

Pelletron Accelerators

The use of neoprene belt and corona discharge had many drawbacks. These were overcome by using a charging chain. The chain consists of steel cylinders (pellets) joined by links of solid insulating material like nylon. The pellets are charged inductively by using a high voltage of the order of 60 kV. Negative potential is used for inducing positive charge on the belt. As charging current is ripple free, the terminal voltage is easily maintained at a precise value. Many belt charged accelerators have been converted to Pelletron charging. In India the 14 UD pelletron accelerator at Tata Institute of Fundamental Research (TIFR) can provide medium heavy ion beams from lithium to nickel. Negative ions from the ion source enter the accelerating tube and get accelerated in two stages. For example, a negative ion of carbon C^- gains 14 MeV in the first stage and gets additional 14 x q MeV energy in the second stage, where q is the charge state of the carbon ion. If all 6 electrons are stripped off, then the energy of C^{+6} ion will be 14(6+1) = 98 MeV. Beam currents around 100 nA are available from this pelletron.

Insulated Core Transformer Accelerator

This type of accelerators are extensively used for electron beam processing in industry. Normal three phase (440V) line power drives the primary coil of the power supply transformer. The voltage is magnetically coupled by an iron core to the secondary coils

which are connected to rectifier decks as mentioned earlier. The rectifiers are flat and circular which can be stacked one above the other to make a large stack. Electron energies in the range of 0.3 to 3 MeV with beam power of upto 100 kW is achievable.

Dynamitron Accelerator

Another cascade rectifier system called Dynamitron was invented by Cleland. The power source is a high voltage radio frequency (100 kHz) oscillator. The two terminals of this source are connected to two large semi cylindrical (RF) electrodes housed in the accelerator tank. There are two capacitor banks on either side of the rectifiers, as shown in Fig. 11.1. The capacitors are connected to each other in parallel with each capacitor connected to the RF electrode on its side. Half rings on the accelerator column provide capacitive coupling between the rectifiers and the large RF electrodes. These accelerators are also widely used for electron beam processing with electron energy ranging from 0.5 to 1.5 MeV and power of 50 to 100 kW.

Linear Accelerators (LINAC)

Generation of high voltage for accelerating charged particles was a serious challenge and voltages beyond a few MV were very difficult to obtain. A different approach to the problem is the repeated acceleration of the ions through relatively small potential difference. A radio frequency oscillator sends RF power to a wave guide and generates electric potential differences that accelerate the ions. If the RF wave and the particle move synchronously, then the particle continues to gain energy. A schematic of a linear accelerator is given in Fig. 11.5. The acceleration occurs in a metallic drift tube made up of several sections of increasing length. Alternate sections of this drift tube are connected to the RF source having frequency of about 200 MHz for proton acceleration and about 3,000 MHz for electron acceleration. Microwave power for this purpose is produced by high frequency vacuum tube amplifiers (klystrons) which may have power output from a kW to MW range. The ion

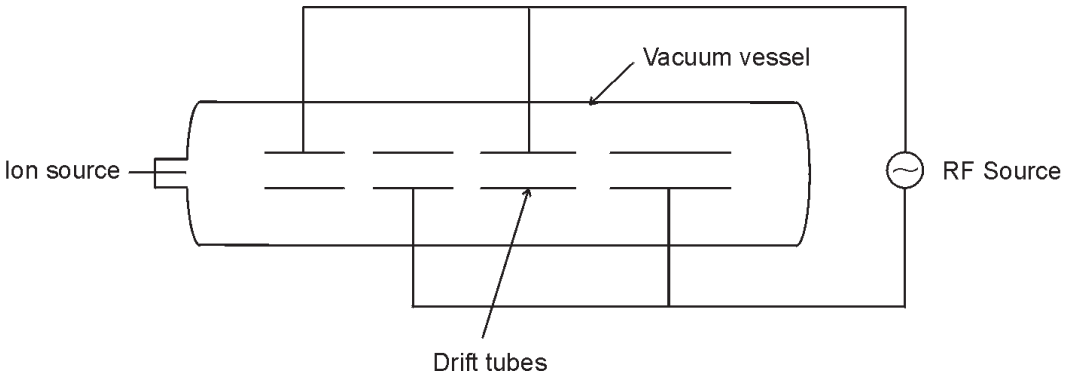

Fig. 11.5 Schematic of a linear accelerator.

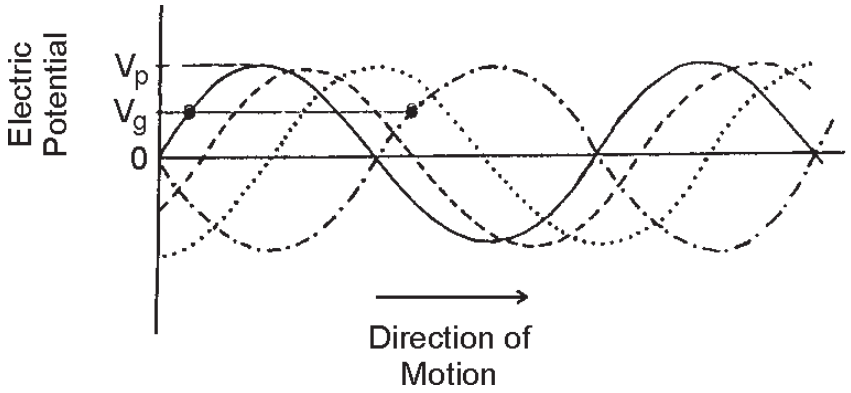

Fig. 11.6 Four different phases of the electric potential of an RF wave, and a charged particle riding in phase with the RF wave in a linear accelerator.

source releases the charged particles into the drift tube. For a 3000 MHz machine the cycle repeats every 1/3000 μs and the field reverses every 1/6000 μs. The direction of the field between the gaps alternates as shown in Fig. 11.6. Each time a particle crosses the gap, it should find an accelerating field so that it will gain energy. This can be achieved by designing the separation between successive acceleration gaps to equal the distance travelled by the particle during one half cycle. This length L is given by

$$L = \frac{v}{2f} \tag{11.1}$$

where v is the particle velocity and f is the frequency of the electric field. As the particle gains energy, v increases and therefore L must continuously increase. If V is the voltage across the gaps then energy gain (E) by a particle of charge q is

$$E = q\,V \tag{11.2}$$

If particle velocity is in the non-relativistic region, then length of n^{th} segment is given as:

$$L_n = \left[2nq\left(\frac{V}{m}\right)\right]^{1/2} / 2f \tag{11.3}$$

In the case of electrons, the particle velocity approaches that of light and spacing becomes constant

$$L_n = \frac{C}{2f} = \frac{\lambda}{2} \tag{11.4}$$

As the phase angle changes from 0 to π/2, the potential increases from 0 to V_p. From π/2 to π, the potential decreases from V_p to 0. The phenomenon is repeated with a negative sign from π to 2π. It is important that the particle and the wave move in phase. The separation between gaps should be designed such that the particle reaches the next gap exactly after one half

cycle and is subjected to acceleration by voltage V. The same phenomenon will occur at the next gap and so on. It is as if the particle rode a fixed point on the wave, like a surfer. However, if the gap came a little too soon, the potential will be less than V_g and hence the gain in energy will be less. But it will arrive at the next gap a little late and experiences higher potential. Thus a continuous loss and gain occur. This is called phase instability and should be avoided.

Cyclotron

The principle of multiple acceleration by a high frequency magnetic field was employed by Livingston and Lawrence to construct a circular rather than a linear machine. These accelerators are most successful in accelerating positive ions to hundreds of MeV energy. Unlike the linac, the ions in a cyclotron move along a spiral path under the influence of a magnetic field. Hollow drift tubes are replaced by two hollow semicircular electrode boxes called dees. Figure 11.7 shows the heart of a cyclotron schematically. The ions are produced in an ion source near the centre of the gap between the two dees. The dees are enclosed in a high vacuum tank which is located between the circular pole faces of an electromagnet. An RF potential is applied between the dees. Positive ions start from the ion source and move towards the dee having negative charge (let us assume A). On reaching the field free interior of the dee the magnetic field constrains the ion to move with a velocity v in a circular path of radius r given by

$$r = \frac{mv}{He} \tag{11.5}$$

$$\therefore \text{ angular velocity } \omega = \frac{v}{r} = \frac{He}{m}$$

where m and e are the mass and charge of the particle respectively, and H is the magnetic field strength. It is seen that for a fixed magnetic field strength, the angular velocity of a particle depends only on e and m. A radio frequency is chosen such that its period equals the time taken by the particle to complete one revolution. Frequency f $(= w/2\pi)$ at H=15,000 G is 23 MHz. Thus the RF oscillator frequency should be 23 MHz for 1500 G magnetic field. With this frequency, when the proton comes out of the dee A, the dee B will have negative potential and it will again gain energy across the gap. Thus the particle gains energy twice which completes one cycle through both the dees. Each time the diameter of the circle in which the proton moves increases and the process gets repeated several times. The proton thus has a spiral path in the dees. For particles with similar e/m, e.g., deuteron and alpha particle, the frequency of oscillator is the same. The peak voltage of RF oscillator has to be in the range of 50-500 kV for optimum performance. The electric focusing effect observed for static accelerators is also active here but its role becomes small at high particle energy. A magnetic focusing effect across the gap is, however, quite strong. This arises because near the edge of pole faces, the lines of magnetic field are curved and, therefore, the field has a horizontal component. This component provides a restoring force and guides ions above or below the medium plane towards that plane. The focusing is so good that a cyclotron beam is

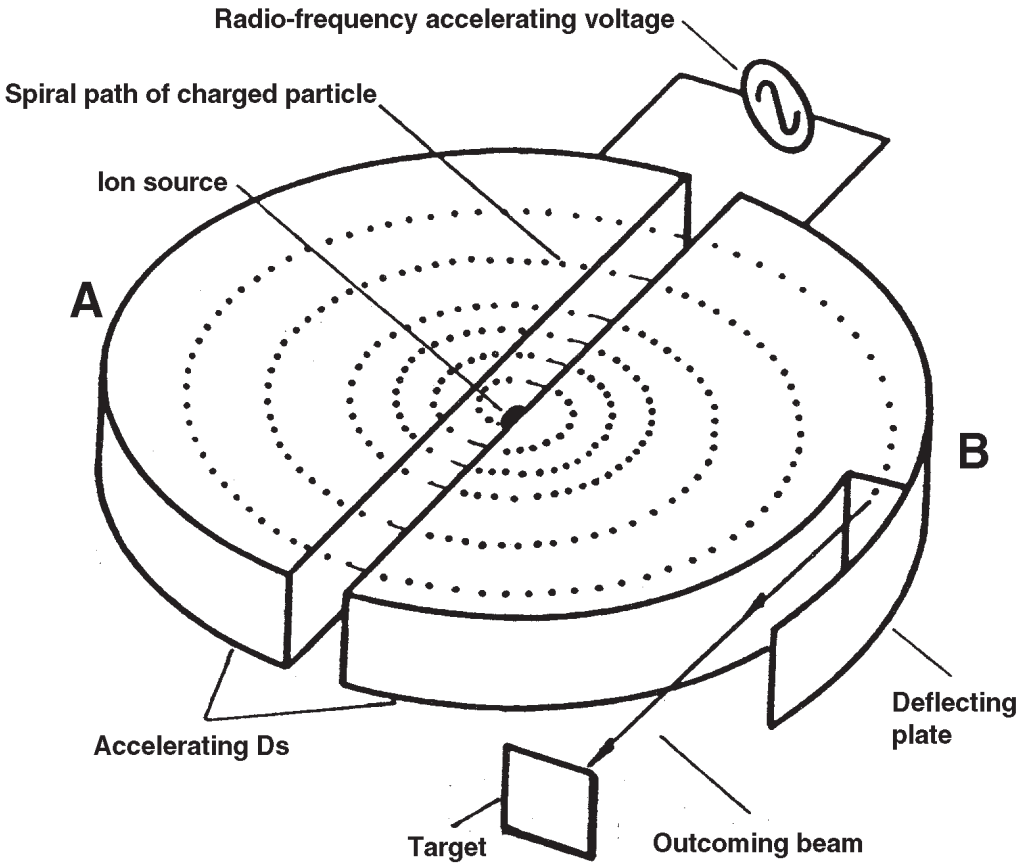

Fig. 11.7a Schematic representation of dees in a cyclotron.

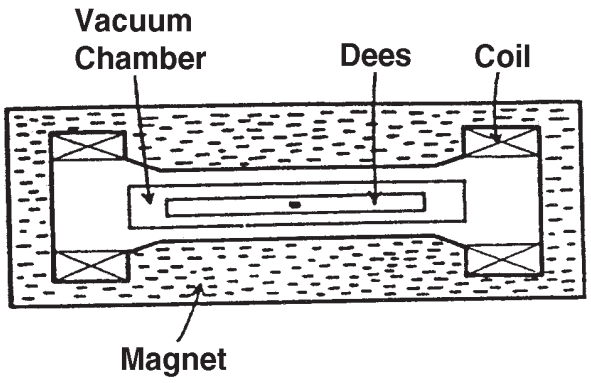

Fig. 11.7b Cross-sectional view of a cyclotron.

generally less than 5 mm diameter at the target. After acceleration of the particle to the desired energy, a deflector is used which causes the particles to exit through a window. The energy spectrum of the particles coming out of a cyclotron is quite often wide and suitable analyser magnets are used to obtain particles of a specific energy.

Constancy of particle mass is the basis of cyclotron principle. However, as the particle energy increases towards the velocity of light, there is an increase in the mass of the particle and decrease in angular velocity of the particle. In machines called synchrocyclotrons, the frequency of the accelerating electric field is steadily decreased to match the decreasing angular velocity of the particle. Proton energies of several hundred MeV are possible with these machines. In another machine called isochronous cyclotron, the magnet is constructed so that the magnetic field is stronger near the circumference than that at the centre. This compensates for the mass increase and maintains particles at a constant frequency of revolution.

The 224 cm variable energy cyclotron (VEC) at Kolkata was commissioned in 1977. It is a sector focused cyclotron. It has been providing α and p beams. α-particle beams of energy 30 to 120 MeV with beam currents of 10 μA have been made use of by researchers. For medical isotope applications, intense internal beam currents of about 100 μA have been made available on regular basis. Currently, this cyclotron is upgraded to provide medium and heavy ion beams upto an energy of 35 MeV/A using Electron Cyclotron Resonance (ECR) heavy ion sources. Neon ion beams of 200-300 MeV are now available with this modification.

Microtron

Cyclotrons are not used for electron acceleration because they reach relativistic velocities, and therefore, a change in mass, at fairly low energies. A modified design, called microtron, is able to overcome this drawback. This device also uses a constant and uniform magnetic field, and a constant RF voltage. The problem was overcome by ensuring that the phase slip at each turn, caused by increase of mass of the electron, corresponds to an integral number of RF cycles. The principle of phase stability helps to overcome small deficiencies in this requirement. The orbits of the electron are not concentric but arranged to have a common tangent at which point an accelerating cavity is placed. The electron trajectory is a series of circles of increasing radius (Fig. 11.8). The relative energy gain per cycle is high, orbits are well separated and beam extraction is straight forward. Electron energies of upto 850 MeV have been obtained in a microtron at Mainz, Germany. Quite often microtrons are used for injecting high energy electrons into other accelerating devices.

Betatron

The betatron is an electron accelerator of resonance type. Path of the electron in a betatron is a circle of fixed diameter (Fig. 11.9) A ceramic high vacuum chamber called a

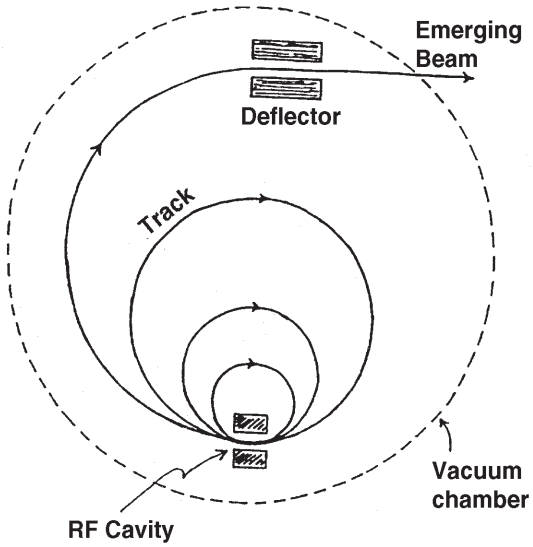

Fig. 11.8 View of the microtron in the plane containing the particle track.

"doughnut" is placed between truncated poles of a magnet that is powered by an alternating current of 50 to 200 Hz.

The electron moves in a circular path inside the doughnut under the influence of the magnetic field. This field is made to increase with time, by passing higher current through coils, to impart energy to the electrons. The field that keeps the electron in the orbit also produces a field in the interior of the orbit. The average field inside the orbit is always twice as strong as the magnetic field in the orbit. As the radius of the orbit remains constant, the acceleration chamber can be made in the shape of a doughnut. The poles of the magnet are tapered to cause the field near the orbit to weaken with increasing radius. This focuses the beam by causing any particles which stray from the orbit to be subjected to forces that restore it back towards its proper path.

To increase the energy of a particle in an orbit of radius r in a magnetic field, the particle must experience an electric field in the direction of its motion. The magnetic field itself can do no work on a charged particle because the force it provides is at right angles to the motion. The principle that a changing magnetic flux (φ) within a loop can create an electric field along the loop is used for acceleration of electrons. A transformer core within the circular orbit provides the voltage ($d\varphi/dt$ volts per turn). The inductance represented by the coil system is usually in a resonant circuit with a large capacitor to store the energy. The particles circulating in the orbit between the poles with a velocity v, experience an electric field E.

$$E = \frac{1}{2}\pi r \cdot \frac{d\varphi}{dt} \cdot \frac{v}{m} \qquad (11.6)$$

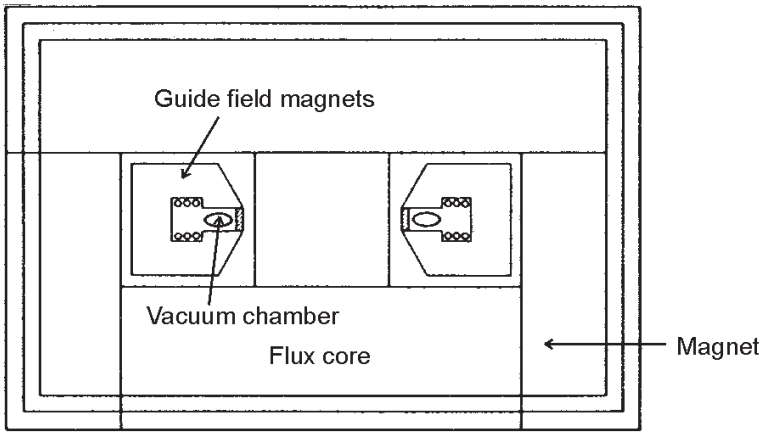

Fig. 11.9a Cross-sectional view of Betatron perpendicular to the plane of particle injection.

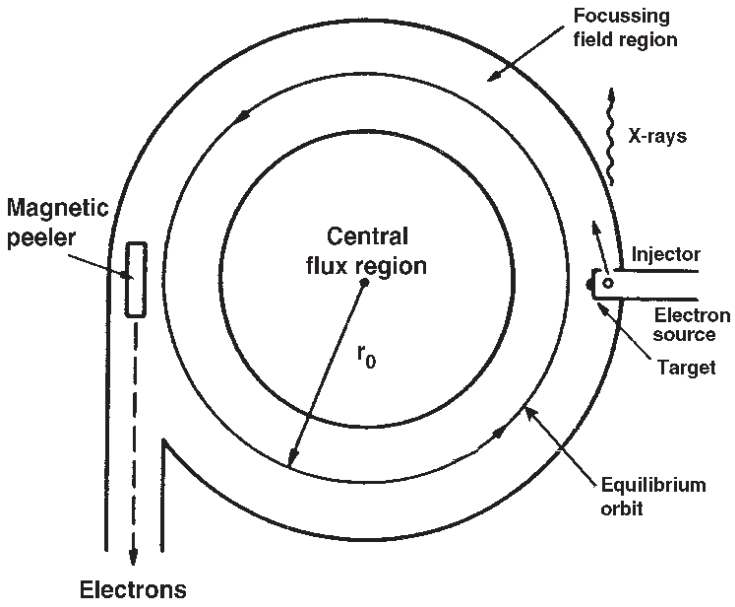

Fig. 11.9b Cross-sectional view of a Betatron perpendicular in the plane of particle motion.

The rate of change of momentum of the particle is given by

$$\frac{dp}{dt} = eE \tag{11.7}$$

As the electron gains energy it tends to move out of the equilibrium orbit. The magnetic field strength is increased to hold the electron in the orbit. This increase in magnetic field strength produces an electric field and the electron gains energy again. This process of increasing

magnetic field and increasing electron energy continues till the alternating current reaches its peak and starts to decrease. Before that happens an iron peeler is inserted to create a magnetic field free region and lets the electron emerge tangentially from the doughnut. In a typical betatron an electron may travel upto 1000 km in 1-4 ms it takes for acceleration. In a 20 MeV betatron, the electron gains about 100 eV per revolution and would travel the orbit 200,000 times during acceleration.

A limitation of the betatron method of magnetically induced acceleration is that, with electrons, centripetal electron energy loss becomes quite high when energies are 100 MeV and above. An ordinary iron-core flux with a rise time of a few milliseconds cannot sustain the energy loss. For example a 300 MeV betatron with a 4 ms rise time has approximately 10% energy loss during acceleration. This radiation is in ultraviolet to soft X-ray region and has proven useful because of its high intensity.

Synchrotron

The basic principle of synchrotron is a blend of principles of betatron and cyclotron. Like in a betatron, the charged particle is made to travel in a vacuum doughnut of fixed radius. To keep the particle orbit fixed, the magnetic field strength increases with the energy of the particle. However, unlike in a betatron, acceleration is produced by an alternating electric field that is synchronous with the orbital frequency as is done in a cyclotron. Physically the main differences are that the doughnut can be very large, ranging in diameter from several meters to hundreds of meters. A series of magnets are placed at appropriate locations along the doughnut to maintain a fixed orbit for the particles. The radio frequency oscillators to impart energy to the particle could be placed at suitable locations along the doughnut. The synchronism is maintained by the principle of phase stability.

Synchrotrons were developed to overcome the energy limits imposed by cyclotrons. These machines are useful when the speed of the particle is near that of light. While that happens for an electron at 2 MeV energy, the energy must be in the range of 4 GeV in the case of protons. In either case, the particles are injected into a synchrotron only after preliminary acceleration in a suitable machine. The idea is to make it go round and pass through the RF cavity repeatedly for successive gain of energy. To make a high energy particle travel in a circle, large magnetic fields and a huge circular magnet are required. The problem is overcome by not having a circle but a polygon as the path for the particle. At each rounded corner of the polygon a magnet forces the particle into the next arm of the polygon. In a four sided polygon the particle has to take a right turn at each corner which would require a strong field. By having a large number of sides, the angle through which the particle track has to be changed becomes smaller. To accommodate the magnets, the diameter of the equivalent circle has to increase and may range from tens of meters to hundreds of meters. The schematic of a typical synchrotron is shown in Fig. 11.10. It is essential to synchronise the rotation of particles in the accelerating tube with the field profile of the RF cavity, as is the case in a cyclotron. The principle of phase stability is helpful in keeping the particles bunch

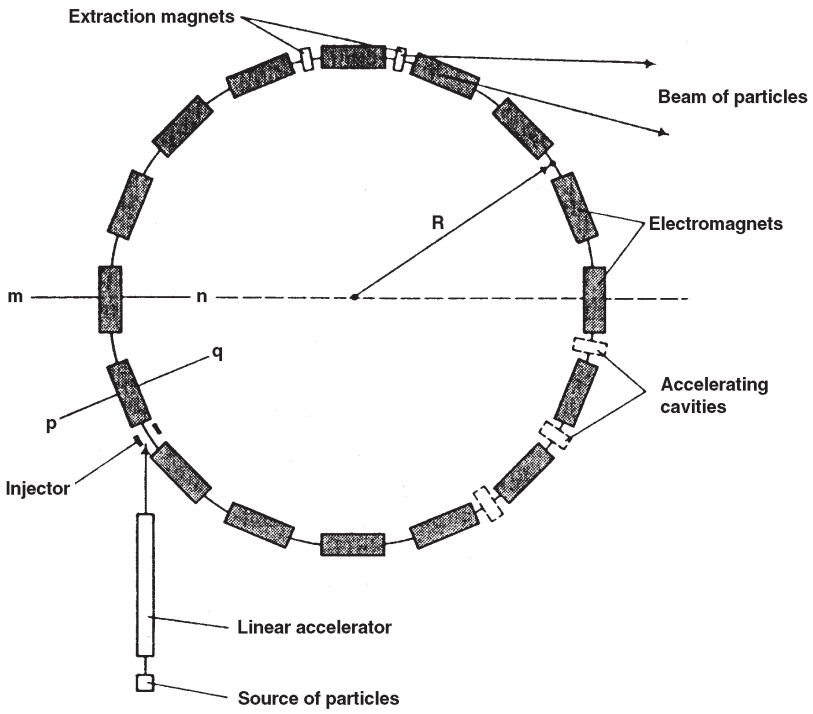

Fig. 11.10a Synchrotron having two types of magnets and alternating gradient focusing.

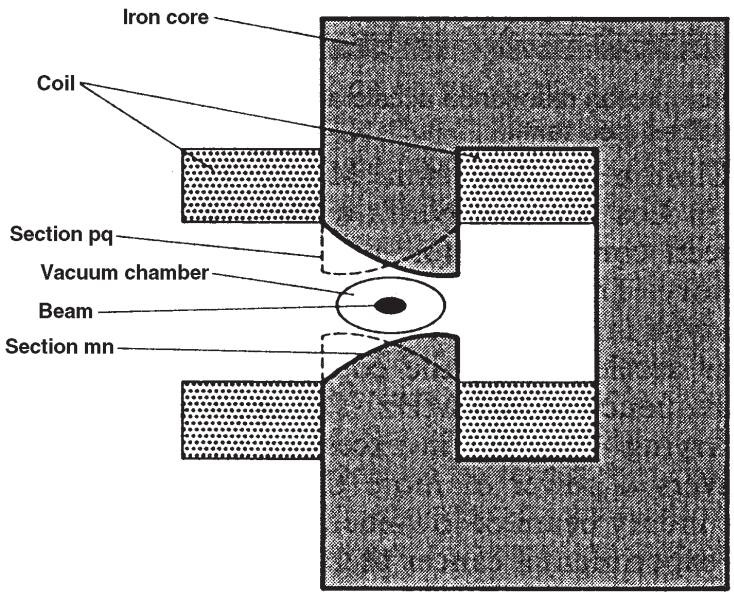

Fig. 11.10b Cross-sectional view of synchrotron with two different configurations for the pole tip.

together over the large number of rotation cycles. Also the peak accelerating voltage is about twice as large as the average energy gain per turn.

The weight and cost of magnets for a synchrotron of a given orbit largely depend on the size of the apertures in which the magnetic field has to be applied. The size of aperture, particularly in a proton machine, is governed by vertical and radial oscillations of the particles round the equilibrium orbit. These oscillations are caused due to various reasons like spread in angle and energy of the particle at injection, gas scattering at low energies, inhomogeneities in the magnetic field and inadequate high frequency control. In order to avoid excessive loss of particles from the beam by collision with the walls, large enough aperture is provided. The aperture can be reduced only by incorporating some focusing system. This is achieved by having shaped magnetic fields which provide bending as well as focusing (strong focusing). In this case the magnetic fields vary strongly with the radius. A magnet with pole tips shaped as shown in Fig. 10.10, cross section 'mn' produces a magnetic field that sharply decreases with increasing radius. In the plane perpendicular to the orbit, this field focuses the beam but at the same time the beam is defocused in the plane of the orbit. A magnet with pole tip shaped as shown in cross section 'pq' (Fig. 11.10), the field is focusing in the vertical direction and defocusing in the radial direction. This defocusing and focusing actions result in net focusing of the beam, similar to that achieved in the drift tubes. Alternate magnets in a machine have pole shapes as shown in cross sections mn and pq.

In an electron synchrotron the speed of the particle is essentially constant and very close to the speed of light. The time taken by the electrons to complete one rotation is fixed and the RF cavity can, therefore, have a single frequency. Electron loses energy on acceleration at the RF cavity or at each corner of the polygon. The emitted synchrotron radiation is quite useful for many investigations. However, this also limits the highest achievable energy. By having the path gently curved, the loss of energy is somewhat reduced. However, this radiation loss is dependent on the fourth power of energy and, therefore, the upper limit is dictated by this consideration. At CERN the large electron-positron collider accelerates electrons and positrons to 50 GeV in a ring of 27 km circumference. Magnetic field is used for beam extraction.

A proton synchrotron differs from an electron synchrotron in two aspects. First, the speed of the proton is not fixed and goes on changing as it gains energy. Because of this, the time taken to complete the orbit changes and in order to have synchronisation, the frequency of the RF cavity has to be modulated. Second, the protons lose much less energy because of their lower speeds. The energy loss of a 5 GeV proton is similar to that of a 3 MeV electron. The limit of energy in a proton synchrotron is dictated by the cost of magnetic ring which has a lower dependence on energy. At Fermi lab two large rings of 1000 meters in radius are used for attaining proton energy of upto 800 GeV. The bending and focusing functions are separated in this machine with 774 bending magnets in each ring. The first ring uses conventional magnets and has 180 focusing magnets. This is used to produce proton beams of energy upto 150 GeV in 1.5 s, which are injected into the second ring. This ring uses more powerful superconducting magnets for bending and focusing and there are 216 focusing magnets. The device gives one pulse energy of protons every minute.

Bibliography

1. M.S. Livingston, J.P. Blewelt, Particle Accelerators, McGraw Hill, New York (1962).
2. S. Humphry Jr., Principle of Charged Particle Acceleration, Wiley-Interscience, New York (1989).
3. W. Scharf, Particle Accelerators and their Uses, Harwood Academic, New York (1986).
4. M.S. Livingston, The Development of High Energy Accelerators, Dover, New York (1966).
5. B.S. Tomar, Guest Editor, Ionising Radiation Sources, IANCAS Bulletin, 15(4) 1999.

Chapter 12
Production and Separation of Isotopes

The isotopes of an element are characterised by a fixed number of protons (Z) and different number of neutrons (N). These isotopes can either be stable or radioactive. The stable isotopes of an element exist in nature in a fixed proportion in most of the cases. Most of the radioisotopes are man-made (artificial). Out of about 2000 isotopes of known elements, 275 are stable, the rest being radioactive with half lives ranging from microseconds to trillion years. Every element in the periodic table has at least one known isotope which is radioactive, while some have as many as 30 radioisotopes. Isotopes are used both in basic sciences and applications like industry and health care. Production of isotopes and their separation are important to understand.

This Chapter consists of two parts, namely, (i) Production of Radioisotopes and (ii) Methods for the Separation of Stable Isotopes.

Production of Radioisotopes

Natural radioactivity of uranium was discovered by Becquerel in 1896 and upto 1934, only naturally occurring radioactive substances were known. The natural radioisotopes are of two kinds. The long lived radioisotopes ^{40}K, ^{87}Rb, ^{235}U, ^{238}U and ^{232}Th survived from the time of creation of the terrestrial elements 4.5×10^9 years ago. Radioisotopes like ^{14}C which are relatively short-lived are continuously formed by the cosmic ray interaction in the upper atmosphere.

A vast majority of radioisotopes which find different applications are artificially produced. The first artificially produced radionuclide was discovered by Curies in 1934 while bombarding aluminium with α-particles from ^{210}Po. The reaction $^{27}_{13}Al\ (\alpha,n)\ ^{30}_{15}P$ yielded radiophosphorus. Subsequent period saw the development of (α,n) neutron sources, such as ^{226}Ra-Be, and accelerators. The efforts were directed towards the acceleration of α-particles, protons and deuterons and bombarding targets to produce and identify new radionuclides. With the construction of nuclear reactors neutrons also became available for isotope production.

General Considerations

Basic Nuclear Process

Stable elements tend to become radioactive when the neutron-proton ratio (N/Z ratio) in the nucleus is altered. Radioisotope production process makes use of altering N/Z ratio of the element by bombarding suitable target material with neutrons or charged particles. Neutron bombardment in general yields "neutron rich" isotopes which usually decay by β^- (negatron) emission and often accompanied by γ-radiation. In contrast, charged particle bombardment produces "neutron deficient" isotopes and they decay either by β^+ (positron) or Electron Capture (EC) mode. This is illustrated in Fig. 12.1

Neutron bombardment of selected targets in reactors is by far the most common route for radioisotope production. Charged particles of sufficient energy yield a product which is not isotopic with the target element and results in high specific activity product.

Neutron Bombardment

Nuclear reactor is a source of neutrons, which provides fluxes of thermal and fast neutrons of the order of 10^{13} - 10^{14} n/cm^2/s. At present there are three research reactors at BARC, Mumbai, namely, Apsara, CIRUS and Dhruva to cater to the needs of isotope production. The maximum neutron flux obtainable in Apsara, CIRUS and Dhruva are 5 x

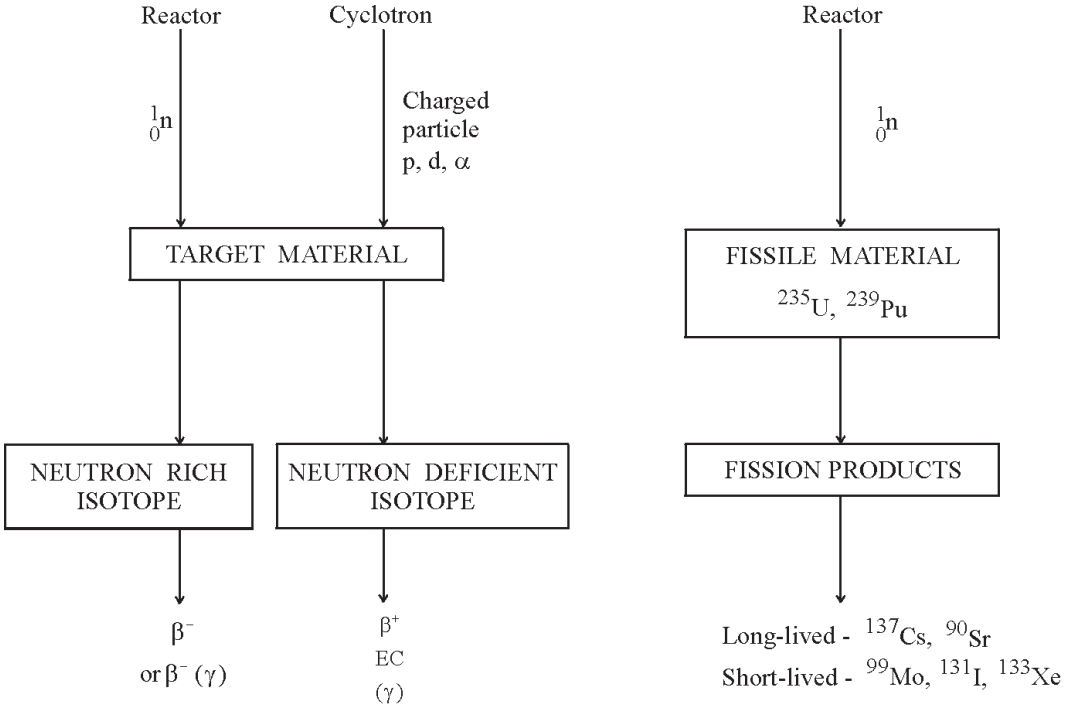

Fig. 12.1 Production of radioisotopes.

10^{12}, 6 x 10^{13} and 1.8 x 10^{14} n/cm^2/s respectively. Neutron being electrically neutral is not subjected to the electrostatic repulsion of the target nucleus. Therefore, even neutrons of low energy (thermal neutrons) cause nuclear reactions like (n,γ), (n,p) and (n,α). Types of neutron induced reactions commonly used for isotope production are briefly discussed.

(n,γ) Reaction

This reaction is called radiative capture and is the most common form of interaction of thermal neutron, with any atomic nucleus. The product is an isotope of the target nucleus with a mass number increased by one unit. Generally the radionuclide formed decays by β^- emission.

The primary product is an isotope of the target element and its chemical separation from stable isotopes is not possible. Specific activity is limited by the available neutron flux and cross section. More than half of the radioisotopes which are in general use are produced by (n,γ) reaction and a few typical reactions are given in Table 12.1.

Table 12.1 - Production of radioisotopes by (n,γ) reactions

Target	Radioisotope	σ_n (b)	$t_{1/2}$	Decay mode
^{59}Co (n,γ)	^{60}Co	36	5.274 y	β^-
^{98}Mo (n,γ)	^{99}Mo	0.14	65.94 h	β^-
^{23}Na (n,γ)	^{24}Na	0.53	14.9512 h	β^-
^{191}Ir (n,γ)	^{192}Ir	370	73.827 d	β^-
^{197}Au (n,γ)	^{198}Au	99	2.69517 d	β^-
^{81}Br (n,γ)	^{82}Br	3.2	35.30 h	β^-

(n,γ) Followed by β^- Decay

Some (n,γ) reactions produce a short lived radioisotope which decays to another radioisotope having a longer half-life. For example, (n,γ) reaction with tellurium yields a product ^{131}I. The product isotope is easily separable from the target and leads to high specific activity.

$$^{130}_{52}\text{Te} \quad (n,\gamma) \; ^{131}_{52}\text{Te} \xrightarrow[25\ \text{min}]{\beta^-} \; ^{131}_{53}\text{I} \xrightarrow[8.02070\ \text{d}]{\beta^-} \; ^{131}\text{Xe} \qquad (12.1)$$

(n,p) and (n,α) Reactions

After a neutron is captured by the target nucleus, emission of charged particle such as proton or α-particle from the compound nucleus (CN) is feasible if sufficient excitation

Table 12.2 - Production of radioisotopes by (n,p) reactions

Target	Radioisotope	σ_n	$t_{1/2}$	Decay mode
^{32}S (n,p)	^{32}P	65 mb	14.262 d	β^-
^{58}Ni (n,p)	^{58}Co	90 mb	70.86 d	β^+, EC
(n,p) reactions with thermal neutrons				
^{14}N (n,p)	^{14}C	1.82 b	5730 y	β^-
^{35}Cl (n,p)	^{35}S	0.35 b	87.38 d	β^-

Table 12.3 - Production of radioisotopes by (n,α) reactions

	Target	Radioisotope	σ_n	$t_{1/2}$	Decay mode
Fast (n)	^{27}Al (n,α)	^{24}Na	0.56 mb	14.9512 h	β^-
Thermal (n)	^{6}Li (n,α)	^{3}H	950 b	12.33 y	β^-

energy is available to the CN. A few examples are cited in Table 12.2 and 12.3. As the product nuclide is non-isotopic with the target, it can be separated from the target and very high specific activity is attainable by this route.

Multistage Neutron Capture Process

This method involves successive neutron capture and is especially important among the heavy elements. Some transuranic isotopes were produced using this route, e.g., ^{241}Am.

$$^{239}_{94}Pu\ (n,\gamma)\ ^{240}_{94}Pu\ (n,\gamma)\ ^{241}_{94}Pu \xrightarrow[14.290\ y]{\beta^-} {}^{141}_{95}Am \qquad (12.2)$$

Fission Reaction

The neutron induced fission of ^{235}U or ^{239}Pu during normal reactor operation provides a wide variety of radioisotopes as by-products. The peak fission yield of 6% corresponds to the isotopes with mass numbers 95-100 and 135-140 (Chapter 9). The specific activities of various isotopes vary from element to element as stable isotopes are also formed during fission in addition to the radioisotopes, e.g., radioisotope ^{99}Mo is a fission product formed along with stable ^{100}Mo.

Long lived fission products (FP) of industrial importance are ^{137}Cs, ^{90}Sr, ^{85}Kr, ^{147}Pm etc. These isotopes can be separated from FP waste solution during nuclear fuel

reprocessing. Short lived fission products (FP) ^{99}Mo, ^{140}Ba, ^{89}Sr, ^{131}I, ^{133}Xe etc. are produced by irradiating natural or enriched uranium targets in nuclear reactors for a short duration followed by conventional radiochemical separation. Fission products ^{90}Sr, ^{106}Ru, ^{132}I, ^{137}Cs and ^{140}Ba cannot be obtained by the (n,γ) route.

Indirect Reaction

The particle emitted from the target in a neutron induced reaction can further initiate a nuclear reaction. For example, energetic tritons are produced by ^{6}Li (n,α) ^{3}H reaction. When lithium carbonate is irradiated in a flux of thermal neutrons, ^{18}F, a positron emitting isotope having $t_{1/2}$ of 110 min is produced as shown below.

$$^{6}\text{Li}(n,\alpha)^{\mathbf{3}}\mathbf{H} \text{ and } ^{16}\text{O}(^{\mathbf{3}}\mathbf{H}, n)^{18}\text{F} \qquad (12.3)$$

The Szilard-Chalmers (SC) Process

The (n,γ) reaction sometimes causes chemical effects, owing to the recoil energy of the nucleus when γ-ray is emitted. The recoil energy is sufficient to rupture chemical bonds. If after the rupture, the product atom exists in a different chemical state and separable from that of the target, then the product can be isolated from the large mass of inactive target. This process is known as Szilard-Chalmers process. This provides a means of obtaining high specific activity product even though the target and the product are isotopic.

Szilard and Chalmers (SC) discovered that when ethyl iodide was irradiated with neutrons, ^{128}I atoms formed from ^{127}I (n,γ) ^{128}I recoil out of the compound and end up as free iodine which could be extracted with water.

$$\underset{\text{ethyl iodide}}{C_2H_5\ ^{127}I} \xrightarrow{n} [C_2H_5\ ^{128}I]^* \xrightarrow{\gamma} \underset{\text{recoil}}{C_2H_5^{\bullet}} + {}^{128}I^{\bullet} \qquad (12.4)$$

The liberated ^{128}I loses its kinetic energy and stabilises as iodine atom or iodide ion. A significant fraction of radionuclide appears in a chemical form different from that of the target (C_2H_5I).

The SC process is employed for isotope production. For example, ^{51}Cr, is produced by irradiating potassium chromate (K_2CrO_4) target in a thermal neutron flux by ^{50}Cr(n,γ)^{51}Cr reaction. Due to the recoil effect following the (n,γ) reaction, ^{51}Cr produced is in +3 oxidation state. This Cr(III) is separated from the Cr(VI) in K_2CrO_4 by precipitation of Cr(VI) as $BaCrO_4$.

In the SC process, enrichment factor is defined as the ratio of specific activity of the recoiled chemical form to that of the target at the end of irradiation. High enrichment factor is necessary for the isotope production (Table 12.4). It has been observed that low or medium neutron flux and short irradiation times are conducive to a high enrichment factor.

Table 12.4 - Examples of the SC process for isotope production

Nuclide	Target	% Yield	Enrichment factor
^{82}Br	$KBrO_3$ $^{81}Br\ (n,\gamma)\ ^{82}Br$	91	2×10^4
^{59}Fe	$K_4Fe(CN)_6$ $^{58}Fe\ (n,\gamma)\ ^{59}Fe$	60	2000 - 9000
^{51}Cr	K_2CrO_4 $^{50}Cr\ (n,\gamma)\ ^{51}Cr$	40	150 - 2500

Charged Particle Bombardment

High energy charged particles like p, d, α and He^{3+}, obtained from accelerators, are used for the production of neutron deficient radionuclides. As the charged particles have small penetrating power (range), the targets in accelerator are in most cases very thin metal foils. Targets are also prepared by depositing oxide layer on a suitable substrate. In accelerator bombardment the product is normally an element different from the target and chemical separation yields a high specific activity product. In the low to medium energy charged particle induced reactions, depending on the energy of the projectile, the following reaction channels are probable.

(i) (p,α), (p,d), (p, xn) (p,xn,yp)

(ii) (d,α),(d,p),(d,xn),(d,xn,yp)

(iii) (α,xn),(α,xn,yp)

where x,y = 1,2,3,...

In the proton induced reaction on ^{127}I, ^{123}Xe, ^{125}Xe and ^{121}Xe are formed by (p,5n), (p,3n) and (p,7n) exit channels respectively. From the knowledge of excitation functions, the energy of the proton beam is so chosen to primarily yield ^{123}Xe by (p, 5n) reaction.

Cyclotron produced isotopes such as ^{67}Ga, ^{111}In, ^{123}I and ^{201}Tl decay by EC and are extensively used in nuclear medicine. Positron emitting isotopes such as ^{11}C, ^{13}N, ^{15}O and ^{18}F are short lived ($t_{1/2}$ in the range of minutes). Their production in cyclotron is followed by rapid radiochemical processing to yield labelled molecules. Some useful cyclotron produced radionuclides are shown in Table 12.5.

Radioisotope Generators

One way of obtaining a short lived radioisotope for use as tracers in medicine and industry, at places far away from nuclear reactors or cyclotron installations, is to use the radioisotope parent-daughter generator. In a generator, a longer lived parent is chemically

Table 12.5 - Some cyclotron produced radioisotopes

Nuclide	$t_{1/2}$	Decay mode	Production
^{22}Na	2.6019 y	β^+ (91%), EC	^{24}Mg (d,α) ^{22}Na
^{57}Co	271.94 d	EC	Ni (p,x) ^{57}Co
^{67}Ga	3.2612 d	EC	^{68}Zn (p,2n) ^{67}Ga
^{111}In	2.8047 d	EC	^{112}Cd (p,2n) ^{111}In
^{123}I	13.27 h	EC	^{124}Te (p,2n) ^{123}I ^{124}Xe (p,2n) $^{123}Cs \rightarrow {}^{123}Xe \rightarrow {}^{123}I$
^{201}Tl	72.912 h	EC	^{203}Tl (p,3n) $^{201}Pb \rightarrow {}^{201}Tl$
^{11}C	20.39 min	β^+	^{14}N (p,α) ^{11}C
^{13}N	9.965 min	β^+	^{16}O (p,α) ^{13}N
^{15}O	122.24 s	β^+	^{14}N (d,n) ^{15}O
^{18}F	109.77 min	β^+	^{18}O (p,n) ^{18}F ^{20}Ne (d,α) ^{18}F
^{103}Pd	16.991 d	EC	^{103}Rh (p,n) ^{103}Pd

fixed, which decays to shorter lived daughter and comes into radioactive equilibrium (Chapter 4). The daughter nuclide is selectively milked out from the generator making use of the difference in the chemical properties of the two elements. Some examples of generator systems are ^{137}Cs - ^{137m}Ba, ^{140}Ba - ^{140}La, ^{99}Mo - ^{99m}Tc, ^{90}Sr - ^{90}Y and ^{113}Sn - ^{113m}In.

The parent radioisotope is either produced in a reactor or in a cyclotron and is normally adsorbed on a material support, for example - an ion exchange resin in a small packed column. The short lived daughter is eluted from the system by using selective solvents. Daughter nuclide continues to grow and reaches a maximum activity after a period of 3 to 4 times its half life. Therefore, repetitive milking is possible.

Reactor or Cyclotron

The choice of the mode of production depends upon several factors. It is important to choose a radionuclide which is suitable for a particular application or experiment taking into consideration half life, decay mode, energy, specific activity, radionuclide purity, processing time etc. For example, ^{24}Na ($t_{1/2}$ = 14.9512 h) cannot be used as a tracer in an experiment when the duration of the experiment is more than a month. In such a case

cyclotron produced ^{22}Na ($t_{1/2}$ = 2.6019 y) is the choice. The possibility of production of a particular radioisotope may then be limited either by the available facility (reactor, flux, charge particles, beam current, target considerations etc.) or by the reaction cross section.

Reactor produced radioisotopes are usually cheaper and easier to obtain on a routine basis as compared to cyclotron produced isotopes. In a reactor, many targets are irradiated simultaneously and radioisotope production in most cases is incidental to normal reactor operation, whereas in cyclotron, normally only one target can be bombarded at a time. Even though the production costs are high, cyclotron offers many important neutron deficient products. Hence the two modes of production are complementary.

Irradiation Yields

It is important to know how much of a radionuclide is formed when the target of an element is subjected to neutron or charged particle bombardment. Number of particles incident/cm^2/s on a target is the flux (ϕ). A beam of charged particles in a cyclotron is usually referred to as beam current rather than flux. Beam current is expressed in amperes (A). Beam current of one ampere corresponds to 6.24 x 10^{18} protons/s or 3.12 x 10^{18} α particles/s.

In a nuclear reactor the entire target is completely immersed in the neutron flux. The rate of production of a nuclide by neutron irradiation in a reactor is expressed as:

$$\frac{dN_1}{dt} = \phi\sigma N_t \qquad (12.5)$$

where N_1 = Number of product atoms at any time t, N_t = Number of target atoms, ϕ = neutron flux (n/cm^2/s) and σ = reaction cross section (cm^2)

In an accelerator the target size is quite often comparable to or larger than the beam dimension. Production rate of nuclide in cyclotron irradiation is given by

$$\frac{dN_1}{dt} = 6.24 \times 10^{18}\ i\ z^{-1}\ \sigma\ N_a \qquad (12.6)$$

where i = beam current in amperes, z = charge on the projectile and N_a = Number of target atoms per cm^2

If the product nuclide is radioactive, it will decay with its characteristic $t_{1/2}$ during the course of its production leading to another product nuclide.

$$a + A \xrightarrow{\sigma} X_1 \xrightarrow{\lambda_1} X_2$$

Let N_1 be the number of atoms of product X_1 present at any time t

$$\frac{dN_1}{dt} = \text{rate of formation - rate of decay} = \phi\ \sigma\ N_t - \lambda_1 N_1 \qquad (12.7)$$

For neutron irradiation, On solving the differential eqn. 12.7, number of product atoms N_1 present after irradiation time t is given by

$$N_1 = \phi \sigma N_t \frac{(1-e^{-\lambda_1 t})}{\lambda_1} \qquad (12.8)$$

Activity of $X_1 = A_1 = N_1\lambda_1$

$$A_1 = \phi \sigma N_t (1-e^{-\lambda_1 t}) \quad (Bq) \qquad (12.9)$$

(i) when $t >> t_{1/2}$, i.e. $\lambda_1 t >> 1$ then $e^{-\lambda_1 t} \approx 0$ and eqn. 12.9 reduces to

$$A_1 (max) = \phi \sigma N_t \qquad (12.10)$$

and is called the saturation activity.

(ii) when $t << t_{1/2}$, exponential term $(1-e^{-\lambda_1 t}) \cong \lambda_1 t$ and eqn. 12.9 reduces to

$$A_1 = \phi \sigma N_t \lambda_1 t \qquad (12.11)$$

From the eqn. 12.9 it can be seen that the activity increases exponentially with time and reaches a maximum value called saturation activity and given by eqn. 12.10. $(1-e^{-\lambda_1 t})$ is called growth factor.

(iii) Irradiation time in terms of $t_{1/2}$

When irradiation is carried out for 1,2 and 3 half lives, the activity formed would be respectively 0.5, 0.75 and 0.875 times the saturation activity. The build up of ^{24}Na activity as a function of time at different neutron fluxes is shown in the Fig. 12.2. Generally for radioisotope production, it is not prudent to carry out irradiation over periods greater than three half lives.

Eqn. 12.8 and 12.9 are valid only when

a) Projectile energy remains constant - therefore reaction cross section is also constant.

b) Number of nuclear reactions taking place is small compared to the total number of target atoms. This ensures N_t to be nearly constant.

c) Flux (ϕ) does not change while passing through the target

The activity equation for cyclotron irradiation can be expressed as

$$A_1 = 6.24 \times 10^{18} i z^{-1} \sigma N^a (1-e^{-\lambda_1 t}) \ (Bq) \qquad (12.12)$$

Two examples are given to explain the method of calculation of activities that could be obtained by reactor and accelerator routes.

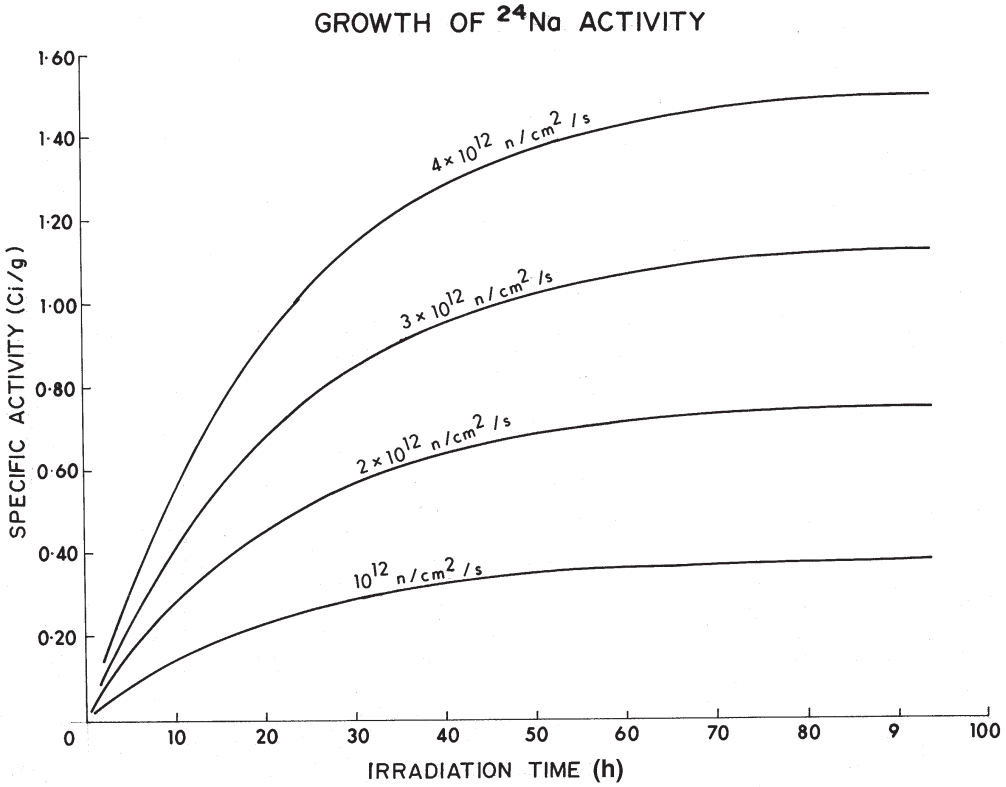

Fig. 12.2 Build-up of ^{24}Na activity.

Sodium-24 ($t_{1/2}$ = 14.9512 h) is produced in the reactor by the reaction $^{23}Na\ (n,\gamma)^{24}Na$. 10 g of Na_2CO_3 (Mol wt = 106) is irradiated in a thermal neutron flux of 10^{13} n/cm^2/s for 45 h. Reaction cross section for ^{23}Na (100% natural abundance) is 0.53 barns. ^{24}Na activity (A_1) at the end of irradiation is calculated using eqn. 12.9 as follows:

$\phi = 10^{13}$ n/cm^2/s, $\sigma = 0.53 \times 10^{-24}$ cm^2, t = 45 h, $\lambda = 0.693/14.9512$ h^{-1}

$N_t = (10 \times 2)/ 106 \times 6.023 \times 10^{23} = 1.136 \times 10^{23}$

$A_1 = 10^{13} \times 0.53 \times 10^{-24} \times 1.136 \times 10^{23} \times 0.875$

$= 5.27 \times 10^{11}$ Bq

^{24}Na can alternatively be produced in an accelerator by deuteron bombardment of magnesium target via $^{26}Mg(d,\alpha)^{24}Na$ reaction. Natural magnesium contains 11% of ^{26}Mg. σ = 25 mb. A 0.01 cm thick Mg foil (Mol. wt. = 24.3, density = 1.74 g/cm^3) is irradiated for 1 h at 100 μA beam current. ^{24}Na activity at the end of bombardment is computed using eqn. 12.12 as follows:

$i = 100 \times 10^{-6}$ amp; $\sigma = 25 \times 10^{-3} \times 10^{-24}$ cm^2, z = 1, t = 1 h, $\lambda = \dfrac{0.693}{14.9512} = 0.0462$ h^{-1}

$$\text{Number of } ^{26}\text{Mg atoms/cm}^2 = \frac{0.11 \times 1.74 \times 6.023 \times 10^{23}}{24.3} \times 0.01$$

$$= 4.742 \times 10^{19}$$

$A_1 = {}^{24}$Na activity

$= 6.24 \times 10^{18} \times 100 \times 10^{-6} \times 25 \times 10^{-27} \times 4.74 \times 10^{19} (1\text{-}e^{-0.0462 \times 1})$

$= 3.33 \times 10^{7}$ Bq

Role of Enriched Targets

Enriched targets are relatively expensive but needed in the following cases.

(a) For obtaining increased yield and higher specific activity. e.g., ^{112}Sn (n,γ) ^{113}Sn : Natural abundance : 1% and ^{18}O (p,n) ^{18}F : Natural abundance : 0.2%

(b) To minimise concomitant reaction(s) leading to unwanted activation product(s).
e.g., ^{185}Re (n,γ) ^{186}Re ($t_{1/2}$ = 3.7183 d); ^{187}Re (n,γ) ^{188}Re ($t_{1/2}$ = 17.005 h)
(37.4%) (62.6%)

One has to let ^{188}Re decay over 85 - 102 hours to use reasonably pure ^{186}Re which amounts to poor utilisation of the reactor irradiation capacity. Similarly, if one wants to use ^{188}Re by the above route, very short irradiation periods followed by immediate use of the product will be needed.

(c) To ensure very high radionuclidic purity of the final product.
e.g., ^{124}Xe (p,2n) ^{123}Cs $\rightarrow$ ^{123}Xe $\rightarrow$ ^{123}I ($t_{1/2}$ = 13.27 h)

If ^{124}Xe (Natural abundance : 0.1%) is not highly enriched (>>99%), ^{126}Xe present in the target would give rise to ^{125}I ($t_{1/2}$ = 59.400 d) by the reaction :

^{126}Xe (p,2n) ^{125}Cs $\rightarrow$ ^{125}Xe $\rightarrow$ ^{125}I

Long-lived isotopic impurity of ^{125}I is not acceptable in ^{123}I products meant for use in humans, except at extremely low level.

Another example is the case of ^{58}Co ($t_{1/2}$ = 70.86 d) production from ^{58}Ni (n,p) ^{58}Co reaction. Natural abundance of ^{58}Ni is 68.077%. Unless one uses nearly pure ^{58}Ni, ^{60}Ni present (26.1%) in natural nickel will yield ^{60}Co ($t_{1/2}$ = 5.274 y) from ^{60}Ni (n,p) ^{60}Co reaction. Long-lived isotopic impurity of ^{60}Co is not acceptable in ^{58}Co.

(d) To avoid high neutron absorption reactions.
e.g., ^{152}Sm (n,γ) ^{153}Sm (σ = 210 b) and ^{149}Sm (n,γ) ^{150}Sm (σ = 41000 b)

Presence of ^{149}Sm along with ^{152}Sm (natural abundances of ^{149}Sm and ^{152}Sm are 13.8% and 26.7% respectively) in the target would place limitations on the quantity of target that can be irradiated per given location in the reactor.

Radiochemical Processing

γ-emitting isotopes such as ^{60}Co and ^{192}Ir are used as radiation sources for industrial radiography. Targets are irradiated in suitable form and the irradiated material is directly used after sealing them in a protective container. When isotope such as ^{46}Sc is used as tracer, scandium, irradiated in suitable chemical form, is used for experiment without any purification. The associated impurities do not interfere in the tracer work. But in majority of cases the irradiated targets are subjected to radiochemical processing steps in order to obtain a radioisotope in a required chemical form and at the desired level of purity (radionuclide and chemical purity). The need for chemical processing stems from the fact that during neutron or charged particle bombardment more than one type of nuclear reactions takes place concurrently such as (n,α), (n,p) and (n,γ). This results in production of different nuclides. In addition, impurities in the target also give rise to a host of other radionuclide products. Selection of pure targets and at times enriched targets is, therefore, necessary.

Radiochemical processing of irradiated target utilises one or more conventional separation methods such as adsorption and coprecipitation, solvent extraction, ion exchange or solid-liquid chromatography, distillation / volatilisation and electrochemical methods. The following factors are to be considered to choose a processing.

(a) Time : Overall processing time limit depends upon the $t_{1/2}$ of the isotope. Rapid radiochemical separation methods are used for short lived isotopes.

(b) Quantity : Generally extremely small quantity of radioactive material is produced and high yield chemical separations at these levels are not very easy. e.g., 0.1 mCi of ^{58}Co is produced by ^{58}Ni(n,p)^{58}Co in one week irradiation at a flux of 10^{12} n/cm^2/s. This is equivalent to 3 x 10^{-12} g of ^{58}Co. Carrier free separations are done at these levels.

(c) Radiation : Due to associated radiation all the chemical operations are carried out inside specially designed facilities, such as glove boxes, lead shielded plants and hot cells depending upon the amount of activity handled and the type and energy of the emitted radiation (see Chapter 21 for details).

Production and Processing of some Reactor Produced Isotopes

Phosphorus-32

It is a pure β^- emitter having β_{max} energy of 1.71 MeV. Its half life is 14.262 d and is used as tracer in agricultural and biological research. It is prepared by two methods.

(a) Neutron irradiation of elemental phosphorus: ^{31}P is of 100% natural abundance. Reaction ^{31}P(n,γ)^{32}P yields contamination free but low specific activity ^{32}P.

(b) Fast neutron irradiation of elemental sulphur: Natural sulphur contains 95% of ^{32}S. Reaction ^{32}S(n,p)^{32}P yields high specific activity product. Typically 100 mCi ^{32}P is produced per 100 g of sulphur when irradiated in a neutron flux of 10^{12} n/cm^2/s for 30

days. A small amount of ^{33}P ($t_{1/2}$ = 25.34) from $^{33}S(n,p)^{33}P$ reaction is an unavoidable radionulcidic impurity. Irradiated sulphur is distilled off under reduced pressure and elevated temperature. Residual ^{32}P, is leached with dil HCl and passed through a cationic exchanger to remove the impurities. The eluent is concentrated, evaporated to dryness, re-dissolved in dil HCl and the product supplied as ^{32}P labelled orthophosphoric acid. This compound is a precursor in the synthesis of labelled nucleotides (biomolecules) such as γ-ATP.

Sulphur-35

It is also a pure β^- emitter having β_{max} energy of 0.167 MeV. Its half life is 87.51 d and is prepared by (n,γ) or (n,p) reactions. In practice, $^{35}Cl(n,p)^{35}S$ reaction is used for production (σ = 0.35 b) of ^{35}S. Typically 220 mCi ^{35}S/g of Cl is obtained when irradiated for 30 days in neutron flux of 10^{12} n/cm^2/s. This is one of the few examples of (n,p) reaction taking place with thermal neutrons. Irradiated target (KCl) is dissolved in dil HCl and passed through an alumina column. ^{35}S is eluted out with 1 N NH_4OH. The ammonium salt is destroyed with conc. HNO_3 and ^{35}S is supplied as $H_2\,^{35}SO_4$.

Molybdenum-99

The importance of the radioisotope ^{99}Mo is due to its daughter technetium-99m (^{99m}Tc), which is widely used for diagnostic studies in nuclear medicine. ^{99}Mo ($t_{1/2}$ = 65.94 h) is in transient equilibrium with ^{99m}Tc ($t_{1/2}$ = 6.01 h).Decay scheme of ^{99}Mo is shown Fig. 12.3.

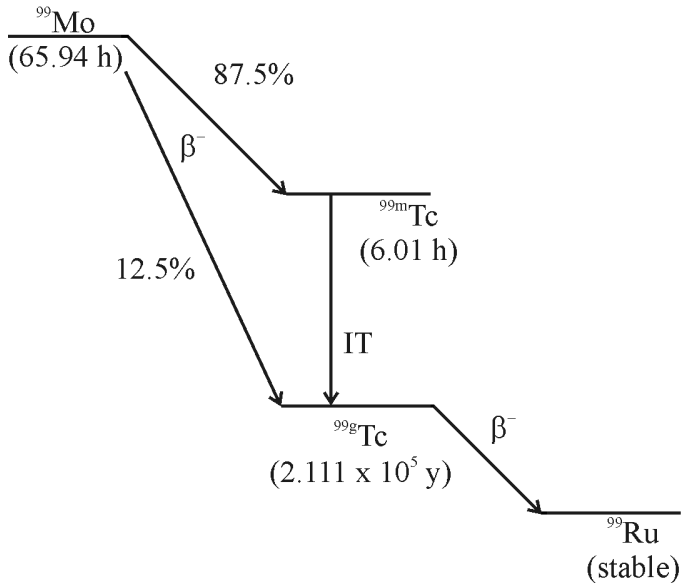

Fig. 12.3 Partial decay scheme of of ^{99}Mo.

^{99}Mo is produced bu two routes. Neutron activation of Mo and neutron induced fission of ^{235}U.

(a) Neutron activation of molybdenum
Molybdenum-99 is produced by ^{98}Mo (n,γ) ^{99}Mo reaction when Molybdenum trioxide (MoO_3) is irradiated with neutrons in a nuclear reactor. Corss section for this reaction is 0.14 with thermal neutron and $\sigma_{effective}$ = 0.5 b (contribution from the epithermal neutrons)

Typically 800 mCi ^{99}Mo/g of natural Mo is produced in one week irradiation at a neutron flux of 5 x 10^{13} n/cm^2/s. Natural molybdenum has 14.8% ^{92}Mo, 9.1% ^{94}Mo, 15.1% ^{95}Mo, 16.7% ^{96}Mo, 9.5% ^{97}Mo, 24.4% ^{98}Mo and 9.6% ^{100}Mo. Of these the neutron reaction cross section for ^{92}Mo is very small and the product ^{93}Mo is very long lived. ^{100}Mo absorbs neutrons to yield short lived (14.61 min) ^{101}Mo. All other isotopes yield stable products. So after a brief period of cooling essentially all the activity is the target is due to ^{99}Mo. The use of enriched targets can give higher specific activity of ^{99}Mo. (n,γ) reactions on the impurities in MoO_3 give rise to radionuclide impurities which get carried with ^{99m}Tc, when separated from ^{99}Mo. For example, the following nuclear reaction takes place if molybdenum target contains tungsten impurity.

$$^{186}\text{W (n,}\gamma\text{) }^{187}\text{W (n,}\gamma\text{) }^{188}\text{W} \xrightarrow[69.4\ \text{d}]{\beta^-} {}^{188}\text{Re} \qquad (12.13)$$

^{188}Re is a radionuclidic impurity which is hard to separate from ^{99m}Tc because of similar chemical properties. Irradiated MoO_3 target is dissolved in hot NaOH and ^{99}Mo is made available as sodium molybdate. ^{99m}Tc (as sodium pertechnetate) is extracted from the alkaline molybdate solution by solvent extraction, with methyl ethyl ketone.

(b) Fission mode: ^{235}U(n,f)^{99}Mo,
Molybdenum-99 is produced in the fission of ^{235}U with an yield of 6.1% and fission cross section is 585 b. Uranium metal or U-Al alloy low enriched uranium (LEU) (<20% ^{235}U) or highly enriched uranium (HEU) (93% ^{235}U) is used as the target.

Typically 20 Ci ^{99}Mo/g of ^{235}U is produced in fission in 7 day irradiation with a neutron flux of 10^{13} n/cm^2/s. The essential difference between (n,γ) ^{99}Mo and (n,f) ^{99}Mo is that the latter gives very high specific activity (>10^3 Ci/g Mo), though not carrier-free. Molybdenum isotopes such as ^{98}Mo (stable) and ^{100}Mo (stable) are formed either during fission or during post irradiation cooling due to decay from the precursors and results in specific activity reduction.

The separation is carried out soon after irradiation, since post irradiation decay produces stable molybdenum isotopes resulting in further reduction in specific activity. Various chemical processes to extract curie quantities of ^{99}Mo have been developed. In one of the processes irradiated enriched ^{235}U target is dissolved in 6 M nitric acid followed by addition of tellurium carrier. The solution is then passed through an alumina column. Molybdenum and tellurium are selectively absorbed while uranium and other fission products go to the effluent during washing. Molybdenum is recovered from the column

eluting with 1 M NH_4OH. The chemical yield is 70%. The major radionuclidic impurities are ^{131}I, ^{103}Ru, ^{89}Sr, ^{90}Sr, ^{137}Cs, ^{141}Ce etc. and should be absent as stringent limits are set for ^{99m}Tc for medical applications. With high specific activity ^{99}Mo the alumina column generators are used. With low specific activity ^{99}Mo, solvent extraction using methyl ethyl ketone (MEK) is used.

Iodine-125

^{125}I undergoes decay by electron capture with a half life of 59.408 d. It emits γ-rays of 35 keV and 28 keV and finds extensive application as tracer in radioimmunoassay (RIA). It is produced by neutron irradiation of natural/enriched xenon gas. Natural abundance of ^{124}Xe is 0.094%

$$^{124}Xe\ (n,\gamma)\ ^{125}Xe \xrightarrow[16.9\ h]{EC} {}^{125}I \xrightarrow[59.400\ d]{EC} {}^{125}Te \qquad (12.14)$$

Typically 130 mCi ^{125}I per g of Xe (natural) is produced when irradiated for 15 days in a neutron flux of 5 x 10^{13} n/cm^2/s. Maximum specific activity attainable is 17 mCi/μg iodine. Apart from other isotopes, natural xenon contains ^{126}Xe which leads to ^{127}I formation and decreases the specific activity of ^{125}I.

$$^{126}Xe\ (n,\gamma)\ ^{127}Xe \xrightarrow[34.4\ d]{EC} {}^{127}I\ (stable) \qquad (12.15)$$

High neutron absorption cross section of ^{125}I ($\sigma = 900$ b) leads to radionuclide impurity ^{126}I.

$$^{125}I\ (n,\gamma)\ ^{126}I\ (n,\gamma)\ ^{127}I$$
$$\downarrow\ EC\ (13.11\ d)$$
$$^{126}Te$$

The formation of ^{126}I can be reduced if large quantities of ^{124}Xe is irradiated for a short period of time. Purification of ^{125}I from ^{126}I is only achieved by allowing the shorter lived ^{126}I to decay. Usually natural xenon gas is irradiated in a specially designed aluminium containers for 15 days. After 30-40 days post irradiation cooling, the container is cooled under liquid nitrogen and xenon gas is allowed to escape while ^{125}I is held on the walls of the irradiation vessel. ^{125}I is leached out when washed with potassium bisulphate solution.

Iodine-131

Iodine-131 decays by β^- emission with a half life of 8.0207 d. The product emits two γ-rays of 364 keV and 637 keV. This is an important radioisotope used in medicine for both therapy and diagnosis. It is produced by neutron irradiation of tellurium metal.

$$^{130}_{52}Te\ (n,\gamma)\ ^{131}Te \xrightarrow[25\ min]{\beta^-} {}^{131}_{53}I \xrightarrow[8.0207\ d]{\beta^-} {}^{131}_{54}Xe\ (stable) \qquad (12.16)$$

Tellurium has many stable isotopes. ^{130}Te (34.5%), ^{128}Te (31.8%), ^{126}Te (18.7%) and smaller percentages of ^{125}Te, ^{124}Te, ^{123}Te, ^{122}Te and ^{120}Te. Typically 100 g Te metal irradiated for 15 days in a neutron flux of 5 x 10^{13} n/cm^2/s yields 35 Ci of ^{131}I. Longer

irradiation though yields more activity, the specific activity of the product decreases because of the formation of inactive (stable) ^{127}I and very long lived ^{129}I.

$$^{128}Te\ (n,\gamma)\ ^{129}Te \xrightarrow[69.6\ min]{\beta^-} {}^{129}I \xrightarrow[1.57 \times 10^7\ y]{\beta^-} {}^{129}Xe \qquad (12.17)$$

$$^{126}Te\ (n,\gamma)\ ^{127}Te \xrightarrow[9.35\ h]{\beta^-} {}^{127}I\ (stable) \qquad (12.18)$$

The irradiated metal target is dissolved in chromic acid/sulphuric acid. Iodine is produced in different oxidation states during irradiation. Addition of oxalic acid reduces different species of iodine to elemental form, which is then distilled off as Na ^{131}I. Oxidation and reduction cycle ensures that all the iodine formed is recovered.

The active waste generated is relatively large in this method. Also, from the reagents and chemicals required for processing, traces of carrier iodine come into the final product. This reduces the specific activity. For example, specific activity of 20 - 40 Ci/mg is obtained contrary to the expected value of 120 Ci/mg.

Use of TeO_2 target and dry distillation technique is an alternate process for the isolation of ^{131}I with reduced waste generation. This also increases the overall chemical purity of iodine, which is good for radioiodination of even sensitive chemical molecules and biological substances.

Cobalt-60

Cobalt-60 is produced by (n,γ) reaction on the mono-nuclidic ^{59}Co target ($\sigma = 36$ b) is the only major radioisotope required in megacuries. Since ^{60}Co has a half-life of 5.274 years, activation of Co target for several years in reactors. One gram of Co, when irradiated in a neutron flux of 5×10^{13} n/cm^2/s for 2 years and 10 years, will yield 114 Ci and 363 Ci of ^{60}Co respectively. In the long irradiation, the self-absorption in Co target becomes appreciable and the activation yield reduces with time. Actual yield is much lower. Annular target container system is preferred for activation, if practicable. Further, very fine pellets of Co (1 mm x 1 mm Ni coated) are used to improve the activation yields. This method gives rise to ^{60}Co of very high specific activity. The alternate target is Co slugs (ϕ 6 mm x 25 mm, Al cladded), which leads to specific activity of about 100-150 Ci/g. High specific activity ^{60}Co (>200 Ci/g) is needed for the preparation of teletherapy sources, while medium specific activity is adequate for preparation of source pencils for use in radiation processing plants.

In India ^{60}Co is produced in the nuclear power reactors such as those at Kota, Narora and Kakrapar. Taking advantage of the long uninterrupted operation of these power reactors, cobalt targets in the form of "adjuster rods"are irradiated. The processing facilities needed for large scale ^{60}Co production would involve a few hot cells, associated equipment / gadgets and an adjoining special water pool to receive and store the activated rods.

Iridium-192, Bromine-82 etc.

^{192}Ir ($t_{1/2}$ = 73.827 d) is another important isotope required in large quantity mainly as a source for gamma radiography cameras (upto 100 Ci per camera) and as ^{192}Ir wire (a few mCi/cm) for brachytherapy of cancer. ^{192}Ir is produced by activation of natural iridium target, ^{191}Ir (n,γ) ^{192}Ir (σ = 370 b). Activation of 1 gram of iridium target (^{191}Ir, 37.3%) at 5 x 10^{13} n/cm^2/s for 1 and 3 months results respectively in 144 Ci and 335 Ci of ^{191}I activity.

^{24}Na and ^{82}Br are the other major radioisotopes of interest, for use as industrial tracers including for field works. They are produced by the activation of Na_2CO_3 and NH_4Br target, respectively. Post-irradiation processing involves simple dissolution and dispensing.

Emerging Need for Therapeutic Radionuclides

There is an increasing role for radionuclide therapy in both cancerous and non-cancerous diseases. Since a large quantity of particle emitting radionuclides is required for this purpose, nuclear reactor becomes a convenient source. Some of them with their production reactions, half-lives, β_{max} and E_γ are given in Table 12.6.

Table 12.6 - Some therapeutic radionuclides

Radionuclide	$t_{1/2}$	Nuclear reaction	$E_{\beta_{max}}$ / MeV	Eγ / keV (%)
^{153}Sm	46.284 h	^{152}Sm (n,γ) ^{153}Sm	0.81	103 (28)
^{166}Ho	26.763 h	^{165}Ho (n,γ) ^{166}Ho	1.85	81 (6)
^{186}Re	90.64 h	^{185}Re (n,γ) ^{186}Re	1.07	109 (9)
^{90}Y	64.0 h	^{89}Y (n,γ) ^{90}Y	2.27	—
^{198}Au	2.69517 d	^{197}Au (n,γ) ^{198}Au	0.96	412

^{153}Sm and ^{166}Ho are produced using research reactor(s) of medium flux. The activation yield is 200-300 mCi/mg in the case of ^{153}Sm and >100 mCi/mg in the case of ^{166}Ho. In the case of ^{186}Re, even after allowing one $t_{1/2}$ period decay after the end of irradiation, [to allow co-produced ^{188}Re ($t_{1/2}$ = 17.005 h) for decay], yield of over 100 mCi/mg is attainable. The post-irradiation processing is relatively simple in the former two cases, while processing the rhenium target needs a few steps as shown below:

$$Re \xrightarrow{HNO_3} Re\text{ - nitrate} \xrightarrow{NH_4OH} NH_4ReO_4 \qquad (12.19)$$

Additionally, extraction of perrhenate into MEK and recovery in aqueous phase would be needed to achieve greater purity for some applications.

Production and Processing of some useful Cyclotron Produced Isotopes

Gallium-67

Gallium-67 decays by electron capture and has a half life of 3.2612 d. It emits γ-rays of 93.3 keV and 186 keV energy among others. Commercial production is carried out by (1) proton bombardment of enriched zinc target, ^{68}Zn (p,2n) ^{67}Ga, E_p = 20-25 MeV and (2) α-particle bombardment of natural copper target, ^{65}Cu (α,2n)^{67}Ga, E_α = 30-32 MeV

Natural copper target is irradiated for the production of ^{67}Ga required for radiopharmaceuticals. Natural copper contains ^{63}Cu - 69.17% and ^{65}Cu - 30.83%. Apart from ^{67}Ga, α-particle bombardment produces following β^+ radionuclides:

^{65}Cu(α,n)^{68}Ga $t_{1/2}$ = 67.629 min (12.20)

^{63}Cu(α,n)^{66}Ga $t_{1/2}$ = 9.49 h (12.21)

^{63}Cu(α,2n)^{65}Ga $t_{1/2}$ = 15.2 min (12.22)

Irradiated targets are cooled for sufficient periods to allow ^{65,66,68}Ga to decay. After four days cooling, the target surface is etched in nitric acid and the nitrates are converted to chlorides of Cu, Zn and Ga. Gallium is separated from other cationic impurities by passing the solution through a cation exchanger. ^{67}Ga chloride solution contains 1% ^{66}Ga as radionuclide impurity. Typical yield is 100 μCi/μA h. The chloride solution is converted to Ga-citrate which is used to image soft tissue tumours.

Thallium-201

^{201}Tl ($t_{1/2}$ = 72.912 h) is produced by 30 MeV proton irradiation of natural Tl target which contains 29.5% ^{203}Tl and 70.5% ^{205}Tl.

$$^{203}\text{Tl (p,3n) } ^{201}\text{Pb} \xrightarrow{9.33\ \text{h}} ^{201}\text{Tl} \qquad (12.23)$$

Typical activation time is a few hours. Enriched ^{203}Tl target is used to increase the yield and minimise impurity products arising from the activation of ^{205}Tl.

In order to ensure higher purity of ^{201}Tl as well as avoid carry-over of toxic Tl target in to final product, ^{201}Pb has to be rapidly separated, immediately after the activation keeping, thallium content to be well within acceptable limits (1-2 ppm) in the separated ^{201}Pb. This ^{201}Pb is allowed to stand for decay over nearly 30 hours and then the second stage separation is done to obtain pure ^{201}Tl from the decayed ^{201}Pb solution. A combination of ion-exchange chromatography and solvent extraction is used in both stages. Also advantage is taken of the variable oxidation states of thallium, thallic and thallous forms, in effecting a clean separation from lead.

Table 12.7 - Nuclear properties of some iodine isotopes

Nuclide	$t_{1/2}$	Decay mode	Main gamma ray energy (keV)
^{123}I	13.27 h	EC	159
^{124}I	4.176 d	EC, β^+	603
^{125}I	59.400 d	EC	35
^{126}I	13.11 d	EC, β^+, β^-	670
^{127}I	(stable)	-	-
^{131}I	8.0207 d	β^-	340

Iodine-123

Iodine-123 decays by electron capture mode with a half life of 13.27 h. The energy of its main γ-ray is 159 keV (Table 12.6). Importance of ^{123}I in medical applications stems from the fact that it gives a lower absorbed dose to the patient when administered and its gamma energy is ideally suited for gamma camera imaging (Table 12.7).

One of the methods for production of ^{123}I in cyclotron is by the reaction: $^{124}Te(p,2n)^{123}I$. Enriched ^{124}Te is used as natural tellurium contains 4.6% of ^{124}Te and 7.0% of ^{125}Te, which gives rise to ^{124}I impurity as $^{125}Te(p,2n)^{124}I$. ^{124}I is also formed with protons of lower energy via $^{124}Te\ (p,n)\ ^{124}I$ and higher beam energy is preferred.

Iodine is recovered from the target by volatilisation. Typically 96.21% enriched ^{124}Te with proton energy of 27 MeV yields 10 mCi of ^{123}I/mAh. The radionuclidic impurity of ^{124}I is about 0.78%.

Iodine-123 in pure form is produced by the decay from its precursor nuclide ^{123}Xe as follows.

$$^{124}Xe\ (p,2n)\ ^{123}Cs \xrightarrow[5.87\ min]{} {}^{123}Xe \xrightarrow[2.08\ h]{} {}^{123}I\ (t_{1/2} = 13.27\ h) \qquad (12.24)$$

The co-produced ^{124}Xe is stable, while the other product nuclide ^{122}Xe and its decay product ^{122}I are short-lived, and decay during processing and transfer to user's end.

Natural abundance of ^{124}Xe is, however, very low at 0.1%. If ^{124}Xe is not very highly enriched (>>99%), ^{126}Xe present in the target would give rise to ^{125}I ($t_{1/2}$ = 59.408 h) by a reaction similar to the above. Highly enriched target is hence used and recycled for production of this vital medical tracer.

Carbon-11

Carbon-11 decays by positron emission and has a half life of 20.39 min. It gives annihilation photons of 511 keV.

It is produced by $^{14}N(p,\alpha)^{11}C$ reaction with protons of 15-18 MeV, with an yield of 90 mCi/μAh. Target is usually nitrogen gas containing traces of oxygen which is continuously flowing through the target holder. Initially ^{11}CN radicals and ^{11}CO are formed. ^{11}CN radicals are the result of interaction of the recoil ^{11}C and N_2 molecule. ^{11}CN radical and most ^{11}CO are oxidised to $^{11}CO_2$ at higher radiation dose. Hence the final product is $^{11}CO_2$ containing about 1% of ^{11}CO. The gaseous mixture is passed through heated CuO tube at 800°C to yield $^{11}CO_2$ product. Because of very short half life, various precursors for the synthesis of labelled ^{11}C compounds are prepared on-line. At higher proton energy, $^{14}N(p,pn)^{13}N$ reaction gives ^{13}N radionuclide as contaminant.

Fluorine-18

Fluorine-18 decays by positron emission with a half life of 109.77 min. The $^{18}O(p,n)^{18}F$ reaction on enriched ^{18}O is the primary mode of production. At E_p = 22 MeV yield of 6 mCi/μAh is obtained with an enriched H_2 ^{18}O target. E_p of 10-16 MeV will also suffice for ^{18}F production for medical use. Under proton bombardment, water decomposes to H_2, O_2 and H_2O_2 and becomes oxidising. Proper target container is chosen so that it is resistant to corrosion under oxidising conditions. ^{18}F is obtained as fluoride. This is the most widely used cyclotron produced isotope in diagnostic nuclear medicine.

Separation of Isotopes

Isotopes of an element have similar (almost) chemical properties but their nuclear properties can be quite different. Separation of isotopes for various applications is a fully developed technology. This is particularly true for the nuclear industry in which separation/enrichment of fissile ^{235}U is carried out on a large scale. Another large scale technology relates to the production of heavy water (^2D_2O) moderator for nuclear reactors. Some important isotopes which are being enriched for use in different fields are listed in Table 12.8. Different methods are employed for isotope enrichment and some typical examples are given in Table 12.9. Small differences in physico-chemical properties of the different isotopes of an element are used for their separation. These include boiling points, diffusion coefficients, rate of electrolysis and spectroscopic properties. The methods which have been developed for isotope separation/fractionation can be divided into two categories (i) equilibrium processes and (ii) rate processes.

In an equilibrium process the isotope effect is small and thus quite often limits their use to the isotope separation of light elements, usually with atomic number less than 10. These processes consume less energy. On the other hand, isotope effects in rate processes are larger and they are based on dynamic phenomena like ion mobility, diffusion, electrolysis,

Table 12.8 - Separated / Enriched isotopes and their uses

Isotope	Natural atom %	Use
^{235}U	0.7205	Fuel for nuclear fission reactors
^{2}H	0.015	D_2O moderator for natural U reactors. Fuel for thermonuclear reactors
^{6}Li	7.5	Source for tritium fuel for thermonuclear reactors
^{7}Li	92.5	As LiOH, water conditioner for water cooled reactors. As metal, possible HTR coolant
^{10}B	19.61	Neutron absorber in control rods
^{13}C ^{15}N ^{17}O	1.107 0.366 0.037	Isotope tracer for living systems. Nuclear magnetic resonance studies of molecular structure
^{18}O	0.204	Tracer for environmental studies. Target for ^{18}F production
^{57}Fe	2.20	Mossbauer studies

Table 12.9 - Methods employed in isotope separation

Method	Applied to
Electromagnetic	All isotopes
Electrolysis	D, Li
Distillation	D, ^{10}B, ^{13}C, ^{15}N, ^{18}O
Chemical exchange	D, Li, ^{10}B, ^{13}C, ^{15}N, ^{18}O
Ion migration	Li
Gaseous diffusion	^{235}U
Thermal diffusion	^{18}O, ^{15}N, inert gas isotopes
Gas centrifuge methods	^{235}U
Aerodynamic methods	^{235}U
Photochemical methods	All isotopes
Ion exchange methods	Light elements and ^{235}U

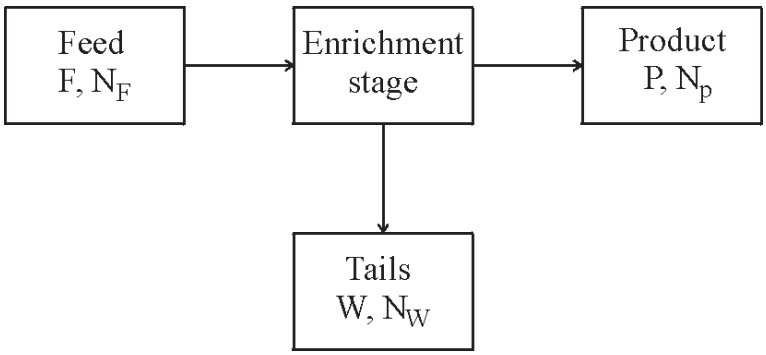

Fig. 12.4 The concept of enrichment.

centrifugation and electromagnetic separation. These are energy intensive processes and, therefore, require large investment.

Separation Factor

Separation factor (α) is defined as the quotient between the isotope ratios of the product and the waste streams (tails). The following illustration explains α for uranium which has two main isotopes ^{235}U and ^{238}U. Uranium hexaflouride gas is used for isotope separation in a number of processes. Schematically enrichment can be represented as shown in Fig. 12.4. F, P and W are the quantities of UF_6 in feed, product and tails streams respectively and N_F, N_P and N_W are the concentrations of ^{235}U in these streams. The ratios of ^{235}U to ^{238}U in these streams can be defined as

$$R = \frac{N}{(1-N)} \tag{12.25}$$

where, N is the atom fraction of ^{235}U.

The separation factor α is then defined as the ratio of R_P in product stream and R_W in the tails stream.

$$\alpha = \frac{R_P}{R_w} = \frac{\dfrac{N_P}{1\text{-}N_P}}{\dfrac{N_W}{1\text{-}N_W}} \tag{12.26}$$

If the product stream is marginally enriched to 0.721% ^{235}U and the tails have 0.7195% ^{235}U.

$$\alpha = \frac{\dfrac{0.721}{99.279}}{\dfrac{0.7195}{99.2805}} = 1.0021$$

Table 12.10 - Separation factors in typical enrichment processes

Process	Property	Separation factors for		
		H_2 - HD	^{14}N - ^{15}N	$^{235}UF_6$ - $^{238}UF_6$
Distillation monothermal	R	1.5	1.033	1.00002
Chemical exchange	K	3.6	1.055	1.0016
Gaseous diffusion	$\sqrt{(m_2 / m_1)}$	1.225	1.017	1.00429
Gas Centrifuge	$\exp \frac{(m_2 - m_1)v^2}{2RT}$	1.056	1.056	1.162

R = relative volatility; K = equilibrium constant

Enrichment factor (E) is calculated from α

$$E = \alpha - 1 \qquad (12.27)$$

In this example enrichment achieved is 0.0021 or 0.21%. Ideal separation factor in a gaseous diffusion is 1.0043 in one stage.

In the case of hydrogen the natural abundance of D in H is about 0.0148% (it depends on the source of hydrogen). If by gaseous diffusion the product D concentration is increased to 0.017% and that of tails decreased to 0.0145%, α can be calculated to be 1.1724. Ideally a separation factor of 1.225 is achievable in a gaseous diffusion process for hydrogen. This can be compared with the separation factor of 3.1 achievable in a chemical exchange process[1]. Ideal separation factors in typical enrichment processes are given in Table 12.10.

Separating Unit and Cascade

The smallest element of an isotope separation plant that effects separation of process material is called a separation unit. For example a centrifuge, an electrolytic cell etc. A stage consists of a number of separating units coupled in parallel, all fed with material of same composition and producing product streams of nearly same composition. The number of units in a stage decides the amount of material that can be processed. In a single stage only a small enrichment is possible in most of the processes. In order to achieve higher enrichment,

---

[1]Isotope exchange reaction between liquid D_2O and hydrogen gas is as follows:

$$H_2(g) + D_2O \rightleftharpoons D_2(g) + H_2O\ (l)$$

For similar concentration the reverse reaction is faster. Under equilibrium conditions the ratio of D/H in liquid is approximately three times the ratio in the gas phase.

a number of stages are coupled together and this is called a cascade. The number of stages in a cascade decides the enrichment factor.

Cascades are generally of two types (i) simple cascade: a cascade in which no attempt is made to reprocess the partially depleted tails streams leaving each stage and (ii) Counter current or recycle cascade: a cascade in which the feed for each stage consists of heads from the previous lower stage and tails from the next higher stage. Recycle cascade is commonly employed. In general as $(\alpha\text{-}1) <<< 1$, in most of the cases, these are also known as close-separation cascades.

Separative Work Unit

Separation capacity is a measure of the rate at which the cascade performs and has the dimensions of flow rate (kg/d). From enrichment point of view, separative work unit (SWU), which is a measure of the amount of separation performed by a cascade is important. Essentially it indicates the amount of work performed to achieve certain enrichment in terms of feed material processed. Assume a plant with a capacity of 1000 te SWU. To obtain 10 te of 3% enriched $^{235}UF_6$, 541 te of natural UF_6 has to be processed if the tails ^{235}U concentration is 0.2%: To produce 10 te of 90% enriched $^{235}UF_6$, in the same plant, 1739 te of natural UF_6 has to processed. This is schematically shown in Fig. 12.5. So high SWU means

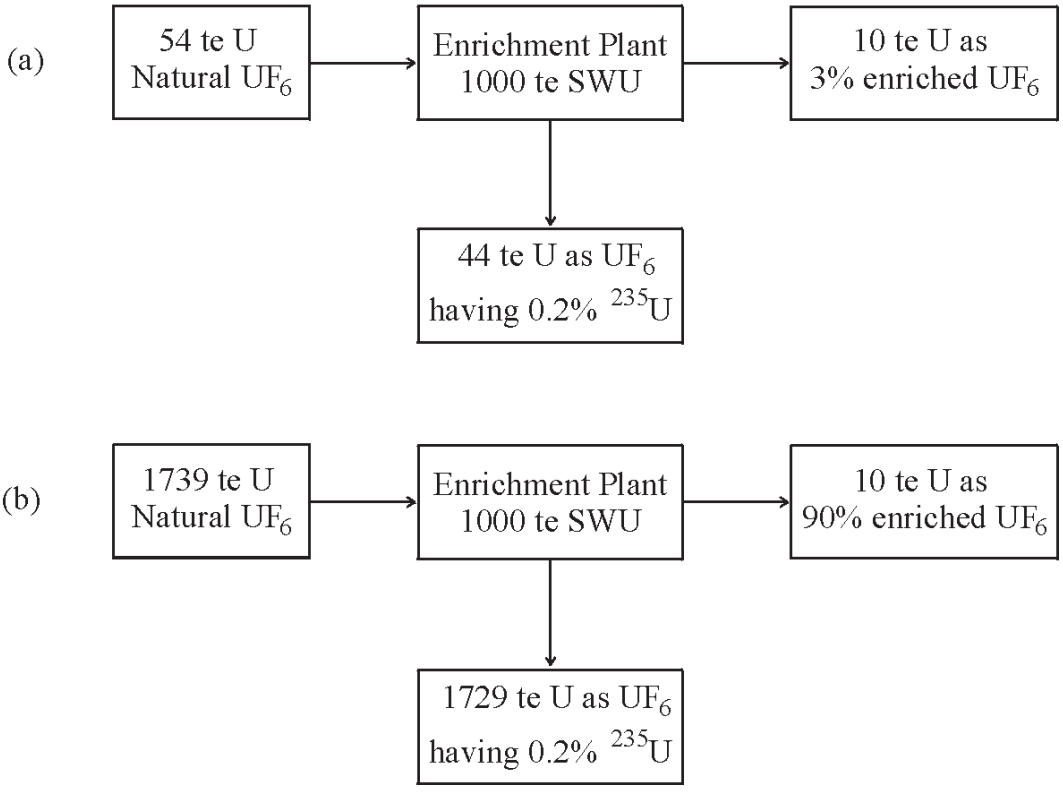

Fig. 12.5 The separative work unit.

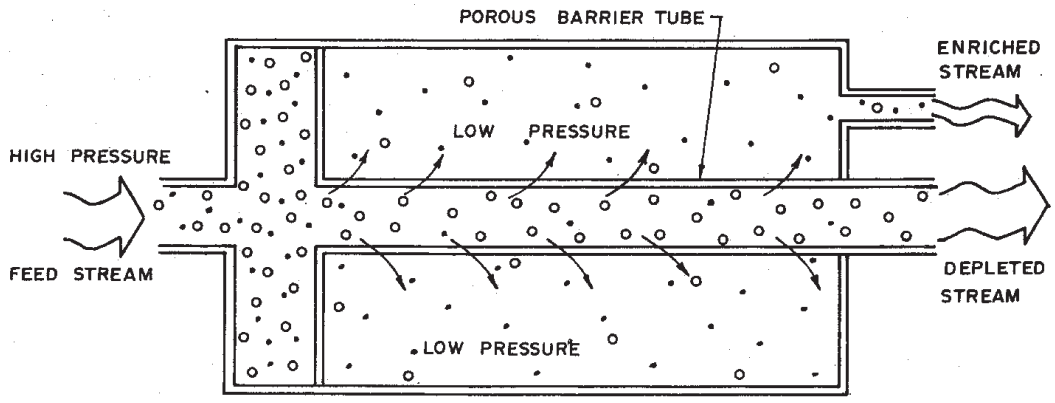

Fig. 12.6 Enrichment by gaseous diffusion method.

obtaining large amounts of low enriched material or smaller amount of high enriched material.

Some details for the production of enriched uranium and heavy water, which are required in the nuclear industry are given below.

Uranium Enrichment

Gaseous Diffusion

On the average $^{235}UF_6$ molecules being lighter (349 amu nominal) have a higher speed than the heavier $^{238}UF_6$ molecules (352 amu nominal) at a given temperature. This forms the basis for enrichment by gaseous diffusion method. If UF_6 is forced to diffuse through a porous barrier with tiny holes, the lighter $^{235}UF_6$ molecules diffuse faster than the $^{238}UF_6$ molecules and the gas coming out of the barrier is slightly richer in $^{235}UF_6$ (Fig. 12.6) Ideal separation factor in single stage of this process is about 1.0043, but in practice, it is only 1.0014. Because of this, an ideal gaseous diffusion plant would have about 1300 stages for producing 3% enriched uranium. Running of a plant based on gaseous diffusion requires tremendous quantities of electricity, about 3000 kWh/kg SWU. This process is in wide scale commercial application.

Gas Centrifuge

We know that under the influence of gravity, the heavier bodies tend to settle at the bottom. If we fill a room with UF_6 gas, then the gas near the ceiling would be richer in $^{235}UF_6$. If the forces acting on the molecules are increased, then the separation factor can be increased. This can be achieved by putting the gas in a high speed centrifuge rotating at a speed of about 50,000 revolutions/minute. The molecules would then be subjected to a force of 250,000 times the force of gravity. Under these conditions, the ratio of isotope abundance

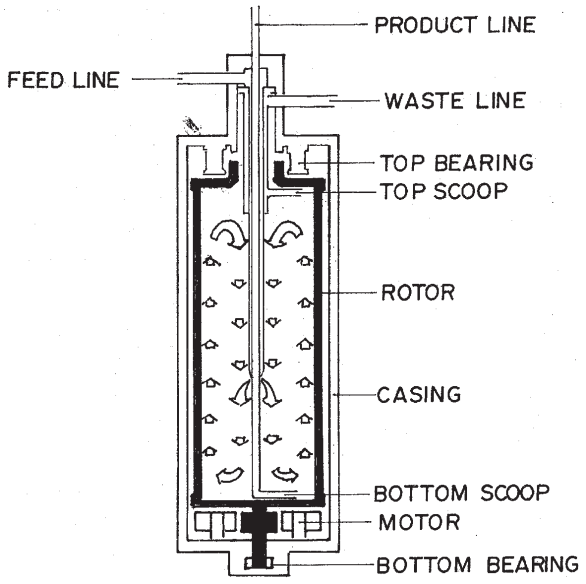

Fig. 12.7 Gaseous centrifuge for $^{235}UF_6$ enrichment.

(q) between the centre of the centrifuge to the outer wall would be 1.147, though there would be very little gas near the centre of the centrifuge. The cylindrical centrifuge bowl can be designed to function as a multistage unit and a single centrifuge can produce separation factors as high as 1.5 (Fig. 12.7). However, because of extremely high speeds at which the centrifuge has to rotate, each of these units has to be small (1.5 m long and 0.2 m dia) and a large number of centrifuges are required to produce quantities of enriched uranium required for reactors. A plant of 1000 te SWU per year capacity would require 66,000 centrifuges. Nevertheless, 3% enrichment can be achieved in about 13 stages. Inspite of large number of units required for the production, the electrical consumption of this process is only 1/10 of the gaseous diffusion process i.e. about 300 kWh/kg SWU. This process is gradually replacing the gaseous diffusion process.

Aerodynamic Methods

These methods are based on the pressure gradients which are generated due to high speed flow of gases along a streamlined curvature. Again, like in a centrifuge, the heavier $^{238}UF_6$ molecules tend to concentrate on the outer side of the curvature. There are two processes based on this principle; the jet nozzle process developed by the Germans and the Helikon process developed by the South Africans.

In the jet nozzle process, a mixture of uranium hexafluoride and hydrogen (96% of H_2) is allowed to expand through a narrow (0.05 mm wide) curved (0.1 mm radius) slit. The high speed gas experiences force equal to 160 million times the gravitational force in the curved nozzle. The stream coming out of the nozzle is divided into lighter and heavier fractions by a very sharp skimmer knife. A tube having about 80 such elements can achieve a

separation factor of 1.0148. About 740 such stages would be required to produce 3% enriched uranium. The energy costs are more than 3,000 kWh/kg SWU.

In the Helikon process, or 'UCOR' process, a mixture of UF_6 and hydrogen (98 to 99% of H_2) is injected, at a very high speed, tangential to the inner wall of a tube. As the gas travels down the tube, the lighter component ($^{235}UF_6$) concentrates near the axis and this enriched uranium can be withdrawn from the central part of the other end of the tube. Stage separation factor of 1.03 has been reported for the process in a 3.5 m dia, 10 m long tube in which many streams having different enrichment flow simultaneously through the tube without mixing. About 100 modules are required to achieve uranium enrichment of 3%. Power consumption in this process is 3,000 - 3,500 kWh/kg SWU which is more than that for gaseous diffusion process. This process has been used in South Africa for producing enriched uranium for power reactors and for highly enriched uranium.

Laser Isotope Separation

The position of electronic levels of uranium atoms, and vibrational levels of molecules, such as UF_6, differ marginally for the isotopes of uranium. The energy difference between two useful levels in uranium atoms is about 2.1eV (red-orange coloured light) and the actual values for ^{235}U and ^{238}U differ by 4.2×10^{-5} eV. The availability of lasers which can be tuned very precisely so as to selectively excite only ^{235}U atoms without affecting the ^{238}U atoms has prompted the development of laser based process.

Atomic vapour laser isotope separation (AVLIS) technique is being investigated by many countries and has the potential for emerging as a new technology in this area. In this technique, selective ionisation of ^{235}U atoms and their collection using electric and magnetic fields are used for isotope separation. Ionisation of ^{233}U atoms requires approximately 6.2 eV of energy and this can be supplied by 3 laser photons of red-orange colour. Vapour of uranium atom is generated by heating uranium metal ingot with electron beam and ^{235}U atoms in vapour are ionised by precise tuning of energies of 3 laser photons. The ionised ^{235}U atoms are deflected on to collector plates for obtaining the product, whereas ^{238}U atoms which are not ionised are later collected on another plate above the source of the vapour. Ideal stage separation factors upto 15 are possible, but 5 to 10 appear practical. Enrichment to 3% ^{235}U in this process may require only a single stage. Further, power consumption is estimated to be only about 100 kWh/kg SWU.

In molecular laser isotope separation (MLIS), $^{235}UF_6$ molecules are first selectively excited with infra-red laser light and then irradiated with ultra-violet laser light to dissociate excited $^{235}UF_6$ to $^{235}UF_5$ and florium. The pentafluoride is a solid and condenses out of the gas stream whereas $^{238}UF_6$ molecules are not affected. Complex spectrum of the UF_6 molecules makes selective excitation quite difficult. Many innovations like jet cooling of UF_6 vapour are under investigation for the development of the process. Currently, no data regarding separation factors have been reported for this process.

Deuterium Enrichment Processes

The differences in physico-chemical properties of hydrogen compounds having hydrogen and deuterium as their constituents, form the basis of all the enrichment processes. Chemical exchange of deuterium between gas/vapour and liquid phases are used for enrichment and important features of some of the processes are given below. The primary source of deuterium is either water or hydrogen available from synthesis gas used in fertiliser plants for the manufacture of ammonia.

Distillation of Water

Deuterium in water can exist as HDO or D_2O. When deuterium content of water is low, it mainly exists as HDO with boiling point of 100.7°C. The vapour of water, therefore, contains slightly less deuterium than the liquid. Water of tropical oceans contains 156 ppm of deuterium. Similarly, when vapour of water partially condenses, the liquid is richer in deuterium. The separation factor for deuterium in the distillation of water is 1.05 at 50°C and 1.026 at 100°C. Production of 99.8% D_2O would, therefore, require about 700 equilibrium stages involving evaporation and condensation. Also because of low deuterium content of water, about 200,000 litres of water would be required to produce one litre of heavy water.

Though distillation is one of the most expensive processes for heavy water production, it is economical for upgrading water having a few percent of D_2O and is, therefore, preferred at many plants. Many heavy water production plants based on other processes produce heavy water having 2 to 40% of D_2O and then up-gradation to 99.8% of D_2O by distillation.

Electrolysis

E.W. Washburn and H.C. Urey were the first to propose electrolysis of water for the production of heavy water in 1932. The first plant in the world was set up by Norsk Hydro, Norway in the year 1934. Another heavy water plant to use electrolysis as one of the process steps for the production of heavy water is located at Nangal in India.

Separation of hydrogen and deuterium is achieved by electrolysis taking advantage of higher mobility of hydrogen ion and slower discharge of deuterium at the cathode. The chemical equilibrium is given by

$$H_2O(l) + HD(g) \rightarrow HDO(l) + H_2O(g) \qquad (12.28)$$

which has an equilibrium constant of 3.8 at 25°C. In this process deuterium tends to concentrate in the liquid phase. As both kinetic and thermodynamic equilibrium phenomena are involved, a number of variables, such as electrode material and cell design, play important role and the separation factor is, therefore, variable. Highest separation factor of 13.2 has been reported at 15°C with iron as cathode. The separation factor decreases with increasing temperature, e.g., 10.6 at 25°C and 7.1 at 75°C. Inspite of the high separation factor, the electrolysis process requires about 220 kWh of energy to produce one gram of

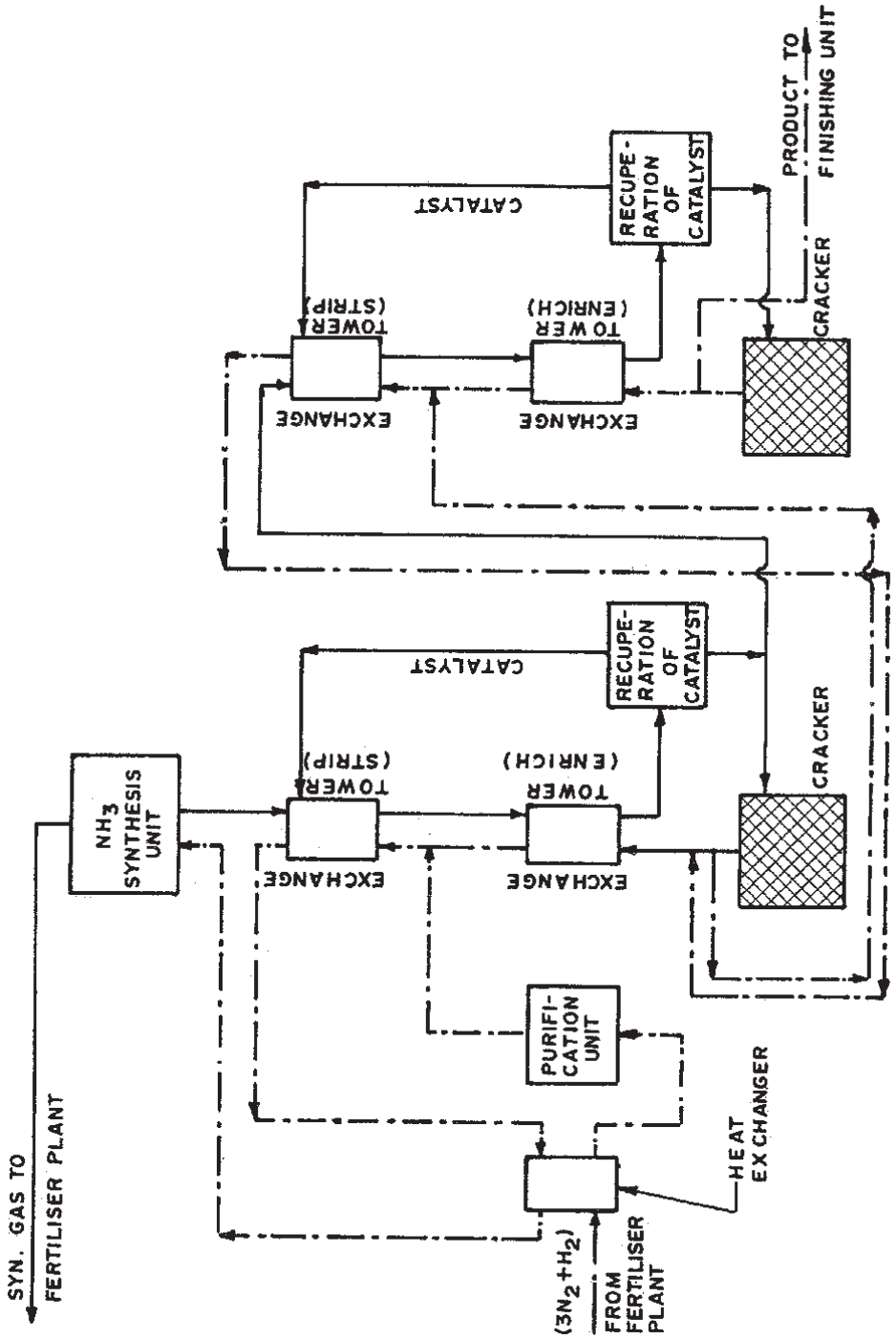

Fig. 12.8 Schematic flow diagram of Heavy Water Plants at Baroda / Tuticorin [Courtesy Heavy Water Board, Department of Atomic Energy, Mumbai, India].

D_2O and is, therefore, practical only where cheap electricity is available. Only Norway and India are currently using this process. At Nangal plant which has a capacity of 14 te D_2O/y, electrolysis is used to produce hydrogen having 450 ppm of deuterium.

Electrolysis, like distillation, uses a lot of energy for enrichment and is not used for primary production of heavy water. However, it is commercially used for upgrading depleted heavy water from nuclear power plants.

Distillation of Hydrogen

Hydrogen gas is converted into liquid by cooling to -252.7°C. During distillation of this liquid, deuterium gets enriched in the liquid phase and the separation factor is 1.5. In view of this high separation factor, this process is attractive but has not been used widely because of the complexities involved in attaining and maintaining low temperatures and also ensuring reliability of the equipment at these temperatures.

Ammonia-Hydrogen Exchange Process

NH_3-H_2 exchange process is designed to extract deuterium from hydrogen used for fertiliser production. Both ammonia and hydrogen required are obtained from the fertiliser plant and, therefore, this type of plants are located at fertiliser plant sites. The extraction of deuterium from hydrogen is achieved by the following chemical reaction:

$$HD(g) + NH_3(l) \Leftrightarrow H_2(g) + NH_2D(l) \qquad (12.29)$$

The separation factor in this process increases with decreasing temperature. Separation factor is 5.2 at -25°C and hydrogen pressure of 350 atm. The exchange reaction does not take place unless an efficient catalyst is present. Potassium amide (KNH_2) dissolved in liquid ammonia is used as a catalyst. A schematic flow diagram of Heavy Water Plant at Baroda is given in Fig. 12.8.

Hydrogen required for fertiliser production is obtained by reforming of natural gas with excess steam when the following equilibria are established.

$$CH_4(g) + H_2O(g) \Leftrightarrow CO(g) + 3\ H_2(g) \qquad (12.30)$$

$$CO(g) + H_2O(g) \Leftrightarrow CO_2\ (g) + H_2(g) \qquad (12.31)$$

Deuterium concentration in this is 115 ppm and exists as HD. Deuterium content in hydrogen returned to the fertiliser plant is about 1.5 ppm.

Presently, India has four operating plants using this technology: Baroda : 45 te/y, Tuticorin : 49 te/y, Thal : 110 te/y and Hazira : 110 te/y. India is the only country in the world currently having the technology to set up large plants based on this process.

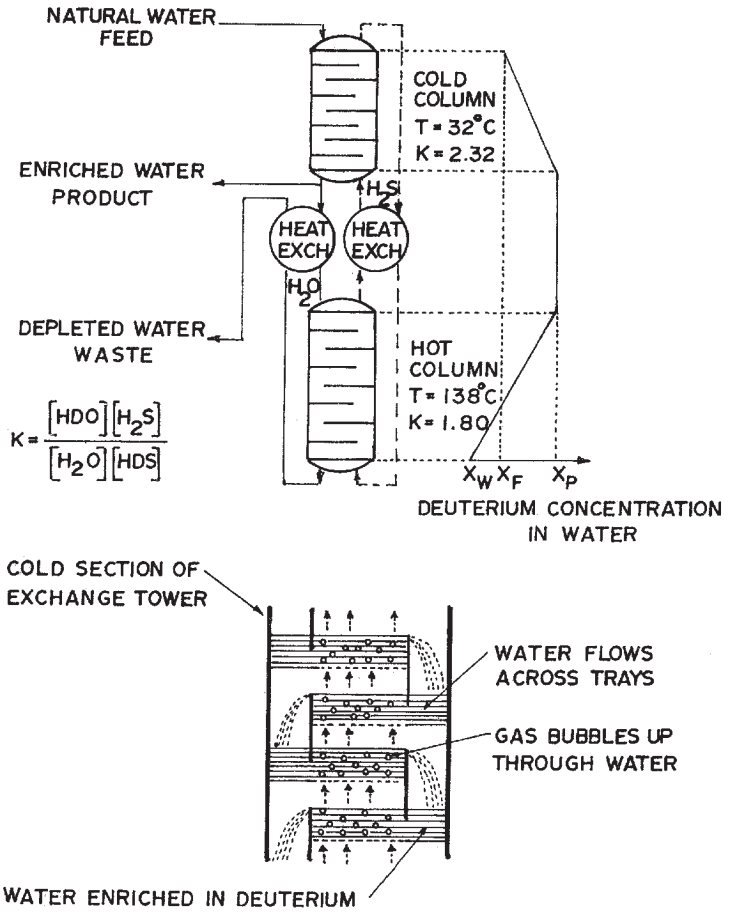

Fig. 12.9 The water-hydrogen sulphide dual-temperature exchange process for enrichment of heavy water [M. Benedict, T.H. Pigford, H.W. Levi, "Nuclear Chemical Engineering", McGraw Hill Book Co., New York (1981)].

Girdler Sulphide Process

Girdler sulphide (GS) process is based on exchange of deuterium between water and hydrogen sulphide gas.

$$H_2O(l) + HDS(g) \Leftrightarrow HDO(l) + H_2S(g) \qquad (12.32)$$

The process is very attractive as the exchange reaction can take place without any catalyst and also the strong dependence of the equilibrium constant on temperature permits the use of a bithermal process which eliminates the need for chemical steps required for providing reflux in the exchange towers. The process uses two towers, a cold tower maintained at 32°C and a hot tower maintained at 138°C. Two plants, based on this process, one of 85 te/y capacity at Kota and the other of 185 te/y capacity at Manuguru are successfully operating in India.

Bibliography

1. S. Glasstone, Sourcebook on Atomic Energy, 3rd Ed., Affiliated East West Press Pvt. Ltd. (1967).
2. G. Friedlander, J.W. Kennedy, E.S. Macias, J.M. Miller, Nuclear and Radiochemistry, 3rd Ed., John Wiley & Sons Inc., New York (1981).
3. H.J. Arnikar, "Essentials of Nuclear Chemistry", 3rd Ed., John-Wiley (1990).
4. Radioisotope Production and Quality Control, IAEA Technical Report Series 128, IAEA, Vienna (1971).
5. Directory of Cyclotron used for Radionuclide Production in Member States, IAEA-TECDOC-1007, IAEA, Vienna (1998).
6. IAEA Training Course Manual for "Research Reactor Utilisation for Production and Applications of Radioisotopes", BARC/IAEA, Mumbai, India (1989).
7. Production Technologies for ^{99}Mo and ^{99m}Tc, IAEA-TECDOC-1065, IAEA, Vienna (1999).
8. N. Ramamoorthy and P. Saraswathy, Radionuclides for Medicine and Research, in "Radiation Safety for Unsealed Sources", Ed. G.S. Pant, Himalaya Publishing House, New Delhi (In Press).
9. K. Cohen, "The Theory of Isotope Separation", McGraw Hill, New York (1951).
10. H. London, "Separation of Isotopes", Newness, London (1963).
11. S. Villani (Ed.), "Isotope Separation", American Nuclear Society, L Grange Park (1976).
12. D.G. Avery, E. Davies, "Uranium Enrichment by Gas Centrifuges", Mills and Boon, London (1973).
13. H.J. Arnikar, "Isotopes in Atomic Age", Wiley Eastern Ltd., New Delhi (1989).
14. G.M. Murphy (Ed.), "Production of Heavy Water", McGraw Hill, New York (1955).
15. E.W. Becker, "Production of Heavy Water", IAEA, Vienna (1961).

Chapter 13

Applications of Radioisotopes in Physico-Chemical Investigations

As the major non-power application of nuclear industry, radioisotopes hold a central place in atomic energy programme. Radioisotopes play an important role in a variety of fields such as health-care, agriculture, industry, hydrology, life sciences, pollution control and research. The radioisotopes have provided a tool to study many problems in chemical, biological and medical fields. Applications of tracers in chemical research cover the studies of reaction mechanism, kinetics, exchange processes and analytical applications such as radiometric titrations, solubility product estimation, isotope dilution analysis and autoradiography. In the field of health-care, both diagnostic and therapeutic applications have been commonplace. Radiotracers have helped in identification of leaks in buried pipelines and dams. Process parameters such as mixing efficiency, residence time, flow rate, material inventory and silt movement in harbours are studied using radioisotopes. ^{32}P and ^{35}S labelled nucleotides have introduced a new chapter in unravelling the mysteries of the very life process. The three main principles of applications of radioisotopes and radiation are:

Tracer Concept

The concept of radioisotope as a tracer was introduced by the pioneering work of the Hungarian scientist Prof. George Hevesy. He applied the tracer concept in many fields, including medicine and biology. In the tracer applications, radioisotopes are firmly tagged to a material and used to trace the path of the material in the system under study, be it a reaction vessel, a plant or even a living species, by either externally measuring the penetrating radiation or measuring radioactivity in the desired state. Modern counting methods permit reliable measurements of radioisotopes at the level of 10^{-18} or 10^{-21} kg depending upon the half-life of the radioisotope.

Scattering and Attenuation of Radiation

The radiation intensity gets reduced as it passes through matter depending on atom density and atomic number. This phenomenon can be used for a variety of applications such as radiography.

Radiation Processing of Materials

Radiation processing is the technology in which radiation energy is used for treating materials like medical products, food items and for the manufacture of certain special materials. Usually, an intense source of ^{60}Co, or in some cases ^{137}Cs, is used. Alternately, electrons or X-rays from accelerators and high voltage generators are also used for radiation processing.

Choice of Radioisotope

The amount of activity handled for the first two types of applications varies from a few nano curies to a few hundred curies. The activity requirement for the third application can be upto several magacuries. The principles guiding the choice of a radioisotope for any particular application are the half-life, radiation characteristics, the ease of production, availability and the cost. For example, the duration of study and the extent of sensitivity of detection would dictate the choice of a radioisotope for use as tracer. The nature of matter (density, mass and effective atomic number) with which radiation interacts would dictate the type and energy of radiation source to be used in applications dealing with scattering and attenuation. High intensity ^{60}Co source is used in radiation processing applications, be it for industrial use or for treatment of cancer patients.

Physico-Chemical Applications of Radioisotopes

The fundamental principle in radiochemical investigations is that the chemical properties of a radioisotope of an element are almost the same as those of the other stable/radioactive isotopes of the element. When radioisotope is present in a chemical form identical to that of the bulk of the element in a chemical process, then any reaction the element undergoes can be directly traced by monitoring the radioisotope. Radioisotope can also be tagged to a molecule or material to follow a process. Radiochemical work involves two main steps (i) sampling of the chemical species to be studied and (ii) quantitative determination of the radiation emitted by the radioisotope in the sample.

The number of atoms of a radioisotope required for any investigation are often so low that the amounts involved are chemically insignificant. For example, 1000 Bq of ^{14}C, which has a half-life of 5730 years, corresponds to 6×10^{-12} kg of ^{14}C. The amounts of this order are adequate for measurement if the isotopes are radioactive. This unique feature of radioisotopes has led to the discovery and study of many new elements apart from enhancing our knowledge in many other areas.

Radioisotopes often find their use in chemistry, in two prominent ways:

As Tracers for Elements

In tracer chemistry the radioisotope is used to follow the behaviour of an element in a chemical reaction. The interest may be in the properties of the element itself, or of a

compound, radical or a group of which it forms a part. This is by far the widest use of isotopes at present.

As Tracers Produced Following a Nuclear Reaction

In nuclear chemistry, the nuclear process itself is employed to initiate reactions which give information of chemical significance. Activation analysis, absorption methods of analysis, X-ray fluorescence, neutron diffraction, radioactive recoil, Mössbauer and nuclear magnetic resonance techniques are widely employed to obtain information on chemical processes. Some of these are discussed in the next Chapter.

Tracer Application

Important characteristics of radioisotope for use as tracer are (i) half-life, (ii) type and energy of radiation and (iii) availability. Short lived isotopes (a few hours to a few days of half life) are preferred as they have high specific activity and the system becomes non-radioactive very soon. If larger amounts of radioactivity (mCi or more) are needed for use, the waste management problem is simpler with short lived isotopes. It is ideal to have a gamma emitting isotope as gamma ray measurement is the simplest and also external monitoring of the process is practicable. Reactor produced radioisotopes are more readily available and are relatively less expensive.

Labelling of a material with radioisotopes for tracer application can be for isotopic or non-isotopic investigations. For studying the chemistry of elements like phosphorus, sodium or hydrogen ^{32}P, ^{24}Na and ^{3}H respectively are used as tracers. Sometimes one has to choose between two or three radioisotopes of the same element depending upon the type of investigation. For example, for sodium, one can choose ^{24}Na (14.959 h) or ^{22}Na (2.6019 y).

^{24}Na would be preferred because of its shorter half life. However, if studies have to be carried out over a period longer than 4-5 days, then ^{22}Na is more suitable. Similarly for studying the metabolism or organ structure of the body, one could use ^{85}Sr, ^{87m}Sr or ^{90}Sr. However, ^{87m}Sr would be preferred because it is a γ-emitter and short lived. Both ^{3}H and ^{14}C emit very low energy beta rays which are more difficult to measure. Studies involving organic compounds or biological aspects, therefore, require great care. ^{11}C (half-life 20.39 min) can be used, but production and utilisation need to be in the same premises, as transporation is ruled out.

For non-isotopic applications, method of counting, internal and external absorption etc. become more important. Suppose one has to trace small particles of a catalyst, V_2O_5+2% K_2SO_4. In this case V and O isotopes are short lived, ^{35}S has a half life of 87.38 d but is a β^- emitter with an energy of 0.167 MeV. Only ^{42}K is useful which can be obtained by irradiation of the catalyst particles in a nuclear reactor.

Depending on the energy and half life, the amount of activity and type of detector have to be chosen. For example, 5000 Bq of ^{32}P and ^{14}C to be made into point sources and counted in a gas proportional counter. The count rate obtained with ^{14}C source would be lower due to

attenuation of low energy β-rays. This problem can, however, be overcome by liquid scintillation counting (LSC), where the geometry of source to detector is nearly 4π.

Sources of Error in Tracer Investigations

Four prominent sources of error can be pointed out. They are due to (i) mass effect, (ii) low concentration effect, (iii) unexpected oxidation state effect and (iv) disturbance of equilibrium of a decay series.

Difference in masses of the isotopes of an element leads to very small differences in their chemical properties, which have been exploited for the separation of isotopes. However, these effects are essentially relevant for low A isotopes.

Amounts of tracers are generally low. Depending on the half life for a given level of activity, weight of the sample varies, e.g., 3.7 MBq of ^{32}P corresponds to 10^{-12} kg of phosphorous. This amount is too small and might be lost in chemical operations. Upto 25% of $^{59}Fe^{3+}$ and ^{110}Ag are known to be lost by adsorption on the walls of the vessels in low concentrations. In carrying out precipitation at tracer levels, one may not exceed the solubility product and hence no precipitation may occur. Use of carriers is, therefore, essential in some operations.

Many elements have multiple oxidation states and any investigation involving tracers must ensure that the oxidation state of tracer is the same as that of the bulk to ensure complete exchange of isotopes.

Some of the β^- emitting nuclides are assayed by measuring the gamma rays emitted by their daughters, e.g., $^{90}Mo/^{99m}Tc$, $^{106}Ru/^{106}Rh$, $^{137}Cs/^{137m}Ba$, $^{144}Ce/^{144}Pr$ etc. In such cases, it is essential to let the radioactive equilibrium be attained before assaying the activity in the sample.

Tracers in Chemical Reactions

The efficiency of any chemical operation such as precipitation, filtration, extraction, separation, chromatography, as well as kinetics, can easily be evaluated using radiotracers due to the sensitivity of measurement of radiation.

Contamination of Precipitates

A common problem in chemical work is the extent to which precipitates are contaminated by adsorption of other species from the supernatant liquid. If tin is being precipitated as SnS_2 from a solution containing cobalt the contamination of Co(II) ion on stannic sulphide precipitates could be measured by adding radiocobalt (^{60}Co) to the aqueous solution before precipitation. After filtration and washing, the activity of the stannic sulphide precipitate is determined, from which the weight of the occluded cobalt is obtained.

Chromatographic Separations

Individual elements of rare earths can be separated from one another using a cation exchanger and eluting them with a chelating agent such as ammonium citrate. Each rare earth element moves as a band at a different speed down the column, although the trailing edge of one band may not be completely separated from the leading edge of the next band. The separation depends on pH, temperature, the exchanger, its grain size and the column length. This investigation is performed by labelling the rare earths with radiotracers. The course of the separation is followed by analysing the effluent fractions for the different radioactivities.

Similar methods have been applied in paper chromatography using radiotracers such as ^{185}W (inorganic) and ^{3}H /^{14}C (organic). In the former case, an equilibrium was facilitated between the different species $HW_6O_{21}^{5-}$ and WO_4^{2-} by dissolving sodium tungstate labelled with ^{185}W in water and adjusting the pH between 5 and 7. These two species were separated by paper chromatography using methanol containing hydrochloric acid as solvent. The equilibrium relationships were established by assaying the activities on the paper chromatograms.

Radiometric Studies of Reactions

Precipitation and Solubility Studies

The sulphate content of a solution may be determined by adding excess of labelled barium of known specific activity, when a precipitate of barium sulphate will be obtained. By measuring the radioactive content of the precipitate, one can determine the amount of barium present in it. From the known stoichiometry, the amount of sulphate is estimated. Alternatively, this can be carried out as a titration as described for chloride ion below.

The titration of chloride ion with ^{110}Ag labelled silver nitrate solution is carried out by taking $AgNO_3$ solution in the burette. The radioactivity of the supernatant solution is measured periodically as the titration proceeds. So long as any chloride ion remains in solution, the ^{110}Ag activity will be carried down with the silver chloride precipitate. As soon as precipitation is complete, the ^{110}Ag activity will begin to rise as excess silver nitrate is added. In place of solution, the precipitate can also be monitored.

Solvent Extraction

Chemically insignificant quantities are quantitatively separated and transferred from one phase to another by solvent extraction. The radioactivity of either or both phases can be followed to monitor the extent of separation. The method has been used for the determination of μg quantities of Hg^{2+}, Pb^{2+}, Co^{2+}, Zn^{2+} and Ni^{2+} from an aqueous solution by extraction with dithizone in CCl_4 solution. The titrant is added from the burette to an aqueous solution containing the metal ion labelled with a suitable radiotracer. The pH of the aqueous solution is adjusted to a value at which extraction of the metal complex into CCl_4 is complete. The end point is reached when the activity in the aqueous phase decreases to zero.

Solvent extraction methods involving radiotracers have also found extensive use in the evaluation of solvent extraction equilibria, analysis and the determination of stability constants of metal ions with different ligands.

Reaction Mechanisms

Radioisotopes are used as research tools to study and elucidate: (i) Reaction mechanisms, (ii) Structure determination / confirmation and (iii) Isotope exchange reactions.

In addition to radioisotopes, some naturally occurring stable isotopes, e.g., ^{2}H (D), ^{15}N and ^{18}O are also used in such studies. Monitoring is done by mass spectrometry in these cases. Traditionally many books refer to these under 'Radioisotope Applications', but are excluded in the present coverage.

Oxidation reaction - Fumaric acid with $KMnO_4$

Fumaric acid is COOH - CH = CH - COOH. Acidified $KMnO_4$ oxidises fumaric acid to CO_2, H_2O and formic acid. It would be interesting to know which 'C' atoms end up as CO_2 and which as formic acid. This was studied with the short-lived ^{11}C isotope ($t_{1/2}$ 20.39 min). $^{11}COOH$-CH=CH-$^{11}COOH$ was used in the study and the resultant formic acid was shown to contain no ^{11}C activity. This implies that one of the methylinic 'C' atoms has gone into forming HCOOH and that both carboxylates are involved in the liberation of CO_2. This is consistent with the expected oxidation process also. The overall reaction can be depicted as,

$$^{11}COOH\text{-}CH=CH\text{-}^{11}COOH + 5(O) \rightarrow 2\,^{11}CO_2 + H_2O + 2HCOOH \qquad (13.1)$$

Confirmation of Intermediate / Precursor Formation in Reactions

There are numerous cases to illustrate the formation of different intermediates in studies of reaction kinetics, which could be identified by appropriate labelling methods.

By the action of caustic soda, phenyl glyoxal is converted to mandelic acid through the formation of an intermediate ion

$$\underset{\text{phenyl glyoxal}}{C_6H_5\,{}^{14}CO.CHO} \xrightarrow{NaOH} \underset{\text{(intermediate ion)}}{C_6H_5.CO(OH).CHO^-} \xrightarrow{Hydrolysis} \underset{\text{Mandelic acid}}{C_6H_5.CHOH.COOH}$$

$$\xrightarrow{degradation} \underset{\text{Benzoic acid}}{C_6H_5\,{}^{14}COOH} + CO_2 \qquad (13.2)$$

The reaction may occur either by migration of the phenyl group or of the hydrogen atom from the aldehyde group. By ^{14}C labelling of the carbon atom adjacent to the phenyl group in the phenyl glyoxal and degrading the product mandelic acid to CO_2 and C_6H_5COOH, less than 1% ^{14}C was found in the CO_2 suggesting that there is no change in the carbon skeleton during the reaction.

Chromplating is a popular technique. In electroplating of metals by chromium, the electrolyte contains chromate i.e. Cr(VI). In the electrolytic reduction, whether Cr(VI) goes

through the intermediate Cr(III) stage or not, was confirmed by using ^{51}Cr tracer in the electrolyte. Two separate experiments are carried out. In each of them, the electrolyte contained both CrO_4^{--} and Cr^{+3} ions with ^{51}Cr as tracer with one of the constituents. It is known that Cr(VI) and Cr(III) do not undergo isotopic exchange. Since the study showed ^{51}Cr active metal deposit only when using chromate - ^{51}Cr tracer, it was concluded that Cr(III) is not an intermediate in the electrolytic reduction of chormate.

Determination/Confirmation of Chemical Structure

It would be interesting to know whether the atoms of the same element in a compound are equivalent or not. For example in the case of thiosulphate, $S_2O_3^{--}$ ions, whether the two sulphur atoms are equivalent or not can be probed using ^{35}S tracer. Elemental sulphur was labelled with ^{35}S tracer. The compound was formed by the reaction,

$$Na_2SO_3 + {}^{35}S \rightarrow Na_2{}^{35}S_2O_3 \qquad (13.3)$$

when this radioactive thiosulphate is oxidatively decomposed to sulphate and sulphide, ^{35}S fraction should be present in both, if the two 'S' atoms are equivalent. The actual results revealed that the entire ^{35}S activity was present in the sulphide precipitate. This showed the non-equivalence of the two 'S' atoms in thiosulphate ion.

Similarly in the molecule PCl_5, it was shown using ^{36}Cl, that all Cl atoms do not occupy structurally equivalent positions. Two of Cl atoms form one set and the other three Cl atoms form another set in terms of structural positions. The reactions studied were:

$$PCl_3 + {}^{36}Cl_2 \rightarrow PCl_5 \text{ and } P^{36}Cl_5 + H_2O \rightarrow POCl_3 + 2H^{36}Cl \qquad (13.4)$$

All the activity was found with HCl and non with $POCl_3$ indicating that bond strength for two Cl atoms is different than the same for other three Cl atoms in PCl_5.

Isotope Exchange Reactions

There are instances wherein two substances having a common atom or ion are together in solution or in solution-precipitate interface. A continuous exchange of the common atom or ion occurs all the while, even as the system remains in equilibrium. Examples are halide-halate (e.g., iodide-iodate), ethyl iodide- (inorganic) iodide, sulphate-thiosulphate and others. The radiotracer procedure is unique in detecting such exchange and helps measure the rate of an exchange. ^{131}I, ^{82}Br and ^{35}S are some of the isotopes used in such reaction studies. Rates of exchange reactions range from very slow to instantaneous. The unique feature is the ability to measure the rates under equilibrium conditions (cf. usual kinetic studies involve measurements away from equilibrium conditions). Separation technique like solvent extraction or precipitation can be employed; e.g., inorganic halide can be precipitated as silver halide from ethyl iodide-iodide system.

If a solution containing sodium bromide labelled with ^{82}Br is added to a solution of ethyl bromide in alcohol and after some time ethyl bromide is separated from the system, it will be found to contain radioactive bromine. No new chemical species is produced and the

concentrations of sodium bromide and the ethyl bromide in the system remain unchanged. The reaction is called isotopic exchange reaction. In this system we are concerned with the behaviour of bromine atoms in two different chemical states, ionic and covalent. Isotopic methods are used to distinguish between them.

The kinetics and mechanism of such exchange reactions involving both homogeneous and heterogeneous systems are studied using radiotracers. Several exchange reactions such as those of the electron transfer type, atom transfer type and dissociative type have been investigated. Some examples are given below

Electron Transfer Type

$$^{59}Fe^{2+} + {}^{56}Fe^{3+} \rightarrow {}^{56}Fe^{2+} + {}^{59}Fe^{3+} \quad (13.5)$$

$$^{239}U^{4+} + {}^{238}U^{3+} \rightarrow {}^{239}U^{3+} + {}^{238}U^{4+} \quad (13.6)$$

$$^{204}Tl^{+} + {}^{205}Tl^{3+} \rightarrow {}^{204}Tl^{3+} + {}^{205}Tl^{+} \quad (13.7)$$

Atom Transfer Type

$$\tfrac{1}{2}\,{}^{36}Cl_2(g) + Cl^{-}(a) \rightarrow {}^{36}Cl^{-}(a) + \tfrac{1}{2}\,Cl_2(g) \quad (13.8)$$

$$*I^{-} + RI \rightarrow RI* + I^{-} \quad (13.9)$$

Dissociative Mechanism

$$^{18}F_2 + UF_6 \rightarrow UF_5\ {}^{18}F + F_2 \quad (13.10)$$

$$[Al(C_2O_4)_3]^{3-} + [{}^{14}C_2O_4]^{2-} \rightarrow [Al(C_2O_4)_2({}^{14}C_2O_4)]^{3-} + [C_2O_4]^{2-} \quad (13.11)$$

Isotope exchange reactions, where concentrations do not change, are easily studied using radiotracers as radioactivity measurement is a nuclear property.

The isotope exchange reactions have been useful for practical applications too. Synthesis of labelled compounds is often carried out taking advantage of this principle. For example, iodine can be introduced as an electrophile ($*I^{+}$) or a nucleophile ($*I^{-}$) in suitable molecules under appropriate conditions of pH and temperature.

$$C_6H_4\,(NH\ COCOOH)\ (I) + Na*I \xrightarrow[\Delta]{pH\ 4\text{-}5} NaI + C6H4\ (NH\ COCOOH)*I \quad (13.12)$$

One can take further advantage of very low concentration of Na*I (nearly carrier-free) and drive the reaction to near quantitative consumption of radioactive *I. Thus at the end of reaction, very little $*I^{-}$ is left in reaction mixture. Radiolabelled compound can be further purified, if needed, by anion exchange chromatography to remove traces of radioactive free iodide. Cu^{++} catalyst has been suggested to enhance the reaction rate and yield. Nucleophilic substitution will need more rigorous reaction conditions, often needing a catalyst and a much higher reaction temperature.

$$\text{3-I - (Benzylguanidine)} + \text{Na*I} \xrightarrow[160\,^{o}\text{C}]{Cu^{+}/Cu^{++}} \text{NaI} + \text{3 - *I - (Benzylguanidine)} \quad (13.13)$$

Solubility of a Sparingly Soluble Substance

The ability of radiometric monitoring of 'chemical mass' is used for measuring solubility product of sparingly soluble substances. Solubilities of AgI, PbI_2 etc. can be measured using $^{131}I^-$ as tracer. KI solution containing ^{131}I of known quantity is taken. Ag I is precipitated by adding excess $AgNO_3$ solutions. Precipitate is separated, filtered and dried. Specific activity, namely, activity per mg of Ag*I is calculated. A finite amount of this precipitate is taken in water (or solvent to be studied) and shaken well at the desired temperature of study. An aliquot of the solution is removed and assayed for radioactivity. Concentration of the solute AgI is calculated from the measured activity and specific activity. The latter gives the extent of solubility under the conditions studied and the solubility product is calculated from the known stoichiometry. Similarly solubility and solubility product are determined for PbI_2 by precipitating it by addition lead acetate solution to KI solution.

Carbon Dating and Other Methods of Age Determination

A long-lived radioisotope, naturally occurring or induced, present in samples in equilibrium with original environment, can be used as an 'age indicator'. The conditions required are: The age (time lapse) is compatible with half-life of the radioisotope (within 3 to 5 times the half-life value) and there is a definite time point of disturbance of the equilibrium (loss of life, total isolation etc.). For example ^{14}C is continuously produced in the atmosphere by the induced cosmic radiation reaction ^{14}N (n, p) ^{14}C . ^{14}C enters the life cycle and about 15 dpm/g is the equilibrium value of activity. Any sample 'dead' since a particular time, would have reduced ^{14}C content. The determination of residual activity of ^{14}C and back calculation will help determine the age of the sample. About 20000-25000 year old samples can be studied since $t_{1/2}$ of ^{14}C is 5730 years.

Similarly, tritiated water HTO, formed in the atmosphere is mixed with large water bodies such as sea and river. The ratio of T/H is constant at equilibrium, about 10^{-18}. If the equilibrium is disturbed or a water body gets totally isolated, this ratio of T/H changes with time, as dictated by the 12.33 year half-life of tritium. In both the above cases, low level soft beta radiation has to be measured. This demands low background liquid scintillation counting system for reliable estimation of residual activity and in turn, the age of the sample.

Similarly the ratio of $^{87}Rb/Sr$ (^{87}Rb, 27.83% natural abundance; $t_{1/2} = 4.75 \times 10^{10}$ y; E_β 0.3 MeV), $^{40}K/Ca$ and $^{40}K/Ar$ (^{40}K 0.0117% natural abundance; $t_{1/2} = 1.277 \times 10^9$ y; β^- 89.28% to ^{40}Ca and EC 10.72% to ^{40}Ar) can be used for the age determination of rocks and minerals. There are, however, difficulties due to the presence of naturally occurring ^{87}Sr, ^{40}Ca and ^{40}Ar, in addition to the 'radiogenic' formation cited above. The age of the earth, rather the 'minimum age', can be computed from the age of the oldest minerals and rocks. The age proposed is 5×10^9 years, based on uraninites found in Canada.

Radiotracer for Optimisation of Chemical Separation Methods

In the case of studies on solvent extraction, ion exchange chromatography, adsorption chromatography, etc., one needs to measure concentration of substances in different phases/components. Radiometric monitoring is simple, reliable and rapid as compared to conventional chemical tests like spectrophotometry / colorimetry. As long as suitable radiotracer is available and chemical forms under study are stable, it is possible to reliably estimate the yield of separation, the extent of separation etc. Table 13.1 shows typical radiotracers used in chemical separation studies. It is also possible to use multi-tracer procedure and follow the radiometric monitoring with high resolution spectrometry so as to simultaneously trace the pathways of more than one element at a time.

There are instances wherein co-produced impurity serves as radiotracer enabling monitoring of radiochemical separation processes. This is particularly true of activation products arising from charged particle reactions. ^{65}Zn produced along with ^{67}Ga when Cu targets are irradiated with alpha particles, serves as tracer for monitoring Zn and Cu removal. ^{202}Tl is co-produced while preparing ^{201}Tl by the reaction ^{203}Tl (p, 3n) ^{201}Pb $\rightarrow$ ^{201}Tl. In the first step of separation, the completion of isolation of thallium target is monitored by assaying ^{202}Tl activity in ^{201}Pb.

Table 13.1 - Radiotracers in chemical separation studies

System	Techniques	Radiotracer(s)
Cu, Zn	Cation exchange chromatography	^{64}Cu, ^{65}Zn
Sn, In, Sb	Ion exchange chromatography	^{113}Sn, ^{124}Sb, ^{113}Sn (^{113m}In)
Mo, Tc, W, Re	Solvent (MEK) extraction	^{90}Mo(^{99m}Tc) $^{186/188}$Re, ^{188}W
Ga, Fe	Solvent (DIPE) extraction / cation exchange chromatography	^{67}Ga, ^{59}Fe
Cs, Ba	Ion exchange chromatography	^{137}Cs (^{137m}Ba) ^{131}Ba, ^{131}Cs
Sm, Eu	Ion exchange chromatography	^{153}Sm, ^{154}Eu
Tl, Pb	Solvent extraction / ion exchange chromatography	^{202}Tl, ^{203}Pb

Radioisotope Powered Battery

The heat associated with the dissipation of radiation energy in a compacted matter can be converted to thermo-electric power in a 'battery' system. The radioisotopes used are ^{90}Sr;

($t_{1/2}$ 28.79 y; E_β 0.54 MeV and 2.27 MeV of ^{90}Y in equilibrium) and ^{238}Pu ($t_{1/2}$; 87.7y E_α 5.4 MeV).

Strontium Ninety Auxiliary Power (SNAP) was developed in USA and used for charging batteries in inaccessible places such as, spacecraft, unmanned laboratory stations in Arctic area, and submarines. ^{238}Pu based battery has also been used in space applications.

Bibliography

1. S. Glasstone, Sourcebook on Atomic Energy, 3rd Ed., Affiliated East West Press Pvt. Ltd. (1967).
2. G. Friedlander, J.W. Kennedy, E.S. Macias, J.M. Miller, Nuclear and Radiochemistry, 3rd Ed., John Wiley & Sons Inc., New York (1981).
3. H.A.C. McKay, Principles of Radiochemistry, Butterworths (1971).
4. H.J. Arnikar, Essentials of Nuclear Chemistry, 3rd Ed., John-Wiley (1990).
5. Experiments in Radiochemistry, Eds. D.D. Sood, S.B. Manohar and A.V.R. Reddy, IANCAS Publication, Mumbai (1994).
6. J. Tölgyessy and M. Kyrs, Radioanalytical Chemistry, Vol. 1 and 2, Ellis Horword Ltd., England (1989).
7. E.A. Evans, M. Muramatsu, Radiotracer Techniques and Applications, Marcel Dekker, New York (1977).

Chapter 14
Radioanalytical Techniques and Applications

Hevesy and Paneth were the first to use radionuclides in the analytical work. In 1913, they determined solubility of lead sulphide in water by using a naturally occurring lead isotope (^{210}Pb). After the discovery of artificial radioactivity, construction of accelerators and nuclear reactors, many radionuclides suitable for analytical work were produced and a great deal of progress in radioanalytical chemistry has been made. Radioanalytical chemistry may be defined as a special branch of chemistry which belongs to both analytical chemistry and applied radiochemistry. Radioanalytical chemistry is concerned primarily with the use of radionuclides and nuclear radiations for analytical measurements. Radioanalytical techniques are based on using a radioisotope as a tracer or utilising the radioactivity produced in the sample by activation (e.g., neutron activation analysis) or measuring the X-ray induced in the sample (e.g., X-ray fluorescence).

Tracers in Analytical Chemistry

Radioisotopes are widely used as tracers in analytical chemistry. This is due to the sensitivity and simplicity of the method involved. It may be noted that certain precautions have to be taken while using tracers to minimise errors. Important factors include (i) mass effect, (ii) low concentration, (iii) unexpected oxidation states and (iv) radioactive daughter products. These are discussed in Chapter 13. Many elements have multiple oxidation states and in the investigations involving tracers, the oxidation state of the tracer must be ensured to be the same as that of the element in the bulk.

Chemical yield in Separations

It is often required to determine the chemical yield in a separation process like precipitation, solvent extraction or ion exchange separation. This could be achieved by adding a known amount of radioisotope prior to separation and measuring the activity in the phase containing the product of interest. The ratio of the measured activity to the original activity gives the chemical yield.

Analysis by Means of Natural Radioactivity

A number of naturally occurring radioisotopes are given in Chapter 1. They can be estimated by measuring the radioactivity, e.g., potassium can be analysed by measuring the activity of ^{40}K (0.0117% natural abundance). ^{40}K has a half-life of 1.277×10^9 y. It undergoes β-decay with a β_{max} of 1.33 MeV and has a γ-ray of 1461 keV. By measuring either γ-activity or β-activity, potassium can be estimated.

Another example is measurement of ^{210}Po. It undergoes α-decay ($E_\alpha = 5.3$ MeV)with a half-life of 138.376 d. Polonium can be separated by many methods. Commonly followed separation technique is its spontaneous deposition on silver foil. Pure polonium is separated by controlled potential electrodeposition and is measured with a windowless gas proportional counter or by α-spectrometry.

Emanation Analysis

Radon isotopes and their respective parents can be analysed by measuring the activity of the emanating gaseous radionuclides like ^{222}Rn, ^{220}Rn and ^{219}Rn. For example, ^{222}Rn is measured as follows. The solid substance like mineral, rock or soil containing radon is brought into solution by fusion with a suitable flux like borax. Air is continuously bubbled through the melt at a constant rate and through the ionisation chamber. Measured ionisation is used to estimate ^{222}Rn and its parent ^{226}Ra. Emanation analysis requires quantitative removal of radon and also attainment of equilibrium with the parent before flushing the emanating radon.

Radiometric Titrations

Precipitation

Radioisotopes are used as the indicators in radiometric titrations. The titration of chloride ion with ^{110}Ag labelled silver nitrate solution is described as an example. Silver nitrate solution is taken in the burette and chloride solution is taken in the beaker. During the titration, AgCl precipitate is formed and settles down. As the titration proceeds, the radioactivity of the supernatant solution is measured. So long as any chloride ion remains in the solution, the ^{110}Ag activity will be carried down with the silver chloride precipitate and the measured radioactivity is only due to background. After the end point is reached, ^{110}Ag remains in the solution and activity of the solution will begin to rise. A typical activity profile is shown in Fig. 14.1. This titration may also be performed with ^{36}Cl labelled chloride. In this case, the activity of the solution decreases continuously and attains a constant value corresponding to the background activity. Volume corresponding to the start of the invariant line is the end point value.

Another example is the use of an insoluble compound like $^{110}AgIO_3$ as indicator in the complexometric titration of calcium by EDTA. $^{110}AgIO_3$ is added to the solution containing Ca^{++}. It is titrated with EDTA solution and the activity of the solution is monitored. EDTA is

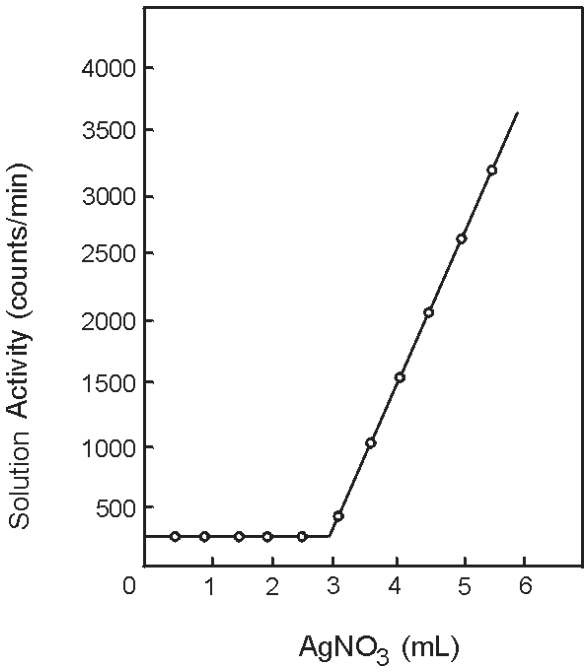

Fig. 14.1 Titration of chloride using a radiotracer as indicator.

removed by Ca^{++} until the end point and after the end point excess EDTA reacts with Ag^{+} to form soluble Ag-EDTA complex. Since silver is labelled with radioisotope, the activity in the solution starts increasing after the end point due to the presence of Ag-EDTA complex in the solution as shown in Fig. 14.2, where the end point is marked as the start of the release of radioactivity.

This simple method has been used for determining the following ions with the precipitants noted in brackets : $CNS^{-}(^{110}Ag^{+})$, $Ag^{+}(^{36}Cl^{-})$, $Cl^{-}(^{110}Ag^{+})$, WO_4^{2-} $(^{60}Co^{2+})$, $Co^{2+}(^{185}WO_4^{2-})$ and $Mg^{2+}(^{32}PO_4^{3-})$. Radiometric methods involving precipitation are limited in sensitivity to quantities which can be handled conveniently, usually >50 mg. However, in some cases, even as low as 10 mg of protein has been assayed by precipitation with tungstic acid.

Solvent Extraction

Sensitivity of radiometric titrations can often be improved by solvent extraction methods, where even chemically insignificant quantities can quantitatively be separated and transferred from one phase to another. The radioactivity of either or both phases is measured to monitor the titration. The method has been used for the determination of microgramme quantities of Hg^{2+}, Pb^{2+}, Co^{2+}, Zn^{2+} and Ni^{2+} by extraction with dithiozone in CCl_4 solution. Solvent extraction methods involving radiotracers have also found extensive use in the evaluation of solvent extraction equilibria, analysis and the determination of stability constants of metal ions with different ligands.

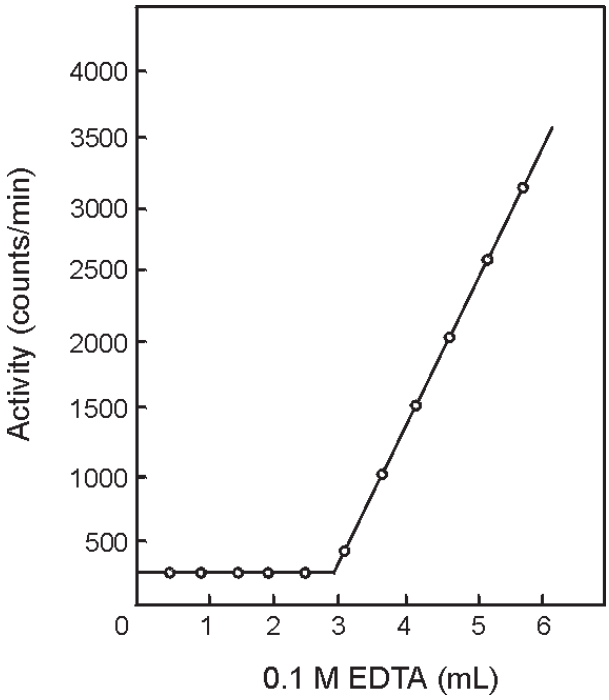

Fig. 14.2 Titration of Ca^{2+} with EDTA using a radiotracer as indicator.

Isotope Dilution Methods

Isotope Dilution Analysis (IDA) is a quantitative analytical technique that was first developed by Hevesy and Hobbe in the late 1930s. IDA is a good analytical method that yields quantitative results. IDA does not need quantitative separation. The basis of IDA is that the specific activity of a mixture of stable and radioisotopes, which is in a constant ratio, does not change by chemical processing. Labelled compounds allow quantitative analysis even with incomplete isolation of the compound.

In this method, a known mass M of the material of known specific activity S is added to a system. Chemical form is chosen such that exchange between the inactive and active species is ensured. The radioactive material is diluted with the inactive material having mass M_x . This results in the reduction of the specific activity. If a part of the material is separated (e.g., by precipitation) and its specific activity S_x is determined, then M_x can be calculated based on the conservation of total activity as follows:

$$M_x = M\left[\frac{S}{S_x} - 1\right] \qquad (14.1)$$

As mentioned above, there is no need for quantitative separation of the precipitate. This is illustrated in Fig. 14.3. Sample contains 12 units of radioactivity and the specific activity is 1. It is diluted with 24 units of inactive material. From the mixture, a portion is

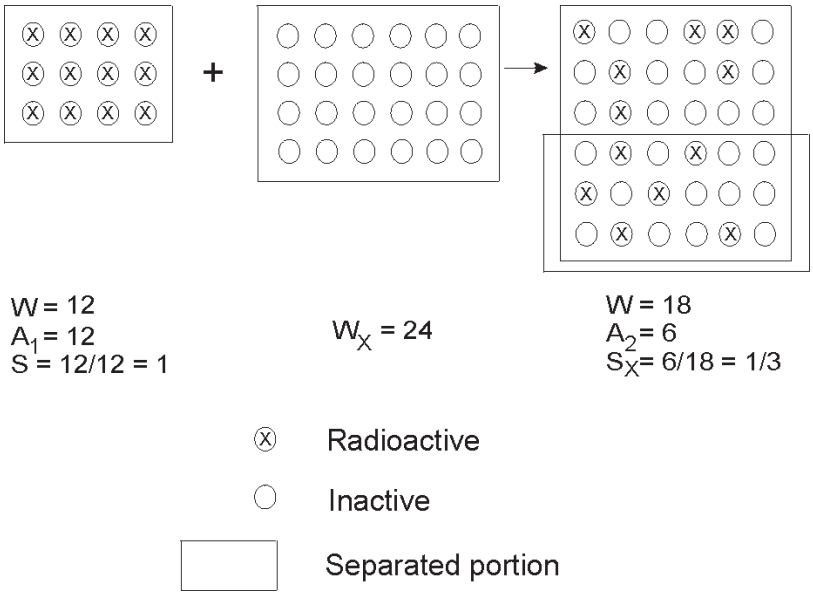

Fig. 14.3 Schematic representation of isotope dilution analysis.

separated having 18 units of weight of which 6 units are radioactive. Thus specific activity is 6/18 = 1/3. Decrease in specific activity is due to isotope dilution. This decrease in specific activity is used to calculate the amount of the material originally present in the sample.

A simple example is worked out here to illustrate the isotope dilution analysis used for the estimation of cobalt present in a solution.

To 10 mL of a solution in which cobalt has to be estimated, a solution containing 7.5 mg of cobalt with a measured activity of 340 cpm was added. From this, cobalt was separated as the metal by electrodeposition. Weight and activity of the isolated Co were 10.3 mg and 178 cpm respectively. Amount (M_x) of Co in the original sample is calculated as follows.

$$\text{Specific activity in the sample (S)} = \frac{340}{7.5} = 45.3 \text{ cpm/mg}$$

$$\text{Specific activity in the separated sample } (S_x) = \frac{178}{10.3} = 17.3 \text{ cpm/mg}$$

$$\text{Using eqn. 14.1, } M_x = \left(\frac{45.3}{17.3} - 1\right) 7.5 = 12.1 \text{ mg.}$$

$$\text{Concentration of Cobalt} = \frac{12.1}{10} = 1.21 \text{ mg/mL}$$

IDA has been effectively used in organic and biomedical investigations where complete separations are often difficult to perform. IDA is being applied in situations where

(i) quantitative isolation of the element is difficult or impossible, (ii) complete separation is time consuming, (iii) amount of the analyte is very small and (iv) it is impossible to obtain the entire sample for analysis. An example representing the situation (iv) is worked out here where total volume of blood in a person is determined by IDA.

One mL of blood from a patient is withdrawn and is labelled with ^{24}NaCl (^{24}Na $t_{1/2}$ = 14.959 h), specific activity being 20,000 cpm/mL. This is injected intravenously into the patient. After about 15 min, 1 mL of blood is withdrawn from the patient for measuring the activity. It gave a specific activity of 4 cpm/mL. The observed decrease is due to dilution of the ^{24}Na activity in the entire volume of the blood (V). By activity balance, volume of the blood of the patient is calculated as

$$20000 \times 1 = 4 (V+1)$$

$$V = 4999 \text{ mL}.$$

Reverse Isotope Dilution Analysis (RIDA)

It is a modification to IDA. In this method, the amount of radioactive substance (M_X) is determined. The specific activity of the sample is S. The sample is diluted with a known amount (M) of inactive isotope. Then the compound is separated and the specific activity (S_1) is measured. The decrease in specific activity ($S-S_1$) is related to the amount of diluent M by eqn. 14.2 and is used to arrive at the amount M_X, originally present in the sample. It requires that the original specific activity S be known.

$$M_x = \frac{MS_1}{S - S_1} \qquad (14.2)$$

RIDA is useful in determining the yields of the products of metabolism of pharmaceuticals. Labelled drugs are fed to experimental animals, the organs of which can be analysed for the original drug, or for one of its metabolic products by adding a known quantity of the appropriate inactive compound to an extract of the organ and then separating the purified sample. For example, the distribution and composition of the degradation products of dicoumarol in experimental animals and of the carcinogen dibenzanthracene (^{14}C-labelled) after application to the skin of mice have been studied by RIDA.

Isotope Derivative Dilution Analysis is a modification of RIDA. When the parent material is inactive, but undergoes chemical reactions with a radioactive reagent to form other derivatives, the latter can be analysed by RIDA after addition of known amount of inactive derivative.

Substoichiometric Isotope Dilution Analysis (SIDA)

The sensitivity of the IDA methods has often been enhanced by the use of sub-stoichiometry technique. The amount of the reagent added is less than the amount required for completing the chemical reaction. It is necessary to have a reagent which reacts quantitatively and selectively with the analyte and also the resulting material, generally a

precipitate, is readily separable. Metallic elements can be precipitated using chelating agents. In this method, separations are performed on the sample and a standard for comparison. A known amount of tracer is added to the solution under investigation and to a standard. Same quantity of the reagent, which is not adequate to separate all the analyte, is then added leading to identical quantities of precipitate. Precipitates from the standard and sample are separated and activities are measured. There is no need to weigh the precipitate. Activity of the sample and standard are related inversely to the amounts present in them. If M_x and M_s are the quantities of the substance in the sample and the standard with respective activities of A_1 and A_2, then $A_1M_x = A_2M_S$. From this, the value of M_x can be calculated. This technique of isotope dilution analysis is finding much use in inorganic analysis. The following example is an illustration of SIDA for calculating Ag present in a sample.

A tracer containing ^{110}Ag is added to a standard solution (20 mg/mL of Ag) and to a sample that is to be analysed. Substoichiometric amounts of dithiozone in chloroform were added to both the solutions. Ag-dithiozone complex from both the solutions were extracted and their activities were measured as 2000 cpm and 1500 cpm respectively.

Since equal amounts of dithiozone were added, the amount of Ag-dithiozone complex would be same. By adding substoichiometric quantities and maintaining proper conditions, complete utilisation of the reagent is ensured. Activity of the complex extracted from the sample is observed to have lower activity. This means that the amount of Ag present in the sample is higher compared to the standard. Amounts of Ag are inversely related to the activities. Thus the concentration of Ag in the sample = 2000 x 20/1500 = 26.7 mg/mL.

Some examples of IDA using radioisotopes and applications are given in Table 14.1.

Radioimmunoassay (RIA)

RIA is a micro radio analytical technique for measurement of substances in biological specimens in low concentrations, e.g., hormones, drugs, vitamins and viruses. It is a substiochiometric IDA which was first developed by Berson and Yalow in 1950s. They used ^{131}I labelled insulin in their studies. RIA technique for the measurement of an antigen concentration is based on competition between labelled antigen and unlabelled antigen (Ag^* and Ag) for the limited binding sites on its specific antibody (Ab).

$$(Ag \text{ and } Ag^*) + Ab \rightarrow (Ag\ Ab) + (Ag^*\ Ab) \qquad (14.3)$$

At the end of the reaction, the antibody bound and the free antigen are separated by a suitable physico-chemical method and the radioactivity is measured. By constructing a standard curve, antigen concentration in the sample is calculated. Details are described in Chapter 16.

Nuclear Activation Analysis

The nuclear activation analysis is based on activation of the isotopes of elements and subsequent measurement of induced radioactivity. It provides information on both

Table 14.1. Typical examples of isotope dilution analysis - some results

Element or compound	Label	Sample	Remarks
Cobalt	^{60}Co	Steel and Ni alloys	On a few g sample containing 0.14-0.154% Co Max. error:0.02%
Vitamin B-12 (Cyano cobalamin)	^{57}Co	Feed supplements, vitamin capsules etc.	For sample down to 100 μg at conc. of 0.1 μg/mL
m-nitrotoluene	^{14}C	Products of nitration of toluene	For > 100 μg sample, accuracy ± 5%
Corticosterone	^{14}C	Human Plasma	For > 100 μg sample, accuracy ±5%
Penicilline	^{35}S or ^{14}C	Production broths	±6% at 95% confidence level
α-isomer of hexachloro-benzene	^{36}Cl or ^{14}C	Mixture with other isomers	±0.15%

qualitative and quantitative chemical analysis of samples. The activating source may be a neutron or a charged particle (e.g., α, p) or a photon (e.g., γ-ray) and the radioactive products decay by emitting radiations like α, β, γ and X-ray or delayed neutron. In 1934, I.J. Currie and F. Joliot discovered nuclear activation by bombarding Al, Mg and B with alpha particles. The neutron induced radioactive product was first reported by Fermi. George de Hevesy and Hilde Levi were first to introduce the neutron activation analysis (NAA) technique in 1936. A few nuclear techniques are listed below and neutron activation analysis is dealt in detail.

Prompt Gamma Neutron Activation Analysis (PGNAA)

In PGNAA, prompt gamma rays emitted by the compound nucleus formed after absorption of the neutron, are measured. This is an on-line technique. Though it is less frequently used, PGNAA is an effective tool for the analysis of many elements including light elements like H, B, N, P and S.

Charged Particle Activation Analysis (CPAA)

In CPAA, the analyte is activated by charged particles like protons or alpha particles. The energy of the activating particles is in the range of a few MeV. Measured activities of activation products are used to determine the concentration of the analyte.

Particle Induced Gamma ray Emission analysis (PIGE)

In PIGE, the prompt gamma rays emitted by the compound nucleus formed after absorption of the charged particle are measured. It is an on-line technique. It is mainly used for the analysis of light elements like Li, Be, B and F.

Instrumental Photon Activation Analysis (IPAA)

Energetic photons in the range of 10-15 MeV are used to activate the analyte. High photon intensities are obtained in electron accelerators. When electron beam is accelerated continuous energy (Bremsstrahlung radiation) photons are produced. This is used as a photon source in IPAA.

Neutron Activation Analysis

Neutron, being a non-charged particle interacts with the nuclei of most of the isotopes and result in nuclear reactions. The product formed in neutron induced reaction is often a radioisotope. By measuring the radioactivity of the radioisotope formed, preferably with a high resolution gamma ray spectrometer, concentration of the isotope that underwent nuclear reaction is measured. Using the isotopic abundance, elemental concentration can be calculated. This is the principle of Neutron Activation Analysis (NAA). In 1936, Prof. Hevesy and his younger colleague Levi determined the sub-mg quantities of dysprosium in yttrium, by bombarding the sample of yttrium with neutrons obtained from a radium-beryllium source. In this reaction, radioisotope ^{165}Dy ($t_{1/2}$ = 2.334 h) was formed and its activity was measured. Measured activity was used to determine the concentration of Dy. This experiment heralded the arrival of the NAA, a powerful and sensitive radioanalytical technique.

Thus NAA is based on irradiation of a sample with neutrons, preferably in a nuclear reactor, and subsequent measurement of the induced radioactivity, most frequently employing a high resolution γ-ray spectrometer[1]. Multi element analysis is carried out by measuring gamma ray activities corresponding to different radioisotopes (elements), present in both samples and standards, using a multi channel analyser.

In NAA, for irradiation the whole reactor neutron spectrum can be used or thermal neutrons can be filtered off using Cd or B filters to achieve selective activation with epithermal and/or fast neutrons (epithermal NAA - ENAA and fast NAA - FNAA,

---

[1]Gamma rays may interact with matter either by photoelectric effect or Compton scattering or pair production. Photoelectric effect is very useful for quantitative measurement of energy and intensity of the gamma rays. A semiconductor detector such as HPGe (high purity germanium) has resolution in the range of 1.6 to 2.0 keV at 1332 keV and thus is very useful for simultaneous measurement of gamma rays that represent different isotopes. A good amplifier, Analog to Convertor (ADC) and a multi channel analyser in combination with HPGe are the major components of a high resolution gamma ray spectrometer.

respectively). FNAA can also be performed using 14 MeV neutrons produced by the (d,t) reaction in neutron generators, or with fast neutrons produced by deuterons / protons induced by (d,p) reactions. Isotopic neutron sources based on either the spontaneous fission of ^{252}Cf or nuclear reactions, such as the (α,n) reactions (e.g., ^{241}Am-Be) or the (γ,n) reaction (e.g., ^{124}Sb-Be) are also used for NAA, although they provide a neutron fluence which is several orders of magnitude lower as compared to that in nuclear reactors.

Activity Formed in Activation

The activity (A) formed at the end of irradiation when a sample is irradiated in a neutron flux (ϕ) for a period of time (t), is given by (see Chapters 8 and 11),

$$A = N_t \sigma \phi \, [1 - e^{-\lambda t}] \qquad (14.4)$$

where, λ = decay constant of the radioisotope formed, $[1-e^{-\lambda t}]$ is the saturation factor and N_t is the number of target atoms which is given by

$$N_t = \frac{N_A \, \theta \, w}{M} \qquad (14.5)$$

where , N_A = Avogadro number, θ = isotopic abundance, w = weight of the sample and M = atomic weight

The activity after a cooling period of T is given by

$$A = \frac{N_A \, \theta \, w}{M} \sigma \, \phi \, [1 - e^{-\lambda t}] \, e^{-\lambda T} \qquad (14.6)$$

By measuring A and using the values of σ, ϕ, λ, t, T, θ, w and M, in eqn. 14.6, the number of atoms (N_A) in the sample can be calculated.

Sensitivity and Detection Limit

The sensitivity (S) of an element in NAA is defined as counts.μg^{-1} for a particular experimental conditions of irradiation (t_i), decay (t_d) and counting (t_c) durations. Depending on the nuclear properties of the isotope of interest, the above parameters (t_i-t_d-t_c) are decided by the analyst. It is clear that the main parameters for sensitivity are σ, ϕ and ε. Since σ is fixed for an isotope, it is needed to use higher ϕ and a detector of higher efficiency.

Detection limit in NAA varies from pg to mg depending on the element of interest, gamma ray background, elemental sensitivity, sample matrix and pre or post chemical separations. The detection limit (L_D) is defined as the three times of the standard deviation of the background counts (C_b) under the photopeak and is calculated using the expression: L_D (counts) = 2.71+3.29x$\sqrt{Cb}$. The counts are then converted to $\mu g.g^{-1}$ with the use of S sample mass (g). The typical detection limit using a flux of 10^{13} n.cm^{-2}.s^{-1} for elements like Eu and Dy, is about 1 pg whereas for Mn, In and Lu it is 10 pg, for Co, Rh, Br, Au, Re and Sm it is 0.1

ng and for elements like Na, Ga, La, K, Sc, Ni, Zr, Rb, Cd, Zn, and Cr the detection limits are between 10 ng to 1 μg.

Different Methodologies of NAA

The NAA technique can broadly be divided into two categories based on whether analysis of sample is carried out without or with any chemical separation. Depending on the sample type, element and nuclide to be analyzed, different approaches are practised.

If elements of interest can be determined without any chemical treatment, the process is called instrumental neutron activation analysis (INAA). This approach is more common and has several advantages like non-destructive in nature, multielement capability, minimal sample handling and no reagent blank correction. When the radioisotope of interest is very short-lived (ms to less than a minute) the cycle of to improve the signal to background ratio (S/B) and discriminate the long-lived interfering elements. This approach is called CINAA and it is carried out using automated equipment. short irradiation, quick transfer and short counting of sample. The process is repeated to get accumulated γ-ray spectra for the same sample for an optimum number of cycles (3-4 cycles) depending on the improvements of S/B ratio, counting statistics and also detection limit. When the concentration of element of interest is lower than the detection limit achieved by INAA, then pre or post chemical separations are often employed. In RNAA radioisotopes of interest are separated. When the element of interest is chemically separated prior to irradiation, the procedure is called preconcentration or chemical NAA (PNAA/CNAA). Another pre-irradiation separation approach where speciation/ oxidation state information is obtained in conjunction with NAA is called speciation NAA (SNAA). For some elements that are poorly determined using conventional NAA or does not have any characteristic gamma lines, derivative NAA (DNAA) is used where the element is chemically exchanged or complexed with an element that is amenable to NAA.

When the element has good nuclear properties and experiences no or minimum interference, the first method of choice is the INAA due to its simplicity. The INAA approach has three different forms depending on the energy of neutron: Thermal INAA (TINAA), Epithermal INAA (EINAA) and Fast INAA (FINAA). The above three INAA methods are named due to activation of isotopes mainly from thermal neutron (most probable energy 0.0253 eV and E_n max up to 0.55 eV), epithermal and resonance neutrons (0.2-500 keV) and fast neutron (>500 keV). In EINAA the total activity due to interfering nuclides such as Na, K, Mn, Cl, Al, Br and La is suppressed. Nuclides of elements, with high resonance integral to thermal neutron capture cross section ratios ($I_0 / \sigma_0 = Q_0$; $Q_0 > 10$), such as Ag, As, Au, Ba, Br, Cd, Cs, Ga, Gd, In, Mo, Ni, Pd, Pt, Rb, Sb, Se, Sm, Sr, Ta, Tb, W, Th and U are analyzed by EINAA. In EINAA the sample is placed inside a cylindrical box of 1-mm thick cadmium (0.55 eV cut-off) or a boron carbide box (cut-off energy 10-280 eV, depending on boron thickness and amount) and irradiated. The Cd or B absorbs thermal neutrons and filter out higher energy neutrons. The detection limit of these elements is comparable or better than TINAA. However, FINAA is capable of determining many

elements including the light elements that are amenable to TINAA or EINAA. The common elements that are determined by FINAA are O, N, F, Mg, Si, P, Fe, Cu, Zn, Zr, Th and U.

Chemical Separations in NAA

NAA in principle is a non-destructive instrumental analysis (INAA). However, when certain elements like Na, K and Br are present as major constituents, the gamma rays from activation products formed would complicate the measurements. Additionally, if the sample contains uranium, it undergoes nuclear fission and the products with Z between 35 and 70 would be formed. Therefore, estimation of these elements would be erroneous. In such situations, it is essential to preconcentrate and remove elements like U prior to irradiation. This procedure is known as Chemical Neutron Activation Analysis (CNAA). In Radiochemical NAA (RNAA), the sample is irradiated and the products of higher abundant matrix elements are removed by chemical methods. The activity is measured by gamma ray spectrometry.

Advantages of CNAA are: (1) sensitivity becomes higher, (2) minimum radiation exposure as chemical separation is done before irradiation and (3) gamma ray spectrum becomes simpler because matrix elements are removed before irradiation. However, reagents used for chemical processing may contain impurities. After irradiation these impurities will produce radioisotopes and the analysis might be affected. This is the main disadvantage of CNNA. This can be overcome by blank correction. Advantages of RNAA are : (1) gamma ray spectrum becomes simpler, (2) blank correction for reagents is not needed as chemical procedures are applied only after irradiation and (3) during chemical process, some carriers can be used without blank correction. The disadvantages of this method are, (i) Radioactive samples have to be handled as the radiochemical separations are carried out after the irradiation. This limits the amount of the sample to be handled; (ii) During separation, short-lived nuclides may decay and their detection is not possible. Therefore radiochemical separation methods should be fast and simple (see Chapter 18).

Standardization Methods of NAA

There are three standardization methods of NAA as described below.

Absolute Method

The mass of the element (m) can be calculated from measured activity directly using the nuclear and reactor based data. The expression for "m" derived from eqn. 14.7 is given below.

$$m = \frac{cps}{SDC} \cdot \frac{M}{N_A \cdot \theta \cdot \gamma} \cdot \frac{1}{\sigma\phi} \cdot \frac{1}{\varepsilon} \qquad (14.7)$$

However, this method is not practised for two reasons: (i) it is difficult to evaluate the absolute values of ϕ and σ since both parameter values vary with neutron energy and (ii)

uncertainties associated with the absolute values of (n,γ) thermal and epithermal neutron cross sections, γ, θ and M contribute to the final results.

Relative Method

In this method, elemental standard is co-irradiated with the sample and the activities from both sample and standard are measured in identical conditions with respect to the detector. This method is simple to arrive at the results, since it does not need the nuclear and reactor based input parameters. Using the mass of the element in standard ($m_{x,std}$) and activities of standard ($cps_{x,std}$) and sample ($cps_{x,sample}$), the mass of the element in the sample ($m_{x,sample}$) is determined for the same counting time by the following equation:

$$m_{x,\ sample} = m_{x,\ std} \cdot \frac{cps_{x,\ sample}}{cps_{x,\ std}} \cdot \frac{D_{std}}{D_{sample}} \qquad (14.8)$$

The $m_{x,\ sample}$ (μg) is converted to concentration (e.g., $\mu g.g^{-1}$ or ppm) by dividing with sample mass (g). Though the relative method is simple and precise, prior knowledge of the elements present in the sample is necessary to prepare multielemental standards or certified reference materials (CRMs) of similar matrices. An example is given below to illustrate the analysis.

A 10 mg sample of dry tea leaves and 10 μg of Mn standard were irradiated in Apsara reactor with a neutron flux of 10^{12} $n/cm^2/s$ for two hours. Sample and standard were counted after cooling periods of 1 and 1.5 h respectively. If the activities of sample and standard are 1500 and 2000 cpm (counts per minute) respectively, the amount of Mn in tea leaves is calculated as follows.

Radioisotope ^{56}Mn is formed in the neutron activation of Mn. Its half-life is 2.5785 h. Since a standard is irradiated along with sample, there is no need to calculate absolute activity formed. Ratio of decay corrected activities is sufficient to arrive at the concentration of Mn in tea leaves.

Corrected activity of Mn in the sample (Cooling period=1 h) = $1500 \text{ X } e^{0.693/2.5785X1}$
= 1962 cpm

Corrected activity of Mn in the standard (Cooling period=1.5 h) = $2000 \text{ X } e^{0.693/2.5785X1.5}$
= 2992 cpm

$\therefore$ The amount of Mn in tea leaves = $\frac{1962}{2992} \times 10$ = 6.6 μg (using eqn. 14.8)

This amount of Mn is present in 10 mg of the sample.

$\therefore$ The concentration of Mn in tea leaves analysed = 6.6 μg/10 mg = 660 μg/g

In fact, certain tea leaves are reported to contain about 0.13 % i.e. 1300 μg/g

Note : Suppose other elements like Na, K and Cl are present in the sample, they can be estimated from the same experiment by irradiating appropriate standards along with the sample. Also k_0 NAA (described in the next section) can be used where the elements present in a sample are not known.

An interesting problem is to measure arsenic in hair. Any arsenic entering human body accumulates in the roots of hair and move along the length of the hair as it grows. Normal growth of hair is about 0.35 mm / day. One can analyse the hair by NAA to arrive at the As amount. This analysis would be very useful in the case if a person dies of As poisoning. By cutting the hair into small pieces, distribution of As as a function of length might provide the time when As was initially ingested by the person (if it is a poisoning case). While normal hair would have 0.8 μg/g, any value in excess of this is considered dangerous. It is reported that 10.4 μg/g of As was found in the hair of Emperor Napoleon.

Single Comparator or k_0-NAA Method

The possibility of using a single element as comparator for multielement NAA (k_0-NAA) is attractive The k_0-NAA involves the simultaneous irradiation of a sample and a neutron flux monitor, such as gold, and the use of a composite nuclear constant called k_0. It obviates the preparation of standards for each element and a priori knowledge of constituents of sample is not necessary. For the calculation of elemental concentrations besides net counts under the peak, input parameters such as (i) sub-cadmium to epi-thermal neutron flux ratio (f), (ii) the epi-thermal neutron flux shape factor (α), (iii) the absolute/relative efficiency of the detector (ε) and (iv) the two nuclear constants: k_0 and Q_0 are used. The reactor based parameters (f and α) are dependent on each irradiation facility, so they must be determined for standardization purposes. The factor k_0 is defined as:

$$k_0 = \frac{M^* \theta \sigma_0 \gamma}{M\theta^* \sigma_0^* \gamma^*} \tag{14.9}$$

where, σ_0 is the 2200 $m.s^{-1}$ (n, γ) cross section. The symbol "*" refers to the corresponding parameters of the comparator (e.g., gold). Gold is frequently used comparator in the k_0-method owing to its favorable nuclear properties. However other elements (e.g., Mn, Co, Zr, Zn etc.) can also be used as a single comparator. The k_0-NAA method has been developed using the Hogdahl convention and the expression for concentration of the i^{th} element (C_i in $\mu g.g^{-1}$) is given by,

$$k_0 = \frac{\frac{N_p / LT}{S.D.C.W}}{\left(\frac{N_p / LT}{S.D.C.w}\right)^*} \cdot \frac{1}{k_0} \cdot \frac{f + Q_0(\alpha)^*}{f + Q_0(\alpha)} \cdot \frac{\varepsilon^*}{\varepsilon} \tag{14.10}$$

where, W and w are masses of sample and single comparator respectively. The k_0-factor is taken from the literature by De Corte. The $Q_0(\alpha)$ ($=I_0(\alpha)/\sigma_0$) is calculated using following expression

$$Q_0(\alpha) = \frac{Q_0 - 0.429}{\bar{E}_r^{\alpha}} + \frac{0.429}{(2\alpha + 1) \cdot E_{cd}^{\alpha}} \tag{14.11}$$

The details of calculations of f, α and elemental concentration in k_0-NAA method can be found in literature. The Hogdahl convention is not valid for non-1/v nuclides like ^{176}Lu and ^{151}Eu. A convention called modified Westcott-formalism is followed to include these nuclides in k_0-NAA method.

The k_0-Based Internal Mono Standard Method

The idea of using an internal mono standard in k_0-NAA is promising in terms of analyzing large and irregular geometry samples. This approach gives relative elemental concentration of element (x) with respect to mono standard (y) as given below,

$$\frac{m^x}{m^y} = \frac{\left((S.D.C.) \cdot (f + Q_0(\alpha))\right)^y}{\left((S.D.C.) \cdot (f + Q_0(\alpha))\right)^x} \cdot \frac{P_A^x}{P_A^y} \cdot \frac{\varepsilon_\gamma^y}{\varepsilon_\gamma^x} \cdot \frac{1}{k_0} \tag{14.12}$$

where, $k_0 = k_{0,Au}(x) / k_{0,Au}(y)$. The relative concentration can be converted to absolute values by using mono standard mass. In special cases where analysis of all major and minor elements is amenable, concentrations can be arrived by material balance.

Advantages and Limitations of NAA

The NAA technique has the advantageous properties like high sensitivity and selectivity, inherent accuracy and precision and low matrix effect in the estimation of many elements. The INAA technique is nondestructive, which helps in minimal sample handling. Both its inherent potentials for accuracy and totally independent principle as a nuclear-based property, which is not the case of many competent techniques, make NAA as an invaluable reference technique. It has self-validation capability, like a particular element has more than one isotope and one isotope has more than one characteristic gamma line, which forms the basis for an unique ability to verify analytical data.

NAA has some limitations as well. It needs a neutron source like nuclear reactor that is available at a few research centers. Determination of elements forming very short-lived, long-lived or only β^- emission isotopes is difficult by conventional NAA. Determination of elements forming long-lived isotopes is time consuming. NAA is insensitive to the nature of chemical species present unless pre-irradiation separation is carried out. Conventional NAA does not provide sufficient information for certain elements like Si, P, Pb, B, Gd and low Z elements.

Interferences in NAA

The types of interferences in NAA are primary, secondary and second order interference reactions, gamma-ray spectral interference, neutron self-shielding, γ-ray self-attenuation and true and random coincidences during gamma ray measurement. If a radionuclide is formed from other than the analyte, then a primary interference reaction occurs as in the case of ^{28}Al, which is produced in the following reactions: ^{27}Al (n,γ) ^{28}Al, ^{28}Si (n,p) ^{28}Al, and ^{31}P (n,α) ^{28}Al. Thus determination of Al in the presence of Si and P is erroneous. However, finding a correction factor or irradiating the sample with and without Cd or B shielding or using a highly thermalized irradiation site can solve these problems. Similarly determination of Mn and Cr in presence of Fe, Na in presence of Al and Mg are other examples. Gamma-ray spectral interferences included 846.8 keV of ^{56}Mn and 844 keV of ^{27}Mg, 279.2 keV of ^{203}Hg and 279.5 keV of ^{76}Se. In such cases other indicator gamma rays are used or one waits for the decay of other nuclide whereever possible.

Experimental Methodology in NAA

In NAA the following steps are involved: (i) sampling, (ii) preparation of sample and standard sample (CRM/ SRM), (iii) preparation of the standard (s) or single comparator, (iv) irradiation of samples and comparator in a reactor, (v) radioactive assay by high-resolution γ-ray spectrometry, (vi) spectral analysis for net peak areas, (vii) evaluation of detection efficiency (for k_0 method), (viii) calculation of elemental concentration, (ix) estimation of uncertainties and (x) interpretation of the results.

Applications of NAA

NAA has found extensive applications in many science and technology fields for macro, micro and trace element analysis in the samples corresponding to the following fields: archaeology, biomedicine, animal and human tissues, environmental science and related fields, forensics, geology and geochemistry, industrial products, nutrition, quality assurance of analysis and certifications reference materials. Two such applications are described here.

Certification of Reference Materials

The NAA methods have played an important role in the certification of inorganic constituents in many environmental certified/standard reference materials (CRMs/SRMs). Since the concentration of an element in CRM/SRM certified by agencies like NIST, IAEA, IRMM and USGS is usually determined by two or three independent analytical methods, the use of INAA as one method eliminates the possibility of common error sources resulting from sample dissolution. Other advantages include: its property in its radiochemical mode of allowing trace element radiochemistry to be performed under controlled conditions by carrier additions, and the ease of obtaining the chemical yield by the carrier recovery or

radiotracer method. More over, the method is theoretically very simple and the sources of uncertainty can be modeled and well estimated as per the international organization for standardization (ISO) guidelines.

The estimation of combined uncertainty is an independent exercise and it is different than the calculation of standard deviation from the mean value of replicate measurements. The different uncertainty components were divided into three steps: pre-irradiation step, irradiation step and gamma ray spectrometry measurement step. An additional step is considered if chemical separation step is done. The sources of uncertainty are identified and then each uncertainty component (u_i) is converted to a standard deviation. The combined uncertainty (u_c) is calculated using error propagation formula. Finally the expanded uncertainty (EU) is calculated using coverage factor of 2 at 95.5% confidence level (CL).

Forensic Applications

INAA/RNAA methods are frequently used for analysis of forensic samples like gun shot residues, glass, hair, ornamental gold, cannabis and paper. Some of the marker elements such as Ba, Sb, Cu, Sb, Ag, Fe, Br, Zn and K are analyzed depending on the sample type.

Multi Element Analysis in Leaves by k_0 NAA

Elemental concentrations of a few varieties of leaves which are used either as a natural ingredient in ayurvedic medicine preparations or as reliable items for human diet are determined using k_0 NAA method. Gold is used as single comparator. Data obtained for neem leaves from Tirupati and Mumbai, along with reference material SRM 1571 (Orchard leaves) are given in Table 14.2. Concentrations varying from 18.9 mg/g (Ca) to 20.2 ng/g (Eu) could be determined using this method.

Palladium and Gold Determination by CNAA

Measurement of trace elements in the presence of large amounts of Fe, Cu and U by NAA is very difficult due to the spectral interferences and due to the fission product contribution from the fission of uranium. In such cases, it becomes imperative to pre-concentrate elements of interest and decontaminate from the major elements and measure the concentrations by NAA. An example of Chemical Neutron Activation Analysis (CNAA) is the measurement of the trace amounts of Au and Pd present in matrices that may contain uranium, copper and iron. Pd and Au could be pre-concentrated on a mini column containing anion exchanger Dowex 1x8 (100-200 mesh) in Cl^- form. By irradiating the column with neutrons and measuring the activities Pd and Au could be determined with improved sensitivities. Standard addition method was used to arrive at the lowest detection limits. Under the ideal interference free conditions, an absolute detection limit of 0.12 ng for Pd and 0. 1 ng for Au are reported.

Table 14.2 - Measured elemental concentration in neem leaves from different sources and a standard

Element	Units	Reference sample : SRM 1571		Neem Leaf from	
		Measured	Reported	Tirupati	Mumbai
Na	μg/g	88.7 ± 6.8	82.0 ± 6.0	100.4 ± 6.5	541.5 ± 17.7
Mg	%	0.59 ± 0.02	0.62 ± 0.02	0.49 ± 0.03	0.76 ± 0.03
Al	μg/g	330 ± 7.5	310-410	116.2 ± 7.2	309.3 ± 21.3
Cl	μg/g	650 ± 30.0	690	5300 ± 400	8300 ± 500
K	%	1.42 ± 0.09	1.47 ± 0.03	2.84 ± 0.09	1.11 ± 0.06
Ca	%	1.89 ± 0.03	2.09 ± 0.03	3.06 ± 0.034	4.02 ± 0.051
Sc	ng/g	86.5 ± 5.1	90.0	-	-
Ti	μg/g	56.9 ± 4.2	-	-	-
V	μg/g	0.52 ± 0.02	-	1.66 ± 0.06	4.26 ± 0.08
Mn	μg/g	87.0 ± 8.2	91.0 ± 4.0	16.97 ± 1.16	36.5 ± 2.1
Zn	μg/g	29.3 ± 4.3	25.0 ± 0.3	-	-
As	μg/g	8.3 ± 0.6	10.0 ± 0.2	-	-
Br	μg/g	8.5 ± 0.7	9.5 ± 1.1	7.07 ± 0.5	3.86 ± 0.24
Sr	μg/g	34.1 ± 1.5	37.0 ± 1.0	115.0 ± 10.1	138.3 ± 4.4
Sb	μg/g	2.6 ± 0.3	2.9 ± 0.3	-	-
I	μg/g	-	-	3.09 ± 0.6	-
Cs	μg/g	-	-	-	1.89 ± 0.13
Ba	μg/g	-	-	74.98 ± 3.41	-
La	μg/g	1.13 ± 0.07	1.1 ± 0.07	0.33 ± 0.005	-
Sm	ng/g	130.0 ± 10.0	114 ± 20	-	-
Eu	ng/g	20.2 ± 2.3	24 ± 3	-	-

[T. Balaji et al., *J. Radioanal. Nucl. Chem.* **234(3)** (2000) 283.]

Determination of Trace Elements in Leaves by RNAA

In many naturally occurring biological materials and minerals, Na is a major element. In leafy materials, in addition to sodium, Br and K are present as major constituents. In NAA, activation products of these elements make the measurements nearly impossible. In view of this, it is essential to either separate these major elements prior to activation (CNAA) or after the activation (RNAA). If the matrix does not contain fissionable materials, then it would be better if the chemical separations are carried out after the activation. Trace elements are determined in leaf samples and in SRM-1571 by RNAA with enhanced sensitivity. Radiobromine was expelled from the activated samples during its digestion in perchloric acid medium. Radiosodium and radiopotassium were separated from the solution by passing it over Hydrated Automony Pentoxide (HAP) column in 8M HNO_3 for Na removal and 1M HNO_3 for K removal. Effluent was monitored to measure the activities due to trace elements which otherwise could not be measured in the presence of K and Na.

X-ray Fluorescence

High energy photons (X-rays, γ-rays) can cause ejection of inner shell electrons of an atom which is followed by emission of X-rays as outer shell electrons fill the vacancy. X-rays emitted have energies characteristic of the element involved and intensity of X-rays is proportional to the concentration of the element and the strength of the ionising source. In X-ray fluorescence (XRF) analysis, concentration of the element in the analyte is determined by measuring the intensity of the X-rays of that element for a given source strength. The energy and intensity of the characteristic X-rays are measured either in wave length or energy mode : the first mode is called wave length dispersive (WD XRF) mode and the second one as energy dispersive (ED XRF) mode. With the advent of semiconductor detectors and advances made in associated electronics, energy dispersive and wavelength dispersive XRF analyses have become powerful analytical methods for multi element analysis.

X-ray Production

X-rays originate from atomic electron transitions and are, therefore, element specific. In the stable atom, electrons occupy discrete energy levels that are designated, in order of decreasing energy, as K, L_1, L_2, L_3, M_1, … M_5, N_1, ... N_7, and so forth. It is possible to remove an electron from an atom by providing energy greater than the binding energy of electron. The vacancy thus created is filled by an electron from an outer orbit. The resultant loss in potential energy may appear as an X-ray whose energy is equal to the difference in binding energies in two states. For example, if a uranium K electron is removed from the U atom, an electron from L_3 falls into its place and if an X-ray is produced, then its energy will be 98.428 keV (=115.591 - 17.163 keV). This X-ray is designated as $K_{\alpha 1}$. Each X-ray has a specific probability (intensity). The L_3 to K transition is most probable and other intensities are expressed relative to $K_{\alpha 1}$. The energy (E) of the X-ray in keV and its wave length (λ) in angstroms are related as $E = 12.396/\lambda$.

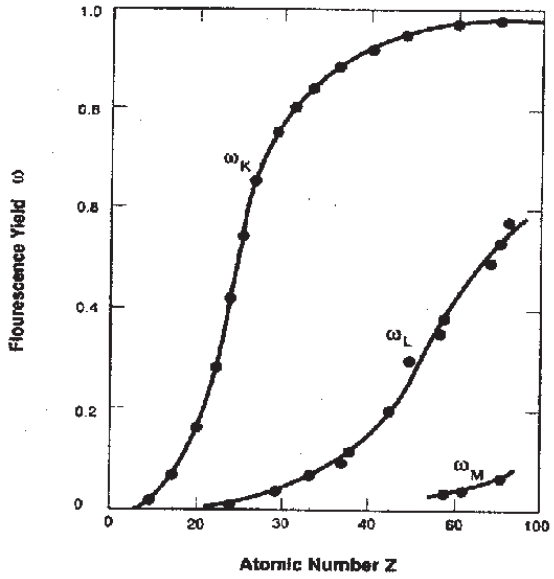

Fig. 14.4 Fluorescence yield as a function of Z [Passive Non-Destructive Assay of Nuclear Materials, Ed. D. Reilly et al., Los Alamos National Lab., USA].

Fluorescence Yield

All ionisations do not result in X-ray emission. The Auger effect is a competing mechanism of atomic deexcitation. If the energy of X-ray is greater than the binding energy of an outer shell electron, then it is possible that the energy is utilised to eject the electron and this electron is known as Auger electron. The ratio of number of emitted X-rays to the total number of ionisations is called fluorescence yield (w_1) and is related to atomic number (Z) as

$$w_1 = \frac{Z^4}{(A_i + Z^4)} \qquad (14.13)$$

where A_i is approximately 10^6 for the K-shell and 10^8 for the L shell. Variation of fluorescence yield as a function of Z is given in Fig. 14.4.

The photon energy must be greater than or equal to the binding energy of the electron to eject that electron due to interaction of photon with matter. The fraction of the photons (F) that interact with the atomic electrons is given by

$$F = 1 - e^{-\mu\rho x} \qquad (14.14)$$

where μ is the mass attenuation coefficient (cm^2/g), ρ is the density of the material (g/cm^3) and x is the thickness of the sample (cm). Variation of mass attenuation coefficient as a function of photon energy is given in Fig. 14.5. The edge corresponds to the energy that is just around the binding energy of the electron that is emitted. Photoelectric effect is the dominant process involved in photon excited X-ray emission interaction.

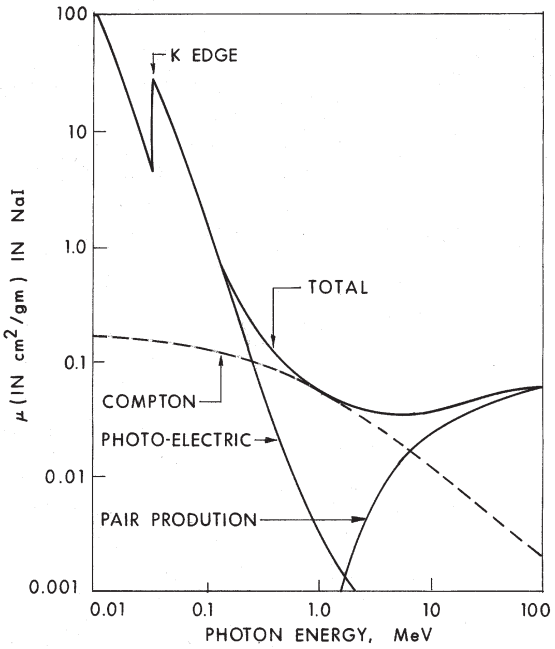

Fig. 14.5 Mass attenuation coefficient as a function of photon energy [G.R. White, Natl. Bur. Stds. (US), Report 1003, 1952].

Types of Sources for XRF Studies

Continuous sources like X-ray generators and discrete γ and X-ray sources like radioisotopes are generally used in XRF measurements. In the X-ray generators, accelerated electron beam strikes a target (anode) material like rhodium, molybdenum and tungsten, and produces X-rays. These X-rays have continuous energy spectrum. This is known as Bremsstrahlung radiation[2]. A Mo X-ray tube with an operating voltage of 25 kV produces a continuous energy radiation from about 3 to nearly 25 keV with varying intensity. In addition K_α and K_β X-rays are also produced. These sources are bulky and need high operating voltage. Small generators with operating voltage of 50 kV and a power output of 50 W are commercially available. Discrete energy sources using radioisotopes are small, stable and simple to operate. This makes XRF an attractive analytical tool. A list of isotopic sources are given in Table 14.3.

Sources that give energy just above or equal to the absorption edge of the element in the analyte is the best choice as the exciting source. When the sample contains many elements, then a single source like X-ray generator or combination of isotope sources are used.

---

[2]When electrons are accelerated in the electric field of a nucleus, emission of radiation with continuous energy takes place and this radiation is known as Bremsstrahlung radiation.

Table 14.3. Radioisotopic sources

Nuclide	Half-life	Decay mode	Type	Energy in keV
^{37}Ar	35.04 d	EC	K X-ray	2.957
^{44}Ti	49 y	EC	K X-ray	4.508
^{55}Fe	2.73 y	EC	K X-ray	5.895
^{57}Co	271.79 d	EC	γ-ray	122, 136
^{109}Cd	462.6 d	EC	Ag K X-ray	22
^{144}Ce	284.893 d	β	K X-ray	36, 134
^{125}I	59.408 d	EC	K X-ray γ	27 35
^{147}Pm	2.6234 y	β	Bremsstrahlung	12 to 45

Instrumentation

In wavelength dispersive method, a crystal spectrometer is used. X-rays emitted by the sample are allowed to impinge on a crystal which diffracts the X-rays according to their wave lengths. These spectrometers offer outstanding energy resolution but are quite expensive and are difficult to use. Instead, an energy dispersive system based on a solid state detector Si(Li), is preferred. The resolution of Si(Li) detectors is good, e.g., 0.15 keV at 5.9 keV of Mn K X-ray. Scintillation detectors are used for X-ray energies above 5 keV. These are not very useful for multielement analysis. Proportional counters using Ar or Xe or methane are used for energy upto 20 keV. However, Si(Li) is most preferred. Elements with atomic number differing by more than 4 units can be simultaneously measured.

Applications of XRF

XRF analysis has been used in analytical chemistry for many years. In most cases, X-ray generator is used rather than radioisotope as an excitation source. Sample preparation is very important in XRF analysis. Sample is homogenised and compressed to form a thin and uniform disc prior to analysis. XRF can yield accurate and precise data with sensitivities in tens of nanogram region. However, one has to account for attenuation correction and interferences. Normally while analysing low Z materials, the sample and detector assembly have to be placed in a vacuum chamber to minimise the attenuation in the path. It is a common practice to analyse a standard along with the sample. Solutions also can be analysed using this technique. Uranium in the range of 0.1 to 200 g/L and Pu upto 50 g/L can be measured reliably.

Many environmental samples like fly ash is made into circular disc samples of size 30 mm dia X 2 mm thick, and are analysed by XRF. Similarly, sediment samples are mixed with

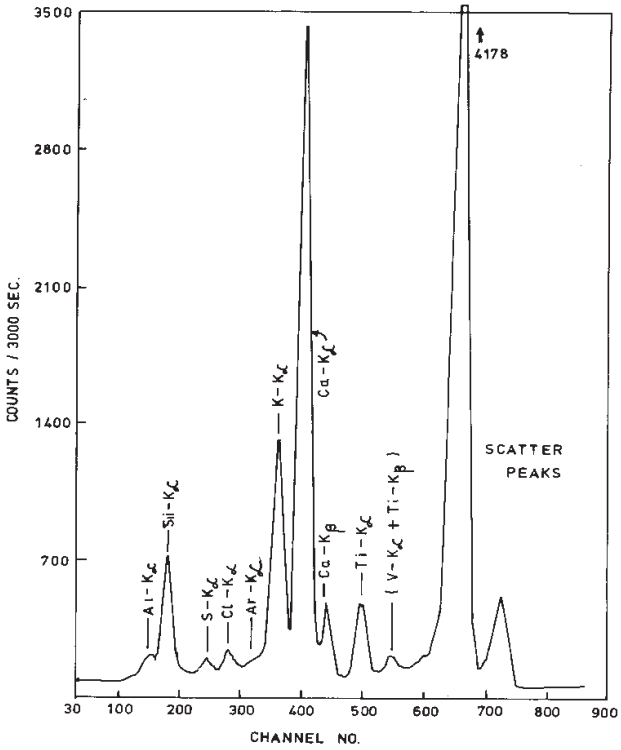

Fig. 14.6 XRF spectrum of an air filter sample using ^{55}Fe excitation source.

a binder like maleic acid and the XRF sample is prepared. In identical conditions, samples from the respective NBS standards are prepared. Measured XRF is compared with the standards after appropriate corrections to arrive at the concentrations of the constituent elements. A typical energy dispersive XRF spectrum of a filter, through which air was sucked, is shown in Fig. 14.6. Radioisotope source ^{55}Fe was used as the excitation source. Comparing with the standard, concentrations of Al, Si, S, Cl, Ar, K, Ca, Ti and V were determined. One of the major limitations is the matrix interference. Trace levels are difficult to measure in presence of major elements without chemical separations.

Ion Beam Analysis Techniques

Elemental analysis is also carried out using ion beams. Radiations produced by ion beam bombardment of the sample are measured and used to arrive at the concentration of the elements present in the sample. These are on-line measurement techniques, i.e., radiation measurement has to be performed while target is being bombarded with the ion beam. Since focused ion-beams are used, micro-analysis can be carried out. Particle induced X-ray/γ-ray emission (PIXE/PIGE), Rutherford Backscattering Spectrometry (RBS) and Nuclear Reaction Analysis (NRA) are important ion beam analysis techniques. In the ion beam analysis techniques light particle ions (p, d and α) of a few MeV/amu, normally produced by

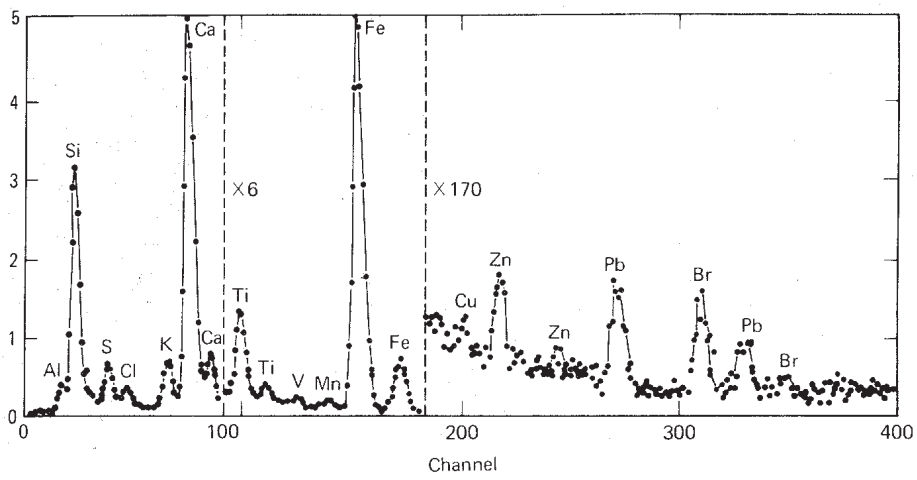

Fig. 14.7 Proton-induced X-ray spectrum of an atmospheric particulate sample. The abscissa scale corresponds to approximately 35 eV per channel. The lead X-rays are L_α and L_β, all others are K X-rays; where there are two K peaks for an element, the left-hand one is the K_α, the right-hand one the K_β peak [J.W. Nelson, "Proton Induced Aerosol Analyses : Methods and Samples" in X-ray Fluorescence Analysis of Environmental Samples (T.D. Dzubay, Ed.), Ann Arbor Science, Ann Arbor, Michigan (1977)].

small accelerators are used. Ion penetration in solid matrices is tens of μm and analytically probed depth can vary from sub-μm to tens of μm. Equipment used in these techniques is generally complex and success depends on good instrumentation. PIXE and RBS techniques are discussed below.

Particle Induced X-ray Emission (PIXE)

A charged particle projectile of a few MeV energy has a high probability to eject an inner shell electron from the orbit of a target atom. The resulting vacancy is rapidly filled by an outer shell electron and a characteristic X-ray of the target atom is emitted. Using energy dispersive X-ray detector, e.g., Si(Li), the intensity of the X-rays are measured, which are used to identify the element and measure its concentration. PIXE is a multielemental, sensitive and quantitative method for analysis of different materials. Due to its capability of probing small dimensions, particulate matter (dia < 20 μm) can be analysed, e.g., air pollution and mining samples. A typical PIXE spectrum of atmospheric particulate sample is given in Fig. 14.7. PIXE is effective for elements with $Z \geq 11$.

Rutherford Backscattering Spectrometry (RBS)

Nuclear backscattering is due to Coulomb repulsion of the incoming charged particle by the nucleus of the target. By measuring the energy of the backscattered projectile, mass of

the target nucleus is analysed. The energy loss suffered by the backscattered projectile varies depending on the depth of the target nucleus, i.e. a projectile scattered by the nucleus from the surface will have more energy compared to that scattered by a nucleus deep in the sample. Thus depth of the scattering nucleus in the sample can be determined from the extent of energy loss suffered by the backscattered projectile as it passes into and out of the sample. Scattering cross-section is proportional to Z^2 of the target. This method, therefore, is more sensitive to high Z elements. RBS is useful for both depth profiling and determining the bulk composition of the material. Protons of a few hundred keV or α-particles of a few MeV are useful projectiles.

Bibliography

1. J. Tölgyessy and M. Kyrs, Radioanalytical Chemistry, Vol. 1 and 2, Ellis Horword Ltd., England (1989).
2. G.D. Chase and J.L. Rabinowitz, Principles of Radioisotope Methodology, Burgess Publishing Co., Minneapolis (1967).
3. H.A.C. McKay, Principles of Radiochemistry, Butterworths (1971).
4. G.F. Knoll, Radiation Detection and Measurement, John Wiley & Sons, New York (1979).
5. Industrial and Environmental Applications of Nuclear Analytical Techniques, IAEA-TECDOC-1121, IAEA, Vienna (1999).
6. G. Friedlander, J.W. Kennedy, E.S. Macias, J.M. Miller, Nuclear and Radiochemistry, 3rd Ed., John Wiley & Sons Inc., New York (1981).
7. S. Glasstone, Sourcebook on Atomic Energy, 3rd Ed., Affiliated East West Press Pvt. Ltd. (1967).
8. J.J.M. De Goej and P. Bode, Proc. of Health Related Environmental Measurements using Nuclear and Isotopic Techniques, Hyderabad, India (1996) pp.3-15.
9. E.P. Bertin, Principles and Practices of X-ray Spectrometric Analysis, 2nd Ed., Plenum Press, New York (1975).
10. M. Pinta, Modern Methods for Trace Element Analysis, Ann Arbor Science, Ann Arbor, Michigan (1978).
11. A.G.C. Nair, A.V.R. Reddy, R.N. Acharya, P.P. Burte and S.B. Manohar, J. Radioanal. Chem., 240 (1999) 877.
12. W.D. Ehmann and D.E. Vance, Radiochemistry and Nuclear Methods of Analysis, John Wiley & Sons (1992).

Chapter 15

Applications of Radioisotopes in Agriculture and Industry

Radioisotopes are used in a variety of studies encompassing basic research and applications. Some of the areas where isotopes used are health care, agriculture, industry and physical sciences. In this Chapter applications in agriculture and industry are described whereas applications in hydrology and waste management are not included.

Agricultural Applications

In agriculture, radioisotopes are used to improve the quality and productivity of agricultural products as well as for optimum utilisation of fertilisers, insecticides and pesticides without harmful effects to plants and mankind. They are also used for insect, pest and disease management and, for preservation of foods and agricultural products. These agricultural applications are based on tracer techniques and utilisation of radiation energy.

Studies on Soil Plant Relationship

The radiolabelled fertilisers have been used to study the uptake, retention and utilisation of fertilisers. Phosphates and sulphates labelled with ^{32}P and ^{35}S, respectively, are used for studying the efficacy, quantity, correct time of application, mode of application, depth of application etc. A known quantity of labelled phosphate is added to the soil in which plants are grown. At certain intervals, the plants are harvested, ashed and phosphorus content is analysed by measuring radioactivity in the ash. This is compared with the initial specific activity of the fertiliser to arrive at the quantity of uptake of phosphate by plants. Such studies helped in arriving at optimal use of fertilisers. The radioisotopes like ^{54}Mn, ^{57}Co, ^{59}Fe and ^{65}Zn are used as radiotracers for the micronutrients. These radiotracers are used to establish the role of nutrients and estimate their optimal amounts. Similar studies can be done using labelled pesticides and insecticides to monitor the fate and persistence of their residues in food items, soil, ground water and environment. These studies have helped to reduce the harmful side effects of the use of pesticides and insecticides.

Genetic Improvement of Crop Plant

In 1930, an American Scientist L.J. Stadler demonstrated the development of genetic variation in plants by exposing seeds to X-rays. The central dogma of the use of *in vitro* techniques is "totipotency" which means that isolated plant cells have the ability to divide and grow into complete plants. The technique of utilising radiation energy for inducing mutations in plant cells is now widely used to obtain a desired variation in the quality of the product. Plants can be genetically altered to produce recombinant proteins such as peptides and vaccines, to improve fruit quality, to increase disease resistance and to improve nutritional quality.

Different types of radiation can be used to induce mutation. However, ^{60}Co is the most commonly used radiation source. Typical radiation dose used for inducing mutation is 10-50 Gy. A proper selection of mutant varieties can lead to improved quality and productivity. Extensive research carried out at BARC has led to the development of a number of high yielding varieties of tur, green gram, black gram, groundnut, jute and rice. About 23 varieties are released in India for cultivation. Most of the ground nut in Maharashtra and urid in India are grown with mutants developed at Bhabha Atomic Research Centre (BARC).

Insect, Pest and Disease Management

Pest control by a technique called "sterile (male) insect technique (SIT)" involves the release of a large number of male flies rendered sterile by γ radiation into the field. They compete with the regular male population in the reproductive process and the eggs produced from their mating are infertile. This process over two or three generations, reduces the overall pest population. This has been effectively utilised in the case of the Mexican fruit fly along the US - Mexican border to prevent flies from entering California.

Food Preservation

Food preservation is needed to minimise wastage as well as increase shelf-life. It has become more relevant with long distances between production and consumption centres. It is estimated that about 25-30% of the world's food production is spoiled or lost due to insects, pests, bacteria, fungi and enzymes that eat, degrade or destroy the crops or stored food. Spoilage can also occur due to chemical and physiological changes in stored food. Also, there is a possibility of food contamination by pathogens and parasites that lead to food borne diseases. This loss of food can be avoided by employing efficient food preservation methods.

Conventional food preservation methods like sun drying, salting and pickling are known since the existence of mankind. Cold storage, canning, pasteurising, vacuum drying and preservation by chemical additives are some of the modern techniques used for food preservation. Each of these techniques has its own merits and demerits. Further development in the area of food preservation is radiation processing of food with ionising radiation like γ-rays from ^{60}Co. When food is exposed to radiation, its interaction with DNA causes the death of microorganisms and insects. Additionally, in food items like onions and potatoes,

the ionising radiation impairs the sprouting processes resulting in longer storage periods. Food preservation by exposing to X-rays was first patented in France in 1930.

Irradiation is a cold process and it does not bring about any change in the freshness and texture of food unlike other methods. It does not leave any harmful residues in food. Irradiation does not produce any significant chemical changes in food. None of the changes known to occur have been found to be harmful. Irradiation does not make the food items radioactive. The nutrition value is least affected by irradiation compared to other methods of food preservation. It is efficient and can be used for pre-packed commodities as well as bulk products. Almost all the packaging materials currently used in food industry, e.g., plastic bags, laminated plastic films with aluminium foil etc. are suitable for irradiation. The process consumes less energy and is eco-friendly. It is however, very important that food included for radiation processing is of good quality and handled and prepared according to codes of good manufacturing practices (GMP) established by national and international standards.

The joint FAO/IAEA/WHO expert committee recommended in 1980 that foods irradiated upto an overall dose of 10 kGy do not pose any toxicological hazard or present any special nutritional or microbiological problems. Over 35 countries have accorded clearance for gamma irradiation of 43 food items. The National Monitoring Agency (NMA) of Government of India has cleared in 1987, radiation processing of onions, spices and frozen sea foods for export.

On the basis of radiation dose deployed, applications are classified into 3 categories. A few examples in each category are listed below.

Low Dose Applications (upto 1 kGy)

1. Inhibition of sprouting in potatoes and onions, garlic and ginger for long term storage, without the use of chemical sprout inhibitors.
2. As an alternative to the use of fumigants for prevention of insect-induced damage to stored grains, pulses, spices, dry fruits, nuts and dry fish and also as a quarantine treatment.
3. Destruction of parasites found in meat and meat products, e.g., entomoeba histolytica and toxoplasma gondi (causative agents of amoebic dysentery and toxoplasmosis respectively) and Trichinae and tape worms.

Medium Dose Applications (1 – 10 kGy)

1. Elimination of spoilage microorganisms present in berry fruits (strawberry), meat, poultry and sea foods to improve shelf-life under refrigeration.
2. Prevention of food poisoning caused by Salmonella, Vibrio and other non-spore forming pathogens present in fresh as well as frozen meat, poultry and sea foods.
3. Shelf-life extension of mushrooms.

4. Hygienisation of whole spices, spice powders and spice mixes by reducing microbial load.

High Dose Applications (10 – 45 kGy)

Destruction of spoilage organisms including bacterial spores to obtain shelf stable sterile products without refrigeration.

Two demonstration plants for Radiation Processing of Spices and onions are in operations in India.

Applications in Industry

The use of radioisotopes in industry ensures good quality products and brings down the cost of manufacture by ways of sensitive non-destructive testing and efficient in-process control. Radioisotopes are also employed in certain manufacturing processes to induce desired chemical reactions, e.g., polymerisation of wood impregnated with monomers. Bactericidal effect of ionising radiation has been employed for sterilisation of medical products and devices. The radioisotope as open sources and in suitable physical and chemical forms are also employed in systems to study their movement, adsorption, retention etc. and monitoring the activity either continuously or after sampling depending on the nature of the study. Thus radioisotopes and radiation have become useful tools and almost every branch of industry uses them.

Industrial applications of radioisotopes and radiation can be broadly classified into three categories, namely, radiation processing, non-destructive testing based on attenuation of radiation and radiotracer applications.

Radiation Processing

High energy ionising radiation has the unique ability to produce very reactive short-lived ionic and free radical species in a variety of substances. These reactive species induce many chemical reactions. This property is beneficially used for various industrial processes. The underlying principles of radiation processing are detailed in Chapter 19.

Radiation Sterilisation of Medical Products

Ionisation radiation has been effectively employed as bactericide for sterilisation of medical products and devices on commercial scale. This technique is mainly a cold process. It is used for disposable medical devices made from heat sensitive plastics. A dose of 25 kGy is given to the sealed packages containing the products to achieve sterilisation. The γ-rays penetrate through these sealed packages and destroy micro-organisms, if present in the product. Major advantages of this process over conventional methods employing steam and chemicals are high inactivation factor, the ability to sterilise the product in its final package, enhancement of shelf-life of the product and no carry over of toxic residues. Some of the products regularly sterilised are syringes, surgical dressing, blades, sutures, absorbent cotton

wool, infusion sets, surgical kits and certain antibiotics and ophthalmic ointments. In India, currently three such plants are in operation in Mumbai, Bangalore and Delhi and offer sterilisation services to industry. The ISOMED plant at BARC completed 25 years of operation in 1999. Nearly 1500 user industries are availing ISOMED services.

Sludge Hygienisation

Sewage sludge is rich in organic matter, nutrients and trace elements and merits recycling for economic considerations. However, the raw sludge contains a very high concentration of pathogens, which are responsible for causing infectious diseases like typhoid, cholera and hepatitis. Hence the sludge needs to be treated before being released for use as manure. The pathogen concentration in sewage sludge is reduced by treatment with about 3-5 kGy of radiation dose. This offers advantages over conventional methods of aerobic and anaerobic digestion, which do not reduce the pathogen concentration to safe levels. Sludge Hygienisation Research Irradiator (SHRI) facility, containing about 150 kCi of ^{60}Co for treatment of sewage has been in operation in Baroda.

Treatment of Flue Gases

Flue gases released from coal or oil fired boilers in power stations and engineering industries contain high concentration of pollutants like sulphur dioxide, oxides of nitrogen and particulate matter. A technique is available using gamma ray irradiation to convert the gaseous pollutants into useful fertiliser constituents like ammonium sulphate and ammonium nitrate. The flue gas from the boiler is passed through a mechanical filter and saturated with water vapour before admission into an irradiation chamber. In the presence of radiation field and ammonia, the oxides are converted to their salts. A radiation dose of around 10-20 kGy is required for this purpose.

Radiation in Manufacturing

Radiation processing technique is used for manufacturing improved quality products like polyethylene foam, cables, treated leather and semi-conductors. Curing of surface coatings and heat shrinkable foams is also brought about by such treatment. The radiation doses required vary widely depending upon a particular treatment. The general advantages are, ease of flexibility in process control, better wear resistance, cost effectiveness and environmental safety. Some important applications are given below.

(i) Radiation is now widely used for vulcanisation of natural rubber latex instead of the conventional method using sulphur, which results in the formation of carcinogen in rubber.

(ii) Radiation cross-linking of polymers imparts dimensional stability to polymers thereby extending the working temperature range.

(iii) When cross-linking is induced in some polymers like polyethylene, it tends to shrink on heating.

(iv) By irradiation with γ-rays or with electron beam (EB), it is possible to impart chain scission in polytetrafluoroethylene (PTFE) which is otherwise extremely resistant to pulverisation. These degraded PTFE products are useful for specialised applications as lubricants.

(v) Value added useful products are prepared by impregnating cheap wood with suitable monomer and subsequent radiation processing.

Radioisotopes in Non-Destructive Testing (NDT)

The difference in the intensity of the radiation after passing through a test material is useful to get information such as thickness, density and defects of the material under study. Based on this principle, the materials are tested non-destructively. Sealed sources of radioisotopes are used for non-destructive testing. The major techniques are radiography, gamma scanning, computer aided tomography and nucleonic gauging system.

Gamma Radiography

The principle in γ-radiography is the same as that of X-ray radiography. When gamma radiations pass through matter, its intensity is reduced and the extent of reduction depends on the density and atomic number of the interposed material. In the case of a metal cast, if there is a crack, then the reduction pattern will be different than in the normal case. Thus γ-radiography is useful for the non-destructive examination of welds and castings and is a well established technique. Highly penetrating gamma rays from radioisotope sources such as ^{60}Co (1173 and 1332 keV) and ^{192}Ir (296, 308, 317 and 468 keV) are used in radiography techniques for examination of a variety of industrial products of greater thickness as in boilers, pressure vessels, ship and aeroplane components. Since gamma ray sources are portable, they are ideal for field works including in construction phases. Gamma radiography cameras containing upto 100 Ci of ^{192}Ir or 20 Ci of ^{60}Co are being used in India in thermal and nuclear power stations, fertiliser and petrochemical plants for checking welds/casts.

Computed Tomography

Computed tomography has been developed for the non-destructive testing of engineering and industrial specimens. This system is useful to obtain cross sectional images of the internal structure of test objects. The computed tomography imaging system consists of a gamma ray source, a collimated detector assembly, a precisely controlled mechanical manipulator and a data acquisition system along with a PC. The method involves collection of transmission data of the penetrating radiation through an object at different planes. Subsequent reconstruction using the two dimensional planar profiles of the effective linear attenuation coefficients at designated points leads to a 3D image. This computer aided tomography is expected to be useful for the non-destructive testing of a number of precision components required for specialised applications such as in space, defence and atomic energy programmes.

Gamma Scanning

The non-performance of an industrial column in the desired way can result in production losses. In conventional tests, it will be essential to shut down the plant before any inspection and trouble-shooting operation can be undertaken, which will result in further production losses. Gamma scanning is used for on-line trouble-shooting of industrial columns without disturbing the on-going production activity.

A collimated source and a detector are positioned in the horizontal plane either across the diameter (in tray type columns) or across the different equal-length chords (in packed bed columns). Both the source and detector are then moved synchronously along the length of the column and radiation intensity is recorded at desired elevations. The analysis of the data with reference to the internal loading and hardware configuration of the column gives information about the column. 'Signature scans' obtained under normal functioning or during pre-commissioning trials are used for comparison and to derive useful information of the internal configuration of the column. Gamma scanning techniques have wide applications in trouble shooting, de-bottlenecking, preventive maintenance and for optimisation of the design of industrial columns. This technology along with specialised services is offered by BARC and Engineers India Ltd. and is now widely availed by the Indian industry.

Nucleonic Gauging

Attenuation of the radiation passing through any material is dependent on the mass interposed. This property can be used to measure and monitor thickness of sheet materials such as films and sheets of metals and plastics during the manufacturing process. A sealed source of suitable radioisotope is placed on one side and the detector on the opposite side. The degree of attenuation of radiation is used for controlling the desired parameters. By a proper selection of the radioisotope and instrumentation, even thin material like papers can be well monitored. The levels of liquids in closed or large tanks can be conveniently measured and controlled using radioisotope gauges kept external to the tanks. Similar concepts are applied in controlling the filling of gases in cylinders and detergent powder in packages.

Radioisotope Smoke Detector

A tiny source of radioisotope (e.g., ^{241}Am) is used in a suitable ionisation chamber in the detector. Interaction of radiation with matter produces ionisation/excitation. The extent of ionisation depends on density and atomic number of the medium. If the density of the medium is increased, ionisation current also increases. e.g., smoke and air. This increase is utilised to trigger an alarm above a set threshold value. Ionisation chamber of smoke detectors is divided into two compartments: one is closed and the other has openings for continuous flow of air. When air containing smoke enters this compartment, the resultant ionisation current is compared with the ionisation emit from the closed compartment. If the difference exceeds the threshold, the alarm is triggered.

Industrial Radiotracer Techniques

The radioisotopes in suitable physical and chemical forms are introduced in systems under study. By monitoring the radioactivity either continuously or after sampling (depending on the nature of study), the movement, adsorption, retention etc. of the tracer, and in turn, of the bulk matter under investigation, can be followed. The radioisotopes preferred for such studies are gamma emitters having half-life compatible with the duration of studies, e.g., ^{24}Na, ^{82}Br. In the case of biochemical and biological applications long lived soft beta emitters ^{3}H and ^{14}C are extensively used. The strength of radioactivity used varies depending on the nature of application. Some typical applications are described below.

Leak Detection

The leakage in long and buried pipelines or those in industrial plants can be monitored with a suitable short-lived isotope like ^{82}Br ($t_{1/2} = 35.3$ h). This involves isolating segments of the pipelines, introducing the tracer and holding the liquid column under pressure, flushing the pipeline and scanning the surface / soil for leaked out radioactivity. Even minute leaks have been detected leading to enormous savings of cost, energy and man-hours. Similarly, leaks in dams and reservoirs can also be detected.

Process Parameters

The mixing time and mean residence time of materials in process containers are of vital importance for production efficiency and product quality in chemical industry. A small quantity of the radiotracer is introduced at the input point and monitored as a function of time to determine the mixing rate and residence time. Such measurements can be made on stream as well as by sampling. These studies are being routinely used in chemical and cement industries.

Material Inventory

The material inventory of mercury in caustic soda plant has been determined using the principle of isotope dilution analysis. The short-lived ^{197}Hg ($t_{1/2} = 64.14$ h) is mixed with the mercury and the measured radioactive concentration after thorough mixing is used for estimating the total quantity of mercury in the cell.

Silt Movement in Harbours

Dredging operations in harbours are carried out periodically for keeping the shipping channels clear. In order to select suitable sites for dumping the dredged silt and for checking the suitability of the alignment of any shipping channel in a new harbour, it is required to study the movement pattern of the silt under water. A radiotracer like ^{46}Sc ($t_{1/2} = 83.79$ d) is mixed with a sample of silt and deposited in the sea bed. The movement of the silt is monitored by measuring radioactivity of ^{46}Sc using underwater radiation detectors. All the major port authorities in India have used such techniques.

Coastal Pollution Studies - Dispersal of Waste

Similarly radiotracers are used to study the pattern of dispersal of waste in water bodies. The timing of and the distance at which discharge is preferred can be reliably established. Such investigations would help ensure safe and acceptable means of waste disposal and improve environmental protection measures. In collaboration with NEERRI, BARC has carried out studies off Mumbai coast.

Bibliography

1. H.J. Arnikar, Isotopes in the Atomic Age, Wiley Eastern Ltd., New Delhi (1989).
2. S. Glasstone, Sourcebook on Atomic Energy, 3rd Ed., Affiliated East West Press Pvt. Ltd. (1967).
3. P.S. Rao, Guest Editor "Nuclear Agriculture and Biotechnology", IANCAS Bulletin, 15(1) (1999).
4. A.K. Sharma, Guest Editor "Preservation of Food by Ionising Radiation", IANCAS Bulletin, 14(1) (1998).
5. G. Harderson, Use of Nuclear Techniques in Soil Plant Relationships, Training Course Series No.2, IAEA, Vienna (1990).
6. IAEA Technical Report Series 336, IAEA, Vienna (1992).
7. D.D. Sood, "Changing Scenarios in Isotope Production and Utilisation", IANCAS Bulletin, 14(1) (1998) vii.
8. Isotopes and Radiation Technology in Industry, Eds. S.M. Rao and K.M. Kulkarni, NAARRI, Mumbai (1994).
9. R.J. Woods and A.K. Pikaev, Applied Radiation Chemistry: Radiation Processing, Wiley Interscience (1994).
10. Applications of Radioisotopes and Radiation in Industrial Development, Eds. D.D. Sood, A.V.R. Reddy, S.R.K. Iyer, S. Gangadharan and Gursharan Singh, NAARRI, Mumbai (1998).

Chapter 16
Applications of Radioisotopes in Healthcare

The applications of radioisotopes in the field of healthcare in general and in medicine in particular have been very extensive. Radioisotope techniques are aiding diagnosis and prognosis in a variety of diseases as well as providing relief by both curative and palliative treatment. The diagnostic techniques are performed *in-vitro* using radioimmunoassay reagents and *in-vivo* using radiopharmaceuticals. The therapeutic procedures could be performed using implanted or externally located sealed sources of radioisotopes or by systemic administration of appropriate radiopharmaceuticals.

Diagnostic Applications

Radioimmunoassay (RIA) and Related Techniques

Radioimmunoassay (RIA) is a versatile radioanalytical technique for the measurement of micromoles to picomoles of substances of clinical interest in biological specimens. Three decades back, Berson and Yalow published their first paper on the measurement of insulin using an antigen-antibody reaction. They called this new assay technique 'Radioimmunoassay' (RIA), as it used a radiolabelled antigen and an antibody for the measurement of the analyte. At about the same time, Ekins developed an assay technique, similar in principle, for the measurement of serum thyroxine, in which he used radiolabelled thyroxine and thyroxine binding globulin (TBG) as binder, instead of a specific antibody because of the high affinity of TBG for thyroxine. He coined a general term for these assays as 'saturation analysis'. The development of an antibody against an antigen is more generalised and it is possible to develop high affinity antiserum for any antigen, irrespective of its nature and concentration in blood. Due to inherent versatility, RIA became a popular technique. Dr. Rosalyn Yalow was awarded the Nobel Prize for medicine in the year 1977. Since its invention, RIA is now used for the measurement of most of the biologically important substances such as hormones, drugs, vitamins and viruses. It has largely contributed to our current knowledge in endocrinology.

Principle of RIA

RIA technique is based on a competitive reaction between the labelled antigen (Ag*) and unlabelled antigen (Ag) (analyte) for the limited (substoichiometric) binding sites on a specific antibody (Ab) (reagent), for the measurement of unknown antigen concentration in a sample.

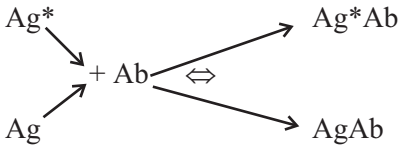

(16.1)

At the end of the reaction, the antibody bound antigen and the free antigen are separated by a suitable chemical method. The bound fraction, containing the labelled and unlabelled antigen, is measured for its radioactivity. A standard curve is constructed (Fig. 16.1) using known concentrations of standards and a limited and fixed amount of labelled antigen and antibody. The amount of radioactivity associated with the bound fraction is inversely related to the concentration of unlabelled antigen. The antigen concentration in the sample is estimated by interpolation in the standard curve.

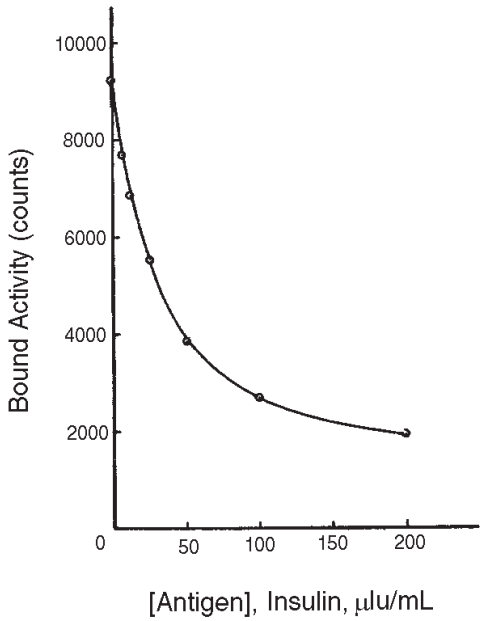

Fig. 16.1 Radioimmunoassay standard curve.

Requirements for setting up RIA

The essential requirements for setting up a radioimmunoassay are (a) Radiolabelled antigen, (b) Specific and high affinity antibody, (c) Standard antigen and (d) Separation system for the separation of free antigen and antibody bound antigen.

(a) Labelled antigen

The radiolabelled antigen is prepared by incorporating an ^{125}I atom into the molecule either directly through a tyrosyl residue available in the antigen or indirectly through a derivative which is attached to the molecule. Iodine-125, a gamma emitting radionuclide with a half life of 59.408 days, is the most convenient radioisotope label due to its low γ-energy (35 keV) and high counting efficiency (~70%), almost 100% isotopic abundance and comparatively long shelf life of the labelled product. The radiolabelled antigen is purified by gel filtration, TLC or HPLC, depending upon the nature of the antigen.

(b) Antiserum (serum containing antibody)

The antibody required for radioimmunoassay is prepared by immunising laboratory animals like guinea pigs, rabbits or goats with the antigen (or a conjugate of the antigen with a carrier protein in case of small antigens) after emulsifying it in a special medium called Freund's adjuvant. The immunised animals show antibody response after 2 to 3 injections which could be given during periodic intervals of 2 to 6 weeks. The immunised animals are bled, the serum separated, checked for its antibody concentration (titre), affinity (avidity) and specificity and stored for use in RIA.

(c) Standard

The standards used in RIA are prepared by diluting the pure hormone obtained from commercial sources with hormone free serum to make the standard as similar as possible to the sample. These standards are then compared with international reference standards distributed by agencies like World Health Organisation (WHO) and National Institute of Health (NIH) to ascertain their potencies.

(d) Separation systems

Various techniques are used for the separation of the antibody bound antigen and free antigen in RIA. These include species specific second antibody, another protein substance called protein A, polyethylene glycol (PEG) etc. for the precipitation of the antibody bound complex or dextran coated charcoal for the separation of the free antigen from the complex (in case of small antigens). A common procedure now in use is the combination technique in which a lower concentration of both the second antibody and PEG are used to achieve an efficient and fast separation. Many of the presently available indigenous kits in India use this separation technique. The first or second antibody immobilised on solid phases (antibody coated polystyrene tubes/beads) are used for efficient, fast separation of antibody bound antigen in solid phase assays. Assays based on the use of antibody coated tubes are the most popular. In the case of coated tubes, upon completion of incubation period, the tubes are

simply inverted and decanted. In another separation system, an alternative solid phase is provided by magnetisable particles attached to the antibody. In this case, assay tubes are placed on a magnetic rack to let form the pellet and be attracted to the magnets, before proceeding to decant.

The reagents required for RIA are formulated in the form of a kit and supplied by manufacturers along with well defined protocols. The development of RIA by itself for any antigen can be a challenging job. The availability and use of kits have popularised this technique and is in routine practice in many pathology laboratories.

Immunoradiometricassay (IRMA)

The radioimmunoassay technique developed by Yalow and Berson and the competitive protein binding assay (CPBA) have been the forerunners for many related techniques that have been developed subsequently. Immunoradiometricassay (IRMA) is one of these techniques.

(a) Principle of Immunoradiometricassay (IRMA)

Sensitivity of an analytical technique would be maximum if all the analyte reacts with the reagent for the formation of the product. In RIA technique, maximum sensitivity derivable from the antigen-antibody reaction is limited due to the competitive nature of the reaction, since only a fraction of the analyte reacts with the antibody. Hence the idea of excess reagent assays using labelled antibody was conceived.

$$Ag + Ab^* \rightarrow Ag.Ab^* \qquad (16.2)$$

The amount of AgAb* formed is directly related to the concentration of the analyte. This type of assays which uses excess concentration of the reagent, i.e. the labelled antibody, is called immunoradiometric assay (IRMA). This technique could not be initially put to practical use since the difference in properties between antigen antibody complex [Ag. Ab] and Ab was not adequate for effective separation. With the advent of hybridoma technique and concept of monoclonal antibodies, the IRMA concept has been translated into a reality. In IRMA, free labelled antibody is separated based on its reaction with an immunosorbant made of an antigen coupled to a solid phase. The concept of 'sandwich' or 'two site' IRMA requires the use of two antibodies for the same analyte antigen and relies on the preliminary immuno-extraction of the analyte by solid phase antibody (capture antibody) followed by reaction with the labelled antibody (detector antibody).

$$\bullet\text{-Ab1} + Ag + Ab2^* \rightarrow \bullet\text{-Ab1-Ag-Ab2}^* + Ab2^* \qquad (16.3)$$
(excess)

A typical standard curve of an IRMA is shown in Fig. 16.2. Two site immunoradiometric assays developed using labelled monoclonal antibodies directed to different antigenic determinants of the same antigen are now widely used, due to their high sensitivity and specificity. An example is the development of highly sensitive assays for thyroid stimulating

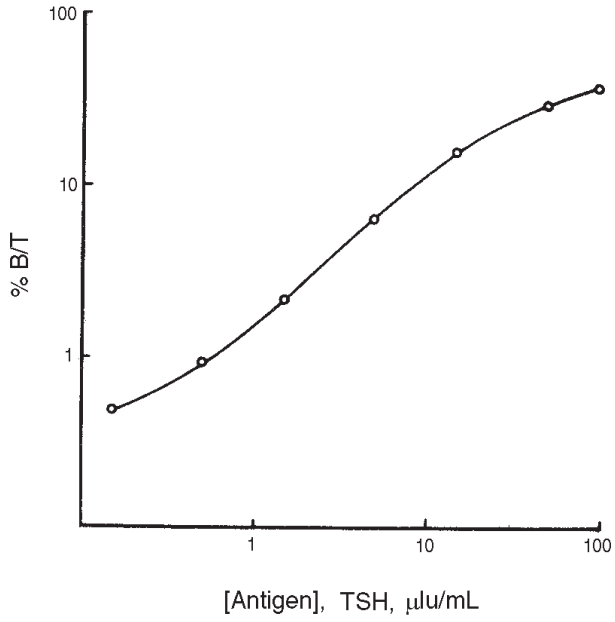

Fig. 16.2 IRMA Standard curve.

hormone (TSH), which can distinguish between hyper and normal thyroid patient samples, indistinguishable by conventional RIA.

Non-Isotopic Immunoassays

Non-isotopic immunoassays with antigen or antibody labelled with an enzyme, a chemiluminescent molecule or a fluorophore are the competing techniques to the radiometric immunoassay techniques. In these assays, instead of radioactivity, enzyme activity or fluorescent or chemiluminescent intensity of the bound antigen is measured. These assays are named after the label used and the labelled moiety. Thus, for example, in enzyme immunoassay, an enzyme is used for labelling the antigen and in an immunofluorimetric assay, a fluorophore is used to label the antibody. At present the most widely used non-isotopic assays are enzyme immunoassys (ELISA) chemiluminescence assays and fluoroimmunoassays.

Applications

The technique of RIA/IRMA is now a standard practice in clinical medicine. The instrumentation is relatively simple with comparatively small investment. Ready to use RIA/ IRMA kits are now available for almost all hormones, drugs and many other important antigens.

Assays of thyroid related hormones (T_3, T_4 and TSH) and hormones of reproductive system (both protein hormones and steroid hormones) have been the ones most frequently carried out. Differential diagnosis of hypothyroidism, diagnosis of neonatal hypothyroidism

Table 16.1 - Applications of radioimmunoassay of important substances

Analyte(s)	Application(s)
Thyroid hormones (T_3 & T_4) and Thyrotropin (TSH)	Diagnosis of thyroid diseases. Screening for neonatal hypothyroidism, differential diagnosis of primary and secondary hypothyroidism
Human Chorionic Gonodotropin (HCG)	Early detection of pregnancy Diagnosis of ectopic pregnancy Monitoring of chemotherapy of choriocarcinoma
Follicle stimulating hormone (FSH) and Luteinizing hormone (LH)	Diagnosis of infertility and aid in in-vitro fertilisation
Prolactin	Diagnosis of pituitary adenomas and in galactoria.
Testosterone	Male infertility investigation
Growth hormone (HGH)	Diagnosis of acromegaly and dwarfism
Angiotensin-1	Renovascular hypertension
Tumour markers (Alpha fetoprotein, Prostate specific antigen, carcinoembrionic antigen)	Screening of high risk population for cancer. Monitoring therapy and staging of patients.
Drugs	Determination of therapeutic window range. Drug analysis and estimation. Evaluation of new drug delivery system and formulations. Bioavailability study and pharmaco- kinetics of drugs.
Bacterial and viral antigens, e.g., Hepatitis B surface antigen (HBs Ag)	Screening high risk populations. Detection of infectious diseases Diagnosis of serum hepatitis. Differential diagnosis
Toxins	Detection of toxins in milk and meat
Pesticides and herbicides	Batch analysis and detection of pesticides and herbicides in the atmosphere, water and vegetation.

by mass screening of new borns, early diagnosis of hyperthyroidism are feasible by the assay of T_3, T_4 and TSH. Many problems of infertility have been successfully managed by the assay of the protein hormones – luteinizing hormone (hLH), follicle stimulating hormone (hFSH) and the steroid hormones, testosterone, estradiol etc. Assays for tumour markers such as, thyroglobulin (Tg), prostate specific antigen (PSA), alpha-fetoprotein (AFP) and carcinoembryonic antigen (CEA) are used in the prognosis/diagnosis of cancer and

screening of patients. The efficacy of treatment while employing toxic/ dose dependent drugs such as digoxin for heart ailments, phenytoin for epilepsy and methotrexate for cancer has been monitored by RIA. In the recent past, radiometric techniques have also been reported for non-clinical applications, such as aflatoxin B, in food industry etc.

Apart from improving the diagnostic accuracy and thereby ensuring better patient care, RIA has served as a valuable research tool. It has contributed to enhancing medical knowledge through continuing research in the fields of endocrinology, oncology, monitoring the drug therapy etc. (Table 16.1). Understanding of different disease processes/ physiological functions have been accomplished by the knowledge gained.

Radiopharmaceuticals

A radiopharmaceutical product can be described as a special radiochemical formulation, of adequate purity and pharmaceutical safety, suitable for oral or intravenous administration to humans for performing a diagnostic test or for treatment. This branch of medicine is called 'nuclear medicine'. Radiopharmaceuticals are 'open source' radioisotope products in the form of solutions, capsules and injections. Sealed sources of ^{60}Co and ^{137}Cs used for teletherapy and brachytherapy for the treatment of cancer, another major area of the use of radioisotopes in medicine, are not traditionally included under radiopharmaceuticals. The diagnostic techniques with radiopharmaceuticals comprise mainly scintigraphy of organs using static, sequential and dynamic imaging procedures. Therapeutic radiopharmaceuticals are employed to achieve therapeutic effect by localisation in the target tissue.

Radioisotopes Used in Radiopharmaceuticals

Diagnostic radiopharmaceuticals employ radionuclides emitting photons, preferably of 100-200 keV energy and minimal or no high LET particulate radiations. Positron emitters from a separate class of radioisotopes used in positron emission tomography. ^{51}Cr, $^{57/58}$Co, $^{52/59}$Fe, **^{67}Ga**, ^{81m}Kr, ^{82}Rb, **^{99m}Tc**, **^{111}In**, **$^{123/125/131}$I**, ^{133}Xe, ^{169}Yb, $^{195m/198}$Au, **^{201}Tl** etc. are some commonly used diagnostic radionuclides. The radioisotopes used in therapy are mostly β-emitters such as **^{32}P**, **^{89}Sr**, **^{90}Y**, **^{131}I**, **^{153}Sm**, **^{166}Ho**, **$^{186/188}$Re**, **^{177}Lu** and ^{198}Au. The important isotopes are shown in bold letters. Table 16.2 shows the details of the nuclear reactions, the commonly used targets (natural/ enriched) etc. for some diagnostic radionuclides.

Classification of Products

The radiopharmaceuticals can be classified into various types depending on the nature of formulation.

Simple Radiochemicals

The application of radioisotopes in medicine started with the use of a few primary isotope preparations as radiopharmaceuticals in the nineteen fifties. These include ^{131}I as sodium iodide and ^{51}Cr as sodium chromate. Of these preparations, ^{131}I sodium iodide is used

Table 16.2 - Important radionuclides for diagnostic radiopharmaceuticals

Radionuclide	$t_{1/2}$, Decay mode	Main Eγ keV (%)	Production route
I. Gamma Emitters			
(a) 'Versatile' Tracers			
^{99m}Tc	6.01 h, IT	140.5 (89)	^{99}Mo-^{99m}Tc Gen.
^{111}In	2.8047 d , EC	171 (90) 245 (94)	Cd(p,xn) ^{109}Ag(α,2n)
^{123}I	13.27 h, EC	159 (83)	^{124}Xe(p,2n) ^{123}Cs → ^{123}Xe →; ^{124}Te(p,2n)
(b) Tracers of 'Specific' Utility			
^{201}Tl	72.912 h, EC	69-80 (95) Hg X-rays 135 + 167 (11)	^{203}Tl(p,3n) ^{201}Pb →;
^{67}Ga	3.2612 d, EC	93 (37) 185 (20)	Zn(p,xn); ^{65}Cu (α,2n)
^{131}I	8.0207 d, β^-	364 (81) 637 (7)	^{130}Te(n,γ)^{131}Te → ^{235}U(n,f)^{131}I

II. β^+ emitters for PET

Radionuclide	$t_{1/2}$ (min)	E_{β^+} (MeV)	511 keV rays %	Method of production
^{11}C	20.39	0.96	200	^{14}N (p,α)
^{13}N	9.965	1.19	200	^{16}O (p,α)
^{15}O	2.037	1.72	200	^{14}N (d,n) ^{15}N (p,n); ^{16}O (p,pn)
^{18}F	109.77	0.635	194	^{18}O (p,n) ^{20}Ne (d,α)

IT : Internal Transition, EC : Electron Capture, β^- **:** β^- decay

even now for the diagnosis of some thyroid disorders and more importantly for the therapy of thyrotoxicosis and thyroid cancer. Other important products of this type include $^{89}SrCl_2$ and $^{201}TlCl$.

Labelled Compounds

Labelled compounds are specific chemicals or biochemicals labelled with ^{131}I, or any other convenient radioisotope, having inherent property to accumulate in specific organs upon systemic administration. Iodine labelled radiopharmaceuticals include $^{123/131}I$ labelled hippuran for kidney function studies and $^{123/131}I$ labelled metaiodobenzylguanidine (MIBG) for neuro-endocrine tumours (Table 16.3). Labelled compounds can be either 'true' (or genuine) labels as in $^{57/58}Co$ labelled cyanocobalamin (Vitamin B_{12}) or 'foreign' labels as in ^{131}I - human serum albumin (HSA). The major products currently in this group include (a) ^{123}I compounds such as p-iodo-N-isopropyl- amphetamine (IMP, IAMP), p-iodo-phenyl-3-methyl-pentadecanoic acid (BMIPP), (b) ^{11}C compounds such as ^{11}C-acetate, ^{11}C-palmitate, ^{11}C-N-methyl spiperone and (c) ^{18}F compounds, 2-fluoro-2-deoxy glucose (FDG) and L-6-^{18}F-fluoro dihydroxyphenyl alanine (F-DOPA).

Table 16.3 - ^{131}I radiopharmaceuticals

^{131}I-Sodium iodide	Thyroid uptake and scan; imaging metastatic thyroid cancer. Treatment of Thyrotoxicosis and metastatic thyroid cancer.
^{131}I-MIBG	Neuro-endocrine tumour imaging and therapy.
^{131}I-Hippuran	Kidney function studies by probe renography.

Coordinate Complexes of Radiometals

This is the most widely used class of radiopharmaceuticals today. Most of the ^{99m}Tc, ^{111}In and $^{186/188}Re$ labelled compounds fall in this category. Almost all the radiopharmaceuticals made from metallic radionuclides are used in the form of their coordinate complexes with chelating agents, a suitable oxidation state of the metal being stabilised by appropriate ligands.

Particulate Formulations

Colloids and macro-aggregates of radiometals with substrate, e.g., ^{198}Au - Gold colloid, ^{32}P - chromic phosphate, ^{99m}Tc labelled macro-aggregated albumin, ^{99m}Tc labelled radio-colloids etc. belong to this category of radiopharmaceuticals. Recent additions are hydroxy apatite particles complexed with ^{166}Ho and ^{153}Sm, and colloidal suspensions of silicates/phosphates of ^{90}Y, ^{186}Re, ^{153}Sm and ^{166}Ho.

Radiolabelled Cells, Proteins and Peptides

^{99m}Tc labelled erythrocytes (red blood cells, RBC) and $^{99m}Tc/^{111}In$ labelled leucocytes (white blood cells, WBC) are well known products. The preparation of the latter requires the

use of lipophilic precursor radiolabel, ^{99m}Tc-d,l-HMPAO and ^{111}In-oxine, respectively. Further, handling of blood and separation of cells are involved. On the other hand, ^{99m}Tc-RBC is formed by pre-tinning of RBC by first injecting using a stannous salt. Pertechnetate injected subsequently leads to *in situ* formation of ^{99m}Tc-RBC for use as blood pool marker.

Monoclonal antibodies (MAb) raised against antigens associated with a cancerous tumour are radiolabelled with *I / radiometal *M (e.g., ^{99m}Tc, ^{111}In for diagnostic use; $^{186/188}$Re, ^{90}Y for therapy) for use as radiopharmaceuticals. MAb which is an immunoglobulin G (IgG) molecule of 150,000 dalton molecular weight is also pre-treated to yield fragments called Fab and $F(ab)_2$ of lower molecular weights (50,000 and 100,000 daltons) for preferential use as carrier molecules, due to relatively faster pharmaco-kinetics in vivo. The attachment of radiometal is done using a bi-functional chelating agent (BCA) containing a chelator group to hold *M and a functional group to covalently bind the MAb or its fragments. 'Direct' labelling of MAb/fragment with ^{99m}Tc is also possible using mild reduction of disulphide bridges of IgG molecule to liberate free thiol groups. Complexation with technetium proceeds via coordination of Tc to S atoms of thiol groups. Recent advances have shown the potential of smaller peptides as carrier molecules to image/treat lesions. ^{99m}Tc, ^{111}In, $^{186/188}$Re and ^{90}Y are the radiolabels in this case too. The sequence of bioactive peptide - spacer molecule - chelating peptide is the preferred method for radiolabelling in the case of peptides.

Preparation of Radiopharmaceuticals

The preparation of radiopharmaceuticals involves application of many chemical principles and techniques. Apart from their being radioactive materials, the chemical quantities of radioisotopes are often very low. Hence, special arrangements for remotely carrying out all the radiochemical steps of preparation, purification, sterilisation and aseptic dispensing are required. Adequate attention to details of both radiation safety and pharmaceutical safety angles is warranted. Codes of Good Manufacturing Practices applicable for conventional pharmaceuticals are equally applicable to radiopharmaceuticals, with necessary revisions incorporated in some cases due to the perishable nature and short shelf-life of these products.

Isotopic Exchange

An inactive atom present in the molecule is exchanged with a radioactive atom. This is done either by refluxing inactive compounds with the radioisotopes under appropriate conditions or by using chemicals which promotes exchange such as an oxidising agent and catalyst. Examples of radiopharmaceuticals prepared by this method include $^{123/131}$I-Hippuran and $^{123/131}$I-MIBG.

Chemical Synthesis

Radioactive atoms are incorporated in one of the synthesis steps, e.g., synthesis of chlormerodrin- $^{197/203}$Hg; ^{11}C-methionine and ^{18}F-fluorodeoxyglucose.

Bio-Synthesis

In biosynthesis, suitable microorganism is allowed to grow in a nutrient medium containing the radioactive isotope. During its growth, the product of interest is prepared (biosynthesis) by the organism. The product formed will then contain radioisotope as a label, e.g., $^{57/58}$Co-Vitamin-B_{12} using *streptomyces olivaceous*.

Complexation

The metallic ion of the desired radioisotope is complexed with the ligand at a suitable pH and in the presence of reducing agents, if necessary, to bring the metal to a reactive lower oxidation state e.g. ^{99m}Tc / ^{111}In - DTPA (diethylene triamine penta acetic acid), ^{99mT}c-DMSA (dimercaptosuccinate), ^{186}Re/^{153}Sm - alkyl phosphonate etc.

Processing and Purification

In many cases, analytical techniques such as solvent extraction, ion exchange and column/ gel permeation chromatography are used for the purification of the radiopharmaceuticals.

In the case of short-lived positron emitters, using suitable pneumatic transfers, the activation products are delivered from the cyclotron to a reaction box in a shielded enclosure. Automated radiochemical processing units are available for established products e.g. ^{18}FDG and water-^{15}O. Automated unit to provide a suitable precursor molecule like $^{11}CH_3I$, $^{11}CH_3MgX$ for the research group are also available. The end product formulated is brought into a clean air containment box, wherein terminal sterilisation (by autoclaving or membrane filtration) and dispensing are carried out.

Hot atom chemistry (recoil labelling technique) is used to make suitable end product or precursor molecules in the gas phase itself in the targetry system doped with the required traces of additive chemical(s), e.g., ^{11}C as CO_2. Using self-shielded gas processing modules, $^{11}CO_2$ can be converted to ^{11}CO, H^{11}CN for direct use or further chemical synthesis.

Quality Control (QC) Aspects

The radiopharmaceuticals prepared are controlled for chemical, radiochemical, radionuclidic and pharmaceutical purity. A typical QC chart is given in Table 16.4.

Unlike conventional pharmaceutical products, radiopharmaceuticals have much shorter shelf-life. The time available to carry out QC tests is much restricted. Tests for pharmaceutical safety in the case of injectables, for certifying for sterility and apyrogenicity require much longer duration in comparison to the half-life of the radionuclide in the product.

Quality Control of accelerator and generator based products is challenging due to short half-life of radionuclides employed. Full fledged quality control is impractical and only important tests are carried out prior to use of the product. However, often tests for sterility and a pyrogenicity are performed post-facto and recorded. Well established and

Table 16.4 - Radiopharmaceutical Quality Control

Physico-chemical control	Radiochemical control	Biological control
1. Physical inspection	1. Radioactive concentration	1. Sterility (for injectables)
2. pH	2. Radionuclidic purity	2. Apyrogenicity (for injectables)
3. Chemical purity	3. Radiochemical purity	3. Organ distribution
4. Particle size (where applicable)		

documented record of previous manufacturing experience provides the basis for release of such products for medical use. This is pertinent with respect to tests for pharmaceutical safety, as most of the products are meant for parenteral administration. For example, no major biological tests would be practicable on most of the final products before actual use for Positron Emission Tomography (PET) applications. Periodic system control checks, exclusive QC test runs, and compliance with Standard Operating Procedure (SOP) / Good Manufacturing Practice (GMP) codes would alone provide the necessary Quality Assurance for the intended medical applications in patients.

Tracer Requirements

The prime requirement of a radiochemical formulation to be accepted as a radiopharmaceutical is its satisfactory distribution in an organ or its ability to trace a particular metabolic or excretory pathway and acceptable excretion features. Apart from this, the product should be suitable for administration to humans, that is, pharmaceutical safety, free from toxic or other reactions in the patients. A variety of mechanisms are exploited for achieving the desired organ specificity. These include active transport, phagocytosis, cell sequestration, capillary blockage and antigen-antibody reaction, amongst others. The general factors influencing the bio-localisation are: binding to serum proteins, blood flow to organs, nature of the tracer in terms of molecular size, charge and lipid solubility.

Type of Investigations and Instruments

The type of investigations using radiopharmaceuticals can be as simple as administering orally 10-50 μCi of ^{131}I as NaI in a capsule and monitoring the uptake in thyroid as a function of time. A suitable probe of NaI(Tl) detector is used for monitoring the activity in the thyroid. One could also carry out a simple procedure like isotope dilution analysis for determining the blood volume (see Chapter 14).

The mapping of the actual distribution of radioactivity in the organ known as 'scintigraphy' was initially done using rectilinear scanners. The moving detector in this case records the activity at each point of the organ, and line by line basis. This is a slow process and not compatible with dynamic physiological functions. There are many situations in which the dynamic changes taking place in the organ are of prime interest apart from a need to probe the actual pathway following administration of the product. 'Gamma camera', which is the most widely used device, fulfils the rapid imaging requirements. It consists of a relatively large but thin crystal of NaI(Tl), 400-550 mm in diameter and 6-12 mm thickness, coupled to an array of photomultiplier tubes. Serial images (time resolved, temporal resolution) and data processing are achieved using a computer. It is also useful to obtain images as tomographic slices for improved vision and for better quantification with SPECT (Single Photon Emission Computed Tomography).

The PET machine uses the coincidence detection technique. It consists of many detector rings, each containing arrays of bismuth germinate (BGO) scintillation crystals and a computer system for reconstruction of image and data processing. Lutetium silicate (LSO) crystal detectors (in lieu of BGO) for PET offer features superior to BGO in terms of sensitivity. The standard dual head SPECT gamma camera; but with thicken (20-25 m) NaI(Tl) crystals, has been advocated for imaging with PET radiopharmaceuticals using coincidence data acquiring software. Although the dual head camera will have inferior resolution compared to PET, clinically useful images/ information are still obtained.

Radioisotope Generators for Short-lived Isotopes

^{99}Mo - ^{99m}Tc Generator

One of the major milestones in the radiopharmaceuticals chemistry was the development of the ^{99m}Tc generator at the Brookhaven National Laboratory, USA in the late fifties. In the ^{99m}Tc generator, parent ^{99}Mo is adsorbed on a small acidic alumina column. Due to the difference in the chemistry of Tc and Mo, the daughter product, ^{99m}Tc is selectively eluted as TcO_4^- with normal saline at periodic intervals. The useful life of this generator is about 2 weeks. The generator needs high specific activity ^{99}Mo, which is obtained from fission of ^{235}U or by the irradiation of enriched ^{98}Mo target in a high flux reactor.

In the case of low specific activity ^{99}Mo produced by irradiation of natural Mo targets in the medium flux reactors, the generator is based on solvent extraction. Technetium as sodium pertechnetate is extracted into methylethylketone (MEK) from an alkaline molybdate solution. MEK is then evaporated and TcO_4^- left behind is reconstituted in normal saline solution and sterilised for use on humans. Gel generator is another system that retains the ease and safety of column operation, but without recourse to expensive fission produced ^{99}Mo. ^{99}Mo of medium specific activity is converted to an insoluble column matrix of zirconium molybdate (ZrMo) gel. ^{99m}Tc is eluted in normal saline or even with water from the ZrMo gel column functioning as a cation exchanger. Fig. 16.3 shows a photograph of ^{99m}Tc generator.

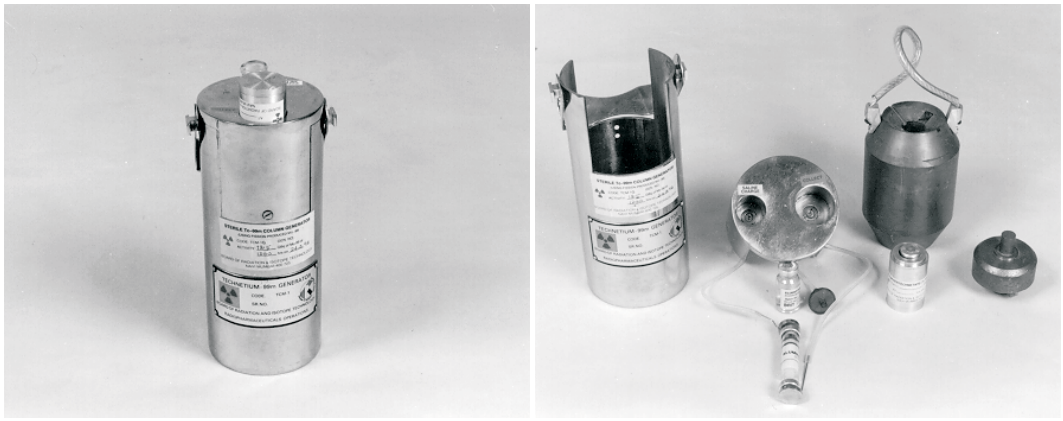

Fig. 16.3 Alumina column chromatography generator for ^{99m}Tc and components.

Advantages of ^{99m}Tc

^{99m}Tc has many favourable properties required for diagnostic use in nuclear medicine. These are:

(a) 140 keV gamma energy of ^{99m}Tc is ideally suited for efficient detection and giving high quality pictures with a gamma camera. The distortion due to attenuation by the body tissues is low.

(b) The decay of ^{99m}Tc is associated with only a small component of particulate emission (internal conversion electrons) and hence upto 30-40 mCi of ^{99m}Tc radiopharmaceuticals can be injected safely into patients. Such a large dose helps in getting better quality images and information of greater reliability.

(c) The 6.01 h half-life of ^{99m}Tc is well suited for most of the nuclear medicine studies.

(d) The multiple oxidation states of technetium allow the chemical formulation of a variety of coordinate complexes.

(e) ^{99m}Tc can be conveniently obtained from a generator system.

(f) The parent ^{99}Mo is available at low cost and hence it is cost effective.

^{99m}Tc is hence the 'work horse' of nuclear medicine and over 70% of all nuclear medicine studies carried out the world over use this single isotope. The sodium pertechnetate ($Na^{99m}TcO_4$) obtained from the generator is used for the preparation of a large number of radiopharmaceuticals by simply mixing with the 'cold kits'. The cold kit contains the ligands needed for chelation along with a reducing agent, buffer and preservatives. On addition of TcO_4^- to the cold kits, pertechnetate is reduced to the appropriate valence state and incorporated into the chelate to form the radiopharmaceutical. The concentration of technetium in these radiopharmaceuticals is of the order of 10^{-7} M only. Presently ^{99m}Tc radiopharmaceuticals are available for most organs and clinical conditions (Table 16.5).

Table 16.5 - Technetium-99m radiopharmaceuticals

Liver scanning	Tc - Sulphur Colloid, Tc -Tin Colloid, Tc-Phytate
Kidney function studies	Tc-Glucoheptonate, Tc-DTPA, Tc-Dimercaptosuccinate Tc-Mercaptoacetyl triglycine, Tc-Ethylene Dicysteine
Bone scanning	Tc-Methylene diphosphonate (MDP)
Hepatobiliary function studies	Tc-Mebrofenin, Tc-Disofenin [iminodiacetic acid (IDA) derivatives]
Lung Scanning	Tc-HSA Microspheres / Macroaggregates, Tc-Aerosols
Cardiac studies	Tc-Red blood cells; Tc-Pyrophosphate; Tc-glucarate, Tc-Sestamibi, Tc-Tetrofosmin
Brain blood flow	Tc-d,l-HMPAO, Tc-L,L-ECD
Infection / Inflammation Imaging	Tc-Leuocytes; Tc-HIgG; Tc-antigranulocyte antibodies; Tc-ciprofloxacin

Cyclotron Based Products

The accelerator based products are classified as (i) gamma emitters for use with planar gamma camera and single photon emission computed tomograph (SPECT), (ii) positron emitters for use with PET and (iii) therapeutic products. First group comprises ^{67}Ga, ^{111}In and ^{201}Tl compounds, as also compounds of ^{123}I ($t_{1/2}$ 13.27 h). ^{11}C, ^{13}N, ^{15}O and ^{18}F compounds belong to PET group of products and require an on-site cyclotron (except ^{18}F). Radiolabelled compounds containing ^{47}Sc, ^{67}Cu, ^{124}I and ^{211}At could be cited under therapeutic products.

^{111}In is a favoured tracer for imaging. ^{111}In labelled peptide called octreotide is used for imaging tumours of neuro-endocrine origin. ^{123}I products show a versatile range of applications, where ^{99m}Tc compounds are not yet available, or not possible to be developed. For example, ^{123}I labelled beta methyl fatty acid analogues (BMIPP) for myocardial metabolic imaging and ^{123}I labelled receptor binding ligands for receptor imaging.

Diagnostic Techniques and Applications

Applications of radiopharmaceuticals cover a vast area (Table 16.6) and some important examples are outlined below.

Table 16.6 - Diagnostic Applications of Radiopharmaceuticals

Brain	Blood Flow (perfusion) imaging: ^{123}I-N-isopropyl iodoamphetamine, ^{18}FDG, ^{99m}Tc-d-l-HMPAO, ^{99m}Tc-ECD Tumours: ^{201}TlCl, ^{99m}Tc-d-l-HMPAO, ^{99m}Tc-GHA, ^{18}FDG Neuro-receptors: ^{18}F-DOPA, ^{13}C-N-Methyl spiperone, ^{11}C-Carfentanil, ^{18}F-fluoro 2-Ty
Thyroid	NaI – $^{131/123}$I ; $^{99m}TcO_4^-$
Lungs	Ventilation : ^{99m}Tc-aerosols, ^{133}Xe; ^{81m}Kr Perfusion : ^{99m}Tc-HSA microspheres / macroaggregates
Heart	Myocardial perfusion : ^{201}TlCl, ^{99m}Tc-Sestamibi, ^{99m}Tc-Tetrofosmin. Metabolism : ^{18}FDG, ^{123}I-FA analogs (BMIPP) Infarcts : ^{99m}Tc-PYP; ^{99m}Tc-glucarate Receptors : ^{123}I-MIBG Blood Pool : ^{99m}Tc-RBC; ^{99m}Tc-HSA
Bone	^{99m}Tc-phosphonate (Tc-MDP)
Liver and Spleen	^{99m}Tc-S colloid; ^{99m}Tc-phytate;
HB System	^{99m}Tc-IDA derivatives
Kidneys	Imaging : ^{99m}Tc-DMSA, ^{99m}Tc-GHA Renography : ^{99m}Tc-DTPA, ^{99m}Tc-MAG_3, ^{99m}Tc-EC
Infection / Inflammation	(i) Infection : ^{111}In / ^{99m}Tc-Leucocytes; ^{99m}Tc-Ciprofloxacin (ii) Inflammation : ^{99m}Tc/ ^{111}In – HIgG, ^{67}Ga-citrate
Tumours	$^{123/131}$I-MIBG, ^{111}In-Octreotide, ^{18}F-FDG, ^{11}C-Methionine, ^{111}In/^{99m}Tc/^{123}I-MoAb, ^{67}Ga-citrate

Organ scintigraphy provides valuable information on the size, shape and location of organs and lesions (Fig. 16.4). In most of the cases the normally functioning tissues take up the tracer and the defective non-functioning areas are seen as 'cold spots'. Examples of this type are thyroid imaging with radioiodine, liver imaging with radiocolloids and imaging of the blood flow to myocardium and brain. In some cases, the tracer is taken up only by the defective tissues but not by the normal ones. The abnormal areas are hence detected as 'hot spots'. Examples of this type are imaging of metastatic sites of thyroid cancer with radioiodine and of infection with ^{67}Ga-citrate/^{111}In-WBC/^{99m}Tc-HIG.

Dynamic imaging procedures are required for the evaluation of renal and cardiac function, wherein time activity curves (e.g., renography) over the region of interest are generated by serially imaging the organ of interest. Quantitative parameters of the organ function, e.g., left ventricular ejection fraction (LVEF) are then calculated from such curves providing vital data to the clinician for diagnosis/prognosis. At times, the data are augmented

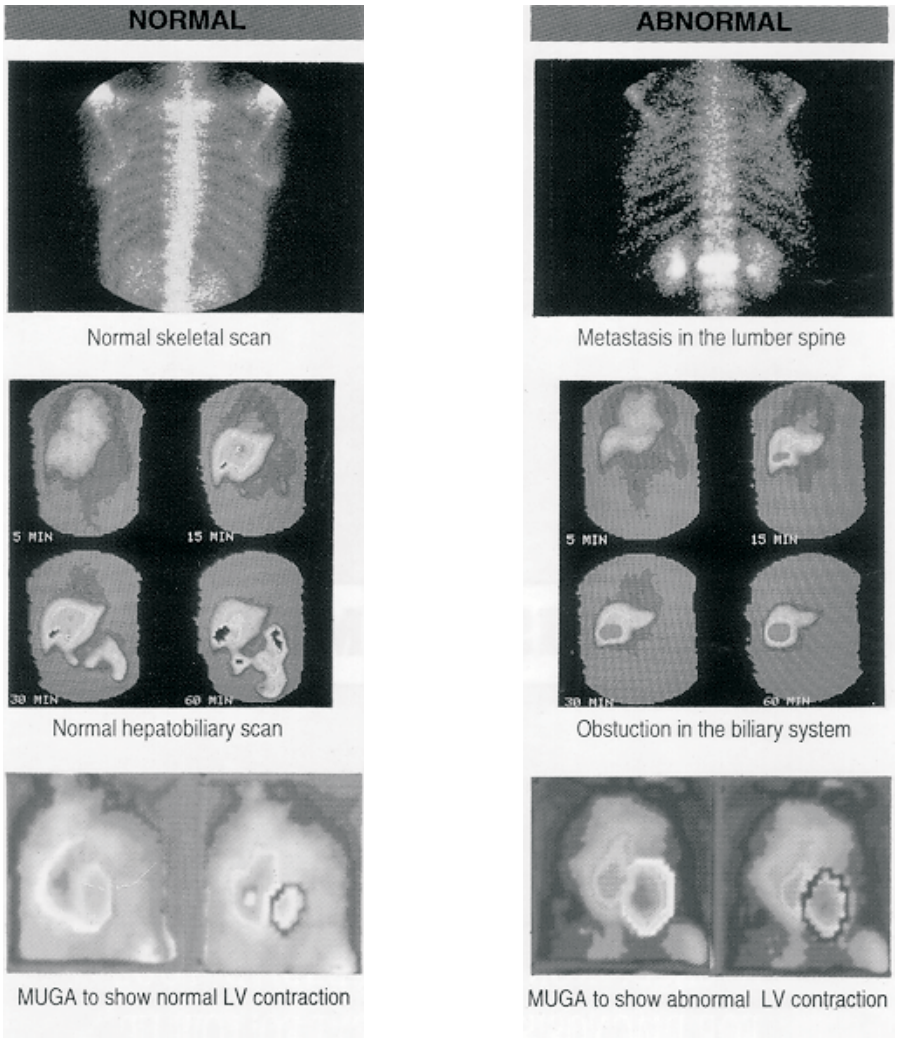

Fig. 16.4 Examples of radionuclide scintigraphy (normal and abnormal) : bone imaging, hepatobiliary function study and cardiac pumping function (MUGA) study.

by interventional procedures using both pharmacological interventions, (drugs for kidney function) and physiological interventions, (stress for cardiac function).

Applications of SPECT / Planar Imaging

Some typical applications of major interest are:

- Bone scanning with ^{99m}Tc-MDP for follow up of metastatis of cancer patients.
- Renography to elicit renal function, study obstruction and evaluate renal transplant.
- Imaging blood flow (perfusion) to myocardium and brain.

- Hepatobiliary function imaging for suspected acute cholecystitis.
- Lung imaging, both perfusion and ventilation functions – pulmonary embolism, chronic obstructive pulmonary disease (COPD).
- Others: gastrointestinal bleeding, infection/inflammation imaging, lymphoscintigraphy

^{99m}Tc compounds described in Table 16.5 are mostly used in all the above cases. Procedures employing ^{99m}Tc products for renal and hepatobiliary functions are commonly employed including paediatric patients.

^{201}Tl is being extensively used as marker for myocardial viability. Imaging of blood flow (perfusion) to the myocardium with ^{201}Tl has an added feature of *re-distribution*. The differential rate of uptake and clearance of tracer from normal myocardial cells versus damaged cells (compromised, but viable) is the basis for the so called *re-distribution*. The ability to pick out stress induced perfusion defects (ischemia) with a single dose of 2-3.5 mCi ^{201}Tl given at peak exercise followed by images acquired immediately and after 3 to 4 hours post-injection, has become the hallmark of "^{201}Tl study". Ischemic zones will show filling with tracer at rest images, while necrotic (dead) tissues will remain cold at both stress and rest. The pharmacological interventional studies in lieu of physical exercise (with adenosine / dipyridamole and nitroglycerine) further increase the diagnostic capability.

^{67}Ga citrate imaging is used for suspected occult infection and for patients with soft tissue tumours. A positive gallium scan is always an indicator of problem, while a clean image need not necessarily exclude a disease / lesion.

Applications of PET Studies

Some of the major applications of PET products are described below. 2-[^{18}F]-fluoro-2-deoxyglucose (FDG) has become synonymous with PET. On entering the cell, FDG gets converted to FDG-6-phosphate by the enzyme hexokinase but, thereafter, not metabolised further. This leads to retention of ^{18}F activity within the cell by metabolic trapping mechanism.

Neurology

^{18}FDG tracer was originally proposed for estimating regional cerebral blood flow (rCBF) and shown as a good index of brain activity during various mental functions (e.g., seeing, thinking, listening to music etc.), since glucose is the only source of energy for brain. ^{15}O labelled water is presently more widely used for brain activation studies. The research findings help understand brain function and brain tissues involvement in disease.

Fundamental aspects of receptor involvement in health and disease have been investigated using ^{11}C labelled receptor radiopharmaceuticals. The link between blood flow/ metabolism with ^{18}F-FDG on one hand and receptor involvement on the other, for example with ^{11}C-N-methylspiperone (for dopamine receptor), has been investigated in neurologic disorders. ^{18}F labelled fluoro-DOPA (6-^{18}F-3,4-dihydroxy phenylalanine) has shown

interesting results in patients of Parkinson's disease (PD) with the degree of uptake in D-2 dopamine receptor regions inversely related to the severity of disease.

Cardiology

There is avid accumulation of ^{18}F-FDG in viable but damaged myocardial tissues, i.e. in blood flow starved, but viable tissues, since they shift to glycolytic pathway for availing glucose as source of energy. This is thus an unequivocal marker of myocardial viability. PET tracers, $^{13}NH_4^+$ and $^{82}Rb^+$, can be used for PET imaging of myocardial perfusion. $^{82}Rb^+$ is a generator produced K^+ analogue, ^{82}Sr being the parent nuclide.

Oncology

^{18}F-FDG is used in tumour metabolism investigation as a better grading/ staging indicator of tumour prognosis. The correlation of response in terms of FDG uptake with tumour prognosis in a large number of clinical studies help choose or avoid surgery. The distinction between necrotic (radiation scar) tumour tissue (FDG absent) versus tumour recurrence (FDG uptake) is facilitated by FDG imaging. ^{11}C labelled amino acid, e.g., ^{11}C-methionine, is useful for estimating the efficacy of response to therapy in cancer patients, the increased rate of utilisation of amino acid by the proliferating malignant cells, providing the basis for the selection / rejection of therapeutic strategy under consideration.

Therapeutic Applications

Radionuclide Therapy

Radionuclides have provided ammunition to the physicians to tackle some diseases since early times, especially cancer. Selective irradiation of the unwanted cells, e.g., cancer cells, is the main aim in these procedures. The ability to target the abnormal tissues with the maximum doses of radiation and at the same time spare the normal cells is a daunting task. Generally well over 100 cGy or more is needed to control cancer cells. The therapeutic radionuclides could be classified on the basis of their half-lives as well as on the type of particulate emissions. There is a choice depending on the volume to be irradiated. The criteria for selection of the therapeutic radionuclide would depend upon whether there is internalisation of the administered product in a lesion or surface uptake on the lesion. The concept of tailored therapy has also been advanced. From practical point of view, it is convenient to classify the radionuclides as alpha emitters, Auger / conversion electron emitters, hard beta emitters and soft beta emitters (Table 16.7). It is possible to confine the delivery of dose over a few μm range to several mm.

Radioiodine Treatment of Thyroid Disorders

The efficacious treatment of thyroid disorders, one benign (thyrotoxicosis) and another malignant (thyroid cancer), with radioiodine, ^{131}I, is well established. Iodide is easily absorbed from the gut and trapped with high efficiency by the thyroid. Typically 5 mCi fixed dose or calculated dose approach is followed for treating hyperthyroidism. Patients are

Table 16.7 - Important radionuclides (RN) for therapy

(A) Alpha emitters				
RN	$t_{1/2}$	E_α (mean), MeV		Method of production
^{211}At	7.214 h	6.76		^{209}Bi (α,2n)
^{212}Bi	60.55 min	7.8		^{224}Ra (3.8 d) $\rightarrow$ ^{212}Pb - ^{212}Bi generator
^{213}Bi	45.59 min	5.87		^{225}Ac (10 d) - ^{213}Bi generator
(B) 'Pure' Beta Emitters				
RN	$t_{1/2}$	E_β (max), MeV		Method of production, % nat. Abundance: σ
^{32}P	14.262 d	1.71		^{32}S (n,p); 95; σ(n,p) = 0.53 b
^{89}Sr[a]	50.53 d	1.46		^{88}Sr (n,γ); 82.6; 0.0058 b
^{90}Y	64.0 h	2.27		Decay of ^{90}Sr (28.3 y); ^{90}Sr - ^{90}Y generator ^{89}Y (n,γ); 100; 1.3 b
^{169}Er[a]	9.4 d	0.34[b]		^{168}Er (n,γ); 26.8; 2 b
(C) Beta emitters with 'Minor Abundance' Gamma Emission				
RN	$t_{1/2}$	E_β (mean), MeV	E_γ / keV (%)	Method of production, % nat. Abundance: σ
^{153}Sm	46.284 h	0.81	103 (28)	^{152}Sm (n,γ); 26.7; 206 b
^{166}Ho	26.763 h	1.5	81 (6.33)	^{165}Ho (n,γ); 100; 58 b
^{186}Re	90.64 h	1.07	137 (9)	^{185}Re (n,γ); 37.4; 106 b
^{188}Re	17.005 h	2.11	155 (15)	^{187}Re (n,γ); 62.6; 73.2 b Decay of ^{188}W (69.4 d) ^{188}W - ^{188}Re generator ^{186}W (n,γ) ^{187}W (n,γ) ^{188}W; 28.6; 37.8 b
(D) Beta emitters with 'Major Abundance' Gamma Emission				
^{131}I	8.0207 d	0.6	364 (81)	^{130}Te (n,γ) ^{131}Te $\rightarrow$; ^{235}U (n,f)
^{67}Cu	61.83 h	0.57	184 (49) 92 (16)	As (p, Spall.) ^{67}Cu
^{47}Sc	3.3492 d	0.6	160 (73)	Ni (p, Spall.) ^{47}Sc
(E) Auger e^- and other Particulate Emitters				
RN	$t_{1/2}$	Decay characteristics and major energy, keV		Method of production, % nat. Abundance: σ
^{124}I	4.176 d	β^+, EC; Auger e^-; Eγ 603		^{124}Te (p,n); ^{125}Te (p,2n)
^{125}I	59.40 d	EC; IC & Auger e^-; Eγ 35		^{124}Xe (n,γ) ^{125}Xe $\rightarrow$;
^{117m}Sn	13.6 d	IT; IC e^- 130, 160; Eγ 159		^{116}Sn (n,γ); 14.7; 0.006 b
^{169}Er	9.4 d	β^-; IC e^- 340		^{168}Er (n,γ); 26.8; 2b

[a]909 keV of ^{89}Sr and 110 keV of ^{169}Er of very low abundance have been ignored.
[b]Energy of the most abundant conversion electron.

treated on out-patient basis in this case. In the case of metastatic thyroid cancer, upto 250 mCi dose is given to the patients after surgical removal of thyroid followed by ablation of any remnant thyroid, in turn, with an ablation dose of ^{131}I (30 to 80 mCi). This technique requires special ward for patient with suitable facilities for containment of radioactive waste and for taking care of accidental contamination and radiation exposure to occupational workers.

Treatment of Metastatic Bone Pain

The palliative treatment of metastatic bone pain in terminal cancer patients with intractable pain and immobility is a significant success of nuclear medicine. ^{32}P as phosphate, $^{89}SrCl_2$ and ^{153}Sm / ^{186}Re - phosphonate complex etc. are the radionuclide products of importance in this regard. Strontium is a calcium analog, while phosphate / phosphonate chemisorb on to the bone mineral constituent, hydroxy apatite. Dosages of 12-14 mCi of ^{32}P as sodium orthophosphate per patient and 1 mCi of ^{153}Sm-EDTMP per kg body weight have been administered for metastatic bone pain palliation without undue myelotoxicity in groups of patients selected on the basis of satisfactory blood cell counts prior to treatment. A cocktail of two therapeutic nuclides, one short-lived and another longer-lived, is used in order to avail the dual benefit of early response of pain relief (from the former nuclide), as well as sustained respite from pain (from the latter nuclide), e.g., $^{153}Sm + ^{89}Sr$, has been advocated.

Radiation Synovectomy

Locally instilled particulate formulation containing a suitable therapeutic radionuclide is used for the treatment of the crippling chronic disease of pain in bone joints due to inflammation of synovium, e.g., rheumatoid arthritis. The procedure called (radio) synoviorthesis or radiation synovectomy is an alternative to surgery. Prof. Gunter Modder, Germany has carried out pioneering work in this field and the procedure is widely practised in Europe for efficacious treatment of patients suffering from joint pain due to rheumatoid arthritis (RA) haemophilic anthitis amongst others, which are, non-responsive to conventional medical therapy. This needs therapeutic radionuclides ranging from soft to hard beta energy (Table 16.7), typically 0.3 MeV of ^{169}Er for small joints like the finger joints, 0.8 MeV / 1 MeV of ^{153}Sm / ^{186}Re for medium sized joints and 2.27 MeV/1.71 MeVof ^{90}Y/ ^{32}P for large joints like the knee. In this technique, insoluble particulate formulations (preferably biodegradable, e.g., hydroxy apatite) of controlled size, usually 2-5 μM, and in a small volume are instilled into the inflamed synovial space of the affected joint under monitoring, with the help of gamma camera in the case of large joints and fluoroscopy for small joints. The immobilisation of the treated joint for at least 48 hours post instillation of the radionuclide, helps prevent leakage of activity from the joint.

Radioimmunotherapy (RIT) and Radiopeptidetherapy (RPT)

The prospects of radioimmunotherapy (RIT) using radiolabelled monoclonal antibodies to tumour associated antigens and radiopeptidetherapy (RPT) using radiolabelled peptides targeted to receptors on the lesions, are the major recent advances in combating

cancer. While many hurdles have yet to be overcome, the approaches are sound and research efforts world over warrant the development of methods for the large scale production of many therapeutic radionuclides of high specific activity (Table 16.7) capable of being attached to these biological carrier molecules in a simple, stable manner. Radionuclide therapy by targeting cellular, and even molecular levels, for internalised cytotoxicity, is being explored. Radiopharmaceuticals with Auger electon emitters have been shown to be very effective if they can be targeted to enter tumor cells. ^{125}I labelled uridine derivatives have been reported in this respect. Loco regional applications of β^- emitter tagged particles being used in countries such as South Koriea for treatment of liver cancers. ^{166}Ho-chitosan is one such example.

Dosimetry Aspects

Therapeutic efficacy depends upon the amount of absorbed radiation dose and radiosensitivity of the irradiated target tissue. The former is influenced by such factors as the radionuclide uptake and residence time at target site, radiation energy characteristics and target volume to be irradiated. Radiation dosimetry aspects are an essential component of the development and acceptance of new therapeutic applications using internally administered / loco-regionally instilled therapeutic radionuclides. Pure particulate emitters are preferred for therapy. In case, accompanying gamma rays are present, irradiation of additional surrounding tissues results. But it is difficult to accurately estimate the absorbed dose from pure beta emitters. Gamma emitters in conjunction with SPECT technique or positron emitters with PET would be desirable for reliable quantitation of uptake and retention. Thus the concept of analogous radionuclides called "surrogate radionuclides" compatible with SPECT/ PET is being used for reliable calculations of internal dosimetry, e.g., using ^{111}In (gamma ray emitter or ^{86}Y (positron emitter) for ^{90}Y. Such dosimetric considerations could promote customised dose delivery to individual patients, in order to maximise the beneficial effects at minimal risk.

Radiotherapy

Radiotherapy deals with treatment of cancer using radiations emitted from radioisotopes or X-ray machines or using high energy electrons. Early research in radiation biology conclusively proved that radiation can destroy the DNA molecule in the cells, thereby making them incapable of further division. A beneficial use of this harmful effect of radiation was the development of methods for the treatment of cancer.

Radiotherapy, surgery and chemotherapy form three pillars in the management of cancer. Radiotherapy is resorted to destroy remnant tumour mass after surgery. Radiotherapy is the only method of treatment for those types of cancer, which are difficult to treat by surgery, e.g., cervical cancer. It is also often used as a palliative treatment in patients with advanced cancer. Radiotherapy is based on the principle that ionising radiation such as gamma rays and X-rays inactivate living cells by interaction with their chromosomes, the extent of killing being higher in rapidly proliferating cells than in normal cells. In general, the cancer cells proliferate more rapidly than the normal cells and hence are much more

susceptible for destruction by radiation. However, in actual radiotherapy, irradiation of normal cells surrounding the cancer cells cannot be completely avoided. Hence various techniques are employed to maximise the radiation dose to tumour cells (role of radiosensitiser) and minimise the dose to surrounding normal cells (role of radioprotector).

Radiotherapy is being practised since the early part of this century, i.e. since the discovery of X-rays and radium. Radiotherapy practice has improved tremendously over the years with the availability of a variety of artificially produced radioisotopes. Today the quality of treatment is of a very high order and radiotherapy is an important component of cancer control programmes all over the world. Radiotherapy is practised in two modes called teletherapy and brachytherapy, depending on the physical location of the radiation source vis-à-vis the patient or the tumour.

Teletherapy

In teletherapy, the radiation source is placed in a shielded housing and a collimated beam of radiation from the source is directed towards the tumour for treatment. The source head can be moved and fixed in any desired position. The patient remains stationary on a couch situated at the centre of the orbit of the source head. The radiation source commonly used is ^{60}Co because of certain desired characteristics like high specific activity, high radiation output per curie and long half-life. A typical teletherapy unit consists of a remotely operated high intensity (~10,000 Ci) of ^{60}Co point source housed inside a shielded container. After placing the patient in position, the source is brought out to focus collimated radiations coming out of it on the tumour tissues. For therapy, a radiation dose of upto 50-60 Gy could be delivered over several sittings. The advantages of ^{60}Co machines include radiation emission at a predicted rate, unaffected by external factors such as temperature and pressure and availability. In fact, ^{60}Co machines are the work-horses in most radiotherapy departments.

Gamma Knife

A recent advance in external radiation therapy is the development of 'Gamma Knife' for stereotactic radiosurgery of tumours and arteriovenous malformations in the brain. Stereotaxy essentially uses the concept that a point can be precisely located if its relationship to three different co-ordinates is known. Radiosurgery refers to the precise delivery of a high dose of radiation exactly to a reconstructed 3D target volume of the tumour. A stereotactic frame or a head-ring serves as a reference platform for reconstructing the patient's head and the target lesion within. A precise, one time dose of radiation is then delivered to the lesion simultaneously from different locations in the gamma knife. The radiation can be X-rays or gamma rays from ^{60}Co sources.

Brachytherapy

Application of small sealed radiation sources in close proximity to the tumour for treatment is called brachytherapy. In this practice, three modes of treatment are commonly used:

- Surface therapy - application of one or more sources on or near an area of body surface which is to be treated, e.g., treatment of cancer of eye., skin cancer
- Intracavitory therapy – placing one or more sources with the help of an applicator or a holding device within a natural body cavity wherein the tissues adjacent to the walls are to be treated, e.g., treatment of cancer of cervix.
- Interstitial therapy – implanting one or more sources into the tissue which is to be treated, e.g., treatment of breast cancer, prostate cancer.

Brachytherapy was initially practised using radium and radon sources. However, with the advent of nuclear reactors, artificially produced radioisotopes with more favourable radiation characteristics became available. This has revolutionised brachytherapy techniques and radium has been almost completely replaced by isotopes like ^{192}Ir, ^{60}Co, ^{198}Au and ^{137}Cs. These isotopes in the form of tubes, needles, wires, seeds etc., are used in applicators with enhanced quality of treatment. Many types of manual and remote loading applicators and machines are available today. ^{125}I sources for brachytherapy of certain intra-ocular tumours affecting the eyes are also in use.

In recent times, an accelerator / cyclotron based radionuclide, ^{103}Pd, ($t_{1/2}$ = 16.991 d, EC decay mode, E_γ = 40 keV) is used for brachytherapy of prostate cancer. A specially designed high current, medium energy (2 - 3 mA, 18 MeV proton) cyclotron called "palladium making cyclotron" is being utilised to produce ^{103}Pd.

Typical Applications

Radiotherapy is effectively used for treating a variety of cancers including those of head and neck, prostate, lungs, stomach, colon, rectum, esophagus, brain, cervix and ovary, either alone or in combination with surgery or chemotherapy. Radiotherapy is very effective in treatment of cancers of head and neck, cervix, colon and rectum and Hodgkin's lymphoma. Cervical cancer which accounts for the largest incidence of cancer among women and which could be treated by crippling surgery only some years back, is now quite successfully treated using brachytherapy, helping these patients to lead a near normal life. Similarly, head and neck cancers widely prevalent in Indian males are also effectively treated using radiotherapy.

Bibliograhy

1. N.P. Alazraki and F.S. Mishkin, Fundamentals of Nuclear Medicine, Society of Nuclear Medicine, New York (1984).
2. R.D. Lele, Principles and Practice of Nuclear Medicine, Arnold-Heinemann, New Delhi (1984).
3. H.N. Wagner Jr., Z. Szabo, J.W. Buchanan, Principles of Nuclear Medicine, 2nd Edition (1995).
4. J.I. Thorell and S.N. Larson, Radioimmunoassay and Related Techniques, C.V. Mosby St. Louis (1978).

5. M.R.A. Pillai, S.D. Bhandarkar, Radioimmunoassay : Principles and Practice, 3rd Edition, BARC, Mumbai (1998).

6. C.B. Sampson, Text Book of Radiopharmacy - Theory and Practice, Gordon and Breach Sci. Pub. (1994).

7. R.J. Kowalsky and J.R. Perry, Radiopharamceuticals in Nuclear Medicine Practice, Appletons Lange (1987).

8. G. Modder, Radiosynoviorthesis, Warlich Druch und Verlagsges, Germany (1995).

9. D.H. Shah, A.M. Samuel, R.S. Rao, Thyroid Cancer in Indian Perspective, Quest Publication, Mumbai (1999).

10. Modern Trends in Radiopharmaceuticals for Diagnosis and Therapy, IAEA-TECDOC 1029, IAEA, Vienna (1998).

11. Therapeutic Applications of Radiopharmaceuticals, IAEA-TECDOC 1228 (2001), IAEA, Vienna.

12. Radiopharamaceuticals and Hospital Radiopharmacy Practices, Eds. N. Ramamoorthy, V. Shivarudrappa, A.A.Bhelose, BRNS, BRIT-DAE, Mumbai (2000).

13. Cancer Therapy with Radiolabelled Antibodies, Ed. D.M. Goldenberg, CRC Press, Boca Raton (1995).

Chapter 17
Applications of Radioisotopes in Biology

During the last 50 years there has been tremendous progress in biochemistry, molecular biology and biotechnology research. The researcher no longer is satisfied with analyzing data at the macro level but is much more focused on obtaining information at the molecular level. This has lead to a demand for labels, which could effectively and accurately convey information about events and processes as they unfold in various biological systems. Radioactive isotopes have served this purpose and contributed a great deal in understanding the various biochemical mechanisms and pathways. In effect radioisotopes have served as "radio tracers" in the field of biology.

In this chapter the application of radioisotopes in biological research is described with a special emphasis on molecular biological techniques utilizing radioisotopes. Nucleic acid and protein labeling techniques are described in detail with some of their applications. An attempt has also been made to bring out certain aspects of applied research wherein radioisotopes are used in day-to-day life.

Characteristics of a Radiotracer

A radiotracer is generated by suitably labeling a biomolecule of interest with the radioisotope of choice. Since, an isotope by definition is a chemically identical moiety, it doesn't alter the function of the biomolecule. A radiolabel is characterized by the type and energy of radiation emitted, its half-life, radiochemical purity and specific activity, which are characteristic of the isotope used and the final chemical form of the label. In Table 17.1 the most commonly used β^- emitting isotopes in biology with their radiochemical characteristics are given.

Any label has to meet two primary requisites. It has to be highly specific and it has to be sensitive. This would enable the use of very small amounts of tracer to obtain accurate information. The sensitivity would be governed by the half-life, energy and specific activity of the isotope whereas its chemical form decides the specificity. Specific activity of a radiochemical is commonly expressed in units of Ci (or mCi) per millimole of the compound. From Table 17.1, it can be seen that the highest specific activities are offered by

Table 17.1 - Some properties of radioisotopes

Sl .No.	Isotope	Half-life	Energy (MeV)	Max. Specific Activity Ci/mmol
1.	^{3}H	12.33 y	0.018	28.9
2.	^{14}C	5730 y	0.156	0.062
3.	^{35}S	87.38 d	0.167	1485
4.	^{32}P	14.262 d	1.72	9086
5.	^{33}P	25.34 d	0.249	5075
6.	^{131}I	8.02070 d	0.361	16,320
7.	^{45}Ca	162.61 d	0.257	801

^{131}I and ^{32}P. This means that for radiation equivalent to 1mCi, the amount of labeled compound needed would be the lowest for ^{131}I and highest for ^{14}C. Since, most of the applications of radioisotopes involve highly specific interactions it is important to have very high radiochemical purities. Radiochemical purity is defined as the percentage of radioactivity present in the desired chemical form. In most cases the impurities may have inhibitory effects in the assays and in the case of *in vivo* studies may be toxic too.

Radiolabels provide a very high degree of sensitivity. It is possible to detect concentrations as low as attomolar (10^{-18}M). Since, radiation is a nuclear phenomenon the radiation emitted is independent of physico-chemical conditions and hence is highly reproducible under variable laboratory conditions.

Labeling Methods in Molecular Biology

Nucleic Acid Labeling

Deoxyribonucleic acid (DNA) is the carrier of the genetic information. These are polymers of deoxynucleotides. Each nucleotide consists of a purine or pyrimidine base, a sugar and a triphosphate molecule (Fig. 17.1). During DNA synthesis, the nucleotides are linked by a phosphate ester, which is formed with the hydroxyl group of the sugar moiety of another nucleotide. A series of such linkages result in the formation of a DNA. The enzyme DNA polymerase carries out this polymerization. The bases are of four types: adenine (A), guanine (G), cytosine (C) and thymine (T). The DNA has a double helical structure, which is formed by a complementary binding of A with T and G with C. In Ribonucleic acid (RNA) the base thymine is replaced with uracil. DNA are the precursors of RNA and RNA are the precursors of proteins. RNA is prepared from DNA by the process called transcription and RNA is converted into proteins by translation. Thus, DNA, RNA and proteins are inter-related and a labeled DNA could give information about the protein function too. One of the phosphorus atoms in the molecule can be labeled with ^{32}P or ^{33}P to obtain the

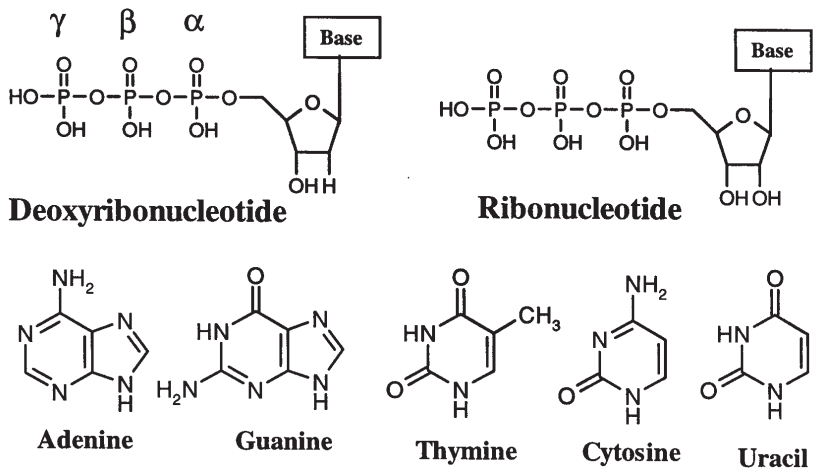

Fig. 17.1 Structure of nucleic acid constituents.

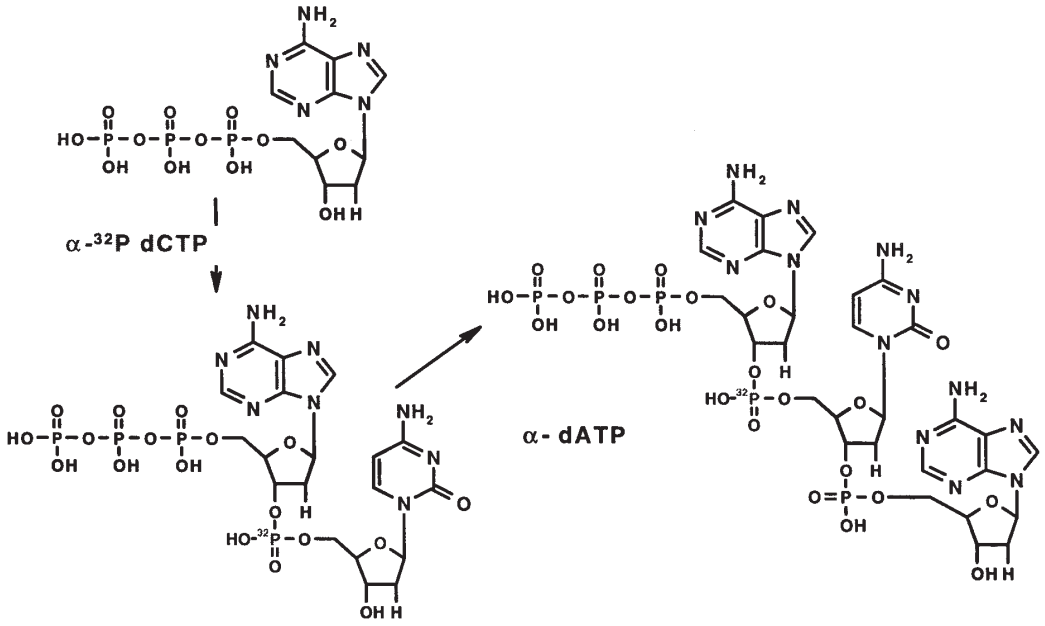

Fig. 17.2 Schematic representation of labeled DNA synthesis.

radiolabeled nucleotide, which can be used for labeling. Schematic representation of synthesis of labelled DNA is given in Fig. 17.2. Thiophosphate analogs can also be prepared by replacing a phosphorus atom with ^{35}S. Since, enzymes cannot distinguish between radiolabeled and unlabeled substrates, nucleic acid labeling can easily be carried out by enzymatic methods. A variety of methods are available for nucleic acid labeling.

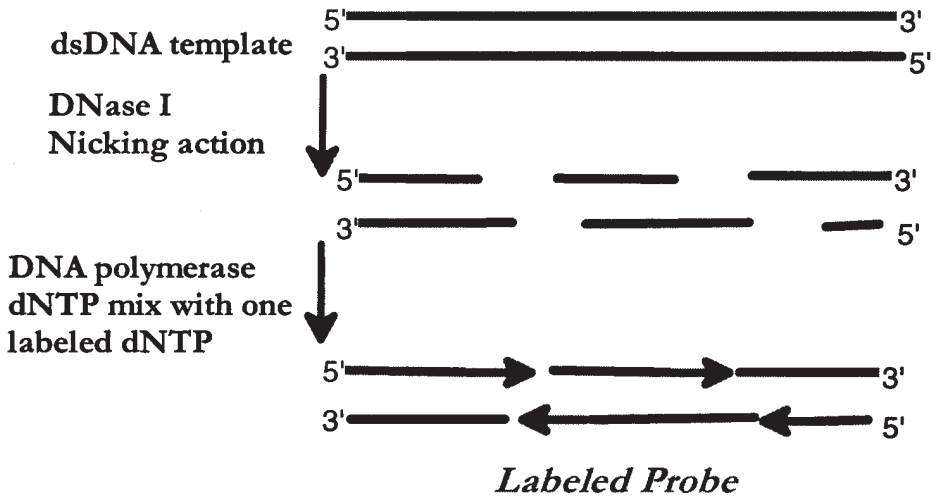

Fig. 17.3 Nick translation.

Nick Translation

This is a method by which a labeled double stranded DNA (dsDNA) is synthesized *in vitro*, from a dsDNA template using two enzymes Dnase I and DNA polymerase. The first enzyme creates nicks in the DNA and the second enzyme extends the DNA from the nicks created. The nucleotides are supplied and one of the nucleotides is a labeled nucleotide, which is incorporated into the DNA during its synthesis. Thus, a labeled DNA probe is obtained (Fig. 17.3).

Random Priming

In this method a DNA is first denatured to obtain single stranded templates. To this random hexanucleotides (random primers) are added. These primers bind to complementary sequences on the template DNA. The enzyme DNA polymerase (Klenow fragment) is then used to extend these primers along the sequence of the template DNA. The nucleotides are supplied and one of the nucleotides is labeled and hence a labeled DNA fragment is obtained (Fig. 17.4).

Oligonucleotide Labeling

Oligonucleotides are sets of nucleotides, which are single stranded. The terminal phosphate group of an oligonucleotide can be labeled with either ^{32}P or ^{33}P. End labeling is carried out by first dephosphorylating the oligo and then phosphorylating it in the presence of γ ATP, using the enzyme T4 polynucleotide kinase (PNK) as shown in Fig. 17.5. This is the simplest method of labeling an oligonucleotide or a DNA. By this method each oligo contains only one label at the terminal position. This method also gives the probes with the highest specific activities.

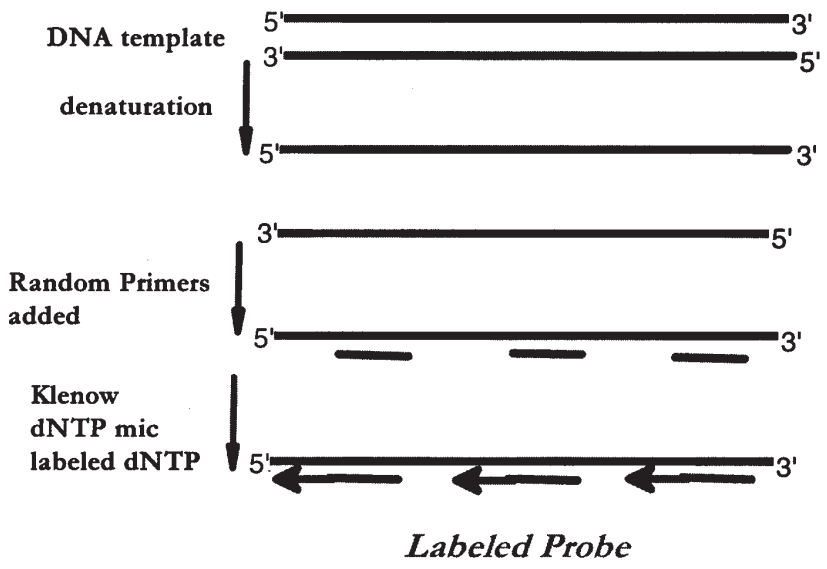

Fig. 17.4 Random priming.

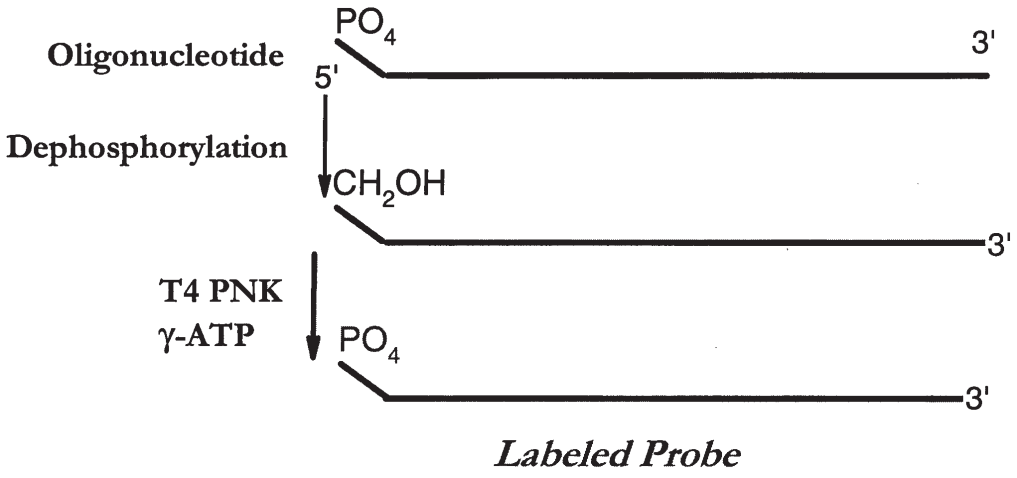

Fig. 17.5 5'-End labeling.

Polymerase Chain Reaction

In most of the cases the amount of DNA available for analysis is extremely low. Polymerase Chain Reaction (PCR) is a tool for amplifying DNA. This technique makes use of the thermostable enzyme Taq DNA polymerase. PCR consists of 3 main cycles : Denaturation, Primer Annealing and Extension. Each of these steps is programmed for about a minute. Several such cycles are carried out and a PCR of 'n' cycles would lead to a 2^n fold amplification of DNA as shown in Fig. 17.6. PCR has now become an indispensable tool in molecular biology. The template DNA is first denatured at high temperature. The primers

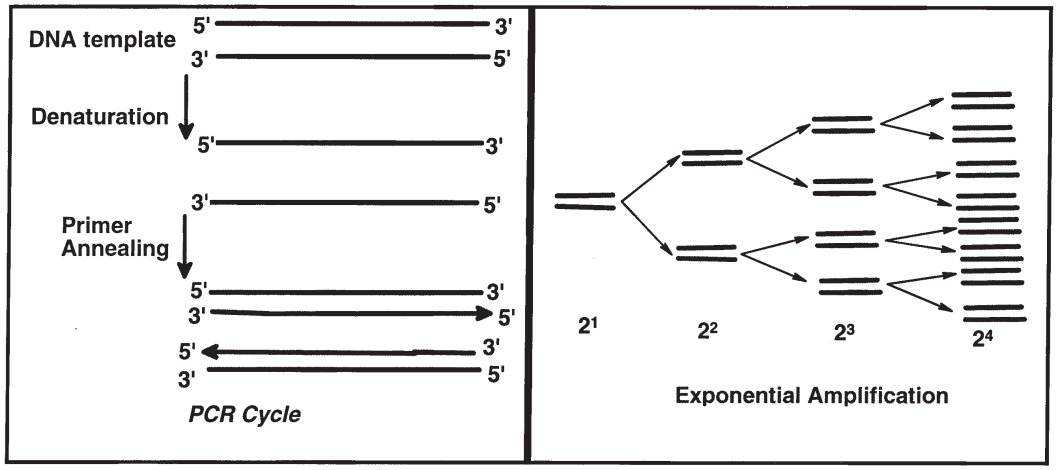

Fig. 17.6 Polymerase chain reaction.

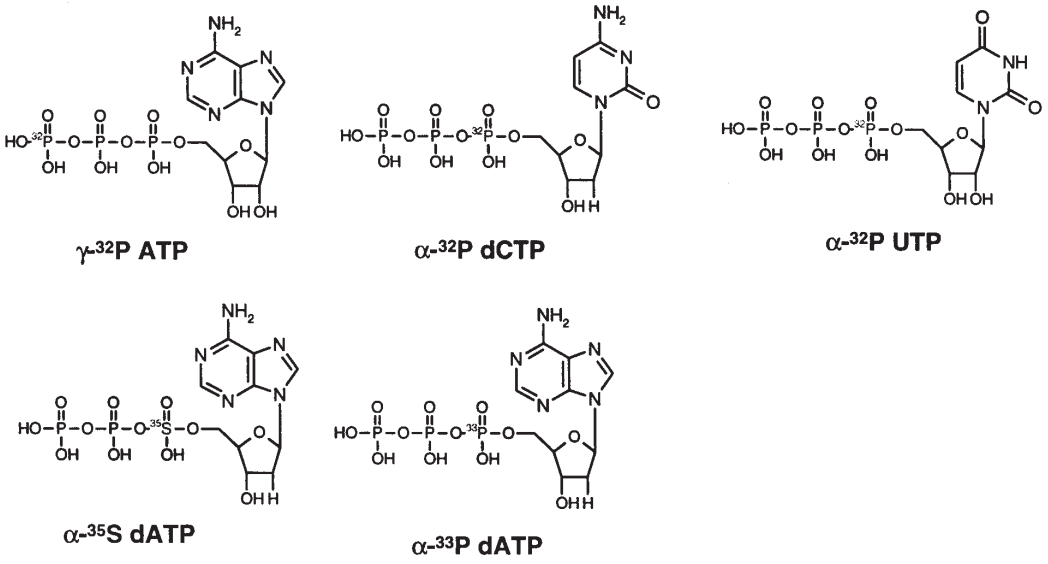

Fig. 17.7 Schematic of some nucleic acids.

then anneal to the ssDNA template. The next step is the extension step by Taq DNA polymerase in which nucleotides are provided. Labeled DNA in PCR can be generated in two ways: (i) by using end labeled primers (labeled with ^{32}P or ^{33}P) and (ii) by supplying a labeled nucleotide as one of the reagents.

The high fidelity amplification in PCR is exponential. Milligram levels of DNA are prepared starting from trace amounts using this technique. PCR is used in a variety of applications where DNA amplification is required. For example, the structures of some of the commonly used nucleic acid labels are shown in Fig. 17.7.

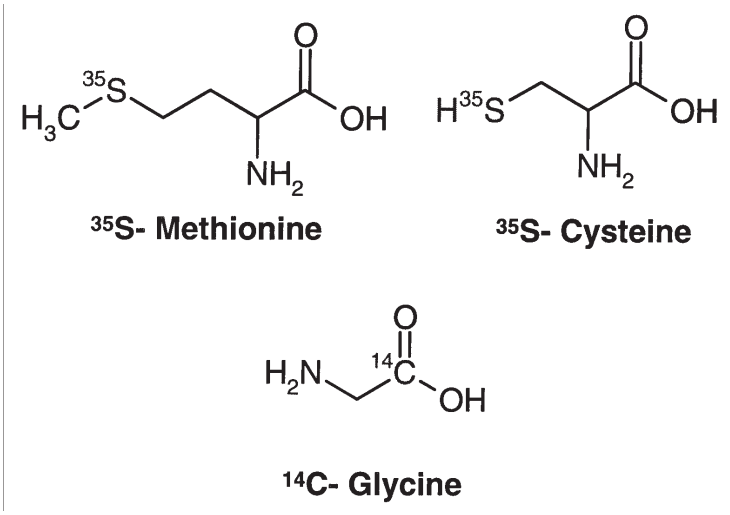

Fig. 17.8 Schematic of labeled amino acids.

Protein Labeling

Proteins are polymers of amino acids. Of all the naturally occurring amino acids, the most commonly used radiolabeled amino acid is ^{35}S methionine. This is used for a variety of applications such as *in vitro* protein translation. In this, the protein is synthesized by supplying amino acids. Labeled methionine is supplied to obtain a protein, which is radiolabeled. Other amino acids labeled with ^{14}C and ^{3}H are also available commercially. *In vivo* protein modifications can also be studied by using ^{3}H, ^{14}C or ^{35}S labeled amino acids in the cell culture medium. Protein labels thus generated are used for studying protein metabolism, protein function and interactions of proteins with antibodies. Modification of proteins such as phosphorylation is carried out using ^{32}P and ^{33}P labeled γATP or γGTP.

^{35}S-Methionine can be used for a variety of applications such as *in vitro* translation. This is also used in protein labeling in cells *in vivo*. Other labeled amino acids like ^{35}S-Cysteine and ^{14}C Glycine too are routinely used. Structures of these labelled acids are given in Fig. 17.8. Some salient features of S-35 are given in Table 17.2.

Chemical Labeling

Chemical synthesis of radiolabeled biomolecules is carried out following conventional organic chemistry. The label is introduced in one of the intermediate steps of the synthetic route by substituting one of the reagents with the radiolabeled reagent. Many labeled synthetic drugs and ligands are synthesized using ^{14}C or ^{3}H labeled reagents.

Table 17.2 - Properties of some commercially supplied radiochemicals

Product	Radioactivity level (mCi/mL)	Specific activity (Ci/mmol)	Applications
γ-^{32}P ATP	10	4000-6000	5'-end labeling of nucleic acids, protein phosphorylation.
α-^{32}P dATP & α-^{32}P dCTP	10	2000-4000	DNA labeling by Nick translation, random priming, PCR
α-^{33} dATP & α-^{33} dCTP	10	2000-4000	DNA labeling by Nick translation, random priming, PCR, cycle sequencing, RT-PCR, *in situ* hybridisation.
^{35}S Methionine	10	1000	*in vitro* protein translation, protein synthesis in cells.

Labeled Probe Applications

The basis of molecular biology research lies in understanding the DNA, RNA and the proteins. Nucleic acid and peptide probes thus generated are used for a variety of applications such as *in situ* hybridization, molecular cloning and screening, preparation of genomic libraries, structural and functional genetics, identification of gene mutations, identification of genetic disorders, molecular diagnosis of diseases and forensic applications such as DNA finger printing

The three primary techniques involved in the detection of DNA, RNA and Proteins are (i) Southern Hybridization/Blots (DNA detection), (ii) Northern Blots (RNA detection) and (iii) Western Blots (Protein detection).

Blotting is a general term for the technique in which the biomolecule separated or purified is transferred onto to solid support such as a nylon membrane. This is probably the most commonly used technique in molecular biology prior to detection. When a DNA or DNA fragments are transferred on to membranes and hybridized with labeled DNA probes the technique is called Southern Blots. When RNA are involved the technique is referred to as Northern blotting. In the case of proteins, it is called Western blotting. Western blots are an important tool in disease diagnosis. Proteins from samples can be transferred to membranes and can be detected by labeled antibodies. Western blots are commonly used in the detection of many viruses including HIV.

In situ hybridization (ISH)

Though, DNA probes were used for *in vitro* techniques it was felt that more accurate information could be obtained by studying the DNA in its actual environment rather than in

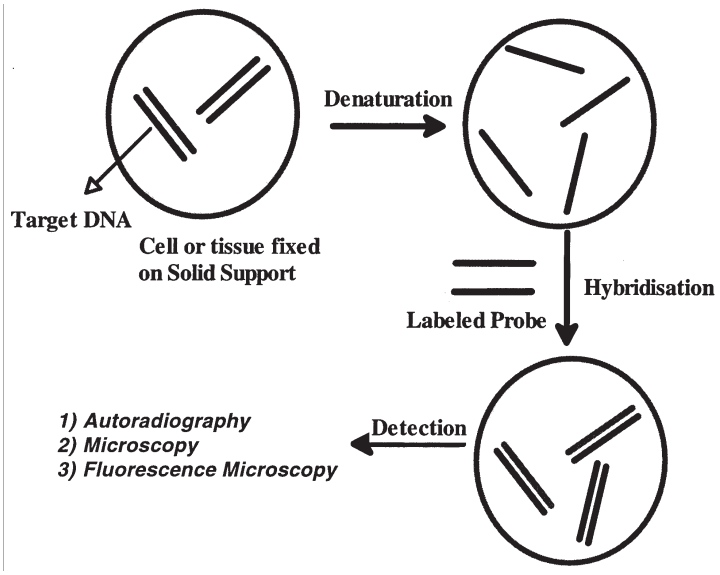

Fig. 17.9 Schematic representation of hybridization process of PNA.

in vitro situations. This required a technique by which a labeled DNA fragment could be delivered to its actual location in the cell or the tissue. This technique of binding a labeled DNA to a target sequence within the cell or tissue is called *in situ* hybridization (ISH). This concept of complementarity provides very high level of specificity to the technique. The target DNA can be immobilized on solid supports such as glass slides retaining its cellular morphology and then hybridized with the labeled DNA (Probe). The probe can be DNA, RNA or more recently PNA (Peptide Nucleic Acid) fragments labeled with radioisotopes. The probes can be generated by any of the methods described above such as Nick translation, random priming or PCR. The entire hybridization process is depicted in Fig. 17.9.

In situ hybridization is used for a variety of applications such as genomic mapping, clinical diagnosis and chromosomal mapping. Using *in situ* hybridization gene mutations can be studied. It is regularly used in pre-natal diagnostic studies using the fetal cells in the mother's blood. This can help identify genetic diseases at a very early stage. ISH can also be used for the detection of viral DNA and RNA. Thus, ISH can be used for developing sensitive assays for the infection and spread of viruses such as HIV. With the introduction of fluorescence probes it is now possible to visualize the entire labeled hybrid. The use of fluorescence labels has given birth to a whole new technique called Fluorescence *in situ* hybridization (FISH). With the advent of FISH, it is now possible to generate visual images. The use of FISH is now predominant.

DNA Finger Printing

One of the biggest applications of PCR in everyday life is in the field of forensics. With the advent of PCR, it is now possible to detect very small quantities of specimen DNA

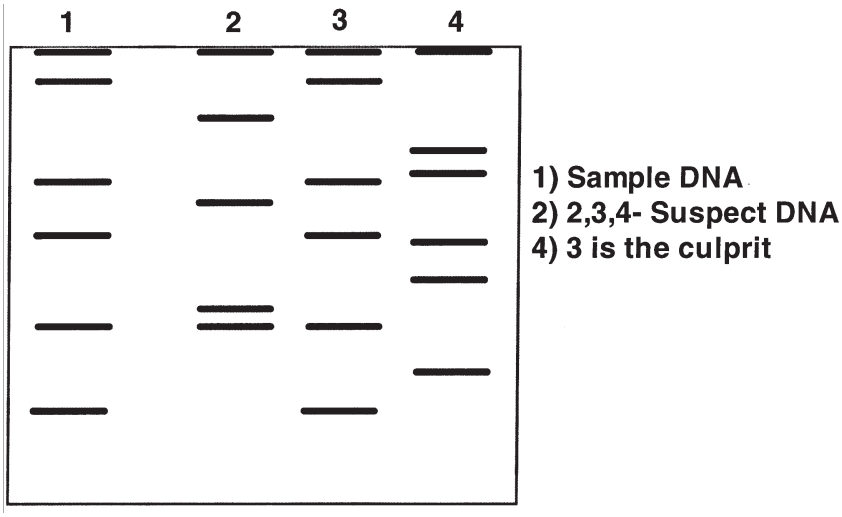

Fig. 17.10 Comparison of sample and suspects DNAs.

that can be extracted from the scene of the crime. The advantage of PCR is that it works on small sequences of DNA and hence a degraded DNA sample too is a good sample. DNA can be extracted from any source such as bloodstains, hair, semen and skin. The DNA is first amplified. The basis of DNA finger printing is that the DNA has regions of repeat sequences called microsatellites. These are specific to individuals. The digested DNA is separated by electrophoresis and visualized. The closer the DNA sequence is, between two individuals, greater will be the number of common bands. Hence, a DNA from crime scene can be matched with DNA of suspected persons (Fig. 17.10). In order to maintain reproducibility in various laboratories standard DNA are used as markers. Similar procedures are adapted for PCR based DNA sequencing, genomic mapping, studying gene mutations etc. PCR has now become an indispensable tool for the molecular biologist.

Molecular Diagnostics

It is now evident that most human diseases have a genetic origin. This has lead to the development of diagnostic methods, which aim at identifying specific genes responsible for the disease. By this method, it is sufficient if structural information of the gene is known. DNA detection techniques such as Southern blots and PCR amplification are the commonly used techniques in molecular diagnostics. Radiolabeled probes would not only maintain the specificity of binding to target sequences but would also provide signals at very low working concentrations of the sample. Kits based on the above principle are available for a variety of diseases such as HIV, hepatitis, tuberculosis and Malaria. The principle of developing such a diagnostic method would involve the following steps. The first step of course would be the knowledge of the genomic sequence of the bacteria or the virus. Once the sequence is known, a target sequence is identified which is common to all the different strains of the bacteria or virus. Primers are designed which are specific to this target sequences. The primers

themselves can be labeled. In the case of PCR, the labeling can be done during DNA synthesis. DNA is isolated from the patient's sample and is then amplified by PCR using labels. The PCR product is then detected. With increasing commercialization of such techniques, it is imperative that high-throughput methodologies are developed. This is possible by having a large number of DNA probes (for various diseases) on a single surface (example a chip) and then allowing the sample to bind to it. The sample will bind specifically to probes for which it has affinity. Thus a large number of diseases can be screened at one go. This is the principle of DNA Microarray.

Therapeutic Applications

The most recent and exciting development in the use of radioisotopes in biology is in the field of therapy. With the identification of the molecular origin of diseases, there has been extensive research in the field of oligonucleotide and peptide based therapy. Oligonucleotide therapy is based on the theory that by identifying specific sequences of the disease causing genome, oligos can be designed and synthesized, which can bind to this sequence and inhibit its expression, thus curing the disease. ^{32}P and ^{33}P labeled oligos are being extensively used in this research. In addition, being β^- emitters they are being used for specifically binding to target tumors and then delivering dose. This is a variation of brachytherapy. Labeled oligos can pinpoint the exact mechanism and function of these synthetic oligos and are a vital tool in their design. Peptide based therapy is also becoming prominent. Peptides act in a similar fashion. In addition, peptides can act as ligands and can carry metals, which are radioactive. This has opened up a whole new branch of metallopharmaceuticals.

Enzyme Assays

Enzymes are biocatalysts, which are vital for biochemical reactions. A thorough understanding of enzyme activity and kinetics can be obtained by the use of radiolabeled enzyme substrates. A wide variety of substrates such as nucleotides (^{32}P, ^{33}P and ^{3}H), carbohydrates (^{14}C and ^{3}H), amino acids (^{35}S), lipids/steroids (^{3}H), labeled synthetic ligands and peptides are available commercially for assays of various enzymes of biological importance.

Drug Discovery

Drug design today is a core area of scientific research. The concept of drug design has evolved from empirical drug screening to a more mechanism-based approach. The central dogma of drug development is the principle of ADME (Adsorption, Distribution, Metabolism, Excretion). These four factors characterize the function of a drug *in vivo*. The studies related to these are termed pharmacokinetics and drug metabolic studies. Radioisotopes play an important role in both these studies. In addition, radiotracers provide vital information with respect to the proof of mechanism of action of the drug *in vivo*. This constitutes the field of pharmacodynamics and provides information of the fate of the drug and its metabolism. Thus, radioisotopes are useful at each and every stage of the ADME

principle and have proved to be a great asset in drug development. In addition to ^{14}C and ^{3}H labeled compounds, there is a huge application of Positron Emission Tomography (PET) in this area.

Detection Methods

The method involves the use of photographic films consisting of an emulsion of silver halide grains. The photographic films are first exposed to radiation. Radiation sensitises silver halide grains which remain intact when they are developed. The intensity of darkening in the developed film is proportional to the radiation received. For example, labeled nucleic acids are first purified by gel electrophoresis. This gel is then dried and exposed to a photographic film to obtain latent images of the DNA. The radiolabeled moiety can also be immobilized on blots, membranes etc. Autoradiography is a widely used technique for visualizing radiolabeled experiments. With the introduction of phosphoimagers, latent images of radiolabeled molecules can be generated without the use of photographic films and without the need for long exposures and developing procedures. Phosphoimagers are highly sensitive instruments, which with the help of Charge Coupled Diodes cameras can easily quantify the labeled biomolecules. The purified radiolabeled biomolecule is also counted using a liquid scintillation counter. Details of counting are given in Chapter 7. Currently, sophisticated instruments are available which give the provision of selecting the isotope so that the counting can be done with 100% efficiency.

Bibliography

1. J. Sambrook, E. F. Fristsch & T. Manniatis; Molecular Cloning: A Laboratory Manual, II edition, Cold Spring Harbor Laboratory Press, New York (1989).
2. George H Keller & Mark M Manak, DNA Probes, II edition, McMillan Press, Stockton, UK. (1993).
3. K. H. Goulding and R. J. Slater, Radioisotope Techniques; in Practical Biochemistry, Principles and Techniques; IV Edition, Eds. Keith Wilson & John Walker, Cambridge University Press (1994).
4. Robert J. Slater; Radioisotopes in Biology; A Practical Approach; II edition, Oxford University Press (2002).
5. Howard J Glenn; Biologic Applications of Radiotracers, CRC Press (1983).

Chapter 18
Radiochemical Separations

Most of the chemical techniques and separation procedures developed over the years have been applied to radiochemistry. Chemical procedures like precipitation, ion exchange, solvent extraction and chromatography are routinely used in a radiochemical laboratory. The apparatus used in a radiochemical laboratory and in a chemical laboratory are similar. Chemical separations and radiochemical separations are based on chemical properties and therefore, are similar. However, in a radiochemical separation one deals with (i) radioelements (isotopes) that emit radiations, (ii) amounts are often in sub-microgram level making radiochemical separations a special art, (iii) separation times range from a few seconds to minutes, depending on the half life of radioisotope to be separated and (iv) need for radionuclide purity. Radionuclides emit ionising radiations like α, β and γ. Therefore radiochemical separations are carried out in special laboratories with provisions for (i) containment of radioisotopes in the unlikely event of spillage and (ii) equipment to monitor radiation (see Chapter 21). Since radiation interacts with matter and causes physical / chemical changes and hence adequate safety precautions have to be taken. While processing high levels of radioactive materials, one has to consider the radiation stability of the chemicals that are required in the chemical processing.

Carriers, Hold Back Carriers and Scavengers

Separation procedures involving precipitation, filtration and centrifugation require a certain minimum quantity of material. Quite often the amount of the element (including the radioisotope) is present in subnanogram quantities and this is likely to be lost by adsorption on the surface of the glassware. Also, in some areas, precipitation may not occur at these low concentrations as the ionic product may not exceed the solubility product. Suppose a sample of ^{99m}Tc (6.01 h) corresponding to a disintegration rate of 10^6 dps has to be isolated from its parent ^{99}Mo. Weight of ^{99m}Tc of this sample would be 5.15×10^{-14} kg. It would be very difficult to separate such tiny quantities by ordinary separation procedures. Similar is the case with the separation of 5×10^4 dps of ^{139}Ba (82.9 min) has to be separated from a host of

fission products formed in the nuclear fission of natural uranium[1]. This corresponds to 3.59 x 10^8 atoms and a weight of 8.28 x 10^{-17} kg. Normally barium is separated from fission products by precipitating it as sulphate or nitrate. It is impossible to separate precipitates at such low concentrations. Additionally, chemical behaviour at low concentrations would be quite different from that of micro and macro concentration.

Low concentrations radioisotopes are separated by the addition of large excess of its inactive isotope(s) called carrier. Milligram quantities of inactive barium ions are added to the solution containing radiobarium. As chemical properties of radiobarium and inactive barium are same[2], both are precipitated together and the lose of radiobarium would be minimal.

Suppose about 10^{10} atoms of barium would be lost by adsorption and other processes. If carrier is not added in the above case, most of the barium atoms would be lost. When a milligram of inactive barium is added, total number of barium atoms corresponds to 4.33 x 10^{18} + 3.59 x 10^8 = 4.33 x 10^{18} atoms. If enough care has been taken to ensure that the chemical state of carrier and the radioisotope are the same and proper isotope exchange is ensured, then even if 10^{10} atoms from this are lost, essentially almost all radiobarium atoms are precipitated. The chemical state of the carrier and the radioelement must be identical for this process to work. For example, in iodine separation radioiodine present in the form of iodide can not be separated with iodate carrier. There are some situations where carriers of same element may not be available, e.g., radium. In such cases a chemical homologue is chosen. It is well known that Hahn and Strassman[3] used barium carrier to precipitate radium which resulted in the separation of radiobarium with barium isotopes as radium was not formed at all.

When a radioisotope has to be separated in pure form from a mixture of radioisotopes of different elements, e.g., from fission products, it becomes necessary to avoid contamination. In such cases, the unwanted radioelements can be held back by using suitable reagents, e.g., fission product iodine is separated by solvent extraction of molecular iodine. To the fission product solution, tellurium and iodide carriers are added. Fission product iodine isotopes may be present in different oxidation states and these are converted to molecular iodine, which is extracted into chlorofom. If tellurium carrier is not added, radiotellurium could enter organic phase by physical adsorption. Here tellurium carrier is added to hold it back in aqueous phase. Carriers used for such purpose are called 'hold back carriers'.

---

[1]Natural uranium consists of three isotopes ^{238}U (99.2745%), ^{235}U (0.720%) and ^{234}U (0.0055%). Only ^{235}U undergoes fission with thermal neutrons.

[2]It is well known that isotopes of an element, in general, behave chemically similar. In the low Z region like hydrogen and lithium, isotope effects are observable.

[3]It is often quoted that, use of barium as carrier for radium separation led to the discovery of fission!! In the fractional crystallisation of sulphates, it was conclusively proved that uranium underwent division.

Often trace impurities are removed by using scavengers. Fe^{3+} acts as a good scavenger. $Fe(OH)_3$ is a gelatanious precipitate and has the property of occluding many ions. For example, to remove impurities from a radiobarium solution, Fe^{3+} carrier is added, the solution is made ammoniacal and Fe^{3+} is precipitated as $Fe(OH)_3$. Most of the unwanted ions are scavenged with $Fe(OH)_3$. From the remaining solution (filtrate), Ba can be precipitated as $BaSO_4$ or $Ba(NO_3)_2$ by acidifying the filtrate. By repeating scavenging and precipitation two or three times, required purity can be achieved.

Time of Separation

Unlike in conventional chemical separations, time of separation becomes often very important parameter in planning a radiochemical separation. If the product formed in a nuclear reaction is very short lived, then the chemical separation has to be fast. In cases where kinetics of the separation process are slow, quantitative separation or chemical yield is sacrificed. In the study of ^{132m}Sb (4.10 min) and ^{133}Sb (2.79 min), antimony isotopes are separated from the fission products and other reaction products by distilling Sb as volatile steben within 30 seconds with a chemical yield around 30%. ^{221}Fr (4.9 min) is a daughter product of ^{225}Ac (10.0 d). Actinium is separated by extracting it into TTA + TOPO in dioxan and purified. This acts as a generator for ^{221}Fr. By contacting with water for 10 s, 80% of ^{221}Fr could be separated and used to determine its half-life and other nuclear properties. Heavy elements like Ha (Z = 105) are separated by using Automated Rapid Chemistry Apparatus (ARCA) based on ion-exchange separations. Separation times are in the range of 2-5 seconds with a chemical yield around 10%.

Radionuclide Purity

In many tracer applications, isotopes with highest purity are required. Both radiochemical purity and radionuclide purity should be ensured. The first one is concerned with chemical form of the isotope and the second one is concerned with the presence of other radioisotopes. Suppose radioiodine is present as iodide (90%) and iodate (10%), then the sample is not radiochemically pure. In many applications, radiochemical purity has to be ensured by adhering to established chemical procedures. On the other hand, radionuclide purity is very crucial as presence of any other radioisotope other than the required one is not acceptable in many applications. Radionuclide purity is established by measuring the half-life and identifying the characteristic α, β or γ ray energies. Presence of other nuclides within the detection limits can be established by spectrometric measurement. However, always care has to be taken at separation stage to eliminate impurities. By choosing appropriate nuclear reaction and energy of the projectile, formation of the required radioisotope is maximised. The best solution is to use enriched isotopes. ^{99m}Tc is an important isotope and is the daughter product of ^{99}Mo (65.94 h). By irradiating MoO_3, ^{99}Mo is produced. Since Mo has stable isotopes of $^{92,94\text{-}98,100}Mo$, two more isotopes, ^{93}Mo (4×10^3 y) and ^{101}Mo (14.61 min) are also formed along with ^{99}Mo. ^{101}Mo is allowed to decay by cooling the irradiated target for a few hours. ^{93}Mo decays by EC and the daughter product

^{93}Nb does not interfere in the chemistry of technetium. Purified molybdenum is loaded on an ion-exchange column and ^{99m}Tc is periodically eluted with required purity for medical use. Details are discussed in Chapter 16.

Specific Activity

Specific activity is the activity per unit weight of the radioisotope. The following examples are worked out for understanding the concept of specific activity in situations where the radioisotope may be present in different chemical forms.

The disintegration rate of one μg of molecular iodine consisting of only ^{131}I isotope will be

$$\frac{6.023 \times 10^{17}}{131} \times \frac{0.693}{8.0207 \times 24 \times 3600}$$

$= 4.6 \times 10^{9}$ Bq $= 4.6 \times 10^{9}$ dps

$\simeq$ 124 mCi (1 Ci $= 3.7 \times 10^{10}$ dps)

$\therefore$ Specific activity = 124 mCi/μg $= 1.24 \times 10^{5}$ μCi/μg

Suppose 10 μCi of carrier free ^{131}I in the form of NaI is administered to a patient for thyroid uptake measurements, the specific activity is calculated as follows.

Activity of ^{131}I (A) = 10 μCi $= 3.7 \times 10^{5}$ Bq

$$\text{No. of I atoms (N)} = \frac{A}{\lambda} = \frac{3.7 \times 10^{5}}{0.693} \times 8.0207 \times 24 \times 3600 = 3.71 \times 10^{11} \text{ atoms}$$

There will be an equal number of Na atoms or NaI molecules. Molecular weight of NaI = 154

$$\therefore \text{ Weight of Na } ^{131}\text{I} = 3.71 \times 10^{11} \times \frac{154}{6.023 \times 10^{23}} = 9.46 \times 10^{-11} \text{ g}$$

$\therefore$ Specific activity = 10 μCi / (9.46×10^{-11} g) $= 1.06 \times 10^{5}$ μCi/μg

Decrease in specific activity from 1.24×10^{5} to 1.06×10^{5} is due to the presence of inactive Na atoms, though in both the cases, samples are carrier free. Depending on the molecular weight of the compound, the specific activity gets modified.

Suppose 10 μCi ^{131}I is separated as molecular iodine by using 5 mg of I^- carrier. The specific activity is calculated as follows:

Total weight of the sample = Weight of the carrier
(assuming that chemical yield is 100%) = 5 mg

The weight of iodine tracer is so small that it can be neglected.

$\therefore$ Specific activity = 10 μCi/5 mg

$= 2 \times 10^{-3}$ μCi/μg

Addition of carrier thus results in low specific activity samples.

For most applications, high specific activity samples are needed. One of the methods is to use non-isotopic carriers in the separation. Yttrium-88 (106.65 d) is separated from the solution of irradiated strontium target by co-precipitating with $Fe(OH)_3$. By two or three cycles of dissolution and precipitation of $Fe(OH)_3$ containing $Y(OH)_3$, the precipitate is dissolved in 9 M HCl and Fe^{3+} is extracted into diisopropyl ether leaving ^{88}Y in aqueous solution. For preparing radioisotope samples of high specific activity, separation procedures like solvent extraction are chosen without addition of inactive carrier.

Some of the separation methods are described below.

Precipitation

Precipitation reactions are useful in radiochemical separations. Carriers are used in the separation scheme based on precipitation. Radioiodine is separated from radiophosphate by precipitating iodine as AgI in the presence of excess nitric acid which prevents precipitation of silver phosphate. AgI precipitate is separated either by filtration or centrifugation. Other activities, if present, invariably get adsorbed on the surface. By washing the precipitate, some of the particulate matter can be removed. Use of the hold back carriers and repeating the cycle of dissolution of precipitate and re-precipitation help in improving the radionuclide purity.

Advantage is taken if an element exists in two or more oxidation states to achieve high decontamination. Cerium exists in Ce(III) and Ce(IV) states. Cerium is precipitated as ceric iodate. If Zr is present it also gets precipitated. Ce(IV) is reduced to Ce(III) and brought into solution whereas Zr remains in Zr(IV) state as zirconium iodate and filtered off. Ce(III) in the filtrate is oxidised to Ce(IV) and ceric iodate is precipitated. By repeating this cycle twice or thrice required purity is obtained.

In the fission product separation, precipitation reactions are useful. Barium and strontium are separated by precipitating as nitrates in presence of Ba and Sr carriers with fuming nitric acid. Separated nitrates are redissolved and impurity activities are removed by using $Fe(OH)_3$ scavenging. Finally, Ba is separated from Sr by chromate precipitation.

Solvent Extraction

If a compound (solute) is soluble in two immiscible solvents, and the solvents and solute are brought into contact, then the solute distributes itself between the two solvents in a definite manner at a certain given pressure, temperature and concentration of the solute. The ratio of the concentration of the solute in the two solvents is called distribution coefficient.

One of the phases is normally organic and the other is aqueous, and this partition is used for selective separation of elements. This technique is known as solvent extraction. Often distribution coefficients are nearly independent of concentrations and, therefore, are very useful for separating carrier free tracers. Solvent extraction separations, in some cases, are quite rapid and particularly applicable for separation of short-lived isotopes. By repeating the cycles of extraction into organic phase and stripping back into aqueous phase, desired radionuclide purity is achieved. Solvent extraction separation is also a useful technique for concentrating the radioisotopes. Gallium is separated from Fe and Tl by extracting $GaCl_3$ in presence of reducing agents by which Fe and Tl are reduced to Fe(II) and Tl(I) and are not extracted. Organo phosphorus compounds like tri-n-butyl phosphate (TBP), tri-n-octyl phosphine oxide (TOPO) and bis-(2-ethylhexyl) O-phosphoric acid (HDEHP) and chelating agents like cupferron, dithizone and thenoyltrifluoroacetone (TTA) are widely used as extractants for radioisotope separations. Optimum conditions for separation of a specific isotope (element) are arrived at by sacrificing yields, separation time etc. For example, although high distribution coefficient for Ac (^{225}Ac) with 0.25 M TTA + 0.25 M TOPO in dioxan was observed at pH = 3.5, decontamination from Ra (^{225}Ra, ^{224}Ra), Bi (^{213}Bi) and Pb (^{208,209}Pb) was found to be maximum at pH = 2. Plutonium and uranium are separated from the irradiated fuel solution by extracting into 30% TBP in kerosene at 3 M HNO_3 in the Purex Process.

Ion Exchange

Ion exchange separation has attained considerable importance as a tool in both fundamental and industrial chemistry. This method has become one of the useful separation techniques for radioelements as it can be applied to tracer as well as macroquantities. Ion exchange is the reversible interchange of ions between a liquid phase and solid material. By choosing proper conditions, ions of the desired material can be exchanged on the column and they can be removed by passing a suitable solution called 'eluent'. Solid ion exchangers have cross linked polymer of high molecular weight as the base and an exchangeable cation or anion. This electrolyte has one very large heavy ion and another small ion with opposite charge that is 'exchangeable'. In the cation exchange resin, for example exchangeable ion is H^+ of sulphonic acid group. In the anionic exchanger, exchangeable ion can be Cl^- or OH^- group. Most popular resins are produced by polymerising styrene in the presence of divinyl benzene. Particle diameters of 0.08-0.16 mm (100-200 mesh size) are commonly used.

A mixture of uranium and thorium is separated using an Dowex-1x8 anion exchange column. Solution containing U and Th is prepared in 6-8 HCl. Uranium, present as anionic species $UO_2Cl_4^{--}$, is exchanged with OH^- on the resin. Thorium does not form anionic species and $ThCl_4$ passes through the column. Uranium can be eluted using dilute HCl (0.1 to 1 M).

Rare earths are exchanged on a cation exchanger column. Individual rare earths are eluted using α-hydroxy isobutyric acid. The rare earths are eluted in the reverse order of their

atomic number. Ion exchangers were used for the isolation of heavy elements in the early experiments of their discovery, e.g., Mandelevium.

Fast Radiochemical Separations

Radiochemical separations performed in a short time period, often comparable to the half-life of short-lived nuclides, are generally called fast or rapid radiochemical separations. The time scale is in the range of a second to few tens of seconds. Separation schemes to isolate radioisotopes in such short time scale are planned based on the type of nuclear reactions, cross-sections, the half-lives, complexity of the reaction products, selectivity of separation and the instrumentation for acquiring data.

Studies on these nuclides provide information on nuclear reaction mechanism and nuclear structure. One of the challenging tasks for nuclear chemists and nuclear physicists is the study of the nuclei far removed from the line of stability and nuclides in the island of stability, if it exists (Fig. 2.5, Chapter 2). Nuclear fission and heavy ion induced reactions are sources for a large number of such radioactive nuclides. To study one or a few nuclides from a complex mixture of products, it is important to transport the reaction products with or without target from the site of their production, to avoid the exposure to high radiation fields, to the site where chemical separations are performed. Since the half-lives are in the order of seconds, transportation systems should be very efficient. Two most commonly used fast transport systems are (i) Gas jet transport system and (ii) Pneumatic Carrier Facility (PCF). Subsequent to transport, the required radioisotope (element) is separated. To achieve separation in short time periods, chemical yield is often sacrificed. However, the selectivity is given utmost priority. Fast radiochemical separation procedures have been developed for many elements produced in nuclear fission and are extended to the separation of heavy elements ($Z > 100$). Most of the elements could be separated in a second or so. Separation procedures are based on techniques like ion-exchange, solvent extraction and volatilisation.

Gas Jet Transport (GJT) System

This is an important transport system in which only reaction products are transported. Target is kept in a chamber which has inlets for carrier gas and an outlet for its exit. Helium gas loaded with a few ppm of fine KCl particles is often used as a carrier gas. Nuclear reaction products produced in the target recoil out of the target. They are thermalised in the carrier gas, get attached to KCl particles and are carried along with the carrier gas in a capillary tube. Reaction products are carried over to distances of 20 meters in a time span of 0.6 to 0.8 second with a yield of 60% and above. Reaction products are deposited over a frit attached to a degassing unit or directly into a solution where mixing and degassing are performed. Selective chemical separation is carried out using this solution. GJT system plays an important role in the studies of heavy elements.

Pneumatic Carrier Facility (PCF)

Target material placed inside a carrier container, called rabbit, is pneumatically sent to the irradiation site, e.g., reactor irradiation position. A timer starts the moment rabbit reaches the irradiation site and after a pre-set time of exposure of the target to neutrons in the reactor, the rabbit is retrieved pneumatically to the chemical processing site. Rabbit travels through a pipe that is very selective to the reactor facility and the diameter of the pipe depends on the size of the rabbit; e.g., 1.2 cm or 2.5 cm. Since the distances between the rabbit shooting and retrieval station, and the irradiation site is fixed, the time taken for retrieval depends exclusively on the pressure of the gas used to carry the rabbit and the distance. The transport time varies between 1 and 5 seconds. In the rabbit irradiation, both target and reaction products are carried back. In the subsequent radiochemical separations, target will also be subjected to chemical processing. This facility is very useful in fission studies and radioanalytical measurements.

Several reviews on fast radiochemical separations are available in the literature. Reviews by Kusaka and Meinke, Herman and Trautmann, Rengan and a monograph by Rengan and Myer are very informative (see Bibliography). Heavy element research not only uses fast radiochemical separations but also it enters into instrumentation for atom-at-a-time chemistry. A review by Wierczinski and Hoffman provides some insight into this area (see Bibliography). Rapid radiochemical separations are broadly separated into batch process and continuous process.

Batch Process

The transportation, chemical separations and data collection are time sequenced and automated using micro processor controlled computers. Hundreds of separation cycles are used to obtain statistically reliable data. An example of this process developed at University of Mainz is described below in which technetium products were separated for nuclear spectroscopic studies. Rabbit containing irradiated plutonium solution with associated fission products was transported and smashed by impact in the chemical apparatus. Fission products Br and I were removed by passing through preformed silver pertechnetate. Washings were collected and oxidised using $(NH_4)_2S_2O_8$ whereby Tc is converted to pertechnetate. This was passed through a layer of chromosorb coated with tetraphenyl arsonium chloride in chloroform into which pertechnetate was extracted. Technetium was removed by washing with 2M HNO_3 and precipitated with $(NH_4)_2ReO_4$; which was filtered, washed and transferred to the counting system. The entire process took 7.5 seconds and a schematic diagram of the entire scheme is given in Fig. 18.1. Many separation schemes are available in literature and references are given in bibliography.

Continuous Processes

Continuous production and separation of radionuclides improves the efficiency of data collection and is applicable with half lives of the order of 1 second or shorter. It involves three steps : (1) continuous production and delivery of reaction products in a time period comparable with the half-life of radionuclide of interest, (2) a system that provides

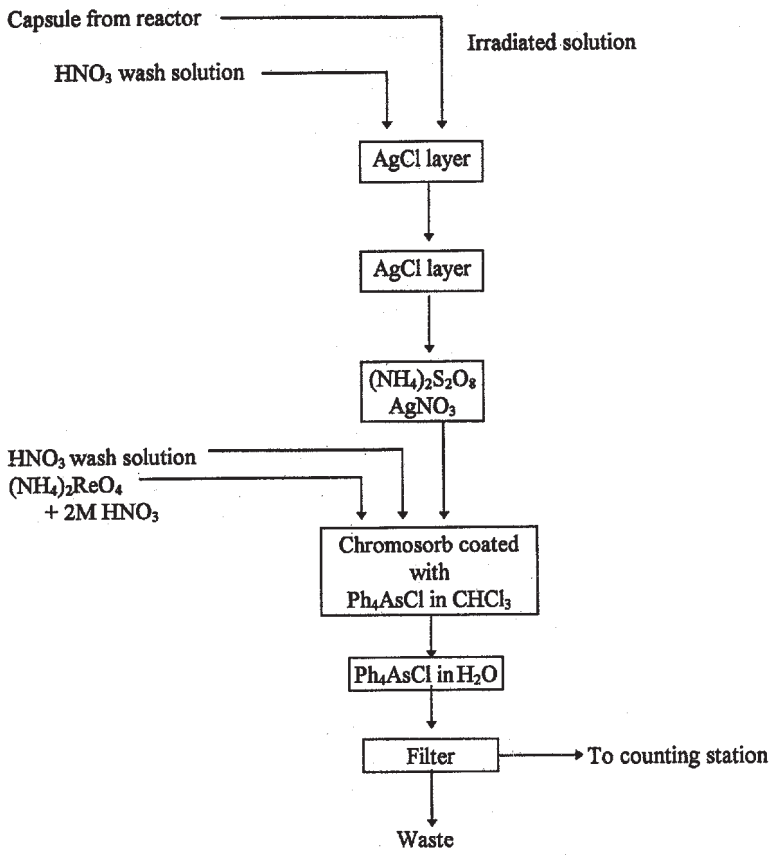

Fig. 18.1 Schematic diagram of technetium separation from fission products. Separation time is 7.5 s [Frontiers in Nuclear Chemistry, Eds. D.D. Sood, A.V.R. Reddy, P.K. Pujari, IANCAS Publication, Mumbai (1996) p.158].

continuous separation and (3) data acquiring system. Solvent extraction based system SISAK (Short lived Isotope Studied by Akufve) proved to be excellent and a number of studies were carried out using this system. It uses small volumes (0.3 mL) H-centrifuges with speeds of 20,000-30,000 rpm and hold up time of 0.05 s. Many short lived fission products were separated using SISAK and of late it is being used in the heavy element studies.

The isotope ^{261}Db produced by ^{243}Am (^{22}Ne,4n) reaction was transported using KCl loaded GJT system to the degasser unit. It was dissolved in 1 M α-hydroxy isobutyric acid and extracted into organic phase trioctylamine in a scintillator. Liquid scintillation detection system was used to measure α, discriminating β-γ activity. A schematic diagram of SISAK 3 is given in Fig. 18.2.

Isothermal gas chromatography is another continuous technique. It is based on the interaction of the reaction products with gases present in the target to form volatile products

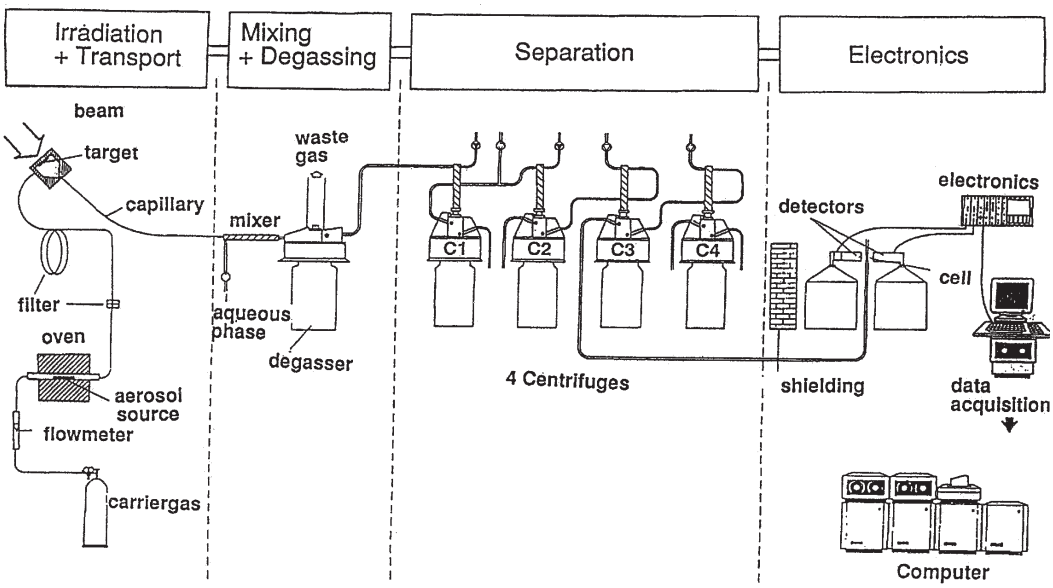

Fig. 18.2 Schematic diagram of SISAK system [Frontiers in Nuclear Chemistry, Eds. D.D. Sood, A.V.R. Reddy, P.K. Pujari, IANCAS Publication, Mumbai (1996) p.185].

which are separated in gas phase to obtain isothermal chromatograms. Details are available in the literature cited in bibliography.

Automated Rapid Chemistry Apparatus (ARCA)

High Performance Liquid Chromatography (HPLC) is very useful for fast radiochemical separations in GJT system. Computer Controlled Automated Rapid Chemistry Apparatus (ARCA) has been successfully used in heavy element studies (see bibliography). The reaction products attached to KCl aerosols are collected on a frit for a fixed period. Then the frit is moved to a position where it is washed by an aqueous phase. While the first frit is washed, collection on another frit takes place. The reaction products are collected in a solvent and pumped onto a microcolumn of 0.5 to 1.7 mm dia and length of 8 mm. After eluting the required product, the solution was collected (0.1 mL volume), evaporated and sent to a detector system. Complete separation takes about 55 s. The entire system is programmed such that one cycle is completed in 1 min. A schematic diagram of ARCA II is shown in Fig. 18.3.

Chemical behaviour of 34 s ^{262}Db produced by ^{249}Bk (^{18}O, 5n) reaction was studied using ARCA II. Trisisooctyl amine on an inert support was used to study anionic halide complex formation and compared with Nb and Ta.

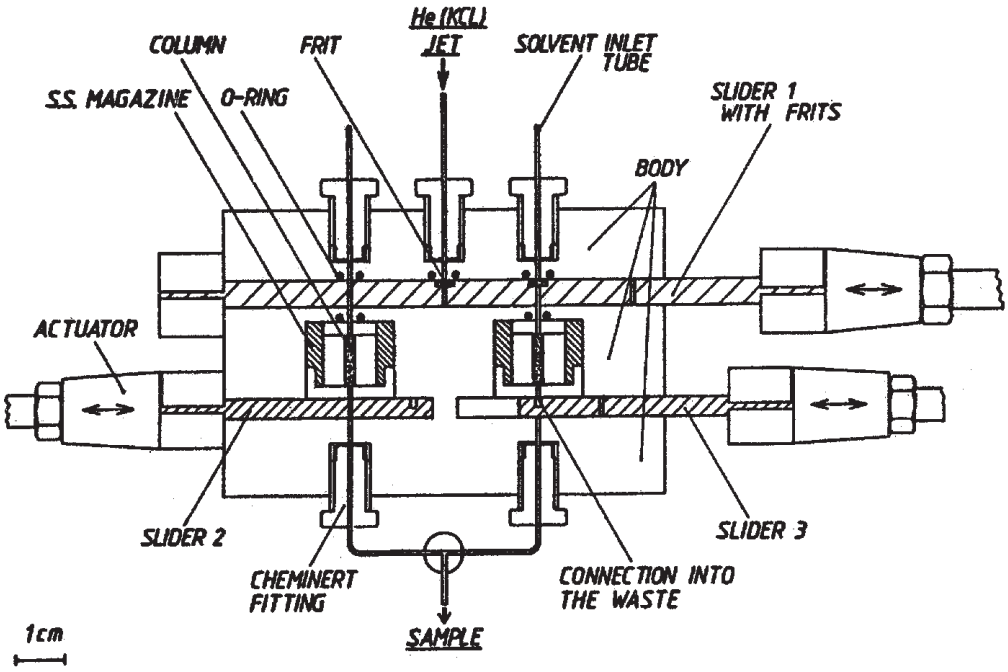

Fig. 18.3 Schematic diagram of ARCA II [Frontiers in Nuclear Chemistry, Eds. D.D. Sood, A.V.R. Reddy, P.K. Pujari, IANCAS Publication, Mumbai (1996) p.181]

Future Outlook

Nuclear chemists are currently interested in the study of nuclides far removed from stability line, particularly, the heavy elements. With half-lives around a second, and production rates of atom-at-a-time, the investigations are really challenging. Planning a chemical scheme, testing that with chemical homologues and applying it in the case of heavy elements provide enough scope to study these elements. Some reactions like $^{249}Bk(^{20,22}Ne,xn)^{266\text{-}268}Ns$; $^{254}Es(^{16,18}O,xn)^{265\text{-}268}Ns$; $^{251}Cf(^{22}Ne,4n)^{269}Hs$ and $^{257}Es(^{20,22}Ne,xn)^{270\text{-}272}Mt$ lead to the products that are expected to belong to the region of deformed stability with half-lives around 1 second giving scope to study these reactions using ARCA, SISAK and gas phase chromatographic techniques.

Bibliography

1. Frontiers in Nuclear Chemistry, Eds. D.D. Sood, A.V.R. Reddy and P.K. Pujari, IANCAS Publication, Mumbai (1996).

2. G. Friedlander, J.W. Kennedy, E.S. Macias and J.M. Miller, Nuclear and Radiochemistry, 3rd Ed., John Wiley & Sons Inc., New York (1981).

3. H.A.C. McKay, Principles of Radiochemistry, Butterworths (1971).

4. J. Tölgyessy and M. Kyrs, Radioanalytical Chemistry, Vol. 1 and 2, Ellis Horword Ltd., England (1989).

5. Y. Kusaka and W.W. Meinke, Rapid Radiochemical Separations, NAS-NS-3104 (1961).

6. G. Herrmann and N. Trautmann, *Ann. Rev. Nucl. Part. Sci.*, **32** (1982) 117.

7. K. Rengan and R.A. Meyer, Ultrafast Chemical Separation, NAS-NS-3118, 49 (1993).

8. M. Schädel et al., *Radiochim. Acta*, **25** (1978) 111.

9. K. Rengan, *J. Radioanal. Nucl. Chem.*, **142** (1990) 173

10. K. Rengan, in 'Frontiers in Nuclear Chemistry', Eds. D.D. Sood, A.V.R. Reddy and P.K. Pujari, IANCAS Publication, Mumbai (1996)

11. B. Wierczinski and D.C. Hoffman, in 'Frontiers in Nuclear Chemistry', Eds. D.D. Sood, A.V.R. Reddy and P.K. Pujari, IANCAS Publication, Mumbai (1996).

12. J.V. Kratz et al., *Radiochim. Acta*, **48** (1989) 121.

13. M. Schädel, in 'Hundred Years of X-rays and Radioactivity (RON-BEC 100), Eds. D.D. Sood, H.C. Jain, A.V.R. Reddy, K.L. Ramakumar and S.G. Kulkarni, BARC, Mumbai (1996).

14. J.V. Kratz, in Proc. of DAE Symposium on Nuclear and Radiochemistry (NUCAR 97), Eds. K.L.Ramakumar, P.K. Pujari, R. Swarup and D.D. Sood, BARC, Mumbai (1997).

Chapter 19
Radiation Chemistry

Ionising radiation interacts with matter and results in a number of physical changes as well as formation of reactive chemical species. In gases an energy 30-35 eV is required for the production of an ion pair. Thus radiation chemistry deals with chemical effects of radiation (β, γ or charged particles) having energy substantially above 50 eV, quite often in the keV to MeV range. Each photon/particle can excite/ionise thousands of molecules along its path and cause the formation of distinct tracks in matter. Neutrons cause chemical effects indirectly through the formation of charged particles by interaction with matter.

Curie and Debierne found, in 1901, that a hydrated uranium salt produced gas continuously. Giesel in 1902 observed the evolution of gas from an aqueous solution of radium bromide and later observed that the gas was a mixture of hydrogen and oxygen. Madame Curie was the first to propose that the primary effect of the ionising radiation is to produce ions that are precursors for chemical changes. Lind put the relation between ionisation and chemical reactions on a firmer ground. In aqueous systems the most prominent reaction is the formation of free radicals H and OH.

$$H_2O \qquad H + OH \tag{19.1}$$

In the CGS system, used until recently, the number of molecules of a product formed or destroyed per 100 eV of absorbed energy was called the G value. In a system, G value is given by

$$G = \frac{M}{N} \times \frac{100}{W} \tag{19.2}$$

where W is the mean energy required to form an ion pair in the liquid and M/N is the ratio of number of molecules undergoing change (M) to the number of ion pairs formed (N) known as the ionic yield. In SI system G is defined as the number of moles of the product form for one joule of energy absorbed and is related to the CGS system as 1 molecule per 100 eV = 0.1036 μmol per joule. G values have been reported for a wide variety of reactions, but these are very sensitive to experimental conditions such as the presence of impurities (e.g., dissolved oxygen in aqueous solutions) and build up of the radiolytic products.

The main steps in radiation induced reactions are the formation of ions and excited molecules, followed by free-radical reactions leading to stable chemical products. Over the years there has been a lot of emphasis on understanding the reaction mechanism of the series of fast reactions which lead to the formation of the final product. For example, in the case of water, the most common reaction medium, the following reactions are known to take place.

$$H_2O \qquad H_2O^+ + e^- \qquad (19.3)$$

$$H_2O^+ + H_2O \rightarrow H_3O^+ + OH^\bullet \qquad (19.4)$$

$$e^- + H_2O \rightarrow H^\bullet + OH^- \qquad (19.5)$$

where $H^\bullet$ and $OH^\bullet$ are free radicals. Free radicals are atoms or molecules having one or more unpaired electrons. Even the simplest of the radiation chemistry reactions involve a variety of reaction intermediates which react at different rates. Pulse radiolysis, mostly using pulses of electrons from an accelerator, has been very useful in understanding the complex reaction pathways.

Primary Radiation Effects

Absorption of ionising radiation by matter results in the formation of tracks of ionised and excited species. The nature of these species does not depend on the nature of the incident radiation and, therefore, the chemical effects are qualitatively similar. However, as the energy transfer per unit length (linear energy transfer, LET) is much more for charged particles like protons and alpha particles, as compared to the gamma-rays or X-rays, the quantities of reaction products depend on the type of radiation. This is particularly true for liquids.

Most often the primary radiation produces electrons which are quite energetic and cause further ionisation. If the energy of the secondary electrons is small (< 100 eV), they are readily absorbed close to the original ionisation site, giving a small cluster (spur) of excited and ionised species. With secondary electrons of 100-500 eV energy a cluster of spurs (blobs) are formed. Secondary electrons having higher energy are called delta (δ) rays and they form tracks on their own, branching from the primary track. For a 1 MeV electron on an average more than 10^4 ion pairs are produced per incident particle.

Specific ionisation, the average number of ion pairs produced in a medium per unit length of track, gives a measure of the rate of energy loss by a charged particle and of the density of ionisation in the particle track. It includes both ions produced in the primary particle track and those produced by δ-rays. For protons, alpha particles etc. the specific ionisation is nearly constant up to 2 MeV and then increases strongly as the particle slows down.

As the quantitative aspects of the chemical reactions depend on the density of ionisation in a track, the concept of linear energy transfer is very important. Some data for aqueous medium are given in the following sentences. For electrons having an energy of

1 MeV and above, LET is approximately 0.2 keV μm^{-1}. Below 1 MeV it increases sharply and is ~100 keV μm^{-1} at 0.1 keV energy. For ^{3}H beta-rays the average is 4-7 keV μm^{-1}. For ^{60}Co gamma-rays LET is approximately 0.23 keV μm^{-1}. For 50 kV X-rays the average value is 6.3 keV μm^{-1}. For 5.3 MeV α-particles the average LET is 43 keV μm^{-1}.

Radiation Dosimetry

Quantitative studies in radiation chemistry require a knowledge of the energy transferred by the incident radiation to the medium under investigation, and if possible, the energy distribution. This subject is called dosimetry. Dosimetry of homogeneous chemical systems is discussed here briefly and dosimetry related to non-homogeneous systems encountered in health physics, radiology and clinical radiobiology are not covered. The unit of absorbed dose is gray (Gy) and it is measured in joules per kilogram (Jkg^{-1}).

Calorimetry

Curie and Laborde used the rise in temperature of a graphite block to measure the energy release by the decay of radium. This principle is successfully used even today and very precise and compact calorimeters are available. Calorimetry is more common for standardising dose for radiation therapy.

Ionisation Measurement

The use of ion chambers for radiation measurement has already been discussed in Chapter 7. Standard free-air ionisation chambers (for radiation of <300 keV energy) and parallel plate ionisation chambers are typical examples for this purpose. The measured ionisation can be converted to absorbed dose using Bragg-Gray cavity principle. Details are available in references cited in the bibliography.

Charge Collection Measurement

For charged particles, the particle fluence rate of a beam can be determined by measuring the total charge using a Faraday cup. A metal block, supported on an insulator block and housed in a vacuum chamber, completely stops the beam and charge acquired by the block causes a flow of current which is proportional to the fluence. The energy of the particles can be known from the characteristics of the source or determined by magnetic deflection. Calorimetry can also be used.

Chemical Dosimetry

In a chemical dosimeter the yield of a chemical species formed due to radiation is measured. This yield is compared with the yield when a known quantity of radiation was incident on the calorimeter. Chemical dosimeters are thus secondary dosimeters.

The primary requirement for a chemical system to be suitable for dosimetry are:

(i) The chemical yield should be proportional to the absorbed dose over a wide range.

(ii) The yield should be independent of the dose rate. The range may vary from a few Gy min^{-1} to 10^{11} Gy s^{-1}.

(iii) The yield should be independent of the LET of radiation.

(iv) The yield should be independent of temperature, and

(v) The yield should be reproducible (Precision ± 1 to 5%)

Some additional criteria are dictated by practical considerations. Two dosimeters which are most often employed are Fricke dosimeter and ceric sulphate dosimeter.

Fricke dosimeter is based on the radiation induced conversion of ferrous ion to ferric ion at low pH and in the presence of oxygen. The standard dosimeter solution contains 1 mol m^{-3} ferrous ammonium sulphate, 1 mol m^{-3} NaCl in 400 mol m^{-3} H_2SO_4 (pH 0.46), and is saturated with air (the concentration of dissolved oxygen is ~0.25 mol m^{-3}). The measured dose is independent of small changes in the concentration of reagents. The solution should not be stored for more than a few days because of slow oxidation of ferrous ion. Impurities, particularly organic, must be strictly avoided. Spectrophotometric measurement at approximately 304 nm is used to measure ferric ions formed and normally spectrophotometric cell with a path length of 0.01 m or higher is used. The G value is taken as $G(Fe^{3+})_{\in 304} = 352 \times 10^{-6}$ m^2 kg^{-1} Gy^{-1} (25°C).

The G value is LET dependent being 1.61 μmol J^{-1} for ^{60}Co γ-rays (average energy is 1.25 MeV). This is also the value for higher energy photons and electrons having energy in the range of 1 to 30 MeV. It reduces to 1.50 μmol J^{-1} for 60 keV photons and to 0.31 μmol J^{-1} for ^{235}U fission fragments. The absorbed dose is kept between 50 and 350 Gy as beyond this the consumption of oxygen inhibits Fe^{3+} formation. Use of oxygen instead of air, and increase in Fe^{3+} concentration to about 20 mol m^{-3} can enhance the range by a factor of 4. The dosimeter response is independent of dose rate up to 2×10^6 $Gy.s^{-1}$.

In ceric sulphate dosimeter the radiation induced reduction of Ce^{4+} to Ce^{3+} is used. Dissolved oxygen is not important and an upper dose limit of 10^6 Gy is set by the complete reduction of Ce^{4+} to Ce^{3+}. Ceric sulphate concentration between 0.01 and 400 mol m^{-3} in H_2SO_4 of 400 mol m^{-3} can be used. At low Ce^{4+} concentrations (< 0.2 mol m^{-3}) spectrophotometric measurements of Ce^{4+} at 320 nm is used. A higher absorbed dose redox titration can yield better results. Some typical G (Ce^{3+}) values are 0.25 μ mol J^{-1} for ^{60}Co γ-rays, 0.326 μ mol J^{-1} for 200 kV X-rays and 0.332 μ mol J^{-1} for ^{210}Po α-rays.

A large variety of other chemical dosimeters are used for specific applications. For example, oxalic acid in-reactor dosimetry and organic dye like methylene blue (which bleaches) for commercial irradiators. Use of solid alanine is also common for commercial irradiators in which the concentration of trapped radicals formed due to radiation is measured by electron paramagnetic resonance.

Radiolysis Intermediates

The first reactive species formed by the interaction of radiation are the ions and excited molecules roughly in equal amounts. These can directly react to give stable chemical products or through formation of intermediate free radicals. After the initial interaction the absorbed energy is rapidly distributed and chemically reactive ions, excited molecules and free radicals are formed by the loss/excitation of less firmly bound outer shell electrons. Examples include nonbonding electrons on oxygen and nitrogen, and p electrons of unsaturated compounds.

Ions

Typical ionisation reactions are:

$$\begin{aligned} CH_4 \quad & CH_4^+ + e^- \\ & CH_3^+ + H + e^- \\ & CH_2^+ + H_2 \text{ (or } 2H) + e^- \end{aligned} \qquad (19.6)$$

For methane the value of W is 27.3 eV which would give about 3 ion pairs per 100 eV of absorbed energy. In polar solvents ions may be stabilised by solvation or a number of other reactions including recombination may take place as discussed below.

Energy rich (excited) polyatomic ions may dissociate to give secondary ions/radicals.

$$(CH_4^+)^* \rightarrow CH_3^+ + H^\bullet \qquad (19.7)$$

$$(C_2H_6^+)^* \rightarrow C_2H_4^+ + H_2 \qquad (19.8)$$

Fragmentation is prominent in gas phase reactions but less in liquids and solids. The ions could also transfer their charge to a neutral atom/molecule.

$$He^+ + Ne \rightarrow He + Ne^+ \qquad (19.9)$$

When the ionisation potential of the incident ion is significantly higher than that of the reacting molecule, charge transfer may be accompanied by dissociation.

$$Ar^+ + CH_4 \rightarrow Ar + CH_3^+ + H^\bullet \qquad (19.10)$$

A third mechanism is the reaction of ions with molecules.

$$CH_4^+ + CH_4 \rightarrow CH_5^+ + {}^\bullet CH_3 \qquad (19.11)$$

$$H_2O+ + H_2O \rightarrow H_3O^+ + {}^\bullet OH \qquad (19.12)$$

$$H_2^+ + O_2 \rightarrow H^\bullet + HO_2^+ \qquad (19.13)$$

$$CH_3^+ + CH_4 \rightarrow C_2H_5^+ + H_2 \quad (19.14)$$

$$C_4H_8^+ + C_4H_8 \rightarrow C_4H_9^+ + {}^{\bullet}C_4H_7 \quad (19.15)$$

$$C_4H_9^+ + C_4H_8 \rightarrow C_8H_{17}^+ \quad (19.16)$$

The last two reactions represent the initiation of radiation induced polymerization of isobutene.

Electrons are sometimes (though rare) captured by some molecules to form new products.

$$CH_3Br + e^- \rightarrow Br^- + {}^{\bullet}CH_3 \quad (19.17)$$

$$O_2 + e^- \rightarrow O_2^- \quad (19.18)$$

$$H_2O + e^- \rightarrow e_{aq}^- \rightarrow OH_{aq}^- + H^{\bullet} \quad (19.19)$$

The ions get neutralised by combining with electrons and many times this may result in the formation of reactive species.

$$C_2H_5^+ + e^- \rightarrow {}^{\bullet}C_2H_5 \text{ or } {}^{\bullet}C_2H_5 * \quad (19.20)$$

$${}^{\bullet}C_2H_5* \rightarrow C_2H_4 + H^{\bullet} \quad (19.21)$$

Neutralisation is delayed by solvation of ions/electrons.

Some molecules have high affinity for ions/radicals and quite often used as scavengers in the study of reaction mechanisms. Lewis bases like ammonia, amines, water and alcohols accept protons from the ionised species.

$$RH^+ + NH_3 \rightarrow R + NH_4^+ \quad (19.22)$$

$$RH^+ + H_2O \rightarrow R + H_3O^+ \quad (19.23)$$

Compounds which undergo electron addition reactions are used as electron scavengers.

$$e_{aq}^- + N_2O \rightarrow N_2O^- \xrightarrow{H^+} N_2 + {}^{\bullet}OH \quad (19.24)$$

$$e_{aq}^- + H^+ \rightarrow H^{\bullet} \quad (19.25)$$

Excited Molecules

Excited molecules may be formed by excitation of one of the electrons in a pair in the ground state. Normally excitation to higher level does not involve any change in spin (singlet state). Radiative loss of a part of energy may result in the change of spin of the excited molecule leading to the formation of triplet excited state. As triplet state has two unpaired electrons, it behaves like a diradical. Unlike in photochemistry, a large fraction of molecules

directly attain triplet state in radiation chemistry. As de-excitation to ground state is a forbidden transition, the excited state is long lived (up to a few seconds) and this along with their diradical character makes molecules in the triplet excited state important in chemical reactions.

Free Radicals

Free radicals are atoms or molecules having one or more unpaired electrons. Breakage of a covalent bond can lead to the formation of two free radicals.

$$R : S \qquad R^{\bullet} + {}^{\bullet}S \tag{19.26}$$

The • on R and S is representing unpaired electron. This is normally omitted for small radicals like H, OH and Cl. Free radicals can also be charged species, e.g., e^{-}_{aq} , O^{-}, O^{-}_{2}, CH^{+}_{4} and $^{\bullet}CH_2CO^{-}_{2}$. The unpaired electron makes free radicals very reactive. Electron transfer and electron pairing are the most common modes of reaction. Radicals such as H, OH and $^{\bullet}CH_3$, have only transient existence, whereas long and bulky organic radicals are relatively stable. Some typical free radical reactions are given below:

(i) Radical rearrangement to give a more stable free radical

$$Ph_3C - CH^{\bullet}_{2} \rightarrow Ph_2C - {}^{\bullet}CH_2Ph \tag{19.27}$$

(ii) Radical dissociation

$$Br_2CH - {}^{\bullet}CHBr \rightarrow Br^{\bullet} + BrCH = CHBr \tag{19.28}$$

$$CH_3CO^{\bullet}_{2}(g) \rightarrow {}^{\bullet}CH_3(g) + CO_2(g) \tag{19.29}$$

(iii) Addition reaction (Reverse of dissociation)

$$Br^{\bullet} + R - CH = CH_2 \rightarrow R - {}^{\bullet}CH - CH_2Br \tag{19.30}$$

(iv) Abstraction reaction

$$^{\bullet}OH + CH_3OH \rightarrow H_2O + {}^{\bullet}CH_2OH \tag{19.31}$$

$$H^{\bullet} + CH_3I \rightarrow HI + {}^{\bullet}CH_3 \tag{19.32}$$

(v) Radical combination

$$2\ {}^{\bullet}CH_3\ (g) \rightarrow C_2H_6(g) \tag{19.33}$$

$$H^{\bullet}(g) + C_2H_5(g) \rightarrow C_2H_6{}^{*}(g) \tag{19.34}$$

(vi) Disproportionation

$$2\ {}^{\bullet}C_2H_5(g) \rightarrow C_2H_6(g) + C_2H_4\ (g) \tag{19.35}$$

$$2\ CH^{\bullet}_{3}CHOH \rightarrow CH_3CH_2OH + CH_3CHO \tag{19.36}$$

(vii) Electron transfer

$$^{\bullet}OH + Fe^{2+} \rightarrow Fe^{3+} + OH^{-} \quad (19.37)$$

(viii) Reaction with oxygen

Oxygen molecule with two unpaired electrons in π^*antibonding molecular orbitals behaves like a molecule with two free radical centres. Some reactions are:

$$R^{\bullet} + {}^{\bullet}O = O^{\bullet} \rightarrow RO_2^{\bullet} \quad (19.38)$$

The peroxy radical $RO_2^{\bullet}$ is relatively stable. Following chain reactions can subsequently take place

$$RO_2^{\bullet} + RH \rightarrow RO_2H + R^{\bullet}$$

$$2RO_2H \rightarrow RO_2^{\bullet} + RO^{\bullet} + H_2O$$

$$RO^{\bullet} + RH \rightarrow ROH + R^{\bullet} \quad (19.39)$$

These reactions are important in drying oil-based paints and deterioration of rubbers and polymers. Peroxy radicals are strong oxidising agents and a few reactions are given below.

$$HO_2^{\bullet} + Fe^{2+} \rightarrow HO_2^{-} + Fe^{3+} \quad (19.40)$$

$$HO_2^{\bullet} + NO \rightarrow OH + NO_2 \quad (19.41)$$

$$2\ HO_2^{\bullet} \rightarrow H_2O_2 + O_2 \quad (19.42)$$

(ix) Radical scavenging

Scavengers for free radicals are added to attain a concentration of about 1 mol m^{-3}. These include oxygen, nitric oxide, iodine, hydrogen iodide, organic iodides and transition metal salts.

$$R^{\bullet} + I_2 \rightarrow RI + I^{\bullet} \quad (19.43)$$

$$I^{\bullet} + I^{\bullet} \rightarrow I_2 \quad (19.44)$$

However, because of many side reactions of I_2, hydrogen iodide is a better scavenger.

$$R^{\bullet} + HI \rightarrow RH + I \quad (19.45)$$

Radiation Chemistry in Different Media

In reactions involving solutions the solvent is the main recipient of the radiation energy and the reactive species produced from the solvent guide the chemical reactions of the solute. Some typical systems are discussed below.

Aqueous Inorganic Systems

Some prominent reactions with water, as discussed earlier, are

$H_2O \qquad H_2O^+ + e^-$ or H_2O^*

$H_2O^+ + H_2O \rightarrow H_3O^+ + OH$

$H_2O^* \rightarrow H + OH \rightarrow H_2O$

$e^- + H_2O \rightarrow e^-_{aq}$

$$e^-_{aq} + H_2O \rightarrow H + OH^- \qquad (19.46)$$

$$e^-_{aq} + H^+_3O \rightarrow H + H_2O \qquad (19.47)$$

$$H + H \rightarrow H_2 \qquad (19.48)$$

$$OH + OH \rightarrow H_2O_2 \qquad (19.49)$$

$$OH + H_2O_2 \rightarrow H_2O + HO_2 \qquad (19.50)$$

The steady state concentration of the reactive species is quite low and depends upon the LET of the radiation. Free radicals e^-_{aq} and H act as reducing species and free radicals OH, HO_2 as well as molecular H_2O_2 act as oxidising agents. In oxygenated systems e^-_{aq} and H are readily scavenged by dissolved oxygen and perhydroxyl radical (HO_2) becomes important. The species HO_2 is stable at pH 4.5 and lower. At pH 5 and higher, O^-_2 is the main species. HO_2 is a stronger oxidising agent than O^-_2, but it can act both as an oxidising and a reducing agent. It can oxidise ferrous to ferric state but reduces ceric to cerous state.

$$HO_2 + Fe^{2+} \rightarrow Fe^{3+} + HO^-_2 \ (+H^+ \rightarrow H_2O_2) \qquad (19.51)$$

$$HO_2 + Ce^{4+} \rightarrow Ce^{3+} + O_2 + H^+ \qquad (19.52)$$

Hydrogen peroxide can also act as a redox agent

$$H_2O_2 + Fe^{2+} \rightarrow Fe^{3+} + OH^- + OH \qquad (19.53)$$

$$H_2O_2 + Ce^{4+} \rightarrow Ce^{3+} + HO_2 + H^+ \qquad (19.54)$$

Aqueous Organic Systems

The free radicals or other radiolytic products of water are the primary species in aqueous organic systems. Whereas in inorganic systems the redox reactions are the main focus, in the organic systems abstraction and addition reactions take place. The primary radiolytic products tend to react with the functional groups in organic molecules to produce organic radicals and stable products. Unsaturated groups and thiol group have a higher tendency for reactions. Typical reactions with alcohols are as follows:

$$H + CH_3OH \rightarrow H_2 + {}^{\bullet}CH_2OH \quad (19.55)$$

$$OH + CH_3OH \rightarrow H_2O + {}^{\bullet}CH_2OH \quad (19.56)$$

$$2\,{}^{\bullet}CH_2OH \begin{cases} \rightarrow CH_3OH + HCHO \\ \rightarrow (CH_2OH)_2 \end{cases} \quad (19.57)$$

Reactions of amino acids are important as they are constituents of proteins. Reaction of glycine (NH_2CH_2COOH) in near neutral solutions, where it exists as $NH_3^+CH_2CO_2^-$, are as follows:

$$e_{aq}^- + NH_3^+CH_2CO_2^- \rightarrow NH_3 + {}^{\bullet}CH_2CO_2^- \quad (19.58)$$

$$H + NH_3^+CH_2CO_2^- \rightarrow H_2 + NH_3^+\,{}^{\bullet}CHCO_2^- \quad (19.59)$$

$$OH + NH_3CH_2CO_2^- \rightarrow H_2O + NH_3\,{}^{\bullet}CHCO_2^- \quad (19.60)$$

$$NH_3^+\,{}^{\bullet}CHCO_2^- + {}^{\bullet}CH_2CO^- \rightarrow NH_2^+ = CHCO_2^- + CH_3CO_2^- \quad (19.61)$$

Organic Systems

Chemical effects of radiation on polar organic compounds are similar to those on water as the electrons and secondary positive ions are stabilised by solvation and ion recombination is delayed. In non-polar solvents, the ion recombination occurs before the expansion of the spur.

Irradiation of alcohol gives H_2, CO, aldelydes and secondary or tertiary alcohols. In the absence of oxygen, glycols are formed. Among non-polar solvents cyclohexane yields hydrogen, cyclohexene and bicyclohexyl

$$C\text{-}C_6H_{12} \qquad c\text{-}C6H_{11}^{\bullet} + \quad (19.62)$$

$$H + c\text{-}C_6^{\bullet}H_{11} \rightarrow c\text{-}C_6H_{10} + H_2 \quad (19.63)$$

$$2\ c\text{-}C_6^{\bullet}H_{11} \rightarrow C_{12}H_{22} \quad (19.64)$$

In the case of normal hexane, there is a larger number of products in C_1-C_5 and C_7-C_{11} range. Other straight chain hydrocarbons have similar reactions.

Among chloro-hydrocarbons carbon tetrachloride yields mainly chlorine and hexachloroethane.

$$CCl_4 \qquad CCl_4^+ + e^- \quad (19.65)$$

$$e^- + CCl_4 \rightarrow {}^{\bullet}CCl_3 + Cl^-$$

$$CCl_4^+ + Cl^- \rightarrow CCl_4 + Cl$$

$$2\ {}^{\bullet}CCl_3 \rightarrow C_2Cl_6 \qquad (19.66)$$

In unsaturated hydrocarbons the yield of hydrogen is lower and that of high molecular weight products are higher. Liquid and solid aromatic compounds are much more resistant to radiation damage than alkanes and alkenes. Aromatic groups act as energy sinks. Dimeric and polymeric products are formed by irradiation.

Radiation in Chemical Processes

The formation of reactive free radicals has potential for application in many chemical processes. However, the G value in most chemical reactions is less than 1 μ mol J^{-1} and any process would be uneconomical unless a chain reaction increases the value to 10^2-10^3 μ mol J^{-1} or higher. Over the years many synthetic and polymeric reactions have reached the industrial scale but only polymeric reactions are currently in use for a variety of products.

Synthetic Reactions

One of the simplest reactions is the reaction of H_2 and Cl_2 to form HCl with a G value of 10^3 - 10^4 μ mol J^{-1}

$$Cl_2 \qquad 2C \qquad (19.67)$$

$$Cl + H_2 \rightarrow HCl + H$$

$$H + Cl_2 \rightarrow HCl + Cl$$

$$H + Cl \rightarrow HCl \qquad (19.68)$$

This reaction was used for several years in the former USSR to eliminate H_2 from the chlorine stream of an electrolyser.

The largest plant (450 te/y) to use radiation for chemical synthesis was set up by Dow Chemicals, and operated for 8 years, for making bromoethane by the reaction of HBr and $CH_2 = CH_2$

$$Hbr \qquad H + Br \qquad (19.69)$$

$$Br + CH_2 = CH_2 \rightarrow {}^{\bullet}CH_2\text{-}CH_2Br$$

$${}^{\bullet}CH_2 - CH_2Br + HBr \rightarrow CH_3CH_2Br + Br \qquad (19.70)$$

G value ranges 10^3-10^4 μ mol J^{-1} for this reaction.

Another reaction exploited commercially (175 te/y) in the USSR for many years is the reaction of ethylene with CCl_4 to get tetrachloropropane and tetrachloropentane

$$CCl_4 \qquad Cl + {}^{\bullet}CCl_3 \qquad (19.71)$$

$$^{\bullet}CCl_3 + CH_2 = CH_2 \rightarrow {}^{\bullet}CH_2 - CH_2 - CCl_3$$

$$^{\bullet}CH_2 - CH_2 - CCl_3 + CCl_4 \rightarrow ClCH_2 - CH_2 - CCl_3 + {}^{\bullet}CCl_3$$

$$^{\bullet}CH_2 - CH_2 - CCl_3 + CH_2 = CH_2 \rightarrow {}^{\bullet}CH_2 - CH_2 - CH_2 - CH_2 - CCl_3 \qquad (19.72)$$

$$^{\bullet}(CH_2 - CH_2)_2 - CCl_3 + CCl_4 \rightarrow Cl - CH_2 - (CH_2)_3 - CCl_3 + {}^{\bullet}CCl_3 \qquad (19.73)$$

G value of the reaction was approximately 200 μmol J^{-1}

Another commercial plant operated in the USSR was for sulphochlorination of alkanes to obtain sulphonyl chlorides.

$$RH \qquad R^{\bullet} + H \qquad (19.74)$$

$$R^{\bullet} + SO_2 \rightarrow RSO_2^{\bullet}$$

$$RSO_2^{\bullet} + Cl_2 \rightarrow RSO_2Cl + Cl$$

$$Cl + RH \rightarrow HCl + R^{\bullet} \qquad (19.75)$$

G values of 10^3-10^4 were obtained.

Polymerisation Reactions

Many simple organic molecules, for example ethylene, can undergo a chain reaction to yield polymeric compounds having a wide range of industrial application. Chemical techniques to initiate and propagate a chain reaction involve the use of sensitisers or catalysts. However, radiation induced free radical can fulfil the same role in a more effective manner and, therefore, gamma-rays and electrons are extensively used for the manufacture of special polymers.

Industrial Applications of Radiation

Radiation is widely used for a variety of applications in industry and a few applications are briefly described.

Radiation Processing of Polymers

Crosslinking of Polyethylene

The classical example of the radiation processing in polymer chemistry is polyethylene (PE) cross-linking. Industrial production of insulating materials based on irradiated PE in the form of sheets was developed in early 1950s in the USA. Radiation cross-linking of PE increases the mechanical strength, as well as the heat and environmental stability, which greatly extend the field of application for PE.

When polymers are irradiated with ionising radiation, very reactive intermediates in the form of excited molecules, ions and free radicals are formed, which are the precursors of further chemical transformations. This results in fundamental changes in the chemical structure and hence, in the properties of polymers. Typical reactions leading to the cross-linking of PE when irradiated with ionising radiation can be given as:

$$-CH_2-CH_2- \rightarrow (-CH_2-CH_2-)^* \rightarrow -CH_2-\overset{\bullet}{C}H- + \overset{\bullet}{H} \qquad (19.76)$$

Recombination of two macro-radicals produces cross-linked structures:

$$\begin{matrix} -CH_2-CH_2-\overset{\bullet}{C}H-CH_2 \\ \\ CH_2-CH_2-\overset{\bullet}{C}H-CH_2 \end{matrix} \rightarrow \begin{matrix} -CH_2-CH_2-CH-CH_2 \\ \quad\quad\quad\quad\quad\quad\quad\quad | \\ -CH_2-CH_2-CH-CH_2 \end{matrix} \qquad (19.77)$$

The properties of a cross-linked polymer are determined by the network density. By increasing the absorbed radiation dose, it is possible to control the network density and thus the polymer properties. Shape stability, and resistance to heat, solvents and aggressive chemical agents increases with increased cross linking of PE. The heat stability of PE cross linked by chemical agents and by radiation is as follows:

	Chemical cross linking	Radiation cross linking
Maximum temperature of long term service (^oC)	90	150
Maximum temperature of short term service (^oC)	250	350

In addition to its technical superiority, other advantages of the radiation induced cross-linking over the traditional techniques are the higher throughput and decrease in energy expenditure and waste production. Radiation cross-linking of PE is used for the production of heat shrinkable materials, polyethylene foam and polyethylene hot water distribution pipes.

Heat-Shrinkable Materials

Many semi-crystalline thermoplastics exhibit a so-called “memory effect”. This effect, discovered by A. Charlesby, is the ability of the irradiated and deformed polyethylene (or any other polymer having some crystallinity) to return to the initial state after heating. A PE sample is first exposed to irradiation, forming a three dimensional network and then heated above the softening temperature and allowed to deform. During subsequent cooling, the sample is recrystallised and the chains are fixed in a new configuration. This sample retains its shape for any period of time as long as it is kept at ambient temperatures. This is due to the effect of crystalline phase superimposed on the deformed structure of the previously cross-linked material. If the sample is heated again, the sample softens and returns to its initial shape under the influence of intermolecular cross-links it had before deformation. Polyethylene excels other polymers in exhibiting memory effect. The effect of heat shrinkage is widely used, mainly for the production of various heat-shrinkable tubes, couplings, films for impermeable casings, jackets and various packaging materials.

Heat-shrinkable tubes are increasingly used for insulation and sealing of cable joints. A stream of hot air from a blower or slight exposure to a burner flame are sufficient for the tube to insulate and seal the required parts as a result of heat shrinkage.

Polymer Foams

Radiation technology is also used for the production of polyethylene based foamed polymers. Cross-linked PE foam can be obtained in a continuous process contrary to the batch chemical process. Generally electron accelerators are used for this purpose. In continuous production of PE foam, different ingredients are mixed. A foaming agent like diazocarbonamide is used, which can produce about 200 cm^3 of gas (60% N_2 and 25% CO_2) per gram at 200^oC. Cross-linking takes place at doses of 20-100 kGy, and cross-link density can be easily controlled. Upon subsequent heating under conditions of hot pressing, foam can be obtained in any desired shape. Articles made from PE foam are used in civil engineering, automobile industry and in the manufacture of sports goods.

Radiation Processing in Cable, Wire and Tyre Industries

In the wire and cable industry, many types of polymers are used for electrical insulation. The most common insulation materials include polyethylene, polyvinyl chloride and ethylene-propylene rubber. Some constraints arise in the use of these materials because of the physical properties of these thermoplastics which include; plastic flow at elevated temperatures, environmental stress cracking, poor solvent resistance and low softening temperatures. By linking the polymer chains into a network via cross-linking, the toughness, flexibility, impact resistance, chemical resistance and working temperatures are greatly improved. Both physical and chemical cross-linking processes are used in the wire and cable industry. Physical cross-linking technology uses ionising radiation whereas chemical cross-linking technology either uses peroxide and heat or silane and water systems as tools for cross-linking. Radiation cross-linked PE is widely used for computer wiring, hook-up wiring, building and appliance wiring, automobile wires, power cables, power station control cables and communication wires. Unmodified PE can easily be radiation cross-linked without the need for any special additives. Radiation cross linked polymers with insulation temperature ratings of up to 150^oC are available. The usual antioxidants for wire and cable do not impede the radiation process. The dose required, however, may be as high as 300 kGy if a very high degree of cross-linking (80%) is required. For many applications a dose of 200 kGy or less yields adequate cross-linking. Radiation sensitising additives, usually multifunctional monomers such as triallyl cyanurate, polyethylene glycol dimethacrylate or tri methylol propane tri methacrylate may reduce the necessary dose by a factor of two or more (100-150 kGy). However, additives to provide flame retardancy tend to retard the radiation cross-linking.

The best known radiation cross-linked application for PVC insulation is in main frame switchboard (communications- telephone) wiring. Since unmodified PVC does not cross-link with radiation, multifunctional monomer additives are essential, and these also help in reduction of dose to only 50-80 kGy. Small gauge wires are cross-linked at a very high speed (>300m/min) by medium voltage high current accelerators. Other applications

are in hook-up wire, coax and shielded cable, business machines, aircraft, computer and internal appliance wiring. The growing interest all over the world in using electron beam accelerators for the cross-linking of wire and cable insulators has been due to the following advantages:

- Depending on the plant, the throughputs attained with electron beam accelerators are two to five times as high as those of conventional cross-linking plants.
- Electron beam accelerators use approximately half the energy required by chemical cross-linking plants.
- The amount of scrap produced during start-up and slow-down in chemical cross-linking is appreciably reduced or completely eliminated.
- In most of the cases electron beam cross-linking plants require less space.
- Of the total manufacturing costs of a production unit, the percentage spent on cross-linking is less when the modern electron beam system is fully loaded.

Radiation induced vulcanisation of rubber has several advantages over conventional thermal-chemical vulcanisation. The properties of rubbers due to network formation are easily controlled by the absorbed radiation dose without any change in the mix composition. The formulations of the mixes become much simpler because they do not contain vulcanising agents, chemical accelerators and other additives. The application of electron accelerators to rubber vulcanisation leads to a considerably higher process rate. Vulcanisates with C - C and sulphur cross-links formed by the combined application of radiation and thermochemical vulcanisation exhibit good properties. The process is often carried out in two stages corresponding to the above two vulcanisation methods. Because of the complex structure, tyres are not irradiated as a whole as different parts behave differently under irradiation. Only single tyre elements should be considered for radiation induced vulcanisation. Thus, these elements (tread, casing and inner layers) are radiation pre-vulcanised at a low absorbed dose (10-100 kGy). In this way high shape stability of tyres or their parts and a significant decrease in their weight are obtained. As a result of the increasing cohesive strength of the uncured rubber mix, spoilage is almost completely eliminated and the production time is reduced by 20%. The combination of radiation and thermochemical technology favours an increase in the mechanical properties or the rubber: residual elongation decreases, dynamic modulus, abrasion and fatigue resistance increase, and tyre life increases by 15-20%.

Sterilisation of Medical Products

Radiation sterilisation is still considered a relatively new process although its origins go back to the discovery of X-rays in the 1890s. In 1896 it was first reported that X-rays could kill micro-organisms. In 1930s the effects of radiation on micro-organisms were quantified. In 1956 the first attempt to use radiation for sterilisation came from the company Ethicon, an affiliate of Johnson and Johnson using a 2 MeV Van de Graff electron accelerator. In the following year a 7 MeV Linac was used for the same purpose. Although Linac was an

Table 19.1 - Comparison of sterilisation of packaged goods by ethylene oxide and radiation

Factor	Ethylene oxide	Radiation
Process parameter	Temperature, time, humidity, ethylene oxide concentration, vacuum/pressure	Time
Retention of sterilant	Yes	No
Post-process treatment	Aeration to remove ethylene oxide	NA
Residual toxicity	Yes	Nil
Sterility test	Required	Not required
Quarantine	14 days	NA
Penetration through packaging	Problem	NA
Choice of packaging	Narrow	Wide
Batch/continuous	Batch	Both
Environmental pollution	Yes	Nil

NA = Not applicable

effective steriliser, due to short klystron lifetime and other hardware problems it was operated only until 1964 when it was replaced with a ^{60}Co irradiator.

Micro-organisms exhibit a wide range of resistance to radiation. The radio-resistance of microbes and the impact of this on the minimum sterilising dose requirement have been a subject of on-going debate since the late 1950s. The first studies established 25 kGy as an effective sterilising dose for sutures and this has evolved into a widely accepted sterilising dose for a variety of products in many countries. Radiation sterilisation has a number of advantages over other techniques as the products can be sterilised after packaging, thus avoiding problems of recontamination. The technical, economic and environmental advantages of radiation processing make it the method of choice for industrial sterilisation. Heat sterilisation is very energy intensive and many products cannot withstand the high temperatures. Ethylene oxide gas sterilisation may leave behind carcinogenic residues and requires long quarantine periods in addition to other disadvantages. A comparison between the two major industrial sterilisation processes, namely radiation sterilisation versus ethylene oxide sterilisation is given in Table 19.1.

Today, millions of tonnes of single-use medical products from scalpels to syringes are being sterilised in more than 200 irradiation facilities in about 50 countries. In Western world radiation is used to treat about 50% of the total disposable medical products and its use

will expand to a large extent in many countries in the near future. Because of this growing use of gamma radiation sterilisation by the medical device industry, guidelines have been established by the Association for the Advancement of Medical Instrumentation and the IAEA. These guidelines help assure that processing by this method is conducted in a manner consistent with providing sterile products of the highest quality.

Radiation Technology for the Conservation of Environment

One of the emerging applications of ionising radiation is in the conservation of the environment. Some of the problems that can be solved by using radiation-chemical methods are:

- Conversion of NO_x and SO_2 in combustion gases into fertilisers in the presence of ammonia.
- Disinfection and decomposition of pollutants in drinking water.
- Degradation of biologically resistant harmful substances in industrial wastewater.
- Disinfection of sludge and conversion into manure.
- Recycling of plastic wastes.

Flue Gas Treatment

The potential of using ionising radiation to remove the toxic gases SO_2 and NO_x from flue gas effluents using accelerated electron beams was first investigated by Japanese institutes in the seventies of last century. The method has been developed from the laboratory to pilot and large demonstration scale by research and development projects in Japan, Germany, USA and Poland. Any exhaust gas is a complex mixture of gases containing nitrogen, oxygen, water vapour and carbon dioxide as the main ingredients as well as small amounts of pollutants such as oxides of sulphur and nitrogen, which are known to be the precursors of acid rain. When such an exhaust gas is irradiated with accelerated electrons, most of the electron beam energy is absorbed by the main components, promoting radiation induced chemical reactions. The radicals produced initially through direct and ionic decomposition processes are OH, N, HO_2, O and H. These radicals react instantaneously with SO_2 and NO_x which are good radical scavengers and oxidise them into corresponding acid forms. In this process of electron beam scrubbing of exhaust gases the nitric and sulphuric acids produced are reacted with previously added ammonia to produce powdery ammonium nitrate and ammonium sulphate which can be removed using an electrostatic precipitator. The main reaction paths to remove these two pollutants are given in Fig. 19.1.

The process has numerous advantages over currently used conventional processes:

- The process simultaneously removes SO_2 and NO_x at high efficiency levels
- It is a dry process which is easily controlled and has an excellent load-following capability

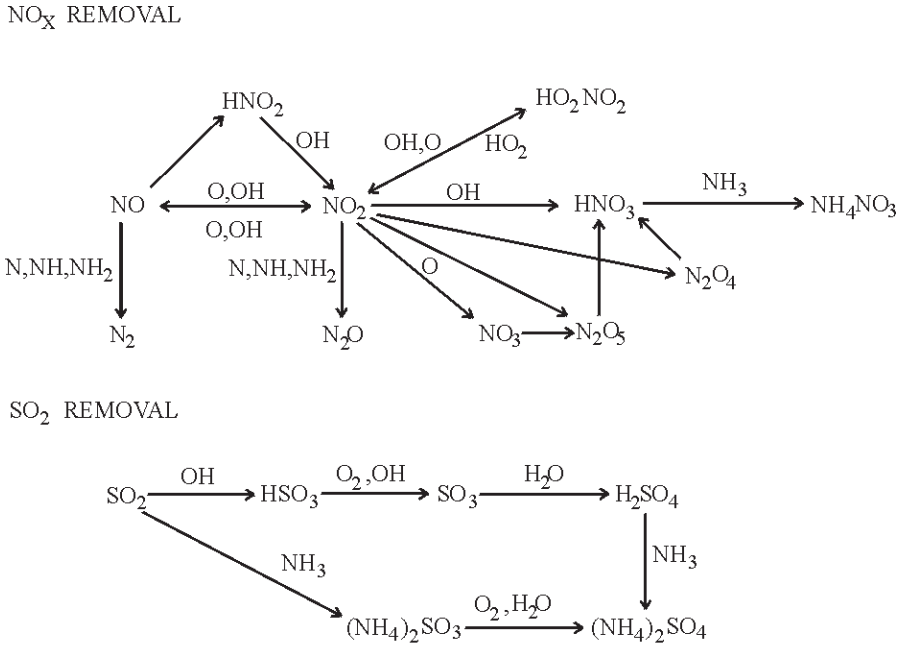

Fig. 19.1 Main reaction paths for NO_x and SO_2 removal.

- The pollutants are converted into saleable agricultural fertilisers.

Based on the results of pilot tests, the world's first full scale plant has started its operation in Chengdu, China in September 1997. This plant can treat half of the 600,000 Nm^3/h of exhaust gases produced in the 200,000 kW coal power generation boilers. The exhaust gas is cooled to 65°C and irradiated with electron beam from two electron accelerators (800 kV, 400 mA) in the presence of ammonia at 3 to 4 kGy thus removing 80% of the 1800 ppm of sulphur dioxide and obtaining 2.5 tons per hour of by-products. A plant has been constructed to treat 620,000 Nm^3/h of exhaust gases produced from the crude oil-fired boiler with a power output of 220,000 kW of a plant in Nagoya, Japan.

It was also recently shown that the present technique of using electron beams is also effective in treating exhaust gases with very high sulphur dioxide concentrations (5000 ppm or higher) which are produced during the combustion of high sulphur content lignite.

Water and Wastewater Treatment

For thousands of years human beings used water as a convenient site to dump wastes. The pollution comes from many sources, including untreated sewage, chemical discharges, petroleum leaks and spills, and agricultural chemicals that are washed off from farm fields.

Chemically or micro-biologically contaminated solutions often percolate through certain soils or soil fissures into ground water or are discharged, in principle, after some remedial treatment, into surface reservoirs thus endangering potable water supplies.

Ionising radiation has been demonstrated to be very effective, as such or in combination with other agents such as ozone and heat, the decomposition of refractory organic compounds in aqueous solutions and in the effective removal or inactivation of the pathogenic micro-organisms and protozoan parasites.

The basic mechanisms of radiolysis of water have been extensively studied and fairly well understood. When dilute aqueous solutions are irradiated practically all the energy absorbed is deposited in water molecules and the observed chemical changes are brought about indirectly via the radical species formed.

The primary reactions of water radiolysis and the G-values of the primary products are given below:

$H_2O \rightarrow$ e_{aq}, H, OH, H_2, H_2O_2, H^+, OH^-

G value (2.7) (0.6) (0.8) (0.45) (0.7) (3.2) (0.5)

The presence of both very strong oxidising and reducing species in irradiated aqueous systems makes this technique unique among other waste or drinking water treatment systems. For example, the following reactions illustrate complete demineralisation of chloroform pollutant by radiation treatment of air saturated water.

$$e_{aq} + CHCl_3 \rightarrow Cl^- + {}^{\bullet}CCl_3 \quad (19.78)$$

$$^{\bullet}OH + CHCl_3 \rightarrow H_2O + {}^{\bullet}CCl_3 \quad (19.79)$$

$$^{\bullet}CCl_3 + 2H_2O + O_2 \rightarrow CO_2 + {}^{\bullet}HO_2 + 3HCl \quad (19.80)$$

$$^{\bullet}CHCl_2 + H_2O + O_2 \rightarrow CO_2 + {}^{\bullet}OH + 2HCl$$

Radiation treatment of water and wastewater should not, however, be considered as a stand-alone process. Radiation processing when coupled with other unit processes, leads to economically viable treatment systems.

Following is the list of typical examples of large scale operations:

- Groundwater containing chlorinated organic compounds in lower Austria was successfully treated utilising electron beam radiation in conjunction with ozone addition. Complete demineralisation of pollutants have been achieved and all toxicity tests on treated water proved negative (2400 m^3/d).
- The city of Voronezh in Russia utilised ionising radiation for treating groundwater which contained a detergent from an industrial process (5000 m^3/d).
- A mobile electron beam accelerator developed in the USA has been used to demonstrate treatment of all forms of aqueous wastes. Highly contaminated groundwater in Germany

and ground water contaminated with a petroleum additive in California have been successfully treated with this mobile system (200 m^3/d).

- The effluent of a large chemical company in Brazil has been treated on pilot scale with electron beams (75 m^3/d).
- A pilot plant constructed in textile dye wastewater plant in Korea has proved technologically successful in treating the effluent at 1000 m^3/day.

Bibliography

1. J.W.T. Spinks and R.T. Woods, 'An Introduction to Radiation Chemistry', Wiley, New York (1976).
2. P.J. Ausloos, 'Fundamental Processes in Radiation Chemistry', Interscience Publishers, New York (1968).
3. R.J. Woods and A.K. Pikaev, 'Applied Radiation Chemistry : Radiation Processing', Wiley, New York (1974).
4. J.H. O'Donnel and D.F. Sangster, 'Principles of Radiation Chemistry', Edward Arnold, London (1970).
5. Y. Tabata, Y. Ito and S. Tagawa, 'CRD Handbook on Radiation Chemistry', CRC Press, Boca Raton (1991).
6. G. Hughes, 'Radiation Chemistry', Clarenden Press, Oxford (1973).
7. A.J. Swallow, 'Radiation Chemistry of Organic Compounds', Pergamon Press, Oxford (1960).
8. R. Bradley, 'Radiation Technology Handbook', Marcel Dekker, New York (1984).
9. A. Chapiro, 'Radiation Chemistry of Polymer Systems', Wiley Interscience, New York (1962).
10. A. Charlesby, 'Atomic Radiation and Polymers', Pergamon Press, Oxford (1960).
11. J.E. Wilson, 'Radiation Chemistry of Monomers, Polymers and Plastics', Marcel Dekker, New York (1974).
12. Radiation Curing of Polymers, Ed. D.R. Randell, The Royal Society of Chemistry, London (1987).
13. Radiation Processing of Polymers, Eds. A. Singh and J. Silbermann, Hansen Verlag, München (1992).
14. The Study of Fast Processes and Transient Species by Electron Pulse Radiolysis, Eds. J.H. Baxendale and F. Busi, Reidel, Dordrecht (1982).
15. A.J. Swallow, 'Radiation Chemistry : An Introduction', Longman, London (1973).

Chapter 20
The Actinide Elements

The search for elements beyond uranium led to the discovery of a series of elements called the actinides. Out of the fifteen elements starting with actinium and ending with Lawrencium, only uranium and thorium are present in nature. Actinium and protactinium isotopes are all radioactive and the longest lived ^{227}Ac ($t_{1/2} = 21.773$ y) and ^{231}Pa ($t_{1/2} = 32760$ y) are decay products of ^{235}U and coexist with uranium in trace amounts. Before the discovery of tansuranic elements these four elements were classified as members of the fourth transition element series with electrons progressively filled in the 6 d shell as against the 5f shell. This classification was justified due to the similarity of some chemical properties of thorium with Hf/Zr, Pa with Ta/Nb and of uranium with W/Mo. Chemistry of transuranic elements Np, Pu and Am, however, did not fit into the transition metal mould. The concept of actinides, similar to the lanthanides, suggested by Seaborg, was instrumental in devising the chemical procedures for the separation of ultra-trace quantities (a few atoms) of transuranics leading to their discovery and identification. Many similarities in the chemistry of lanthanides and actinides were discovered subsequently.

Discovery of Actinide Elements

In 1899 Debierne, while working on the isolation of various fractions during the processing of uranium ores, discovered a radioactive substance concentrating in the rare-earth fraction which was named actinium. The amount of actinium was extremely small. One te of pure pitchblende contains only 0.15 mg of ^{227}Ac. Milligram amounts of ^{227}Ac could be prepared in 1950 by the transmutation of ^{226}Ra by neutron induced reactions .

$$^{226}_{88}\mathrm{Ra}\,(n,\gamma)\,{}^{227}_{88}\mathrm{Ra} \xrightarrow[42.2\ \mathrm{min}]{\beta^-} {}^{227}_{89}\mathrm{Ac} \xrightarrow[21.733\ \mathrm{y}]{} \qquad (20.1)$$

Thorium is the most abundant among the actinide elements with outer layer of earth having 12 parts per million of thorium. It was discovered by Berzelius in 1828 in a Norwegian mineral which contained the thorite ($ThSiO_4$). In India, thorium mainly occurs on the beach sands of Kerala and Orissa states as monazite which is a mixed phosphate of thorium and rare earths.

Protactinium (^{231}Pa) was discovered by O. Hahn and L. Meitner in 1917 and also by F. Soddy and J.A. Cranston at around the same time. ^{231}Pa is present only to the maximum extent of 0.34 ppm in uranium ore and weighable amounts were first isolated by A.V. Grosse. As in the case of actinium, protactinium can also be produced by neutron irradiation.

$$^{230}_{90}\mathrm{Th}(n,\gamma)\ ^{231}_{90}\mathrm{Th} \xrightarrow{\beta^-} {}^{231}_{91}\mathrm{Pa} \xrightarrow[32760\ \mathrm{y}]{\beta^-} \qquad (20.2)$$

Uranium was discovered in 1789 by M.H. Klaproth in a specimen of pitchblende. Average concentration of uranium in the earths crust is about 4 parts per million which is higher than elements like Cd, Mg, Hg and Bi.

The first transuranium element Neptunium was discovered in 1940 by McMillan and Abelson. When uranium is bombarded with neutrons, in addition to fission products, activation product $^{239}_{92}$U was also produced as shown in eqn. 20.3. When this uranium foils were irradiated, energetic fission products passed through the foil whereas $^{239}_{92}$U (23.45 min) was retained in the toil. The target foil after irradiation had another activity with a half-life of 2.3565 d attributed to ^{239}Np.

$$^{238}_{92}\mathrm{U}(n,\gamma)\ ^{239}_{92}\mathrm{U} \xrightarrow[23.45\ \mathrm{min}]{\beta^-} {}^{239}_{93}\mathrm{Np} \xrightarrow[2.3565\ \mathrm{d}]{\beta^-} {}^{239}_{94}\mathrm{Pu} \qquad (20.3)$$

Neptunium-237 the longer lived isotope of neptunium ($t_{1/2}$ = 2.144 x 10^6 y) is formed in significant quantities in the nuclear power reactors by the following reactions and can be isolated during spent fuel reprocessing.

$$^{238}_{92}\mathrm{U}(n,2n)\ ^{237}_{92}\mathrm{U} \xrightarrow[6.75\ \mathrm{d}]{\beta^-} {}^{237}_{93}\mathrm{Np} \qquad (20.4)$$

$$^{235}_{92}\mathrm{U}(n,\gamma)\ ^{236}_{92}\mathrm{U}(n,\gamma)\ ^{237}_{92}\mathrm{U} \xrightarrow[6.75\ \mathrm{d}]{\beta^-} {}^{237}_{93}\mathrm{Np} \qquad (20.5)$$

During the discovery of neptunium, it could be indirectly inferred that the daughter product would be ^{239}Pu. However, the fact could not be established because the amount of ^{239}Pu produced was very small and it has a half-life of 24110 y. The first isotope of plutonium to be discovered was ^{238}Pu. Seaborg, McMillan, Kennedy and Wahl bombarded uranium with a deuteron beam from an accelerator to produce ^{238}Pu as shown in eqn. 20.6.

$$^{238}_{92}\mathrm{U}(d,2n)\ ^{238}_{93}\mathrm{Np} \xrightarrow[2.117\ \mathrm{d}]{\beta^-} {}^{238}_{94}\mathrm{Pu} \xrightarrow[87.70\ \mathrm{y}]{\alpha} {}^{234}_{92}\mathrm{U} \qquad (20.6)$$

The half-life of ^{238}Pu is short and activity produced was adequate which enabled to follow it even in trace amounts. ^{239}Pu was subsequently identified, in 1941, as a decay product of ^{239}Np produced in large amounts by exposure of uranium foil to a strong neutron beam produced by neutron reaction in an accelerator.

Americium, the next transuranium element was discovered in 1944 by Seaborg, James, Morgan and Ghiorso. It was formed by successive neutron capture by ^{239}Pu to produce ^{241}Pu which decays to ^{241}Am.

$$^{239}_{94}\text{Pu}\,(n,\gamma)\,^{240}_{94}\text{Pu}\,(n,\gamma)\,^{241}_{94}\text{Pu}\xrightarrow[14.290\ \text{y}]{\beta^-}\,^{241}_{94}\text{Am}\xrightarrow[432.2\ \text{y}]{\alpha} \qquad (20.7)$$

Curium was discovered, in early 1944, in the alpha induced reaction of

$$^{239}_{94}\text{Pu}\,(\alpha,n)\,^{242}_{96}\text{Cm}\xrightarrow[162.8\ \text{d}]{\alpha}\,^{238}_{94}\text{Pu} \qquad (20.8)$$

Subsequently ^{242}Cm has also been produced by reactor irradiation of ^{241}Am.

The discovery of the next transuranium element, Berkelium took almost five years. Thompson, Ghiorso and Seaborg discovered ^{243}Bk by bombardment of ^{241}Am with 35 MeV alpha particles, which undergoes electron captive to form $^{243}_{96}$Cm.

$$^{241}_{95}\text{Am}\,(\alpha,2n)\,^{243}_{97}\text{Bk}\xrightarrow[4.5\ \text{h}]{\text{EC}}\,^{243}_{96}\text{Cm} \qquad (20.9)$$

Berkelium-247 with a half-life of 1380 y and ^{249}Bk with a half-life of 330 d are more suited for chemical investigations.

Californium was discovered by Thompson, Street, Ghiorso and Seaborg by bombardment of microgram quantities of ^{242}Cm with 35 MeV alpha particles as shown in eqn. 20.10.

$$^{242}_{96}\text{Cm}\,(\alpha,n)\,^{245}_{98}\text{Cf} \qquad (20.10)$$

Einsteinium and Fermium were discovered as products formed following the multiple neutron capture by uranium during the Mike thermonuclear explosion. It is postulated that ^{253}U was formed after capturing 15 neutrons, which eventually decayed to ^{253}Fm ($t_{1/2}$ = 3.0 d). These were subsequently produced by neutron irradiation of ^{239}Pu in high flux reactors.

Mendelevium was first synthesised by irradiation of ^{253}Es with 41 MeV alpha particles.

$$^{253}_{99}\text{Es}\,(\alpha,n)\,^{256}_{101}\text{Md} \qquad (20.11)$$

Only a few atoms of this element were produced and these were identified on the basis of cation exchange chromatography and nuclear properties. ^{256}Md decays by electron capture ($t_{1/2}$ = 77 min) to ^{256}Fm which undergoes by spontaneous fission with a half-life of 2.63 h.

Element nobelium was produced at the Nobel Institute of Physics in Stockholm, by a large international team, by bombarding ^{244}Cm with 90 MeV ^{13}C ion beam. Two isotopes ^{251}No and ^{253}No were produced as shown in eqn. 20.12.

$$^{244}_{96}\text{Cm}\left(^{13}_{6}\text{C},6n\right)\,^{251}_{102}\text{No}\ \text{ and }\ ^{244}_{96}\text{Cm}\left(^{13}_{6}\text{C},4n\right)\,^{253}_{102}\text{No} \qquad (20.12)$$

Both the nobelium isotopes were short lived and decayed by α-emission. Subsequent measurements established the half-life of ^{251}No as 0.8 s and that of ^{253}No as 1.62 min. A few atoms of No produced were identified following the procedure for Md.

Lawrencium was discovered by Ghiorso, Sikkeland, Larsh and Latimer in 1961 using a boron ion beam on a californium target, as shown in eqn. 20.13.

$$^{252}_{98}\mathrm{Cf}\left(^{10}_{5}\mathrm{B},5\mathrm{n}\right)\ ^{257}_{103}\mathrm{Lr} \qquad (20.13)$$

Electronic Structure

The chemical properties of elements are dictated by their electronic structure. The electronic structure of gaseous atoms and trivalent ions of actinides, beyond radon shell, are given in Table 20.1.

Table 20.1. Electronic structure of gaseous actinide elements and ions

Element	M(g)	M^{3+} (g)	Element	M(g)	M^{3+} (g)
Ac	$6d^1\ 7s^2$	[Rn]	Cm	$(5f^7\ 6d^1\ 7s^2)$	$5f^7$
Th	$6d^2\ 7s^2$	$5f^1$	Bk	$5f^9\ 7s^2$	$5f^8$
Pa	$5f^2\ 6d^1\ 7s^2$	$5f^2$	Cf	$5f^{10}\ 7s^2$	$5f^9$
U	$5f^3\ 6d^1\ 7s^2$	$5f^3$	Es	$5f^{11}\ 7s^2$	$5f^{10}$
Np	$5f^4\ 6d^1\ 7s^2$	$5f^4$	Fm	$5f^{12}\ 7s^2$	$(5f^{11})$
Pu	$5f^7\ 7s^2$	$5f^5$	Md	$(5f^{13}\ 7s^2)$	$(5f^{12})$
Am	$5f^7\ 7s^2$	$5f^6$	No	$(5f^{14}\ 7s^2)$	$(5f^{13})$
			Lr	$(5f^{14}\ 6d^1\ 7s^2)$	$(5f^{14})$

Unlike in the case of lanthanides, where the inner 4f shell starts filling from cerium onwards, for actinides 5f shell starts filling only at protactinium. Also Am which has $5f^7\ 7s^2$ configuration does not display divalency as europium with $4f^7\ 6s^2$. But nobelium with $5f^{14}7s^2$ structure shows divalency as does Yb with $4f^{14}6s^2$ structure. Similarly one of the stable oxidation states of berkelium is Bk(IV) ($5f^7$ configuration) as is the case with Tb. In general, the shielding of 5f electrons, from the fields of neighbouring outer electrons is lower than that of 4f electrons. The actinides, particularly the early members upto Am, display a richer chemistry than do the lanthanides due to the participation of 5f electrons in bonding. From curium onwards, there is considerable resemblance between the actinide and lanthanide chemistry. This is because with increasing nuclear charge the 5f shell contracts and the

shielding of 5f electrons by outer electrons becomes more effective in the heavier end of the actinides and they tend not to take part in bonding.

Oxidation States

The possible oxidation states of the actinides in solution and solid state are given in Table 20.2.

Table 20.2. Oxidation states of actinides elements

Ion	Metal														
	Ac	Th	Pa	U	Np	Pu	Am	Cm	Bk	Cf	Es	Fm	Md	No	Lr
M^{2+}							(2)			(2)	(2)	2	2	<u>2</u>	
M^{3+}	<u>3</u>	(3)	(3)	3	3	3	<u>3</u>	<u>3</u>	<u>3</u>	<u>3</u>	<u>3</u>	<u>3</u>	<u>3</u>	3	<u>3</u>
M^{4+}		<u>4</u>	4	4	4	4	4	4	4	(4)					
MO_2^+			<u>5</u>	5	<u>5</u>	5	5								
MO_2^{2+}				<u>6</u>	6	6	6								
MO_2^{3-}					7	7	(7)								

Underline indicates most stable oxidation state.
Parentheses indicate either only in solid state or not well characterised.

The first element actinium is trivalent but this oxidation state does not become stable till americium is reached. Thorium is predominantly tetravalent and the most stable oxidation state being (V) for Pa and (VI) for U. Thus elements from Ac to U tend to attain f^0 state for forming most stable ions. The trend starts reversing from neptunium with most stable oxidation states being Np(V), Pu(IV) and Am(III). The 5f shell not only contracts with increasing nuclear charge but also with increasing ionic charge. After americium, all actinide elements other than nobelium show (III) as the most stable (or the only) valence state. Tetravalency is exhibited by curium and californium in the solid state (CmO_2/CfO_2 and CmF_4/CfF_4) and berkelium in the solution. Divalency is the stable oxidation state of nobelium and is also observed for fermium and mendelevium. Actinides thus show a greater tendency towards the stability of (II) state due to increasing bonding of 5f (or 6 d) electrons upon approaching the end of the series. Pentavalent and hexavalent actinides exist as oxycations MO_2^+ and MO_2^{++}. The actinyl oxygen is strongly bound and remains unchanged through a variety of chemical reactions. The heptavalent state has been observed only for neptunium and plutonium under highly oxidising conditions and in alkaline media. The ionic species are NpO_5^{3-} and PuO_5^{3-}. In acidic solution, these ions immediately oxidise water.

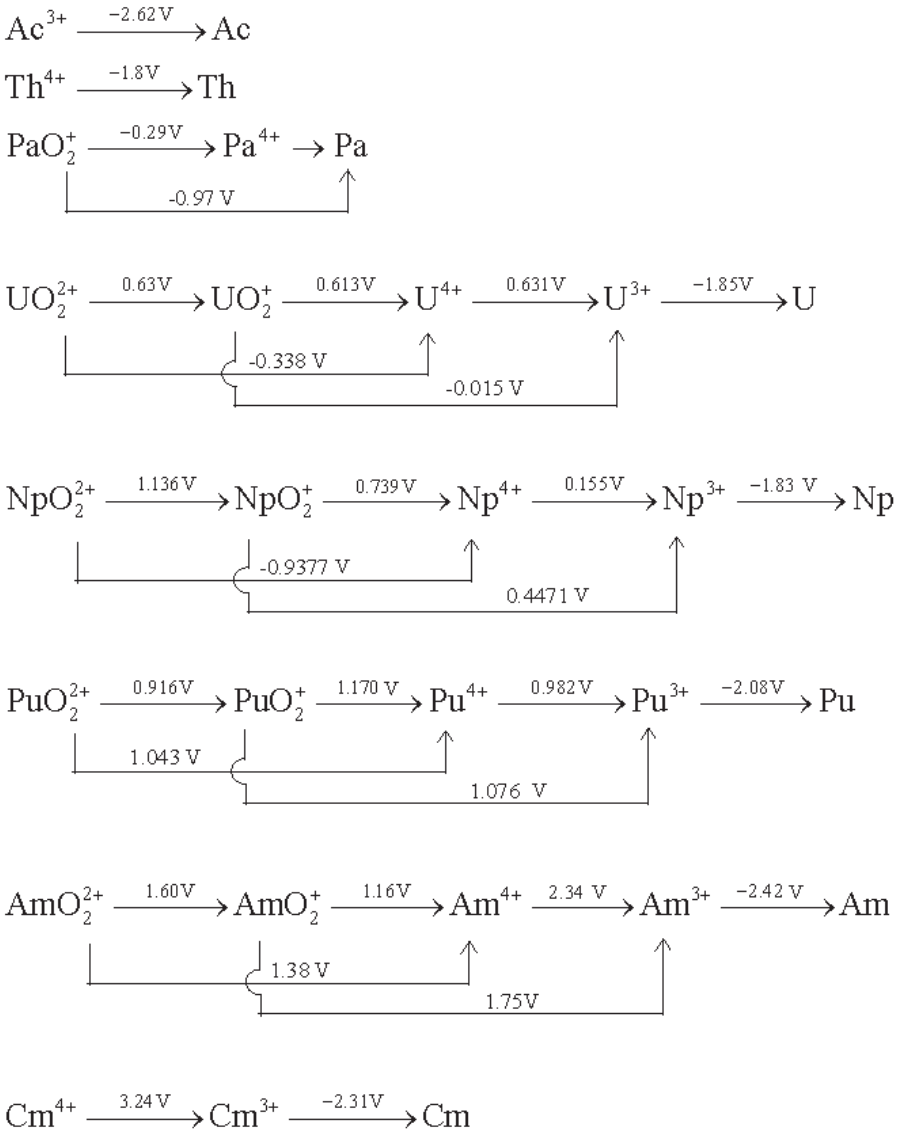

Fig. 20.1 Formal reduction potentials of some actinides in 1 M $HClO_4$.

The relative stability of various actinide ions in aqueous solution can be judged from the formal reduction potentials of these ions. In 1M $HClO_4$ medium, formal reduction potentials Ac to Cm are given in Fig. 20.1.

The closeness in redox potentials of an element in different oxidation states lead to a number of disproportionation reactions which are among the most intricate known in chemistry. Further the presence of complexing agents (SO_4^{--}, NO_3^- etc.) significantly modifies the redox potentials and can stablise oxidation states not otherwise stable.

Hydrogen ion concentration also affects the redox equilibria particularly those involving actinyl ions.

The phenomenon of disproportionation can be explained by taking the case of plutonium. At high acidities, PuO_2^+ can disproportionate to (Pu^{4+} + PuO_2^{2+}) or (Pu^{3+} + PuO_2^{2+}). Equilibrium constant (K) for these reactions are high.

$$2PuO_2^+ + 4H^+ \rightarrow Pu^{4+} + PuO_2^{2+} + 2H_2O \qquad \log K = 4.29 \qquad (20.14)$$

$$3PuO_2^+ + 4H^+ \rightarrow Pu^{3+} + 2PuO_2^{2+} + 2H_2O \qquad \log K = 5.40 \qquad (20.15)$$

When pH of the solution is increased then (at pH 2) not only PuO_2^+ but also Pu^{4+} is unstable. Pu^{4+} can disproportionate to Pu^{3+} + PuO_2^+ / PuO_2^{2+}

$$3Pu^{4+} + 2H_2O \rightarrow 2Pu^{3+} + PuO_2^{2+} + 4H^+ \qquad \log K = -2.08 \qquad (20.16)$$

$$Pu^{4+} + PuO_2^+ \rightarrow Pu^{3+} + PuO_2^{2+} \qquad \log K = 1.11 \qquad (20.17)$$

Thus under certain conditions, all oxidation states of plutonium can be present in significant amounts, as shown in eqn. 20.17.

Complexes of Actinide Ions

Besides the redox behaviour, complexing characteristics of various actinide ions play an important role in their solution chemistry. All actinide ions are electron acceptors and many anions, and neutral molecules with lone pair of electrons, form complexes with actinide cations. At times several complexes may co-exist in a solution, depending upon their relative stability constants. The magnitude of a stability constant increases with increasing charge and with decreasing size of the actinide ions. The tetravalent ion, therefore, form the strongest complexes. For actinyl ions MO_2^{2+} and MO_2^+, the effective charge on the actinide atom M is considerably higher than 2 or 1 but significantly lower than 6 or 5. The complexing characteristic of actinide ions can lead to preferential stabilisation of one of the valence states.

Ligands with electron donating atoms like halogens, O, N and S form complexes with actinides. O and N are normally constituents of complex ions. Common inorganic anions making complexes include F^-, Cl^-, NO_3^-, SO_4^{2-}, CO_3^{2-} and PO_4^{3-}. All actinide ions are hydrated in aqueous solution, the degree of hydration increasing with increasing charge and decreasing size of the ion. Trivalent actinide hydrates are 9 coordinated like lanthanides. Co-ordination number of 8 is most common for tetravalent ions. MO_2^+ and MO_2^{2+} ions co-ordinate to 4, 5 or 6 ligands in solution, thus exhibiting co-ordination number between 6 to 8. Ionic radii for six co-ordinated ions of some actinides are given in Table 20.3.

Table 20.3 - Ionic Radii (nm) of actinides (6-coordination)

Element	M^{3+}	M^{4+}	MO_2^+	MO_2^{2+}
Ac	0.1076	-	-	-
Th	-	0.0984	-	-
Pa	-	0.0944	-	0.171
U	0.1005	0.0929	-	-
Np	0.0986	0.0913	0.198	-
Pu	0.0974	0.0896	0.194	-
Am	0.0962	0.0888	0.192	-
Cm		0.0886	-	-

For any actinide the relative tendency for complex formation decreases in the order of $M^4+ > MO_2^{++} > M^{3+} > MO_2^+$. Among the common monopositive anions the complexing power is in the order $F^- > NO_3^- > Cl^- > ClO_4^-$. For divalent anions the order is $CO_3^{2-} > C2O_4^{2-} > SO_4^{2-}$.

Because of the highly complexing characteristics many water molecules can get co-ordinated to the actinide ions. For example, ions of the type $UO_2(H_2O)_4^{2+}$ and $Th(H_2O)_9^{4+}$ have been identified. The hydrated actinide ions act like Bronsted acids. Due to reactions in hydration shell, there is a tendency to split off protons and this tendency increases with increasing ionic charge, being strongest for the tetravalent ions. Hydrolysis of Pu(IV) starts even in dilute acidic solution (~0.1 M). Hydrolysis tendency of actinides follows the trend observed for their complex formation.

Colour and Spectra

Solutions of many actinides ions (uranium to americium) are brightly coloured due to selective absorption of certain wavelength of visible light. These solutions also possess absorption bands in visible and infra-red regions. These vivid colours are generally due to electron transfer (charge transfer) from the 5f levels of the actinide to the orbitals of the co-ordinated ligand. These transitions are markedly affected by environmental influence resulting in broad and intense charge transfer bands in the ultraviolet and visible regions. Electronic transitions also occur between 5f and 6d levels leading to fairly intense absorption in ultraviolet region (molar absorption coefficient = 1000 cm^{-1} M^{-1}). The absorption bands are broad due to the influence of the ligand field on the many energy states that take part in

the absorption. Intra-shell transitions 5f shell (f → f), though Laporte forbidden, occur when there is no change in spin multiplicity. These bands are weak (molar absorption coefficient = 10-50 cm^{-1} M^{-1}) and can occur in ultraviolet to near infra-red regions. Typically colours for plutonium ions in dilute acid medium are Pu(III) → Blue, Pu(IV) → brown, Pu(V) → reddish purple and Pu(VI) → orange pink. In strong nitric acid medium (> 3M) Pu(IV) exhibits green colour.

Extraction of Thorium, Uranium and Plutonium

Thorium, uranium and plutonium are important in the atomic energy programme. Only two actinide elements, thorium and uranium, are available in nature in significant quantities. Thorium is a fertile material, which can be converted to fissile uranium-233 by irradiation in a reactor.

$$^{232}_{90}\mathrm{Th}(n,\gamma)\,^{233}_{90}\mathrm{Th} \xrightarrow[22.3\ \mathrm{min}]{\beta^-} {}^{233}_{91}\mathrm{Pa} \xrightarrow[26.967\ \mathrm{d}]{\beta^-} {}^{233}_{92}\mathrm{U} \xrightarrow[1.592 \times 10^5\ \mathrm{y}]{\alpha} {}^{229}_{90}\mathrm{Th} \qquad (20.18)$$

Uranium has two important isotopes ^{235}U (0.7204%) and ^{238}U (99.2742%). ^{235}U is fissile. ^{238}U is converted to ^{239}Pu as shown in eqn. 20.2. The spent fuel from nuclear reactors contains significant quantities of plutonium and several hundred tonnes of plutonium have been recovered by reprocessing the spent fuel all over the world. The methods of their separation followed in India are briefly discussed.

Thorium

India's thorium resources of 363,000 tonnes are more than five times the uranium resources and it has great interest in utilising the same for producing nuclear energy via conversion to ^{233}U. Thorium is present as monazite in the beach sands of Kerala and Orissa states. These beach sands are being processed for the recovery of ilmenite (for TiO_2 based paints) and monazite for the recovery of rare-earths. Thorium is essentially a byproduct with small use in gas mantle industry and as a minor alloying constituent. Monazite contains about 9% of ThO_2, 60% of rare earth oxides, 0.4% of UO_2 and 27% of phosphorous pentaoxide. Thorium hydroxide and rare earth (RE) hydroxides are formed when monazite is treated with sodium hydroxide.

$$Th_3(PO_4)_4 + 12\ NaOH \rightarrow 3\ Th(OH)_4 + 4\ Na_3PO_4 \qquad (20.19)$$

$$R.E.(PO_4) + 3\ NaOH \rightarrow R.E.(OH)_3 + Na_3PO_4 \qquad (20.20)$$

Thorium and rare earth hydroxide precipitate is dissolved in hydrochloric acid. Thorium is precipitated as sulphate with 50% sulphuric acid and purified by another dissolution/precipitation step. Thorium sulphate is then treated with ammonium carbonate to obtain thorium hydro-carbonate which is dissolved in nitric acid to obtain mantle grade thorium nitrate. Purification of this thorium nitrate can be achieved by extraction with TBP.

Uranium

The main minerals of uranium are uraninite ($UO_2 + UO_3$), pitchblende ($UO_{2.2}$-$UO_{2.67}$), coffinite ($U(SiO_4)_{1-x}$ $(OH)_{4X}$) and carnotite ($K_2.2UO_3.V_2O_3.2H_2O$). In India most of the deposits have oxide base mineralisation. Largest deposit is in Singbhum district in Bihar. A mine and mill was established at Jaduguda and operations are being expanded to Narwapahar. Significant deposits of uranium have been identified at Domiasiat in Meghalaya and Cuddapah/Nalgonda districts of Andhra Pradesh. All deposits of uranium, identified so far in India, on an average have a maximum uranium concentration of 0.1%. Jaduguda mill processes an ore with an average grade of 0.07% U_3O_8.

The uranium ore mined at Jaduguda looks like granite stones used for road making. Small quantities of uranium are present in the mineralised viens and can be leached out only after fine grinding (~200 mesh). The crushed ore also contains some copper and molybdenum as sulphide which is recovered by froth flotation. In terms of oxides the ore mainly contains $SiO_2 = 67.2\%$, $FeO/Fe_2O_3 = 13.2\%$, $Al_2O_3 = 5.5\%$, $(CaO+MgO) = 7.6\%$ and $U_3O_8 = 0.07\%$. Dilute sulphuric acid (equivalent to 30kg of Conc. H_2SO_4 per tonne of ore) and MnO_2 (6kg per tonne of ore) are added to obtain a pH of 1.8 for leaching uranium.

$$UO_3 + H_2SO_4 \rightarrow UO_2(SO_4) + H_2O \qquad (20.21)$$

$$UO_2 + O \text{ (from } MnO_2) + H_2SO_4 \rightarrow UO_2(SO_4) + H_2O \qquad (20.22)$$

By proper selection of conditions, uranium is preferentially leached out with a very little of gangue material. The leach liquor having 0.0006 - 0.0008 kg/L of U_3O_8 is then processed for the recovery of uranium by the anion exchange method. In the leach liquor, uranium is present as anionic species $UO_2(SO_4)_3^{4-}$ and readily displaces the chloride ions on the anion exchanger

$$4RCl + UO_2(SO_4)_3^{4-} \rightarrow R_4\,UO_2(SO_4)_3 + 4Cl^- \qquad (20.23)$$

Uranium is then eluted out with a solution of common salt, and precipitated as MgU_2O_7 (yellow cake) with dolomite.

$$MgO + 2UO_2SO_4 + 2H_2O \rightarrow MgU_2O_7 + 2H_2SO_4 \qquad (20.24)$$

The yellow cake is processed at Nuclear Fuel Complex (NFC), Hyderabad for obtaining nuclear purity uranium oxide suitable for the manufacture of nuclear reactor fuel. Solvent extraction with 30% TBP in odourless kerosene is used for the purification step.

Plutonium

Currently 436 reactors with a total installed capacity of 336,000 MWe are supplying electricity in the world. The annual generation of plutonium for a 1000 MWe light water reactor (the type at Tarapur) is about 0.22 te. The total annual generation therefore is 74 te of plutonium. For a pressurised heavy water reactor (the type at Kota, Madras, Narora etc.) the annual generation of plutonium for the same capacity is nearly double. This plutonium can

be separated, along with residual uranium, from the fission products by reprocessing. This step also helps in the isolation of highly radioactive fission products which can be subsequently immobilised for safe storage and disposal. More than 99% of the radioactivity produced in nuclear power generation is safely contained within the spent fuel which has an activity level of a few million curies per tonne of the spent fuel.

The fuel discharged from the reactor is stored in specially designed pools of water to allow the decay of short lived fission products. Water of the pool provides the cooling which is essential and also the biological shielding from radiation. After about an year, the spent fuel is transported, in specially designed shielded containers, to the reprocessing plant. The spent fuel is unloaded into the storage pool of the reprocessing plant. Reprocessing has to be carried out in specially designed buildings which ensure adequate safety of operating personnel from the radiation present in the spent fuel. The walls of the process cells in which the reprocessing equipment is installed are more than 2 m thick. As these cells are likely to become contaminated with radioactivity, and virtually inaccessible for any repairs, the equipment design is such that it does not need replacement throughout its life. Nevertheless, the design permits replacement by remote methods in case it becomes essential. Most operations cannot be seen, but in areas where visual information is essential, special thick lead glass windows are installed. Closed circuit television is also used for monitoring some operations.

Many processes were used in the initial phase of spent fuel reprocessing but currently 'Purex' (Plutonium refining by extraction) process is almost universally used for the recovery of plutonium from spent fuel. The fission product elements present cover almost half of the periodic table with noble gases, alkali metals, alkaline earth metals, rare earths, and many transition elements like Zr, Nb and Mo.

The objective of the Purex process is to recover uranium and plutonium quantitatively and to have high decontamination factors from the fission product elements. High recoveries would ensure that the valuable fissile materials as well as fertile materials are recovered and also that they do not go into the waste streams which have to be subsequently treated for safe disposal. High decontamination factors ensure that the uranium and plutonium products can be handled without requiring extensive shielding or remote operations. The process should also ensure that while handling thousands of curies of radioactivity daily within the plant, the operating staff is not exposed to any radiation. Also the radioactivity released to the environment through various effluent streams is well within the internationally agreed recommendations. The reprocessing operations can be classified into the following major steps:

(i) Fuel decladding and dissolution

(ii) Extraction of uranium and plutonium

(iii) Partitioning of uranium and plutonium and their subsequent purification

(iv) Solvent recycling

(v) Waste handling

A chop leach process is used for dissolving fuel materials. The fuel elements in this process are cut into small pieces about 5cm long and treated for dissolution. The dissolution is carried out in nitric acid at about 100°C when the following reactions take place.

$$2\ U + 3\ O_2 + 4\ HNO_3 \rightarrow 2\ UO_2\ (NO_3)_2 + 2\ H_2O \qquad (20.25)$$

$$2\ UO_2 + 4\ HNO_3 + O_2 \rightarrow UO_2\ (NO_3)_2 + H_2O \qquad (20.26)$$

The dissolution is carried out in the presence of air with a view to minimising the loss of nitric acid as nitrogen oxide gases. Uranium metal and UO_2 dissolve readily. After dissolution, the zirconium cladding which is not attacked by acid, is separated from the solution and separately disposed off as high active waste. The solution is filtered off to remove suspended particles and treated for recovery of uranium and plutonium.

Tributyl phosphate (TBP) solution in paraffin diluent is used for extraction. Pu(III), Pu(IV), Pu(VI), U(IV), U(VI), Nb, Zr, Th and RE as a function of nitric acid concentration. Before starting the extraction it is necessary to ensure that plutonium is present in the tetravalent state in the solution to be extracted. This is achieved by treating the solution with oxides of nitrogen or sodium nitride which stabilise the tetravalent plutonium. These reagents have no effect on uranium which continues to be present in the hexavalent state. The acid concentration of the solution after dissolution is maintained at 2 M to maximise the extraction of uranium and plutonium and minimise the extraction of fission products (Fig. 20.2). The solution is then fed to the extraction column in which 99.9% of uranium and 99.98% of plutonium get extracted into the organic phase with less than 0.5% of the fission products.

$$Pu(NO_3)_4\ (aq) + 2\ TBP\ (org) \rightarrow Pu(NO_3)_4\ .\ 2\ TBP\ (org) \qquad (20.27)$$

$$UO_2(NO_3)_2\ (aq) + 2\ TBP\ (org) \rightarrow UO_2(NO_3)_2\ .\ 2\ TBP\ (org) \qquad (20.28)$$

Bulk of the fission products (99.5%) are left behind in the aqueous solution and are treated separately for immobilisation and safe storage. An important precaution which is required to be taken when dealing with concentrated fissile materials like plutonium is that under optimum conditions less than 500 g of plutonium in solution is adequate to attain criticality and sustain a fission chain reaction. Special attention is paid to criticality control.

Partitioning of uranium and plutonium is based on the non- extractability of trivalent plutonium into TBP. The organic solution is thus contacted with an aqueous solution having a reducing agent like ferrous sulphamate or tetravalent uranium nitrate. These reagents selectively reduce tetravalent plutonium to trivalent plutonium without affecting uranium. Reduction of plutonium causes back extraction of this species into the aqueous phase leaving uranium in the organic phase. Both uranium and plutonium streams at this stage have some amount of fission products and need further purification. The purification of uranium stream is always carried out by another cycle of solvent extraction just like the first step. The purification of plutonium is either carried out by solvent extraction method or by ion

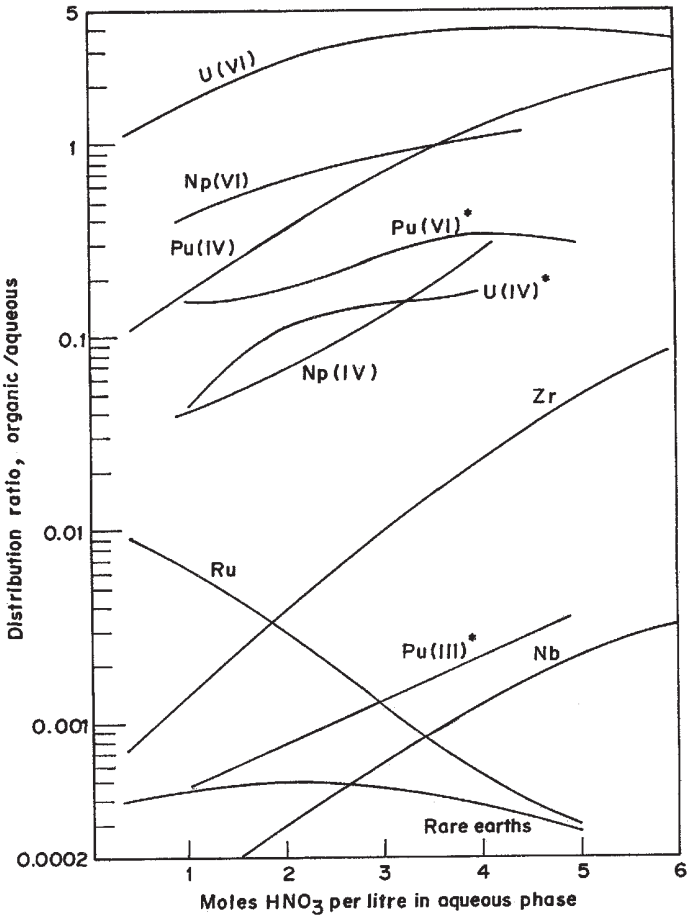

Fig. 20.2 Effect of nitric acid concentration on distribution ratios in 30 v/o TBP 80 percent saturated with uranium (~100 g/l) at 25°C
**Unpublished data from BARC.*

exchange method. In ion exchange technique the property of tetravalent plutonium ion to combine with nitrate ion is used. When the concentrations of nitric acid is increased to 7M, each plutonium ion combines with 6 nitrate ions to make species of the type $Pu(NO_3)_6^{2-}$. Very few metallic ions form this kind of species and, therefore, separation of plutonium from a large number of impurities can be readily achieved by using anion exchange method. When the solution of tetravalent plutonium in 7M nitric acid is passed through an anion exchange column, plutonium is selectively retained on the resin. This column is washed with 6-7 M nitric acid to remove impurities and plutonium is then removed from the column by using dilute nitric acid (0.5 M) which breaks the anionic complex leading to its release from the resin. A typical flow chart of PUREX process is given in Fig. 20.3.

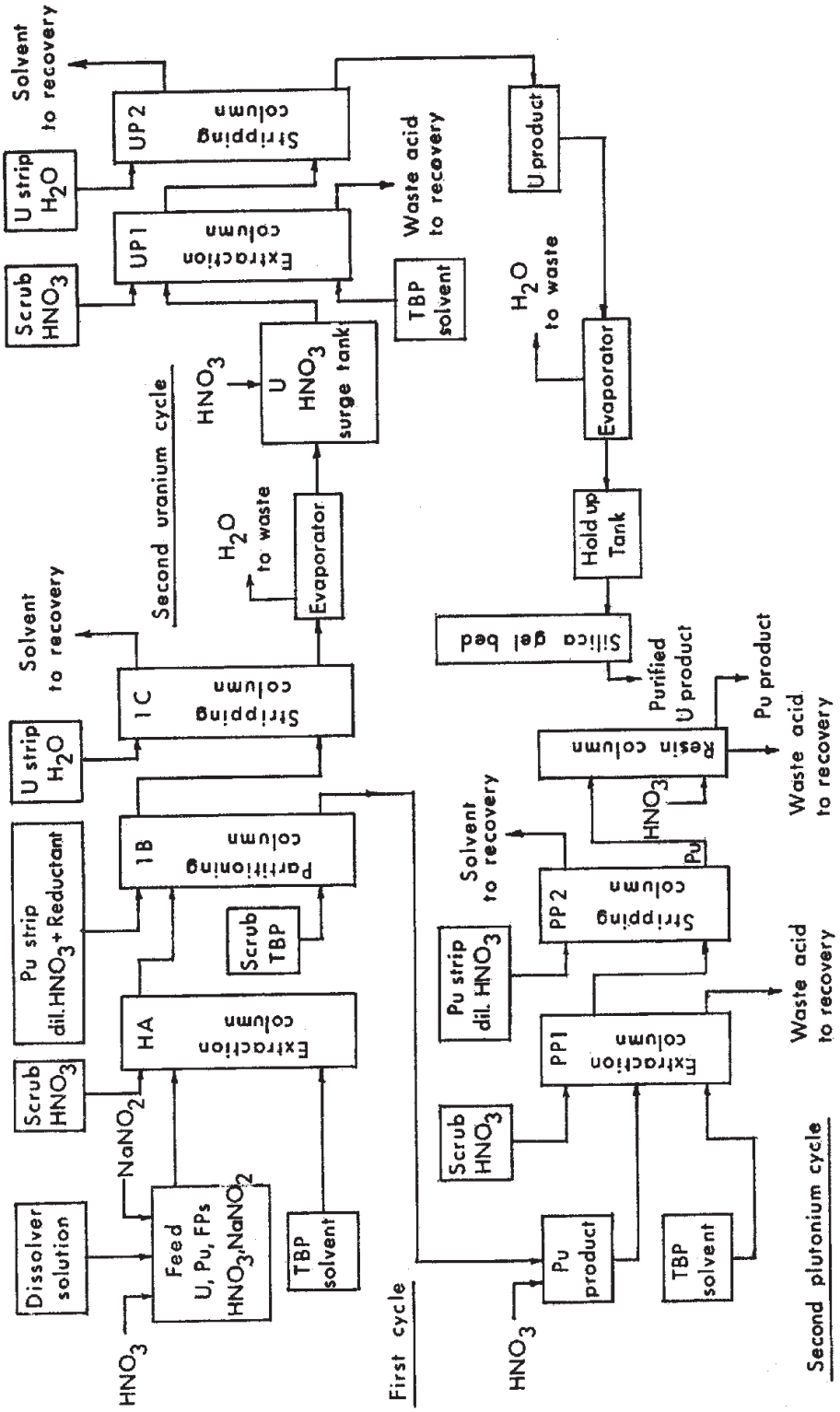

Fig. 20.3 Flow sheet of PUREX process.

Tributyl phosphate as well as organic diluents are subjected to high radiation emitted by the fission products. This results in the production of degradation products, some of which can have detrimental effect on the extraction properties of the solvent. In view of the cost as well as the need for keeping the waste volumes low, it is customary to use the solvent many times before it is discarded. In order to recycle the solvent, it is essential to treat it for the removal of the degradation products. One of the most common methods used for this purpose is a wash with sodium carbonate solution. During this step the degradation products as well as uranium, plutonium and fission products retained by the solvent as complex species are back extracted into the sodium carbonate solution and the solvent gets purified. The solvent is then given a dilute nitric acid wash before sending it back for re-use.

Separation of Other Transuranium Elements

Liquid high active waste (HAW) generated from nuclear fuel reprocessing contains long lived alpha emitters like Np, Am and Cm in addition to the residual U and Pu. Removal of these actinides from HAW would substantially reduce the long term radiological risk from this waste. ^{237}Np is a starting material for producing ^{238}Pu which is useful for isotope batteries for space and remote applications. Many reprocessing plants have modified 'Purex' flow sheet for recovering Np in addition to Pu and U. In dissolver solution, Np exists mainly as Np(V) which is not extracted by TBP. Np(VI) and Np(IV) are extractable in TBP. At low HNO_2 concentration (10^{-3} - 10^{-4} M) Np is oxidised to Np(VI) and co-extracted with U and Pu. When HNO_2 concentration is > 10^{-2} M, Np follows the raffinate along with the fission products. So processes have been designed to recover Np from the organic phase or the aqueous raffinate essentially making use of the redox and extraction behaviour of Np.

Many schemes have been proposed for the removal of Am and Cm from the HAW. One of the earliest methods was based on the extraction with liquid cation exchanger di-2-ethylhexyl phosphoric acid (HDEHP) at low acidity. Use of bifunctional organophosphorus extractant like octyl (phenyl)-N, N diisobutyl carbamoyl methylphosphineoxide (CMPO)) permits extraction of all valence states III, IV and VI of actinides directly from HAW. In transuranic extraction (TRUEX) process, Np is reduced to Np(IV) and all actinides, as also lanthanides, are extracted into 0.2-0.25 M CMPO + 1-1.2 M TBP in a hydrocarbon diluent. Trivalent actinides (Np, Am) are back extracted with 0.04 M HNO_3 followed by back extraction of tetravalent actinides (Np and Pu) using 0.05 M HNO_3 + 0.05 M HF. U(VI) is removed from the solvent during solvent washing step with Na_2CO_3 solution.

Nuclear Properties of Actinides

The nuclear properties and more specifically the decay modes of actinide isotopes primarily arise due to Coulomb instability of the nuclei with high atomic numbers. In the actinide region N/Z ratio is around 1.5 and this increases asymmetry instability.

The ground state of actinides is deformed. Unambiguous characteristic of deformed nucleus is its quadrupole moment. Quadrupole moment is observed for the nuclei having spin more than 1/2. For odd-Z actinides, e.g., ^{227}Ac, ^{241,243}Am etc. large quadrupole moments were observed. This can be due to coupling of odd proton with even-even core. Even Z nuclei also show evidence for ground state deformation. For even-even actinides, however, quadrupole moment is zero but gamma spectrum of the excited states indicates collective rotational bands of spin states 0^+, 2^+, 4^+ ..... etc. with large E2 transition probabilities. A typical rotational band spectrum for ^{238}Pu is given in Fig. 20.4.

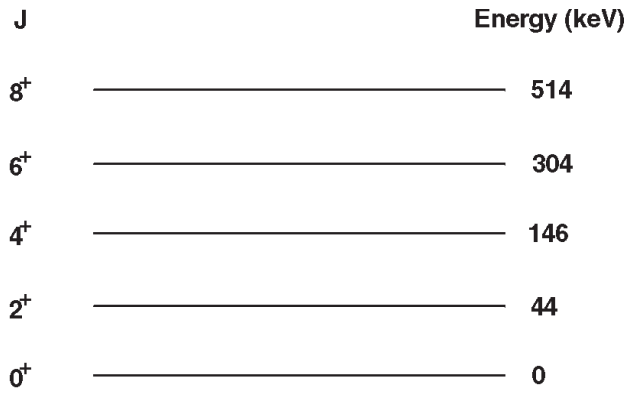

Fig. 20.4 Rotational levels of ^{238}Pu.

Decay Modes of Actinides

Half-lives of actinides vary over a large range from 69 nanoseconds for ^{217}Ac to 1.405 x 10^{10} y for ^{232}Th. The predominant decay modes of the major actinide isotopes are α-decay and spontaneous fission. In the cases where N/Z is greater than 1.56, β-decay is the major mode of decay. For lower N/Z ratios, electron capture is a competing decay mode. Variation of Q_β with A is shown in Fig. 20.5.

For a family of isotopes, α-energy (E_α) decreases with increasing mass number (A) while it increases with the atomic number (Z) in a family of isobars. These aspects can be clearly understood from LDM. Due to increasing Coulombic instability with higher Z for a given A, E_α increases. With increasing A, the α- energy (E_α) increases for a given element (Z). The variations of E_α with A is given in Fig. 20.6.

The other decay mode of actinides is the spontaneous fission where the actinide nuclide in its ground state breaks-up into two fragments of comparable mass and charge. The spontaneous fission half-life of a nuclide is decided by penetrability of the fission barriers depending on their heights and widths. For heavier actinides, shorter spontaneous fission half-life is expected. The variation of $t_{1/2}$ for SF is given in Fig. 20.7.

The spontaneous fission half-lives show a smooth variation for even-even nuclides. For odd A and odd-odd nuclei particularly, these half-lives are still longer than expected

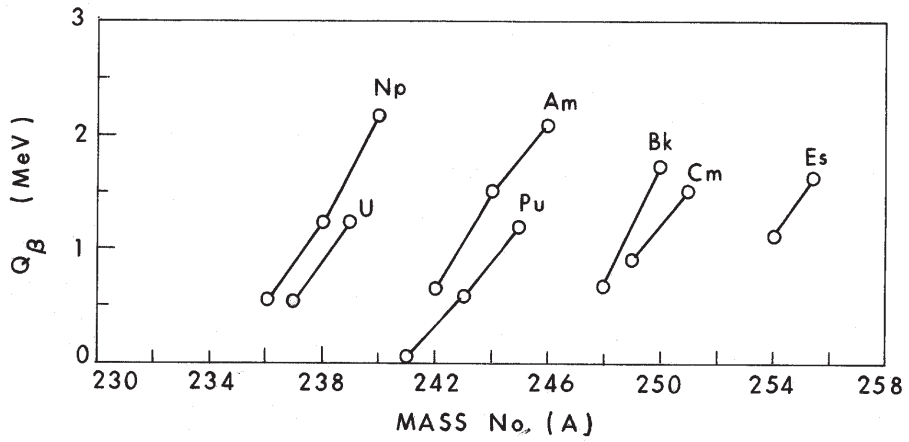

Fig. 20.5 Systematics of beta decay energies of actinides.

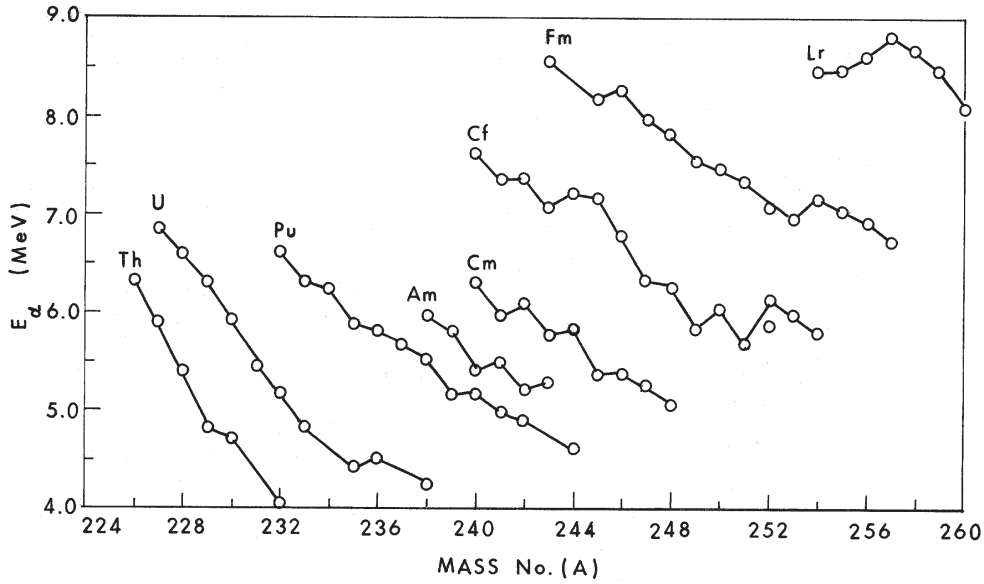

Fig. 20.6 Systematics of alpha decay energies of actinides

from systematics. The odd nucleon in odd A isotope of actinides, is unpaired. In the fission mode, during the deformation of the nucleus, the energy level corresponding to unpaired nucleon does not get altered with increasing deformation. Hence some energy (known as specialisation energy) is tied up i.e., not available in the fission mode. This results in the decrease of the penetrability of barrier and in longer SF half-life. For even-even nuclei, the spontaneous fission half-lives vary from 10^{21} y for ^{232}Th to 400 μs for ^{258}Fm. For the actinides, fission barrier heights vary within a close range of 6.5 to 4.8 MeV upto Z = 98. The two barriers (Chapter 9) for actinides have comparable heights though the second barrier

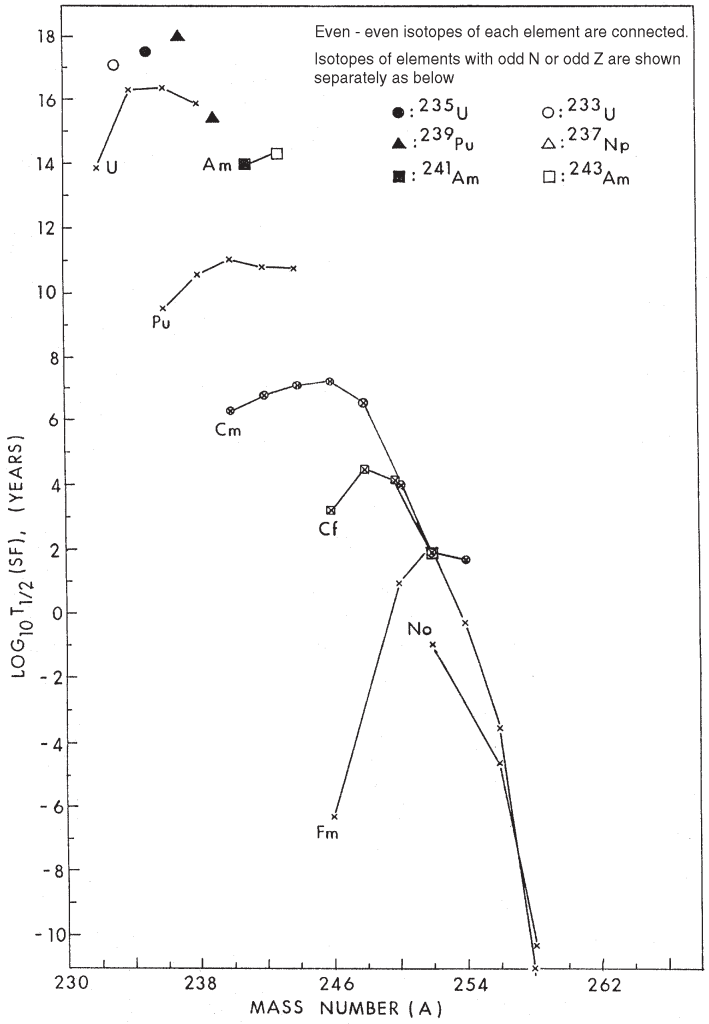

Fig. 20.7 Ground state spontaneous fission half-lives of actinides.

becomes smaller compared to the first barrier for heavier actinides. Even small decrease in the barrier heights increases the penetrability of barrier by orders of magnitude and hence the half-lives are reduced.

Another important feature of actinides with $92 < Z < 98$ is the occurrence of isomeric fission. Nuclei trapped in the valley region between the two barriers in the potential energy surface, at higher deformation, (see Chapter 9) penetrate second barrier and decay by fission. Since isomers are formed during deformation, they are called shape isomers. High deformation of these isomeric nuclei is confirmed from their rotational spectra. In the isomeric fission of actinide isotopes, the systematics of mass, charge and kinetic energy distribution are similar to the thermal neutron induced fission characteristics, except that the

isomeric fission is delayed compared to the neutron induced fission. Various half-lives of some of the actinides are given in Table 20.4.

Table 20.4 - Comparison of isomeric and ground states half-lives of actinide isotopes

Nuclide	Total $t_{1/2}$	$t_{1/2}$ (SF)	$t_{1/2}$ (isomeric fission)
^{232}Th	1.405 x 10^{10} y	10^{21} y	-
^{236}U	2.342 x 10^{7} y	2 x 10^{16} y	116 ns
^{238}U	4.468 x 10^{9} y	8.2 x 10^{15} y	195 ns
^{237}Np	2.144 x 10^{6} y	10^{18} y	45 ns
^{238}Pu	87.70 y	4.77 x 10^{10} y	0.5 ns
^{240}Pu	6564 y	1.34 x 10^{11} y	3.8 ns
^{242}Pu	3.733 x 10^{5} y	6.75 x 10^{10} y	3.5 ns
^{244}Pu	8.08 x 10^{7} y	6.55 x 10^{10} y	380 ps
^{241}Am	432.2 y	1.15 x 10^{14} y	1.5 μs
^{243}Am	7370 y	2.0 x 10^{4} y	5.2 μs
^{242}Cm	162.8 d	6.09 x 10^{6} y	180 ns
^{244}Cm	18.1 y	1.35 x 10^{7} y	100 μs
^{249}Bk	330 d	1.87 x 10^{9} y	-
^{252}Cf	2.645 y	87.9 y	-

All isotopes except ^{249}Bk given in the table undergo α-decay and ^{249}Bk undergoes β-decay

Actinide Synthesis by Heavy-Ion Reactions

Use of heavy ion reactions in the synthesis of rare and higher actinide isotopes has become feasible with the availability of heavy ion accelerators providing projectiles upto ^{238}U at energies upto 10 MeV/u. The most commonly expected reaction channel of complete fusion is not much of a success due to (i) high Coulomb barrier, (ii) high excitation energy of the resultant nuclei and (iii) increased probability of fission. Reactions between two very heavy nuclei, e.g., ^{238}U + ^{238}U, ^{136}Xe + ^{248}Cm at energies 7-8 MeV/u lead to the formation of many actinide isotopes with cross-section in the range of 10^{-33} to 10^{-27} cm^2. These reactions proceed through extensive exchange of nucleons between the target and projectile via deep inelastic collisions. The cross-section for production of some heavy actinides in the most promising deep-inelastic collision is given in Fig. 20.8. It is possible to produce these nuclei

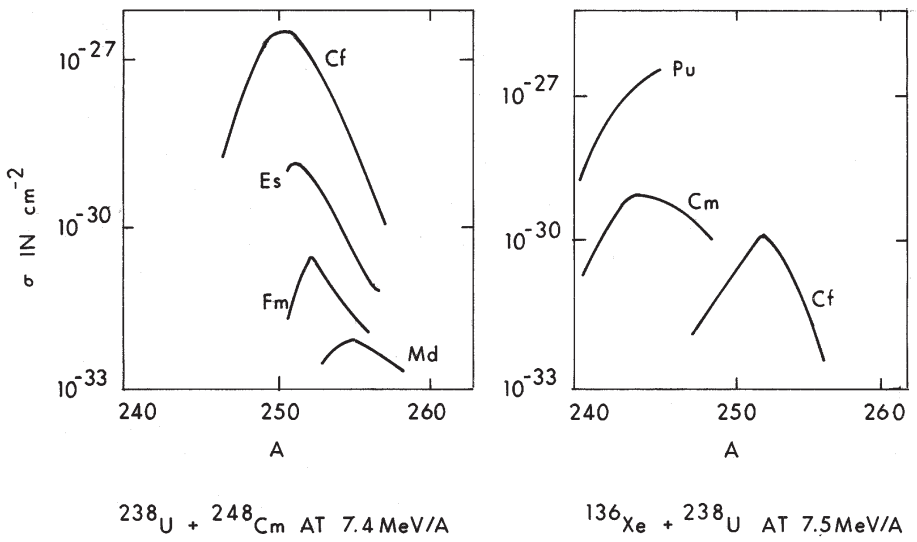

Fig. 20.8 Cross-sections for production of heavy elements.

by multinucleon transfer using smaller projectiles, e.g., ^{18}O, ^{22}Ne etc. on heavy targets, e.g., ^{238}U, ^{248}Cm, ^{249}Cf etc. or by fusion reaction with low excitation energy known as cold fusion.

Bibliography

1. G.T. Seaborg, In Handbook of Physics and Chemistry of Rare Earths: Lanthanides Actinides: Chemistry, Vol.18,(Eds., K.A. Schneider, Jr., L. Eyring, G.R. Choppin and G.H. Lander), Elsevier Science, Amsterdam (1994).

2. J.J. Katz, G.T. Seaborg and L.R. Morss, The Chemistry of Actinide Elements, Vol. 1 and 2, 2nd Ed., Chapman and Hall, New York (1986).

3. A.J. Freeman and G.H. Lander, Handbook of Physics and Chemistry of Actinides, North Holland Amsterdam, Vol. 1 (1984), Vol.2 (1985) and Vol.5 (1987).

4. A.J. Freeman and C. Keller, Handbook of Physics and Chemistry of Actinides, North Holland Amsterdam, Vol.3 (1985), Vol.4 (1986), and Vol.6 (1991).

5. Comprehensive Inorganic Chemistry, (Eds., J.C. Bailer, H.J. Emeleus, R. Niytron and A.F. Trotman-Dickman), Pergamon Press Vol.5 (1976).

6. C. Keller, The Chemistry of Transuranium Elements, Verlag Chemie GmbH, Germany (1971).

7. M. Fred, In Lanthanide/Actinide Chemistry, Adv. Chem. Series 71, Chapter 14, Am. Chem. Soc., Washington D.C. (1967).

8. M.C. Edelson, E.L. Dekalb, R.K. Winge and V.A. Fassel, *Spectrochimica Acta*, **B-41** (1986) 475.

9. W.T. Carnall and H.M. Crosswhite, In Chemistry of Actinide Elements (Eds., J.J.Katz, G.T. Seaborg and L.R. Morss), Chapman and Hall, London, New York, Vol.2, Ch.XVI (1986).

10. N.M. Edelstein and J. Goffart, In The Chemistry of Actinide Elements, (Eds., J.J. Katz, G.T. Seaborg and L.R. Morss), Chapman and Hall, London, New York, Vol.2, Ch.XVIII (1986).

11. B.R. Judd and M.A. Suskin, *J. Opt. Soc. Am.*, **B-1** (1984) 261.

12. G.T. Seaborg and D'E.Hobart, Summary of the Properties of Lanthanide and Actinide Elements' in 'Frontiers in Nuclear Chemistry', Eds. D.D. Sood, A.V.R. Reddy and P.K. Pujari, IANCAS publication, Mumbai (1996)

Chapter 21
Health Physics

Health physics is the discipline that deals with the protection of radiation workers, as well as general population, against the harmful effects of radiation. The application of ionising radiation started soon after the discovery of X-rays by Röntgen in December, 1895. Three years later, in December 1898, Marie Curie and Pierre Curie discovered radium. These two sources of intense radiation were immediately used in the field of medicine for diagnostics and therapy. In most of the applications the concept on radiation exposure was not known nor were the harmful effects of radiation. By 1920 many of the early radiologists and technicians had developed skin cancer and others died of anaemia (probably leukaemia). This led to the concept of a "tolerance dose" for radiation worker and may be termed as the birth of the science of health physics and radiological protection..

Radiation Units

Exposure Unit

Röntgen (R), the first unit for radiation exposure was proposed in 1928 at the Second International Congress on Radiology. It was defined as the amount of X or γ radiation which will produce one electrostatic unit of change of either sign ($1/3 \times 10^{-9}$ coulomb) in one cm^3 of air at 0^oC and at one atmosphere pressure (0.001293 g). The SI exposure unit X is defined as the amount of radiation which causes the formation of ions having one coulomb of charge (either sign) in 1 kg of air.

1 X unit = 1 coulomb/kg

1 R = 1 e.s.u./0.001293 g

$= 1/3 \times 10^{-9}$ C / 1.293×10^{-6} kg $= 2.578 \times 10^{-4}$ C kg^{-1}

$\therefore$ 1 X unit = 3879 R (21.1)

However, Röntgen continues to be widely used as a unit of radiation exposure. This unit is normally limited to X or γ-rays with energies less than 3 MeV. At higher photon

energies the exposure is measured in terms of watt-second per m^2 and exposure rate is watt per m^2.

Absorbed Dose

The effects of radiation on a person are not dependent on the exposure, but on the dose absorbed in the body. The dose is measured in terms of the amount of energy absorbed per unit mass of the tissue. In CGS system the unit is rad.

$$1 \text{ rad} = 100 \text{ erg/g} \tag{21.2}$$

The SI unit for absorbed does is gray (Gy) which is defined as

$$1 \text{ Gy} = 1 \text{ J/kg} \qquad \therefore\ 1 \text{ Gy} = 100 \text{ rad} \tag{21.3}$$

Knowing the fact that a single ion has a charge of 1.6×10^{-19} C and on an average 34 eV (or 5.44×10^{-18} J) is required to produce one ion pair, we get the relation

$$\therefore\ 1 \text{ X unit} = 34 \text{ Gy (in air)} \tag{21.4}$$

It is possible to get an idea about absorption of radiation in 1 kg of tissue from the following discussion. Energy absorption is approximately proportional to the electron density of the absorber. The electron density of air is 3.01×10^{23} electrons per gram. The muscle tissue with a specific gravity of about 1, consists mainly of hydrogen, oxygen and nitrogen atoms with a composition of H = 5.99×10^{22} atoms, O = 2.75×10^{22} atoms and N = 0.172×10^{22} atoms per gram of muscle. It will have an electron density of 3.28×10^{23} electrons per gram. Hence the tissue will absorb more energy for the same radiation exposure, the ratio being 3.28/3.01.

$$\therefore 1 \text{ X unit} = 34 \times 3.28 / 3.01 = 37 \text{ Gy (in tissue)} \tag{21.5}$$

In CGS unit the values for 1 R exposure would be 87.8 erg/g in air and 95 ergs/g in muscle tissue which is very close to 100 erg/g defined for rad. One Röntgen is, therefore, loosely considered to be the same as rad though it is not so.

The absorption of energy by various constituents of the body depends on the part which is exposed and on the radiation energy. A typical correlation is given in Fig. 21.1.

Equivalent Dose

In addition to the energy of radiation and the absorber, the radiation effects also depend upon the type of radiation. For example an alpha particle, with the energy in the range of 4 to 9 MeV moves with slower speed as compared to the electron of similar energy and has double the charge. The linear energy transfer by α-particle is thus much higher which causes enhanced damage to the tissue. Typical LET values in water for some radiations are given in Table 21.1.

Alpha and other heavy particles have very low range and do not pose the hazard of external exposure. But they are very hazardous as they quantitatively transfer energy if

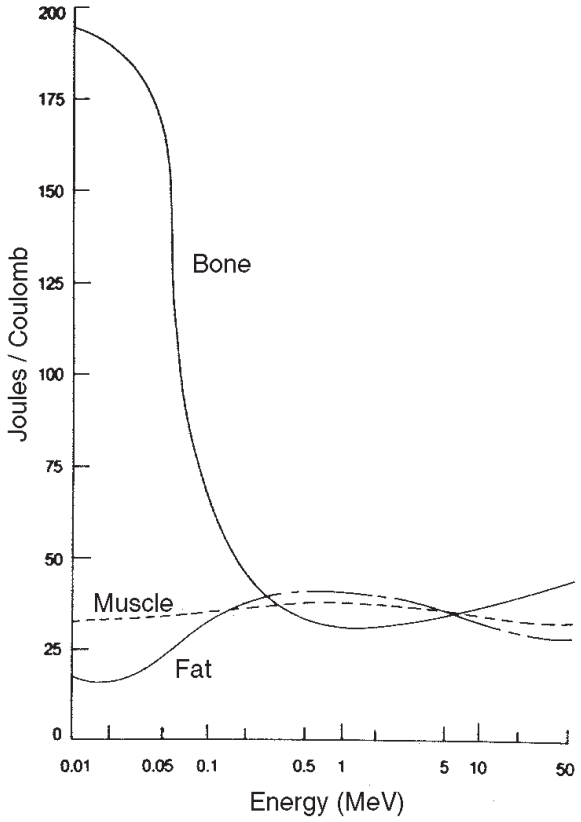

Fig. 21.1 Absorbed dose (J/kg) per X unit (C kg^{-1}) exposure for several tissues [H.E. Johns, 'Radiation Therapy : Depth Dose' in Medical Physics Vol.II, Ed. Otto Glasser, The Year Book Publishers, Chicago (1950) p.791].

Table 21.1 - Linear energy transfer data of α, β and protons in water

Particle	Energy (MeV)	Velocity (cm/s)	LET (MeV/cm)	Range (μm)
Electron	0.1	0.59×10^{10}	23.2	2.5
	1.0	2.82×10^{10}	4.2	140.0
	10.0	2.998×10^{10}	2.0	4,300.0
Proton	1.0	1.4×10^{9}	268	23
	10.0	4.4×10^{9}	47	1,180
Alpha	1.0	0.7×10^{9}	1,410	7.2
	5.3	1.6×10^{9}	474	47

Table 21.2 - International Commission on Radiation Protection (ICRP) radiation weighting factors

Type and energy range		W_R
Photons upto 20 MeV		1
Photons	> 20 MeV	5
Electrons and muons of all energies		1
Neutrons	< 10 keV	5
	10 keV - 100 keV	10
	> 100 keV - 2 MeV	20
	> 2 MeV - 20 MeV	15
	> 20 MeV	5
Alpha particles, fission fragments and heavy nuclei		20

[1990 Recommendations of International Commission on Radiation Protection, ICRP Publication 60, Ann 1-3, Pergamon Press, Oxford (1991)].

ingested internally. The concept of dose equivalent has been introduced to take into account the higher damage potential of such radiation. For equivalent amounts of biological effect, the ratio of the amount of energy of 200 keV X-rays to the amount of energy of heavy ion is called relative biological effectiveness (RBE). For simplification the absorbed dose is multiplied by a radiation weighting factor W_R as given in Table 21.2. The SI unit for equivalent absorbed dose is called Sievert

In the case of internal contamination, there may be a non-uniform distribution of the radionuclide within the body. Also sensitivity of the tissues of different organs / parts of the body is not the same. For calculating the absorbed dose this is taken into account by defining a tissue weighting factor W_T.

$$\text{Sievert} = \text{gray} \times W_R \times W_T \qquad (21.6)$$

W_T is discussed subsequently. The CGS unit of equivalent dose was Rem (Röntgen equivalent man) as defined below

$$\text{Rem} = \text{Rad} \times W_R \times W_T \qquad (21.7)$$

1 Sv = 100 Rem

For a mixture of different types of radiation the corresponding weighting factors are used. For example in a cyclotron facility the dose rate outside the shielding was 5 μGy/h due to gamma rays, 2 μGy/h due to thermal neutrons and 1 μGy/h due to fast neutrons. The equivalent dose to a person would be:

Equivalent Dose = $(5 \times 1 + 2 \times 5 + 1 \times 20)$ μSv/h = 35 μSv/h

Measurement of Exposure and Dose

External Dosimetry

Radiation exposure due to X and γ-rays is obtained by directly measuring the ionisation of air. A parallel plate free air ionisation chamber is a typical device used for this purpose. However, since the range of X and γ-rays is large, and complete absorption of photon energy is essential to determine the exposure, the dimensions of the chamber have to be quite large. For example, for a 300 kV X-ray a cubical ionisation chamber with 0.5 m side is required. This type of equipment is, therefore, used in reference laboratories for the calibration of practical dosimeters.

One of the early instruments for measuring personnel exposure is a self-reading condenser type ionisation chamber. In this dosimeter air in the ionisation chamber is replaced by an electrically conducting plastic (Fig. 21.2). A central metallic thin rod acts as anode and the plastic tube filled with air acts as a condenser which can be charged by connecting the anode to a high voltage (+ve) source of about 200 V. When radiation interacts with the wall (~5 mm thick) of the plastic tube, Compton electrons are produced (X and γ-ray energy 300 keV to 3 MeV). These reach the air cavity and cause ionisation of the air and partial discharge of the condenser. The decrease in voltage at the anode is directly related to the exposure. By a proper choice of wall material and thickness, it is possible to make the dosimeter response independent of energy. A pocket dosimeter would use a chamber of volume of about 2 cm^3.

These dosimeters can also read exposure due to β-rays above 1 MeV energy. By coating the inside chamber with boron, it is possible to make the dosimeter sensitive to neutrons.

Condenser type instruments require a separate device for obtaining the reading. A direct reading dosimeter (DRD) is based on the gold leaf electroscope principle. A quartz

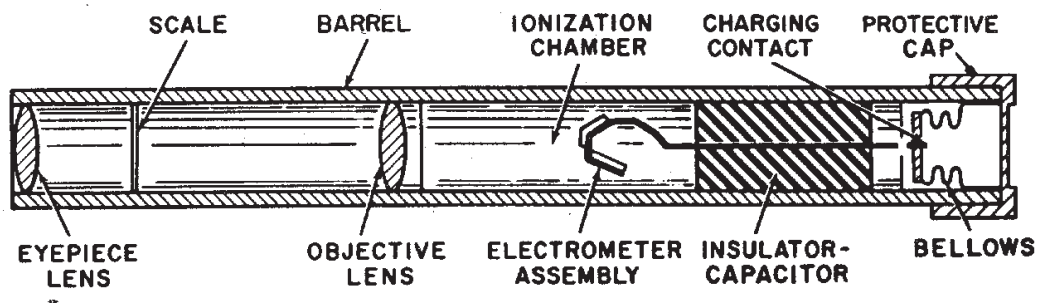

Fig. 21.2 Condenser-type pocket ionisation chamber

fiber is displaced electrostatically by charging to a potential of about 200 V. The image of the fiber is focused on a scale. Exposure to radiation discharges the fiber and the resultant displacement is proportional to the exposure. Commercially available system can read exposure in the range of 0-200 mR and with a provision for audio alarm above a set limit. A schematic of a typical instrument is given in Fig. 21.2.

Another very commonly used personnel monitoring device, used extensively until recent past, is the film badge. It is a small photographic plate wrapped in light-tight paper and mounted in a plastic/metal container. Radiation darkens the film and the degree of darkening, as read with a densitometer, is proportional to the absorbed dose. The general energy range of the radiation can be deduced by incorporating copper, lead and plastic filters on the film and the information used for calculating tissue dose from the film dose. Suitably designed film badges are still used for measuring neutron doses.

Thermoluminescent dosimeters (TLD) are almost universally used for personnel dose measurement and have been discussed in Chapter 7. These dosimeters respond to X-rays, γ-rays, β^- particles and protons over a dose range of 0.1 mGy to 1000 Gy. LiF based TLDs are approximately tissue equivalent (effective atomic number of LiF is 8.1 as against 7.4 for soft tissue).

Internal Dosimetry

Human body has a number of radioisotopes like ^{40}K, ^{14}C and ^{3}H. Also a number of diagnostic or therapeutic procedures in nuclear medicine involve the administration of radioisotopes inside the body. It is, therefore, essential to understand the principles of internal dosimetry. The calculation is straight forward when the radiation is completely absorbed in the tissue. One normally defines the energy absorbed per unit mass per transformation as specific effective energy (SEE). For alpha and β^- radiations, which are completely absorbed in the tissue,

$$\text{SEE} = \frac{\text{Energy delivered per unit time}}{\text{mass of the tissue in kg}}$$

Suppose the testes (weight 18 g) has 6660 Bq of ^{35}S distributed uniformly in the organ after a medical test. Then the daily dose due to this source of ^{35}S can be calculated as follows:

^{35}S is a pure β^- emitter with an average energy of 0.0488 MeV (β^-_{max}=0.1674 MeV)

$$\text{Time} = 8.64 \times 10^4 \text{ s (= 1 day)}$$

$$\text{Dose} = \frac{6660 \times 4.8 \times 10^{-2} \times 8.64 \times 10^4}{18 \times 10^{-3}} \text{ MeV} \,/\, \text{kg/d}$$

$$= 1.56 \times 10^9 \text{ MeV/kg/d} = 2.5 \times 10^{-4} \text{ Gy/d}$$

($\because$ 1 MeV = 1.6×10^{-13} J and 1 Gy = 1 J/kg)

However, the quantity of ^{35}S in testes continuously decreases due to radioactive decay and biological elimination. If λ_R is the radioactive decay constant and λ_B is the biological elimination constant then quantity of radioisotope Q after time t is given by

$$Q = \left(Q_o\ e^{-\lambda_R t}\right)\left(e^{-\lambda_B t}\right) = Q_o\ e^{-(\lambda_R+\lambda_B)t}$$

$$= Q_o\ e^{-\lambda_E t} \qquad (21.8)$$

where $\lambda_E = \lambda_R + \lambda_B$ is called the effective elimination constant. Effective half-life (T_E) is given by

$$\frac{1}{T_E} = \frac{1}{T_R} + \frac{1}{T_B} \qquad (21.9)$$

For ^{35}S, T_R (radioactive half-life) = 87.51 days and T_B = 623 d

$\therefore T_E = 76.4$ d and $\lambda_E = 0.009\ d^{-1}$

The dose due to ^{35}S is therefore not constant and the total dose received over a period τ can be calculated as follows:

Instant dose rate $= \dot{D}_o e^{-\lambda_E t}$

where, $\dot{D}_o$ is the initial dose rate

$$D = \dot{D}_o \int_0^{\tau} e^{-\lambda_E t} \cdot dt$$

$$= \frac{\dot{D}_o\left(1 - e^{-\lambda_E \tau}\right)}{\lambda_E} \qquad (21.10)$$

For large values of τ (about six half-lives), $e^{-\lambda_E \tau} \to 0$.

$$D \simeq \frac{\dot{D}_o}{\lambda_E}$$

So the total dose due to ^{35}S present in the body due to medical procedure would be :

$$D = \frac{2.5 \times 10^{-4}}{0.009} = 0.028 \text{ Gy (or 2.8 rads)}$$

This dose is called the dose commitment.

In the preceding example, ^{35}S was localised in the testes and behaved as if stored in a single compartment. In many cases the radioisotope gets distributed into more than one organ and each organ may have a different clearance rate. For example ^{137}Cs, though

uniformly distributed in the body, behaves as if it was distributed in two compartment in the ratio 1:9. The compartment with 10% ^{137}Cs has a biological half-life of 2 days whereas the major fraction has a biological half-life of 110 d. As ^{137}Cs has a radioactive half-life of 30.07 years, decrease in its activity due to decay can be ignored for calculating internal dose upto about an year.

$$\lambda_{B_1} = \frac{0.693}{2}\, d^{-1} \text{ and } \lambda_{B_2} = \frac{0.693}{110}\, d^{-1}$$

$$D = \frac{0.1\, \dot{D}_o \left(1 - e^{-\lambda_{B_1} T}\right)}{\lambda_{B_1}} + \frac{0.9\, \dot{D}_o \left(1 - e^{-\lambda_{B_2} T}\right)}{\lambda_{B_2}}$$

In the case of α and β particles and for low energy photons which are completely absorbed, dose can be calculated without any corrections. However, in many cases of γ emitters only a fraction of the energy is dissipated inside the body. This must be taken into account while calculating the dose commitment.

Take the case of a 70 kg reference man who is intravenously injected with 1 MBq of $^{24}NaCl$. This gets readily distributed uniformly in the body. ^{24}Na decays by β^- decay to ^{24}Mg. It has a mean β^- energy of 0.555 MeV (β_{max} = 1.392) and two gamma rays having energy of 2.754 and 1.368 MeV. The radioactive half-life is 14.959 h and biological half-life is 11 days. In this case, instead of integrated dose, integrated disintegrations ($\overline{A}$) over a long period have to be calculated to arrive at the dose.

$$\overline{A} = A_o \int_0^\infty e^{-\lambda_E t} \cdot dt = \frac{A_o}{\lambda_E} \qquad (21.11)$$

where, A_o is the initial disintegration rate per second.

λ_E can be calculated to be $1.37 \times 10^{-5}\ s^{-1}$

$$\therefore \text{ Total } ^{24}Na \text{ disintegrations} = \frac{10^6}{1.37 \times 10^{-5}} = 7.3 \times 10^{10} \text{ Bq-s}$$

Using tables/figures from literature which give the fraction φ of the energy absorbed for radiations of different types and dose δ received per disintegration (Bq-s) we get the following :

Radiation	Energy (MeV)	φ	δ kg-fGy/Bq-s	φδ kg-fGy/Bq-s
Beta	0.555	1.0	88.64	88.64
γ_1	1.369	0.31	218.91	67.86
γ_2	2.754	0.265	440.08	116.62
				273.12

[From H. Cember, Introduction to Health Physics, 2nd Ed., Pergamon Press, (1983)]

Hence dose for a man of 70 kg is

$$D = \frac{7.3 \times 10^{10}\ \text{Bq} - \text{s}}{70\ \text{kg}}\ 273.12\ \text{kg} - \text{fGy} \,/\, \text{Bq} - \text{s} = 0.285\ \text{mGy}$$

Iodine-131 is often used in diagnosis and therapy of thyroid malfunction. This isotope has a complex decay scheme as given in Fig. 21.3. Among the β and γ rays, β_4 (89.9%) and γ_6 (83.6%) are the most abundant, the next in importance being β_3 (7.27%) and γ_8 (7.17%).

Certain organs are more sensitive to damage than the others. This has led to the concept of effective dose (ED). Strictly, this concept applies both to external and internal radiation. However, since specific organs are more often subjected to radiation by internal ingestion/inhalation, it is treated in this section. The concept of ED takes into account the chance effects (stochastic effects) of ionising radiations. A weighting factor W_T is defined by which the dose equivalent to an organ must be multiplied to obtain dose to the total body. Some typical weighting factor data are given in Table 21.3.

Let us consider an example. In a radioisotope laboratory accidental release of ^{131}I resulted in the deposition of 370,000 Bq of ^{131}I in a technician. Of that 74,000 Bq was found in the thyroid and 296,000 Bq in the rest of the body. From bio-assay and body scanning the health physicist calculated a dose of 126 mGy for thyroid and 0.26 mGy for the whole body. The effective dose can be calculated using data from Table 21.3 as follows.

ED = 0.05 x 126 + 0.95 x 0.26 = 6.55 mSv

For bone seeking radionuclides like ^{90}Sr and ^{239}Pu, which emit particulate radiation, estimates on radiation effect are based on ^{226}Ra for which a large body of past data exists from watch industry. Maximum permissible body burden of 0.1 μg has been considered for radium.

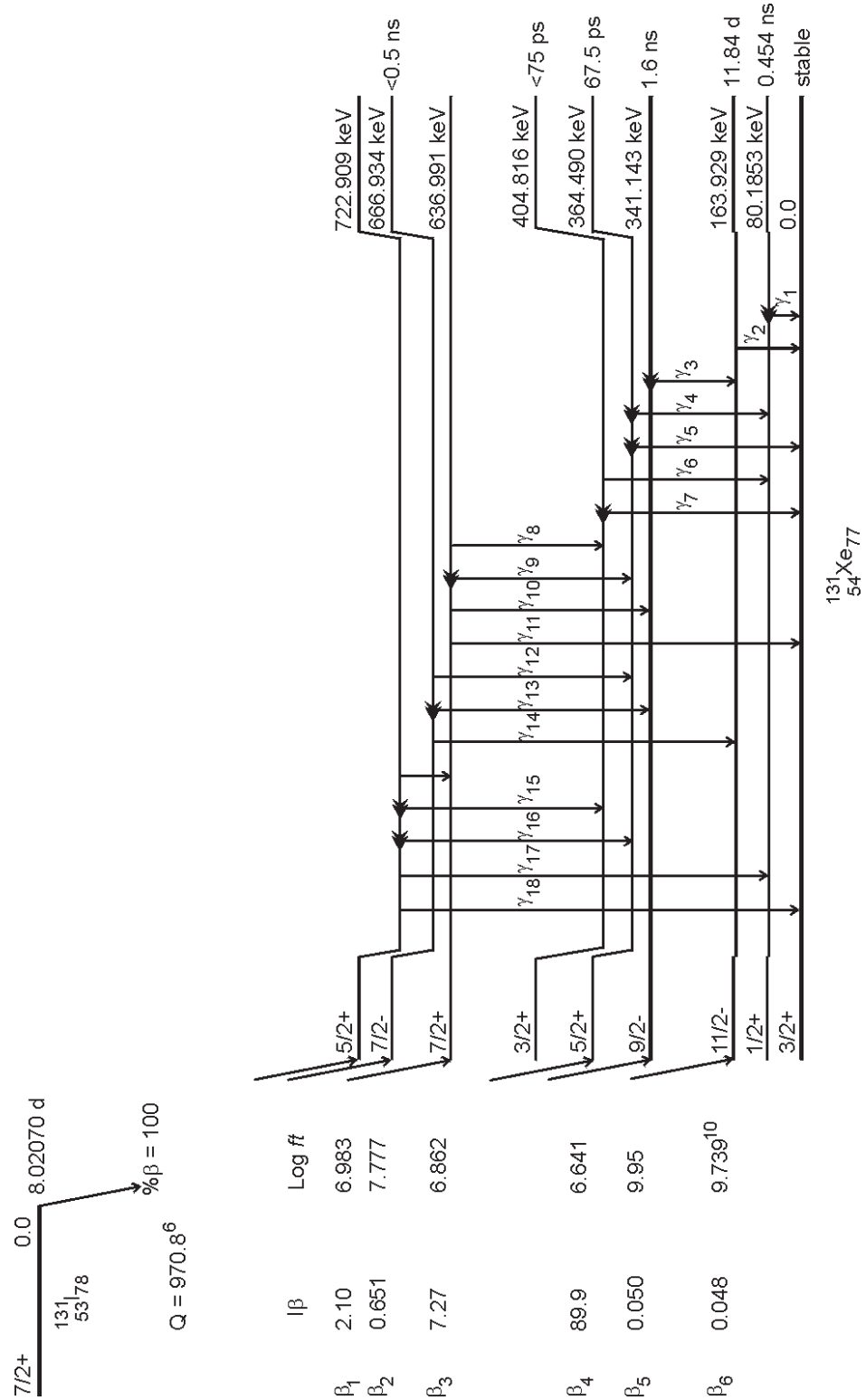

Fig. 21.3 Decay scheme of ^{131}I dosimetry [Courtesy : Nuclear Data Section, IAEA].

Table 21.3 - ICRP tissue weighting factors

Organs	Bone surfaces Skin	Bladder Breast Liver Oesophagus Thyroid[a]	Colon Lung Red bone marrow Stomach	Gonads
WT	0.01	0.05	0.12	0.20
Total	0.02	0.30	0.48	0.20

[a]Also for muscle, kidneys, pancreas, spleen, uterus bladder wall, thymus etc.
[1990 Recommendations of International Commission on Radiation Protection, ICRP Publication 60, Ann 1-3, Pergamon Press, Oxford (1991)].

Doses from Various Sources of Radiation

External Dose due to Natural Sources

Nuclear reactions are the prime sources of energy in the universe. The sun and the stars continuously emit energy, which is released during nuclear fusion reactions. In the process of the formation of solar system, there must have been a stage when there were a large number of radioactive nuclei. Most of them have decayed to stable products. The main radioisotopes left are ^{235}U, ^{238}U, ^{232}Th (along with their daughter products) and ^{40}K as all of them have long half-lives. It is estimated that when earth was formed several billion years ago, the ^{235}U concentration was about 14% which decreased to 0.72% now because the half-life of ^{235}U is less than that of ^{238}U. Uranium and thorium, widely distributed in earth's crust, are sources of exposure to man, as are their decay products particularly radium and radon. In addition, the cosmic radiation, which increases with altitude, is another major source of natural radiation exposure to man. Background dose due to these external sources is estimated to be in the region of 0.9 to 1 mSv per year at sea level. The cosmic radiation is attenuated significantly by the mass of air surrounding us which is equivalent to shielding by 10.3 meters of water. However, if we go to higher altitudes this shielding is decreased and dose is increased. **At a place having 3000 m altitude, the background dose would be about 1.7 mSv/y and will increase to 44 mSv/y in a supersonic jet flying 18 km above the ground.**

In regions of the world which have near surface deposits of uranium or thorium or where natural uranium concentration is significantly above 2-3 ppm, the dose levels are substantially higher. Typical data averaged for British population is given in Table 21.4.

The corresponding average value for India is 2490 μSv/y with much larger internal and external doses, and smaller medical and other doses. Certain specific areas in China, India and Brazil have reported levels in the range of 100-200 mSv/y compared to legal limit of 20 mSv/y for a radiation worker. In coastal areas of Kerala, a large area having thorium

Table 21.4 - Averaged radiation dose to common man in UK

Source	Radiation / Radioisotope	μSv/y
Atmosphere	Rn, ^{137}Cs	800
Rocks and Buildings	U, Th	400
Food/body	^{40}K, ^{14}C, ^{137}Cs	370
Cosmic Rays	Subnuclear Particles	300
Medical Tests	X-rays	250
Everyday Source	Coal, tobacco, air travel	10
Weapons Tests	^{90}Sr	10
Occupational Exposure	X-ray	8
Nuclear Power	U	2
Total		2150

[A. Holmer-Siedel, L. Adams, 'Handbook of Radiation Protection', Oxford University Press, Oxford (1993)].

bearing monazite sand is heavily populated. In Chavara area household dosimetry measurements showed that annual dose was in the range of 10-20 mSv/y.

Internal Dose due to Natural Sources

The body contains several radionuclides of natural origin. There is about 140 g of potassium in standard reference man (70 kg) and out of which 0.0164 g is ^{40}K. It decays with a half-life of 1.28 billion years. 266,000 atoms of ^{40}K decay in our body every minute. Branching fraction for β^- decay is 89.28%, a part of it decays to excited state of ^{40}Ca and the remaining decays to ground state of ^{40}Ca with a β_{max} of 1.33 MeV. Branching fraction for EC is 10.72% and it populates an excited state of ^{40}Ar which deexcites by emitting 1.46 MeV γ-ray. It is estimated that the dose due to ^{40}K is about 0.18 mSv per year.

Another radioactive constituent of body is ^{14}C. It is a soft β-emitter (β_{max} = 156 keV) and has a half- life of 5,730 y. It is continuously formed in air by ^{14}N (n,p) reaction. About 193,000 atoms of ^{14}C decay every minute in our body leading to a dose of about 0.01 mSv per year. Other important natural radioisotopes are ^{226}Ra and ^{210}Po which deposit primarily in bone. ^{210}Po gives about 0.6 mSv and ^{226}Ra about 0.14 mSv to the bone per year.

The atmosphere always contains short-lived ^{222}Rn and ^{220}Rn, from the decay chains of uranium and thorium, along with their decay products (see Figs. 1.1, 1.2 and 1.3). Annual

dose due to these sources to lungs is 6.8 mSv. Thus lung receives the highest radiation exposure from natural sources.

External Dose from Medical X-rays

Different parts of human body receive varying doses due to X-ray examinations. For example, abdomen and thorac spin receive on an average 1.39 and 0.92 mSv in one examination. The upper and lower equivalent dose levels for some common X-ray examinations are given in Table 21.5.

Internal Dose due to Medical Procedures

As mentioned earlier, a number of medical investigations use radioisotope based pharmaceuticals for diagnostics and therapy and body receives does due to these examinations. Some typical values for effective dose equivalents of dose commitment are given in Table 21.6.

Radiation Effects

Biological effect of radiation can be classified into two broad classes: (i) deterministic effects and (ii) stochastic effects. The deterministic effects are the visible changes which manifest themselves within a short period of radiation exposure. These have been observed only at high doses above 1 Gy and occur within the first few weeks of exposure. The stochastic effects are the biological changes produced by chance; these may or may not occur in an individual but in a large population some will manifest this effect. The time required for the effect to be seen can range from several years to several decades.

Deterministic Effects

Deterministic effects are classified into two types : somatic and genetic. As the names indicate somatic effects are seen in the individual receiving radiation exposure. Genetic effects are seen in the progeny of the person exposed.

Somatic Effects

Data on somatic effect has been obtained from Hiroshima/Nagasaki victims, patients treated by teletherapy for cancer, and from animal experiments. In nuclear technology exposures which can cause somatic changes would occur only in the case of severe radiation accident. Some effects are discussed below:

(a) Haematologic Changes

At a dose of about 0.25 Gy haematologic changes are detectable but similar changes may occur even with a common cold. Noticeable changes occur above 1 Gy. There is a decrease in lymphocytes and, its depression and rate of recovery in the initial 48 hours are useful in prognosis. White blood cell count (lymphocytes + granulocytes) decreases rapidly

Table 21.5 - Effective equivalent dose (mSv) for common X-ray examinations.

	Mean	Minimum	Maximum
Lumbar spine			
Whole examination	2.15	0.37	7.37
Anteroposterior only	0.9	0.09	6.87
Lateral only	0.53	0.07	3.14
L5-S1 lateral	0.50	0.05	2.06
Chest			
posteroanterior and lateral (1.3 films)	0.05	0.01	1.32
posteroanterior only	0.02	< 0.01	0.18
Lateral only	0.13	0.01	1.20
Skull			
Three views	0.15	0.01	0.50
Anteroposterior only	0.05	0.01	0.21
Lateral only	0.03	0.01	0.13
Abdomen			
Anteroposterior	1.39	0.12	9.94
Thoracic spine			
Two views	0.92	0.16	4.39
Anteroposterior only	0.48	0.07	3.13
Lateral only	0.29	0.01	1.42
Pelvis	1.22	0.09	5.77
Intravenous urogram			
(8 films)	4.4	1.4	35
Barium meal			
(8 films; including average screening time)	3.8	0.6	24
Barium enema			
(8/9 films)	7.7	2.9	34
Cholecystography			
(4/5 films)	1	0.1	5

[S. Plant, 'Radiation Protection in the X-ray Department', Butterworths Heinemann (1993)]

Table 21.6 - Effective dose commitment in diagnostic imaging.

Organ	Compound (Isotope)	Quantity (Bq)	Organ dose (mGy)	Effective dose (mSv)
Bone	Pyrophosphate (^{99m}Tc)	10^9	63	8.0
Brain	Gluconate (^{99m}Tc)	10^9	56	9.0
Liver	Sulphur Colloid (^{99m}Tc)	1.5×10^8	11.2	2.1
Lung	Macroaggregated Albumin (^{99m}Tc)	1.5×10^8	9.9	1.77
Heart (Cardiac output)	Erythrocytes (^{99m}Tc)	10^9	23	8.5
Renal	Gluconate (^{99m}Tc)	5×10^8	28 (bladder)	4.5
Thyroid	Pertechnetate (^{99m}Tc)	3.5×10^8	8.0 2.2 (bladder)	4.5
Thyroid (uptake 35%)	NaI (^{131}I)	2×10^6	720	22
Thyroid scan (35% uptake)	NaI (^{123}I)	7.5×10^6	34	1.1
Heart	Thallous chloride (^{201}Tl)	7.5×10^7	4.1 (testes)	17

[From J. Shapiro, 'Radiation Protection - a Guide for Scientists and Physicians', Harvard University Press, Cambridge, 1990]

for a week and the decrease may continue upto 5 weeks if exposure is high. If the patient survives, the blood count gradually returns back to normal.

Bleeding may occur in a few days if exposure is several Gy and this is associated with decrease in platelets.

(b) Hemopoietic Syndrome

This involves nausea and vomiting several hours after exposure has occurred. Gamma dose above 2 Gy causes depression or ablation of bone marrow. Epilation (loss of hair) is also seen after 2-3 weeks. At doses of 4-6 Gy complete ablation of bone marrow occurs. If the patient survives, there is a spontaneous regrowth of bone marrow. Doses above 7 Gy quite often lead to irreversible bone marrow loss.

(c) Gastrointestinal Syndrome

At doses above 10 Gy, in addition to the above signs, intestinal epithelium is damaged and diarrhoea occurs and death is likely within 1-2 weeks.

(d) Central Nervous System

Doses above 20 Gy cause lethal damage to the central nervous system. Unconsciousness occurs within a a few minutes and death is more probable.

(e) Other Acute Effects

Skin is most commonly affected by radiation exposure. Dermatitis of hands and face were most common among radiologists of the past. Gonads are sensitive and a single dose of 0.3 Gy to testes causes temporary sterility among men. 3 Gy exposure to ovaries produces temporary sterility. Eyes are also very sensitive. A local dose of several grays results in acute conjunctivitis and keratitis.

(f) Delayed Effects

Radiation can induce cancer and this effect is most commonly observed in the hemopoietic system, in the thyroid, in the bone and in the skin. Tumour induction time ranges between 5 and 20 years. Prominent among the cancers are leukaemia, bone cancer and lung cancer. At Hiroshima a dose of 0.2 to 0.5 Gy led to increased incidence of leukaemia.

Genetic Effects

All radiation effects listed are due to injury to human cells. However, chromosomal injury to germ cells can cause genetic effects. A number of studies have been carried out on groups of individuals exposed to high radiation. These include Hiroshima/Nagasaki bomb blast victims exposed to doses more than 2 Gy, and individuals in France receiving teletherapy dose of 4.5 to 14 Gy. There is no conclusive evidence of any hereditary effects. In the case of unconfirmed animal experiments, where males were given a high level of dose to gonads, no mutation effects were noted in the colon. Radiobiological surveys of plants and animals around nuclear test sites at Bikmi and Eniwetok atolls failed to reveal any definite mutation anomalies. Laboratory experiments on animals have, however, established that radiation can cause mutation. However, the type of mutations observed were similar to those observed without radiation. The relative frequency of mutation is the same for radiation induced or spontaneously occurring mutations. On the basis of these laboratory studies it was concluded that 0.5 to 2.5 Gy of dose would be required to increase the frequency of mutation by a factor of 2. It is estimated that chances for spontaneous mutation (without radiation) in a dominant gene trait are 320 per million. If a parent were irradiated to a dose of 0.01 Gy the probability will increase to 323 units per million.

Stochastic Effects

Stochastic effects are those which occur by chance. They may occur among the people who are not exposed to radiation as well as among people exposed to radiation. These can not be directly attributed to a specific agent. For example, the incidence of cancer is much higher among smokers as compared to non-smokers and the difference is dependent on the intensity of smoking. However, most smokers do not develop lung cancer. There is enough data available at high dose rates but at low doses the results on carcinogenic effects of radiation are not consistent. The reason is that on an average there are 206,000 cancer deaths per million in normal population. Effect of any radiation induced carcinoma on this number is not detectable. Therefore, it is assumed that radiation induced effects will decrease with dose linearly and there is no threshold for cancer induction. Based on this assumption it has been concluded that exposure to 1 mSv of radiation, above the background, would increase cancer related deaths by 125 per million. Certain areas in China, India and Brazil have reported natural radiation level in the range of 100-200 mSv per year compared to legal limit of 20 mSv/y for a radiation worker. Epidemiological studies in China and India, even in the areas having 10 times higher dose than UK, have not proven any correlation between radiation dose and incidence of cancer or genetic mutation. The data on the effects of continuous exposure to low doses of radiation are thus not conclusive and, therefore, extrapolation of data on effects at high doses of radiation is resorted to.

Radiation Protection Guides

Principles

Most countries formulate their radiation protection standards based on the recommendations of the International Commission on Radiation Protection (ICRP). These are based on : (i) prevention of deterministic effects by keeping doses below their threshold level and (ii) assuming that reasonable actions are taken to limit the occurrence of stochastic effects to acceptable levels.

Activities which add to radiation exposure are called ‘practices’. This involves essentially all normal activities in nuclear technology. Activities which help to reduce/subtract radiation exposure are called ‘intervention’, for example counter measures during an emergency/accident.

The principles recommended by the ICRP for ‘practices’ are :

- A practice involving exposure should produce sufficient benefit to offset the radiation detriment it causes - **justification**.
- For any source, doses or likelihood of being exposed should be As Low As Reasonably Achievable (ALARA) and constrained by doses to individual and risks to individuals from potential exposures - **optimisation**.

- Individual exposures from all sources, susceptible to control are subject to dose limits and some control of risk from potential exposures - **dose and risk limits**.

The general principles of 'intervention' are

- Any intervention must do more good than harm so the radiation detriment must exceed the harm and social cost of intervention.
- The scale and duration of the intervention should be such that the net benefit of the reduction in dose, less the cost of intervention, should be as large as reasonably achievable.

ICRP believes that 'effective dose' is an adequate surrogate for detriment to an individual and collective effective dose for a population.

Dose Limits

ICRP dose limits are applicable to occupational and public exposures. The dose limit is set such that continued exposure at a dose just above the limit would be unacceptable or any reasonable basis for continued exposure below the limit is tolerated but not encouraged, such that acceptable doses are somewhat below the limit.

Radiation Workers

Limits apply to all occupational situations including mishaps and misjudgements in plant operation and, planned and unplanned maintenance and decommissioning of a nuclear plant.

(a) Deterministic Effects

Annual limits for workers are 150 mSv for the eye lens and 500 mSv for the skin and extremities.

(b) Stochastic Effects

The dose limits are based on the total estimated detriment due to fatal cancer, non-fatal cancer and hereditary defects. Accordingly

- Effective dose to an individual should not exceed 1 Sv over a working life.
- The rate of delivery of radiation is not to exceed 50 mSv in any single year or 100 mSv in any five years period (20 mSv/y averaged over 5 years).
- Occupational exposure to non-pregnant women are the same as for men. Additional controls are necessary for pregnant women. Conception should be protected by applying a dose limit of 2 mSv to the woman's abdomen for the remainder of the pregnancy.

Public

(a) Deterministic Effects

Limits on annual dose of 15 mSv to lens of the eye and 50 mSv to skin or hands.

(b) Stochastic Effects

Annual effective dose of 1 mSv over any five consecutive years.

Allowed Limits of Intake (ALI)

For a common man as well as for radiation workers, the external dose may not be significant but ingestion or inhalation of radioisotopes may contribute to radiation exposure. Accordingly ICRP has defined the allowed limits of intake of radioisotope through breathing or drinking water. The total effective dose from all sources, external or internal, should not exceed the limits specified by ICRP. In the case of internal intake the chemistry of the radioisotopes comes into play and some of them like ^{90}Sr and ^{239}Pu concentrating in the bone while others like ^{137}Cs distributing all over the body. The tissue weighting factors, individual clearance half-lives are considered in the case of distribution to specific tissue/tissues.

For example, for ^{90}Sr, in equilibrium with ^{90}Y, 1 Bq would correspond to 6.78×10^7 disintegrations in 50 years. Knowing that $^{90}Sr/^{90}Y$ concentrate in the bone (~5 kg) the total dose commitment per Bq is 0.70 mSv/g. So ALI for 50 mSv (1 mSv for 50 y) is 71 Bq/g. With weight of 5 kg and assuming 30% of intake accumulating in bone, ALI is $(71 \times 5000)/0.3 \simeq 1 \times 10^6$ Bq.

For deriving concentration of ^{90}Sr in water one can assume that the person drinks 2.2 litres of water per day. Similarly for derived air concentration one assumes that a person breaths 20 litres of air per minute and he is exposed to 2000 hours in a year.

Measures for Radiation Protection

Handling / Using Radiation Sources

X-ray machines, ^{60}Co teletherapy units and ^{192}Ir radiographic cameras are strong sources of ionising radiation. Great care is taken in handling these sources to keep exposure to personnel within permissible limits. Shielding of radiation, as well as separation of operator from the equipment, are used to minimise radiation exposure. The principles of radiation attenuation have already been discussed. The attenuation coefficients (m) for X/γ-rays are given in Table 21.7.

Quite often the concept of half value thickness is used for practical purposes. For example, the half value thickness of lead for ^{137}Cs (0.66 MeV) gamma rays is 0.55 cm. To reduce radiation exposure by a factor of 8, three half value thickness (1.65 cm) of lead is required. Also as the intensity of photon radiation is inversely proportional to the square of

Table 21.7 - Attenuation coefficients for photons in different materials.

Energy (MeV)	μ (cm^{-1})			
	Water	Iron	Lead	Concrete
0.1	0.168	2.69	59.4	0.400
1.0	0.071	0.469	0.776	0.150
10	0.022	0.235	0.549	0.054

the distance (assuming no absorption by air), use of long tongs for handling radiation sources helps to minimise radiation exposure.

Special Facilities for Handling Radioisotopes

Authorisation from national regulatory bodies is required for handling radioisotopes above a certain limit. This limit is 10 μCi (3.7×10^5 Bq) for most of the radioisotopes, with higher value of 100 μCi for some like ^{35}S, ^{198}Au and ^{14}C, and lower value of 1 μCi for ^{131}I, ^{125}I and ^{60}Co. Above this limit special work environment is required depending upon the amount and the type of radioisotope handled particularly in the form of unsealed sources.

Generally a well designed and well maintained chemistry laboratory is sufficient with some additional precautions. Precaution should be taken to handle radioactive sources in a fumehood with exhaust such that the opening has an air velocity of 30 m/min. This ensures that radioactive particles do not enter the laboratory. Handling is normally done in a tray lined with plastic film. Glassware and tongs used for radioactive materials are kept separately. Latex gloves should be used to carry out operations in a fumehood. Wearing a laboratory coat is a must. This type of arrangement can be used for handling upto 10 mCi (3.7×10^8 Bq) of less hazardous β^- emitters. In order to handle larger amounts, more precautions are required and accordingly the laboratories have been classified into three types namely, A, B and C. The amount of radioactivity permitted to be handled depends on the radiotoxicity of the isotope. Some typical data are given in Table 21.8. The quantities of radioisotopes permitted for handling in various laboratories are given in Table 21.9.

Design Features of a Class C Laboratory

The type of laboratory discussed above is a Class C laboratory. Any chemical laboratory in a college can be converted to a class C laboratory. It is desirable to make the following provisions.

(a) Amenability of surfaces to easy decontamination: Floors, wall, ceilings and table tops should be smooth. Floor could be covered with PVC tiles and surface painted with washable smooth paint. Furniture should preferably be stainless steel/painted steel.

Table 21.8 - Radiotoxicity classification of radionuclides

Highly Toxic	Medium Toxic (A)	Medium Toxic (B)	Low Toxic
$^{232,233,234}U$, $^{238,239,240,241}Pu$, $^{226,228}Ra$, $^{241,243}Am$, ^{244}Cm, ^{210}Po	^{45}Ca, ^{54}Mn, ^{60}Co, $^{89,90}Sr$, ^{95}Zr, $^{129,131}I$, ^{137}Cs, ^{192}Ir, ^{210}Bi	^{14}C, ^{24}Na, ^{32}P, ^{41}Ar, ^{51}Cr, ^{59}Fe, ^{65}Zn, ^{90}Y, ^{99}Tc, ^{198}Au, ^{203}Hg	^{3}H, ^{58m}Co, ^{69}Zn, ^{85}Kr, ^{87}Rb, ^{99m}Tc, ^{133}Xe, ^{147}Sm, ^{Nat}U, ^{Nat}Th

Table 21.9 - Quantities of radioisotopes permitted for handling, in different types of laboratories.

Type of Lab	Quantity of radioisotope handled			
	Slightly or low toxic	Medium toxic		Highly toxic
		Sub Group B	Sub Group A	
Type C	0.37 GBq (10 mCi)	37 MBq (1 mCi)	3.7 MBq (100 μCi)	0.37 MBq (10 μCi)
Type B	370 GBq (10 Ci)	37 GBq (1Ci)	3.7 GBq (100 mCi)	0.37 GBq (10 mCi)
Type A	More than Type B			

(b) Decontamination / Washing Facility

Stainless steel sink preferred over porcelain. Tap should be operable with elbow.

(c) Laboratory Liquid Effluent

Average laboratory effluent is expected to be < 3.7 MBq (or 100 μCi) per m^3 and waste volume is small. It is therefore allowed to mix with the general effluents from the locality which can provide a dilution factor of more than 100.

(d) Forced Ventilation

Laboratory should have a fumehood for handling the radioisotopes. The exhaust system of the fumehood should provide about 3 air changes per hour which would dilute any activity release. Further, it should be assumed that linear velocity of air across the opening in the fumehood is more than 0.5 m/s to prevent entry of radioactive particles into the laboratory. The exhaust is directly discharged to atmosphere and activity is expected to be quite low (<3.7 Bq/m^3).

(e) Counting Room Facility

A separate area/room is preferred for housing the radiation measuring equipment. This would help in keeping the equipment contamination free with a low background.

(f) Storage Facility

If several isotopes are handled in the laboratory, a separate storage space (e.g., corner of the room) should be allocated for storing radioisotopes. The dose outside the storage area (at 10 cm) should not exceed 10 μSv/h.

(g) Monitoring Instruments

It is desirable to keep a continuous check on the level of contamination of the work place and the personnel. A G.M. survey meter and a beta-gamma contamination monitor are required for this purpose.

(h) Personnel may be provided with TLD badges depending on the advice of the regulatory authorities.

Design Features of Class B Laboratory

This type of laboratory becomes essential when the quantities of radioactive materials being handled exceed frequently the limits prescribed for type C laboratories. If the limits are exceeded by factors less than an order of magnitude, the type B laboratory will be a simple modified version of a type C laboratory. For larger amounts, a separate facility coming under type B laboratory must be designed.

Type B laboratory meets all the specifications of a type C laboratory. In addition, the following points need careful evaluation.

(a) Ventilation System

The ventilation system for the active area must be independent of the other ventilation systems in the building. It may also be necessary to provide for filtration of the fumehood exhaust air before it is released into the atmosphere. This exhaust air should be released at the tallest point of the building or a few meters above it through a stack. Siting of exhaust and supply points should be so chosen to prevent recirculation of exhausted air under the prevailing conditions of local terrain. The degree of filtration of the exhaust air will have to be worked out in advance and suitable filtration system installed accordingly. The capacity of the ventilation system should be adequate to provide 5-7 air changes/h in the laboratories.

(b) Use of Glove Boxes

Radioactive operations are shifted from fume hoods to glove boxes whenever the quantities of radioactive materials involved exceed the limits set for operations in fumehood or wherever materials are handled in dry form. Glove boxes are discussed under containment systems.

(c) Gamma Shielding

This may be necessary for creating a regular storage facility or providing shielding in a fumehood or glove box if the radiation field for personnel working in operation areas exceeded the derived working limits. For the storage area the floor loading capacity should be adequate to support the weight of lead or mild steel which are commonly used for gamma shielding. This requirement should be considered while facility is under construction. Similarly the fumehood/glove box floor or the tables used to support them should be strong enough to withstand the weight of the lead bricks used to make shielded enclosures within these handling facilities. Areas requiring heavy gamma shielding are always located on the ground floor or basement.

(d) Provision of a Change Room

Type B laboratories require provision of a change room at the entrance of the active area which is delineated by providing a physical barrier. Shoe covers must be worn beyond the barrier and laboratory coats must be picked up from the change room before proceeding to the laboratories. Wash basins and contamination monitors are also installed in the change room.

(e) Laboratory Liquid Effluents

The activity content of the waste arising from these laboratories may be high enough to prohibit its discharge directly into the public sewer. This problem is tackled by taking the following steps (a) Effort is made to collect high active liquid waste into separate plastic carbuoys or glass bottles instead of discharging it directly into the sink. Such waste is then allowed to decay by storage or handed over to a centralised waste management facility and (b) by providing a separate liquid effluent delay/hold-up tank facility at site. The waste from such a tank can be analysed for its activity level and then discharged into public sewer directly if the activity level is within limits or after dilution if the activity level is high.

(f) Provision of Additional Monitoring Instruments/Protective Equipment

The first and foremost in this case is providing hand, foot and clothing monitors. Provision for routine air monitoring in critical laboratory areas should also be made. Respiratory protective equipment, i.e. dust respirators should also be made available in the change room for use when required. TLD/Film badges may also become necessary for all individuals in the laboratory.

For type B facilities outside the Department of Atomic Energy (DAE), a constant interaction may be necessary between operating agency and the authorising agency to deal with situations not clearly spelt out otherwise.

Design Features of a Class A Laboratory

Type A laboratory requires careful planning and design as there is no upper limit on the radioactivity that can be handled there. Each project, is therefore, examined separately

and the largest quantities of materials likely to be encountered are identified. Necessary facilities are then built accordingly taking into account the operational requirements.

Thus all the specifications discussed above in the case of type C and B facilities must be met in this case. In addition, the following points require careful consideration (Radiological laboratories at Bhabha Atomic Research Centre (BARC), Mumbai are typical examples for Class A laboratories).

(a) Layout of the Laboratory Area

From consideration of safety and operational efficiency, the design of overall laboratory should group together areas according to the degree of contamination hazard posed by them. Such grouping involves, classification of areas into following zones.

(i) *White (Inactive) Area* : It consists of unrestricted areas of the laboratory facility, e.g., office room, reception room, workshop etc. No radioactive material is kept, stored or handled here. Probability of contamination is nil in this area except under accidental conditions.

(ii) *Green (Potentially Active) Area* : No radioactive materials are handled in this area but small quantities in sealed containers may be stored. Possibility of contamination in this area (which is otherwise clean) can not be ruled out by virtue of its proximity to active areas. Counting room, health physics room, personnel corridors etc. constitute this zone. Access to this and other areas described below is restricted to laboratory staff and the supporting staff only.

(iii) *Amber (Low Active) Area* : It is the actual laboratory area where work benches, fume hoods, glove boxes, etc. are located. It also includes the active personnel corridors and the change room. Possibility of contamination in this area always exists by virtue of its proximity to red zone. A physical barrier separates it from the green zone.

(iv) *Red (Active) Zone* : The area where the radioactive material is actually present and handled i.e. interior of a fumehood, glove box or shielded cell. This zone is always highly contaminated and operations here are manipulated by personnel standing in amber area. Entry in this are is forbidden except under special circumstances and with prior authorisation.

The zoning philosophy in type B and C laboratories is also similar. While the red zone gets clearly demarcated, boundaries of other zones may be less rigid or sharp. In type C laboratories, the green and white zones overlap each other very often.

(b) Containment Systems

The spread of activity or contamination from red zone to amber zone is prevented/minimised by designing the red zone as a containment system. It consists of fumehoods and glove boxes.

(i) *Fumehood* : Fumehood is a partial enclosure and the opening of the panel provides an access to material being handled. Directional air movement through the panel opening maintained at 30 cm from the bottom prevents the materials from reaching operators' environment. Operations are carried out in fumehood when the amounts of radioactive materials being handled are limited, nature of operation is simple and contamination hazard is not significant.

(ii) *Glove Box* : A glove box is a miniature laboratory within a laboratory. It provides for total containment of material being manipulated. It is a leak tight assembly which completely isolates the hazardous material from the operator's environment. It is operated at a negative pressure of 12-25 mm water gauge. The manipulation is effected through gauntlet gloves fixed on the viewing panels of glove box. Transfer ports and bagging ports are provided on glove boxes for taking the materials in or out without affecting containment's integrity. Glove boxes are used when the activities handled exceed the limits prescribed for fume hoods or when the nature of operation is hazardous.

(iii) Shielded glove boxes and hot cells are essentially extended versions of glove boxes. Thus they provide not only total containment of materials being handled but also provide shielding to personnel when radiation levels encountered are high. The high radiation levels in these cases preclude operations by hands through gauntlet gloves. The operations are then carried out by tongs and master slave manipulators in shielded glove boxes and hot cells respectively. Further detailed description of these two containment systems lies outside the scope of this book.

(c) Ventilation System

The ventilation system is the most important and expensive part of the entire radioactive laboratory system. The general ventilation system in a laboratory consists of a balanced air supply and exhaust, such that the air always flows from potentially less active to high active area. The quantum of air supply and exhaust (number of air changes) is governed primarily by the number of fume hoods provided in the laboratory. The inlet air is filtered to avoid large dust loads. Filtration of the exhaust air is determined on the basis of likely release of materials into the atmosphere. Separate systems are provided for laboratory areas (which include fume hoods), glove boxes (including shielded boxes) and hot cells.

The ventilation system in a class A laboratory has a once through conditioned air supply system. The general laboratory ventilation system consists of a balanced supply and exhaust. The air flow always follows the pattern: from white area to green area to amber area to red area, to prevent spread of air borne contamination. The capacity of the ventilation system should be adequate to provide about 3, 5 and 10 air changes in white, green and amber areas respectively. This large air-volume can pose dust problems in the active laboratories. The supply air is, therefore, filtered through coarse filters which remove 85 to 95% of the atmospheric dust load. This air is exhausted through fume hoods. Since the quantities of activities handled in fume hoods are relatively large (as compared to those in type B or C laboratories), the exhausted air is filtered through a bank of high efficiency particulate air

(HEPA) filters which has a filtration/retention efficiency of greater than 99.5% (for the bank as a whole) for particles of 0.3 μm size (for individual filters the efficiency is ≥ 99.98%). The filtered air is released to the atmosphere through a stack, which should be taller than the tallest building in that area.

The glove box and hot cell exhaust systems have no separate air supply. They draw air from the surrounding areas through leakages and in certain cases, through designed air inlet points. Since the activities handled in these enclosures are very high, the exhausted air undergoes filtration through HEPA filters twice: first while leaving the enclosure and second before discharging to stack. The stack height is decided based on dilution needed for the exhausted air by the time it reaches ground level.

Because the type A laboratories are very expensive facilities, their continuous operation and utilisation is very essential. For this purpose, the ventilation systems generally have 50% to 100% standby capacities to take care of any break downs/shut downs. The glove box and hot cell ventilation systems also have standby diesel power supply which takes over if and when normal power supply fails.

(d) Liquid Effluent System

From type A laboratories, no effluent is discharged directly into the public sewers or into the sea or river. These laboratories have their low level liquid waste systems, which consists of waste lines and storage tanks. The collected effluents are monitored for radioactivity content and then pumped to effluent treatment plant for further treatment and discharge. This waste contains alpha, beta and gamma activities.

All the high level liquid waste which can not be directly put into the sinks (activity > 3.7 MBq or 100 $\mu Ci/m^3$) is taken in carbuoys and separately handed over to Waste Management Facility for further treatment. Alpha bearing waste is collected separately.

Solid Radioactive Waste

The waste arising from red and amber zone is treated as radioactive waste. It consists of gloves, tissue papers, polyethylene sheets, glassware and anything else in the laboratory that has been used for active work and is no longer required. Waste is segregated in two categories (i) compressible waste consisting of paper, rubber, PVC etc and (ii) non-compressible waste consisting of glass, metal etc. A further categorisation is also made based on radiation levels i.e. < 2, 2-20 and > 20 mSv/h for beta-gamma waste. Alpha bearing waste is collected separately.

The waste is doubly sealed in polyethylene/PVC bags to withstand rough handling during transportation. All non-compressible waste requires further packing in cardboard boxes. Each waste bag must have a proper transit tag that shows the waste category and the level of radiation field on its surface. The waste from type A laboratories is always handed over to a centralised waste management facility for further treatment.

Similar waste categorisation is also carried out at type B and C laboratories. These laboratories, those outside DAE, may have their own burial pits for wastes of low activity level. High activity level waste, if any, must however, be transported to the nearest centralised waste management facility.

Operational Procedures and Practices

Success in the operation of a radiochemical facility depends on many factors in addition to intrinsic safety inculcating discipline to adhere to regulations. They are: evolving good operational practices, their scrupulous implementation, respect for administrative controls, etc. These are directly linked to the level of awareness of staff working in the facility. A healthy working atmosphere, therefore, becomes a prerequisite to achieve positive end results.

Further, to avoid any inadvertent internal contamination and as a matter of abundant caution the following are banned in all the areas except white areas.

(a) use of eatables, beverages and snuff, and smoking.

(b) use of chewing materials like pan, chewing gum etc.

(c) use of personal hand kerchiefs and napkins in amber areas and

(d) use of cosmetic items.

Direct fountain type water coolers (non storage type) may, however, be permitted in green areas.

It is essential to follow certain stipulated procedure to minimise contamination in the laboratory and working place. The necessary instructions are as follows:

(a) As described earlier, the radioactive area (Amber Zone) is separated from the Green Zone by a barrier. Persons entering the amber zone should wear the protective clothing like shoe covers and coats (Class B and Class A).

(b) All work should be carried out in a fumehood or a glove box. Polythene sheet must be spread in the fumehood/glove box before starting experiment to help in rapid clean up (All classes).

(c) Eating, drinking, smoking and using snuff are prohibited in the laboratory (All classes).

(d) All operations with exposed sources of radioactivity must be carried out in a fumehood with proper ventilation. Personnel should wear surgical gloves during these operations to avoid direct physical contact with the radioactive substances (All classes).

(e) No work with radioactive material should be carried out by anybody having an open cut, skin lesion or injury (All classes).

(f) Pipetting of any solution should not be done by mouth in a radioactive laboratory. Pro-pipette or a syringe should be used (All classes).

(g) Any spillage of radioactive solution, contamination of personnel or work area by any accident must be reported to the laboratory-in-charge (All classes).

(h) All wastes of liquids and solids must be separated and stored in containers (Class B and Class A).

(i) All active materials must be stored, sealed and labelled properly, with date and persons name written on it (All classes).

(j) Active samples should not be removed from the laboratory without the permission of laboratory in-charge (All classes).

(k) After removing the gloves, hands should be washed with detergent solution and water (All classes).

(l) Hands should be monitored using hand monitors provided in the green zone of the radioactive laboratory. Only when the hands are free from contamination one should leave the laboratory (Class B and Class A).

(m) A film badge or a TLD for personnel monitoring of radiation exposure must be worn by the person while working in the active laboratory (Class B and Class A).

Measurement of Radiation Exposure

Despite all the radiation safety precautions and procedures, individuals might be exposed to radiation. It must, however, be ensured that these exposures are within the prescribed limits. They arise from external and internal radiation exposures.

External radiation exposure is measured for each individual by providing the individual with a TLD/film badge. It is worn on the trunk of the body and is processed at a certain predetermined periodicity. Internal radiation exposures, which are generally small due to intrinsic safety features of the laboratory, are measured by bioassay techniques and/or in-vivo whole body burden measurements. Sum of the two exposures is the total exposure of each individual.

Bibliography

1. 1990 Recommendations of International Commission on Radiation Protection, ICRP Publication 60, Ann 1-3, Pergamon Press, Oxford (1991)

2. Nuclear Regulatory Commission. Standards for Protection against Radiation. Final Rule. Report No. 10 CFR Pt.20. US NRC, Washington (1991)

3. Risk Estimates for Radiation Protection: Recommendations of National Committee of Radiation Protection and Measurement. The Council, Bethesda (1993)

4. B. Shleren, 'The Health Physics and Radiological Health Handbook', Scinta, Silver Spring (1992)

5. H. Cember, 'Introduction to Health Physics', Pergamon Press, New York (1983)

6. A. Holmer-Siedel and L. Adams, 'Handbook of Radiation Protection', Oxford University Press, Oxford (1993)

7. D.J. Rees, 'Health Physics: Principles of Radiation Protection'. Butterworths, London (1967)

8. K.Z. Morgan and J.E. Turner, 'Principles of Radiation Protection: a Textbook of Health Physics, Wiley New York (1967)

9. J.E. Turner, 'Problems and Solutions in Radiation Protection', Pergamon Press (1988)

10. J.J. Bevelacqua, 'Contemporary Health Physics, Problems and Solution. J. Wiley and Sons (1995)

11. K.J. Connor and I.S. Mclintock, 'Radiation Protection Handbook for Laboratory Workers', H and H Scientific Consultants Ltd. (1994)

12. B. Dörochel, V. Schuricht and J. Stener, 'The Physics of Radiation Protection', Nuclear Technology Publishing, Ashford (1996)

13. W.H. Hallenbeck, 'Radiation Protection', Lewis Publishers, Boca Raton (1994)

14. D. Delacorise, 'Radionuclide and Radiation Protection Handbook 1998.' Nuclear Technology Publishing, Ashford (1998)

15. A.D. Martin and A.S. Harbison, 'An Introduction to Radiation Protection' (4th ed.), Chapman and Hall Medical, London (1996)

16. J. Shapiro, 'Radiation Protection - A Guide to Scientists and Physicians'. Harward University Press, Harvard (1990)

17. S. Plant, 'Radiation Protection in the X-ray Department', Butterworths Heinemann (1993)

18. E.M. Noz and G. Q. Maguire, 'Radiation Protection in Radiologic and Health Sciences' (2nd Ed), Lea and Febigh, (1985)

19. R.L. Katherine and P.L. Ziemer, 'Health Physics, a backward glance, Thirteen Original Papers on the History of Radiation Protection' Pugamor, New York (1980)

20. Pushparaja (Guest Editor), Radiation and Safety Aspects, IANCAS Bulletin 15(3), 1999.

Chapter 22
Radioactive Waste Management

Introduction

Radioactive wastes are generated in various stages of nuclear energy production, in R&D and in production and applications of radioisotopes. There are numerous waste streams having different physical and chemical properties as well as quantities of radioisotopes. Schemes for proper management of these waste streams have been in place from early days of the nuclear industry and there is continuous R&D to improve these schemes. Nevertheless, there is a general perception among the people that the present waste management technology does not address this issue completely. Like other areas in nuclear technology, there is a need to reduce the communication gap with the public.

The primary objective of radioactive waste management is to protect humans and environment from any harmful effects of ionising radiation. Radioactive waste isolation and management criteria have been derived from the general radiation protection goals and radiation exposure limits defined by International Commission on Radiation Protection (ICRP). Permissible exposure dose limit from all sources of artificial radioactivity has been set at 1 mSv per annum. National authorities in many countries define the waste management objective such that the individual dose commitment does not exceed 0.1 mSv per annum (0.3 mSv per annum in some countries like the USA). ***At this dose level, the total annual dose to the world population would be 500,000 man-Sv which is one third of the annual dose received due to X-ray examinations and 1/200 of the dose due to natural radiation sources.*** The protection goals are in fact applied to the 'critical' groups most likely to be exposed. The level of protection for future generations should be at least equivalent to that of present generation. Also safety should not depend upon the active maintenance of the disposal system by future generations beyond a limited period of active surveillance, typically 300 years.

All radioactive wastes are collected and transferred to treatment and conditioning facilities for volume reduction, removal of radioactive constituents if feasible and stabilisation of their chemical and physical forms. The treated wastes are contained appropriately and placed in a suitable environment (disposal), which ensures proper isolation of the waste from the biosphere. The selection of the process/procedure ensures

minimum exposure to the operator (As Low As Reasonably Achievable (ALARA) principle) and operational safety is given high importance.

Classification of Radioactive Waste

Gaseous, liquid and solid waste streams can be contaminated by radioactive nuclides. It is necessary to classify them for the purpose of defining the process of treatment and disposal. In India, the categories of different wastes are defined by the Atomic Energy Regulatory Board (AERB) and are given in Table 22.1.

Table 22.1 - Categorisation of Waste by AERB, India

Category	Solid Surface dose (mGy/h)	Liquid Activity (Bq/m^3)	Gaseous Activity (Bq/m^3)
I	< 2	$< 3.7 \times 10^4$	< 3.7
II	2 - 20	3.7×10^4 to 3.7×10^7	3.7 to 3.7×10^4
III	> 20	3.7×10^7 - 3.7×10^9	$> 3.7 \times 10^4$
IV	Alpha bearing	3.7×10^9 - 3.7×10^{14}	-
V	-	$> 3.7 \times 10^{14}$	-

[S.K. Samanta (Guest Editor), Nuclear Waste Management, Practices and Trends, IANCAS Bulletin, 13(1) (1997)].

Most countries have similar classification. For example, in UK the solid waste is classified into four categories.

Very Low Level Waste (VLLW)

Waste which can be safely disposed of with ordinary refuse is called VLLW. Each 0.1 m^3 of this waste should not contain more than 400 kBq beta/gamma activity or a single item containing less than 40 kBq beta/gamma activity.

Low Level Waste (LLW)

Waste containing more than 400 kBq beta/gamma per 0.1 m^3 but not exceeding 4 GBq/t alpha or 12 GBq/t beta/gamma is called LLW.

Intermediate Level Waste (ILW)

Waste having radioactivity above the LLW level but the decay heat is small and does not require attention for designing storage or disposal facilities is called ILW.

High Level Waste (HLW)

Waste in which radioactive decay heat may lead to significant rise in temperature of the waste is called HLW. This aspect is an important design parameter for storage and disposal facilities.

The current IAEA classification of radioactive wastes is given in Table 22.2.

Table 22.2 - IAEA classification of radioactive wastes

Waste classes		Typical characteristics	Disposal options
1.	Exempt waste(EW)	Activity levels at or below clearance levels which are based on an annual dose to members of the public of less than 0.01 mSv	No radiological restrictions
2.	Low and intermediate level waste (LILW)	Activity levels above clearance levels and thermal power below about 2kW/m^3	Disposal in controlled sites after suitable treatment
2.1	Short lived waste (LILW-SL)	Restricted long lived radionuclide concentration (limitation of long lived alpha emitting radionuclides to 4000 Bq/g in individual waste packages and to an overall average of 400 Bq/g[a] per waste package)	Near surface or geological disposal facility
2.2	Long lived waste (LILW-LL)	Long lived radionuclide concentration exceeding limitation for short lived waste	Geological disposal facility
3.	High level waste (HLW)	Thermal power above about 2kW/m^3 and long lived radionuclide concentration exceeding limitation for short lived waste	Geological disposal facility

[a]Upper range of concentration of ^{226}Ra in the earth's crust. *[Classification of Radioactive Waste Safety Series No.111-G-1.1 IAEA (1994)]*

Origin of Radioactive Waste

A 1000 MWe nuclear power station can meet electricity requirements of 2 million people if per capita consumption is 500kW/y (presently in India it is 300 kW/y). Annually, in a plant of this size, 1.2 te of uranium/plutonium would fission to produce the required electricity and result in the production of 1.2 te of fission products. This is equal to an annual production of radioactive products in a nuclear reactor of 0.6 g per person. This may be compared with a coal fired station of similar capacity in which annually 500,000 tonnes of

ash containing 100 te of chemically toxic metals and 5 million tonnes of gaseous wastes (mainly CO_2 but also SO_2, NO_x) are produced. Further, the fission products in a nuclear power plant are dispersed in the fuel and hence contained. They can be treated suitably for isolation from the environment.

Almost the entire radioactivity produced in a nuclear power plant is contained in the nuclear fuel. However, small amounts of activation products produced during the reactor operation and/or the activity leaking out from the pin-hole type defects (very rare) in the fuel element enter the ventilation system and the coolant system of the reactor, which are continuously purified by using high efficiency particulate air (HEPA) filters (see Chapter 21) in the case of gases, and ion-exchange column for coolant water. Both HEPA filters and spent resins constitute a waste stream. In addition, the coolant/moderator contain radioactivity, due to any leakage, and produces a waste stream. The spent fuel is stored in special water pools (atleast for initial few years) where water is continuously cicrulated to remove decay heat. The water is also purified to control chemistry, such that spent fuel clad is not corroded, and to remove radioactivity released from the spent fuel having defects. This also has to be treated as a radioactive waste stream. The spent fuel contains more than 99.9% of the total radioactivity produced in reactor operation and this comes into solution during reprocessing and distributes in various gaseous and liquid streams.

The basic philosophy of waste management is to isolate/remove the radioactive constituents from the waste streams so that bulk of the fluids become essentially free from radioactivity and can be discharged to the environment as per regulatory guidelines. The concentrates obtained from this treatment as well as other more active streams are treated for volume reduction and for fixation/immobilisation of radioactivity. This concentrated/ isolated radioactive material is then fixed in a suitable matrix which acts as a primary barrier and prevents release of radioactivity to the environment. These are contained and stored in suitable disposal sites. Some typical data for annual waste production from a 1000 MWe LWR are given in Table 22.3.

Treatment of Radioactive Waste Streams

The waste treatment processes can broadly be classified into the following categories

(a) Transfer Technologies : These are processes that remove radioactive species from a waste stream and transfer them to another medium. For example, filtration, ion exchange and reverse osmosis.

(b) Concentration Technologies : These are processes which reduce the waste volume. For example, evaporation, crystallisation, precipitation and centrifugation.

(c) Transformation Technologies : These are processes that concentrate radioactive waste by changing its physical form. The processes include incineration, calcination and compaction.

Table 22.3 - Radioactive waste production in the nuclear fuel cycle : Solid or solidified waste related to the operation of a 1000 MWe LWR during one year

Origin and type		Volume in m^3 (after treatment, conditioning and encapsulation)	Activity or weight
1.	Uranium mining and milling	~60 000 or 30 000 - 40 000 if Pu is recycled	3.7×10^8 Bq.m^{-3} (0.01 Ci.m^{-3})
2.	Conversion, enrichment and fuel fabrication - UO_2 fuels - UO_2 and PuO_2 fuels (for an annual reload of 500-700 kg of Pu)	 - ~ 100	 Negligible 5-10 kg Pu
3.	Reactor - Various solid wastes and conditioned resins	200-600[a]	3.7×10^9 to 3.7×10^{11} Bq.m^{-3} (0.1-10 Ci.m^{-3}) β-γ
4.	Reprocessing - Solidified HLW - Compacted cladding hulls - LLW and ILW : beta-gamma solid waste - Solid and solidified alpha waste	 10 3 ~80 ~10	 5×10^{18} Bq (150 MCi) β-γ[b] + actinides (2 kg Pu for UO_2 fuels, 5-10 kg Pu for UO_2 and PuO_2 fuels) 5×10^{16} Bq (1.5 MCi) β-γ[b] + actinides 4×10^{14} Bq (0.01 MCi) β-γ + α 1-5 kg Pu

[a]Depending on reactor type and conditioning process
[b]150 days after fuel discharge from the reactor
[from Radioactive Waste Management, An IAEA Source Book, IAEA, Vienna (1992) p.16]

Gaseous effluents

All areas where significant quantities of radioisotopes are handled, or where there is a possibility of release of radioactivity, have controlled ventilation (once through in most cases). Exhaust air from such areas is filtered through HEPA filters to remove all dust particles upto 0.3 μm size. As radioactivity is mainly associated with such dust particles/aerosols, the filtered air is essentially free of radioactivity and can be discharged to atmosphere. Leakage from reactor cover gas and coolant/moderator into reactor environment results in radioactivity in air. Proper design of the filtration system can ensure good and clean work environment.

During fuel reprocessing the fission gases like Kr, Xe and iodine are released in the dissolution step. Iodine is retained by using silver impregnated zeolites. Noble gases (only ^{85}Kr is having long half life of 10.78 y) are retained by cryogenic retention. Solubilization by fluorocarbons is another possible method for noble gas removal.

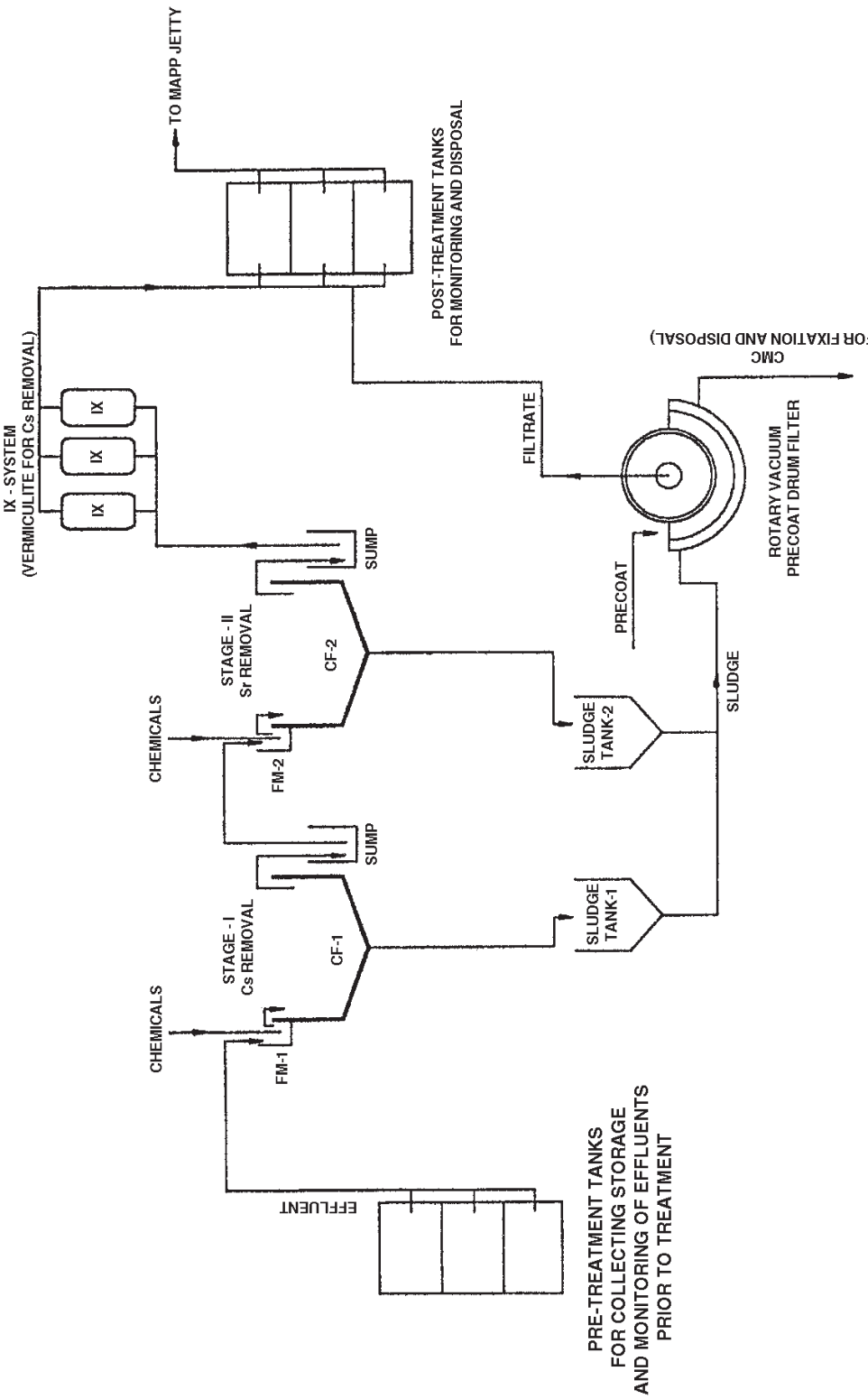

Fig. 22.1 Chemical Treatment Plant at Centralised Waste Management Facility, BARC, Kalpakkam [from Nuclear Waste Management, Practices and Trends, S.K. Samanta (Guest Editor), IANCAS Bulletin, 13(1) (1997)].

Low and Intermediate Level Liquid Effluents

Low and intermediate level waste is generated in most of the facilities connected with nuclear technology. The largest source for this type of waste is the demineraliser regenerants. Sulphate wastes result from regeneration of resins in BWRs and PWRs. In the case of PWRs borate wastes are produced due to the use of boric acid in the primary coolant system. These wastes can either be concentrated (e.g., by evaporation) to obtain concentrates which can be solidified for safe disposal or the radioactivity in the waste removed by techniques such as precipitation and ion exchange.

In order to minimise the requirement of waste treatment, low conductivity water (for BWRs) is collected and treated separately. These are filtered for removing particulates and purified by ion exchange before being returned for reuse. Liquid waste from floor drains requires extensive treatment.

Precipitation Methods

The treatment plant at Kalpakkam (capactiy : 250 m^3/d) is a typical example where precipitation method is used (Fig. 22.1). In the first stage, the effluent from one of the pre-treatment tanks is pumped to Flash Mixer (FM-1), where $K_4Fe(CN)_6$ and $CuSO_4$ solutions are added along with $Fe(NO_3)_3$ solution. The pH of the effluent is adjusted to 8.5 by the addition of NaOH solution and the total content is mixed thoroughly using a turbine type stirrer, operating at 60 rpm. The chemical dosing is as follows: 20 ppm of Cu^{2+} as $CuSO_4$, 30 ppm of Fe^{2+} as $K_4Fe\ (CN)_6$ and 25 ppm of Fe^{3+} as $Fe(NO_3)_3$ solutions.

$$2\ CuSO_4 + K_4Fe(CN)_6 \rightleftharpoons Cu_2Fe(CN)_6 + 2K_2SO_4 \qquad (22.1)$$

The ferric hydroxide formed helps in the coagulation of the precipitate. The precipitate of $Cu_2Fe(CN)_6$ scavenges ^{137}Cs from the effluents. The mixture is let into the flocculating compartment. A retention time of about 4.5 h is provided for efficient growth of the particles and removal of Cs. The overflow is pumped to FM-2.

In the second stage, 75 ppm of Ca^{2+} as $CaCl_2$, 130 ppm of PO_4^{3-} as Na_3PO_4 and 25 ppm of Fe^{3+} as $Fe(NO_3)_3$ are added in the form of solutions, to the effluent in FM-2, followed by the addition of NaOH solution to maintain the pH at 10.5. This results in the precipitation of calcium hydroxy phosphate, $Ca_5(OH)(PO_4)_3$ and other phosphates.

$$5\ Ca^{2+} + 3PO_4^{3-} + OH^- \rightleftharpoons Ca_5(OH)(PO_4)_3 \qquad (22.2)$$

$$3\ M^{n+} + nPO_4^{3-} \rightleftharpoons M_3(PO_4)n \qquad (22.3)$$

M represents Fe^{3+} and some transition metals, lanthanides and actinides. The bulk precipitate of Ca-phosphate / Fe-phosphate carries traces of Sr. As the precipitation is carried out at high pH (10.5), the flocculation of the phosphate is aided by the precipitation of hydroxides of metals present in the system.

The suspension is taken to clariflocculator and the overflow is sent to ion-exchanger for further treatment. The settled mass of suspended solids in the clariflocculators is

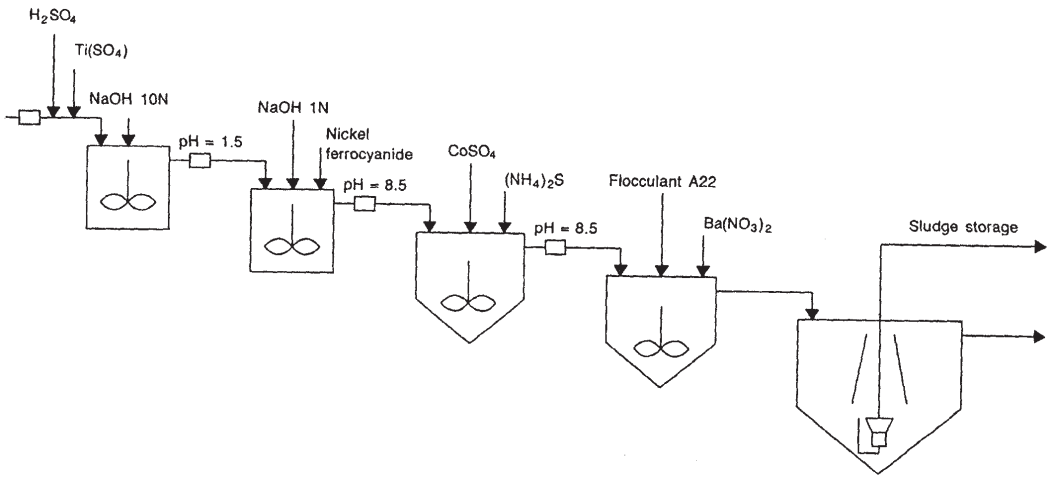

Fig. 22.2 Cogema waste treatment facility.

removed with the help of diaphragm pumps and stored separately in sludge storage tanks installed in filter room. The sludge is filtered using precoat vacuum rotary drum filter, to ensure utmost clarity of filtrate and the solid cake is collected in standard 205 litre drums and sent for concreting prior to disposal. The filtrate is pumped either to post-treatment tank or pre-treatment tank for further treatment depending upon the specific activity.

The cumulative decontamination factor (DF) is calculated by multiplying the DF values obtained in the two stages and may range from 10 to 100.

At the Cogema waste treatment facility (Fig. 22.2) at La Hague, France the intermediate level treatment consists of the following stages.

- addition of sulfuric acid;
- hydrazine pretreatment to destroy nitrites which otherwise interfere with ruthenium decontamination;
- addition of titanium sulphate to precipitate hydrous titanium oxide for improving decontamination from antimony.
- adjustment to pH = 1.5 by using sodium hydroxide;
- addition of preformed nickel ferrocyanide;
- adjustment to pH = 8.5 by using sodium hydroxide;
- addition of sodium sulfide and cobalt sulphate to precipitate cobalt sulfide;
- addition of barium nitrate to precipitate barium sulphate and
- addition of polyelectrolyte.

The ferrocyanide absorbs caesium, cobalt sulfide removes ruthenium and strontium is removed by co-precipitation with barium sulphate. The supernatant liquors are filtered

through a sand filter. The effluent from low level wastes is finally processed by ion exchange. The DFs obtained are 1000 for α, 20-50 for β-γ, 6-30 for Ru, 100 for Sr and 100 for Cs. A volume reduction factor of about 30 is achieved after one decantation stage.

Ion Exchange

Ion exchange resins of different types can be used to trap radioactive ions and reduce radioactivity in the effluent. The concentration of radionuclides is quite often very small and in order to remove these, it is essential that the concentration of other ionic species is also small so that radionuclide uptake is facilitated. Ion exchange resin (cationic and anionic) are thus used to treat effluents which have less than 1000 ppm of total dissolved solid, mainly from different water circuits in a reactor and the water of spent fuel storage pools. After a certain level of use, these resins have to be discarded and treated as waste.

Conventional organic ion exchangers with groups like $-SO_3H$ or $-N(CH_3)_3Cl$, with exchangeable cations (H^+) and anions (Cl^-), respectively, are most commonly employed. Specific ion exchangers have also been developed by many groups for some applications. For example, a phenolic resin made from resorcinol-formaldehyde polycondensate (RFPR) has been developed to remove Cs from alkaline waste streams of a reprocessing plant. Incorporation of iminodiacetic acid ($-CH_2-N(CH_2COOH)_2$) functional group has been found to retain Sr by chelation. The resin has been used to treat several hundred cubic meters of alkaline waste at Tarapur. A commercially available resin Amberlite IRC-718 is also known to be Sr selective in presence of bulk sodium. Use of resins with other chelating groups like aminophosphoric acid is also under investigation for radioactive waste management.

Many of the naturally occurring inorganic ion exchangers, mostly aluminosilicates, have fairly selective properties for absorbing a number of cations of interest in the waste management. These include layer structured clays and zeolites. In layer structured clays there are alternate layers of silicatetrahedra and aluminate octahedra, and the examples include illite, montmorillonite and vermiculite. Of these, vermiculite, $[Mg_3(AlSi_3)O_{10}(OH)_2.nH_2O]$, a natural alteration of mica (about 50% mica), is quite often used for the retention of radioisotopes such as ^{137}Cs, ^{90}Sr, ^{133}Ba and ^{58}Co. Pure vermiculite has an exchange capacity of 1-15 meq/g. It is quite often used in exfoliated (expanded) form in which its density decreases from 0.87 g/cm^3 to 0.21 g/cm^3. Most cations are irreversibly trapped in this matrix due to lattice contraction following adsorption. Among zeolites $[M_{x/n}((AlO_2)_x(SiO_2)_y)zH_2O$, where M is the exchangeable metal ion of valency n, the prominent systems of interest are clinoptilolite, mordenite and philipsite. Sellafield plant in United Kingdom is routinely using clinoptilolite (Majore desert, California) to remove Cs and Sr from water in Magnox spent fuel storage pool. Decontamination factors of 2000 and 500 are reported for Cs and Sr respectively. The ion exchanger is not regenerated but used as a filler in cementation operations. A number of synthetic zeolites are also being investigated for LILW treatment. For example, a mixture of 60% Linde Ionsiv IE-96 and 40% Linde A-51 is used to remove ^{137}Cs and ^{90}Sr at Three Mile Island after the accident, to treat contaminated water. Radionuclides can be fixed in zeolite matrices by thermal/hydrothermal treatment and, therefore, are useful media for radioactive waste disposal.

Treatment of Organic Liquid Effluent

Tributyl phosphate (TBP) diluted with odourless kerosene (70-80%) or with dodecane is used for reprocessing of spent fuel. This solvent loses some of its properties as an extractant after a certain number of cycles and has to be disposed off. Bulk of the radioisotopes in the solvent can be removed by washing with 0.25 M Na_2CO_3 and 7.3 M NaOH. One of the processes which is currently favoured for treating the solvent at Sellafield is based on hydrolysis with strong aqueous NaOH.

$$(C_4H_9O)_3\ PO + NaOH \rightarrow (C_4H_9O)_2PO(ONa) + C_4H_9OH \qquad (22.4)$$

The reaction yields three phases : (i) Aqueous sodium hydroxide containing bulk of the radioactivity and metal contaminants, (ii) Sodium dibutyl phosphate (Na DBP) containing virtually all the remaining contaminants and (iii) Odourless kerosene/dodecane phase. The alkali phase can be used for managing other waste streams. Kerosene and butanol are incinerated. In the case of dodecane, recycle is possible. One of the possibilities for treating NaDBP phase is by acid hydrolysis.

$$(C_4H_9O)_2\ PO(ONa) + HNO_3 \rightarrow NaH_2PO_4 + \text{organic fragments} \qquad (22.5)$$

However, by proper pretreatment steps, it is possible to obtain NaDBP phase suitable for direct disposal.

Treatment of Concentrates and Wet Solids

Many processes of treating LILW results in concentrates and wet solids which require treatment to fix the radioactivity in a matrix suitable for disposal. The concentrates include those from regeneration of dimineralisers in reactor which may contain 8-25% Na_2SO_4 at pH 3-6 as well as boric acid wastes from the primary system of PWR which may contain 5-22% borate at pH 4-8. The wet solids include sludges from precipitation processes and ion exchangers (organic and inorganic). Treatment of combustible solid wastes also results in ash which requires further treatment. A number of methods have been investigated to treat these waste streams and these include incorporation in cement, organic polymer matrices and bitumen. However, cementation is most widely applied method.

Cements are normally made by heating calcarious (lime or sea shells) and argillaceous (clays, silica or iron ore) materials together at 1400-1600^oC. The main ingredients are tricalcium silicate ($3CaO.SiO_2$), dicalcium silicate ($2\ CaO.SiO_2$), tricalcium aluminate ($3CaO.Al_2O_3$) and tetracalcium aluminoferrite ($4CaO.Al_2O_3.Fe_2O_3$). In Ordinary Portland Cement (OPC) the respective percentages of these compounds are about 44, 31, 7 and 13 respectively. Different types of cements can be obtained by changing the relative composition of these constituents. The main cementing component is tobermarite gel ($3CaO.2SiO_2.3H_2O$) produced by the hydrolysis of the calcium silicate in which $Ca(OH)_2$ is the second reaction product. The other two compounds react with $Ca(OH)_2$ and water forming tetracalcium aluminium hydrate and calcium aluminoferrite hydrate. All these phases could incorporate the radionuclide from the waste. The radioactivity becomes fixed in cement after setting and not readily leached. Some specific ingredients are added to

improve the setting properties, strength, quantity of waste incorporated, porosity of the solidified mass and leachability characteristics. Additives include blast furnace slags (BFS), pulverised fuel ash (PFA), pozzolons (like diatomaceous earth), clays and slaked lime. A combination of BFS and OPC has been adopted by many plants of LILW management. BFS is a cementitious material and reacts with water to form a hardened mass. In combination with OPC it produces a totally hydrated system better than OPC alone with lower permeability and pore size for a given water content. In India, a slag based cement has been developed to treat LILW from reprocessing plant. Small amounts of vermiculite are added in the cement to improve retention of Cs.

At some reactor sites in India, polyester based polymer is used to fix ion exchange resins.

Treatment of Solid Wastes

The main operations in solid waste management are reduction in volume and suitable encapsulation of the resultant concentrate. Combustible items like rags, paper, plastics and rubber are quite often incinerated which results in substantial reduction in volumes. In most cases, the incineration is carried out at 800- 1100^{o}C in the presence of excess air (50-75% more). This type of incinerators have the problem of carrying burnable solid particles to the off gas and also the quality of off gas is not controllable. In controlled air incinerators or pyrolising incinerators, the waste is first heated in oxygen deficient conditions at 500-600^{o}C followed by combustion of the resultant material in excess of air.

Compaction is another mode of volume reduction which is particularly applicable to volume reduction prior to disposal. By using a compacting force of upto 10 MN, waste volume density of 400-800 kg/m^3 is possible. At times the waste is directly compacted in a drum/box with a compressive force in the range of 0.01 to 0.5 MN. High force (>10 MN) compression can yield a product with more than 90% theoretical density and is used in some facilities.

For metallic scraps various melting techniques have been proposed for volume reduction but it should always be ensured that secondary wastes from off gas chimney etc. do not increase the waste volume.

High Level Waste Management

During fuel reprocessing, the process of spent fuel dissolution in nitric acid brings almost the entire radioactivity produced during reactor operation into solution. After the extraction of uranium and plutonium with TBP solution, the aqueous raffinate contains bulk of the fission products and traces of U, Pu and other transuranics like Np, Am and Cm. This solution is quite often concentrated and stored in high integrity stainless steel tanks, with cooling arrangement, to allow some of the shorter lived radionuclides to decay. This waste is then solidified in a suitable matrix of high integrity (to store the resultant waste form) in engineered facilities under surveillance. A number of glass and ceramic matrices have been

investigated for immobilisation of HLW. Presently borosilicate glass based systems are most prominent though investigation on ceramic systems is being pursued in many laboratories.

In borosilicate glass the SiO_2 tetrahedral units and B_2O_3 triangular units make a three dimensional network into which elements from HLW occupy suitable positions. Upto 15% of waste oxides can be loaded into a good borosilicate glass composition without detriment to its properties as a stable waste form. The steps involved in the process are evaporation, denitration, calcination, addition of glass former and modifier, and finally preparation of glass. Both batch and continuous processes are used for vitrification. In one of the continuous processes HLW is calcined in a rotary calciner along with minor additives for improving the rheology of the calcine. This calcine and the glass forming additives in the form of primary glass (frit) are fed to the metallic melter. The metallic pot melter is heated by induction furnace. The glass pouring is triggered by heating the freeze valve zone by induction heating. Pouring continues until the decreasing glass level inside the pot reaches the upper level of freeze valve and the pouring stops by itself, since the heating is switched off. The canister is provided with lid and welded. Afterwards the canister is decontaminated externally and sent to interim storage. In France, the vitrification plant AVM (Fig. 22.3) at Marcoule, based on this process is operating since 1978 and three scaled up similar facilities, namely R7 and T7 at La Hague, France and WVP at Sellafield, UK, have been set up.

The Waste Immobilisation Plant (WIP), Tarapur, India is based on pot glass process. The waste is concentrated in a thermosyphon evaporator and is then fed to the metallic

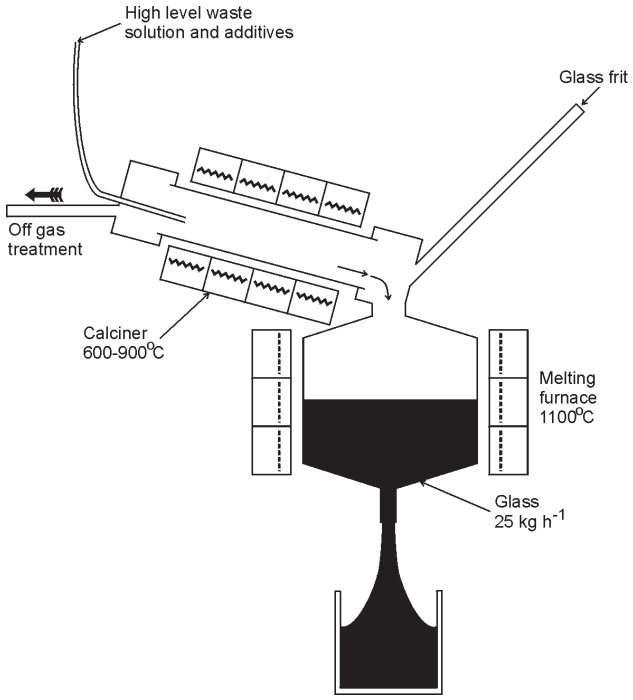

Fig. 22.3 The French continuous vitrification process.

melter. Glass forming chemicals are also fed to the melter in the form of slurry and heated in a multizone induction furnace. The process pot is made of inconel and incorporates a freeze valve section which is operable by the independent induction coil. The susceptor temperature is initially maintained at 600^{o}C. There are simultaneous processes of evaporation and calcination of the HLW, so that solid-liquid interface moves vertically upward. The levels of the glass, calcine and liquid are sensed by the thermocouples located at different heights in the process pot. Temperature of the bottom zone is increased to 950^{o}C so that the calcined mass is fused into glass. Thus three distinct zones, e.g., glass, calcine and waste are established in the process pot. When the pot is filled to about 60% of the capacity with glass, the feed is stopped and the glass is allowed to be soaked at 950-1000^{o}C for 6-8 hours to achieve homogenisation. The molten mass is drained into an insulated canister by operating freeze valve.

The storage canister is 324 mm in diameter, 775 mm long and is made from SS 304 L. The filled canister after 40 hours of cooling is sealed with a lid by pulsed gas tungsten arc welding. The integrity of the welding is ensured by helium leak detection technique. Two such storage canisters are placed in carbon steel overpack of 356 mm dia, 2M long and stored in Solid Storage Surveillance Facility for interim storage.

Radioactive Waste Disposal

The philosophy of radioactive waste management is given in the introductory part of the chapter. Except the very dilute streams, all radioactive wastes are converted into stable solid form which is then kept/disposed off in a suitable repository. The “concentrate and confine” principle is used to ensure isolation of the radioactive material from the biosphere. To achieve this isolation, a multiple barrier enclosure concept is followed. Engineered barriers are important for a period of a few hundred years and are used for isolating activities with half lives of < 30 y. This covers essentially all the fission products radionuclides including ^{137}Cs and ^{90}Sr. Natural geological barriers are essential for long lived nuclides which may require isolation for several thousand years. Use of over-packs made from steel, titanium, lead or copper are under consideration with a view to sealing the waste from the environment. The main route of dispersal of radioactivity from a site is through water which may come in contact with the waste form and leach the radioactivity. This radioactivity may reach the biosphere. The key conditions for characterising a geological environment are:

- Physical isolation and stability
- Hydrological transport processes
- Geochemical conditions and processes.

Annual quantities of low level radioactive waste generated in a nuclear power plant of 1000 MWe are given in Table 22.4

For the purpose of disposal, the Department of Energy, USA has classified low level wastes into three classes A, B and C for disposal in land. For short-lived nuclides, the limits

Table 22.4 - Annual volume and activity of LLW by waste stream and reactor type per 1000 MWe power

Waste stream	BWR		PWR	
	m^3/y	Ci/y	m^3/y	Ci/y
Spent resin	74.1	4,203	32.2	1,326
Filter sludges	547.0		1.2	
Filter cartridges	-		9.2	
Evaporator bottoms	334.7	10,820	494.2	6,006
Compactible trash	917.4		559.0	
Non-compactible trash	133.4		70.4	
Irradiated components	36.0		8.9	
Total	2,042.6	15,023	1,166.2	7,332

[Department of Energy Report DOE/RW-0006 Rev. 2 (1986)]

Table 22.5 - Limits on short lived nuclides in LLW for land disposal.

Nuclide	Class A Bq/m^3	Class B Bq/m^3	Class C Bq/m^3
$t_{1/2} < 5$ y	2.8×10^4	-	-
^3H	1.6×10^3	-	-
^{60}Co	2.8×10^4	-	-
^{63}Ni	1.4×10^2	2.8×10^3	2.8×10^4
^{63}Ni (in metal)	1.4×10^3	2.8×10^4	2.8×10^5
^{90}Sr	1.6	6.0×10^3	2.8×10^5
^{137}Cs	40	1.7×10^3	1.8×10^5

[Low Level Waste Treatment Technology Handbook, DOE/LLW-13TC Department of Energy, Washington (1984)]

are given in Table 22.5. In each of these classes an upper limit is specified for the long lived nuclides, as given in Table 22.6.

Further all classes of waste must (i) contain less than 1% free liquid, (ii) not undergo deterioration, reaction or explosion, (iii) not generate toxic gases, (iv) not be pyrophoric and (v) not contain pathological or infectious waste material. There are no other strict regulations on the physical characteristics of class A wastes. More than 90% of the LLW falls into this

category and include much of the transit, protective clothing and laboratory glassware. Almost all medical low-level waste is class A waste. Radioactivity in these wastes would decay in a few days to a few decades. Class B wastes have radioactivity which may last a few hundred years. Since they are more radioactive and remain radioactive longer, class B wastes must be in a form that remain solid and stable for atleast 300 years. They must be safely packaged and isolated from the environment. Examples include water purification filters in nuclear power plants and aircraft exit signs. Class C wastes may take upto 500 years to decay to safe level at the disposal site. Special attention is paid to shielding and disposing of these wastes. Examples include worn-out nuclear power plant parts. Federal regulations require that these wastes be placed atleast 5 metres beneath the land surface and have barriers which will remain intact for 500 years. Wastes having activity higher than that specified for class C are not acceptable for near surface disposal.

Disposal of Low and Intermediate Level Waste

Table 22.6 - Limits on long lived nuclides for disposal of LLW in land.

Nuclide	Ci/m^3	Nuclide	Bq/g
^{14}C	8	Transuranic ($t_{1/2} > 5$ y)	4000
^{59}Ni (in metal)	220	^{241}Pu	1.4×10^5
^{14}C (in metal)	80	^{242}Cm	8×10^5
^{94}Nb (in metal)	0.2		
^{99}Tc	3		
^{129}I	0.08		

All radioactive wastes are disposed off at controlled sites with adequate provision for continuous monitoring for any release of radioactivity. The site is separated from the rest of the area by a buffer zone in which entry is regulated. Low and intermediate level wastes are disposed off in surface or near surface facilities. For class A wastes (low/suspected radioactivity or short lived radioactivity) simple shallow land burial is quite useful. Some of the possible options are as follows:

(a) Shallow land burial: This approach uses a long, narrow trench 10-15 meters deep with a properly designed protective floor. Waste containers (mostly steel drums) are placed in the trench and spaces between containers backfilled with sand. The trench is sealed with a thick layer of clay or other water repelling materials.

(b) Modular concrete canister: This design is similar to the shallow land burial but the waste drums are placed inside concrete canisters for greater structural stability.

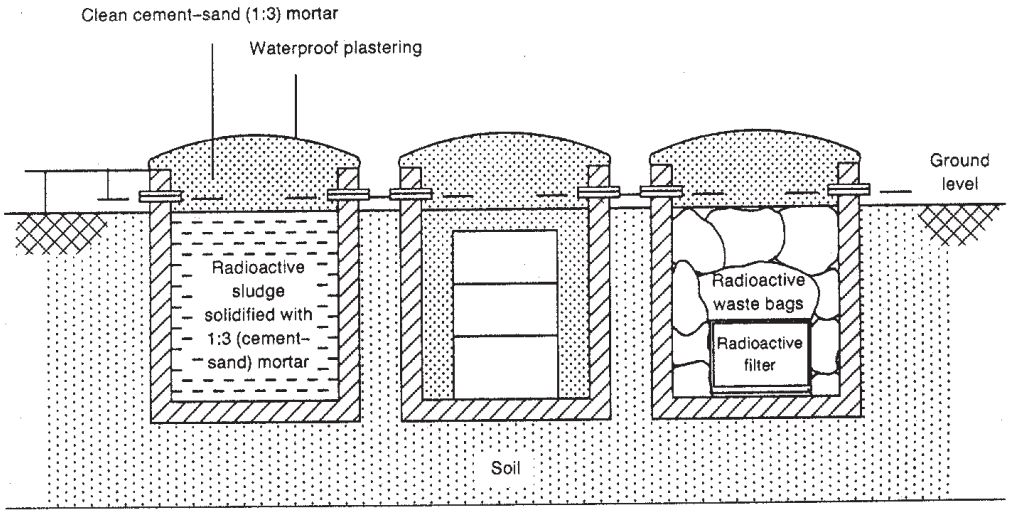

Fig. 22.4 Cross-section of spun concrete receptacles in unlined earth trenches, Tarapur, India.

Cement grount is poured to fill the void space between the waste drum and concrete canister to make a single monolith. These canisters are then placed in the shallow trench, spaces filled with sand and the trench sealed with a water-proof earthen cover.

(c) Concrete vault above or below ground: In this concept a large concrete vault is built from reinforced concrete with 0.7 to 1 m thick walls and floor. Waste drum is put in concrete canisters (as above) and placed inside the vault. The spaces between canisters are filled with sand or grout. The vault is sealed with a poured concrete roof, covered with water-proof membrane and closed with an earthen cap.

In India, it is a practice to have LILW repository at each nuclear site. A brief description of practice at Tarapur is as follows:

The facility accepts solid waste from the nearby Tarapur Nuclear Atomic Power Station and reprocessing plant, which do not generate significant heat and pose no criticality problem. The 100000 m^2 site receives approximately 1000 m^3 of waste per year.

Unlined trenches are only used for suspected active wastes and short lived wastes. Spun concrete receptacles in unlined trenches are used for short lived low and intermediate level trash (see Fig. 22.4). Reinforced concrete trenches of proven design and special waterproof tiling are used for the remaining low and intermediate level wastes and for alpha contaminated wastes in limited amounts (Fig. 22.5).

Tile holds, which are steel lined spun concrete receptacles of high integrity and with waterproof tiling, are used for all wastes with high radioactivity content and for alpha wastes (Fig. 22.6). The unlined trenches are often totally covered with clayed soil while the tile holes are totally filled with concrete and waterproof treatment is used as a top sealing.

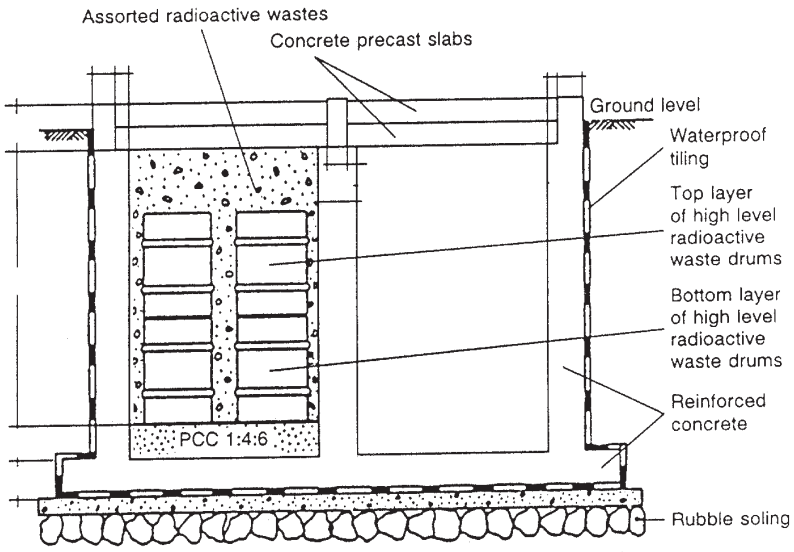

Fig. 22.5 Typical cross-section of a reinforced cement concrete trench (PCC: precast cement concrete), Tarapur, India.

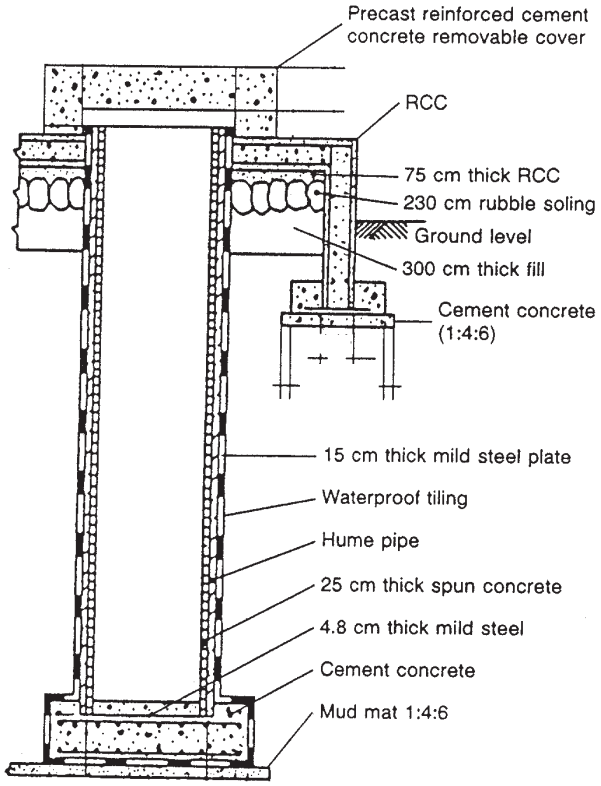

Fig. 22.6 Typical details of a tile hold (RCC: reinforced cement concrete), Tarapur, India.

For regular monitoring of the ground water, special wells are drilled in a grid pattern in the repository. The performance of the site is checked by regular inspection.

Storage of High Level Waste

As described earlier, the current practice for treatment of high level waste, generated during reprocessing of spent nuclear fuel, is to incorporate it in non-leachable form in the glass matrix. The glass is normally placed in steel/stainless steel container. This container is sealed with a lid and the weld integrity is checked by helium leak testing. The container is then put into a secondary container (overpack) mostly made from steel which provides a barrier for leakage of water into and of radioactivity out of the waste form. The steel overpack also provides the mechanical strength required for emplacing the container deep underground. Some countries are pursuing the idea of covering the overpack with a layer of copper or titanium which are known to have high corrosion resistance in the natural environment. The present philosophy is to store these containers in an engineered facility with adequate cooling and surveillance for 30-50 years. In India, the first Safe Storage and Surveillance Facility (SSSF) is already functioning at Tarapur.

Disposal of High Level Waste

High level waste forms require long periods of isolation from natural or man made disruptive forces. Burial of wastes in deep (1 km or more) stable geological formations, provides them an environment where all natural processes which can affect waste behaviour are very slow. One is looking for an isolation period of a few hundred years if the waste does not contain very long lived radioisotopes (particularly Np, Am and Pu isotopes) and several thousand years if these long lived isotopes are present. The main mechanism for the transport of the radioactivity from the waste form to the biosphere would be through water. The corrosion of various protective layers of the waste form, leaching of the radioactivity from glass and migration of contaminated water upto the normal water table which supports biological activity is the scenario of importance for assuming isolation effectiveness. One can also superpose the effect of severe natural phenomena (earthquakes etc.) on this process. The geological properties that make a particular formation a good candidate for repository include scarcity of ground water, low permeability, freedom from joint and faults, good ion exchange capability, freedom from seismic activity and remoteness from biosphere. Rock types which are under consideration include (a) evaporative beds like salt formations, (b) fine grained sedimentary rocks like shale which have good plasticity, low permeability and good ion exchange characteristics, and (c) igneous and metamorphic rocks like granite and basalt. Multi-barrier retention of radionuclides in simulated repository environment (Fig. 22.7) is being studied by many countries and it should be possible to isolate HLW from biosphere for extended periods.

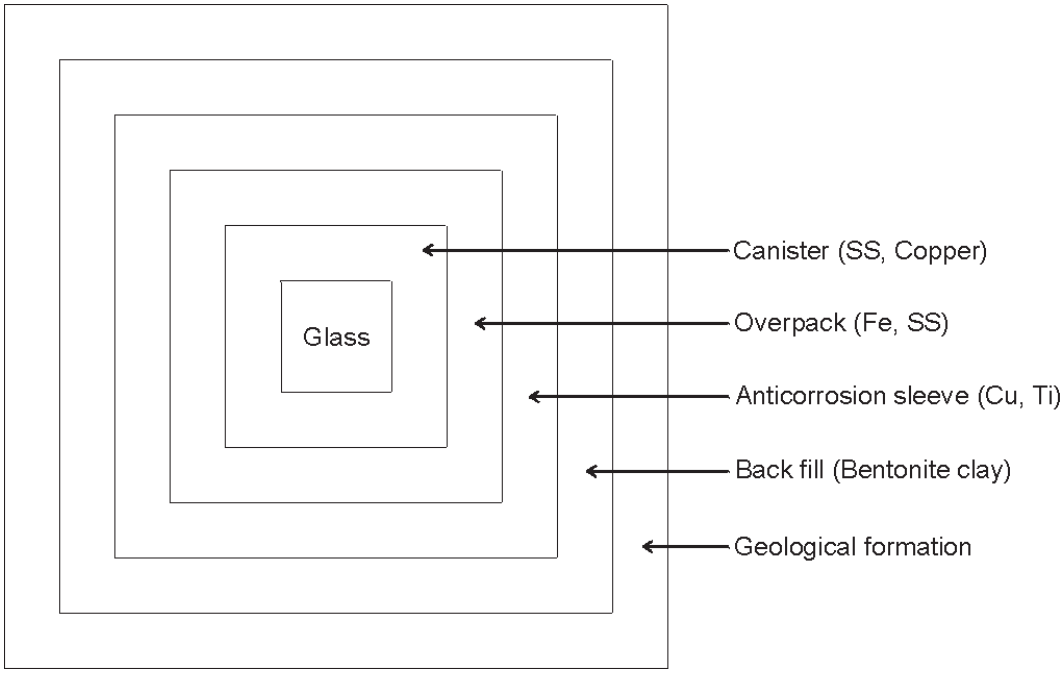

Fig. 22.7 Different barriers for containment of radioactive wastes.

Waste Storage and Disposal Procedures for non-DAE Institutions

A number of hospitals, industrial units and research laboratories use small quantities of radioisotopes. Guidelines for waste disposal in Department of Atomic Energy (DAE), India are briefly given here.

Solid and liquid radioactive wastes containing significant amounts of long lived radioactivity (half-life of the order of years) should not be buried locally or disposed off into the sewerage system. These wastes should be sent to Head, Isotope Applications Division, BARC, Mumbai, after obtaining prior consent.

However, short-lived solid and liquid wastes can be disposed off in conformity with the guidelines given here under.

Solid Waste

1. Solid radioactive waste may be accumulated in the laboratory in suitable receptacles and subsequently buried locally in the pits.
2. An exclusive burial ground for solid radioactive waste should be located in an isolated area and this area should be duly fenced off.

3. While choosing the area for burial, (i) usage of ground and surface waters in the surrounding areas and (ii) the accidental dispersal of the waste to nearby vegetation should be taken into account.

4. The size of the pits may be 120 cm x 120 cm. The depth of the burial pits should be so chosen that the waste containing the activity have a top layer of earth of minimum 120 cm thickness when the pit is finally closed.

5. Normally, after a period of 7 to 10 half-lives, the radioactivity will decay sufficiently so as to permit the contents of a pit, to be disposed off into municipal dump as normal waste. The same pit may be reused for further burial of radioactive materials.

The limits for burial are as shown in Table 22.7.

Table 22.7 - Disposal limits for ground burial and for sanitary sewage system

Sl. No.	Ground Burial					Sanitary Sewage System	
	Radionuclide	Maximum activity in a pit		Maximum limit on total discharge per day		Average monthly conc. of radionuclide	
		(MBq)	(μCi)	(MBq)	(μCi)	(MBq/m^3)	($\mu Ci/cm^3$)
1.	^{3}H	9250	250,000	92.5	2500	3700	1×10^{-1}
2.	^{14}C	1850	50,000	18.5	500	740	2×10^{-2}
3.	^{32}P	370	10,000	3.7	100	18.5	5×10^{-4}
4.	^{35}S	1850	50,000	18.5	500	74	2×10^{-3}
5.	^{45}Ca	370	10,000	3.7	100	10.1	3×10^{-4}
6.	^{60}Co	37	1,000	0.37	10	37	1×10^{-3}
7.	$^{90}Sr + {}^{90}Y$	37	1,000	0.037	1	0.148	4×10^{-6}
8.	^{131}I	37	1,000	3.7	100	22.2	5×10^{-5}
9.	$^{137}Cs + {}^{137m}Ba$	37	1,000	0.37	10	14.8	4×10^{-4}
10.	^{210}Po	3.7	100	0.037	1	0.74	2 x 10

Liquid Waste

1. All radioactive material to be released in normal sewage system must be soluble or easily dispersible in water.

2. It is to be ensured that the concentration and the total quantity of the liquid radioactive waste disposed off into the sanitary sewage system does not exceed the limits shown in Table 22.7.

3. The total activity of all radioisotopes discharged in the sanitary sewage system in one year should not exceed 1 Ci.

4. Liquid radioactive waste containing long lived isotopes (other than ^{3}H and ^{14}C which have short effective half-life) should not be released into the normal drains without the approval of Health, Safety and Environment Group, BARC, Mumbai.

Bibliography

1. S.K. Samanta (Guest Editor), Nuclear Waste Management, Practices and Trends, IANCAS Bulletin, 13(1) (1997).

2. Classification of Radioactive Wastes, Safety Series No.III-G-1.1, IAEA, Vienna (1994).

3. Radioactive Waste Management, An IAEA Source Book, IAEA, Vienna (1992).

4. P.D. Wilson (Ed.), The Nuclear Fuel Cycle - From Ore to Wastes, Oxford Press, Oxford (1996).

5. Department of Energy Report DOE/RW-006 Rev. 2 (1986).

6. Low-level Waste Treatment Technology Handbook, DOE/LLW-13TC Department of Energy, Washington (1984).

7. Management of Small Quantities of Radioactive Waste, IAEA, Vienna (1998).

8. K.W. Carley-Macauley, 'Radioactive Waste: Advanced Management Methods for Medium Active Liquid Wastes', Harwood Academic Publishers, New York (1981).

9. Y.S. Tang and H.J. Saling, 'Radioactive Waste Management' Hemisphere Publishing Corporation, New York (1990).

10. R.E. Berlin and C.C. Stanton, 'Radioactive Waste Management', Wiley Interscience, New York (1989).

11. Radioactive Waste Management at Savannah River Plant: A Technical Review, National Academy Press, Washington (1981).

12. Radioactive Waste Management in Perspective Nuclear Energy Agency, OECD, Paris (1996).

13. D.C. Stewart, 'Data for Radioactive Waste Management and Nuclear Applications', John Wiley & Sons, New York (1985).

14. R.L. Murray and J.A. Powell 'Understanding Radioactive Waste (4th Edition), Batelle Press (1982).

15. Foo-Sun Lau, 'Radioactivity and Nuclear Waste Disposal', John Wiley & Sons Inc. New York (1987).

16. M.H. Campbell, 'High Level Radioactive Waste Management', American Chemical Society, Washington D.C. (1976).

17. Nuclear Power: Management of High-Level Radioactive Waste, World Health Organisation, Copenhagen (1982).

18. C.B. Amphlett, 'Treatment and Disposal of Radioactive Wastes', Pergamon Press, New York (1961).

19. Radioactive Waste (Proc. of 21st Annual Meeting), National Council on Radiation Protection and Measurements, Bethesda (1986).

20. Z. Dlouby, 'Disposal of Radioactive Wastes', Elsevier Scientific Publishing Company, Amsterdam (1982).

21. N.A. Champan, I.G. McKinley and M.D. Hill, 'The Geological Disposal of Nuclear Waste', John Wiley & Sons (1987).

22. 'The Principles of Radioactive Waste Management' Safety Series No.111-F, STI/PUB/989, IAEA, Vienna (1995).

23. 'Partnership Under Pressure-Managing Commercial Low-Level Radioactive Waste', Office of Technology Assessment, Congress of the United States (1989).

24. Report on the Radioactive Waste Disposal STI/DOC/10/349, IAEA, Vienna (1993).

25. 'Low-level Radioactive Wastes', US Council for Energy Awareness, Washington (1993).

26. L.C. Runyon, B. Foster and J.B. Reed, 'Low Level Radioactive Waste - A Legislator's Guide', National Conference of State Legislatures (1994).

27. A.H. Kibbay and H.W. Godbee, 'State-of-the-art report on low-level waste treatment', Report ORNL-TM-7427, Oak Ridge National Laboratory, Oak Ridge (1980).

28. M.W. Carter, A.A. Moghissi and B. Kaln (Eds.) 'Management of Low-level Radioactive Wastes Vol.1&2, Pergamon Press Inc., New York (1979).

29. 'Nuclear Science and Technology - Technological Progress in Management of Radioactive Waste' Report EUR-6699, Commission of European Communities, Brussels (1980).

Appendix I

Fundamental Constants

Quantity	Symbol	Value	SI unit
Speed of light in vacuum	c	299792458	ms^{-1}
Electronic charge	e	1.602176×10^{-19}	C
Planck constant	h	$6.6260693 \times 10^{-34}$	J s
Boltzman constant	k	$1.3806505 \times 10^{-23}$	JK^{-1}
Avogadro Number	A	6.0221415×10^{23}	mol^{-1}
Atomic mass unit (amu)	u	$1.66053886 \times 10^{-27}$	kg
Electron rest mass	m_e	$9.1093826 \times 10^{-31}$	kg
Proton rest mass	m_p	1.67262×10^{-27}	kg
Neutron rest mass	m_n	$1.6749286 \times 10^{-27}$	kg
Faraday constant	F	96485.3383	$C\ mol^{-1}$
Fine structure constant	α	$7.297352568 \times 10^{-3}$	
Molar gas constant	R	8.314472	$J\ mol^{-1}K^{-1}$
Gravitational constant	G	6.6742×10^{-11}	$m^3kg^{-1}s^{-2}$
Acceleration due to gravity	g	9.80665	ms^{-2}
Bohr magneton	μ_B	$9.27400949 \times 10^{-24}$	JK^{-1}
Nuclear magneton	μ_N	$5.05078343 \times 10^{-27}$	JK^{-1}
Electron magnetic moment	μ_e	$-9.28476412 \times 10^{-24}$	JK^{-1}
Proton magnetic moment	μ_p	$1.41060671 \times 10^{-26}$	JK^{-1}
Neutron magnetic moment	μ_n	$-0.96623645 \times 10^{-26}$	JK^{-1}
Compton wavelength of electron		$2.426310238 \times 10^{-12}$	m

Appendix II

Some Conversion Factors

1 Atomic mass unit (u)	=	931.494043 MeV
Electron rest mass (m_e)	=	0.510998918 MeV
Proton rest mass	=	938.272029 MeV
Neutron rest mass	=	939.565360 MeV
1 Joule	=	6.7005361×10^{9} u
	=	$6.24150947 \times 10^{18}$ eV
	=	2.77778×10^{-7} kWh
	=	2.38846×10^{-4} k Cal
1 eV	=	$1.60217653 \times 10^{-12}$ erg
Number of seconds per day	=	86400
One atmosphere pressure (atm)	=	101325 Pa
	=	1.01325 bar
	=	760 torr
Energy-wavelength product	=	12398.5 eV Å
Temperature corresponding to 1 eV	=	1.160450×10^{4} K

Appendix III

Some α-emitting Radioisotopes Used for Energy Calibration

Isotope	Half-life	Alpha energy (MeV)	% Branching
^{235}U	7.038 x 10^8 y	4.598 ± 0.002	4.6
		4.401 ± 0.002	56
		4.374 ± 0.002	6
		4.365 ± 0.002	12
		4.219 ± 0.002	6
^{231}Pa	3.276 x 10^4 y	5.0590 ± 0.008	11
		5.0297 ± 0.008	20
		5.0141 ± 0.008	25.4
		4.9517 ± 0.008	22.8
^{239}Pu	2.411 x 10^4 y	5.1554 ± 0.007	73.3
		5.1429 ± 0.008	15.1
		5.1046 ± 0.008	11.5
^{240}Pu	6.564 x 10^3 y	5.1683 ± 0.002	76
		5.1238 ± 0.002	24
^{241}Am	432.2 y	5.4857 ± 0.001	85.2
		5.4430 ± 0.001	12.8
^{244}Cm	18.1 y	5.80496 ± 0.005	76.4
		5.76284 ± 0.003	23.6

Appendix IV

Some Pure Beta Emitters

Isotope	Half-life	β_{max} (MeV)
^{3}H	12.33 y	0.0186
^{14}C	5730 y	0.156
^{32}P	14.262 d	1.710
^{33}P	25.34 d	0.248
^{35}S	87.51 d	0.167
^{45}Ca	162.61 d	0.252
^{63}Ni	100.1 y	0.067
^{90}Sr	28.78 y	0.546
^{90}Y	64.1 h	2.27
^{147}Pm	2.6234 y	0.224
^{204}Tl	3.78 y	0.766

^{90}Y is the daughter product of ^{90}Sr. Its half-life is 64.1 h. In about 10 days time of purification of ^{90}Sr, its daughter ^{90}Y attains equilibrium with ^{90}Sr.

Appendix V

Some Isotopes Used as Gamma Ray Energy Calibration Standards

Source	Energy (keV)	Source	Energy (keV)
^{241}Am	59.536 ± 0.001	^{192}Ir	468.060 ± 0.010
^{109}Cd	88.034 ± 0.010	Annihilation	511.003 ± 0.002
^{182}Ta	100.106 ± 0.001	^{207}Bi	569.690 ± 0.030
^{57}Co	122.046 ± 0.020	^{208}Tl	583.139 ± 0.023
^{144}Ce	133.503 ± 0.020	^{192}Ir	604.378 ± 0.020
^{57}Co	136.465 ± 0.020	^{192}Ir	612.430 ± 0.020
^{141}Ce	145.442 ± 0.010	^{137}Cs	661.615 ± 0.030
^{182}Ta	152.435 ± 0.004	^{54}Mn	834.840 ± 0.050
^{139}Ce	165.852 ± 0.010	^{88}Y	898.023 ± 0.065
^{182}Ta	179.393 ± 0.003	^{207}Bi	1063.655 ± 0.040
^{182}Ta	222.110 ± 0.003	^{60}Co	1173.231 ± 0.030
^{212}Pb	238.624 ± 0.008	^{22}Na	1274.550 ± 0.040
^{203}Hg	279.179 ± 0.010	^{60}Co	1332.508 ± 0.015
^{192}Ir	295.938 ± 0.010	^{140}La	1596.200 ± 0.040
^{192}Ir	308.440 ± 0.010	^{124}Sb	1691.022 ± 0.040
^{192}Ir	316.490 ± 0.010	^{88}Y	1836.127 ± 0.050
^{131}I	364.491 ± 0.015	^{208}Tl	2614.708 ± 0.050
^{198}Au	411.792 ± 0.008	^{24}Na	2754.142 ± 0.060

Appendix VI

Some Gamma Ray Emitting Radioisotopes with Nuclear Data used as Detection Efficiency Standards

Isotope	Half-life	Gamma ray (keV)	% intensity
^{22}Na	2.601 y	1274.6	99.9
^{40}K	1.277 x 10^9 y	1460.8	10.7
^{57}Co	271.79 d	122.1 136.5	85.6 10.6
^{60}Co	5.274 y	1173.2 1332.5	100 100
^{75}Se	119.779 d	121.1 136.0 264.6 279.5 400.6	16.3 55.6 58.2 24.6 11.1
^{88}Y	106.65 d	898.0 1836.0	94.0 99.4
^{106}Ru	373.59 d	511.8	20.6
^{110m}Ag	249.79 d	657.7 677.6 706.7 763.9 884.7 937.5 1384.3 1505.0	94.7 10.7 16.7 22.4 72.9 34.3 24.3 13.1
^{125}Sb	2.7582 y	427.9 463.4 600.6 635.9	29.4 10.5 17.8 11.3
^{134}Cs	2.0648 y	569.3 604.7 795.8	15.4 97.6 85.4
^{137}Cs	30.07 y	661.6	85.1

Isotope	Half-life	Gamma ray (keV)	% intensity
^{133}Ba	10.5588 y	81.0 302.9 356.0	32.8 18.6 62.3
^{152}Eu	13.537 y	121.8 244.7 344.3 411.1 444.0 778.9 867.4 964.1 1085.9 1112.1 1408.0	28.4 7.37 26.6 2.16 3.02 13.0 4.14 14.6 10.2 13.6 20.8
^{208}Bi	3.68 x 10^5 y	2614.6	100
^{241}Am	432.2 y	59.5	35.9

Foot note 1: A multigamma emitting ^{152}Eu is often used to check the detection efficiency and for energy calibration of gamma ray detectors.

Foot note 2: Radium-226 (1600 y half life) in equilibrium with its daughter product can be used as a multi gamma ray source. Energy of gamma rays span from 186.21 keV to 2447.86. However, ^{226}Ra has to be calibrated against a standard source for the γ-ray intensities.

Appendix VII

Q Value Equation of Nuclear Reaction

The Q value equation for a nuclear reaction is an analytical relationship between the energy (Q) associated with a nuclear reaction and the kinetic energy of the projectile, ejectile and the product, as measured in the laboratory coordinates.

In Fig. A7.1 the dynamics of a nuclear reaction with projectile (a) on target (A) forming an intermediate C from which ejectile b is emitted and the remaining is the product B is shown. M_1, M_2, M_3 and M_4 are the masses of a, A, b and B respectively. $M_c = M_1 + M_2$, θ and ϕ are the emission angles of b and B respectively with respect to the projectile beam direction. E_1, E_3 and E_4 are kinetic energies of a, b and β, respectively and target is stationary ($E_2 = 0$)

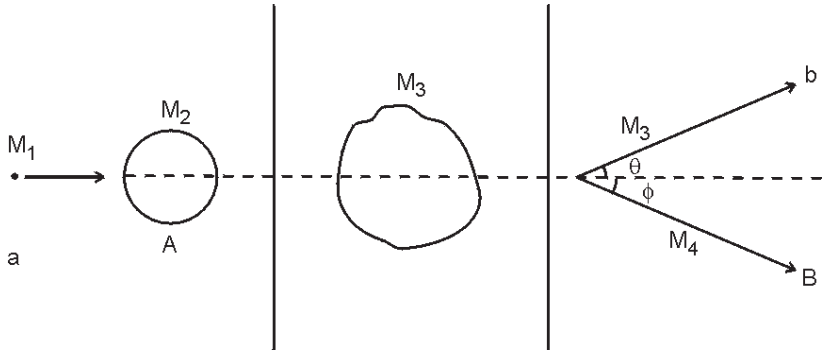

Fig. A7.1 Schematic diagram of the dynamics of a nuclear reaction A(a,b)B

Conservation of mass/energy is related as

$$E_1 + Q = E_3 + E_4 \qquad \text{(A7.1)}$$

Conservation of linear momentum in the direction of incident particle is given by

$$\sqrt{2M_1E_1} = \sqrt{2M_3E_3}\cos\theta + \sqrt{2M_4E_4}\cos\phi \qquad \text{(A7.2)}$$

Conservation of linear momentum in the direction perpendicular to incident particle direction is given by

$$0 = \sqrt{2M_3E_3}\sin\theta - \sqrt{2M_4E_4}\sin\phi \qquad \text{(A7.3)}$$

From eqns. A7.1, A7.2 and A7.3 the Q value can be deduced as

$$Q = E_1\left(\frac{M_1}{M_4} - 1\right) + E_3\left(\frac{M_3}{M_4} + 1\right) - \frac{2\sqrt{M_1M_3E_1E_3}}{M_4}\cos\theta \qquad \text{(A7.4)}$$

This equation is same as that of eqn. 8.7 in Chapter 8. This equation is quadratic in $\sqrt{E_3}$ and when solved gives a formula for E_3 as a function of the projectile kinetic energy (E_1) and the angle of emission of b

$$E_3 = v \pm \sqrt{v^2 + w} \tag{A7.5}$$

$$\text{where } v = \frac{\sqrt{M_1 M_3 E_1}}{M_3 + M_4} \cos\theta \tag{A7.6}$$

$$w = \frac{M_4 Q + E_1 (M_4 - M_1)}{M_3 + M_4} \tag{A7.7}$$

Thus the desired value of E_3 can be obtained by a suitable choice E_1 and θ.

The value of $\sqrt{E_3}$ should be real and positive for a nuclear reaction to take place. The conditions under which $\sqrt{E_3}$ can be imaginary are

(i) Negative Q value

(ii) $M_4 < M_1$ and

(iii) Large θ, so that cos θ becomes negative.

Appendix VIII

The Laboratory and Center of Mass Coordinate Systems

In nuclear reactions, centre of mass system is used rather than laboratory system. It helps in reducing many body system, which is the case in nuclear reactions, relative velocity of two reacting particles, (projectile and target), and the reduced mass are considered representing the system.

In laboratory (L) system of coordinates, the origin is fixed in laboratory and is at rest. In center of mass (CM) system, the origin is fixed at the centre of mass, which can have inertial motion with respect to an observer from the laboratory system coordinates. In Fig. A8.1 relationship between velocity of particles M_1 and M_2 in L system and CM system is given.

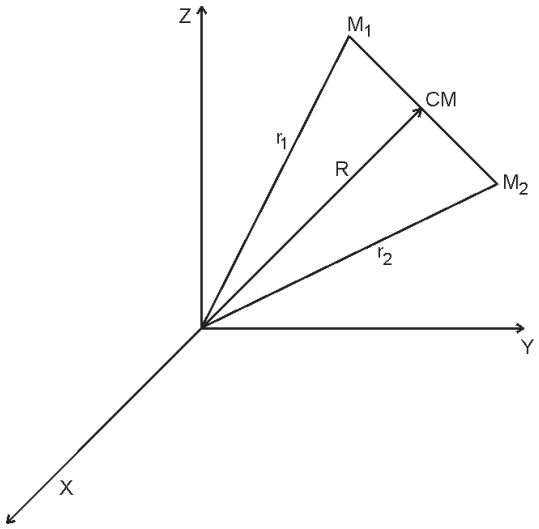

Fig. A8.1 Relationship between velocity of particles M_1 and M_2 in L system and CM system..

Consider two particles of mass M_1 and M_2 moving with velocities V_1 and V_2 before collision and with velocities V_1' and V_2' after collision in L system as shown in the above figure. The same in CM system are denoted by v_1, v_2 and V_1', V_2', respectively.

The center of mass lies on the line joining M_1 and M_2 and its radial distance from the origin of L-system is,

$$R = \frac{M_1 r_1 + M_2 r_2}{M_1 + M_2} \qquad \text{(A8.1)}$$

Since the linear momentum is conserved in both the coordinate systems,

$$M_1V_1 + M_2V_2 = (M_1 + M_2)\, V = M_1V_1' + M_2V_2' \qquad \text{(A8.2)}$$

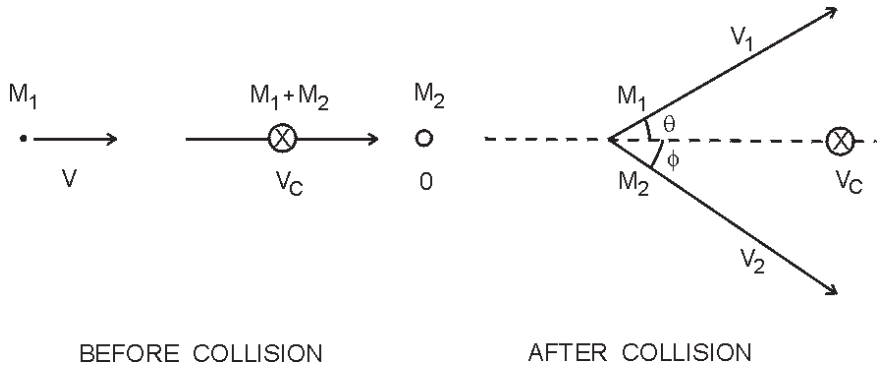

Fig. A8.2 Reaction dynamics of a binary nuclear reaction in L system.

which gives $$V = \frac{M_1 V_1 + M_2 V_2}{M_1 + M_2} \quad \text{(A8.3)}$$

In the Fig. A8.2 dynamics of a binary nuclear reaction in L system is shown. The projectile of mass M_1 moves with a velocity V_1 in L system towards a stationary target of mass M_2 and the two are scattered at angles θ and ϕ with velocities V_1 and V_2 respectively. The center of mass is denoted by X which moves with a velocity V_c in L system.

Conservation of linear momentum gives

$$M_1 V_1 = (M_1 + M_2)\, V_c \quad \text{(A8.4)}$$

In CM system M_1 approaches CM with a velocity equal to V_1-V_c where V_1 and V_2 are relative velocities of M_1 and M_2 respectively.

$$\begin{aligned} M_1 V_1 + M_2 V_2 &= M_1(V_1 - V_c) - M_2 V_c \\ &= M_1 V_1 - (M_1 + M_2)\, V_c \\ &= 0 \end{aligned} \quad \text{(A8.5)}$$

Thus the sum of the momenta before collision is zero. Therefore, for conservation of momentum it will be zero after the collision also. As a result, the particles always move in opposite direction in CM system.

In Fig. A8.3 the dynamics of a binary nuclear reaction in CM-system is given. Let us now calculate the kinetic energy available in the CM system.

In CM system

$$V_1 = V_1 - V_c = V_1 - \frac{M_1}{M_1 + M_2}\, V_1 = \frac{M_2}{M_1 + M_2}\, V_1 \quad \text{(A8.6)}$$

$$V_2 = V_c = \frac{M_1}{M_1 + M_2}\, V_1 \quad \text{(A8.7)}$$

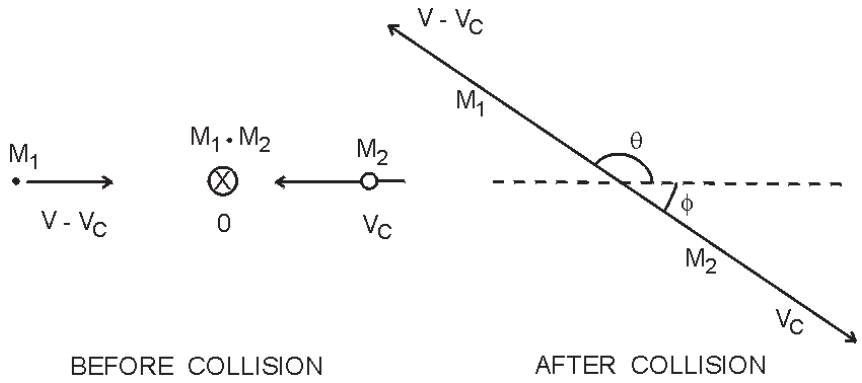

Fig. A8.3 Reaction dynamics of a binary nuclear reaction in CM system.

The kinetic energies of projectile and target in center of mass system are

$$T_1 = \frac{1}{2}M_1V_1^2 = \frac{1}{2}M_1V_1^2\left(\frac{M_2}{M_1+M_2}\right)^2 = \left[\frac{M_2}{M_1+M_2}\right]^2 T_1 \qquad \text{(A8.8)}$$

$$T_2 = \frac{1}{2}M_2V_2^2 = \frac{1}{2}M_2V_2^2\left(\frac{M_1}{M_1+M_2}\right)^2 = \frac{M_1M_2}{(M_1+M_2)^2} T_1 \qquad \text{(A8.9)}$$

$$\therefore T_c = T_1 + T_2$$

$$= T_1\left[\left(\frac{M_2}{M_1+M_2}\right)^2 + \frac{M_1M_2}{(M_1+M_2)^2}\right]$$

$$= T_1\left[\frac{M_2(M_1+M_2)}{(M_1+M_2)^2}\right] = \frac{M_2}{M_1+M_2} T_1 \qquad \text{(A8.10)}$$

The energy T_c is available for inducing nuclear reaction. The energy T_1-T_c is utilised to set CM into motion V is not available. It is given by

$$= \frac{M_1}{M_1+M_2} T_1 \qquad \text{(A8.11)}$$

The only energy that is useful for inducing a reaction is that available in CM system.

For example, let two accelerators provide beams of identical particles of same knietic energy, say T. IF the beams are travelling in opposite direction and meet at a point, the KE in C system is 2T, the same is T/2 of the two are travelling in the same direction.

Appendix IX

Angular Momentum in Nuclear Reactions

The collision between a particle and a nucleus is characterised classically by an impact parameter (b) which represents the distance of closest approach between them. The angular momentum of the system is related to the impact parameter as

$$L = p.b = b\frac{h}{\lambda} \qquad \text{(A9.1)}$$

where p is the relative momentum between the particle and the target nucleus. The impact parameter can vary between zero (head on collision) and R, the sum of the radii of projectile and target nuclei (grazing collisions).

Classically L can vary continuously between zero and R h/λ. However, according to quantum mechanics only discrete values of L are allowed.

$$L = l\,h\,; \qquad l = 0, 1, 2, ... \qquad \text{(A9.2)}$$

Thus a range of b values corresponds to the same value of angular momentum. Thus

$$l\,ƛ < b < (l + 1)\ ƛ \qquad \text{(A9.3)}$$

will have the same angular momentum (l). This can be visualised as each l corresponding to a circular strip of a disc of radius (R) as shown in Fig. A9.1.

The cross section for corresponding to a l wave particles is given by the area of the strip between the radii $l\,\lambda$ and $(l + 1)ƛ$

$$\therefore \sigma_l = \pi[(l + 1)\,ƛ]^2 - (l\,ƛ)^2] \qquad \text{(A9.4)}$$

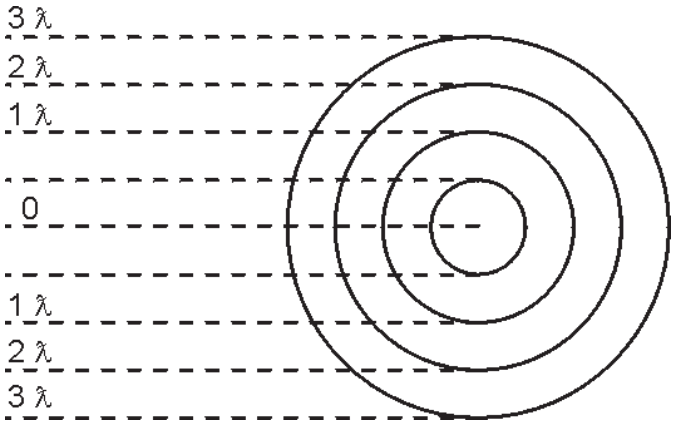

Fig. A9.1 Cross-sectional are as associated with different partial l - waves.

$$\sigma_l = \pi\lambda\!\!\!^{-2}(2l+1) \tag{A9.5}$$

The reaction cross section is the sum of cross sections for all possible l values.

$$\therefore \sigma_R = \pi\lambda\!\!\!^{-2}\sum_{l=0}^{l_{max}}(2l+1) = \pi\lambda\!\!\!^{-2}(l_{max}+1)^2 \tag{A9.6}$$

$$l_{max} = \frac{R}{\lambda\!\!\!^{-}} \qquad \therefore \sigma_R = \pi(R+\lambda) \tag{A9.7}$$

For low energy neutrons, $\lambda\!\!\!^{-} > R$ and therefore

$$\sigma_R \simeq \pi^2\lambda\!\!\!^{-2} \tag{A9.8}$$

For high energy projectiles $R >> \lambda\!\!\!^{-}$ Cross section is given as

$$\sigma_R = \pi R^2 \tag{A9.9}$$

Eqn. A9.5 assumes that every collision leads to reaction. Quantum mechanical treatment however shows that each l wave has a transmission coefficient (T_l) for penetrating the surface of the potential offered by target nucleus. Thus

$$\sigma_l = \pi\lambda\!\!\!^{-2}(2l+1)\,T_l \tag{A9.10}$$

where $0 < T_l < 1$

The transmission coefficients are calculated using the scattering theory.

Angular Momentum Barrier

When a particle approaches the target nucleus with an angular momentum (l), there exists a centrifugal barrier (V_l) given by

$$V_l = \frac{l(l+1)\hbar^2}{2\mu R^2} \tag{A9.11}$$

where R is the sum of the radii of projectile and target. The particle can enter the target nucleus only if its kinetic energy is more than V_l.

Cross Sections for Charged Particle Induced Reactions

When a charged particle collides with a target nucleus, it must overcome the Coulomb barrier (V_c) in order to induce nuclear reaction where V_c is given by eqn. 8.9 (Chapter 8)

$$V_c = \frac{Z_1 Z_2 e^2}{R_1 + R_2}$$

Thus the particle must have a kinetic energy (E_1) greater than V_c. The initial momentum of the particle is $p = \sqrt{2\mu E_1}$ As the particle approaches the target, relative momentum of the system decreases and at the point of contact, it becomes

$$p = \left|2\,\mu(E_1 - V_c)\right|^{1/2} = 2(\mu E_1)^{1/2}\left|1 - \frac{V_c}{E_1}\right|^{1/2} \qquad \text{(A9.12)}$$

The maximum angular momentum (l_m) corresponds to the impact parameter when the projectile and target are just touching. Thus

$$l_m = pR = R(2mE_1)^{1/2}\left|1 - \frac{V_c}{E_1}\right|^{1/2} \qquad \text{(A9.13)}$$

However initial angular momentum $l_m = pb_m$

$$\text{Thus } b_m = R\left|1 - \frac{V_c}{E_1}\right|^{1/2} \qquad \text{(A9.14)}$$

$$\sigma = \pi b_m^2 = \pi R^2\left|1 - \frac{V_c}{E_1}\right| \qquad \text{(A9.15)}$$

This shows that as $E_1 \to V_c$, $l_m \to 0$ and the reaction cross section vanishes at $E_1 < V_c$.

Appendix X

Breit - Wigner Relation

The decay of discrete excited nuclear states follows the independent hypothesis and the mode of decay depends only on the total decay width (Γ) and the partial decay widths (Γ_i) for different exist channels. For a nuclear reaction in which compound nucleus (CN) is formed, CN is in excited state. Breit and Wigner derived a formula for the cross sections in the resonance region. According to this,

$$\sigma_{A\to C} = \pi\lambda\!\!\!^{-2} \frac{2I_C + 1}{(2I_A + 1)(2I_a + 1)} \frac{\Gamma_{aA}\,\Gamma}{(E - E_0)^2 + (\Gamma/2)^2} \qquad \text{(A10.1)}$$

where, I_a, I_A and I_C are the spins of a, A and the compound nucleus respectively.

The total width is the sum of all partial widths. The cross section for channel (a,b) is given by,

$$\sigma(a,b) = \sigma_c\, W_B \qquad \text{(A10.2)}$$

where $W_B = \frac{\Gamma_{Bb}}{\Gamma}$. Thus,

$$\sigma_{A\to C\to B} = \pi\lambda\!\!\!^{-2} \frac{2I_C + 1}{(2I_A + 1)(2I_a + 1)} \frac{\Gamma_{aA}\,\Gamma_{Bb}}{(E - E_0)^2 + (\Gamma/2)^2} \qquad \text{(A10.3)}$$

The cross sections for the (n,γ) reactions in the vicinity of resonances can now be expressed as,

$$\sigma_{(n,\gamma)} = \pi\lambda\!\!\!^{-2} \frac{2I_C + 1}{(2I_A + 1)(2I_a + 1)} \frac{\Gamma_n\,\Gamma_\gamma}{(E - E_0)^2 + (\Gamma/2)^2} \qquad \text{(A10.4)}$$

where E_0 is the resonance energy and E is the neutron energy at which the cross section is calculated.

Appendix XI

Table of Nuclides

Explanation of Table

Column 1, Isotope (Z, El, A)

Nuclides are listed in order of increasing atomic number (Z), and are subordered by increasing mass number (A). All isotopic species are included as well as all isomers with half-life ≥0.1 s, and some other isomers which decay by SF or α emissions. A nuclide is included even if only its mass estimate or its production cross section is available. For the latter nuclides $T_{1/2}$ limit is given *[1]*.

Isomeric states are denoted by the symbol "m" after the mass number and are given in the order of increasing excitation energy. The ^{235}U thermal fission products, with fractional cumulative yields $\geq 10^{-6}$, are italicised in the table. The information on fission products is taken from the ENDF/B-VI fission products file *[2]*.

The names for elements Z=104-109 are those adopted by the American Chemical Society Nomenclature Committee. The symbols Rf (Rutherfordium) and Ha (Hahnium) have, not been accepted internationally due to conflicting claims about the discovery of these elements.

Column 2, Jπ

Spin and parity assignments, without and with parentheses, are based upon strong and weak arguments, respectively. See the introductory pages of any January issue of Nuclear Data Sheets *[3]* for description of strong and weak arguments for Jπ assignments.

Column 3, Mass Excess, Δ

Mass excesses, M-A, are given in MeV with $\Delta(^{12}C)=0$, by definition. For isomers the values are obtained by adding the excitation energy to the Δ(g.s.) values. Wherever the excitation energy is not known, the mass excess for the next lower isomer (or g.s.) is given. The values are given to the accuracy determined uncertainty in Δ(g.s) (maximum of three figures after the decimal). The uncertainty is ≤ 9 in the last significant figure. An appended "s" denotes that the value is obtained from systematics.

The authors are grateful to Dr. Jagdish K. Tuli, National Nuclear Data Center, Brookhaven National Laboratory, USA, who has kindly permitted to freely use the data from Nuclear Wallet Cards July 1995 edition.

Column 4, $T_{1/2}$, Γ or Abundance

The half-life and the abundance (in **bold face**) are shown followed by their units ("%" symbol in the case of abundance) which are followed by the uncertainty, in *italics*, in the last significant figure. For example, 8.1 s *10* means 8.1±1.0 s. For some very short-lived nuclei, level widths rather than half-lives are given. There also, the width is followed by units (e.g., eV, keV, or MeV) which are followed by the uncertainty in *italics*, if known.

Column 5, Decay Mode

Decay modes are given in decreasing strength from left to right, followed by the percentage branching, if known ("w" indicates a weak branch). The percentage branching is omitted where there is no competing mode of decay or no other mode has been observed.

The various modes of decay are given below:

β-	β^- decay
ε	ε (electron capture),, or $\varepsilon+\beta^+$,, or β^+ decay
IT	isomeric transition (through γ or conversion-electron decay)
n, p, α, ...	neutron, proton, alpha, ... decay
SF	spontaneous fission
2β-, 3α, ...	double β^- decay ($\beta^-\beta^-$), decay through emission of 3 α's, ...
β-n, β-p, β-α, ...	delayed n, p, α, … emission following β^- decay
εp, εα, εSF, ...	delayed p, α, SF, … emission following ε or β^+ decay.

References

1. NUBASE: A Database of Nuclear and Decay Properties, G. Audi, O. Bersillon, J. Blachot and A.H. Wapstra, Int. Symposium to Radionuclide Metrology and its Applications (1995).

2. Evaluation and Compilation of Fission Product Yields 1993, T.R. England and B.F. Rider; Rept. LA-UR-94-3106 (1994). ENDF/B-VI evaluation; MAT #9228, Revision 1.

3. Nuclear Data Sheets - Academic Press, San Diego, Evaluations published by mass number for A=45 to 266. See page ii of any issue for the index to A-chains.

3. *Nuclear Physics* - North Holland Publishing Co., Amsterdam - Evaluations by F. Ajzenberg-Selove and by D.R. Tilley et al. For A = 3 to 20.

4. Energy Levels of A = 21-44 Nuclei (VII), P.M. Endt, *Nuclear Physics* A521, 1 (1990).
Supplement, *Nuclear Physics* A633, 1 (1998).

5. *Nuclear Science Reference File* - a bibliographic computer file of nuclear science references continually updated and maintained by the National Nuclear Data Center, Brookhaven National Laboratory, Recent literature scanned by D. Winchell and A. Sonzogni.

6. Table of Isotopes, 8th edition (1996), Editors: R. Firestone, V. Shirley, C. Baglin, F. Chu, and J. Zipkin, John Wiley, New York.

7. Spontaneous Fission Half-lives for Ground State Nuclides, N.E. Holden and D.C. Hoffman, Pure Appl. Chem. 72 (2000), to be published.

8. NUBASE evaluation of Nuclear and Decay Properties, G. Audi, O. Bersillon, J. Blachot and A.H. Wapstra, *Nuclear Physics* A624, 1 (1997)

9. The 1995 update to the atomic mass evaluation, G. Audi and A.H. Wapstra, computerized list of recommended values based on authors' publication, *Nuclear Physics* A595, 409 (1995).

10. N.E. Holden, private communication, December, 1999. *Table of Isotopes* (2000).

11. Evaluation and Compilation of Fission Product Yields 1993, T.R. England and B.F. Rider; Rept. LA-UR-94-3106 (1994). ENDF/B-VI evaluation; MAT #9228, Revision 1.

12. *Table of Isotopes* (1978), 7th edition, Editors: C.M. Lederer, V.S. Shirley, Authors: E. Browne, J.M. Dairiki, R.E. Doebler, A.A. Shihab-Eldin, J. Jardine, J.K. Tuli, and A.B. Buyrn, John Wiley, New York.

13. CODATA Values of the Fundamental Physical Constants: 1998, J. Mohr and B.N. Taylor, *Jl. of Physical and Chemical Reference Data* (to be published). Data taken from http://physics.nist.gov/constants (September 1, 1999).

About the Authors

***Dr. D.D. Sood**, after graduating from Training School of the Bhabha Atomic Research Centre (BARC) in 1959, joined Radiochemistry Division, BARC. He studied cation diffusion in uranium and thorium oxides at Imperial College of Science and Technology, London during 1966 and worked on the molten salt reactor concept at Oak Ridge National Laboratory, USA during 1970-72. He is an expert in chemistry and metallurgy of plutonium with special reference to plutonium based fuels. He has published more than 150 research papers and 25 technical reports. He was a member of the Advisory Board of the Journal of Chemical Thermodnyamics. He has held the designations of Head, Fuel Chemistry Division, BARC and Director, Radiochemistry and Isotope Group, BARC. He served as Director, Division of Physical and Chemical Sciences, IAEA, Vienna during 1998-2003. He was president IANCAS for two terms. He has authored/coauthored 3 books, Nuclear Materials, Introduction to Radiochemistry and Experiments in Radiochemistry. He is recipient of many awards including IANCAS Dr. M.V. Ramaniah Memorial Award for the outstanding and life time achievements in the field of Nuclear and Radiochemistry.*

***Dr. A.V.R. Reddy** after graduating from BARC Training School in 1976-77, joined Nuclear Chemistry Section, RCD and was its Head from 1998. He is at present Head, Analytical Chemistry Division, BARC. His main areas of research are nuclear fission, nuclear reactions, radiochemical separations, neutron activation analysis and general analytical chemistry. He has about 350 publications in journals and symposia. He is a co-author of the books, Experiments in Radiochemistry and Introduction to Radiochemistry. He is a professor of Homi Bhabha National Institute. He served as Secretary (1991-1993) and Editor (2000-2003) of IANCAS. He has worked as a visiting scientist for an year on the extension of Periodic Table in the Institut für Kernchemie, Mainz, Germany. Dr. Reddy served as a Technical Officer during 1999-2000 in the Division of Physical and Chemical Sciences, IAEA, Vienna. He is a fellow of IUPAC (International Union of Pure and Applied Chemistry) and was a commission member of IUPAC's Commission on Radiochemistry and Nuclear Techniques during 1996-2002. He served as an IAEA expert and visited many countries to provide advice on nuclear analytical techniques and radiochemistry.*

***Dr. N. Ramamoorthy** after graduating from BARC Training School during 1971-72 joined Isotope Division, BARC. He worked on technetium chemistry at Nuclear Research Centre, Julich, Germany. He obtained his Ph.D. in 1988 from University of Bombay. He held the positions of Head, Radiopharmaceuticals Division, BARC (1999-2000), Associate Director, Isotope Group, BARC and Chief Executive of Board of Radiation and Isotope Technology (2000-2003). Since October 2003, he is serving as Director, Division of Physical and Chemical Sciences, at the IAEA, Vienna and oversees the IAEA programme on Nuclear Science and on Radioisotope Production and Radiation Technology. His research interests and contributions are in the areas of reactor and cyclotron produced radioisotopes, radiopharmaceuticals and radiation technology. He has published about 160 papers in journals and national/international meetings, co-authored a book, edited 3 manuals. He served as an IAEA expert and as a Visiting Assistant Professor in the University of Missouri-Columbia, USA. Dr. Ramamoorthy is a Founder Fellow of the Indian College of Nuclear Medicine (FICNM), a Fellow of Maharashtra Academy of Sciences and was the President of the Society of Nuclear Medicine, India during 2000-2001 and an active member of IANCAS.*